

Vulnerability-Based Seismic Assessment and Retrofit of One- and Two-Family Dwellings

Volume 3 - Background Documentation

FEMA P-1100-3 / October 2019



FEMA



Vulnerability-Based Seismic Assessment and Retrofit of One- and Two-Family Dwellings

Volume 3 – Background Documentation

Prepared by
APPLIED TECHNOLOGY COUNCIL
 201 Redwood Shores Parkway, Suite 240
 Redwood City, California 94065
www.ATCouncil.org

Prepared for
CALIFORNIA EARTHQUAKE AUTHORITY
 Janiele Maffei, Chief Mitigation Officer
 Erin Waters, Research Program Coordinator
 Sacramento, California

FEDERAL EMERGENCY MANAGEMENT AGENCY
 Michael Mahoney, Project Officer
 Robert D. Hanson, Subject Matter Expert
 Washington, D.C.

ATC MANAGEMENT AND OVERSIGHT
 Jon A. Heintz
 Ayse Hortacsu

PROJECT TECHNICAL COMMITTEE
 Colin Blaney (co-Project Tech. Director)
 Kelly Cobeen (co-Project Tech. Director)
 Thomas Anderson
 Vikki Bourcier
 Michael Cochran
 Daniel Dolan
 Andre Filiatrault
 Brian McDonald
 John Osteraas
 Weichiang Pang

PROJECT STEERING COMMITTEE
 David Bonowitz (Chair)
 Ifa Kashefi
 Philip Line
 Thor Matteson
 Bill Nagel
 Steve Pryor
 Frank Rollo
 Williston Warren (ATC Board Contact)

WORKING GROUP
 Angela Arias
 Gaurav Bali
 Michael Ty Billings
 Brent Crawford
 Steve Fedorchak
 Gayle Jensen
 Kari Klaboe
 Dave Laverdiere
 David McCormick
 Javier Pascacio
 Michael Stoner
 Doug Thompson
 Taylor Vincent
 Dave Welch

October 2019



FEMA



Notice

Any opinions, findings, conclusions, or recommendations expressed in this publication do not necessarily reflect the views of the Applied Technology Council (ATC), the Department of Homeland Security (DHS), or the Federal Emergency Management Agency (FEMA). Additionally, neither ATC, DHS, FEMA, nor any of their employees, makes any warranty, expressed or implied, nor assumes any legal liability or responsibility for the accuracy, completeness, or usefulness of any information, product, or process included in this publication. Users of information from this publication assume all liability arising from such use.

Overview

Purpose and Scope

This document serves as a supplement to FEMA P-1100, *Vulnerability-Based Seismic Assessment and Retrofit of One-and Two-Family Dwellings, Volume 1 – Prestandard*, and assists engineers in understanding the technical basis of the prestandard.

This Volume is organized in Parts, each of which is written to stand on its own, including relevant reference sections. Where necessary, Parts may refer to archived project files in Volume 4, available upon request from the California Earthquake Authority.

Acknowledgements

This Volume presents the body of information developed by the ATC-110 project team over three years. ATC is indebted to the co-Project Technical Directors Colin Blaney and Kelly Cobeen for their leadership and technical expertise, and to the members of the Project Technical Committee consisting of Tom Anderson, Vikki Bourcier, Michael Cochran, Dan Dolan, Andre Filiatrault, Brian McDonald, John Osteraas, Frank Rollo, and Weichiang Pang. Angela Arias, Gaurav Bali, Ty Billings, Brent Crawford, Steve Fedorchak, Gayle Jensen, Kari Klaboe, Dave Laverdiere, David McCormick, Javier Pascacio, Michael Stoner, Doug Thompson, Taylor Vincent, and Dave Welch provided assistance in the development of the design examples as members of the Project Working Groups. ATC gratefully acknowledges the members of the Project Steering Committee consisting of David Bonowitz (chair), Ifa Kashefi, Phil Line, Thor Matteson, Bill Nagel, Steve Pryor, and Bill Warren (ATC Board Contact) who provided advice and assistance at key stages of the work.

ATC also gratefully acknowledges funding provided by the California Earthquake Authority and the Federal Emergency Management Agency, the guidance and support provided by Janiele Maffei (CEA Chief Mitigation Officer), Erin Waters (Research Program Coordinator), Michael Mahoney (FEMA Project Officer), and Bob Hanson (FEMA Subject Matter Expert). Carrie J. Perna (ATC) provided report production services.

Table of Contents

Overview	iii
List of Figures.....	xiii
List of Tables	xix
1. Software Recommendations and Applications	1-1
1.1 Introduction.....	1-1
1.2 Available Software Considered.....	1-1
1.3 Overview of <i>Timber3D</i>	1-2
1.3.1 General Features	1-2
1.3.2 Building Modeling.....	1-5
1.3.3 Non-linear Wall “Building Blocks”	1-5
1.3.4 Modeling of Semi-Rigid Connectivity between Wood Sill Plate and Concrete Foundation.....	1-6
1.3.5 Modeling of Semi-Rigid Connectivity between Vertical Studs and Sill Plate	1-7
1.3.6 Modeling of Semi-Rigid Connectivity from Hold-Down Rods	1-8
1.3.7 Modeling of Semi-Rigid Connectivity from Conventional Hold-Down Devices	1-8
1.3.8 Modeling of Semi-Rigid Connectivity from Steel Straps	1-9
1.3.9 Modeling of Non-linear Soil Springs.....	1-10
1.3.10 Modeling of Inelastic Steel and Concrete Elements	1-10
1.3.11 Modeling of Semi-rigid and Rigid Diaphragms	1-11
1.4 Analysis Methods.....	1-14
1.5 Comparisons of Predictions of Timber3D with a Simplified Model of a Light-Frame Wood Hospital Building.....	1-14
1.6 Applications of Timber3D	1-18
1.7 References	1-19
2. Performance Criteria for Numerical Studies	2-1
2.1 Introduction.....	2-1
2.2 Indicators of Performance	2-1
2.2.1 Collapse Indicators	2-2
2.2.2 Continued Occupancy Indicators.....	2-4
2.2.3 Level of Repair Indicator.....	2-5
2.3 Performance Criteria Selected.....	2-5
2.3.1 Primary Criterion	2-5
2.3.2 Secondary Criteria	2-6
2.4 References	2-7

3.	Assessment and Retrofit Design Criteria	3-1
3.1	Introduction	3-1
3.2	Retrofit Design Methodologies and Criteria	3-1
3.3	Recommendations	3-5
3.4	References	3-5
4.	Material Characterization for Numerical Studies.....	4-1
4.1	Introduction	4-1
4.2	Wall Building Block Data	4-1
4.2.1	Upper Story Characterization.....	4-4
4.2.2	Characterization of Lower Stories.....	4-5
4.3	Recommendations for Modeling	4-6
4.3.1	Stucco plus Gypsum Wallboard.....	4-6
4.3.2	Gypsum Wallboard	4-9
4.3.3	Stucco.....	4-10
4.3.4	Horizontal Lumber Sheathing or Siding	4-11
4.3.5	Wood Structural Panel Sheathing with Tie- Downs	4-12
4.3.6	Wood Structural Panel Sheathing without Tie- Downs	4-14
4.3.7	Material Designations	4-21
4.3.8	Horizontal Diaphragms	4-22
4.3.9	Anchorage of Foundation Sill Plates.....	4-24
4.3.10	Sill Plate Toenails	4-25
4.3.11	A35 Clips	4-27
4.3.12	Considerations of Effective Length for Wall Material Properties	4-28
4.4	Numerical Modeling Methods.....	4-31
4.4.1	Overview	4-31
4.4.2	Procedure for Extraction of Hysteretic Parameters from Test Data.....	4-33
4.4.3	Hysteretic Parameters for Stucco and Gypsum Walls	4-35
4.4.4	Hysteretic Parameters for Wood Structural Panels	4-43
4.4.5	Hysteretic Parameters for Horizontal Wood Siding	4-47
4.4.6	Hysteretic Parameters for 3×16d Toenails	4-48
4.4.7	Hysteretic Parameters for A35 Clips.....	4-49
4.5	Modeling Data Specific to Dwelling Types	4-51
4.6	References	4-51
5.	Protocol for Numerical Studies	5-1
5.1	Introduction	5-1
5.2	Overview	5-1
5.3	Modal (Free Vibration) Analyses	5-2
5.4	Non-linear Static Pushover Analyses	5-2
5.4.1	FEMA P-795 Characteristic Parameters	5-2
5.5	Incremental Dynamic Analyses and Performance Evaluation.....	5-3
5.5.1	Analysis Procedures	5-3
5.5.2	Correction for 3D Effect	5-4
5.5.3	Correction for Spectral Shape Factor	5-4

5.6	5.5.4 Correction for Global Dispersion Factor	5-6
	References	5-10
6.	Median Dwelling Configuration Study	6-1
6.1	Introduction	6-1
6.2	Information Collected on Older Single-family Dwellings....	6-2
6.2.1	Dwelling Configurations Considered	6-2
6.2.2	Geometrical Data Collected from Configuration Set	6-6
6.3	Determining Physical Configuration Properties	6-12
6.3.1	Selected Physical Properties for Configuration Study	6-12
6.3.2	Superstructure Strength and Weight Properties from Configuration Study	6-17
6.4	Developing Baseline Archetypes for Numerical Analysis..	6-25
6.4.1	Baseline Archetype Configurations	6-25
6.4.2	Modification Factors to Represent Configuration Data	6-31
6.4.3	Summary Properties of Superstructure Configurations	6-35
6.5	Geometric Information Collected from All Configurations.....	6-38
6.6	References	6-44
7.	Over-strength Factor for Retrofit Load Path Design	7-1
7.1	Introduction	7-1
7.2	Development of Over-strength Factor	7-1
7.2.1	Numerical Study Evaluation of Over-strength Factor	7-1
7.2.2	FEMA P-695 Approach and Discussion.....	7-2
7.2.3	Alternate Derivation of Over-strength Factor	7-4
7.3	References	7-7
8.	Simplified Overturning Assumptions.....	8-1
8.1	Introduction	8-1
8.2	Development of Simplified Overturning Assumptions.....	8-1
8.3	Numerical Study Evaluation of Overturning Assumptions...	8-2
8.4	References	8-10
9.	Crawlspace to Hillside Dwelling Transition Study	9-1
9.1	Introduction	9-1
9.2	Potential Hillside Failure Modes.....	9-1
9.3	Numerical Studies by the Crawlspace Dwelling Working Group	9-3
9.3.1	Archetypes Considered for Transition Study.....	9-4
9.3.2	Considerations for Resistance at the Uphill Wall Line	9-7
9.3.3	Analysis Results for Cripple Wall Dwellings Considered in the Transition Study.....	9-13
9.4	Numerical Studies by the Hillside Dwelling Working Group	9-17
9.5	Transition Considerations	9-19

9.6	Calculations to Check Capacity of L30 Clips for Out-of-Plane Resistance at the Uphill Wall Line for Zero-height Cripple Walls.....	9-21
9.7	References	9-22
10.	Development of Retrofit Provisions for Masonry Chimneys and Fireplace Surrounds	10-1
10.1	Introduction	10-1
10.2	Prescriptive Retrofit Provisions Based on Progressive Risk.....	10-2
10.3	Technical Background.....	10-5
10.3.1	Description of Typical Chimney Construction ...	10-5
10.3.2	Chimney Failure Modes Considered.....	10-6
10.3.3	Concepts that Guided Development of the Provisions.....	10-8
10.4	Engineering Considerations.....	10-10
10.5	Summary of Key Building Code Prescriptions for Residential Masonry Chimneys.....	10-12
10.6	References	10-13
11.	Development of Vulnerability-Based Retrofit Provisions for Crawlspace Dwellings	11-1
11.1	Introduction	11-1
11.2	Dwelling Stock Represented	11-1
11.2.1	Obtaining Superstructure Strength and Mass Characteristics for Cripple Wall Dwellings	11-2
11.2.2	Superstructure Configurations used for Numerical Analysis.....	11-6
11.2.2	Geometry Variations for Archetype Models.....	11-9
11.3	Modelling and Analysis Procedures	11-9
11.3.1	Overview	11-10
11.3.2	Crawlspace Project Nomenclature	11-10
11.3.3	Weight Take-off Assumptions for Cripple Wall Dwellings.....	11-12
11.3.4	Hysteretic Behavior of Existing Building Materials.....	11-13
11.3.5	General Modeling Approach for Cripple Wall Dwellings	11-18
11.3.6	Determination of Median Collapse Intensity	11-20
11.3.7	Wood Structural Panel Materials for Cripple Wall Retrofit.....	11-22
11.4	Model Performance	11-27
11.4.1	General Trends in Collapse Performance.....	11-28
11.4.2	Summary of Archetype Performance	11-34
11.5	Selected Retrofit Design Parameters and Methods	11-39
11.6	Cripple Wall to Hillside Transition Based on Expert Opinion.....	11-47
11.7	Archived Files	11-47
11.8	References	11-50

12. Development of Vulnerability-Based Retrofit Provisions for Living-Space-Over-Garage Dwellings.....	12-1
12.1 Introduction.....	12-1
12.2 Dwelling Stock Represented	12-1
12.3 Dwelling Configurations Used in Numerical Modeling	12-3
12.4 Analysis Procedures	12-6
12.4.1 Overview.....	12-7
12.4.2 Living-space-over-garage Project Nomenclature.....	12-8
12.4.3 Weight Assumptions and Un-Retrofitted Configurations	12-8
12.4.4 Hysteretic Behavior of Existing Building Materials	12-12
12.4.5 General Modeling Approach for Living-Space Over Garage dwellings	12-18
12.4.6 Determination of Median Collapse Intensity....	12-19
12.4.7 Hysteresis Behavior of Steel Wide-Flanged Retrofits	12-20
12.4.8 Hysteresis Behavior of Proprietary Wall Retrofits	12-23
12.4.9 Description of Models Run by WG5	12-24
12.5 Analysis Results.....	12-26
12.5.1 Sample Analysis Results from Model 5-HOG3-M-E.....	12-26
12.6 Selected Retrofit Design Parameters and Methods	12-29
12.7 Archived Files	12-29
12.8 References	12-30
13. Development of Vulnerability-Based Retrofit Provisions for Hillside Dwellings.....	13-1
13.1 Introduction	13-1
13.2 Dwelling Stock Represented	13-1
13.3 Dwelling Configurations Used in Analytical Modeling	13-4
13.4 Numerical Study Procedures.....	13-8
13.4.1 Hillside Dwelling Numerical Study Nomenclature.....	13-8
13.4.2 Weight Assumptions.....	13-9
13.4.3 Numerical Models.....	13-10
13.4.4 Hysteretic Behavior of Existing Building Materials/Fasteners	13-13
13.4.5 Hysteretic Behavior of Wood Structural Panel Cripple Walls	13-14
13.4.6 Hysteresis Behavior of Anchorage Elements ...	13-14
13.4.7 Modeling Procedures for Flexible Diaphragms	13-17
13.4.8 Superstructure Modeling.....	13-19
13.4.9 Concrete Foundation and Soil Assumptions....	13-19
13.4.10 Determination of Median Collapse Intensity	13-20
13.5 Numerical Results	13-21
13.5.1 Model 6-1H0-M-S	13-23
13.5.2 Model 6-1H04-M-E	13-23
13.5.3 Model 6-1H04-M-R1	13-24
13.5.4 Model 6-1H04-M-R2S.....	13-25

13.5.5	Model 6-1H04-M-R2	13-26
13.5.6	Model 6-1H04-M-R3	13-27
13.5.7	Model 6-1H010-M-R4	13-28
13.5.8	Model 6-1H04-M-R5	13-29
13.5.9	Model 6-1H04-M-R=1	13-29
13.5.10	Model 6-1H010-M-R=1	13-30
13.5.11	Model 6-1H010-M-R=2	13-31
13.5.12	Model 6-1H04-M-R=M2	13-32
13.5.13	Model 6-1H010-M-R=M2	13-33
13.5.14	Model 6-1H04-M-R=M1	13-33
13.5.15	Model 6-1H010-M-R=M1	13-34
13.5.16	Model 6-1H016-M-R=M1	13-34
13.5.17	Model 6-1H016-M-R=M1R	13-35
13.6	Selected Retrofit Design Parameters and Methods	13-36
13.7	Archived Files	13-37
13.8	References	13-38
13A.	Hillside Dwelling Design Example	13A-1
13A.1	Example Dwelling Configuration.....	13A-2
13A.2	Retrofit Terminology	13A-8
13A.3	Eligibility to Use Prestandard Chapter 6	13A-10
13A.4	Assessment	13A-12
13A.5	Simplified Engineered Seismic Retrofit Introduction	13A-13
13A.6	Construction Materials and Dwelling Weight	13A-13
13A.6.1	Unit Weight of Dwelling Assemblies	13A-13
13A.6.2	Weight of Building Tributary to Base Level Diaphragm.....	13A-17
13A.7	Seismic Base Shears for Retrofit	13A-19
13A.8	Primary Anchor Forces.....	13A-21
13A.9	Secondary Anchor Forces.....	13A-22
13A.10	Shear Anchor Forces	13A-23
13A.11	Crawlspac Wall Forces	13A-24
13A.12	Design of Primary Anchors	13A-26
13A.12.1	Main Lateral Load Resisting Element.....	13A-27
13A.12.2	Grade Beam Design for Primary Anchor	13A-31
13A.12.3	Collector Design.....	13A-33
13A.13	Design of Secondary Anchors	13A-43
13A.13.1	Design of Channel for Secondary Anchor	13A-44
13A.13.2	Design of Anchor Bolts for Secondary Anchors	13A-45
13A.13.3	Check Floor Joists for Secondary Anchor Force.....	13A-47
13A.14	Design of Shear Anchors	13A-50
13A.14.1	Design of Anchor Bolts for Shear Anchors ...	13A-50
13A.14.2	Check Bolts for Combined Shear and Tension	13A-51
13A.14.3	Check Concrete Pullout of Bolts	13A-52
13A.15	Design of Crawlspac Walls	13A-56
13A.15.1	Downhill Crawlspac Wall	13A-56
13A.15.2	Side Crawlspac Wall	13A-57
13A.15.3	First Story Wall Above Uphill Foundation....	13A-58

References..... R-1

Project ParticipantsP-1

List of Figures

Figure 1-1	CUREE hysteretic rule for modeling force-displacement response of wood shear walls under cyclic loading	1-3
Figure 1-2	Modification of CUREE hysteretic rule for modeling residual strength.....	1-4
Figure 1-3	Schematic illustration of one-story, light-frame wood building model in <i>Timber3D</i>	1-5
Figure 1-4	Schematic illustration of vertical wall building block	1-6
Figure 1-5	Schematic illustration of modeling of semi-rigid connectivity between the wood sill plate and the concrete foundation	1-7
Figure 1-6	Schematic illustration of modeling of semi-rigid connectivity between the end studs and the sill plate	1-7
Figure 1-7	Schematic illustration of modeling of semi-rigid connectivity introduced by hold-down rods	1-8
Figure 1-8	Schematic illustration of modeling of non-linear hold-down devices.....	1-9
Figure 1-9	Schematic illustration of modeling of non-linear steel straps	1-9
Figure 1-10	Schematic illustration of modeling of non-linear soil springs.....	1-10
Figure 1-11	Schematic illustration of modeling of an inelastic moment-resisting frame rigidly anchored to an elastic concrete foundation.....	1-11
Figure 1-12	Generalized illustration of inelastic moment-rotation relationship for F2F rotational link elements.....	1-11
Figure 1-13	Rigid diaphragm elements implemented in <i>Timber3D</i>	1-12
Figure 1-14	Schematic illustration of modeling of a rigid diaphragm	1-12
Figure 1-15	Schematic illustration of modeling of a semi-rigid diaphragm	1-13

Figure 1-16	Illustration of one-story commercial base line building model considered for the comparisons of predictions between <i>Timber3D</i> and the simplified model	1-15
Figure 1-17	Pushover curves for base line building model predicted by <i>Timber3D</i> and simplified model	1-16
Figure 1-18	Pushover curves for base line building model predicted by <i>Timber3D</i> and simplified model	1-17
Figure 1-19	Incremental dynamic analysis curves for base line building model under three selected ground motion records predicted by <i>Timber3D</i> and simplified model.....	1-18
Figure 2-1	Relating performance criteria to assessment and retrofit criteria	2-2
Figure 3-1	Relating numerical study performance criteria to retrofit criteria.	3-2
Figure 4-1	Plot of applicable test data and approximate backbone for stucco plus gypsum wallboard.....	4-9
Figure 4-2	Plot of applicable test data and approximate backbone for gypsum wallboard	4-10
Figure 4-3	Plot of applicable test data and approximate backbone for stucco.....	4-11
Figure 4-4	Plot of applicable test data and approximate backbone for horizontal lumber sheathing	4-12
Figure 4-5	Plot of available test data for wood structural panel shear walls with an aspect ratio of one and tie-downs	4-13
Figure 4-6	Plot of applicable test data and approximate backbone for wood structural panel shear walls with an aspect ratio of one or less and with tie-downs	4-14
Figure 4-7	Plot of Salenikovich test data for full anchorage and intermediate anchorages of 8 feet tall walls ranging from 12 to 2 feet in length.....	4-17
Figure 4-8	Illustration of the simplified relationship proposed by Salenikovich (2000) to account for panel aspect ratio and number of panels to estimate the fraction of the total bottom fastener resistance developed by shear walls with intermediate anchorage	4-18
Figure 4-9	Illustration of different wood structural panel brace length requirements when designing cripple wall retrofits of various heights with intermediate anchorage	4-20

Figure 4-10	Plot of applicable test data and approximate backbone for wood structural panel shear walls with intermediate anchorage	4-21
Figure 4-11	Plot of applicable test data and proposed linear stiffness of numerical description of semi-rigid diaphragms	4-23
Figure 4-12	Plot of applicable test data and load-deflection behavior of anchor bolts in-plane	4-24
Figure 4-12	Plot of applicable test data and load-deflection behavior of anchor bolts in-plane	4-25
Figure 4-14	Plot of applicable test data and load-deflection behavior for a single 16d common toenail/nail in shear	4-27
Figure 4-15	Backbone curve for Test Specimen FC1-A of cyclic response of shear transfer connections between shearwalls and diaphragms in woodframe construction.....	4-28
Figure 4-16	Illustration of different perforation factors to account for strength and stiffness reduction due to openings in exterior wall lines.....	4-29
Figure 4-17	Calculation of sheathing area ratios for the exterior walls of the CUREE Small House	4-30
Figure 4-18	CUREE hysteretic rule for modeling force-displacement response of wood shear walls under cyclic loading.....	4-32
Figure 4-19	Modification of CUREE hysteretic rule for modeling residual strength.....	4-33
Figure 4-20	Illustration of procedure to extract CUREE hysteretic parameters based on equal cumulative energy absorbed	4-34
Figure 4-21	Test data and recommended backbone curves for walls sheathed with gypsum.....	4-35
Figure 4-22	Test data and recommended backbone curves for walls sheathed with stucco	4-36
Figure 4-23	Test data and recommended backbone curves for walls sheathed with a combination of interior gypsum and exterior stucco	4-36
Figure 4-24	Comparison of hysteretic response and cumulative dissipated energy for test data and optimized CUREE parameters for walls sheathed with lower bound gypsum.....	4-38

Figure 4-25	Comparison of hysteretic response and cumulative dissipated energy for test and optimized CUREE parameters for walls sheathed with best estimate gypsum	4-39
Figure 4-26	Comparison of hysteretic response and cumulative dissipated energy for test data and optimized CUREE parameters for walls sheathed with lower bound stucco.....	4-39
Figure 4-27	Comparison of hysteretic response and cumulative dissipated energy for test data and optimized CUREE parameters for walls sheathed with single/upper story stucco + gypsum.....	4-40
Figure 4-28	Comparison of hysteretic response and cumulative dissipated energy for test data and optimized CUREE parameters for walls sheathed with lower story stucco + gypsum.....	4-42
Figure 4-29	Test data and recommended backbone curves for wood structural panels with tie downs	4-44
Figure 4-30	Test data and recommended backbone curves for cripple walls wood structural panels without tie downs	4-45
Figure 4-31	Comparison of hysteretic response and cumulative dissipated energy for test data and optimized CUREE parameters for wood structural panels	4-46
Figure 4-32	Example hysteretic response for horizontal wood siding using the CUREE hysteretic model and inputs parameters used within the ATC-116 project.....	4-48
Figure 4-33	CUREE hysteretic model parameters for 3-16d common toenails in lateral shear.....	4-49
Figure 4-34	CUREE hysteretic model parameters for A35 clips with in-plane shear loading	4-50
Figure 4-35	Fitting of SAWS hysteretic model to A35 clip testing conducted by Ficcadenti et al. (2004). NOTE: The test shown is for three clips in parallel	4-50
Figure 5-1	Definition of period-based ductility factor.....	5-5
Figure 6-1	Example of housing catalogs used to obtain superstructure information ranging from 1900 to 1969	6-2
Figure 6-2	Plan drawings for the three one-story configurations considered for each construction era. Images are not to relative scale.....	6-4

Figure 6-3	Plan drawings for the first and second stories of the two-story configurations selected for each construction era. Images are not to relative scale	6-5
Figure 6-4	Example of one-story 1910 configuration measurements within ATC-110 cripple wall dwelling superstructure study.....	6-6
Figure 6-5	Floor areas of one-story configurations. Average value is 1125 ft ²	6-7
Figure 6-6	Floor areas of two-story configurations. Average value is 1918 ft ²	6-7
Figure 6-7	Exterior wall criteria for one-story configurations	6-9
Figure 6-8	Interior wall criteria for one-story configurations.....	6-9
Figure 6-9	Exterior wall criteria for the first floor of two-story configurations	6-10
Figure 6-10	Interior wall criteria for the first floor of two-story configurations	6-10
Figure 6-11	Exterior criteria for the second floor of two-story configurations	6-11
Figure 6-12	Interior criteria for the second floor of two-story configurations	6-11
Figure 6-13	Comparing normal and lognormal distribution fits to interior wall density data for one-story cases.....	6-12
Figure 6-14	Sample of configuration data collected across different eras of construction showing the average superstructure strength to seismic weight ratios for all one-story configurations	6-13
Figure 6-15	Illustration of the different building materials assumed when considering the existing building stock of cripple wall dwellings. Data shown is the average strength-to-seismic weight ratios for the one-story configurations	6-14
Figure 6-16	Illustration of the SAWS hysteretic model	6-15
Figure 6-17	SAWS backbone curves for best-estimate materials used in superstructure study for analysis of cripple wall dwellings. Backbones reflect best-estimate properties	6-15
Figure 6-18	Example of simplified pushover analysis and modal pushover analysis conducted in <i>Timber3D</i> using three-dimensional models	6-17

Figure 6-19	Total weight-to-plan area ratios for one-story configurations.....	6-18
Figure 6-20	Strong-to-weak direction strength ratios for one-story configurations.....	6-19
Figure 6-21	Strength-to-seismic weight ratios for one-story configurations.....	6-20
Figure 6-22	Strength-to-plan area ratios for one-story configurations.....	6-20
Figure 6-23	Total weight-to-plan area ratios for two-story configurations.....	6-21
Figure 6-24	Second-to-first-story wall weight ratios for two-story configurations.....	6-22
Figure 6-25	Strong-to-weak direction strength ratios for the bottom story of two-story configurations	6-23
Figure 6-26	First-to-second-story strength ratios for two-story configurations.....	6-23
Figure 6-28	Strength-to-area ratios for the bottom story of two-story configurations.....	6-25
Figure 6-29	Rendering of one-story superstructure baseline configuration used in numerical modeling.....	6-26
Figure 6-30	Rendering of baseline two-story superstructure configuration on two-foot cripple-wall used in numerical modeling.....	6-27
Figure 6-31	Plan view of the one- and two-story configurations selected for modeling of cripple-wall dwellings	6-27
Figure 6-32	Illustration of the basic modelling components of a cripple wall dwelling.....	6-28
Figure 6-33	Example of the effective length assumption used for accounting for openings within building block of exterior wall lines	6-29
Figure 6-34	Building block discretization for exterior wall lines of archetype buildings	6-30
Figure 6-35	Locations of interior walls assumed in archetype configurations.....	6-31
Figure 6-36	Example calculation for modifying the one-story baseline configuration with stucco and gypsum materials to the pre-1950's Median superstructure parameters	6-34

Figure 6-37	Pushover curves for the one-story pre-1950's Median Superstructure	6-36
Figure 6-38	Pushover curves for the two-story pre-1950's Median Superstructure	6-36
Figure 6-39	Pushover curves for the one-story post-1950's Median- β Superstructure.....	6-37
Figure 6-40	Pushover curves for the two-story post-1950's Median- β Superstructure.....	6-37
Figure 6-41	Pushover analysis comparison of all four superstructure configurations considered for cripple wall dwelling analysis.....	6-38
Figure 7-1	Derivation of overstrength factors for connectors	7-5
Figure 8-1	Illustration of simplified overturning assumptions for the design of cripple wall retrofit.....	8-2
Figure 8-2	Illustration of different construction and testing phases of the two-story house tested by Fischer et al. (2001) focusing on major changes to the East and West walls	8-3
Figure 8-3	Example of documented anchorage uplift forces from the test by Fischer et al. (2001; 2002).....	8-5
Figure 8-4	Assumed locations of anchor bolts and hold-downs for calculation of overturning moments from shake table testing by Fisher et al. (2001; 2002)	8-6
Figure 8-5	Illustration of assuming the neutral axis at the center of full-height wall segments to determine anchorage locations in tension for a direction of loading.....	8-7
Figure 8-6	Example of anchorage elements assumed in tension for north loading	8-8
Figure 8-7	Example of anchorage elements assumed in tension for north loading	8-8
Figure 8-8	Example of anchorage elements assumed in tension for north loading	8-9
Figure 8-9	Sample calculation of overturning proportions for in-plane and out-of-plane walls for Test 10.S.5 with north loading assumed.....	8-9
Figure 9-1	Short cripple wall at the uphill side of the dwelling in combination with the tall downhill cripple wall	9-2
Figure 9-2	Illustrations of hillside dwellings failing by tearing away at the uphill diaphragm connection causing global	

	collapse following the 1994 Northridge, California earthquake	9-2
Figure 9-3	Floor diaphragm case examples	9-3
Figure 9-4	Illustration of the two control archetypes on constant height cripple walls used for comparison in the transition study	9-5
Figure 9-5	Illustration of the two orientations of the uphill wall line considered for transition study archetypes	9-5
Figure 9-6	Illustration of the two variations of sloped cripple walls with a maximum downhill height of eight feet: Case 8'-2'0" with large single transition height, Case 8'-6"-4'-2'-0" with evenly distributed height transition	9-6
Figure 9-7	Fitting of SAWS hysteretic model to A35 clip testing conducted by Ficcadenti et al. (2004)	9-8
Figure 9-8	Assumed material backbones for in-plane (IP) and out-of-plane (OOP) resistance at the retrofit joist-to-sill connection at the uphill wall line of sloped cripple wall with a zero-height condition.....	9-9
Figure 9-9	Illustration of the out-of-plane (OOP) connection at the sill plate and the placement of equivalent L30 clip elements along the foundation beam	9-10
Figure 9-10	Modeling assumptions for creating the foundation beam at the uphill wall line	9-10
Figure 9-11	Rendering of Timber3D model representing a one-story cripple wall dwelling with a ‘zero-height’ condition	9-11
Figure 9-12	Illustration of interaction surface assumed for in-plane (IP) resistance at uphill wall line conditioned on peak out-of-plane (OOP) displacement history	9-12
Figure 9-13	Example of using out-of-plane (OOP) displacement to relate to non-simulated collapse in addition to global collapse returned from structural analysis.....	9-13
Figure 9-14	Collapse performance summary at the MCE level for all transition study archetypes	9-15
Figure 9-15	Deformed shape for monotonic uphill push.....	9-18
Figure 9-16	Maximum out of plane crawl space wall drift ratio values for monotonic study	9-19
Figure 9-17	Base level diaphragm behavior for cross-slope loading.....	9-20

Figure 9-18	Page one of calculations for out-of-plane resistance at uphill wall line	9-21
Figure 9-19	Page two of calculations for out-of-plane resistance at uphill wall line	9-22
Figure 10-1	Example of ineligible chimney—corner construction with plan dimension greater than 40 inches.....	10-2
Figure 10-2	Chimney retrofit by removing masonry to the roof level and capped	10-4
Figure 10-3	Chimney retrofit by removing masonry to the top of the smoke chamber and installing a factory-built metal flue in a light-frame chase.....	10-4
Figure 10-4	Common failure of two-story exterior chimney	10-7
Figure 10-5	Typical failure at roof line	10-7
Figure 10-6	Atypical failure of reinforced, one-story interior chimney.....	10-8
Figure 10-7	Masonry residential chimney fragility functions derived from various sources show that the collapse vulnerability is much higher than the implicit performance goal of the building code	10-11
Figure 11-1	Overview of the 42 plan configurations considered in the superstructure strength study for cripple wall dwellings.....	11-2
Figure 11-2	Example of one-story 1910 configuration measurements within ATC-110 cripple wall dwelling superstructure study.....	11-3
Figure 11-3	Sample of configuration data collected across different eras of construction showing the average superstructure strength to seismic weight ratios for all one-story configurations	11-4
Figure 11-4	Illustration of the different building materials assumed when considering the existing one story building stock of cripple wall dwellings.....	11-5
Figure 11-5	Rendering of one-story superstructure baseline configuration on two-foot cripple wall used in numerical modeling	11-6
Figure 11-6	Rendering of two-story superstructure baseline configuration on two-foot cripple wall used in numerical modeling	11-7

Figure 11-7	Plan view of the one- and two-story baseline configurations selected for modeling of cripple wall dwellings	11-7
Figure 11-8	Modal pushover analysis comparison of all four superstructure configurations considered for cripple wall dwelling analysis	11-9
Figure 11-9	Illustration of the residual strength hysteretic model used in <i>Timber3D</i> for modeling the behavior of wall materials	11-14
Figure 11-10	Illustration of the SAWS hysteretic model.....	11-16
Figure 11-11	Assumed hysteretic behavior for stucco plus gypsum wallboard.....	11-17
Figure 11-12	Assumed hysteretic behavior for best estimate stucco and lower bound stucco.....	11-17
Figure 11-13	Assumed hysteretic behavior for best estimate gypsum wallboard and horizontal wood siding.....	11-17
Figure 11-14	Illustration of the basic modelling components of a cripple wall dwelling.....	11-18
Figure 11-15	Example of the effective length assumption used for accounting for openings within building block of exterior wall lines	11-20
Figure 11-16	Illustration of process used for estimating the collapse fragility of a cripple wall dwelling according to the FEMA P-695 procedure	11-22
Figure 11-17	Hysteretic behavior of baseline wood structural panels assuming full anchorage conditions with tie-downs	11-23
Figure 11-18	Comparison of wood structural panel displacement capacity based on cripple wall height	11-24
Figure 11-19	Comparison of hysteretic responses of wood structural panel WSP6 for a 6 foot tall cripple wall	11-27
Figure 11-20	Trends of probability of collapse at the MCE intensity level versus the average peak strength-to-baseline weight ratio: One-story median pre-1950 superstructure	11-29
Figure 11-21	Trends of probability of collapse at the MCE intensity level versus the average cripple wall-to-superstructure strength rat.....	11-30

Figure 11-22	Trends of probability of collapse at the MCE intensity level versus the average peak strength-to-baseline weight ratio	11-31
Figure 11-23	Trends of probability of collapse at the MCE intensity level versus the average cripple wall-to-superstructure strength ratio	11-31
Figure 11-24	Trends of probability of collapse at the MCE intensity level versus the average peak strength to baseline weight ratio	11-32
Figure 11-25	Trends of probability of collapse at the MCE intensity level versus the average cripple wall to superstructure strength ratio	11-33
Figure 11-26	Trends of probability of collapse at the MCE intensity level versus the average peak strength-to-baseline weight ratio	11-33
Figure 11-27	Trends of probability of collapse at the MCE intensity level versus the average cripple wall-to-superstructure strength ratio	11-34
Figure 11-28	Summary of performance criteria: two-foot tall cripple wall cases	11-36
Figure 11-29	Summary of performance criteria: four-foot tall cripple wall cases	11-37
Figure 11-30	Summary of performance criteria: six-foot tall cripple wall cases	11-38
Figure 11-31	Mapping of material weight combinations into weight classifications for cripple wall constructability analysis	11-41
Figure 11-32	Example of constructability tables for all weight combinations, plan dimensions, and number of sheathed panels per wall line	11-43
Figure 11-33	Typical table for two-story structure in constructability spreadsheet.....	11-43
Figure 11-34	Illustration of the original measure of constructability to count conflicts for retrofit of cripple wall dwellings	11-45
Figure 11-35	Illustration of the revised or “new” measure of constructability to count conflicts for retrofit of cripple wall dwellings	11-46
Figure 12-1	Typical rectangular living-space-over-garage dwelling ..	12-2

Figure 12-2	Typical L-shaped living-space-over-garage dwelling	12-2
Figure 12-3	First floor plan of house-over-garage without living space at ground floor	12-3
Figure 12-4	Elevation views of house-over-garage configurations	12-4
Figure 12-5	First floor plan view of house-over-garage with living space at the ground floor	12-5
Figure 12-6	First floor plan view of existing room-over-garage configuration	12-6
Figure 12-7	Typical existing wall layouts for the first story of HOG configurations.....	12-10
Figure 12-8	Typical existing wall layouts for the first story of HOG configurations.....	12-10
Figure 12-9	Rendering of typical HOG configuration with garage door opening.....	12-10
Figure 12-10	Timber3D rendering of HOG existing configuration....	12-11
Figure 12-11	Typical existing wall layouts for ROG configurations.....	12-12
Figure 12-12	Illustration of the residual strength hysteretic model used in Timber3D for modeling the behavior of wall materials	12-13
Figure 12-13	Illustration of the modified STEWart hysteretic model used in Timber3D for modeling the behavior of wall materials	12-14
Figure 12-14	Hysteretic parameters for stucco and stucco+gypsum ...	12-16
Figure 12-15	Hysteretic parameters for gypsum and horizontal siding.....	12-17
Figure 12-16	Hysteretic parameters for wood structural panels	12-17
Figure 12-17	Illustration of modeling components of HOG dwelling including a rendering of actual dwelling and Timber3D components	12-18
Figure 12-18	Conversion of raw collapse information to full FEMA P-695 collapse fragility curve	12-20
Figure 12-19	Steel backbone behavior from ASCE 41-13	12-21
Figure 12-20	Backbone behavior of steel retrofits with and without stiffness decrease.....	12-22

Figure 12-21	Hysteresis behavior of W12×35 steel retrofit	12-22
Figure 12-22	Points used for backbone of proprietary wall systems based on ICC acceptance criteria	12-23
Figure 12-23	Hysteresis behavior of ICC AC proprietary and wood structural panel walls	12-24
Figure 12-24	Plotted mode shapes for 5-HOG3-H-5SW configuration.....	12-26
Figure 12-25	Non-linear static pushover analysis for 5-HOG3-H-5SW	12-27
Figure 12-26	Lateral displacement time history of control roof node for retrofitted and un-retrofitted configuration of HOG3.....	12-28
Figure 13-1	Hillside dwelling of the configuration addressed by FEMA P-1100.....	13-2
Figure 13-2	Hillside dwelling schematic illustration of the underfloor area enclosed with sheathed side walls	13-2
Figure 13-3	Hillside dwelling schematic illustration of the underfloor area with diagonal bracing and open area crawl space.....	13-3
Figure 13-4	Dwelling elevation—downhill.....	13-4
Figure 13-5	Dwelling elevation—side	13-4
Figure 13-6	Dwelling occupied base level story plan for all models except Model 6-1H016-M-R=M1R	13-5
Figure 13-7	Dwelling occupied story plan for rotated model.....	13-5
Figure 13-8	Hillside dwelling isometric with applicable terminology	13-7
Figure 13-9	Hillside dwelling schematic illustration of retrofit elements	13-9
Figure 13-10	Numerical modeling nomenclature.....	13-9
Figure 13-11	Roof diaphragm seismic weight distribution to diaphragm nodes based on tributary area.....	13-10
Figure 13-12	Example 0'-16' hillside retrofit model in Timber3D.....	13-11
Figure 13-13	Hysteresis plots for exterior walls sheathed with best estimate gypsum and stucco.....	13-13

Figure 13-14	Hysteresis plots for downhill cross-slope cripple walls sheathed with WSP3 parameters	13-14
Figure 13-15	Hysteresis plots for a wood to steel ½" bolt specimen tested at Washington State University	13-15
Figure 13-16	Example secondary anchor detail in plan view	13-16
Figure 13-17	Primary and secondary anchor parameters for Model 6-1H04-M-R=1	13-17
Figure 13-18	Shear anchor parameters for Model 6-1H04-M-R=1	13-17
Figure 13-19	Diaphragm mesh for an example hillside model.....	13-18
Figure 13-20	Simplified floor plan for modeling purposes	13-19
Figure 13-21	Example horizontal ground motions components shown for an earthquake included in the 22-far field ground motions.....	13-20
Figure 13-22	Example of an estimated raw data fragility curve being modified with FEMA P695's various seismic performance factors.....	13-21
Figure 13-23	Existing model (6-1H04-M-E) crawl space configuration	13-24
Figure 13-24	Secondary anchor displacement distribution for Model 6-1H04-M-R1 at peak loading when subjected to an out-of-hill monotonic push.....	13-25
Figure 13-25	Criteria plot for the various hillside retrofit models illustrating performance criteria	13-37
Figure 13A-1	First floor plan.....	13A-3
Figure 13A-2	Roof plan.....	13A-4
Figure 13A-3	Foundation and crawlspace plan	13A-5
Figure 13A-4	First floor framing plan	13A-6
Figure 13A-5	Downhill elevation	13A-6
Figure 13A-6	Cross slope elevation.....	13A-7
Figure 13A-7	Existing uphill foundation section.....	13A-7
Figure 13A-8	Hillside dwelling isometric with applicable terminology	13A-9
Figure 13A-9	Hillside dwelling schematic isometric of dwelling	13A-9

Figure 13A-10 Interior uphill foundation corner isometric showing primary anchors, secondary anchors, and shear anchors	13A-10
Figure 13A-11 Building wall locations	13A-17
Figure 13A-12 Primary anchor configuration	13A-21
Figure 13A-13 Secondary anchor configuration	13A-22
Figure 13A-14 Shear anchor configuration.....	13A-23
Figure 13A-15 Downhill crawlspace wall configuration	13A-24
Figure 13A-16 Side crawlspace wall configuration	13A-25
Figure 13A-17 Example dwelling elevation showing primary members.....	13A-27
Figure 13A-18 Example dwelling concrete wall elevation	13A-28
Figure 13A-19 Strain in wall plan view	13A-29
Figure 13A-20 Assumed compression block.....	13A-30
Figure 13A-21 Grade beam.....	13A-31
Figure 13A-22 Example dwelling concrete wall elevation	13A-33
Figure 13A-23 Saddle embed plates.....	13A-35
Figure 13A-24 Saddle connection elevation	13A-36
Figure 13A-25 Collector beam to saddle connection diagram	13A-37
Figure 13A-26 Primary anchor detail.....	13A-38
Figure 13A-27 Primary anchor detail at concrete wall.....	13A-39
Figure 13A-28 Primary anchor detail at grade beam	13A-40
Figure 13A-29 Primary anchor grade beam to uphill foundation.....	13A-41
Figure 13A-30 Collector beam splice detail.....	13A-42
Figure 13A-31 Secondary anchor.....	13A-43
Figure 13A-32 Secondary anchor.....	13A-44
Figure 13A-33 Secondary anchor uphill force diagram	13A-45
Figure 13A-34 Secondary anchor downhill force diagram	13A-46
Figure 13A-35 Secondary anchor force summary.....	13A-46

Figure 13A-36 Secondary anchor collector diagram	13A-49
Figure 13A-37 Shear anchor elevation	13A-50
Figure 13A-38 Secondary anchor punching shear.....	13A-52
Figure 13A-39 Existing uphill foundation detail	13A-53
Figure 13A-40 Secondary and shear anchor detail	13A-54
Figure 13A-41 Secondary anchor collector detail	13A-55
Figure 13A-42 Downhill crawlspace wall force diagram.....	13A-56
Figure 13A-43 Uphill superstructure wall location	13A-58
Figure 13A-44 Exterior wall 2 elevation	13A-59

List of Tables

Table 1-1	Assessment of Software for ATC-110 Project.....	1-2
Table 1-2	Definition of Hysteretic Parameters of CUREE Hysteretic Rule	1-4
Table 1-3	Natural Periods and Mode Shape Directions for Base Line Building Model Predicted by <i>Timber3D</i> and Simplified Model	1-17
Table 2-1	Summary of Applicable FEMA P-58 Fragility Functions.....	2-7
Table 4-1	Vertical Wall Building Blocks—Upper Story Characterization Priorities	4-5
Table 4-2	Vertical Wall Building Blocks—Lower Story Characterization Priorities	4-6
Table 4-3	Cripple Wall Peak Capacities and Drift Ratios for Applicable Subset Tested by Chai et al. (2002).....	4-16
Table 4-4	Material Designations for Approximate Backbone Properties	4-22
Table 4-5	Comparing Different Perforation Factor Relationships Applied to the Exterior Wall Lines of the CUREE Small House	4-5
Table 4-6	Definition of Hysteretic Parameters of CUREE Hysteretic Rule	4-32
Table 4-7	CUREE Hysteretic Parameters for Walls Sheathed with Gypsum and Stucco	4-37
Table 4-8	RESST Hysteretic Parameters Based on 10% Residual Strength for Walls Sheathed with Gypsum and Stucco ...	4-43
Table 4-9	CUREE Hysteretic Parameters for Wood Structural Panels	4-46
Table 4-10	RESST Hysteretic Parameters Based on 10% Residual Strength for Wood Structural Panels	4-47
Table 4-11	CUREE Hysteretic Parameters for Horizontal Wood Siding	4-48

Table 4-12	CUREE Hysteretic Parameters for 3-16d Toenails in Shear.....	4-49
Table 4-13	CUREE Hysteretic Parameters for Single A35 Clip with In-Plane Shear Loading.....	4-50
Table 5-1	Values of Spectral Shape Factor Applicable to Building Archetypes with Elastic Fundamental Periods $T \leq 0.5$ sec and Designed for Seismic Design Category SDC- D_{max}	5-5
Table 5-2	Values of Spectral Shape Factors Applicable to Building Archetypes with Elastic Fundamental Periods $T \leq 0.5$ sec and Designed for Seismic Design Category SDC- D_{max}	5-6
Table 5-3	FEMA P-695 Quality Rating of Design Requirements.....	5-7
Table 5-4	FEMA P-695 Quality Rating of Test Data.....	5-8
Table 5-5	FEMA P-695 Quality Rating of Modeling Uncertainty	5-8
Table 5-6	Proposed Quality Ratings and Dispersion Factors for Assessment and Retrofit Purposes	5-9
Table 6-1	List of Housing Catalog References.....	6-3
Table 6-2	Summary of Weight Take-Off Assumptions for Superstructure Study for Analysis of Cripple Wall Dwellings	6-14
Table 6-3	SAWS Backbone Parameters Used in Superstructure Configuration Study	6-16
Table 6-4	Summary of Total Weight-to-Plan Area Ratios for One-Story Configurations	6-18
Table 6-5	Summary of Strong-to-Weak Direction Strength Ratios for One-Story Configurations	6-19
Table 6-6	Summary of Strength-to-Seismic Weight Ratios for One-Story Configurations	6-20
Table 6-7	Summary of Strength-to-Plan Area Ratios for One-Story Configurations	6-21
Table 6-8	Summary of Total Weight-to-Plan Area Ratios for One-Story Configurations	6-21
Table 6-9	Summary of Second-to-First-Story Wall Weight Ratios for Two-Story Configurations	6-22
Table 6-10	Summary of Strong-to-Weak Direction Strength Ratios for the Bottom Story of two-Story Configurations	6-23

Table 6-11	Summary of Second- to-First-Story Strength Ratios for Two-Story Configurations	6-24
Table 6-12	Summary of Strength-to-Seismic Weight Ratios for the Bottom Story of Two-Story Configurations	6-24
Table 6-13	Summary of Strength-to-Area Ratios for the Bottom Story of Two-Story Configurations	6-25
Table 6-14	Effective Lengths of Exterior Building Blocks for the Superstructure Modeling of Archetype Dwellings	6-30
Table 6-15	Building Block Discretization and Effective Lengths for Interior Superstructure Walls	6-31
Table 6-16	Configuration Data Used for Modification Calculations	6-33
Table 6-17	Modification Factors Applied to Baseline Superstructure Configurations to Target Era-Specific Assumptions.....	6-34
Table 6-18	Summary of Superstructure Configuration Properties for the Analysis of Cripple Wall Dwellings. Structural Models Assume A Rigid Base (Pinned Connection) to the Ground Level	6-35
Table 6-19	Exterior Wall Summary for One-Story Configurations...	6-39
Table 6-20	Interior Wall Summary for One-Story Configurations	6-40
Table 6-21	Exterior Wall Summary for the First Story of Two-Story Configurations.....	6-41
Table 6-22	Exterior Wall Summary for the Second Story of Two-Story Configurations.....	6-42
Table 6-23	Interior Wall Summary for the First Story of Two-Story Configurations.....	6-43
Table 6-24	Interior Wall Summary for the Second Story of Two-Story Configurations.....	6-44
Table 7-1	Calculation of Over-Strength Factors for Work Group 4 Retrofitted Archetypes based on FEMA P-695 Methodology	7-3
Table 7-2	Calculation of Over-Strength Factor for Existing Finishes	7-6
Table 8-1	Brief Description of Construction Phases in the Testing Conducted by Fischer et al. (2001; 2002).....	8-4

Table 8-2	Summary of Overturning Proportions of In-plane and Out-of-plane Tension Demands Estimated from Shake Table Tests by Fischer et al. (2001; 2002)	8-10
Table 9-1	SAWS Hysteretic Parameters for A35 Clips Used for In-plane Resistance of Crawlspace Retrofit at the Joist-to-sill Connection	9-8
Table 9-2	SAWS Hysteretic Parameters for L30 Clips Used for Out-of-plane Resistance of Crawlspace Retrofit at the Joist-to-sill Connection	9-9
Table 9-3	Summary of Different Configurations Analyzed for the Cripple Wall to Hillside Transition Study.....	9-14
Table 9-4	Modal Period and Pushover Summary for Transition Study Archetypes	9-14
Table 9-5	Collapse Performance Summary for Transition Study Archetypes—Counted Collapse Cases at the DE and MCE Intensity Levels and Adjusted Probability of Collapse at the MCE Level	9-16
Table 10-1	History of Key Prescriptive Requirements for Masonry Chimneys in the UBC	10-12
Table 11-1	Summary of Superstructure Configuration Properties for the Analysis of Cripple Wall Dwellings.....	11-8
Table 11-2	Summary of Weight Take-Off Assumptions for Analysis of Cripple Wall Dwellings	11-13
Table 11-3	RESST Hysteretic Parameters for Existing Wall Materials Modeled in Timber3D for the Analysis of Crawlspace Dwellings.....	11-15
Table 11-4	SAWS Parameters for Best Estimate Horizontal Wood Siding.....	11-16
Table 11-5	Strength Reduction Factors Based on Aspect Ratio of Wood Structural Panel Shear Walls without Tie-Downs	11-23
Table 11-6	RESST Hysteretic Parameters for Wood Structural Panel Materials Used for Cripple Wall Retrofit without Aspect Ratio Reduction Factors Applied	11-26
Table 11-7	Percent Improvement in Collapse Probability for the MCE versus Computed R-Factors for One-Story Dwellings	11-39
Table 11-8	Percent Improvement in Collapse Probability for the MCE versus Computed R-Factors for Two-Story Dwellings	11-40

Table 12-1	Weight (psf) Assumptions Used in WG5 Numerical Studies.....	12-9
Table 12-2	HOG Configuration Summary	12-11
Table 12-3	SAWS (or MSTEW) Parameters Used to Represent Horizontal Siding	12-15
Table 12-4	RESST Parameters for Best Estimate Stucco, Best Estimate Gypsum, and Best Estimate Stucco+Gypsum.....	12-15
Table 12-5	RESST Parameters Used to Represent Wood Structural Panels	12-16
Table 12-6	Steel Modeling Parameters from ASCE 41-13	12-21
Table 12-7	Analysis Models Run.....	12-25
Table 12-8	Period of First Three Mode Shapes for 5-HOG3-H-5SW	12-26
Table 12-9	FEMA P-795 Parameters of 5-HOG3-H-5SW	12-27
Table 12-10	Archived Files for WG5	12-30
Table 13-1	Unit Weight Summary	13-9
Table 13-2	Hillside Dwelling Numerical Models	13-12
Table 13-3	Numerical Model Monotonic and Dynamic Results.....	13-22
Table 13-4	Hillside Dwelling Related Archived Files	13-38
Table 13A-1	Example Dwelling Compliance with Eligibility Requirements (from Volume 1, Table 1.8-1).....	13A-10
Table 13A-2	Example Dwelling Compliance with Eligibility Requirements (from Volume 1, Table 6.1-1).....	13A-11
Table 13A-3	Suggested Roof Design Dead Loads—Gravity/ Seismic Flat Weight Takeoff (from Volume 1, Table L-1)	13A-14
Table 13A-4	Suggested Floor Design Dead Loads (from Volume 1, Table L-2)	13A-15
Table 13A-5	Suggested Exterior Wall Design Dead Loads (from Volume 1, Table L-3)	13A-15
Table 13A-6	Suggested Exterior Cripple Wall Design Dead Loads (from Volume 1, Table L-4)	13A-16

Table 13A-7	Suggested Interior Wall Design Dead Loads (from Volume 1, Table L-5).....	13A-16
Table 13A-8	Dwelling Weight	13A-18

Part 1

Software Recommendations and Applications

1.1 Introduction

The ATC-110 Project relied heavily on full-building, three-dimensional numerical studies for developing the FEMA P-1100 prestandard for the evaluation and retrofit of one- and two-family light-frame wood residential buildings. A software program capable of capturing the most important aspects of the seismic response of these buildings needed to be selected. It was also desired that the same software program be used, when practical, to model the different types of light-frame wood residential building construction to be investigated by the different working groups of the project. In addition to this primary analysis program, alternate software programs were also used for detailed numerical studies or sub-assembly studies. This document provides a brief description of the different available software programs that were reviewed by the ATC-110 Project team Working Group 1 (WG1) and provides the basis for the selection of the software that was used for the full-building, three-dimensional numerical studies. This document was initially developed early in the project, and is provided as Volume 3, Part 1 in order to serve as a record of considerations.

1.2 Available Software Considered

A number of different software programs were reviewed and considered by the ATC-110 Project team WG1 at the start of the project in 2015. The pros and cons of these programs are listed in Table 1-1. Based on the summary information provided in this table, it was recommended to use the open-source program *Timber3D* as the main software program for all full-building, three-dimensional numerical studies. This recommendation was based on the following two primary reasons: 1) the ability of *Timber3D* to model flexible roof and floor diaphragms was thought to be the only way to practically capture the behavior that needed to be studied, particularly in living-space-over-garage and hillside dwelling configurations; and 2) the general frame elements included in *Timber3D* were thought to be necessary to model likely retrofits in both room-over-garage and hillside dwelling configurations.

These were anticipated to include cantilevered columns, steel moment frames and anchorage to an uphill foundation.

A brief description of the *Timber3D* software capabilities is provided in the next section.

Table 1-1 Assessment of Software for ATC-110 Project

Software	Availability	Pros	Cons
SAP2000 (v18) ETABS 2015 and PERFORM-3D (v5)	Commercially from Computers and Structures, Inc.	Widely used by practicing earthquake engineers.	Not developed to easily model light-frame wood construction. Not developed to efficiently conduct incremental dynamic analyses.
SAWS (v2.1)	Open source from the State University of New York at Buffalo	Configured specifically for shear-wall type light-frame wood construction. Version 2.1 specifically configured to conduct incremental dynamic analyses efficiently. Simple data input. Computationally efficient.	Does not model semi-rigid connectivity between framing elements (e.g. hold-down, uplift, rocking, etc.). Does not model bending in framing elements. Assumes rigid floor or roof diaphragms.
OpenSees	Open source from the Pacific Earthquake Engineering Center, University of California at Berkeley.	Widely used by researchers in earthquake engineering.	Not developed to easily model light-frame wood construction. Does not include specific hysteretic models for light-frame wood construction.
Timber3D (v1)	Open source from Clemson University	Configured specifically for shear-wall type light-frame wood construction. Models semi-rigid connectivity between framing elements (e.g. hold-down, uplift, rocking, etc.) through general six degrees-of-freedom Frame-to-Frame (F2F) link elements. Models the bending in framing elements. Models in-plane or out-of-plane flexibility of floor or roof diaphragms by equivalent beam elements.	Recently developed program with limited usage.

1.3 Overview of *Timber3D*

This section describes the approach and capabilities of the *Timber3D* software. See also Section 6 for discussion of how the software was used in the ATC-110 Project.

1.3.1 General Features

The *Timber3D* analysis program is a three-dimensional (3D) model originally developed as part of the NEES-Soft project (van de Lindt *et al.* 2012) to capture the non-linear dynamic response and seismic collapse

mechanisms of light-frame wood buildings. This three-dimensional (3D) model is an extension of detailed two-dimensional (2D) models developed earlier for the collapse analysis of light-frame wood shear walls (Pang *et al.* 2012; Christovasilis and Filiatrault 2010, 2013).

The *Timber3D* model operates on the Matlab platform using a co-rotational formulation and large displacement theory. The horizontal floor and roof diaphragms are modelled using co-rotational 3D, two-node, 12-DOF elastic beam elements, which accounts for geometric non-linearity. Using a co-rotational formulation allows proper consideration of the in-plane and out-of-plane motions of the diaphragms under large deformations.

The elastic flexural and axial stiffness of vertical wall studs are modeled using 3D, two-node, 12-degrees-of-freedom (DOF) elastic frame elements. The vertical wall panel-to-framing assemblies are modeled using 6-DOF, Frame-to-Frame (F2F) link elements. Only one (lateral) DOF of the F2F link element needs to be activated to model the lateral non-linear cyclic response of vertical walls sheathed with wood panels and other (non-structural) materials.

The non-linear lateral cyclic response of vertical walls is captured by the CUREE hysteretic rule (Folz and Filiatrault 2001), as illustrated in Figure 1-1. The loading force-deformation paths OA and CD follow a non-linear exponential monotonic envelope curve, while all other unloading and re-loading paths exhibit a linear relationship between force and deformation. This hysteretic rule allows for stiffness and strength degradation as well as post-capping reducing strength.

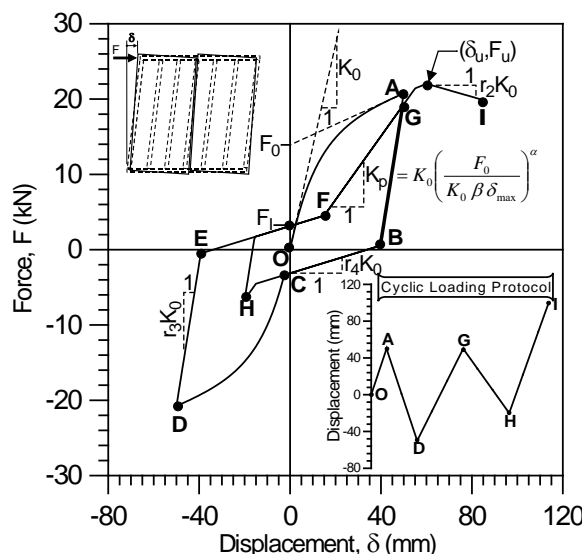


Figure 1-1 CUREE hysteretic rule for modeling force-displacement response of wood shear walls under cyclic loading.

The CUREE hysteretic rule is completely determined by ten physically identifiable parameters, as defined in Table 1-2 and identified in Figure 1-1.

Table 1-2 Definition of Hysteretic Parameters of CUREE Hysteretic Rule

Parameter (see Figure 1)	Definition
K_0	Initial stiffness
F_0	Force intercept of the asymptotic stiffness at ultimate strength
F_I	Zero-displacement load intercept
δ_u	Displacement at ultimate load
r_1	Asymptotic stiffness ratio under monotonic load
r_2	Post-capping strength stiffness ratio under monotonic load
r_3	Unloading stiffness ratio
r_4	Re-loading pinched stiffness ratio
α	Hysteretic parameter for stiffness degradation
β	Hysteretic parameter for stiffness degradation

A modified version of the CUREE hysteretic rule is also available within Timber3D in order to introduce a user-defined residual strength for vertical walls. The post-capping strength stiffness ($r_2 K_0$) is replaced by a reversed S-shaped curve anchored at a displacement D_x and converging to a pre-determined residual strength level at large displacements, as shown in Figure 1-2.

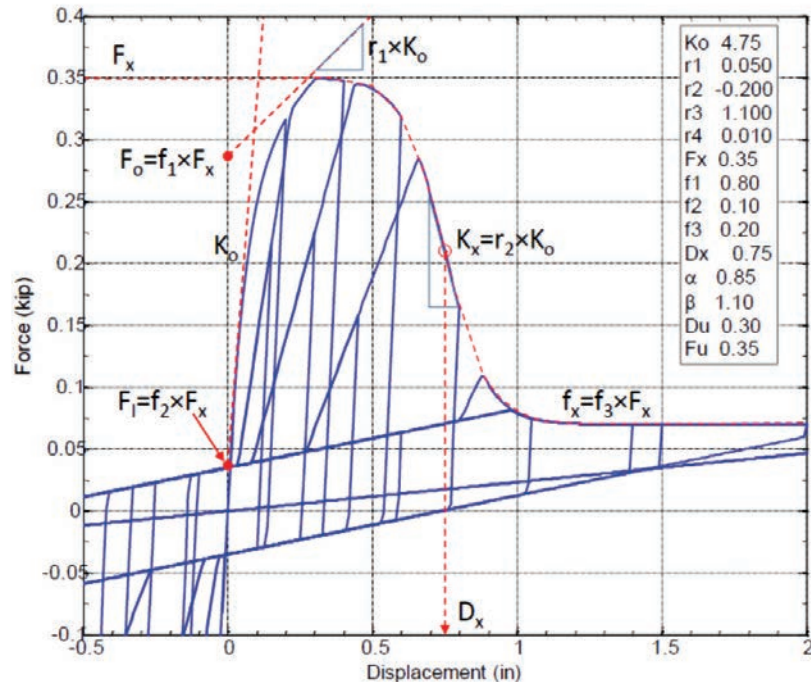


Figure 1-2 Modification of CUREE hysteretic rule for modeling residual strength.

1.3.2 Building Modeling

Figure 1-3 illustrates a single-story light-frame wood building configuration modelled using the *Timber3D* analysis program. As described above, the horizontal roof diaphragm is modelled using co-rotational 3D, two-node, 12-DOF elastic beam elements. The model includes vertical wall elements composed of a limited number of standard non-linear wall “building blocks”. The sill plate and concrete foundation attached to the bottom nodes of the building blocks are modeled with elastic beam elements. Anchored bolts and hold-down devices are modeled with F2F link elements. Similarly, the semi-rigid connectivity (i.e., uplift) between the studs and the sill plate and the sill plate and the concrete foundation are also modeled with F2F link elements. Finally, F2F link elements can also be used to model non-linear soil springs. The modeling methods and physical properties assigned to these individual elements are briefly described in the following sections. Section 6 discusses use of these elements in the ATC-110 project.

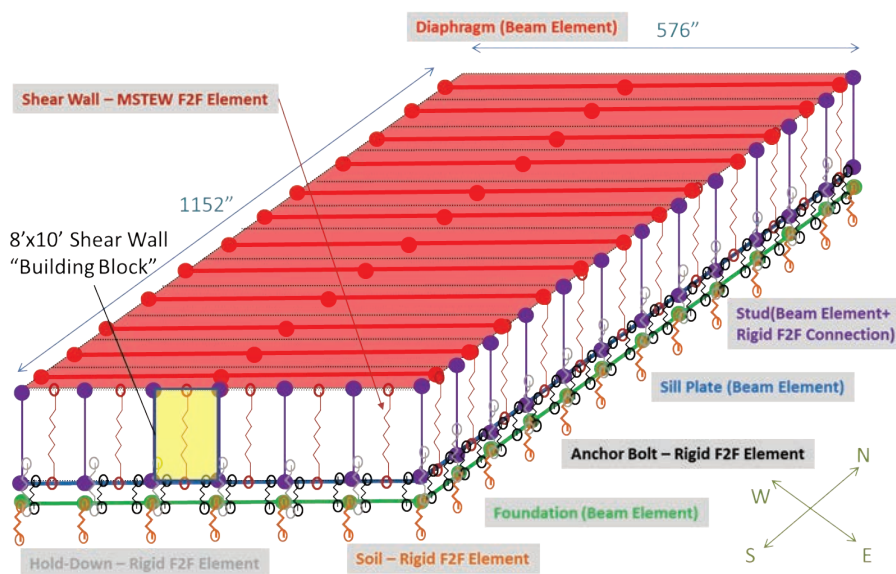


Figure 1-3 Schematic illustration of one-story, light-frame wood building model in *Timber3D*.

1.3.3 Non-linear Wall “Building Blocks”

Modeling of all vertical walls (including both structural and non-structural wall finishes) is based on non-linear wall building blocks made of various common sheathing and framing materials and of variable dimensions depending on the problem at hand. A typical 4 or 8-foot wide by 10-foot tall wall building block is illustrated in Figure 1-4. Each building block is composed of four nodes with two vertical end studs and two horizontal plates modelled by elastic frame elements along with a F2F link element representing the non-linear lateral cyclic response of vertical walls by the

CUREE hysteretic rule, as described above. Each wall building block can model:

- The axial and in-plane flexural deformation of the end studs.
- The in-plane flexural deformation of the top and bottom plates.
- The non-linear lateral cyclic response of the sheathing-to-framing assembly.
- The semi-rigid connectivity (e.g., uplift) between the end studs and the sill plate.

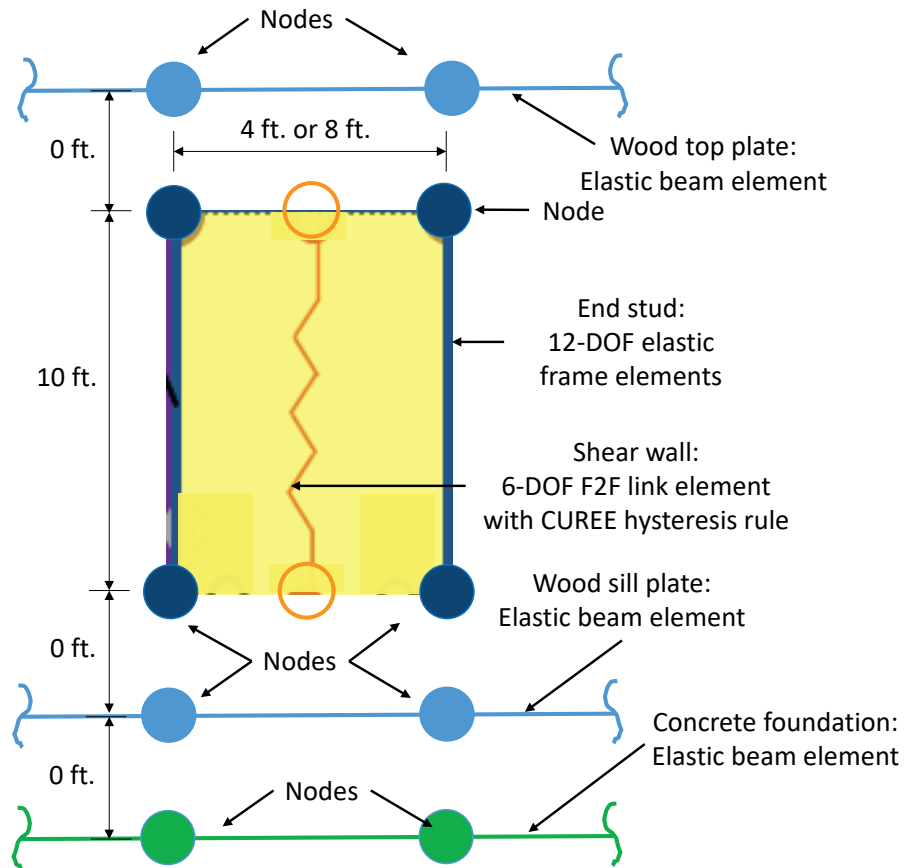


Figure 1-4 Schematic illustration of vertical wall building block.

1.3.4 Modeling of Semi-Rigid Connectivity between Wood Sill Plate and Concrete Foundation

To model the influence of semi-rigid connectivity between the wood sill plate and the concrete foundation on the response of light-frame wood buildings, linear F2F link elements are introduced between the concrete foundation and the wood sill plate, as illustrated in Figure 1-5. The F2F link elements represent the axial response of the anchor (shear) bolts introduced at various locations between the concrete foundation and the wood sill plate.

The wood sill plate is modelled by elastic beam elements. The vertical DOFs of the F2F link elements are released to model the separation between the wood sill plate and the concrete foundation.

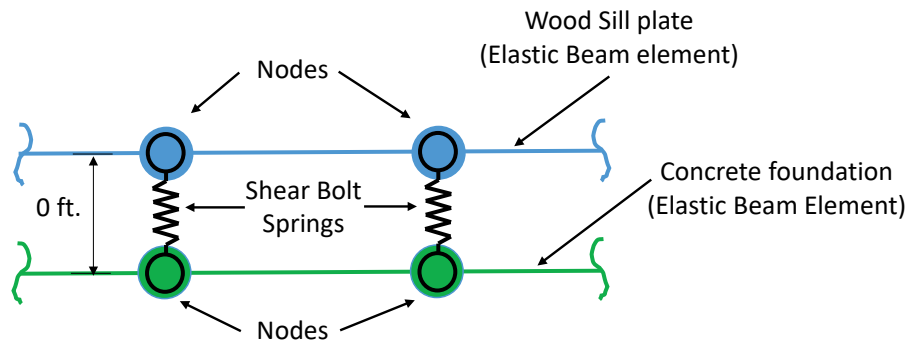


Figure 1-5 Schematic illustration of modeling of semi-rigid connectivity between the wood sill plate and the concrete foundation.

1.3.5 Modeling of Semi-Rigid Connectivity between Vertical Studs and Sill Plate

To model the influence of semi-rigid connectivity between the vertical studs and the sill plate on the response of light-frame wood buildings, non-linear F2F spring elements are introduced between the end studs and the sill plate, as illustrated in Figure 1-6. The F2F end studs spring elements represent the restraint on the uplift of the studs caused by some portion of the wood sheathing nailed to the wood sill plate. The sill plate is modelled by elastic beam elements.

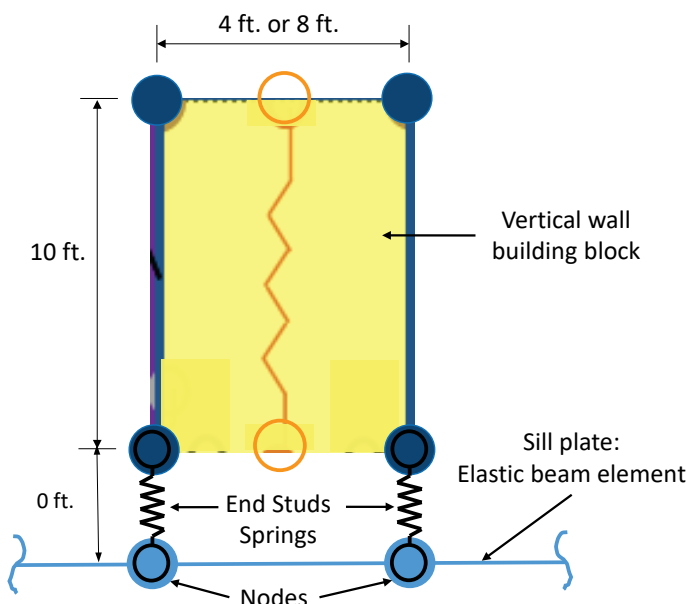


Figure 1-6 Schematic illustration of modeling of semi-rigid connectivity between the end studs and the sill plate.

1.3.6 Modeling of Semi-Rigid Connectivity from Hold-Down Rods

To model the influence of hold-down rods on the non-linear seismic response of light-frame wood buildings, non-linear F2F spring elements are introduced between adjacent floors, as illustrated in Figure 1-7. The vertical DOFs of the F2F link elements are released to model the non-linear axial tensile response of the hold-down rods.

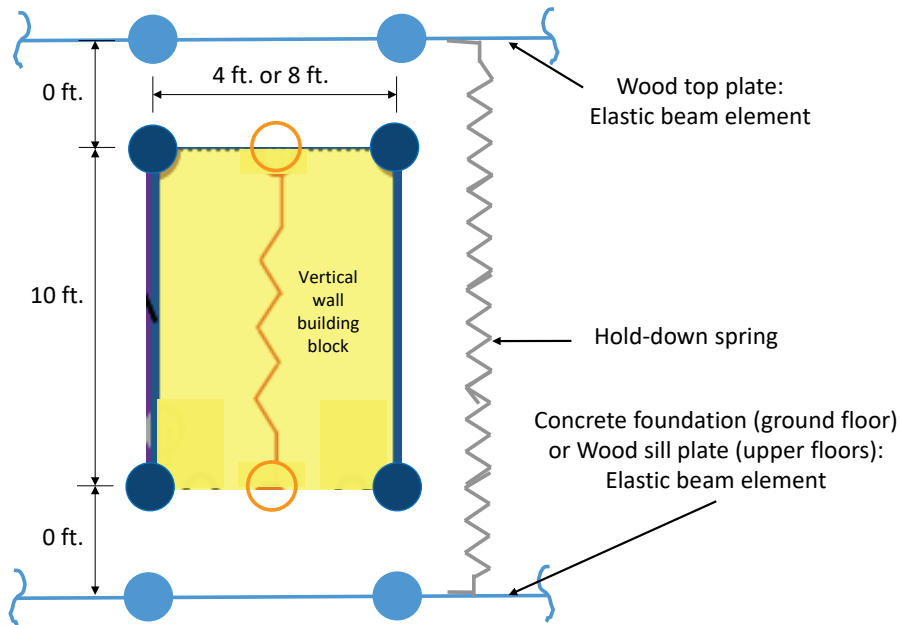


Figure 1-7 Schematic illustration of modeling of semi-rigid connectivity introduced by hold-down rods.

1.3.7 Modeling of Semi-Rigid Connectivity from Conventional Hold-Down Devices

To model the influence of conventional hold-down devices on the non-linear seismic response of light-frame wood construction, non-linear F2F spring elements are introduced between the end studs of vertical wall building blocks and the concrete foundation, as illustrated in Figure 1-8. The concrete foundation is modeled as an elastic beam element. The vertical DOFs of the F2F link elements are released to model the non-linear axial tensile response of the conventional hold-down devices.

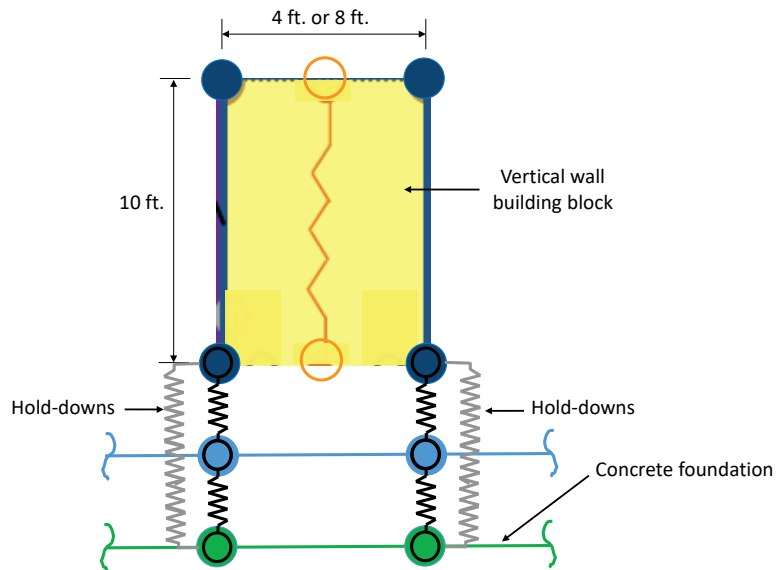


Figure 1-8 Schematic illustration of modeling of non-linear hold-down devices.

1.3.8 Modeling of Semi-Rigid Connectivity from Steel Straps

To model the influence of steel straps on the non-linear seismic response of light-frame wood construction, non-linear F2F link elements are introduced between the end studs of vertical wall building blocks and the top and bottom wood sill plates in the upper floors, as illustrated in Figure 1-9. The wood sill plates are modeled as elastic beam elements. The vertical DOFs of the F2F link elements are released to model the non-linear axial tensile response of the steel straps.

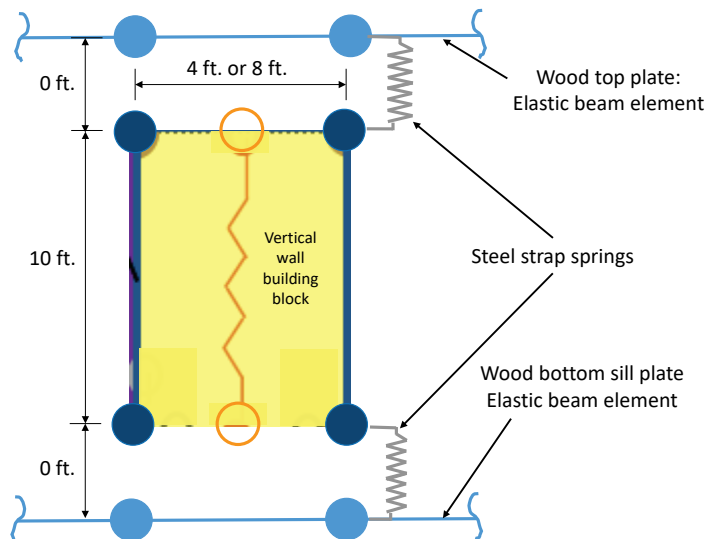


Figure 1-9 Schematic illustration of modeling of non-linear steel straps.

1.3.9 Modeling of Non-linear Soil Springs

Soil-structure interaction effects can be modeled approximately in *Timber3D* by introducing non-linear soil springs between the concrete foundation and fixed base nodes, as illustrated in Figure 1-10. F2F spring elements are used to model the soil springs. Three DOFs of the F2F link elements are released to model the soil springs in the two horizontal and vertical directions. The concrete foundation is modeled as an elastic beam element with high flexural stiffness.

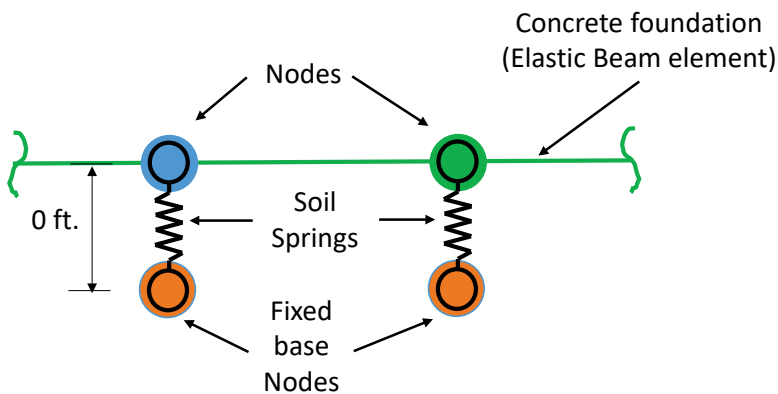


Figure 1-10 Schematic illustration of modeling of non-linear soil springs.

1.3.10 Modeling of Inelastic Steel and Concrete Elements

The modelling of existing and retrofitted full-building configurations may involve the consideration of inelastic elements made of other materials than wood (steel or concrete). For example, a steel moment-resisting frame could be considered as an attractive alternative for the retrofit of hill-side constructions. Also, the consideration of cantilevered configurations may require the consideration of the inelastic response of concrete elements. These inelastic steel and concrete elements can be modeled in *Timber3D* by combinations of elastic frame elements and F2F rotational spring elements. For example, Figure 1-11 illustrates the modeling of an inelastic moment-resisting frame rigidly anchored to an elastic concrete foundation in *Timber3D*. The inelastic response of the frame is modelled by lumped plasticity using F2F spring elements for which only one rotational degree-of-freedom is released. The elastic response is obtained through the elastic properties of the frame elements and the non-linear moment-rotation hysteretic response at each joint between adjacent frame elements and the frame elements and the foundation is obtained through the F2F spring elements. Generalized non-linear moment-rotation relationships can be implemented in *Timber3D*, as illustrated in Figure 1-12.

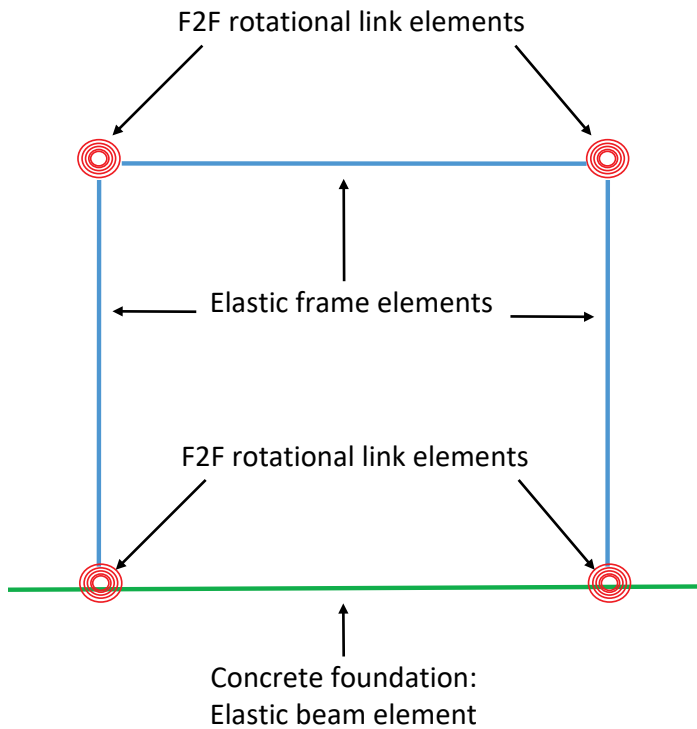


Figure 1-11 Schematic illustration of modeling of an inelastic moment-resisting frame rigidly anchored to an elastic concrete foundation.

Moment, M

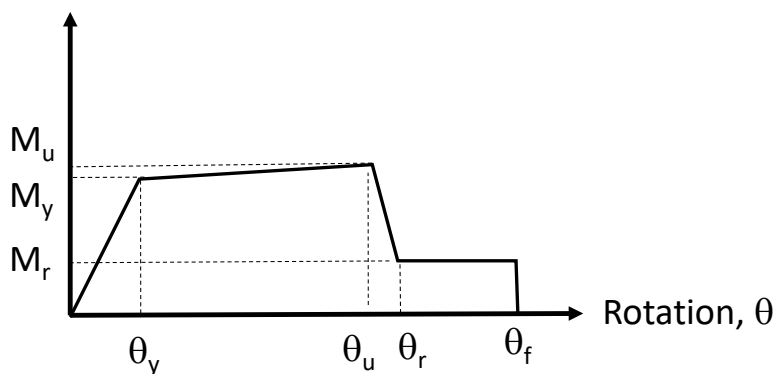


Figure 1-12 Generalized illustration of inelastic moment-rotation relationship for F2F rotational link elements.

1.3.11 Modeling of Semi-rigid and Rigid Diaphragms

Two modelling techniques were developed for diaphragms in Timber3D to capture the behavior of rigid and flexible diaphragms. When rigid diaphragms were required based on the assumption of the structure's behavior, 2-node 12-degrees-of-freedom frame elements were used to represent the main diaphragm components. An example of a rigid diaphragm

element implemented in Timber3D is shown in Figure 1-13. The rigid diaphragm frame elements were assigned the length (L), width (W), and depth (h) of the diaphragm segment they were meant to represent based on the layout of the Timber3D model (see Figure 1-14).

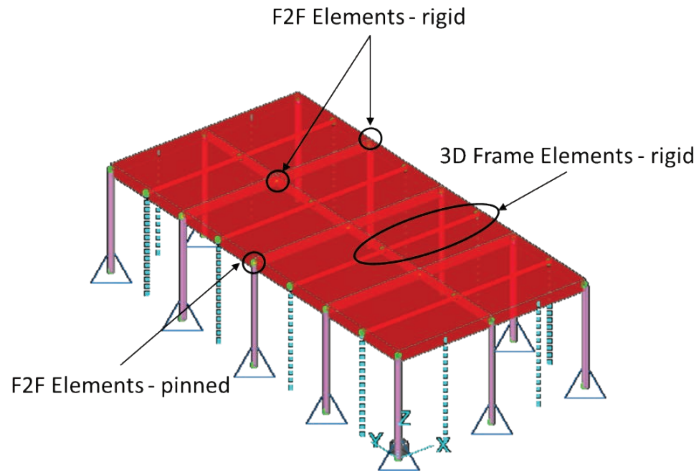


Figure 1-13 Rigid diaphragm elements implemented in *Timber3D*.

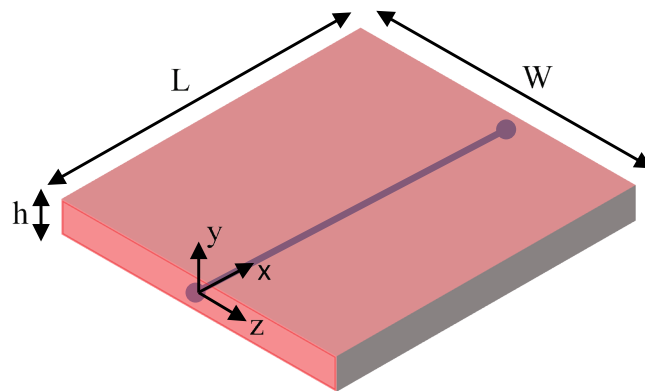


Figure 1-14 Schematic illustration of modeling of a rigid diaphragm.

Section modifiers were used to change the values of the rectangular cross-section properties, A , A_{sy} , A_{sz} , I_y , I_z , and J . A is the cross sectional area normal to local x -axis. A_{sy} and A_{sz} are the shear areas normal to the local y - and z -axes, respectively. I_y and I_z are the moment of inertias for bending about the y - and z -axes, respectively. J is the torsional constant for twisting about the x -axis. For rigid diaphragms, these modifiers were set to large values to ensure the rigid behavior of the diaphragm elements. Frame elements used to model the diaphragm were connected to each other using frame-to-frame (F2F) elements that acted as rigid connections between

section of the diaphragm. The diaphragm frame elements were connected to stud elements using F2F elements that represent a pin-connection.

When it was necessary to model the stiffness of the diaphragm elements explicitly (i.e. semi-rigid diaphragm), the rigid diaphragm model shown in Figure 1-14 was replaced by the semi-rigid diaphragm model shown in Figure 1-15. Four rigid boundary members were attached with pinned F2F connections to allow the semi-rigid diaphragm to deform into parallelogram shape (i.e. pure shear deformation). An equivalent shear beam, modeled using 3D frame element (see Figure 1-15) with reduced element width (b) and depth/thickness (h), was utilized to obtain the desired in-plane shear stiffness. Note that any arbitrary element width and depth can be used to calibrate the in-plane shear stiffness. In this example, b and h were both set to 8 in. The equivalent shear beam (frame element) was fixed to two parallel rigid boundary members, as shown in Figure 1-15.

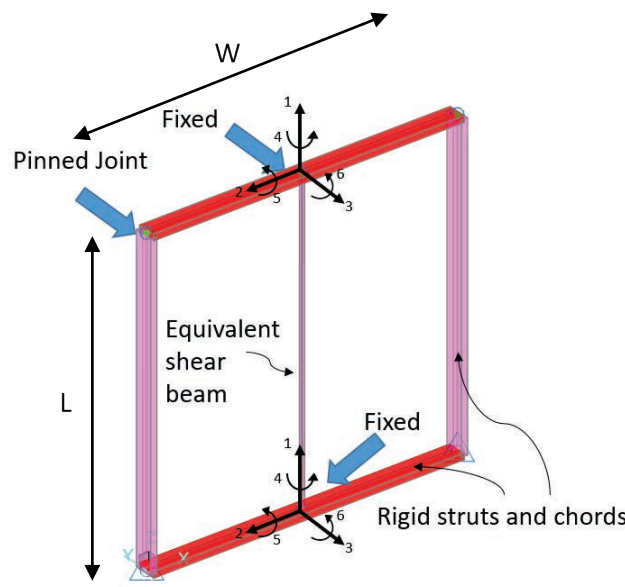


Figure 1-15 Schematic illustration of modeling of a semi-rigid diaphragm.

The in-plane shear stiffness of the diaphragm configuration can be controlled by manipulating the stiffness matrix value associated with the in-plane deflection of the diaphragm controlled by degree of freedom 2. Because the rotation of the equivalent shear beam is fixed, only the term contributing to the deflection of the node at either end contributed to the shear stiffness. The term in the stiffness matrix is controlled by the moment of inertia, I_z , as shown in Eq. (1). Where L and W are the actual length and width of the semi-rigid diaphragm. A_{sy} is the shear area computed using the user assigned element width and depth ($A_{sy} = 2/3 \times b \times h$). G_a is the desired in-plane shear stiffness of the semi-rigid diaphragm, determined based on experimental

testing of unblocked wood diaphragms performed by CUREE and DFPA (see Volume 3 Part 4 document). Based on conservative estimates of the materials used in house- and room-over-garage configurations (Working Group 5), a shear stiffness value of 8 kip/in per foot of diaphragm width was used. G in Eq. (1-1) is the shear modulus, computed using Eq. (1-2), where E is the elastic modulus (1400 ksi), and ν is the Poisson ratio (0.3). The I_z modifier (K_{Iz}) shown in Eq. (1-3) was used to adjust the bending moment of inertia (I_z) of the equivalent shear beam, computed using Eq. (1-1), such that the in-plane shear stiffness of the semi-rigid diaphragm (parallelogram) matches the desired shear stiffness (G_a) obtained from full-scale diaphragm test.

$$I_z = \frac{A_{sy}G G_a L^2 W}{12E(A_{sy}G - G_a W)} \quad (1-1)$$

$$G = \frac{E}{2(1 + \nu)} \quad (1-2)$$

$$K_{Iz} = \frac{12I_z}{bd^3} \quad (1-3)$$

1.4 Analysis Methods

The following analysis methods of light-frame wood buildings are available within Timber3D:

- Modal (free vibration) analyses to evaluate elastic natural periods and mode shapes.
- Non-linear static pushover analyses.
- Linear and non-linear dynamic analyses.
- Non-linear incremental dynamic analyses (IDAs) according to the FEMA P-695 methodology (FEMA 2009) for a defined set of ground motion intensities.

1.5 Comparisons of Predictions of *Timber3D* with a Simplified Model of a Light-Frame Wood Hospital Building

In the first phase of the ATC-116 Project - *Solutions to the Issues of Short-Period Building Seismic Performance*, the predictions of the *Timber3D* software were compared to those of a simplified model used for a pilot study on the Templeton Hospital, a one-story light-frame wood hospital building (Tokas and Lobo, 2012). Some of these comparative results were reviewed

by the ATC-110 Project Team WG1 to get a sense of the capabilities of the of the *Timber3D* software.

For the simplified model, the numerical framework developed *recently* by Koliou et al. (2015) for rigid wall-flexible roof diaphragm structures was utilized. The numerical modeling framework is based on a three step sub-structuring approach including: (1) a hysteretic response database for roof diaphragm connectors; (2) a two-dimensional inelastic roof diaphragm model incorporating hysteretic connector response; and (3) a simplified building model incorporating hysteretic diaphragm model response. The RUAUMOKO2D software (Carr, 2007) was used for the development of the simplified building model.

Figure 1-16 illustrates the one-story commercial base line building model considered for the comparisons of predictions between *Timber3D* and the simplified model. The building dimensions are 48 ft. \times 96 ft. in plan and 10ft. in height. The vertical elements of the seismic force-resisting system (SFRS) of the building consists of perimeter wood shear walls. The vertical wood shear walls consist of 2 \times 6 studs at 16" o.c. sheathed with $\frac{1}{2}$ -inch plywood on one side. The horizontal elements of the SFRS of the building model consists of perimeter wood roof diaphragms sheathed with $\frac{1}{2}$ -inch plywood (no openings). The building model is assumed to be founded on concrete grade beams located below the wood shear walls and on top of a 5-in. thick concrete slab on grade. The roof seismic weight was assumed equal to 21 psf.

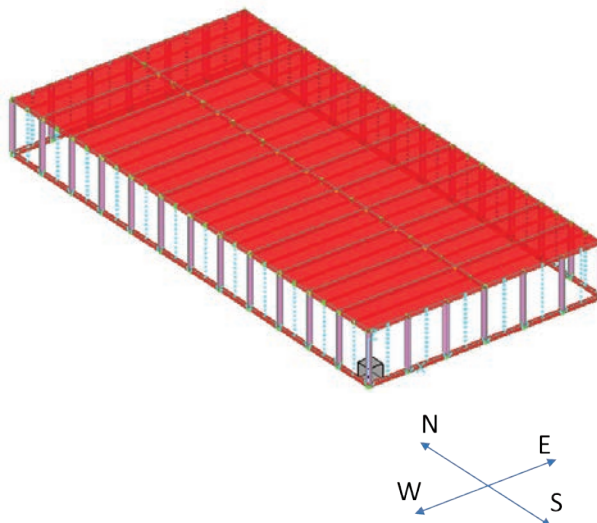


Figure 1-16 Illustration of one-story commercial base line building model considered for the comparisons of predictions between *Timber3D* and the simplified model.

It is important to note that none of the complex behaviors described in Sections 3.4 to 3.10 were activated in *Timber3D* for these limited comparisons.

Figure 1-17 shows the pushover curves in each principal direction of the base line building model predicted by *Timber3D* and the simplified model. Both models predict seismic coefficients (base shear / seismic weight) at peak strength larger than 0.9 in both directions, indicating a very laterally strong building. Both models predict peak strength values at a drift ratio of 2% in the East-West direction and at 2.2% in the North-South direction. The peak strengths predicted by *Timber3D* are slightly higher than that predicted by the simplified model. This is the result of the differences in the modeling of the roof diaphragm by the two models. The simplified model considered the in plane yielding of the roof diaphragm, which controlled the lateral peak strength of the building model. The roof diaphragm is assumed to behave elastically in *Timber3D*.

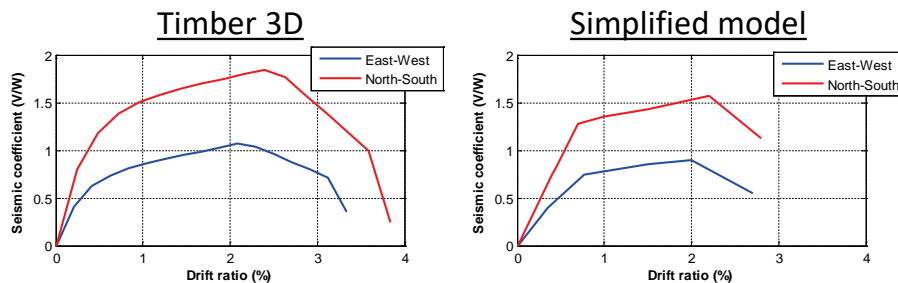


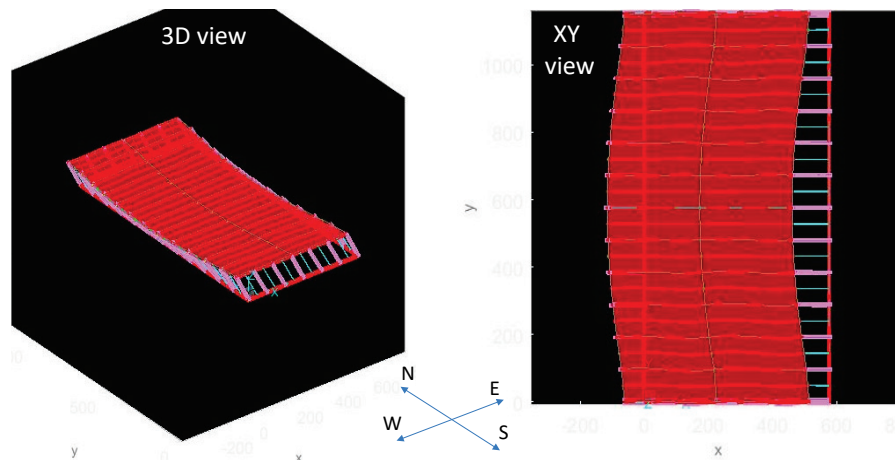
Figure 1-17 Pushover curves for base line building model predicted by *Timber3D* and simplified model.

Table 1-3 compares the first three natural periods and associated mode shape directions of the base line building model predicted by *Timber3D* and by the simplified model. The mode shapes predicted by *Timber3D* are also illustrated in Figure 1-18. Both models predict very similar natural periods and mode shape directions. The influence of the flexibility of the roof diaphragm on the deformed shapes of the building model is evident.

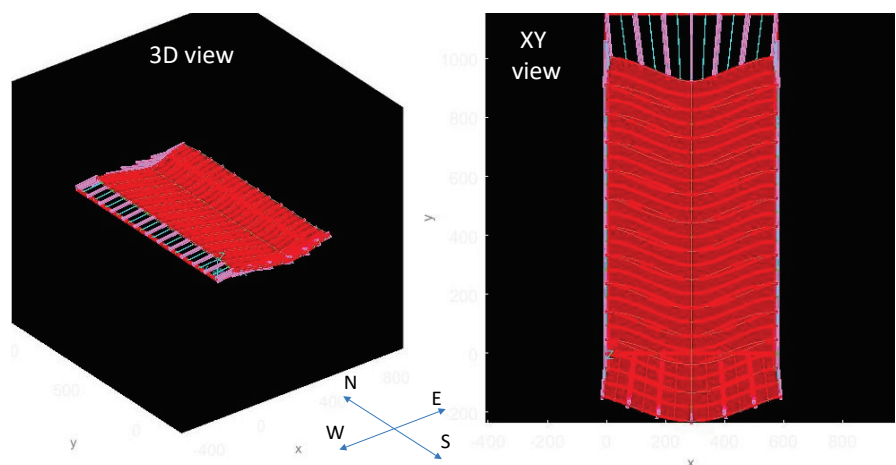
Table 1-3 Natural Periods and Mode Shape Directions for Base Line Building Model Predicted by *Timber3D* and Simplified Model

Mode	Natural Period (sec)		Mode Shape Direction	
	<i>Timber3D</i>	Simplified Model	<i>Timber3D</i>	Simplified Model
1	0.197	0.195	Translational East-West	Translational East-West
2	0.133	0.130	Translational North-South	Translational North-South
3	0.102	0.090	Torsional	Torsional

Mode 1: 0.197 sec.



Mode 2: 0.133 sec.



Mode 3: 0.102 sec.

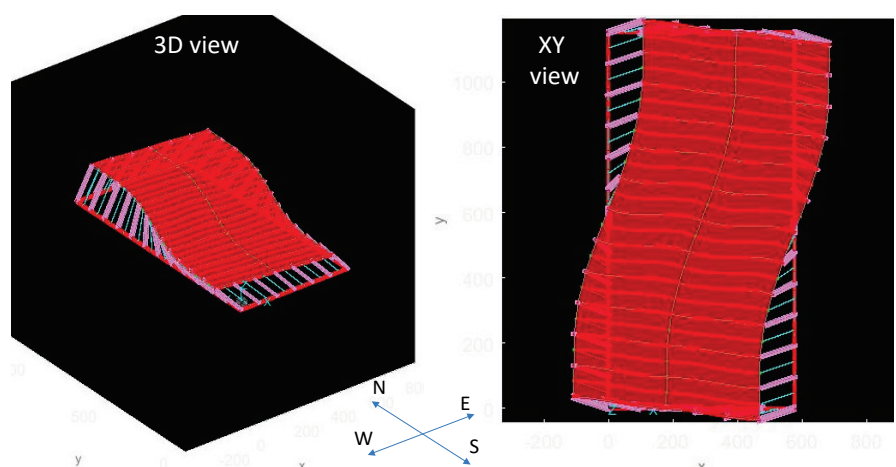


Figure 1-18 Pushover curves for base line building model predicted by *Timber3D* and simplified model.

Figure 1-19 compares the results of incremental dynamic analyses (IDA) on the base line building model obtained with *Timber3D* and the simplified model. The analyses were conducted for three records that are part of the FEMA P695 far-field ground motions set (FEMA, 2009). The first record, designated as “GM median Sa” in Figure 1-13, was selected to best match the 5% damped median spectral acceleration of the entire 44 ground motions set at a period of 0.25 sec. The other two records, designated as “GM median Sa + stdv” and “GM median Sa - stdv” in Figure 1-13, were selected to best match the 5% damped median plus and minus one standard deviation spectral acceleration, respectively, of the entire 44 ground motions set at a period of 0.25 sec. Both models predict very similar IDA curves across the entire range of seismic intensity, all the way to collapse.

The limited comparisons presented above provided some confidence on the capabilities of the *Timber3D* software to model accurately the seismic response of three-dimensional buildings for the numerical studies conducted in the ATC-110 Project.

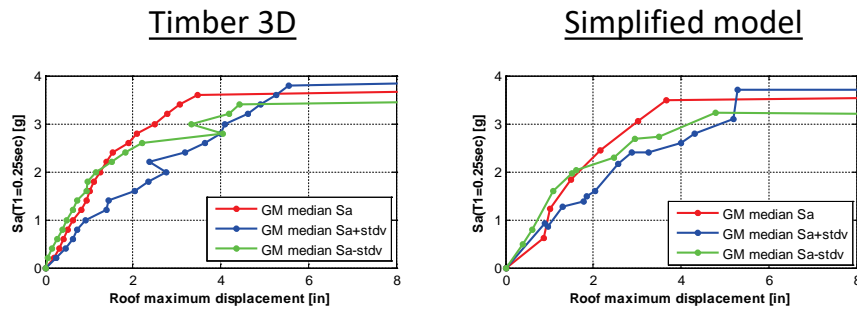


Figure 1-19 Incremental dynamic analysis curves for base line building model under three selected ground motion records predicted by *Timber3D* and simplified model.

1.6 Applications of *Timber3D*

The approach to use *Timber3D* within the project was to keep the modeling as simple as possible whenever possible, and only turning on features of the software when specifically deemed necessary. The basic models included: (1) diaphragm flexibility; and (2) hysteretic wall elements that include combined shear and overturning behavior from component tests. All other sources of semi-rigid connectivity and non-linear behavior were turned off unless specifically required. This allowed the analysis to use the needed sources of flexibility that were best established through previous validations. Some of the semi-rigid connectivity modelling in *Timber 3D* described in Section 3 had not been validated yet. Shear wall building blocks from the concurrent ATC-116 Project were adjusted as necessary to reintroduced into

the wall building blocks the displacements due to overturning that had been removed in the ATC-116 wall building blocks.

Other features of the software were turned on an as-needed basis, with a specific validation of the resulting behavior. Where tie-downs were specifically modeled, shear wall building blocks were adjusted to remove overturning displacement from their cyclic behavior. The items that were included only as necessary are the studs and anchor bolts. Where extra features were needed, modeling properties were carefully developed by the modelers in collaboration with the working groups.

1.7 References

- Christovasilis, I.P. and Filiatrault, A. 2010. "Two-Dimensional Seismic Analysis of Multi-Story Light-Frame Wood Buildings," *9th US National & 10th Canadian Conference on Earthquake Engineering: Reaching Beyond Borders*, Toronto, Canada, Paper No. 69, 10 p.
- Christovasilis, I.P. and Filiatrault, A. 2013. "Numerical Framework for Non-linear Analysis of Two-Dimensional Light-Frame Wood Structures," *Ingegneria Sismica: International Journal of Earthquake Engineering*, Vol. XXX, No. 4, 5-25.
- Carr, A. J. 2007. "RUAUMOKO-Inelastic Dynamic Analysis Program." Dept. of Civil Engineering, Univ. of Canterbury, Christchurch, NZ.
- FEMA. 2009. "Quantification of Building Seismic Performance Factors," FEMA P695, Prepared by the Applied Technology Council for the Federal Emergency Management Agency, Washington, DC, 421 p.
- Folz, B., and Filiatrault, A. 2001. "Cyclic Analysis of Wood Shear Walls", *ASCE Journal of Structural Engineering*, 127(4), 433-441.
- Koliou, M., Filiatrault, A., Kelly, D.J. and Lawson, J. 2015. "Distributed Yielding Concept for Improved Seismic Collapse Performance of Rigid Wall-Flexible Diaphragm Buildings," *ASCE Journal of Structural Engineering* DOI: 10.1061/(ASCE) ST.1943-541X.0001386.
- Pang, W., Ziaeい, E. and Filiatrault, A. 2012. "A 3D Model for Collapse Analysis of Soft-story Light-Frame Wood Buildings," *12th World Conference on Timber Engineering*, Auckland, New Zealand, 7 p.

Tokas, C. and Lobo, R. 2012. "Hospital Seismic Safety Program and Strong Motion Instrumentation," *Proceedings of SMIP12 Seminar on Utilization of Strong-Motion Data*, Sacramento, CA, 111-124.

van de Lindt, J., Symans, M.D., Pang, W., Shao, X., and Gershfeld, M. 2012. "Seismic Risk Reduction for Soft-story Woodframe Building: The NEES-Soft Project," *121th World Conference on Timber Engineering*, Auckland, New Zealand, 8p.

Part 2

Performance Criteria for Numerical Studies

2.1 Introduction

The ATC-110 Project relied heavily on numerical studies to develop the FEMA P-1100 Prestandard for the assessment and retrofit of one- and two-family light-frame wood dwellings. Numerical studies were conducted on a limited number of example (archetype) buildings, both with and without seismic retrofit, with the intent of identifying building characteristics, acceptance criteria, and design criteria that lead to acceptable seismic performance. In order for the numerical studies to be performed, it needed to be decided what constituted acceptable seismic performance for purposes of this prestandard. This document discusses options considered and identifies the performance criteria selected for use. This document was first developed early in the project, and is provided as Volume 3, Part 2 to serve as a record of considerations.

The performance criteria discussed in this section were used by the researchers for numerical studies. Separate criteria were developed to be used by designers in development of retrofit designs, as discussed in Volume 3, Part 3. Figure 2-1 presents a flowchart that differentiates the use of numerical study performance criteria, assessment criteria, and retrofit design criteria.

2.2 Indicators of Performance

This section describes indicators of performance considered for this project. Included in the discussion are examples of indicators that have been used in past studies, along with their pros and cons. The indicators generally fall into three categories: relating to safety against collapse, structural safety for continued occupancy, and level of repair. The indicators selected for use by the ATC-110 Project are provided in Section 3.

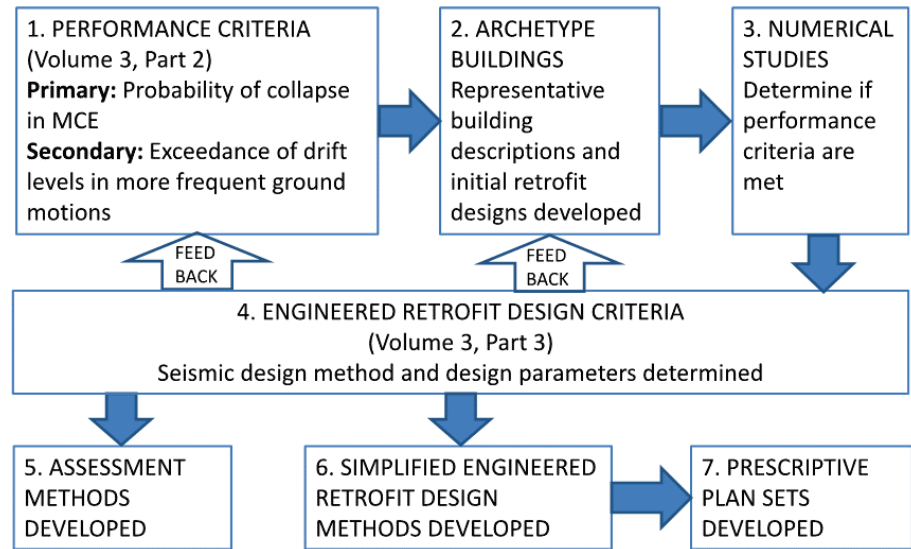


Figure 2-1 Relating performance criteria to assessment and retrofit criteria.

2.2.1 Collapse Indicators

Possible collapse indicators are:

Probability of Collapse. Recent studies for development of seismic provisions for new buildings have almost exclusively judged acceptable seismic performance in terms of a probability of collapse under a prescribed seismic intensity level. This methodology was widely implemented in FEMA P-695 (FEMA, 2009) and follow up studies and has since been used to introduce new lateral-force-resisting systems for new construction. The computer programs used in this project have the ability to explicitly model side-sway collapses caused by P- Δ effects.

Pro: This indicator will be most easily aligned with and related to performance targets for new buildings.

Pro: This indicator is consistent with performance-based design trends in the profession, and results can be compared to recent studies such as FEMA P-695 and P-58 (FEMA, 2012b).

Con: As the ATC-110 project was getting started, numerical studies were recognized to in general predict higher levels of collapse than have been generally seen in the existing building inventory or predicted by the limited available shake table testing; the results of these studies are generally believed to be upper bound, but their bias has not yet been quantified. This observation was the genesis of the ATC-116 project that focused on the seismic performance of short-period buildings. For purposes of the ATC-110 Project, one way identified to deal with this issue was to focus on

performance of pre- and post-retrofit buildings being studied, without specifically stating probabilities of collapse, thus providing a relative measure of improvement. This approach presumes that the bias is similar for vulnerable and properly retrofitted buildings.

Con: Numerical models predicting probability of collapse rely on description of the load-deflection hysteretic behavior of components that make up the building. Numerical modeling to collapse requires data from component testing to large displacements. As the ATC-110 Project was getting started there was very little test data extending to the displacements that would need to be modeled, so expert judgment must be relied on to develop full modeling parameters.

Probability of Exceeding a Drift Level Indicator of Collapse. This approach retains the concept of probability of collapse, but substitutes a judgment-based drift as a collapse criterion for explicit computer modeling of collapse.

Pro: This approach would separate the work of this project from the work of ATC-116 and others, allowing the work of the ATC-110 project to be completed and judged without creating reliance on the work of the ATC-116 Project.

Con: There is very little information to rigorously derive collapse drifts, so the criteria would be heavily dependent on expert opinion.

Con: This approach would have the same concerns regarding availability of component hysteresis data as does the explicit modeling of collapse.

Probability of Exceeding a Drift Associated with Onset of Strength Loss. This would set aside the probability of collapse and instead choose a drift level associated with another behavior such as onset of strength loss in bracing systems. This approach was used in FEMA P-807 (FEMA, 2012a), with onset of strength loss for systems deemed to be more ductile identified to occur at 4% drift. The FEMA P-807 project and a very similar project for the British Columbia Ministry of Education (BC Ministry of Education et al., 2012), combined criteria related to drifts and pre-run nonlinear analysis data bases to develop computer assessment and retrofit tools.

Pro: This could allow the numerical studies to focus on displacement ranges for which more component testing data is available and will provide higher confidence in the results of the numerical studies.

Con: Understanding and communicating the level of safety established using this criterion would be difficult, as the relationship between this criterion and more commonly used measures of safety is not known. A limited numerical

study of performance relative to IEBC and ASCE 41 was conducted (Buckalew et al., 2015) for weak-story wood buildings using P-807 criteria as adopted by the City of San Francisco for their soft-story retrofit program; however, this was at a notably lower performance level than used for the ATC-110 project and so does not help to inform performance for this project.

Probability of Exceeding Strength Criteria at Design Level Earthquake. This would conceptually revert back to the type of measures considered prior to the current focus on probability of collapse.

Pro: This could allow the numerical studies to focus on displacement ranges for which more component testing data is available and will provide higher confidence in the results of the numerical studies.

Pro: This would align and more directly translate into current procedures for the assessment and retrofit of dwellings.

Con: This would not be making use of most current concepts and numerical tools.

2.2.2 Continued Occupancy Indicators

This criterion was intended to relate to possible post-earthquake tagging of the building, based on expert judgement. The purpose was to estimate the probability of exceeding a drift level used as a surrogate for likelihood that continued occupancy would be prohibited. Possible approximate indicators of acceptability for continued occupancy included:

Peak Transient Drift. The peak transient drift can be measured using nonlinear response history analyses. The permissible drift would be selected based on available information relating peak transient drift to damage observed. A level of damage would need to be judged to result in enough loss of strength that likelihood of significant structural damage in an aftershock is high.

Pro: This approach may be simple in concept to convey to the public.

Con: This approach is not aligned with current codes and new building expectations.

Con: Continued occupancy is a high standard and dependent upon more than structural performance of the main dwelling (i.e. some level of functioning utilities).

Peak Residual Drift. The residual drift remaining following a seismic event is currently considered in post-earthquake safety assessment procedures,

when there is an objective of determining whether or not a building is safe to occupy.

Pro: This is easily incorporated into post-earthquake safety assessments, so appropriate criteria can be implemented.

Con: The accuracy with which residual drifts can be predicted is not understood and is feared to be poor.

2.2.3 Level of Repair Indicator

A level of repair indicator would be related to economic consequences, and in particular address the desire to track increased damage that could potentially occur in upper stories as a function of the level of retrofit of lower stories. Because damage to the finish and bracing materials in buildings is primarily a function of transient drift level, this indicator is thought to be a transient drift level criterion that would likely change with different finish materials.

While this is not a primary focus of the prestandard, the occurrence of elevated levels of damage in the superstructure has been brought up as a concern for which at least some numerical investigation is indicated. Developing cost information is beyond the scope of prestandard work, so use of a level of repair indicator would have to consider repair and cost in an approximate way using available information.

2.3 Performance Criteria Selected

ATC-110 selected one primary performance criterion as the basis for development of assessment and retrofit recommendations, and as the primary focus of ATC-110 efforts. ATC-110 also selected two secondary criteria that were defined and tracked for consideration. These secondary criteria were primarily intended to allow discussion in the prestandard and/or associated commentary. These primary and secondary criteria were used as overarching performance criteria, common to all working groups.

2.3.1 Primary Criterion

The primary criterion selected was the probability of collapse with explicit modeling of side-sway collapse in the numerical models. Both “raw” collapse results (i.e. collapse rates obtained directly from the numerical analyses) and collapse results with FEMA P-695 corrections (see Volume 3, Part 5) were generated for consideration by the working groups.

This criterion made best use of most current numerical tools. The noted concern related to over prediction of collapse was not found insurmountable; relative

improvement in performance was emphasized over absolute probabilities of collapse. The noted con related to lack of component testing to high drift levels is being compensated for by use of judgment in defining material characteristics for numerical modeling.

Demand level: Maximum Considered Earthquake (MCE) intensity level was used, consistent with requirements for new construction.

Accepted probability: Ten percent probability of exceedance, as currently used for new construction, was recommended as an initial target. This number was increased to approximately 20 percent for cripple wall houses because it was found impractical to provide the amount of sheathing and fasteners needed to achieve this goal (e.g., full cripple wall sheathing or more was required) and because this represented a significant improvement in performance relative to dwellings that were not retrofit. For the modeled living-space-over-garage and hillside archetype buildings, the probabilities of collapse with retrofit being predicted by the numerical studies were found to fall closer to the 10 percent that was initially targeted. As previously discussed, these probabilities were only relied on for general guidance, and more emphasis was placed on improvement of performance with retrofit.

2.3.2 Secondary Criteria

Two secondary drift criteria were selected to be captured from the numerical studies. These were applied to the subset of dwellings that had not already collapsed at the point that the demand level for this secondary criteria was reached.

One secondary drift criterion selected was termed “drift as a level of repair indicator.” This included tracking of transient drift in both unoccupied and occupied stories. The purpose was to estimate the probability of exceeding a drift level used as a surrogate for damage to finish materials, and compare the influence of different retrofits on this probability. The bases for the selected drift are FEMA P-58 fragility functions, as shown in Table 2-1, and CUREE EDA-02 (CUREE, 2007).

Transient Drift Level: 0.75%

Demand level: 30% probability of exceedance in 50 years (140-year mean return period).

The other secondary criterion selected was drift as it relates to structural safety for continued occupancy. This criterion was chosen as a way to relate to possible post-earthquake tagging of the building, based on expert judgement. The purpose was to estimate the probability of exceeding a drift

level used as a surrogate for likelihood that continued occupancy would be prohibited, and used to compare the influence of different retrofits on this probability. Bases for the selected drift include CUREE EDA-02 and FEMA P-807 Appendix D.9.

Transient Drift Level: 1.5 %

Demand level: 10% probability of exceedance in 50 years (475-year mean return period).

The secondary criteria were used to help inform decisions about which R factor was most appropriate for each retrofit type.

Table 2-1 Summary of Applicable FEMA P-58 Fragility Functions

P-58 Number	P-58 Description	Damage State	Drift Ratio (%)	Damage Description	Consequence Description
B1071-041	Exterior walls full height wood studs with gypsum wallboard	1	0.21	Screws pop, minor cracking of wall board, warping, cracking of tape	Re-tape
		2	0.71	Moderate cracking or crushing of gypsum wallboard (typically at corners or at opening corners)	remove and replace wall board
		3	1.2	Significant cracking or crushing of wall board, buckling of studs, tearing of tracks	rebuild wall
B1071-002 B2011.102	Light-frame wood walls with structural panels sheathing and stucco	1	0.25	Cracking of stucco	clean, patch and paint cracks
		2	0.52	Spalling of stucco, separation of sheathing and stucco from studs	remove and patch spalled stucco
		3	2.52	Fracture of studs, major sill plate splitting	rebuild wall
B2011.101	Exterior walls light-framed wood with structural panels and gypsum wallboard	1	1.0	Slight separation of sheathing from framing	Remove siding, re-nail sheathing
		2	1.75	Permanent rotation of sheathing panels, tear out of sheathing nails	Remove siding, remove and replace sheathing
		3	2.5	Fracture of studs and sill plates	rebuild wall

2.4 References

BC Ministry of Education, 2012. Structural Engineering Guidelines for the Performance-Based Seismic Assessment and Retrofit of Low-rise British Columbia School Buildings, British Columbia Ministry of Education, Professional Engineers and Geoscientists of BC, University of British Columbia, British Columbia, Canada.

Buckalew et al,2015. *Case Studies of Soft-Story Retrofits Using Different Design Guidelines*, SEAONC Special Projects Initiative Report, Structural Engineers Association of Northern California, San Francisco, CA.

CUREE, 2007. *General Guidelines for the Assessment and Repair of Earthquake Damage in Residential Woodframe Buildings* (CUREE EDA-02), Consortium of Universities for Research in Earthquake Engineering, Richmond, CA.

FEMA, 2009. P-695, Quantification of Building Seismic Performance Factors, June 2009.

FEMA, 2012a. Seismic Evaluation and Retrofit of Multi-Unit Wood-Frame Buildings with Weak First Stories (FEMA P-807), Federal Emergency Management Agency, Washington, D.C.

FEMA, 2012b. *Seismic Performance Assessment of Buildings* (FEMA P-58), Federal Emergency Management Agency, Washington, D.C.

Part 3

Assessment and Retrofit Design Criteria

3.1 Introduction

A primary goal of the ATC-110 project was to develop criteria for retrofit of seismic vulnerabilities in one- and two-family light-frame wood dwellings. Engineered retrofit procedures were intended to be simple to use. Where possible, prescriptive retrofit provisions were to be pre-engineered using the selected engineered retrofit criteria. As discussed in FEMA P-1100 Volume 3, Parts 1, 2 and 5, the improvement in dwelling seismic performance using the selected retrofit criteria was validated through numerical studies of representative example (archetype) dwellings.

The objective of this background paper was to inform selection of initial overarching retrofit design methodologies and design criteria, with the understanding that each project working group (WG) would have to, as necessary, revisit and revise the overarching criteria. This background paper discusses potential retrofit methodologies and criteria that were considered by the project, and the selected methodology and criteria. This document was initially developed early in the project, and is provided as volume 3, Part 3 to serve as a record of considerations.

The retrofit methodology and criteria have been selected with the intent of providing seismic performance consistent with the numerical study performance criteria of Volume 3, Part 2. The project numerical studies were used to verify this performance. Figure 1-1 presents a flowchart that differentiates the use of numerical study performance criteria and retrofit design criteria.

3.2 Retrofit Design Methodologies and Criteria

This section discusses possible retrofit design methodologies and criteria that were considered by the ATC-110 project team. Section 3 discusses the selected retrofit methodology and criteria.

Force-Based Design - Equivalent Lateral Force Procedure. The equivalent lateral force (ELF) procedure, as included in the NEHRP Provisions (FEMA, 2015) and ASCE/SEI 7 standard (ASCE, 2017a), was

considered for determination of design forces for retrofit, with the project numerical studies used to develop appropriate R-factors.

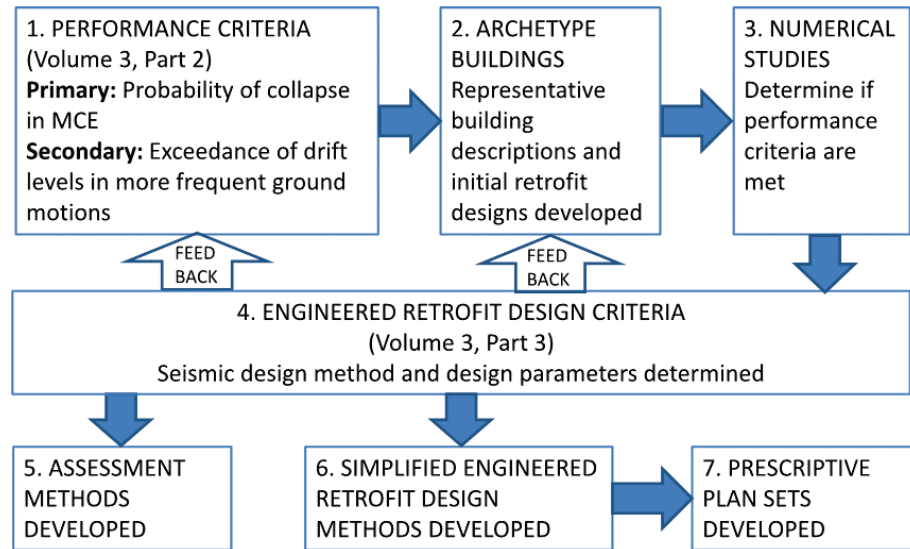


Figure 3-1 Relating numerical study performance criteria to retrofit criteria.

Discussion: The R-factor to be used for retrofit design is understood to be a function of the deformation capacity and ductility of the main seismic force-resisting system (SFRS) bracing materials. Because the materials that serve as the bracing in dwellings vary significantly in deformation at peak load and deformation capacity, it was anticipated that consideration of deformation capacity might be necessary. It was also anticipated that this might result in R-factors varying with the bracing materials and building types.

Pro: Because the ELF procedure is widely used by practicing engineers, this would be the most easily implemented approach, providing the least barrier to widespread use by practicing engineers, plan reviewers and building officials.

Pro: Supporting engineering design data generally used in the design of wood light-frame construction, such as published capacities for members and connections, could be implemented directly.

Pro: Use of an approach based on R-factors calculated for retrofit design from a procedure such as FEMA P-695 (FEMA, 2009), and based upon combinations of finish materials could also inform future R-factors for new construction.

Con: This methodology tends to focus attention on force and strength rather than deformation aspects. If used, drift criteria might have to be built into the methodology.

Con: This methodology has historically been associated with new construction rather than retrofit work and is not consistent with current trends for the retrofit of existing buildings such as ASCE/SEI 41 (ASCE, 2017b).

Con: The use of R-factors that may differ from currently published values may cause confusion.

Con: The conventional approach for new buildings which incorporate R-factors assumes a SFRS that is generally constructed of the similar materials in each direction and each story. This assumption is often not consistent with existing residential construction where various combinations of finishes are present.

Probabilistic Design Using FEMA P-695 Methodology. This approach involves running nonlinear analysis on dwellings and applying the adjusted collapse margin ratio approach implemented in FEMA P-695 to determine acceptable performance.

Pro: This approach would provide the most detailed and technically advanced consideration of performance.

Con: Design of individual dwellings using this methodology would require an extraordinary amount of effort and will not realistically be implemented.

Probabilistic Design Using Pre-run Database. This approach was used for the FEMA P-807 (FEMA, 2012) weak-story tool. Simplified parameters were derived to match building characteristics to the results of a large set of pre-run nonlinear analyses. The building characteristics captured included the combined load-deflection behavior of bracing materials, vertical distribution of strength and stiffness, and torsion.

Pro: This approach allows the implementation of a probabilistic methodology, thought by many to be the most technically advanced consideration of earthquake performance.

Con: This approach is well suited to buildings with one main building block; it becomes significantly more difficult to address the behavior of buildings with more sections or wings that might have varying behavior. This more complex type of geometry was anticipated to occur in a number of the dwellings of interest for the ATC-110 project, so the development of a relevant database might be problematic.

Con: It may be difficult to address the very significant torsional behavior that is anticipated to occur in moderate-to-steep hillside conditions.

Con: The level of analytical effort required to develop the database for the FEMA P-807 weak-story tool was very significant. It is anticipated that the effort would be much larger for the ATC-110 project due to the significant variations in building stock and construction type.

Con: The database was only able to determine whether the bracing met or did not meet the performance criteria. Once this has been determined, the designer needs some additional method or criteria with which to check the entire load path to make sure that the bracing elements can perform properly. With the approach used in FEMA P-807, the concept of capacity-based design was put forward to check the load path, but there was insufficient data and documentation of this approach to allow it to be systematically and uniformly implemented in FEMA P-807. Significant additional guidance would need to be developed in order for this methodology to be implemented for this prestandard.

ASCE 41 Linear Static Methodology. The ASCE/SEI 41 linear static methodology could be implemented. This procedure brings with it demand criteria developed for existing buildings that could serve as a starting point for discussion. Attention would focus on appropriate demand levels and derivation of appropriate m-factors. Consideration would need to be given to applicability and implementation of force- versus deformation-controlled criteria.

Pro: This would have the advantage of using a methodology that has been developed for existing buildings.

Pro: ASCE/SEI 41 could be directly referenced in whole or in part as deemed appropriate as a reference document.

Pro: The use of component by component-based evaluation approach is ideally suited to existing components which differ in expected strengths and ductility in each direction and possibly within each direction.

Con: ASCE 41 is not perceived to be a more accurate tool for wood light-frame structures than design per ELF procedures using R-factors and is less familiar to practicing engineers.

Con: As with R-factors, it is anticipated that a unique set of m-factors would be derived for the materials and combinations of materials that commonly occur in existing dwellings. These likely would be different than those currently contained in the ASCE/SEI 41 methodology and could result in designer confusion.

Con: Like the ELF procedure this methodology tends to focus attention on force and strength rather than deformation aspects. If used, applicable deformation limits or drift criteria may need to be built into the methodology.

ASCE/SEI 41 Nonlinear Static Methodology. The ASCE/SEI 41 nonlinear static methodology could be implemented. This procedure similarly brings with it demand criteria developed for existing buildings that would serve as a starting point for discussion. Attention would focus on derivation of appropriate target displacements for portions of the dwelling to be assessed or retrofit, construction of push-over curves and determination of appropriate deformation limits.

Pro: This would have the advantage of using a methodology that has been developed for existing buildings.

Pro: This would have the advantage of explicitly including consideration of deformation capacity.

Con: Available methods to derive target displacements are not perceived to be of good accuracy.

Con: While an admirable goal, the level of effort is substantial and could potentially take all the resources of the ATC-110 project.

3.3 Recommendations

Based on the ATC-110 project technical committee discussions and work performed as part of this project, a forced-based ELF procedure was selected as the method for design of seismic retrofits.,

The ELF retrofit design procedure was selected because it is the most commonly used and best understood by practicing engineers involved in design of seismic retrofits for one- and two-family dwellings. The ELF procedure is anticipated to require significantly less effort than an ASCE/SEI 41 approach. Reduced effort is an important consideration, in order to keep design cost moderate and allow sufficient attention to be paid to detailing aspects critical to performance. The project validation/calibration of selected ELF retrofit design R-factors using numerical studies, means that the retrofit design procedures have a performance-based design basis.

3.4 References

ASCE, 2017a. *Minimum Design Loads and Associated Criteria for Buildings and Other Structures*, 2016 Edition (ASCE/SEI 7-16). American Society of Civil Engineers, Reston VA.

ASCE, 2017b. *Seismic Evaluation and Retrofit of Existing Structures*, 2017 Edition (ASCE/SEI 41-17), American Society of Civil Engineers, Reston VA.

FEMA, 2009. *Quantification of Building Seismic Performance Factors* (FEMA P695), Federal Emergency Management Agency, Washington, DC.

FEMA, 2012. Seismic Evaluation and Retrofit of Multi-Unit Wood-Frame Buildings with Weak First Stories (FEMA P-807), Federal Emergency Management Agency, Washington, DC.

FEMA, 2015. NEHRP Recommended Seismic Provisions for New Buildings and Other Structures, 2015 Edition (FEMA P-1050), Federal Emergency Management Agency, Washington, DC.

Part 4

Material Characterization for Numerical Studies

4.1 Introduction

As part of the ATC-110 Project, full-building three-dimensional numerical studies were used for evaluation of dwellings before and after retrofit. As described in FEMA P-1100 Volume 3, Part 1, the software program *Timber 3D* was selected for the full building numerical studies. This discussion addresses the development of information to characterize material properties for input into the *Timber 3D* numerical studies. The primary material properties needed include the wall building blocks that describe in-plane bracing wall hysteresis, and the horizontal diaphragm load-deflection behavior. In addition to these primary material-modeling properties, specialized modeling properties were developed by each of the ATC-110 working groups to allow more detailed description of member and connection load-deflection behavior, as well as material descriptions specific to particular dwelling retrofit methods. This document describes the modeling parameters that were common across the working groups. See Volume 3, Parts 11, 12, and 13 for description of additional modeling parameters specific to the individual working group studies.

4.2 Wall Building Block Data

The concept of wall building blocks, used in the numerical studies to model vertical seismic force-resisting elements, was introduced in FEMA P-1100 Volume 3, Part 1. This section discusses assignment of hysteretic properties to the wall building blocks. It is necessary to rely on available component testing to derive the wall building block data, as conducting new component testing was outside of the scope of the ATC-110 project. Over the last 20 years, understanding of aspects important to component testing has evolved, with testing having been conducted at various points in that evolution. As a result, there is no complete perfect set of data from which modeling properties can be derived. Instead, there is a pool of available testing information from which the most representative data must be selected and prioritized, and modeling properties derived with the use of judgment.

Items considered in selection and prioritization of information included in wall building blocks include:

- Test loading protocol: Cyclic testing using the CUREE Ordinary (Krawinkler et al., 2002) or a similar test loading protocol was preferred as this protocol is believed to be most representative of demand on wood light-frame structures from earthquakes and results in failure modes matching those seen in damage following earthquakes. In particular, testing using the Sequential Phased Displacement (SPD) protocol (SEAOSC, 1996; Porter, 1987) has been identified to show failure modes significantly different from observed in earthquakes. In some cases, only monotonic or limited cyclic test data was available. In these cases, the envelope curves could usually be quantified, but judgment was required in assigning hysteretic degradation properties based on those of materials judged most similar.
- Test boundary conditions for finishes: The inclusion of realistic boundary conditions for finish materials, such as returns at corners and at ceilings, was preferred, as this was thought to best describe constructed conditions, and inclusion of such boundary conditions has a notable effect on wall component capacity and displacements at peak and post-peak capacities. Even the installation of trim at openings was found to effect test results (McMullin and Merrick, 2002). Components with less representative boundary conditions are thought to represent lower bound properties.
- Test overturning restraint: Testing with overturning restraint representative of as-built conditions is important to properly capture load-deflection relationships. For full-story height plywood or OSB walls, it was preferred that tie-down devices similar to those that would be used in dwelling construction were used. For plywood cripple wall sheathing without overturning restraint and other material types, overturning devices are not typically used in construction, and overturning restraint would primarily be gained from perpendicular walls, resistance of structural elements or dead load above. Sheathing materials other than plywood and OSB have been tested with a range of overturning restraint types and load levels. Overturning contribution to displacement of the vertical walls was included in the wall building blocks, mirroring the overturning restraint included in the component testing from which wall building block hysteretic parameters were derived.
- Displacement range and post-peak residual strength: In most recent numerical analysis studies, emphasis has come to focus on explicit modeling of building collapse. This has created a need for testing components to much higher displacements than thought necessary in the

past. As a result, component testing with as large imposed displacement as possible was sought. At the time data was being selected for numerical studies, data from testing to large displacements was very limited. Based on limited studies of full buildings, it is believed that some portion of the peak bracing system capacity remains to very large post-peak displacements. This behavior is believed to be in part a system behavior that cannot be fully captured in component testing results. The ATC-110 project team chose to incorporate the concept of post peak residual capacity using the same modeling as was being studied in the concurrent ATC-116 project studies of wood light-frame structures. The percentage of retained post-peak capacity was chosen to be 10% of the peak capacity by the Project Technical Committee in May, 2016. This still recognized the post-peak behavior, but was more conservative than the 30% that was incorporated into baseline studies in the ATC-116 project. The decision to include 10% post-peak residual capacity balanced the desire to not drive the analysis to needlessly conservative results (based on the charge to provide practical results), with the recognition that in the cripple wall or open front stories that are the primary focus of the studies, there is little beyond the items already specifically modeled that contribute to system redundancy and reserve capacity. More detailed discussion of post-peak residual strength can be found in ATC-116 reports, when available.

- Condition of tested materials: Most component tests have been conducted on new wall components specifically constructed in the laboratory for purposes of testing. These component tests must be recognized as representing materials in good condition, with the understanding that while components in existing dwellings might be of similar condition, there will be occurrences of deterioration in dwellings. Deterioration of materials was not specifically taken into account in the determination of building block properties for purposes of numerical studies. It is a consideration in the assessment of existing dwellings, as discussed in FEMA P-1100 Volume 3, Part 3.
- Materials used in combination: Most dwelling components have more than one bracing material installed on opposite sides and sometimes on the same side of the wall. For instance, including combinations of structural sheathing and finish sheathing materials. This is particularly true in occupied portions of the dwelling that as a minimum have both exterior and interior finish materials. Numerical analysis studies in the past have approached this by developing hysteretic descriptions of each of the materials separately, and then developing rules for combining the materials. One such rule used for the FEMA P-807 (FEMA, 2012) methodology allowed combining 100% of the capacity of the stronger

material to 50% of the capacity of the weaker materials. These would be summed for each displacement increment considered. Recent studies (Bahmani and van de Lindt, 2014) have shown that (for the lower-bound boundary conditions used in the Bahmani study) the P-807 approach tends to underestimate the peak capacity and overestimate the post-peak capacity; it is not known whether this pattern would repeat with more realistic boundary conditions. Based on the Bahmani results, however the preferred method for the ATC-110 project, will be to define shear wall building blocks directly developed from testing of combined materials. This approach was taken especially for the superstructure where testing of combined materials is most readily available. Where test results are not available for material combinations, each working group individually selected the preferred method of establishing modeling parameters for the combinations. See Volume 3 Parts 11, 12 and 13 for details.

The following sections discuss the selection and prioritization of wall building block information. Given the variability that occurs in available test data, descriptions of upper and lower bounds and best estimates of material properties were developed reflecting the best available data at the time.

4.2.1 Upper Story Characterization

Combinations of wall bracing materials considered for characterization of vertical wall building blocks for occupied upper stories are shown in Table 4-1. The materials presented in the table are those that are typically found in the superstructure of dwellings that were built between 1900 and today.

Because retrofit of the upper stories is not a focus of this pre-standard, the material combinations considered here are existing construction without inclusion of retrofitting materials. Because the number of options listed is far more than could reasonably be analyzed for this project, material combinations were identified by the Project Technical Committee as priorities for development of modeling properties. Decisions regarding most representative materials were in the end made by each of the working groups relative to the building stock that was being modeled.

Table 4-1 Vertical Wall Building Blocks—Upper Story Characterization Priorities

Exterior Finishes	Interior Finishes		
	Gypsum Wallboard	Plaster on Gypsum Lath	Plaster on Wood Lath
New Stucco - Stapled with Drip Screeds	High - commonly occurring in 1980s and later building stock	Low	Low
Old Stucco - Nailed and Run Down Foundation	High - commonly occurring in older building stock 1950s to 1980s	Low	High - upper bound strength and stiffness 1900s to 1950s
Horizontal Wood Siding	Medium - commonly occurring in older building stock with remodeling	Low	Low
Fiber-Cement or Vinyl Siding	High - lower bound of strength and stiffness - siding might be treated as zero strength and stiffness	Low	Low
New Stucco over Plywood or OSB	Low	Low	Low
Old Stucco over Diagonal Lumber Sheathing	Low	Low	Low

4.2.2 Characterization of Lower Stories

Wall bracing materials and combinations considered for characterization of wall building blocks for lower stories (cripple wall or crawlspace stories or garages) are shown in Table 4-2. The materials presented in the table are those that are typically found in the lower unoccupied stories of dwellings that were built between 1900 and today. Because retrofit of the lower stories is intended, the material considered here was existing construction alone and in combination with wood structural panel sheathing used for retrofitting. Because the number of options listed is far more than could reasonably be analyzed for this project, priorities were identified by the Project Technical Committee. Decisions regarding most representative materials were in the end made by each of the working groups relative to the building stock that was being modeled.

Also of importance for this group of building blocks were scaling of the properties for cripple walls of varying heights, and treatment of wood structural panel sheathed cripple walls without tie-down devices. These modeling aspects will be discussed in following sections.

Table 4-2 Vertical Wall Building Blocks—Lower Story Characterization Priorities

Exterior Finishes	Priority	Priority Combined with Wood Structural Panel (Plywood or OSB)
New Stucco - Stapled with Drip Screeds	High	High
Old Stucco - Nailed and Run Down Foundation	High	High
Horizontal Wood Siding	Medium	Low
Fiber-Cement or Vinyl Siding	Low	Low
New Stucco over Plywood or OSB	High - priority for assessment of existing dwellings	Low
Old Stucco over Diagonal Lumber Sheathing	Low	Low

4.3 Recommendations for Modeling

This section describes the available test data considered and the resulting approximate backbone curves used to develop numerical models. Section 4 discusses the development of detailed hysteretic modeling parameters bounded by the Section 3 approximate backbone curves. The data considered and resulting approximate backbone curves build on the data and modeling parameters developed for FEMA P-807 (FEMA, 2012). Where additional information has been identified, it has been incorporated and new backbone curves derived. In particular, backbone curves derived from testing of combined materials were not considered in FEMA P-807 and have been added.

The approximate backbone curves discussed in this section for bracing walls are intended to reflect the behavior of the bracing material, including the load path connections transferring load into the top of the wall (nailing, shear clips, etc.) and from the bottom of the wall to the foundation or floor framing (nailing, anchor bolts, etc.). Except for unusual cases such as hillside dwelling anchorage, none of the load path connections were explicitly incorporated into the numerical models.

4.3.1 *Stucco plus Gypsum Wallboard*

Backbone curves from testing of combined stucco and gypsum wallboard were not developed for FEMA P-807. Available combined material data includes CUREE EDA-03 (Arnold et al, 2003a), CUREE EDA-07 (Arnold et al, 2003b), Bahmani and van de Lindt (2014), and Pardoen et al. (2003) Tests 14A and 15A, described below.

CUREE EDA-03 and CUREE EDA-07, *Cyclic Behavior and Repair of Stucco and Gypsum Woodframe Walls: Phase I, Phase II*: This series of tests used three-coat stucco (Portland-cement plaster) fastened with furring nails in combination with gypsum wallboard attached with 5d cooler nails. The test setup used eight-foot high by sixteen-foot long walls, one configuration with two window openings and the other configuration with one window and one door. The wall with two window openings had a total of eight feet of full-height wall, while the wall with the window plus door had 9'-4" of full-height wall. The gypsum board boundary conditions included returns to confine the gypsum board at wall ends and at the top of the wall, representing the ceiling, but there was no confinement at the wall base due to the practice of holding the bottom up from the unfinished floor during installation. The stucco boundary conditions included wrapping the stucco around the posts at either end. No stucco confinement was provided at wall top or bottom. In addition to typical anchor bolts, overturning restraint was provided by a series of steel rods that introduced gravity loads at a series of three or four concentrated loads, which were maintained constant through the testing. No specific additional tie-down devices were provided. CUREE-CEA Walls 1 and 2 (Arnold et al., 2003a) were intended to represent the bottom story of a two-story residence. The gravity load applied during this testing was 450 plf applied in three concentrated loads. The loading was distributed to the wall with a W10 loading beam. CUREE-CEA Walls 5 through 8 (Arnold et al., 2003b) were intended to represent the top story of a two-story or a single-story dwelling. A dead load of 250 plf was applied in four concentrated loads and the loading beam was replaced with a 3/8-inch steel strap. These were considered to be the upper bound of capacity from available testing. Two aspects of the test are thought to contribute to this. One is the introduction of boundary conditions, which are thought to increase strength and stiffness. The other is the perforated shear wall condition; because the stucco was strong and stiff enough to mobilize the full-perforated shear wall instead of just the full height piers, additional fasteners were mobilized and additional overturning resistance was engaged. For this reason, it was decided that it may not be appropriate to compare the capacity of this testing with that of an eight-foot long full-height wall, such as tested by Bahmani and van de Lindt (2014). It might be most appropriate to think of a per-foot of length strength including both full height wall and openings, and apply it in this manner to dwellings with similar opening density. The tested configuration with openings is generally very representative of the dwelling configurations being modeled.

Bahmani & van de Lindt, *Experimental and Numerical Assessment of Woodframe Sheathing Layer Combinations for Use in Strength-Based and*

Performance-Based Design, ASCE Journal of Structural Engineering (Bahmani and van de Lindt, 2014): This series of tests was developed for the express purpose of evaluating rules for analysis of combined sheathing materials. Stucco testing was conducted on an eight-foot by eight-foot wall with standard stud framing and standard tie-down devices (HDU8) for overturning restraint at each end of the shear wall. Fastener type and spacing between stucco and framing is not known, but said to be representative of 1920s or 1930s construction. No confining boundary conditions were provided, allowing the stucco to slip past the framing on all edges. The loading was not CUREE or SPD, but set displacement cycles. For wall components with higher numbers of cycles, this likely introduced lower peak strengths and lower displacement capacities, similar to use of the SPD protocol. Because the stucco did not reach high capacity, the effect of protocol is judged to not be significant. For purposes of the ATC-110 project, these tests were thought to represent a lower bound of capacities that might be achieved with stucco in good condition, representing stucco in isolated piers with minimal continuity.

Pardoen Tests 14 & 15 CUREE W-25, *Testing and Analysis of One-Story and Two-Story Walls Under Cyclic Loading* (Pardoen et al., 2003): These are two tests from a larger series of tests using three-coat stucco (Portland-cement plaster) fastened with staples in combination with gypsum wallboard attached with cooler nails. The test setup used eight-foot high by sixteen-foot long walls, Test 14 with a garage door opening (two 3'-0" wide piers for a total of six feet of full height bracing wall) and Test 15 with a pedestrian door opening (two 6'-6" wide piers for a total of 13 feet of full height bracing wall). Testing used the CUREE protocol. Stucco stops were provided at all boundaries, but the stucco was free to slide past the framing. Significant slip between stucco and framing occurred, resulting in retained strength at drift levels much higher than seen in other stucco testing. The high residual strength at high displacements is not thought to be representative of anticipated behavior in real dwellings. The strength levels, however, are thought to reasonably represent a mid-level capacity of stucco in good condition, between the upper bound of the CUREE-CEA testing and the lower bound of the Bahmani testing.

Illustrated in Figure 4-1 are approximate backbone curves using this combined material data. For purposes of comparison, stucco-only data from FEMA P-807, including City of Los Angeles (CoLA, 2001), Schmid (2001), and Pardoen et al. (2003) Tests 16A and 17A are also included in Figure 4-1. Additionally, the approximate backbones used for ATC-110 analysis are illustrated in Figure 4-1; included are lower bound, best estimate, upper

bound top story and upper bound lower story approximate backbone curves. The lower bound backbone is based primarily on Bahmani et al. and CoLA data; this curve captures a lower bound due to lack of restraint at edges of finish materials, large number of loading cycles, and isolated shear wall piers without openings. The best estimate is based on Pardoen Tests 14A to 17A, of longer shear walls with openings, loaded with the CUREE protocol, but with low confinement of stucco at the panel edges. The upper bound upper/single story curve is based primarily on CUREE-CEA top story walls 5 through 8, shear walls with openings with full restraint at edges tested with the CUREE loading protocol. The upper bound lower story curve is based on CUREE-CEA Walls 1 and 2, similar to the top story tests, but with higher gravity load and a stiffer loading beam. This group of four curves was provided for the working groups to choose from as appropriate for each numerical analysis study.

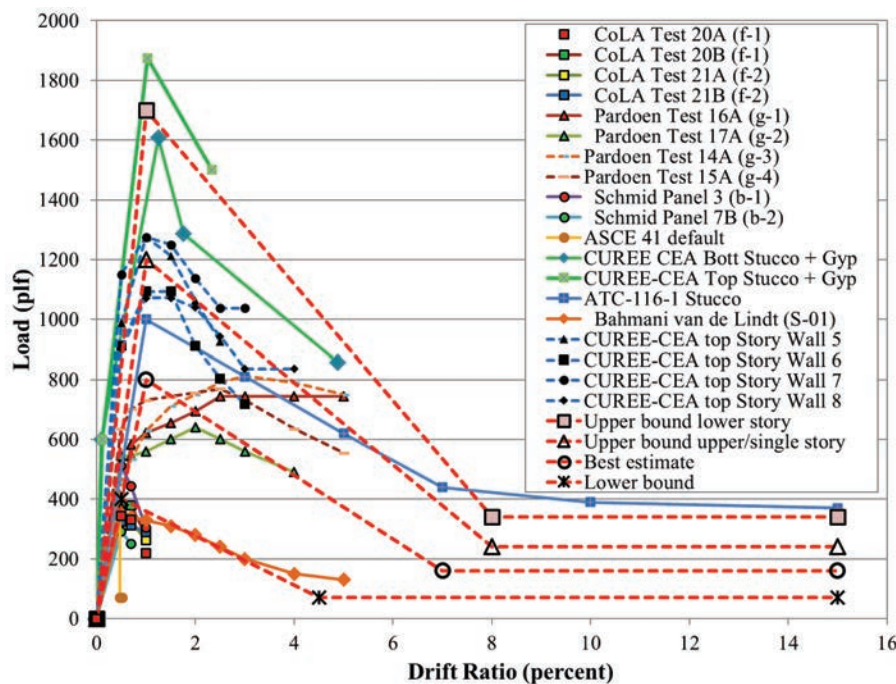


Figure 4-1 Plot of applicable test data and approximate backbone for stucco plus gypsum wallboard.

4.3.2 Gypsum Wallboard

Backbone curves from testing of gypsum wallboard were developed for FEMA P-807, however available data was added from Bahmani and van de Lindt (2014), and Gatto & Uang (2002). The approximate backbones used for ATC-110 analysis are illustrated in Figure 4-2; included are lower bound, best estimate, and upper bound approximate backbone curves. The lower bound backbone is based primarily on Bahmani et al. and Gatto & Uang

data; this curve captures a lower bound due to lack of restraint at edges of finish materials, and isolated shear wall piers without openings. The best estimate is based on an average of McMullin and Merrick (2002) tests of longer shear walls with openings, loaded with the CUREE protocol and with confinement of gypsum wallboard at the panel edges. The upper bound curve is based primarily on McMullin Test 11 and the positive quadrant of McMullin Test 6. This group of curves was provided for the working groups to choose from for each numerical study.

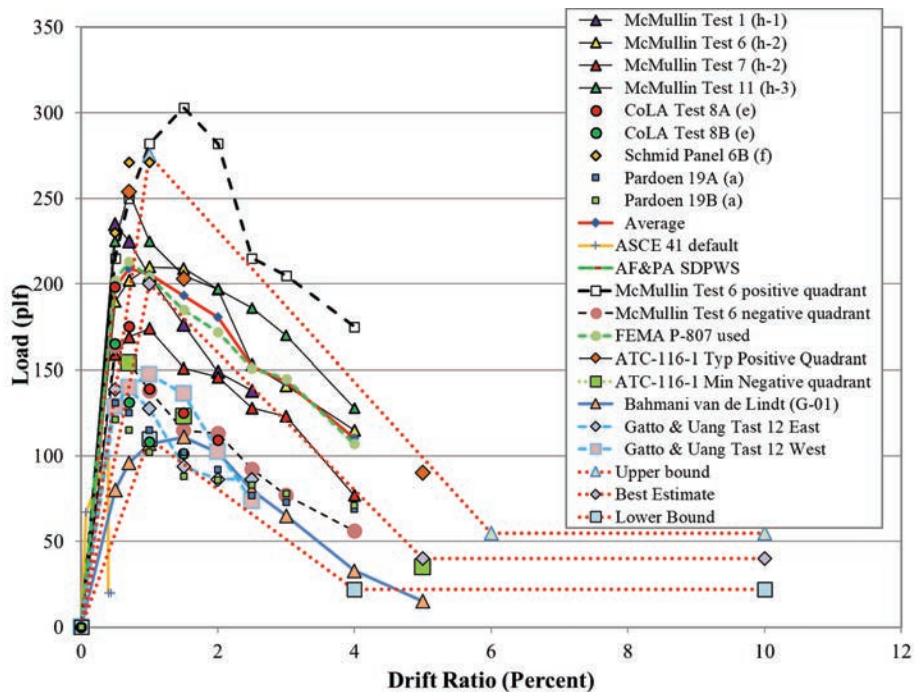


Figure 4-2 Plot of applicable test data and approximate backbone for gypsum wallboard.

4.3.3 Stucco

Where it is necessary to use properties for stucco without gypsum wallboard interior finish, the curves were generated by taking the curves for stucco plus gypsum wallboard and subtracting the matching gypsum wallboard curves. This was done because the data set for stucco plus gypsum is more complete than for stucco alone; in addition, it avoids having significant variation between the stucco and stucco plus gypsum properties. When stucco and gypsum are combined, the behavior of the stucco is believed to control the load-deflection behavior the most. The approximate backbones used for ATC-110 analysis are illustrated in Figure 4-3; included are lower bound, best estimate, upper bound top story and upper bound lower story approximate backbone curves, each derived from the matching stucco plus gypsum wallboard curve.

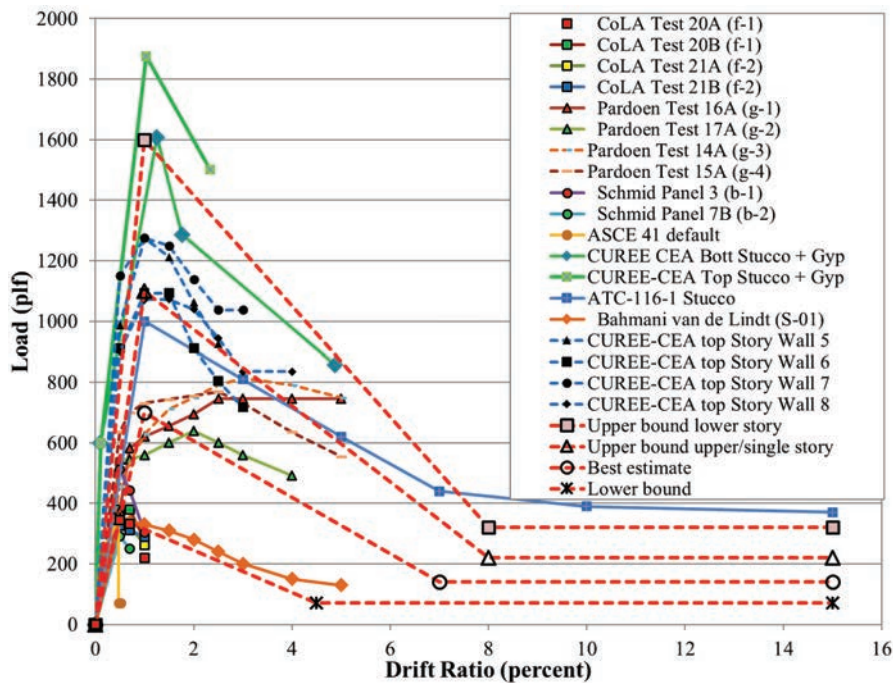


Figure 4-3 Plot of applicable test data and approximate backbone for stucco.

4.3.4 Horizontal Lumber Sheathing or Siding

A backbone curve from testing of horizontal lumber sheathing was developed for FEMA P-807 based on tests conducted between 1940 and 1958 at the Forest Products Laboratory (FPL), however available data was added from Carroll (2006), and Forintek (Ni and Karacabeyli, 2007) to supplement the previously available data.

Carroll tested lumber sheathed walls extracted from dwellings being demolished. Houses 1, 3 and 5 were constructed in 1948, 1945 and 1950, respectively. Walls with a length of four feet and a height just under eight feet were extracted for testing in the lab. The horizontal sheathing was attached with nails most closely resembling 8d nails. The walls were tested monotonically. The only dead load resisting uplift was provided by the self-weight of the loading beam. Supplemental uplift anchorage does not appear to have been provided. The four-foot length of the wall tested may account for the capacity being lower than tests by FPL, which used walls approximately 14 feet in length.

Forintek tested three horizontal (transverse) lumber sheathed shear walls approximately eight feet tall by sixteen feet long. Walls 12 and 13 were sheathed with 1x6 horizontal sheathing, and Wall 14 with 1x10. All walls were nailed with 8d common nails. Walls 12 and 14 were tested monotonically and Wall 13 cyclically. Wall 13 had gypsum wallboard

attached to the opposite side of the specimen from the sheathing while Walls 12 and 14 had horizontal sheathing only. Tie-downs were provided on end studs for all tests, and no dead load was superimposed. Plots of the load and deflection at peak load only are shown in Figure 4-4, to provide a limited comparison to other available information.

The approximate backbone curve used for ATC-110 analysis is shown in Figure 4-4, representing a best estimate. The best estimate is taken as the wood sheathing/siding backbone curve used in the ATC-116 project. This backbone was selected since it provides a balanced estimate based on available testing. Previous FPL tests fall above this best estimate backbone, and the Carroll Houses (1, 3 and 5) fall below in terms of peak normalized strength. The stiffness of the best estimate curve also has a balance between FPL testing and tests conducted by Carroll. There was not sufficient data to justify defining additional approximate backbone curves.

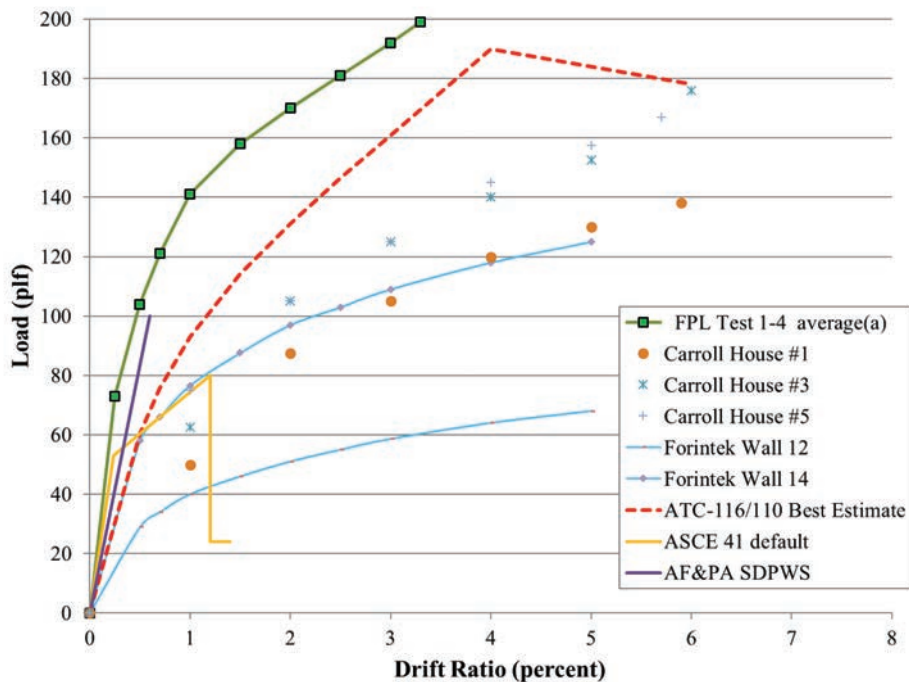


Figure 4-4 Plot of applicable test data and approximate backbone for horizontal lumber sheathing.

4.3.5 Wood Structural Panel Sheathing with Tie-Downs

Backbone curves for shear walls with wood structural panel sheathing with tie-downs were developed for FEMA P-807 from the testing results by Pardoen, Gatto & Uang, CoLA, and others. It was decided, however, to take a different approach for constructing curves for ATC-110 analysis. Databases of existing wood structural panel shear wall test data had been compiled by others in order to allow evaluation of seismic performance of new proprietary

alternatives to code-designed shear walls (all a separate effort not related to this project). Documentation of these databases can be found in Line et al. (2008) and Line et al. (2014). As part of a recent unpublished effort contributing to ATC-114, Phil Line of the American Wood Council created plots of shear wall backbone curves, created in accordance with ASTM E2126, and created normalized curves for shear walls of varying aspect ratios (height over length) (Line, 2016). The various curves accumulated for shear walls with aspect ratios of one are shown in Figure 4-5, normalized to peak capacity. Also shown in Figure 4-5 is the normalized load-deflection curve recommended by Phil Line. It was chosen to use this normalized load-deflection curve for wood structural panel sheathed walls with aspect ratios of one or less; these walls will primarily be used for retrofit shear walls with tie-downs in the cripple wall or lowest story of dwellings being analyzed. Based on accumulated data, the best estimate of the peak unit shear capacity of wood structural panel shear walls with aspect ratios of one and tie-downs is the nominal capacity for wind loading listed in the Special Design Provisions for Wind and Seismic (SDPWS, AWC, 2015) document.

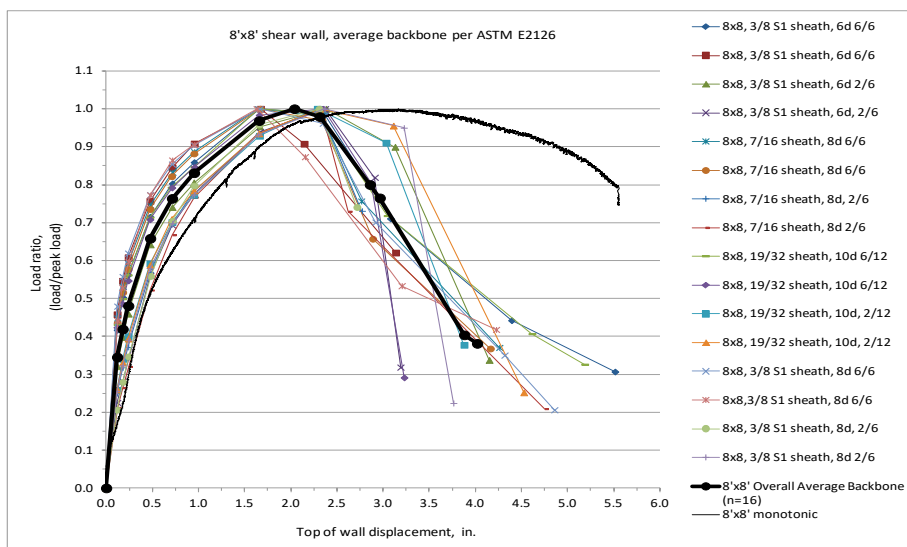


Figure 4-5 Plot of available test data for wood structural panel shear walls with an aspect ratio of one and tie-downs (Line, 2016). Shown in the heavy black line is the recommended normalized curve.

Shown in Figure 4-6 are three approximate backbone curves for ATC-110 analysis, representing high, medium and low unit shear capacities. The baseline curve (Phil Line normalized curve in Figure 4-6) for 8d common nails at six inches on center is also shown with peak capacities of applicable tests from Salenikovich (2000) for comparison. Notably, the unadjusted baseline curve (8d at 4 inches on center) has a peak strength of 616 plf at a drift ratio of 2.1%. The low unit shear capacity represents the sheathing and

nailing combination most commonly used in existing prescriptive cripple wall retrofit provisions; i.e. 7/16-inch rated sheathing with 8d common nails at four inches on center. The medium capacity uses 15/32-inch rated sheathing with 8d common nails at three inches on center. The high capacity used 15/32-inch Structural I sheathing with 8d common nails at two inches on center. These are selected for the purposes of numerical analysis studies only, and are not meant to limit choices for design of retrofits. The choices are limited to 8d common nails due to concerns regarding splitting of framing members where 10d common nails are used.

For shear walls with tie-downs, it is intended that the drift ratios be treated as constant as the wall height varies between two and seven feet, resulting in linearly varying peak drift with height for walls with tie-downs.

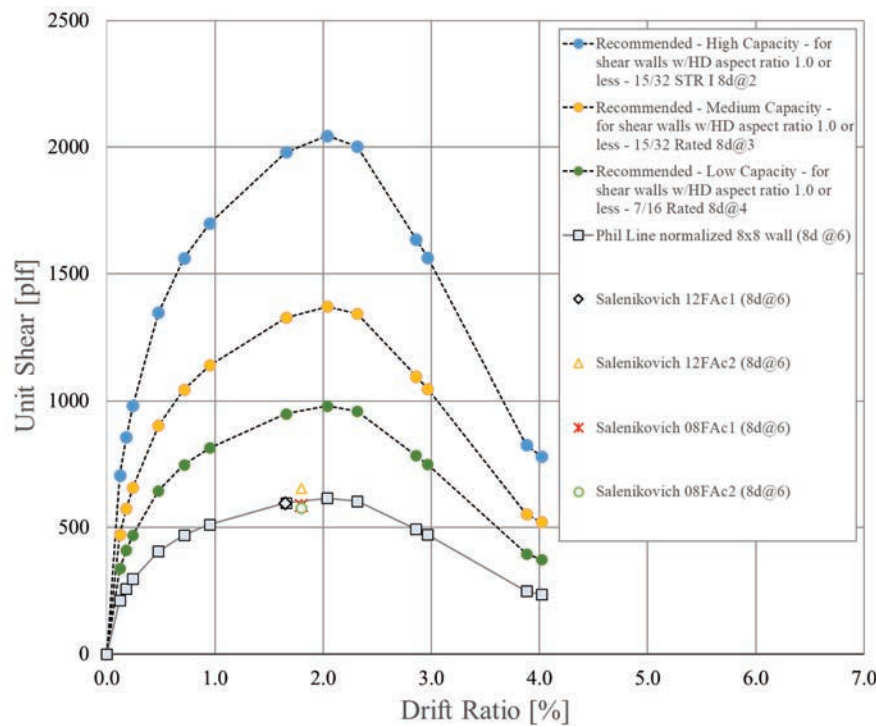


Figure 4-6 Plot of applicable test data and approximate backbone for wood structural panel shear walls with an aspect ratio of one or less and with tie-downs.

4.3.6 Wood Structural Panel Sheathing without Tie-Downs

Backbone curves from testing of wood structural panel shear walls without tie-downs were not developed for FEMA P-807. The primary intended use of wood structural panel sheathing without tie-downs for this project was numerical modeling of cripple wall retrofits using wood structural panel sheathing. This was considered in part because currently available prescriptive methods for design of cripple wall retrofits seldom require use of

tie-down devices. Two different sources of information were used to develop approximate backbone curves for this sheathing type: testing of cripple walls conducted by Chai et al. (2002), and testing of walls of various aspect ratios and anchorage conditions by Salenikovich (2000).

Chai et al. (2002) tested level and stepped cripple walls with varying heights and bracing materials for specimens with a full framed length of 12 feet. Tests were conducted with wood structural panel (WSP) retrofit bracing only that was comprised of 15/32" OSB with 8d common nails at 4 inches on center; tests were also conducted with OSB in combination with a stucco finish. A subset of applicable tests with WSP-only are summarized in Table 4-3. The subset consists of four level cripple walls (Specimens 1, 4 7 and 10) and four stepped cripple walls (Specimens 15, 15A, 16 and 19). The subset of stepped cripple walls consider only those with 1:3 slope that had three four-foot long panels of varying height (i.e., 2, 3.33 and 4.67 feet). The remaining stepped tests assuming a 1:2 slope over a 12-foot length had individual WSP panels of 2.67 feet (i.e., two stud bays) or less which were assumed to not be representative of typical installation requirements. The information provided in Table 4-3 includes the assumed gravity loading, average peak load in positive and negative loading directions, and corresponding drift capacity. Additionally, the drift capacity observed beyond peak loading before losing 5% of peak strength is also annotated to illustrate the ability of shorter cripple walls to maintain appreciable capacity beyond peak loading.

Average values of peak loads, drifts at peak load and drifts within 5% strength loss are provided in Table 4-3 for all tests considered and with Specimens 4 and 10 excluded. This was done to highlight that Specimens 4 and 10 are likely lower bound capacities for cripple walls with 8d common nails at four inches on center. In addition to lower gravity loading, this is due to detailing having two isolated four feet long sheathing panels at each end with the central portion of the framing being unsheathed. Chai et al. (2002) report a larger portion of loading being carried by the central panel for fully sheathed specimens, suggesting that the isolated end panels (Specimen 4) may not represent realistic interaction between individual segments of an actual retrofit layout. Further, the WSP-only specimens had the perimeter nailing directly to the sill plate on the exterior of the wall instead of fastening to additional blocking on the inside to accommodate a sill plate that is wider than the cripple wall framing. This was reported to cause significant sill splitting in the four-foot case (Specimen 10) when compared to the fully sheathed case (Specimen 7).

Table 4-3 Cripple Wall Peak Capacities and Drift Ratios for Applicable Subset Tested by Chai et al. (2002)

Specimen	Height [ft] ¹	Sheathing Length [ft]	Gravity Load [plf]	Average Peak Load [plf]	Average Drift at Peak Load [%]	Average Drift within 5% Strength Loss [%]
1	2	12	450	838	4.01	4.96
4 ²	2	8	100	774	4.09	4.09
7	4	12	450	897	2.03	2.91
10 ²	4	8	100	663	2.01	2.33
15	3.33	12	450	989	3.59	3.59
15A	3.33	12	450	951	3.00	3.50
16 ³	3.33	12	450	1083	3.58	3.58
19	3.33	12	100	908	3.09	3.75
Average				888	3.17	3.59
Average excluding Tests 4 and 10				944	3.22	3.72

¹ Cripple wall height, average height for stepped cases (three equal 4 feet panel lengths with heights of 2 feet, 3.33 feet and 4.67 feet)

² Specimens 4 and 10 assumed as a lower bound due to low gravity loading, sill nailing and isolated 4 feet long brace segments

³ Specimen 16 is the only test shown using the CUREE near-field loading protocol, all others use the ordinary loading protocol, details are similar to Specimen 15 other than loading

⁴ All tests have 15/32" OSB with 8d at 4 inches on center

The average peak loads listed in Table 4-3 suggest that cripple walls with 8d common nails at 4 inches on center provide a similar average capacity to the target full capacity of 980 plf for shear walls with tie-downs (see Section 3.5). Without further testing data, it is assumed that cripple walls with sill anchor bolts but no tie-downs can achieve the same peak capacity as the fully anchored condition (e.g., with tie-downs) provided that the failure mode is not controlled by local overturning failure. In terms of peak drift capacity, the results of Table 4-3 suggest that WSP braced cripple walls with a height of less than five feet can achieve a larger drift at peak load than the baseline value of 2.1% drift associated with full height walls with tie-downs (see Section 3.5). The following paragraphs discuss issues associated with overturning for shear walls without tie-downs.

Salenikovich (2000) tested a series of shear walls eight feet high, with variation in wall length (two feet to twelve feet) and variation in wall anchorage, intended to describe commonly constructed conditions for both engineered and conventional or prescriptive construction walls. The three anchorage levels were full anchorage (FA) using anchor bolts and tie-downs,

intermediate anchorage (IA) using anchor bolts only without tie-downs as would be common for conventional construction supported on a foundation, and no anchorage (NA) using a nailed sill plate connection as would occur for conventional construction supported on a floor platform. All shear walls were sheathed with 7/16 inch OSB sheathing with 8d common nails at 6 inches on the perimeter and 12 inches in the field. The tests were performed in complete absence of gravity loading (i.e., plane of wall parallel to laboratory floor) as a conservative measure to represent shear walls running parallel to floor framing. In other words, not even the self-weight of the materials contributed to axial loading of stud framing. The results of these tests were used to access the effect of intermediate anchorage (no tie-downs) on the peak capacity of the shear wall. The approximate backbone curves of IA data for eight-foot high walls with wall lengths ranging from two to twelve feet are shown in Figure 4-7, resulting in aspect ratios between four and 0.67 when combining multiple panels for the aspect ratio of the entire wall. The figure illustrates the aspect ratio effect on peak capacity of IA walls. Plots of the three data points for peak capacity of FA walls with length from four to twelve feet are also shown in Figure 4-7.

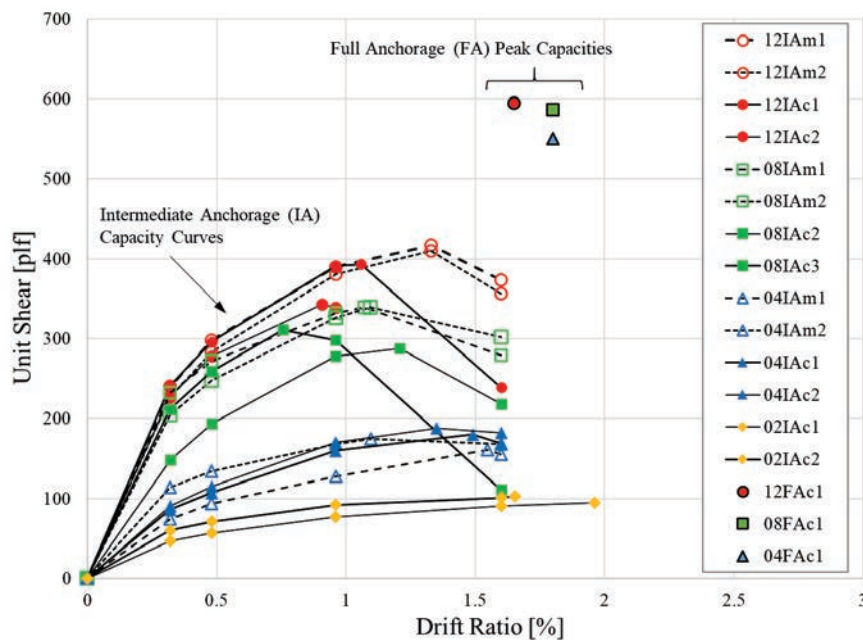


Figure 4-7 Plot of Salenikovich test data for full anchorage (FA) and intermediate anchorages (IA) of 8 feet tall walls ranging from 12 to 2 feet in length. Following the IA designation, "m" denotes monotonic loading, "c" denotes cyclic loading.

Salenikovich (2000) fitted a simplified ultimate strength model to the test data in order to describe the relationship between fully anchored shear walls and those with intermediate anchorage. This was done using a reduction

factor (r) that represented the portion of the total fastener capacity at the bottom row of nailing (i.e., at sill) that was able to be developed by the shear wall at ultimate strength (v/v_{max}). The proposed relationship for shear walls with various panels is reported in Salenikovich (2000) as Equation 6.57 and reproduced here as Equation 3-1:

$$r = v/v_{max} = (1+(2\alpha/n)^2)^{-0.5} \quad (3-1)$$

where α is the aspect ratio of the *panel* comprising the shear wall and n is the number of panels. Notably, the work by Salenikovich (2000) found that v/v_{max} for fully anchored shear walls was slightly less than unity (i.e., 0.96), yet can be assumed to be unity for the purposes of this discussion. Using Equation 3-1, a few example scenarios are plotted in Figure 4-8 for illustration of the main trends from the study.

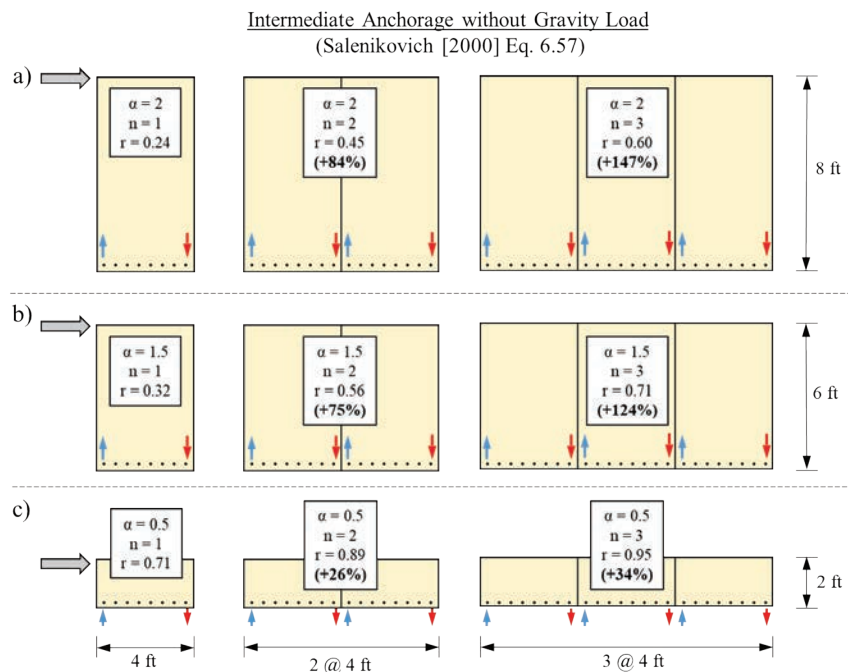


Figure 4-8 Illustration of the simplified relationship proposed by Salenikovich (2000) to account for panel aspect ratio (α) and number of panels (n) to estimate the fraction of the total bottom fastener resistance developed by shear walls with intermediate anchorage (r). a) 8 feet by 4 feet panels (panel size tested); b), c) panel sizes common for cripple wall retrofit with heights of 6 feet and 2 feet, respectively. Percentages in bold show relative increase in normalized per linear foot capacity due to addition of panels compared to single panel.

The case of 8-foot by 4-foot panels oriented vertically with $n=1$, 2 and 3 panels is shown in Figure 4-8a. These wall geometries correspond to those tested by Salenikovich (2000) (not including the 2ft long walls). The 6 feet

and 2 feet tall wall panels which would be representative of different cripple wall heights considered in ATC-110 analysis are shown in Figure 4-8b and 4-8c. Moving from left to right in each sub-figure, the expected reduction factor (r) using Equation 3-1 is annotated. Additionally, the *relative* increase in expected capacity (in normalized units based on wall length) due to additional panels from a single panel wall are shown in bold. The significant increase in capacity that is expected for full-height (i.e., eight feet) with the addition of more panels is shown in Figure 4-8a. As discussed by Salenikovich, this is due to the cancelling of the uplift forces at the end of panels by compressive forces of adjacent panels, where the inclusion of four adjacent panels (in the model) tended toward fully anchored conditions in the end panel in compression (e.g., rightmost panels of Figure 4-8). Recalling that both the tests and model are devoid of gravity loads, this behavior is produced only by the local couples of the perimeter fasteners around the panel.

Also illustrated by the model of Salenikovich is the increase in shear wall capacity with intermediate anchorage with reduced height (i.e., reduced panel aspect ratio). Comparing the single panel variations in the left of Figure 4-8, the reduction factor (r) increases considerably (i.e., more fastener lateral capacity development) when moving from an eight-foot wall to a two foot wall. This is rather intuitive since the effects of overturning would reduce with a reduced lever arm. More importantly, the right side of Figure 4-8, assuming three panels, shows two important trends:

- The addition of panels has a greater net effect (larger % increase in Figure 8-3) for eliminating uplift for taller walls; and,
- More panels are necessary to reach the same r factor for taller walls than shorter walls.

Now, consider the assumption that WSP braces with intermediate anchorage can achieve the same nominal capacity (based on nail spacing and sheathing) as the fully anchored case with tie-downs. This assumption can only be valid if the effects of overturning and uplift failure are prevented in the design process. As an example, a one-story, 1200 ft², house is assumed to be located in an area of very high seismicity ($S_{DS}=1.5g$). The house is assumed to have light exterior, interior and roof materials (i.e., small restoring force to resist overturning). The house is assumed to have varying cripple wall heights of two, four and six feet, which must be retrofitted without the use of tie-downs for this example. The governing panel lengths (for each corner and side of the house) to resist the lateral shear forces are 8 feet for all cripple wall heights as shown in the left of Figure 4-9. In order to prevent uplift, the six and four feet walls require the braced length to be increased by 67% and 33%, respectively.

The two-foot cripple wall design is not governed by overturning and requires the original braced length as when considering shear alone. The combined designs for intermediately anchored WSP braces are shown in the right portion of Figure 4-9 (in terms of required brace length only).

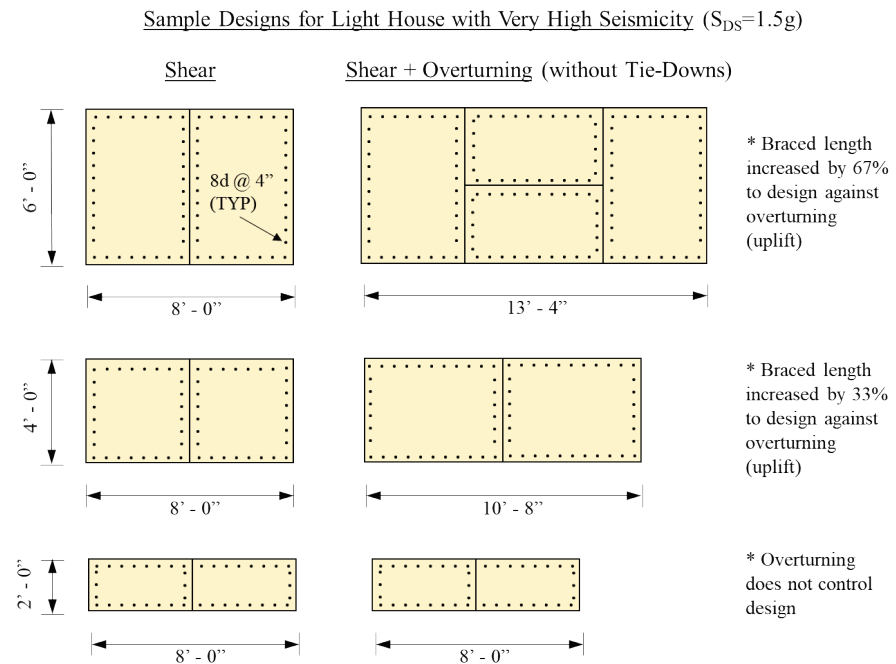


Figure 4-9 Illustration of different wood structural panel brace length requirements when designing cripple wall retrofits of various heights with intermediate anchorage: shear only (left); shear and overturning (right). Wall lengths would be applied in every corner and side of the dwelling. Designs on the right would represent those modeled in numerical studies for the given dwelling and site.

The previous example clearly shows good agreement with the relative trends observed by Salenikovich (2000) for walls with intermediate anchorage. The large difference is the application of expected gravity load in the calculations to design against uplift due to overturning. Notably, testing conducted by Johnston et al. (2006) illustrated that intermediately anchored walls (8-foot by 8-foot) approached cyclic capacities of equivalent walls with tie-downs when gravity loads were increased. More information on design assumptions for cripple wall dwellings can be found in FEMA P-1100 Volume 3, Parts 3, 7 and 8.

For purposes of ATC-110 modeling of wood structural panel sheathed walls without tie-downs, it was selected to use the same low, medium and high capacity walls used for wood structural panel shear walls with tie-downs. To adjust for intermediate anchorage, retrofit designs must have wall lengths

sized to avoid uplift failure due to overturning. To adjust for the range of displacement capacity that might be seen for wall heights between two and seven feet, two curves were generated for each capacity; one follows the normalized curve used for the wood structural panel walls with tie-downs and an aspect ratio of one (Capacity A). The second multiplies the drift ratio at each load increment by 1.5 (Capacity B), based on data from Chai et al. (2002) (see Table 4-3), as seen in Figure 4-10. Capacity A was applied to walls with heights greater than five feet (aspect ratio greater than 0.67 assuming an 8 feet length). Capacity B was applied to walls with a height of five feet or less (aspect ratio less than or equal to 0.67 assuming an 8 feet length).

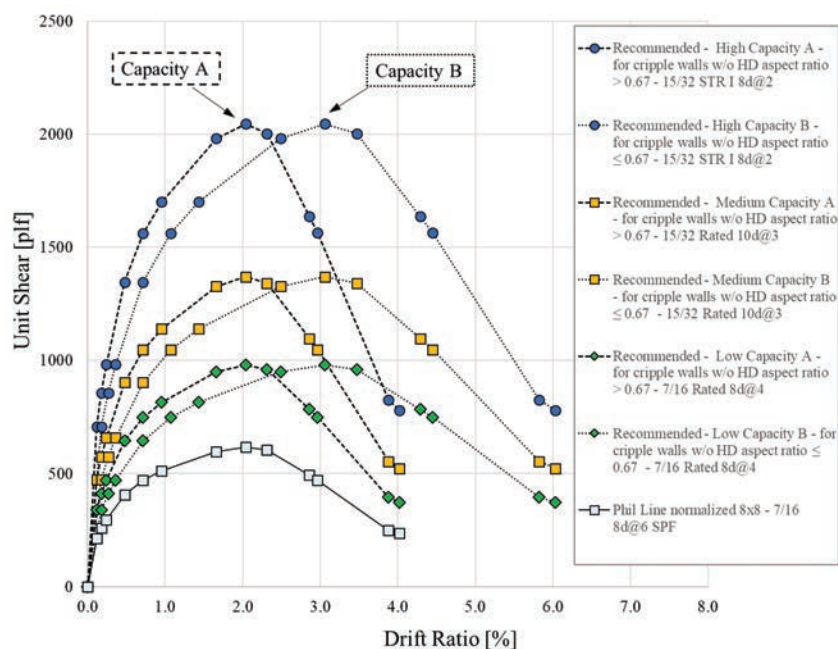


Figure 4-10 Plot of applicable test data and approximate backbone for wood structural panel shear walls with intermediate anchorage.

4.3.7 Material Designations

The approximate backbone curves for material characterization used for development of numerical models is summarized in Table 4-4. Material designations are provided; these designations are used consistently throughout the numerical studies. The drift ratio at peak load used in numerical modeling is provided for completeness. Plywood nominal capacities for purposes of retrofit design are noted, as these differ from the peak capacity for purpose of modeling.

Table 4-4 Material Designations for Approximate Backbone Properties

Material	Designation	Characterization	Numerical Modeling Peak Capacity [plf]	Numerical Modeling Peak Drift [%]	Retrofit Nominal Capacity [plf]
Horizontal Wood Siding	HS1	Best Estimate	190	4.0	N/A
Gypsum Wallboard (Gypboard)	G1	Lower Bound	109	1.0	N/A
	G2	Best Estimate	199	1.0	N/A
	G3	Upper Bound	271	1.0	N/A
Stucco	S1	Lower Bound	347	0.5	N/A
	S2	Best Estimate	695	1.0	N/A
	S3	Top Story Upper Bound	1089	1.0	N/A
	S4	Lower Story Upper Bound	1570	1.0	N/A
Stucco + Gypboard	SG1	Lower Bound	397	0.5	N/A
	SG2	Best Estimate	794	1.0	N/A
	SG3	Top Story Upper Bound	1188	1.0	N/A
	SG4	Lower Story Upper Bound	1673	1.0	N/A
Wood Structural Panel ¹ , Fully Anchored, Aspect Ratio = 1	WSP1	High Capacity (15/32" STR 1 w/ 8d@2")	2037	2.1	1460
	WSP2	Medium Capacity (15/32" Rated Sheathing w/ 8d@3")	1364	2.1	980
	WSP3	Low Capacity (7/16" Rated Sheathing w/ 8d@4")	976	2.1	700
Wood Structural Panel Type A, Intermediate Anchorage ² , Aspect Ratio > 0.67	WSP4	High Capacity	2037	2.1	1460
	WSP5	Medium Capacity	1364	2.1	980
	WSP6	Low Capacity	976	2.1	700
Wood Structural Panel Type B, Intermediate Anchorage ² , Aspect Ratio ≤ 0.67	WSP7	High Capacity	2037	3.15	1460
	WSP8	Medium Capacity	1364	3.15	980
	WSP9	Low Capacity	976	3.15	700

¹ Aspect ratios reflect height to width ratio assuming 8 feet of shear wall length (giving 1.0 for an 8-foot tall wall)

² Intermediate anchorage wood structural panels must be designed against uplift due to overturning to achieve full capacity

4.3.8 Horizontal Diaphragms

ATC-110 numerical analyses were conducted to assess the influence of both rigid and semi-rigid diaphragms on performance of dwellings. This assessment informed for what building configurations inclusion of semi-rigid modeling was important in order to properly capture seismic performance. Due to the limited testing data available and high computational effort, where

used in analysis, semi-rigid diaphragm load-deflection behavior was described as linear-elastic based on an estimated line from zero to the nominal capacity, as seen in Figure 4-11. Data in Figure 4-9 is from testing of unblocked wood structural panel diaphragms by FPL, CUREE literature review 1.1.1 (CUREE, 2001; Fischer et al., 2001) and CUREE literature review 1.4.2 (CUREE, 2001; Dolan et al., 2003). The FPL and Fischer tests were monotonic, the Dolan tests were cyclic to low displacements. No available data from cyclic testing to peak capacity has been identified at this time.

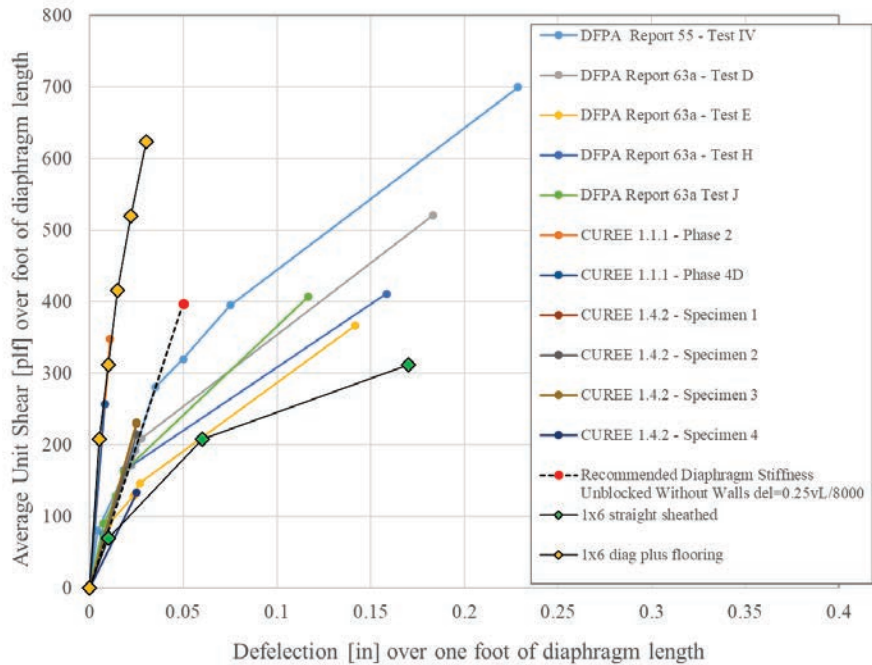


Figure 4-11 Plot of applicable test data and proposed linear stiffness of numerical description of semi-rigid diaphragms. Units are inches per foot increment of diaphragm span, plotted relative to average unit shear over that foot.

From Figure 4-11, the in-plane shear stiffness (G_a) of an unblocked diaphragm was estimated at 8000 lbs/in per foot of diaphragm depth, with the diaphragm deflection calculated using only the shear part of the SDPWS three-part diaphragm deflection equation. Testing confirms that when small sections of walls are located along the diaphragm perimeter, the displacement components related to chord member elongation and chord splice slip are very small (Dolan et al, 2003). For this reason, only the shear deformation component was considered and used in applicable numerical models. Chord member anchorage was investigated separately as part of the hillside dwelling numerical studies.

4.3.9 Anchorage of Foundation Sill Plates

For cripple wall homes on sloped lots, it is common for the floor framing to be sitting directly on top of the foundation sill plate on the uphill foundation. For this configuration, hysteretic modeling properties were necessary for the foundation sill plate connection to the foundation. The modeling properties needed to reflect both the load-deflection behavior, and the peak capacity of the anchorage. In addition, loading directions in-plane (along the length of the foundation) and out-of-plane (perpendicular to the foundation) were considered, as loading and displacements occur in both directions.

For in-plane loading, available testing information includes Mahaney and Kehoe (2002) from the CUREE-Caltech Woodframe Project, which specifically studied foundation anchorage and sill plate splitting issues. Plotted in Figure 4-12 is load-deflection data for an initial series of anchorage tests, conducted on a short wall with loading beam approximately one foot above the anchorage. Failure modes were for the most part brittle. Based on this data a recommended load-deflection curve for ATC-110 analysis is shown as a capacity of 2600 pounds per bolt at a displacement of 0.3 inches. Also shown is Testing by SEAONC and Simpson (Fennell et al., 2008), related to providing an alternative to use of ACI 318 Appendix D for wood wall anchorage. This testing used a test setup with only the sill plate, and significantly more fixity than the Mahaney tests.

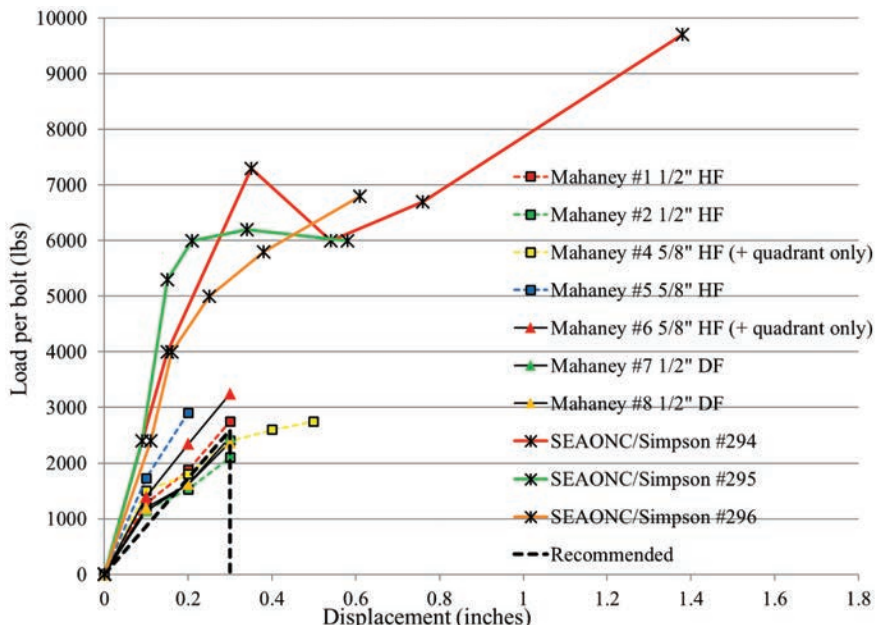


Figure 4-12 Plot of applicable test data and load-deflection behavior of anchor bolts in-plane.

The out-of-plane behavior was primarily used for the uphill foundation of hillside dwellings. When the more flexible downhill walls deflect, this causes rotation in the diaphragm, which in turn causes out-of-plane tension and compression forces on the uphill foundation. There is no available test information looking specifically at this out-of-plane behavior. The best available information comes from testing of shear walls; these shear walls can be envisioned as diaphragms rotated to vertical, and the uplift displacement on the shear wall can be equated to the out-of-plane deflection between the diaphragm and deflection. Some available information for description of this load-deflection behavior is shown in Figure 4-13. The data primarily comes from Mahaney and Kehoe (2002), with a limited check against data from Salenikovich (2000). The recommended in-plane capacity is 2000 pounds per bolt at a displacement of 0.4 inches as shown in Figure 4-13.

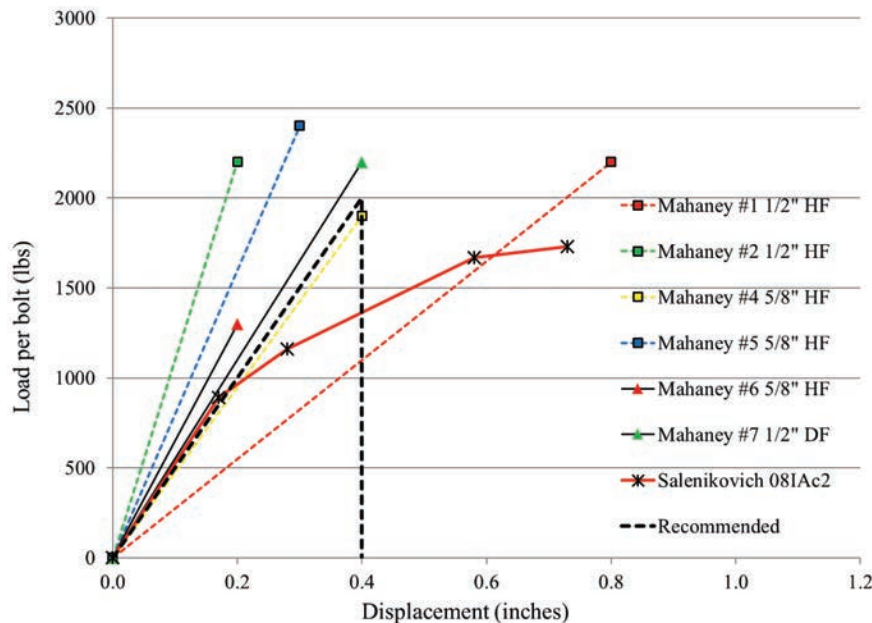


Figure 4-13 Plot of applicable test data and load-deflection behavior for anchorage out-of-plane.

4.3.10 Sill Plate Toenails

When a sloped cripple wall or hillside dwelling rests directly on an uphill foundation sill plate, it is common construction practice for the base-level diaphragm floor joists and uphill perimeter rim to be fastened to the uphill foundation sill plate with 16d toenails. Hysteretic modeling properties were of interest for these elements because they or the uphill foundation sill bolts can be the governing failure mechanism at the uphill mudsill. These elements were only considered for existing condition models and were not to be included in any retrofit models because they are an unreliable source of

capacity due to potential installation errors or decay of the uphill existing foundation sill plate.

For 16d nails in lateral shear, available testing information included Ficcadenti et al. (2004) from the CUREE-Caltech Woodframe Project, where tests were performed with an 8-foot wide by 20-foot long horizontal diaphragm configuration and Douglas-Fir Larch framing members. Four out of the five tests were performed on an unblocked diaphragm, and these tests were primarily of interest due to unblocked diaphragms being typical for residential framing construction. Two specimens were evaluated in a parallel framing application, where a 2x12 floor joist was bearing directly on top of a shear wall double top plate and fastened with 16d sinker toenails at 8 inches on center (i.e., 12 nails total). Similarly, two specimens were also evaluated in a perpendicular framing configuration, where blocking members were fastened to a shear wall double top plate with 16d sinker toenails at 8 inches on center. Cyclic testing was performed with the CUREE protocol and hysteretic plots were developed for each testing specimen.

Additional monotonic testing data in a perpendicular framing-to-framing lateral shear application (Smart, 2002) was also considered for further verification purposes. It is worth noting that this testing was not performed in a toenail configuration and was performed with Spruce Pine-Fir lumber and 16d common nails, as opposed to the Douglas-Fir Larch lumber and 16d sinker nails used for the CUREE testing. The backbone curves from the CUREE toenail specimen (TN-1A) and the Smart's perpendicular framing-to-framing testing are illustrated together in Figure 4-14. Note that the CUREE toenail testing backbone curve was modified to represent a singular nail by dividing the original curves data points by the total number of nails installed for the test. An additional plot with the NDS toenail shear reduction factor applied to Smart's testing data is also shown for reference for further comparison. Note that minor capacity differences are observed between the similarly shaped backbone curves due to differences in lumber specific gravity and nail types. Testing data suggests that a properly installed 16d nail has a peak capacity between 350 and 400 lbs.

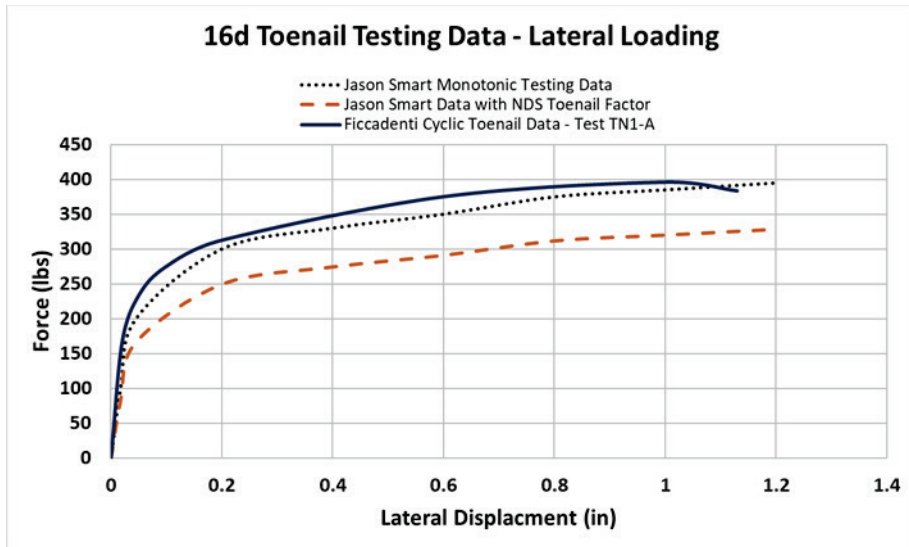


Figure 4-14 Plot of applicable test data and load-deflection behavior for a single 16d common toenail/nail in shear.

4.3.11 A35 Clips

Similar to foundation sill bolts and 16d toenails, hysteretic parameters for A35 clips were of interest for the case where a sloped cripple wall dwelling rests directly on an uphill foundation sill plate. The uphill foundation perimeter rim can be attached to the uphill foundation sill plate with A35 clips for retrofit purposes and numerical modeling.

For A35 clips with in-plane shear loading, available testing information included Ficcadenti et al. (2004) from the CUREE-Caltech Woodframe Project exclusively. Similar to the testing described in Section 3.10 for the 16d toenails, cyclic tests with the CUREE loading protocol were performed on 8-foot wide by 20-foot long horizontal diaphragms that were constructed with Douglas-Fir Larch framing members. Four specimens were analyzed with an unblocked diaphragm, where two specimens had 3-A35 clips connected between a 2x12 floor joist and a shear wall double top plate (i.e., parallel framing configuration), and two specimens had 3-A35 clips connected between floor joist blocking members and a shear wall double top plate (i.e., perpendicular framing configuration). The backbone curve for one of the parallel framing configuration specimens, FC1-A, is illustrated in Figure 4-15. In general, the different specimens had similar load-deflection shapes which suggested that A35 clips have a peak capacity of 2000 pounds which tends to occur near a $\frac{1}{2}$ inch of deflection.

(3) A35 Clips - Backbone for Test Specimen FC1-A

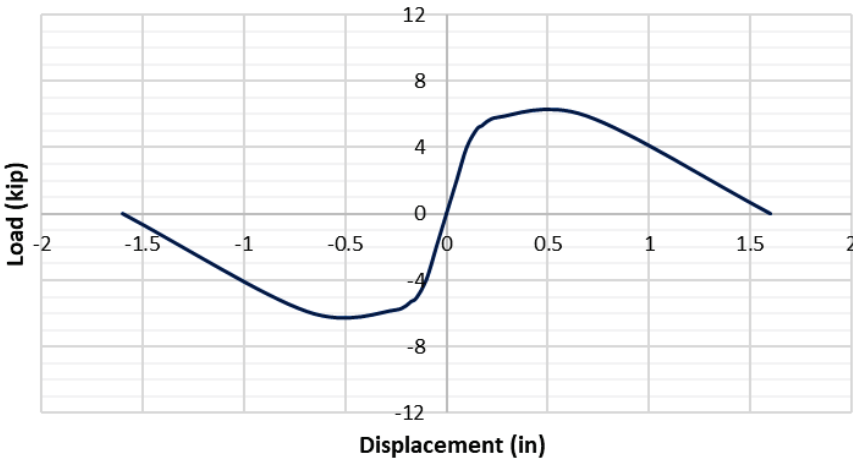


Figure 4-15 Backbone curve for Test Specimen FC1-A of cyclic response of shear transfer connections between shearwalls and diaphragms in woodframe construction (Ficcadenti et. al, 2004).

4.3.12 Considerations of Effective Length for Wall Material Properties

The treatment of wall openings in exterior wall lines assumes that only full height wall sections (i.e., full wall piers) contribute to the effective length (L_{eff}) of a given building block section as proposed by Patton-Mallory *et al.* (1985). Despite numerous additional relationships existing in the literature for treatment of openings of plywood shear walls (e.g., Yasamura and Sugiyama, 1984; Sugiyama and Matsumoto, 1994; Johnson, 1997; FEMA, 2012) the full-height effective length assumption was the most convenient to keep consistent when considering numerous material types and configurations for archetype development. The necessity of this assumption in part reflects the lack of available information for existing finish materials that encompass the scope of the project archetypes. In addition, the approach selected for ATC-110 numerical studies kept the numerical modeling general to the total length of full height wall, rather than tying it to specific wall and opening layouts. The quantification of the total length of full height wall is consistent with FEMA P-1100 Volume 3, Part 6, *FEMA P-1100 Median Configuration Study*. Tracking of individual wall opening configurations would have created significant additional complexity in the numerical studies.

The full-height effective length assumption was carried through from the collection and interpretation of material backbone property data to the applied material properties within numerical models. In other words, if a set of wall tests contains openings, the material properties (e.g., strength in

pounds per linear foot) are based on the effective full-height wall length before combining with other tests that may not have openings. In this way, the general effect of the openings is built into the numerical studies.

While not used in the numerical studies, for background information a subset of the available perforation factor relationships to treat openings in exterior wall lines is illustrated in Figure 4-16. Notably, all relationships besides the “full-pier height” effective length assumption proposed by Patton-Mallory et al. (1985) require the calculation of a sheathing area ratio (r) (see Figure 4-16).

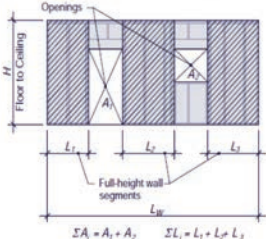
Sheathing Area Ratio (r) (Sugiyama and Matsumoto, 1994)			
<ul style="list-style-type: none"> • Accounts for ratio of sheathed to unsheathed areas in a wall 			
	$r = \frac{1}{1 + \frac{\sum A_i}{H \sum L_j}}$	ΣL_j = “effective length” used in ATC-110	
Perforation Factors			
<ul style="list-style-type: none"> • Factors to adjust full wall without openings for same length L_W 			
α_K = stiffness factor α_F = strength factor			
α_K	α_F	Suggested Drift (θ)	
<i>Patton-Mallory et al. (1985)</i>	$\alpha_{K,F} = \frac{\sum L_j}{L_W}$	Not specified	
<i>Johnson (1997)</i>	$\alpha_K = e^{2.37r - 2.37}$	$\alpha_F = e^{2.24r - 2.24}$	Not specified
<i>Yasumura and Sugiyama (1984)</i>	$\alpha_{K,F} = \frac{r}{3 - 2r}$	$\theta = 1/100 \text{ rad}$	
<i>Sugiyama and Matsumoto (1994)</i>	$\alpha_{K,F} = \frac{3r}{8 - 5r}$ (1)	$\theta = 1/300 \text{ rad}$	
	$\alpha_{K,F} = \frac{r}{2 - r}$ (2)	$\theta = 1/100 \text{ to } 1/60 \text{ rad}$	
<i>FEMA P-807 (2012)</i>	$\alpha_F = 0.92r - 0.72r^2 + 0.8r^3$		

Figure 4-16 Illustration of different perforation factors to account for strength and stiffness reduction due to openings in exterior wall lines.
Note: these relationships are developed based on testing of wood structural panel shear walls and intended for similar application.

In order to illustrate the expected variability due to the treatment of openings, the perforation factor relationships shown in Figure 4-16 are applied to the exterior walls of the original CUREE Small House (Isoda et al., 2002) used for numerical analysis within the CUREE-Caltech Woodframe Project (see Figure 4-17). The corresponding sheathing area ratios for the CUREE Small House are presented in Figure 4-17. As shown in the figure, the values range from 0.81 for the east wall to 0.73 for the north wall. The corresponding

perforation factors (α) using the relationships in Figure 4-16 are compared to the full-pier height effective length assumption in Table 4-5. The estimates can vary as much as 23% when compared to the effective length assumption, yet the differences are within 15% for a majority of the comparisons.

Notably, the relationship proposed in FEMA P-807 Equation 4-3 (FEMA, 2012) was found to give similar results as those obtained using the simpler full wall pier height assumption. This is important since the P-807 guidelines are intended to assess the existing condition of older structures with a variety of materials similar to the ATC-110 numerical studies.

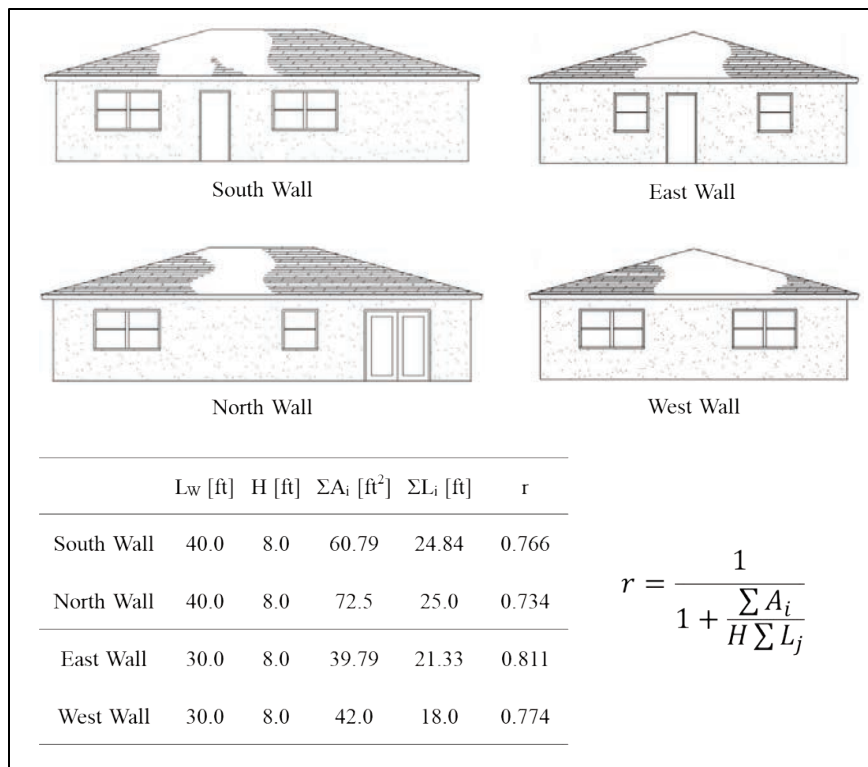


Figure 4-17 Calculation of sheathing area ratios (r) for the exterior walls of the CUREE Small House (Isoda et al., 2002)

Table 4-5 Comparing Different Perforation Factor Relationships Applied to the Exterior Wall Lines of the CUREE Small House

Relationship Source ¹	Factor	Wall Line of CUREE Small House ³			
		South	North	East	West
Patton-Mallory et al. (1985) ²	L_{eff}/L_W	0.62	0.63	0.71	0.60
FEMA P-807 Eq. 4-3	α_F	0.64 (+3%)	0.60 (-3%)	0.70 (-2%)	0.65 (+9%)
Johnson (1997)	α_F	0.59 (-5%)	0.55 (-12%)	0.66 (-8%)	0.60 (0%)
Johnson (1997)	α_K	0.57 (-8%)	0.53 (-15%)	0.64 (-10%)	0.59 (-2%)
Yasamura and Sugiyama (1984)	$\alpha_{F,K}$	0.52 (-16%)	0.48 (-23%)	0.59 (-17%)	0.53 (-11%)
Sugiyama and Matsumoto (1994) (1)	$\alpha_{F,K}$	0.55 (-11%)	0.51 (-19%)	0.62 (-13%)	0.56 (-6%)
Sugiyama and Matsumoto (1994) (2)	$\alpha_{F,K}$	0.62 (0%)	0.58 (-7%)	0.68 (-4%)	0.63 (+5%)

¹ Refer to Figure 4-16 for details; ² The full-height effective length assumption is adopted within ATC-110 numerical studies; ³ See Figure 4-17 for wall line details

² Percentages show the relative difference to the full-height effective length assumption adopted for ATC-110 numerical studies

4.4 Numerical Modeling Methods

4.4.1 Overview

The *Timber3D* analysis program was used in this project to capture the nonlinear dynamic response and seismic collapse mechanisms of full-building three-dimensional models. In this program, the vertical wall panel-to-framing assemblies are modeled using 6-DOF, Frame-to-Frame (F2F) link elements. For this project, however, only one (lateral) DOF of the F2F link element is activated to model the lateral nonlinear cyclic response of vertical walls sheathed with various bracing materials.

The nonlinear lateral cyclic response of vertical walls is captured by the CUREE hysteretic rule (Folz and Filiault 2001), as illustrated in Figure 4-18. The loading force-deformation paths OA and CD follow a nonlinear exponential monotonic envelope curve, while all other unloading and re-loading paths exhibit a linear relationship between force and deformation. This hysteretic rule allows for stiffness and strength degradation as well as post-capping reducing strength (i.e., negative post-peak backbone stiffness). The CUREE hysteretic rule is governed by 10 physically identifiable parameters defined in Table 4-6.

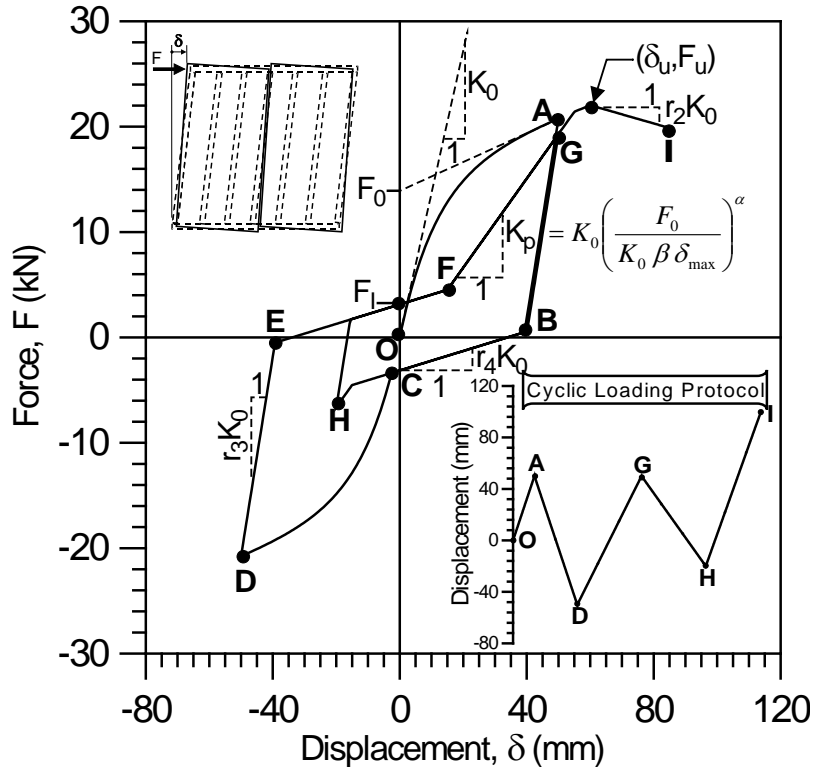


Figure 4-18 CUREE hysteretic rule for modeling force-displacement response of wood shear walls under cyclic loading.

Table 4-6 Definition of Hysteretic Parameters of CUREE Hysteretic Rule

Parameter (see Figure 4-18)	Definition
K_0	Initial stiffness
F_0	Force intercept of the asymptotic stiffness at ultimate strength
F_I	Zero-displacement load intercept
δ_u	Displacement at ultimate load
r_1	Asymptotic stiffness ratio under monotonic load
r_2	Post-capping strength stiffness ratio under monotonic load
r_3	Unloading stiffness ratio
r_4	Re-loading pinched stiffness ratio
α	Hysteretic parameter for stiffness degradation
β	Hysteretic parameter for stiffness degradation

The CUREE hysteretic rule was modified for this project in order to introduce a user-defined residual strength of vertical walls. The post-capping strength stiffness ($r_2 K_0$) is replaced by an S-shaped curve anchored at a displacement D_x and converging to pre-determined residual strength level at large displacements, as shown in Figure 4-19. The final hysteretic model

incorporating residual strength (referred to as the RESST model in *Timber 3D*) is defined by the 12 parameters defined in Figure 4-19.

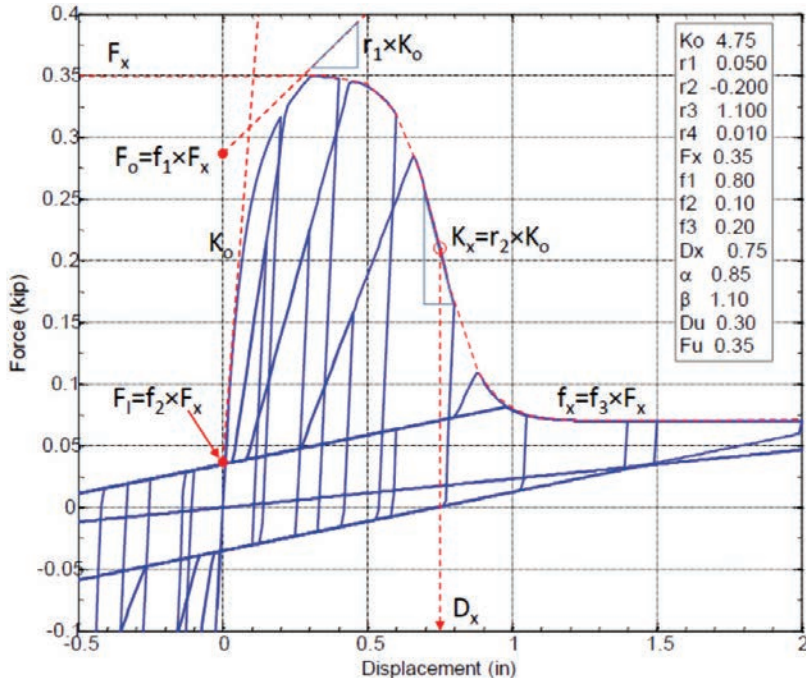


Figure 4-19 Modification of CUREE hysteretic rule for modeling residual strength (RESST hysteresis model in *Timber3D*).

The RESST backbone is defined by the initial stiffness (K_0), peak asymptotic force (F_x), post-peak displacement (D_x) and a series of force and stiffness factors (f_{1-3} , r_{1-4}) that define the backbone in terms of either K_0 or F_x as shown in Figure 4-19. Notably, D_x defines the inflection point of the exponential “S-Curve” that transitions from peak load to the desired residual strength. A constant intercept force and stiffness to model pinching behavior and two parameters to control stiffness degradation upon reloading from the pinched intercept to the backbone curve define cyclic behavior. The factor β defines the next reloading displacement on the backbone curve as a multiplier of the previous maximum displacement (e.g., $\Delta_{i+1}=\Delta_i\beta$). The factor α is an exponent controlling the reloading stiffness (K_p) as a function of initial stiffness (e.g., $K_p=K_0(\Delta_y/\Delta_i+1)\alpha$). The theoretical yield displacement (Δ_y) is defined by the initial stiffness divided by the force F_0 shown in Figure 4-19.

4.4.2 Procedure for Extraction of Hysteretic Parameters from Test Data

The procedure used in this project to extract the hysteretic parameters from test data involves three different phases. In Phase 1, the CUREE parameters for monotonic backbone curves (K_0 , F_0 , δ_u , r_1 and r_2 in Table 4-6) are visually

fitted to recommended backbone curves representing various combinations of test data.

In Phase 2, the CUREE cyclic hysteretic parameters (F_i , r_3 , r_4 , α and β in Table 4-6) are fitted to test data based on an equal energy absorbed (dissipated) approach, as illustrated in Figure 4-20. In this approach, the parameter optimization is obtained by tracking the squares of the error in cumulative absorbed energy at every displacement step of a particular test, then adding the summation of this squared of the errors for all tests. The best set of hysteretic parameters is the one minimizing this cumulative squared error in energy absorbed, E_{CEA} , given by:

$$E_{CEA} = \sum_{j=1}^{NT} \sum_{i=1}^{NP_j} (E_{test,i,j} - E_{model,i,j})^2 \quad (4-1)$$

where, $E_{test,i,j}$ is the absorbed energy measured at displacement i in test j , $E_{model,i,j}$ is the absorbed energy predicted by the CUREE hysteretic model with a selected set of hysteretic parameters at displacement i in test j , NP_j is the number of displacement points in test j and NT is the number of tests considered in the optimization.

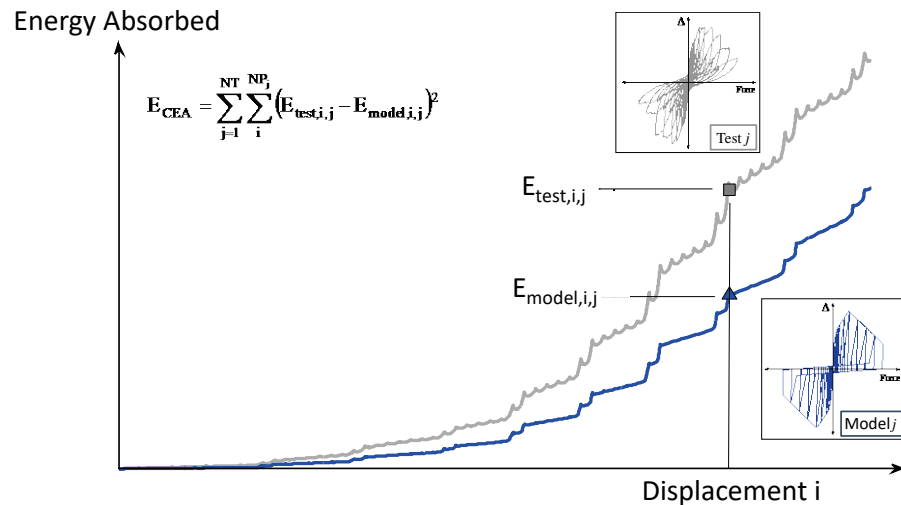


Figure 4-20 Illustration of procedure to extract CUREE hysteretic parameters based on equal cumulative energy absorbed.

The parameter optimization procedure includes the following assumptions:

- Initial ranges of parameters were quantified through visual inspection of test data.
- Tests involving more than one effective wall length assumes the same average wall lengths for all tests (normalized appropriately).
- Two iterations on the hysteretic parameters were carried out. The first iteration used coarse parameter intervals. The second iteration used finer

parameter intervals around the best fitting parameters obtained in the first iteration.

- Test data is trimmed to the first cycle showing a 50% decrease from peak strength if applicable. This trimming was to ensure that the unloading and reloading stiffness ratios (r_3 and r_4) are not biased by large cycles near failure.
- The optimization of hysteretic parameters was based on minimizing the cumulative squared error in energy absorbed, E_{CEA} , across all tests considered for a single material (see Equation (4-1)).

4.4.3 Hysteretic Parameters for Stucco and Gypsum Walls

Figures 4-21 to 4-23 show the test data considered and the recommended backbone curves for walls sheathed with gypsum, exterior stucco and interior gypsum + exterior stucco, respectively. For walls sheathed with gypsum, three different backbone curves are recommended for simulating lower bound, best estimate and upper bound properties. For walls sheathed with exterior stucco and a combination of interior gypsum and exterior stucco, four different backbone curves are recommended for simulating lower bound properties, best estimate properties, upper bound properties of lower stories and upper bound properties of upper stories of multi-story buildings or of single-story buildings.

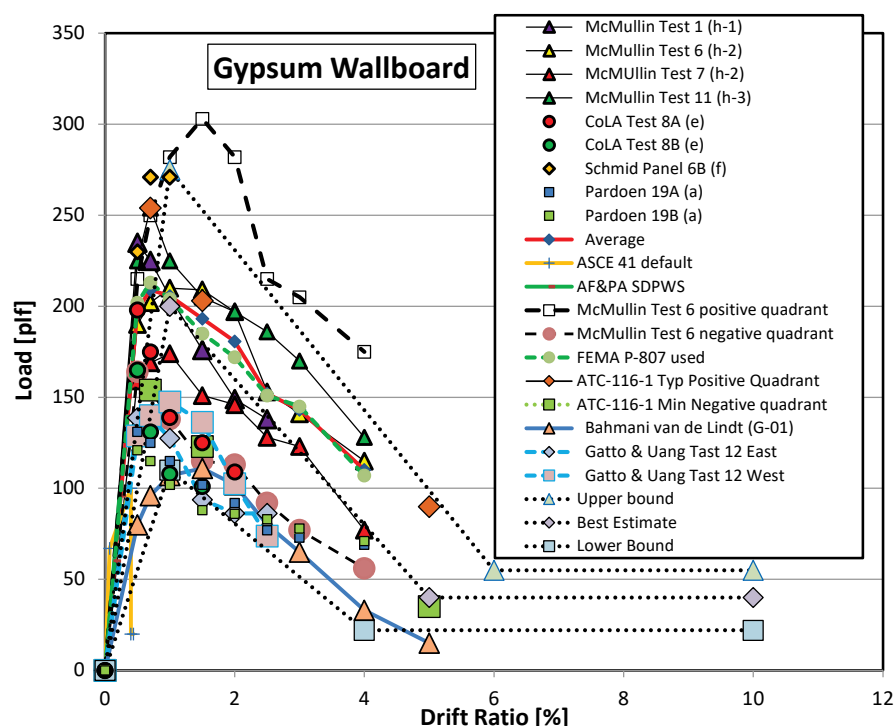


Figure 4-21 Test data and recommended backbone curves for walls sheathed with gypsum.

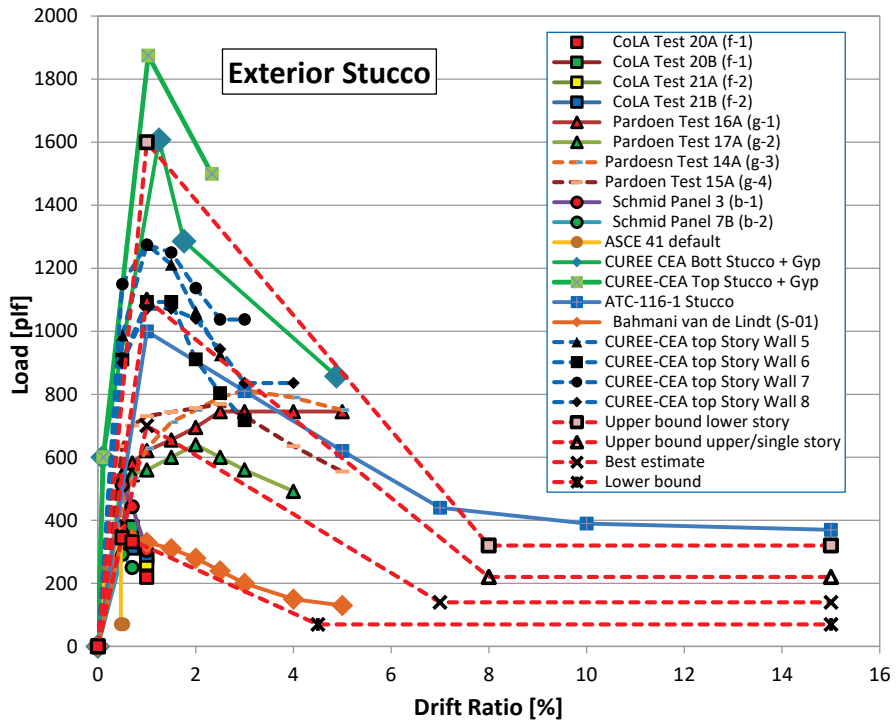


Figure 4-22 Test data and recommended backbone curves for walls sheathed with stucco.

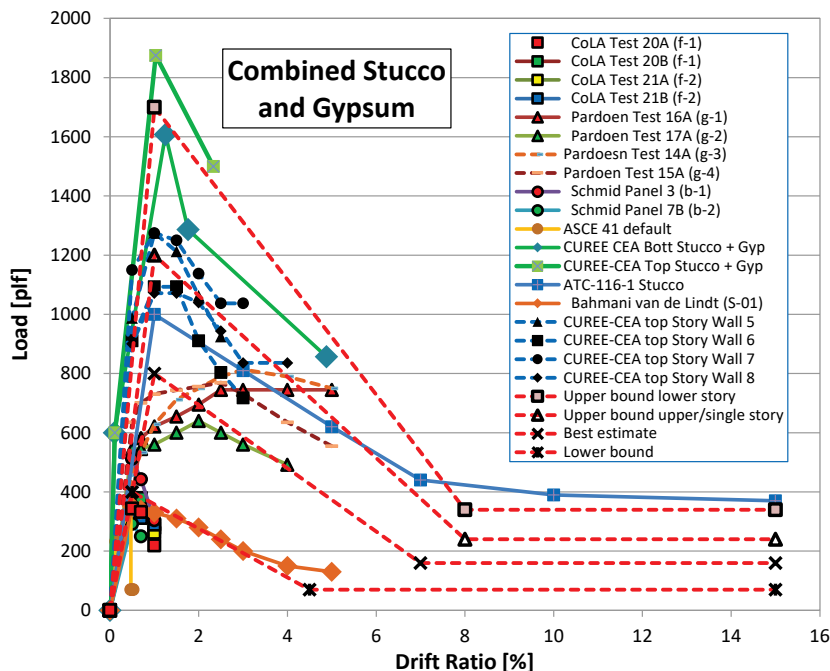


Figure 4-23 Test data and recommended backbone curves for walls sheathed with a combination of interior gypsum and exterior stucco.

The extracted CUREE hysteretic parameters for the wall building blocks sheathed with gypsum and stucco based on the equal absorbed energy approach (i.e., dissipated energy) are listed in Table 4-7. The parameters are provided for normalized lateral load-displacement curves (pounds per linear foot vs percentage of drift).

Because of incomplete test data, the optimum CUREE hysteretic parameters shown in Table 4-7 were based on the following further assumptions.

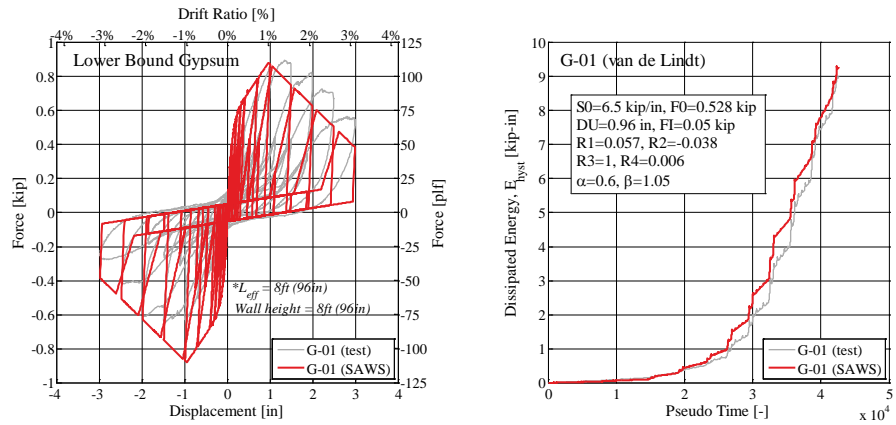
- The hysteretic cyclic parameters for the best estimate gypsum are assigned to the upper bound gypsum. The parameter F_1 was scaled in proportion to the parameter F_0 .
- The hysteretic cyclic parameters for the single/upper story stucco + gypsum were assigned to the best estimate stucco + gypsum. The parameter F_1 was scaled in proportion to the parameter F_0 .
- The hysteretic cyclic parameters for the various properties of stucco were assigned the cyclic parameters for the corresponding properties of stucco + gypsum. This assumes that the stucco dominates the unloading and reloading characteristics of walls sheathed with stucco and gypsum.

Table 4-7 CUREE Hysteretic Parameters for Walls Sheathed with Gypsum and Stucco

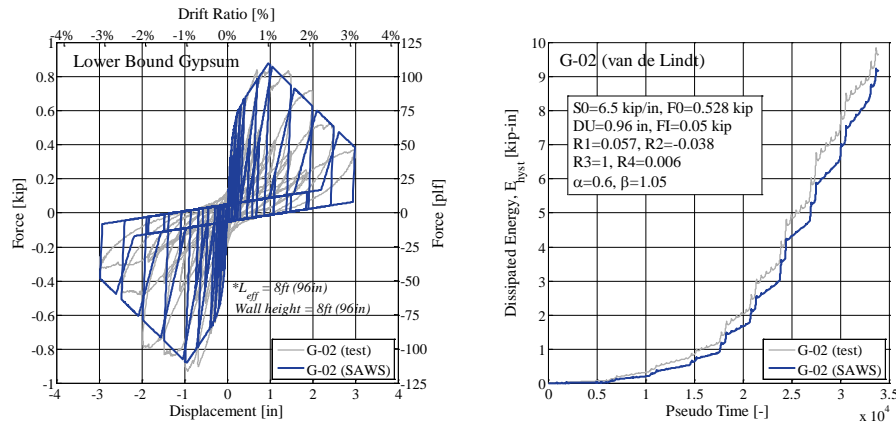
Material / Property	K_0 [lb/%-ft]	F_0 [lb/ft]	r_1	r_2	δ_u [θ%]	F_1 [lb/ft]	r_3	r_4	α	β	
Gypsum	G1 - Lower Bound	780	66.0	0.0565	-0.0376	1.0	6.3	1.0	0.006	0.60	1.05
	G2 - Best Estimate	780	120.0	0.1030	-0.0513	1.0	15.4	1.0	0.040	0.60	1.20
	G3 - Upper Bound ¹	780	165.1	0.1410	-0.0560	1.0	21.1	1.0	0.040	0.60	1.20
Stucco	S1 - Lower Bound	3750	175.0	0.0935	-0.0187	0.5	20.0	1.0	0.012	0.70	1.00
	S2 - Best Estimate	3750	350.0	0.0935	-0.0213	1.0	100.8	1.0	0.025	0.70	1.30
	S3 - Single/Upper Story	3750	550.0	0.1470	-0.0335	1.0	158.4	1.0	0.025	0.70	1.30
	S4 - Lower Story	3750	800.0	0.2130	-0.0481	1.0	325.6	1.0	0.080	0.90	1.30
Stucco + Gypsum	SG1 - Lower Bound	4530	220.0	0.0795	-0.0182	0.5	25.0	1.0	0.012	0.70	1.00
	SG2 - Best Estimate ³	4530	440.0	0.0795	-0.0235	1.0	126.7	1.0	0.025	0.70	1.30
	SG3 - Single/Upper Story	4530	660.0	0.1190	-0.0302	1.0	190.4	1.0	0.025	0.70	1.30
	SG4 - Lower Story	4530	935.0	0.1690	-0.0425	1.0	380.6	1.0	0.080	0.90	1.30

¹Cyclic parameters taken from best estimate gypsum; ²Cyclic parameters estimated from corresponding stucco + gypsum case; ³Cyclic parameters estimated from single story case

Comparisons of the hysteretic response and cumulative absorbed energy from test data and those obtained with the optimized CUREE parameters for walls sheathed with the various properties of gypsum and stucco listed in Table 4-7 for which test data are available are illustrated in Figures 4-24 to 4-28. The model reproduces reasonably well the hysteretic test data response and predict very well the sequence of energy dissipated in all tests.



a) Test G-01



b) Test G-02

Figure 4-24 Comparison of hysteretic response and cumulative dissipated energy for test data (Bahmani and van de Lindt, 2014) and optimized CUREE parameters (see Table 4-7) for walls sheathed with lower bound gypsum.

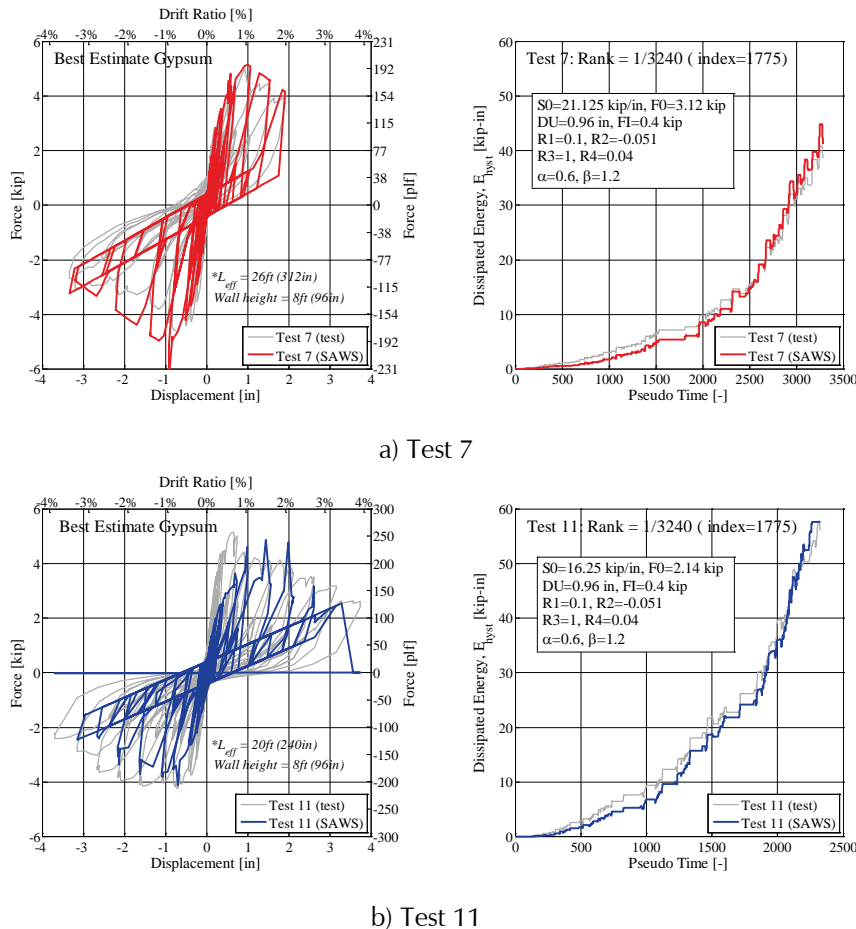


Figure 4-25 Comparison of hysteretic response and cumulative dissipated energy for test data (McMullin and Merrick, 2002) and optimized CUREE parameters (see Table 4-7) for walls sheathed with best estimate gypsum.

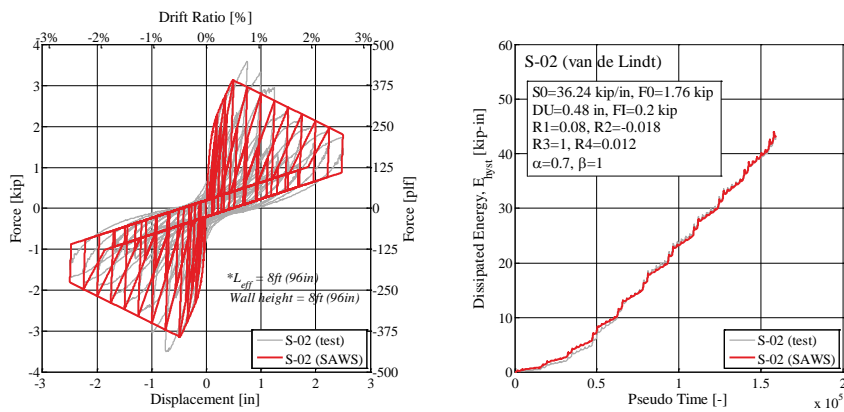


Figure 4-26 Comparison of hysteretic response and cumulative dissipated energy for test data (Test S-02 from Bahmani and van de Lindt, 2014) and optimized CUREE parameters (see Table 4-7) for walls sheathed with lower bound stucco.

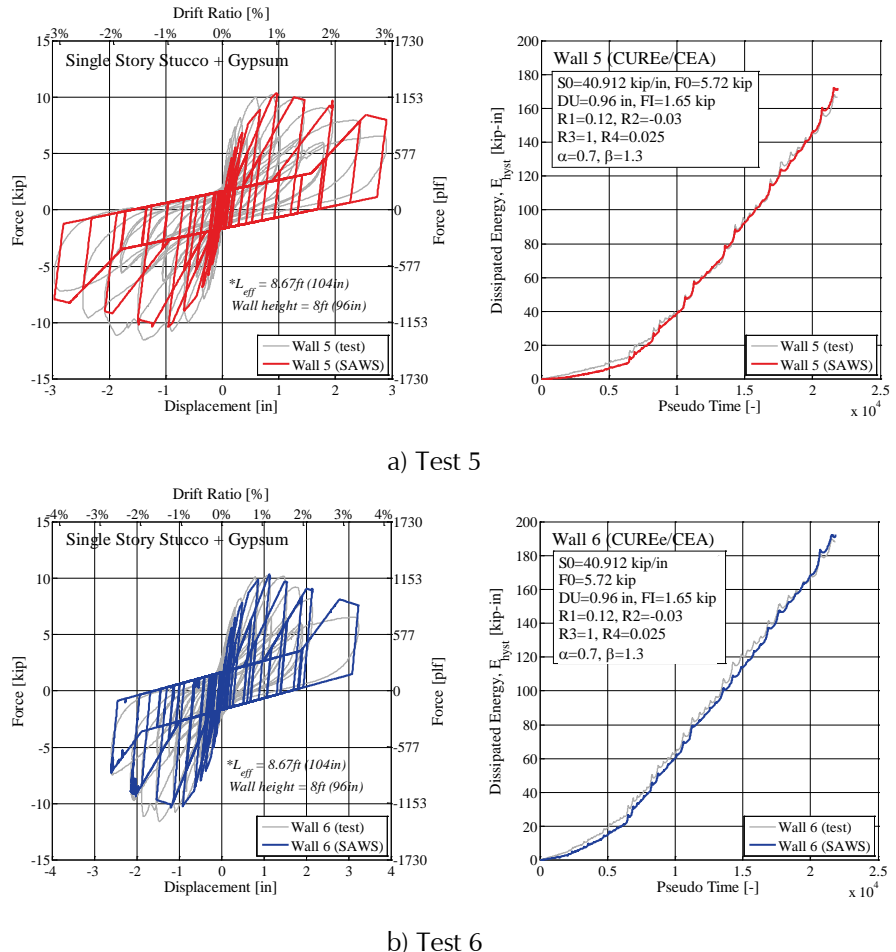
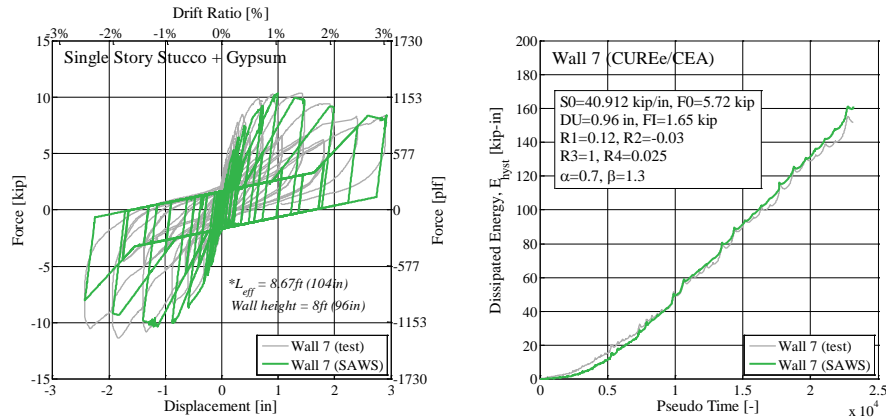
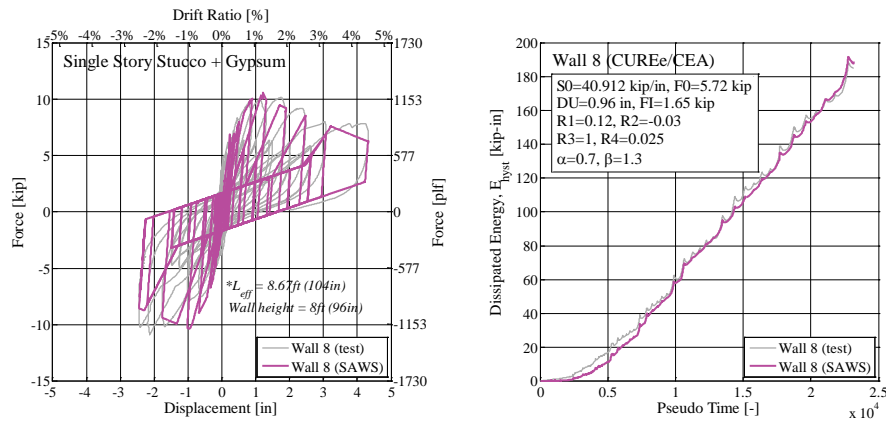


Figure 4-27 Comparison of hysteretic response and cumulative dissipated energy for test data (Tests 5 and 6 from Arnold et al., 2003b) and optimized CUREe parameters (see Table 4-7) for walls sheathed with single/upper story stucco + gypsum.



c) Test 7



d) Test 8

Figure 4-27 (ctd) Comparison of hysteretic response and cumulative dissipated energy for test data (Tests 7 and 8 from Arnold et al., 2003b) and optimized CUREe parameters (see Table 4-7) for walls sheathed with single/upper story stucco + gypsum.

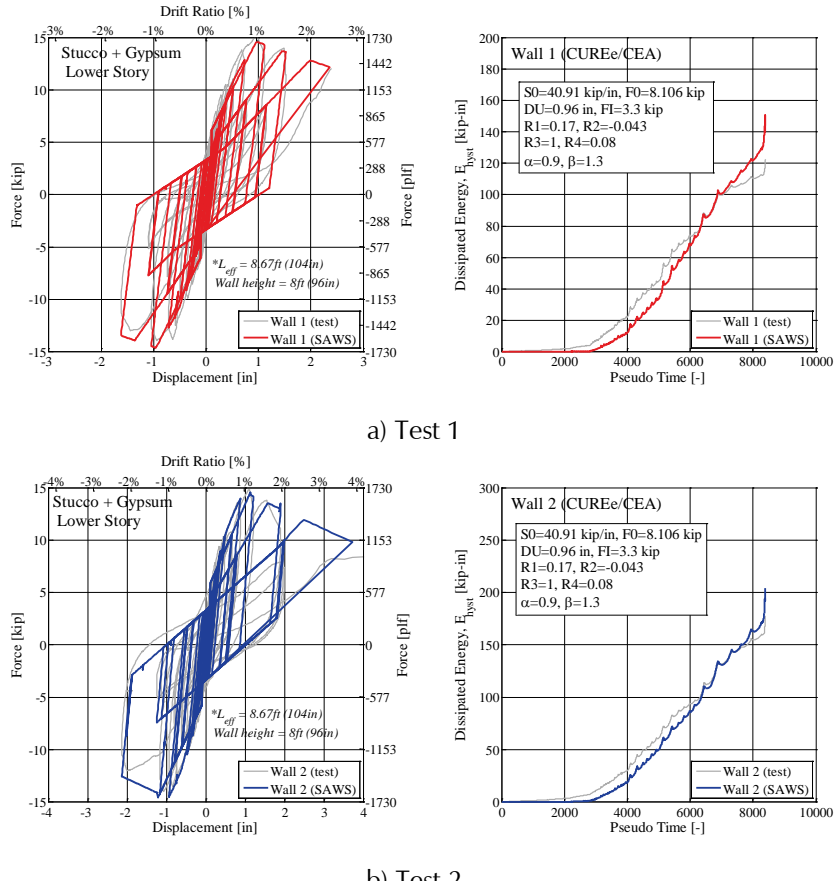


Figure 4-28

Comparison of hysteretic response and cumulative dissipated energy for test data (Arnold et al., 2003a) and optimized CUREe parameters (see Table 4-7) for walls sheathed with lower story stucco + gypsum.

The final *Timber3D* RESST hysteretic parameters based on 10% residual strength for the different varieties of walls sheathed with gypsum and stucco are listed in Table 4-8.

Table 4-8 RESST Hysteretic Parameters Based on 10% Residual Strength for Walls Sheathed with Gypsum and Stucco

Material / Property	K ₀ [lb/%-ft]	r ₁	r ₂	r ₃	r ₄	F _x [lb/ft]	f ₁	f ₂	f ₃	D _x [%]	α	β	
Gypsum	G1 - Lower Bound	780	0.057	-0.054	1.0	0.006	124.3	0.531	0.051	0.1	2.22	0.60	1.05
	G2 - Best Estimate	780	0.103	-0.074	1.0	0.040	225.9	0.531	0.068	0.1	2.62	0.60	1.20
	G3 - Upper Bound ¹	780	0.141	-0.081	1.0	0.040	307.8	0.536	0.069	0.1	3.03	0.60	1.20
Stucco	S1 - Lower Bound	3750	0.094	-0.027	1.0	0.014	395.6	0.442	0.051	0.1	2.12	0.75	1.05
	S2 - Best Estimate	3750	0.094	-0.031	1.0	0.025	785.3	0.446	0.128	0.1	3.85	0.70	1.30
	S3 - Upper Bound Single/Upper Story	3750	0.147	-0.049	1.0	0.025	1233.1	0.446	0.128	0.1	3.85	0.70	1.30
	S4 - Upper Bound Lower Story	3750	0.213	-0.070	1.0	0.080	1789.1	0.447	0.182	0.1	3.81	0.90	1.30
Stucco + Gypsum	SG1 - Lower Bound	4530	0.080	-0.026	1.0	0.014	451.8	0.487	0.055	0.1	2.08	0.75	1.05
	SG2 - Best Estimate ²	4530	0.080	-0.034	1.0	0.025	901.6	0.488	0.141	0.1	3.44	0.70	1.30
	SG3 - Upper Bound Single/Upper Story	4530	0.119	-0.045	1.0	0.025	1342.7	0.492	0.142	0.1	3.85	0.70	1.30
	SG4 - Upper Bound Lower Story	4530	0.169	-0.063	1.0	0.080	1891.2	0.494	0.201	0.1	3.85	0.90	1.30

4.4.4 Hysteretic Parameters for Wood Structural Panels

The test data considered and the recommended backbone curves for walls sheathed with wood structural panels with and without tie-downs, respectively are shown in Figures 4-29 and 4-30.

The test data for walls with tie-downs apply for a maximum aspect ratio (height/width) of 1.0 based on an 8-foot length.

For each wall type (i.e. with and without tie downs), three different backbone curves are recommended for simulating low, medium and high strengths. All the recommended backbone curves shown in Figures 4-29 and 4-30 were obtained by scaling Line's normalized backbone curve for 8x8 walls (Line et al., 2008) also shown in the figures. Note that this normalized backbone curve was multiplied by a factor of 0.92 to adjust for SPF species used in the tests.

For walls without tie-downs, two different types of displacement capacities (A and B) are included to consider the significant dispersions in displacement capacities observed in different testing programs. The displacements of Type B walls were obtained by multiplying the displacements of the corresponding Type A walls by 1.5. Refer to Section 3.6 for discussion of wood structural panels without tie-downs.

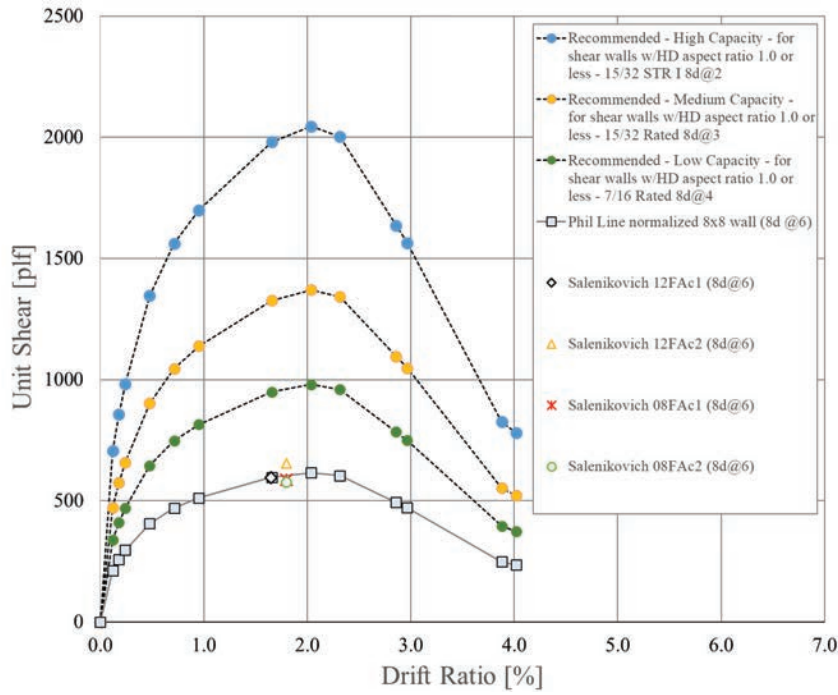


Figure 4-29 Test data and recommended backbone curves for wood structural panels with tie downs.

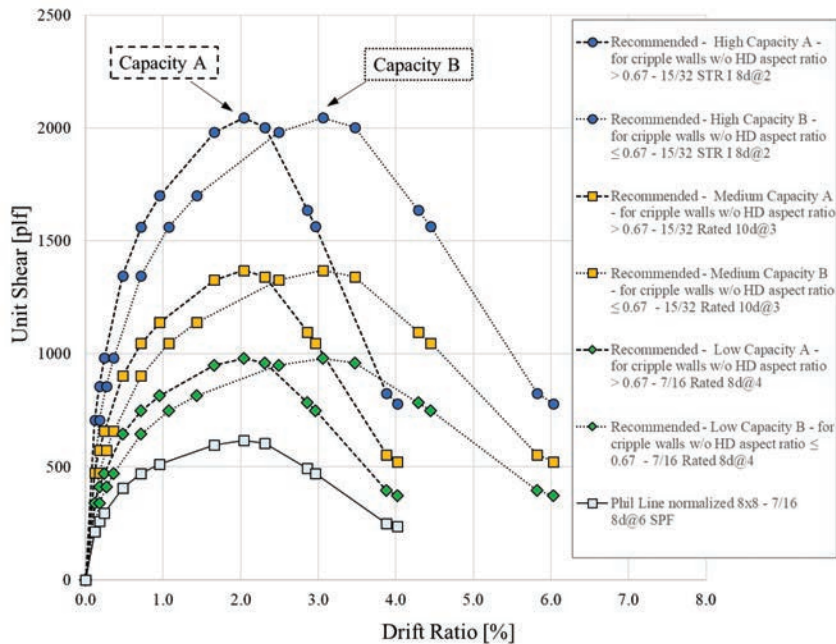


Figure 4-30 Test data and recommended backbone curves for cripple walls wood structural panels without tie downs.

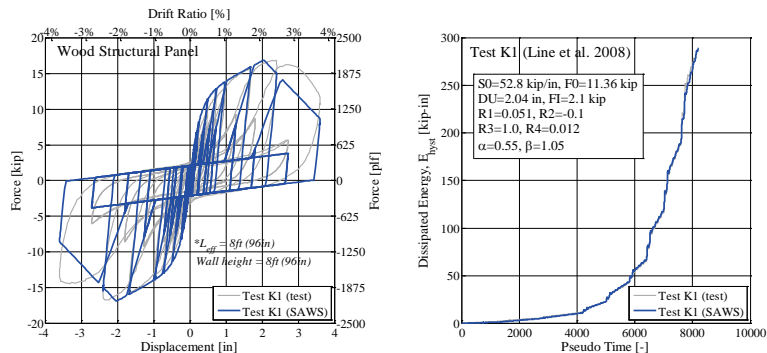
The extracted CUREE hysteretic parameters for the different varieties of wood structural panels based on the equal absorbed energy approach are listed in Table 4-9. The parameters are provided for normalized lateral load-displacement curves (pounds per linear foot vs percentage of drift).

Comparisons of the hysteretic response and cumulative absorbed energy for test data and optimized CUREE parameters for wood structural panel are shown in Figure 4-31. Note that the hysteretic parameters listed in Table 4-9 are derived from two tests conducted by Line et al. (2008) (tests K1 and K2 in Figure 4-31). The model reproduces well the hysteretic test data response and predict very well the sequence of energy dissipated in the two tests considered.

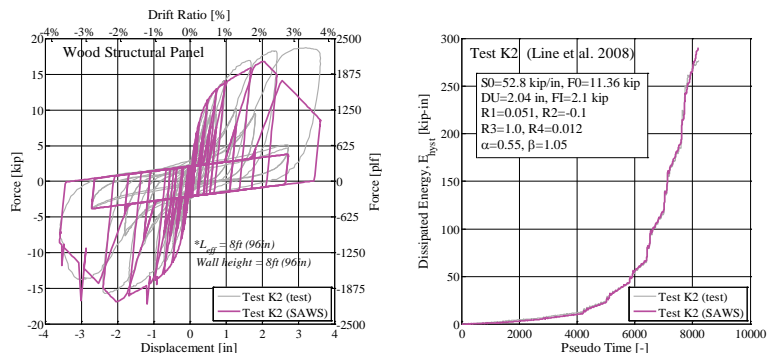
Table 4-9 CUREE Hysteretic Parameters for Wood Structural Panels

Properties	Strength	K_0 [lb/%-ft]	F_0 [lb/ft]	r_1	r_2	δ_u [θ%]	F_l^1 [lb/ft]	r_3	r_4	α	β
Hold Downs, Max. Aspect Ratio ≤ 1	WSP1 - High	6130	1375	0.0515	-0.10	2.12	254.4	1.0	0.012	0.55	1.05
	WSP2 - Medium	4107	921	0.0515	-0.10	2.12	170.4	1.0	0.012	0.55	1.05
	WSP3 - Low	2935	659	0.0515	-0.10	2.12	121.9	1.0	0.012	0.55	1.05
No Hold Downs, Capacity A, Aspect Ratio ≤ 0.67	WSP4 - High	6130	1375	0.0515	-0.10	2.12	254.4	1.0	0.012	0.55	1.05
	WSP5 - Medium	4107	921	0.0515	-0.10	2.12	170.4	1.0	0.012	0.55	1.05
	WSP6 - Low	2935	659	0.0515	-0.10	2.12	121.9	1.0	0.012	0.55	1.05
No Hold Downs, Capacity B, Aspect Ratio ≤ 0.67	WSP7 - High	4087	1375	0.0515	-0.10	3.19	254.4	1.0	0.012	0.55	1.05
	WSP8 - Medium	2738	921	0.0515	-0.10	3.19	170.4	1.0	0.012	0.55	1.05
	WSP9 - Low	1957	659	0.0515	-0.10	3.19	121.9	1.0	0.012	0.55	1.05

¹ F_l estimated from a constant F_l/F_0 ratio of 0.185.



a) Test K1



b) Test K2

Figure 4-31

Comparison of hysteretic response and cumulative dissipated energy for test data (Line et al., 2008) and optimized CUREE parameters (see Table 4-9) for wood structural panels.

The final *Timber3D* RESST hysteretic parameters based on 10% residual strength for the different varieties of shear walls with wood structural panels are listed in Table 4-10.

Table 4-10 RESST Hysteretic Parameters Based on 10% Residual Strength for Wood Structural Panels

Properties	Strength	K_0 [lb/%-ft]	r_1	r_2	r_3	r_4	F_x [lb/ft]	f_1	f_2	f_3	D_x [θ%]	α	β
Hold Downs, Max. Aspect Ratio = 1	WSP1 - High	6130	0.052	-0.144	1.0	0.012	2309.8	0.595	0.110	0.1	3.21	0.55	1.05
	WSP2 - Medium	4107	0.052	-0.144	1.0	0.012	1547.3	0.595	0.110	0.1	3.21	0.55	1.05
	WSP3 - Low	2935	0.052	-0.144	1.0	0.012	1106.7	0.595	0.110	0.1	3.21	0.55	1.05
No Hold Downs, Capacity A, Aspect Ratio > 0.67	WSP4 - High	6130	0.052	-0.144	1.0	0.012	2309.8	0.595	0.110	0.1	3.21	0.55	1.05
	WSP5 - Medium	4107	0.052	-0.144	1.0	0.012	1547.3	0.595	0.110	0.1	3.21	0.55	1.05
	WSP6 - Low	2935	0.052	-0.144	1.0	0.012	1106.7	0.595	0.110	0.1	3.21	0.55	1.05
No Hold Downs, Capacity B, Aspect Ratio ≤ 0.67	WSP7 - High	4087	0.052	-0.144	1.0	0.012	2309.8	0.596	0.110	0.1	4.81	0.55	1.05
	WSP8 - Medium	2738	0.052	-0.144	1.0	0.012	1547.3	0.596	0.110	0.1	4.81	0.55	1.05
	WSP9 - Low	1957	0.052	-0.144	1.0	0.012	1106.7	0.595	0.110	0.1	4.81	0.55	1.05

4.4.5 Hysteretic Parameters for Horizontal Wood Siding

The hysteretic parameters for horizontal wood siding were obtained directly from the ATC-116 draft project documents using the CUREE (SAWS) hysteretic model. The original ATC-116 parameters were provided for ten-foot tall by eight-foot long building blocks. These values were normalized into equivalent parameters expressed in terms of pound per linear foot and percent drift for strength and displacement, respectively. An example of the normalized hysteresis for horizontal wood siding is shown in Figure 4-32.

The corresponding CUREE hysteretic parameters are provided in Table 4-11.

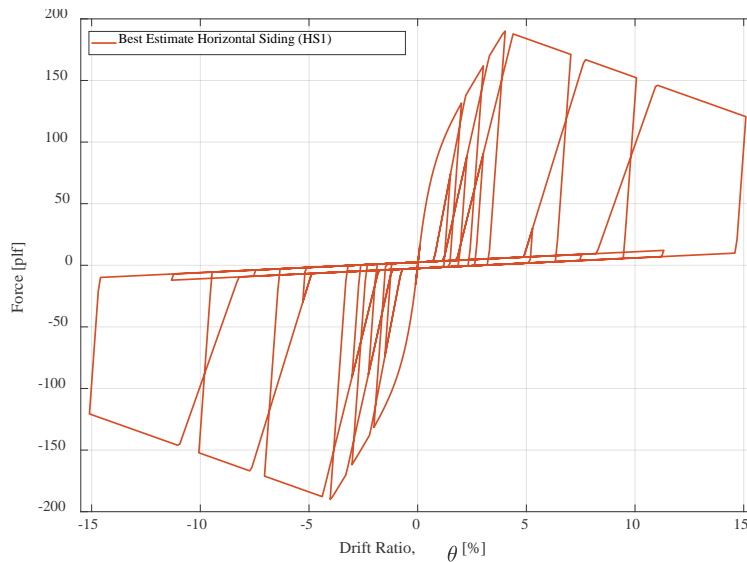


Figure 4-32 Example hysteretic response for horizontal wood siding using the CUREE hysteretic model and inputs parameters used within the ATC-116 project.

Table 4-11 CUREE Hysteretic Parameters for Horizontal Wood Siding

Material	K_0 [lb/%-ft]	F_0 [lb/ft]	r_1	r_2	δ_u [θ%]	F_1 [lb/ft]	r_3	r_4	α	β
Horizontal Wood Siding	169.5	75.0	0.17	-0.037	4.0	2.5	1.45	0.005	0.38	1.09

4.4.6 Hysteretic Parameters for 3×16d Toenails

As illustrated in Figure 4-33, hysteretic parameters were produced for 3-16d toenails in lateral shear. To obtain hysteretic parameters for these toenails, hysteretic parameters were pulled from MCASHEW2's hysteresis database (Pang and Shirazi, 2013) for (2) 16d nails in lateral shear in a perpendicular framing-to-framing application. The backbone shape of this hysteresis plot was then verified with monotonic testing data from *Capacity Resistance of Performance of Single-Shear Bolted and Nailed Connections* (Smart, 2002). The K_0 and F_0 CUREE hysteretic parameters were then modified to account for the following capacity changes:

- Multiplied by NDS toenail shear reduction factor of 0.83
- Multiplied by 3/2 to adjust from (2) 16d toenails to (3)
- Multiplied by reduction factor of 0.50 to account for potential existing mudsill decay and installation errors

The CUREE hysteretic parameters for the 16d toenails are provided in Table 4-12.

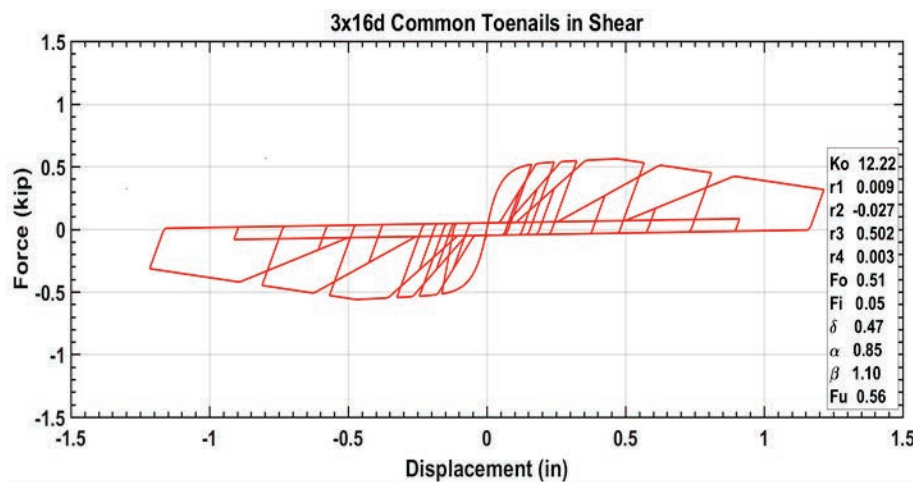


Figure 4-33 CUREE hysteretic model parameters for 3-16d common toenails in lateral shear.

Table 4-12 CUREE Hysteretic Parameters for 3-16d Toenails in Shear

Material	K_0 [kip/in]	F_0 [kip]	r_1	r_2	δ_u [in]	F_1 [kip]	r_3	r_4	α	β
3-16d toenails	12.22	0.51	0.009	-0.027	0.47	0.05	0.502	0.003	0.85	1.10

4.4.7 Hysteretic Parameters for A35 Clips

Hysteretic parameters for in-plane shear loading of A35 clips were developed using the CUREE hysteretic model and parameters are illustrated in Figure 4-34 and tabulated in Table 4-13. The hysteretic properties of these clips were based on testing data from Specimen FC1-A in *Cyclic Response of Shear Transfer Connections Between Shearwalls and Diaphragms in Woodframe Construction* (Ficcadenti et al., 2004). This specimen was selected because it was believed to be a strong average representative out of the four specimens discussed in Section 3.11. The hysteretic fitting was carried out visually to Specimen FC1-A as shown in Figure 4-35. The CUREE hysteretic model was adjusted in order to give a failure displacement of 1.6 inches, after which the element has zero-resistance as shown in Figure 4-35.

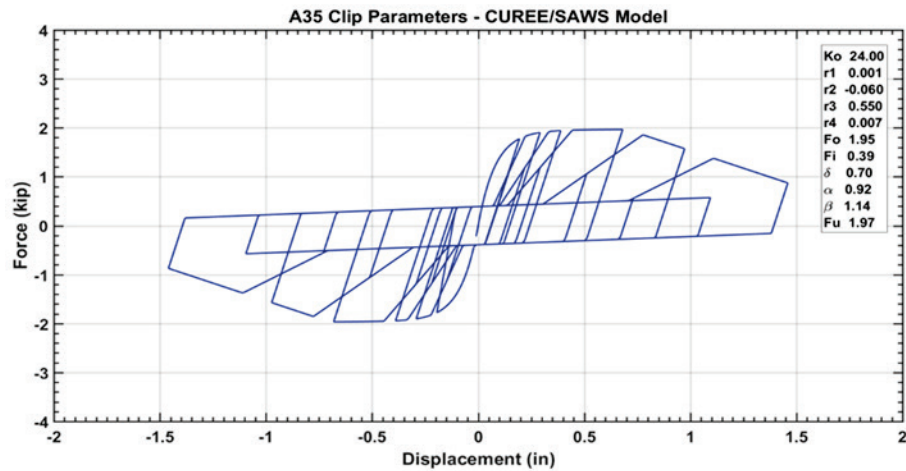


Figure 4-34 CUREE hysteretic model parameters for A35 clips with in-plane shear loading.

Table 4-13 CUREE Hysteretic Parameters for Single A35 Clip with In-Plane Shear Loading

Material	K_0 [kip/in]	F_0 [kip]	r_1	r_2	δ_u [in]	F_1 [kip]	r_3	r_4	α	β
A35 Clip (in-plane shear)	24.0	1.95	0.001	-0.06	0.7	0.39	0.55	0.007	0.92	1.14

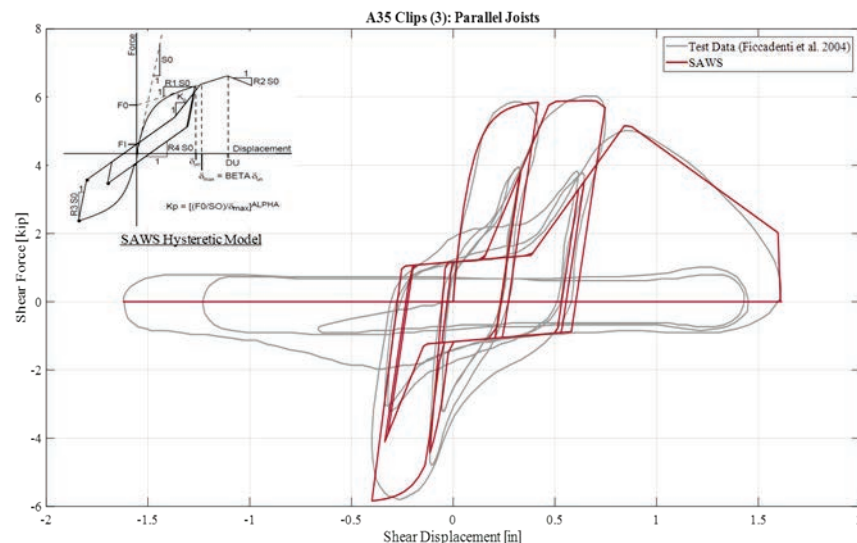


Figure 4-35 Fitting of SAWS hysteretic model to A35 clip testing conducted by Ficcadenti et al. (2004). NOTE: The test shown is for three clips in parallel.

4.5 Modeling Data Specific to Dwelling Types

Where specific dwelling types generated unique retrofit approaches that were not wall bracing based, appropriate hysteretic modeling was produced. Examples include steel moment frames or cantilevered columns for the living-space-over-garage configuration, and base level diaphragm anchorage for the hillside configuration.

4.6 References

- AWC, 2015. Special Design Provisions for Wind and Seismic. American Wood Council, Washington, D.C.
- Arnold, A.E., Uang, C-M. and Filiatrault, A. 2003a. "Cyclic Behavior and Repair of Stucco and Gypsum Woodframe Walls: Phase I," CUREE Publication No. EDA-03, Consortium of Universities for Research in Earthquake Engineering, Richmond, CA, 268 p.
- Arnold, A.E., Uang, C-M. and Filiatrault, A. 2003b. "Cyclic Behavior and Repair of Stucco and Gypsum Woodframe Walls: Phase II," CUREE Publication No. EDA-07, Consortium of Universities for Research in Earthquake Engineering, Richmond, CA, 341 p.
- Bahmani, P. and van de Lindt, J. 2014. "Experimental and Numerical Assessment of Woodframe Sheathing Layer Combinations for Use in Strength-Based and Performance-Based Design." ASCE Journal of Structural Engineering, 10.1061/(ASCE)ST.1943-541X.0001134, E4014001.
- Carroll, C. T. 2006. Wood Materials and Shearwalls of Older Light-Frame Residential Structures, A thesis submitted to Oregon State University in partial fulfillment of the requirements for the degree of Master of Science, February, 2006.
- Chai, Y.H., Hutchinson, T.C., Vukazich, S.M. 2002. "Seismic Behavior of Level and Stepped Cripple Walls," *CUREE Publication W-17*, CUREE-Caltech Woodframe Project, Consortium of Universities for Research in Earthquake Engineering, Richmond, CA.
- CoLA 2001. Report of a Testing Program of Light-Framed Walls with Wood-Sheathed Shear Panels, Final Report to the City of Los Angeles Department of Building and Safety, 2001.
- CUREE. 2001. Woodframe Project Testing and Analysis Literature Reviews, A. Filiatrault (ed.), CUREE Publication No. W-03, CUREE-Caltech

Woodframe Project, Consortium of Universities for Research in Earthquake Engineering, Richmond, CA.

- Dolan, J.D., D. Carradine, J. Bott, and W.S. Easterling. 2003. Design Methodology of Diaphragms, CUREE Publication No. W-27, Consortium of Universities for Research in Earthquake Engineering.
- FEMA, 2012. Seismic Evaluation and Retrofit of Multi-Unit Wood-Frame Buildings with Weak First Stories (FEMA P-807).
- Fennell, W.A., P. Line, G. Mochizuki, K. Moore, T. VanDorpe, and T. Voss. 2008. "Report on Laboratory Testing of Anchor Bolts Connecting Wood Sill Plates to Concrete with Minimum Edge Distance."
- Fischer, D., Filiatrault, A., Folz, B., Uang, C-M.,Seible, F. 2001. Shake Table Tests of a Two-Story Woodframe House, CUREE Publication No. W-06, CUREE-Caltech Woodframe Project, Consortium of Universities for Earthquake Engineering Research, Richmond, CA.
- Folz, B., and Filiatrault, A. 2001. "Cyclic Analysis of Wood Shear Walls", ASCE Journal of Structural Engineering, 127(4), 433-441.
- Gatto, K. and C.M. Uang, 2002. Cyclic Response of Woodframe Shearwalls: Loading Protocol and Rate of Loading Effects, CUREE Publication No. W-13. Consortium of Universities for Research in Earthquake Engineering, 2002.
- Isoda, H., Folz, B., Filiatrault, A. 2002. "Seismic Modeling of Index Woodframe Buildings," CUREE Publication W-12, CUREE-Caltech Woodframe Project, Consortium of Universities for Research in Earthquake Engineering, Richmond, CA.
- Johnson, A.J. 1997. "Monotonic and Cyclic Performance of Long Shear Walls with Openings," MSc Thesis, Virginia Polytechnic Institute and State University, Blacksburg, VA.
- Johnston, A.R., Dean, P.K., Shenton III, H.W. 2006. "Effects of Vertical Load and Hold-Down Anchors on the Cyclic Response of Wood Framed Shear Walls," Journal of Structural Engineering, ASCE, 132(9): 1426-1434.
- Krawinkler, H., Parisi, F., Ibarra, L., Ayoub, A., Medina, R. 2000. "Development of a testing protocol for wood frame structures," CUREE Publication No. W-02, CUREE-Caltech Woodframe Project, Consortium of Universities for Research in Earthquake Engineering (CUREE), Richmond, CA.

- Line, P. 2016. "Backbone Summary for Wood Frame Nailed Wood Structural Panel Shear Walls," private communication, March, 2016.
- Line, P., N. Waltz, and T. Skaggs. 2008. "Seismic Equivalency Parameters for Engineered Woodframe Wood Structural Panel Walls," *Wood Design Focus*, 18(2): 13-19, Summer, 2008.
- Line, P., N. Waltz, T. Skaggs, and E. Keith. 2014. In-Plane Racking Strength of Wood-Frame continuous Sheathed Wood Structural Panel Wall Bracing In Accordance with ICC-ES Acceptance Criteria AC269.1," *Wood Design Focus*, 24(2): 10-21.
- Mahaney, J.A. and Kehoe, B.E. 2002. "Anchorage of Woodframe Buildings: Laboratory Testing Report," CUREE Publication No. W-14, Consortium of Universities for Research in Earthquake Engineering, Richmond, CA, 137 p.
- McMullin, K.K. and Merrick, D. 2002. "Seismic Performance of Gypsum Walls: Experimental Test Program," CUREE Publication No. W-15, Consortium of Universities for Research in Earthquake Engineering, Richmond, CA, 168 p.
- Ni, C. and Karacabeyli, E. 2007. "Performance of Shear Walls with Diagonal or Transverse Lumber Sheathing." *ASCE Journal of Structural Engineering*, December 2007, p. 1832-1842. DOI: 10.1061/(ASCE)0733-9445(2007)133:12(1832).
- Pang, W., Shirazi, S.M.H. 2013. "Corotational Model for Cyclic Analysis of Light-frame Wood Shear Walls and Diaphragms", *ASCE Journal of Structural Engineering*, 139(8): 1303-1317.
- Pardoen, G.C., Waltman, A., Kazanjy, R.P., Freund, R.P. and Hamilton, C. 2003. "Testing and Analysis of One-Story and Two-Story Shear Walls Under Cyclic Loading," CUREE Publication No. W-25, Consortium of Universities for Research in Earthquake Engineering, Richmond, CA, 278 p.
- Patton-Mallory, M., Wolfe, R.W., Soltis, L.A. 1985. "Light-frame shear wall length and opening effects," *Journal of Structural Engineering*, ASCE, 111(10): 2227-2239.
- Porter, M.L. 1987. "Sequential Phased Displacement (SPD) Procedure for TCCMAR Testing, Proceedings of 3rd Meeting of the Joint Technical Coordinating Committee on Masonry Research, US-Japan Coordinated Research Program.

Salenikovich, A.J. 2000. The Racking Performance of Light-Frame Walls. Dissertation submitted to the faculty of the Virginia Polytechnic Institute and State University in partial fulfillment of the requirements for the degree of Doctor of Philosophy in Wood Science and Forest Products, August, 2000.

Schmid, B. 2002. "Results and Ramifications of Cyclic Tests of Typical Sheathing Materials Used on One and Two Story Woodframe Residences," hand out at SEAOC 2002 convention.

Sugiyama, H., Matsumoto, T. 1994. "Empirical Equations for the Estimation of Racking Strength of a Plywood-Sheathed Shear Wall with Openings," Architectural Institute of Japan (AIJ).

SEAOSC. 1996. "Standard method of cyclic (reversed) load test for shear resistance of framed walls for buildings," Structural Engineers Association of Southern California, Whittier, CA.

Yasamura, M., Sugiyama, H. 1984. "Shear properties of plywood-sheathed wall panels with opening," Transactions of the Architectural Institute of Japan, 338(4): 88-98.

Part 5

Protocol for Numerical Studies

5.1 Introduction

The ATC-110 Project relied heavily on full-building, three-dimensional numerical studies for developing the FEMA P-1100 Prestandard for the evaluation and retrofit of one- and two-family light-frame wood residential buildings. The software program *Timber3D*, capable of capturing the most important aspects of the seismic response of these buildings was selected for conducting the analyses¹. The intent was to use the same software program, when practical, to model different types of light-frame wood residential building construction to be investigated by the different working groups of the project. There was a need for a similar analysis protocol to be used by the different working groups in order to provide comparable analysis approaches for the study of project variables. This protocol needed to be consistent with the recommendations for performance criteria for the numerical studies² and with the recommendations for retrofit design³ that were developed by the project. Alternate analysis methods were also used by the different working groups for detailed numerical studies or sub-assembly studies, as required. The results of these detailed numerical studies are summarized in the resource papers developed by the different working groups^{4,5,6}. This document serves as a record of the ATC-110 Project analysis protocol for full-building, three-dimensional numerical studies.

5.2 Overview

The following analyses were conducted on each full-building model developed by the ATC-110 Project:

- Modal analyses to evaluate elastic natural periods and mode shapes.
- Non-linear static pushover analyses.

¹ Volume 3 Part 1 - Software Recommendations and Applications for Numerical Studies.

² Volume 3 Part 2 - Performance Criteria for Numerical Studies.

³ Volume 3 Part 3 - Assessment and Retrofit Design Criteria.

⁴ Volume 3 Part 11 - Development of Vulnerability-Based Retrofit Provisions for Crawlspace Dwellings.

⁵ Volume 3 Part 12 - Development of Vulnerability-Based Retrofit Provisions for Living-Space-Over-Garage Dwellings.

⁶ Volume 3 Part 13 - Development of Vulnerability-Based Retrofit Provisions for Hillside Dwellings.

- Non-linear incremental dynamic analyses (IDAs) according to the FEMA P-695 methodology (FEMA, 2009) and for the P-695 far-field ground motion suite incrementally scaled in the time domain.

All these analyses were conducted with the software program *Timber3D*. Details are described in the following sections.

5.3 Modal (Free Vibration) Analyses

Eigenvalue and eigenvector analyses were conducted using elastic properties in order to determine the initial natural periods, T_1 , and mode shapes in each orthogonal direction of each full-building model. The primary objective of the period calculations was to compare the period predictions of the full-building models to that of past numerical studies to evaluate consistency or understand reasons for differences. The majority of the full-building models considered in the project were expected to be in the short-period range ($T_1 < 0.5$ sec), for which design forces would be capped. The period calculations could have been used in simplified retrofit design procedures.

5.4 Non-linear Static Pushover Analyses

Non-linear static pushover analyses were conducted along each direction of each full-building model to extract the overall backbone base shear – roof displacement response and to extract the characteristic parameters defined in Section 4.1 of FEMA P795 (FEMA, 2011). The monotonic pushover analysis was based on a first-mode distribution of lateral forces. Second order (P- Δ) effects was included. These P-795 characteristic parameters could have entered the simplified retrofit procedures that could have been used in simplified retrofit design procedures. The pushover analysis was used for estimation of system overstrength, as discussed in Volume 3, Part 7.

5.4.1 FEMA P-795 Characteristic Parameters

For the purpose of comparison and validation of analysis results as well as for the development of simplified retrofit procedures, a number of characteristic response properties consistent with the FEMA P-795 definitions (FEMA, 2011) were calculated for each pushover curve obtained along each orthogonal direction of each full-building model. Note that FEMA P-795 would require calculating these parameters based on cyclic test results. For simplicity, however, the monotonic pushover curves of the full-building models were used to calculate the response parameters. These characteristic response parameters are:

- The secant stiffness at 40% of the peak strength, K_{40} , in the loading portion of the force-displacement response.

- The drift at 80% of the peak strength, $\Delta_{u,80}$, in the post-capping portion of the force-displacement response.
- The maximum drift, $\Delta_{u,\max}$, in the post-capping portion of the force displacement response corresponding to the start of the residual strength plateau. This response parameter is not included in FEMA P795 but was introduced in the ATC-110 Project because of the consideration of residual strengths in the full-building models.

5.5 Incremental Dynamic Analyses and Performance Evaluation

5.5.1 Analysis Procedures

Non-linear Incremental Dynamic Analyses (IDAs) according to the FEMA P-695 methodology were to be conducted on all full-building models for specific levels of ground motion intensities (intensity stripes). The 22 FEMA P-695 far-field ground motions set, with two horizontal components for each motion, were used in all IDAs. The record set was scaled based on the median spectra intensity (S_T) at the code fundamental period of each building model given by the formulas of Section 12.8.2.1 of ASCE/SEI 7-10 (ASCE 2010), as required by the FEMA P-695 methodology. Alternatively, when comparing the performance of different full-scale building models, a common fundamental period of 0.25 sec was used for scaling the records. This is the shortest period permitted for analysis by the FEMA P-695 methodology and it corresponds to the period range of most full-building models developed by the ATC-110 Project.

For each intensity stripe, three-dimensional (3D) IDAs were conducted by applying the 22 FEMA P-695 far-field (FF) records (two components each) to the archetype model in two orthogonal orientations (i.e., NS- EW and EW-NS orientations) generating 44 response data records for each response parameter of interest. Therefore, the collapse and other statistics were based on 44 analyses. Note that in order to represent realistic dynamic response and collapse mode at large displacements, a very small amount of viscous damping (close to zero) was to be introduced in the archetype building models. The ATC-116-1 Project found that even a small amount of viscous damping generated significant artificial (and unrealistic) restoring forces in light-frame wood building models once the hysteretic damping from vertical wall building blocks were near exhausted close to collapse.

For each archetype building model, the IDAs were to be conducted for intensity stripes starting at $S_T = 0.1$ g. The intensity was to be increased by

increments of 0.1g up to an intensity level for which all (44) ground motions of the record set caused collapse of the building model.

The intensities corresponding to 50% collapse rate was considered to approximate the medians of the collapse fragility curves used to assess the primary performance criterion considered by the ATC-110 Project. This primary criterion is related to structural safety and is defined as the probability of collapse under MCE_R ground motion intensities. The raw collapse fragility data was stored as baselines. Lognormal fragility curves were also constructed based on assumed composite dispersions (β_{TOT}) adjusted for three-dimensional effects (3D) and Spectral Shape Factor (SSF) according to the FEM P-695 methodology, as described in the next sections.

5.5.2 Correction for 3D Effect

Since 3D IDAs were conducted with the 22 record pairs applied twice to each building archetype model, once with the ground motion records oriented along one principal direction, and then again with the records rotated 90 degrees, the calculated median collapse intensities were multiplied by a factor of 1.2 per FEMA P-695 methodology. This factor is introduced to remove the conservative bias of median collapse intensities of approximately 20% for 3D analyses compared to results from 2D analyses.

5.5.3 Correction for Spectral Shape Factor (SSF)

Because the shape of the acceleration response spectrum of a rare intense ground motion is peaked at a predominant period, and drops off more rapidly (and has less energy) at periods that are longer or shorter than the predominant period, structures with sufficient ductility increase their effective periods causing a rapid drop of demands at other periods. This causes rare records to be less damaging than would otherwise be expected based on the shape of the standard design spectrum. To remove this conservative bias, the FEMA P-695 methodology uses a simplified spectral shape factor (SSF), which depends on the fundamental period (T) and period-based ductility factor (μ_T) of a full-scale building model, to adjust its collapse median intensity.

The full-building models to be developed in the ATC-110 Project were used for the assessment of (older) existing buildings and the evaluation of the performance of retrofit buildings. It was expected that the median collapse intensities of older existing buildings would be much lower than those incorporating new retrofit designs. Therefore, different values of SSF were applied to the median collapse intensities of existing buildings being assessed and retrofitted buildings.

For older existing buildings failing at low seismic intensities, the correction for SSF cannot be easily justified. An SSF value of 1.00 was used for the collapse assessment of all existing full-building models developed in the ATC-110 Project.

It was expected that most of the full-building models incorporating retrofit measures developed in the ATC-110 project would have had short fundamental periods ($T \leq 0.5$ sec). Table 5-1 lists the SSF values extracted from Table 7-1b of FEMA P-695 that are applicable to building archetypes with elastic fundamental periods $T \leq 0.5$ sec and designed for Seismic Design Category SDC- D_{max} . The SSF values are capped at 1.33 for $\mu_T \geq 8$.

Table 5-1 Values of Spectral Shape Factor (SSF) Applicable to Building Archetypes with Elastic Fundamental Periods $T \leq 0.5$ sec and Designed for Seismic Design Category SDC- D_{max}

Period-Based Ductility Factor							
1.0	1.1	1.5	2	3	4	6	8
1.00	1.05	1.10	1.13	1.18	1.22	1.28	1.33

The period-based ductility factor is obtained from a pushover analysis of a full-building model and is defined as the ratio of the ultimate roof displacement (δ_u) to the effective roof yield displacement ($\delta_{y,eff}$), as illustrated in Figure 5-1. The ultimate roof displacement is defined as the roof displacement corresponding to a strength of 80% of the peak strength in the post-capping region of the pushover curve. The effective roof yield displacement is defined as the roof displacement corresponding to the extension of the elastic stiffness up to the peak strength of the full-building model.

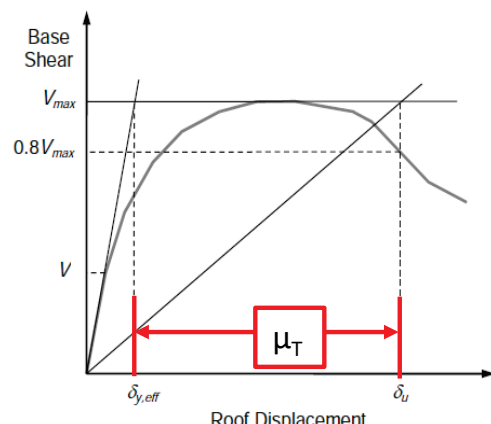


Figure 5-1 Definition of period-based ductility factor (μ_T).

Table 5-2 presents the values of μ_T and corresponding values of SSF computed from the backbone curves (lb. /ft. /rad vs story drift in rad) of the

various material building blocks that were to be used in the ATC-110 models and that were available at the time of writing. The period-based ductility factors are near or above a value of 8.0 for all materials. The average value of the SSF taken across materials is 1.32, which is very close to the maximum SSF value of 1.33. Based on these results and anticipating similar (or larger) values of μ_T for retrofitted full-building pushover curves, the maximum SSF value of 1.33 was used to multiply the median collapse intensities of all retrofitted full-building models developed in the ATC-110 Project.

Table 5-2 Values of Spectral Shape Factors (SSF) Applicable to Building Archetypes with Elastic Fundamental Periods $T \leq 0.5$ sec and Designed for Seismic Design Category SDC-D_{max}

Material	Condition	$\delta_{y,\text{eff}} (\%)$	$\delta_u (\%)$	μ_T	SSF
Gypsum	Upper Bound	0.353	2.260	6.4	1.29
	Best Estimate	0.257	2.000	7.8	1.33
	Lower Bound	0.141	1.751	12.4	1.33
Stucco	Upper Bound: Lower Story	0.426	2.773	6.5	1.29
	Upper Bound: Single/Upper Story	0.294	2.753	9.4	1.33
	Best Estimate	0.187	2.754	14.7	1.33
	Lower Bound	0.093	1.500	16.1	1.33
Stucco + Gypsum	Upper Bound: Lower Story	0.375	2.767	7.4	1.32
	Upper Bound: Single/Upper Story	0.265	2.753	10.4	1.33
	Best Estimate	0.177	2.503	14.1	1.33
	Lower Bound	0.088	1.470	16.7	1.33
Average Value of SSF					1.32

5.5.4 Correction for Global Dispersion Factor (β_{TOT})

According to the FEMA P-695 methodology, the following sources of uncertainty must be considered in the collapse assessment process:

- Record-to-Record Uncertainty (RTR) expressed by a dispersion factor β_{RTR} .
- Design Requirements Uncertainty (DR) expressed by a dispersion factor β_{DR} .
- Test Data Uncertainty (TD) expressed by a dispersion factor β_{TD} .
- Modeling Uncertainty (MDL) expressed by a dispersion factor β_{MDL} .

For the record-to-record uncertainty, the FEMA P-695 methodology allows the use of a fixed value of $\beta_{RTR} = 0.40$ for structures with significant period

elongation (i.e., $\mu_T \geq 3$). The other sources of uncertainty are qualified in terms of quality ratings provided in Tables 5-3, 5-4 and 5-5, respectively.

According to the FEMA P-695 methodology, the global dispersion factor (β_{TOT}) is obtained by combining the individual dispersion factors as follows:

$$\beta_{tot} = \sqrt{\beta_{RTR}^2 + \beta_{DR}^2 + \beta_{TD}^2 + \beta_{MDL}^2} \quad (5-1)$$

Table 5-3 FEMA P-695 Quality Rating of Design Requirements (DR)

Completeness and Robustness	Confidence in Basis of Design Requirements		
	High	Medium	Low
High. Extensive safeguards against unanticipated failure modes. All important design and quality assurance issues are addressed.	(A) Superior $\beta_{DR} = 0.10$	(B) Good $\beta_{DR} = 0.20$	(C) Fair $\beta_{DR} = 0.35$
Medium. Reasonable safeguards against unanticipated failure modes. Most of the important design and quality assurance issues are addressed.	(B) Good $\beta_{DR} = 0.20$	(C) Fair $\beta_{DR} = 0.35$	(D) Poor $\beta_{DR} = 0.50$
Low. Questionable safeguards against unanticipated failure modes. Many important design and quality assurance issues are not addressed.	(C) Fair $\beta_{DR} = 0.35$	(D) Poor $\beta_{DR} = 0.50$	--

The full-building models were used for evaluation of the performance of existing buildings prior to retrofit and of retrofit buildings. The quality ratings listed in Tables 5-3 to 5-5 could vary significantly for older existing buildings and for those incorporating new retrofit designs. Therefore, it was recommended to apply different global dispersion factors (β_{TOT}) to the lognormal fragility curves of existing buildings prior to retrofit and retrofitted buildings. Table 5-6 lists the various quality ratings and dispersion factors that were used. Also shown in the table are the global dispersion factor (β_{TOT}) computed from Eq. (5-1).

Table 5-4 FEMA P-695 Quality Rating of Test Data (TD)

Completeness and Robustness	Confidence in Test Results		
	High	Medium	Low
High. Material, component, connection, assembly, and system behavior well understood and accounted for. All, or nearly all, important testing issues addressed.	(A) Superior $\beta_{TD} = 0.10$	(B) Good $\beta_{TD} = 0.20$	(C) Fair $\beta_{TD} = 0.35$
Medium. Material, component, connection, assembly, and system behavior generally understood and accounted for. Most important testing issues addressed.	(B) Good $\beta_{TD} = 0.20$	(C) Fair $\beta_{TD} = 0.35$	(D) Poor $\beta_{TD} = 0.50$
Low. Material, component, connection, assembly, and system behavior fairly understood and accounted for. Several important testing issues not addressed.	(C) Fair $\beta_{TD} = 0.35$	(D) Poor $\beta_{TD} = 0.50$	--

Table 5-5 FEMA P-695 Quality Rating of Modeling Uncertainty (MDL)

Representation of Collapse Characteristics	Accuracy and Robustness of Models		
	High	Medium	Low
High. Index models capture the full range of the archetype design space and structural behavioral effects that contribute to collapse.	(A) Superior $\beta_{MDL} = 0.10$	(B) Good $\beta_{MDL} = 0.20$	(C) Fair $\beta_{MDL} = 0.35$
Medium. Index models are generally comprehensive and representative of the design space and behavioral effects that contribute to collapse.	(B) Good $\beta_{MDL} = 0.20$	(C) Fair $\beta_{MDL} = 0.35$	(D) Poor $\beta_{MDL} = 0.50$
Low. Significant aspects of the design space and/or collapse behavior are not captured in the index models.	(C) Fair $\beta_{MDL} = 0.35$	(D) Poor $\beta_{MDL} = 0.50$	--

As shown in Table 5-6, the quality rating for the design requirements of existing full-building models prior to retrofit is lower than that for retrofitted building models. Often for existing buildings, design requirements may be inadequate or nonexistent, which would justify a (D) Poor rating. It was expected that the performance of retrofitted buildings be dominated by the presence of retrofit measures, which will be based on modern engineering or prescriptive techniques. Because these retrofit procedures could not be thoroughly evaluated in the ATC-110 Project, a conservative rating of (C) Fair was assigned to retrofitted full-building models.

Table 5-6 Proposed Quality Ratings and Dispersion Factors for Assessment and Retrofit Purposes

Uncertainty Source	Proposed Quality Ratings and Dispersion Factors	
	Prior to Retrofit	With Retrofit
Record-to-Record	$\beta_{RTR} = 0.40$	$\beta_{RTR} = 0.40$
Design Requirements	(D) Poor $\beta_{DR} = 0.50$	(C) Fair $\beta_{DR} = 0.35$
Test Data	(C) Fair $\beta_{TD} = 0.35$	(B) Good $\beta_{TD} = 0.20$
Modeling	(B) Good $\beta_{TD} = 0.20$	(B) Good $\beta_{TD} = 0.20$
Global	0.75	0.60

The test data associated with existing buildings, often incorporating archaic materials, are incomplete. Nevertheless, the ATC-110 Project spent a considerable effort in identifying and scientifically analyzing test data available on a variety of archaic and modern materials. For this reason, a rating of (C) Fair was assigned for assessment purposes in Table 5-6. It was expected that retrofit measures incorporate modern materials (e.g. wood structural panels) for which much more test data is available. For this reason, a high rating of (B) Good was assigned to retrofitted full-building models.

The open-source *Timber3D* software program was used for all full-building, three-dimensional numerical studies conducted within the ATC-110 Project⁷. This recommendation was based on the following two primary reasons:

1. *Timber3D*'s ability to model flexible roof and floor diaphragms was thought to be the only way to capture the behavior that needed to be studied, particularly in room-over-garage and hillside home configurations.
2. The general frame elements included in *Timber3D* were thought to be necessary to model likely retrofits in both room-over-garage and hillside home configurations. These might have included cantilevered columns, steel moment frames and anchorage to an uphill foundation.

Because *Timber3D* represents the state-of-the-art software platform for the non-linear collapse seismic analysis of wood buildings, a rating of (B) Good was assigned to both existing buildings prior to retrofit and retrofit buildings in Table 5-6.

⁷ Volume 3 Part 1 - Software Recommendations and Applications for FEMA P-1100 Numerical Studies.

Based on the above, it was recommended to apply $\beta_{TOT} = 0.75$ to lognormal fragility curves developed for the collapse assessment of existing pre-retrofit full-building models. For lognormal fragility curves developed for the evaluation of retrofitted full-building models, it was recommended to apply $\beta_{TOT} = 0.60$.

5.6 References

ASCE, 2010. *Minimum Design Loads for Buildings and Other Structures*, ASCE Standard ASCE/SEI 7-10, American Society of Civil Engineers, Reston, VA.

FEMA, 2009. *Quantification of Building Seismic Performance Factors*, FEMA P-695, Prepared by the Applied Technology Council for the Federal Emergency Management Agency, Washington, DC, 421 p.

FEMA, 2011. *Quantification of Building Seismic Performance Factors: Component Equivalency Methodology*, FEMA P795, Prepared by the Applied Technology for the Federal Emergency Management Agency, Washington, DC, 292 p.

Part 6

Median Dwelling Configuration Study

6.1 Introduction

The FEMA P-1100 prestandard targets a range of known seismic vulnerabilities for one- and two-family dwellings including those with a crawlspace, living-space-over garage, and dwellings situated on steep sloping known as hillside homes. Of these residential structure types, crawl-space dwellings represent one of the oldest and most types that often sustain damage during moderate to large earthquakes. The commonality of crawlspace dwellings and particularly those with unbraced cripple-walls, reflects the enduring (yet not ubiquitous) construction practice from the turn of the 20th century to the mid 1970's. These dwellings were constructed and elevated on a small perimeter foundation often with the first-floor framing supported on a system of short cripple-wall studs around the exterior and interior posts and footings within the interior. The simplicity of this construction, coupled with a multitude of styles, configurations and construction practices results in an almost endless number of possible configurations and embedded engineering properties with which to study.

This white paper illustrates the efforts taken to better understand the likely configurations and engineering properties of detached one- and two-story dwellings that would be representative of crawlspace dwellings with unbraced cripple-walls. The geometrical data set developed by measuring plan configurations of period homes is discussed in Section 6.2 and Section 6.3 illustrates the process of translating geometrical information into meaningful physical properties (i.e., strength, mass and stiffness) to assist in the development of appropriate superstructure models for numerical analysis of cripple-wall dwellings. Finally, Section 6.4 demonstrates the steps taken to create representative archetype configuration models to adequately capture the range of likely superstructure response of cripple-wall dwellings with seismic retrofit.

6.2 Information Collected on Older Single-family Dwellings

This section discusses the review process taken to better understand the building stock of older wood-frame dwellings. The dwelling configurations are introduced with details of the review and documentation process provided. The extracted information is then summarized before relating the information to engineering parameters in Section 6.3.

6.2.1 Dwelling Configurations Considered

The superstructure configuration study consisted of reviewing home plans and sketches within a time frame of construction between 1900 and 1969. This was deemed appropriate to reflect the range of construction eras that would have raised crawlspaces with unbraced cripple walls in high seismic regions. Archived housing catalogs provided the most useful information since these typically provided a rendering (illustration) of the home, combined with scaled plan drawings of each occupied story such that the particular dwelling could be measured using visual tools.

The target age range of construction (i.e., 1900 to 1969) was sub-divided by decade. Configurations from each decade were obtained, yet no further discretization of the age of construction was possible due to limited catalogs that were available through online search engines. Example cover pages of one catalog from each decade is shown in Figure 6-1. The complete set of housing catalogs utilized in the study are defined in Table 6-1.

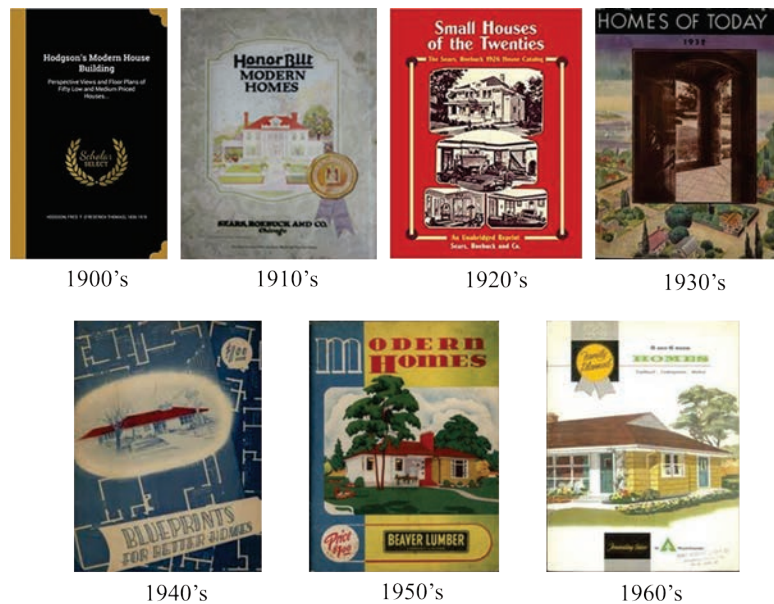


Figure 6-1 Example of housing catalogs used to obtain superstructure information ranging from 1900 to 1969.

Table 6-1 List of Housing Catalog References

Era of Construction	Title	Company	Reference
1900	Hodgson's Modern House Building	Frederick J. Drake and Co.	Hodgson (1905)
1900	Radford's Artistic Bungalows	The Radford Architectural Company	Radford (1908)
1910	Honor Bilt Modern Homes	Sears, Roebuck and Co.	Sears-Roebuck (1918)
1920	Small Houses of the Twenties	Sears, Roebuck and Co.	Sears-Roebuck (1926)
1920	Practical Homes	Carr and Johnston Company	Carr and Johnston (1926)
1930	Homes of Today	Sears, Roebuck and Co.	Sears-Roebuck (1932); reprint by Sears (2003)
1940	Weyerhaeuser 4-Square Book of Homes	Weyerhaeuser Sales Company	Weyerhaeuser (1940)
1940	Blueprints for Better Homes, 1946	Blueprints for Better Homes	BFBH (1946)
1950	Modern Homes	Beaver Lumber Company	Beaver Lumber (1950)
1950	Selected 3-Bedroom Homes	Weyerhaeuser Sales Company	Weyerhaeuser (1957)
1950	Attractive Multi-Level Homes	Weyerhaeuser Sales Company	Weyerhaeuser (1958)
1950	Select Home Designs	The Building Centre Limited	B.C. Ltd. (1959)
1960	54 Homes of Distinction	Home Planners, Inc.	Home Planners (1960)
1960	5 and 6 Room Homes	Weyerhaeuser Sales Company	Weyerhaeuser (1960)
1960	Three Bedroom Homes	National Plan Service, Inc.	NPS (1961)

Thumbnail sketches of each configuration are shown for the one-story and two-story configurations in Figure 6-2 and Figure 6-3, respectively. While the plan images are not set to relative scale, they give the reader an idea of the different plan shapes and interior wall densities considered.



Figure 6-2 Plan drawings for the three one-story configurations considered for each construction era. Images are not to relative scale.

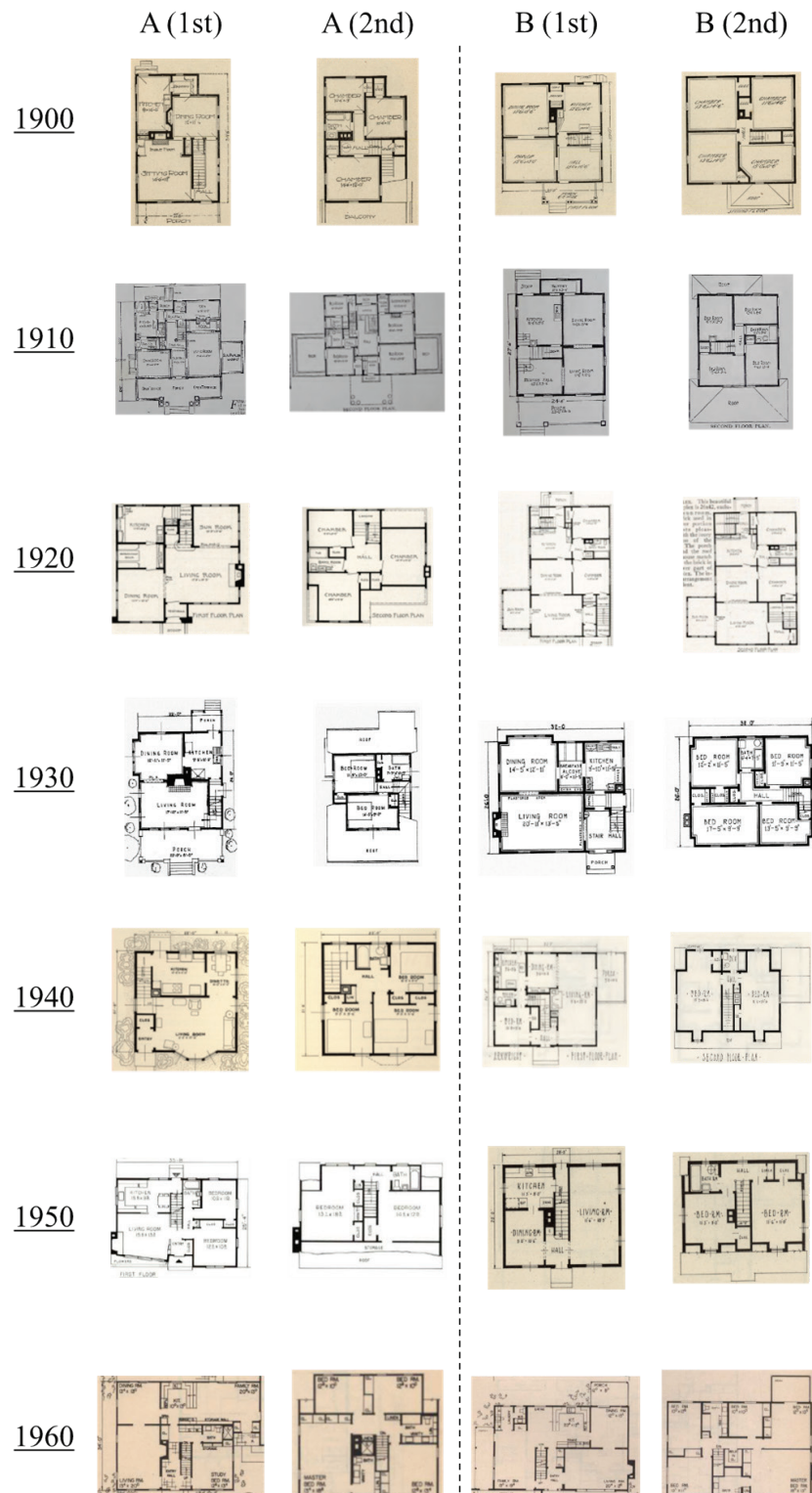


Figure 6-3 Plan drawings for the first and second stories of the two-story configurations selected for each construction era. Images are not to relative scale.

6.2.2 Geometrical Data Collected from Configuration Set

Each configuration was measured and documented for the following geometrical parameters:

- Floor area for each story;
- Length of full-height interior partition walls in each orthogonal direction;
- Length of full-height exterior walls in each orthogonal direction;
- Estimate of roof gable areas, pitch and eave overhangs (for weight take-off).

An example of a measured plan configuration is provided in Figure 6-4 for a 1910's one-story dwelling.



Figure 6-4

Example of one-story 1910 configuration measurements within FEMA P-1100 cripple wall dwelling superstructure study: (a) exterior view of house; (b) plan configuration; (c) plan measured for interior walls; (d) plan measured for exterior walls.

Figure 6-4b shows that configuration 1910-B has a total plan area of 1128 ft². When measuring for interior and exterior wall quantities, only full pier height sections were considered, and the horizontal dimension of each plan was

taken as the “X-Direction” for each case. Figure 6-4c illustrates that the example configuration has 42.5ft of interior wall in the X-direction ($L_{Int,X}$) and 29.5ft in the Y-direction ($L_{Int,Y}$). Similarly, in Figure 2-4d the exterior walls are measured as 63.0ft and 62.0ft in the X- and Y-directions, respectively.

The floor areas of the one-story configurations range from approximately 600 ft² to 1800 ft² with an average of 1125 ft². The two-story configurations range from 950 ft² to 3700 ft² (including both floors) with an average of 1918 ft². The summary of floor areas is provided in Figure 6-5 and Figure 6-6 for one- and two-story configurations, respectively. The figures show that a range of home sizes is considered within the study.

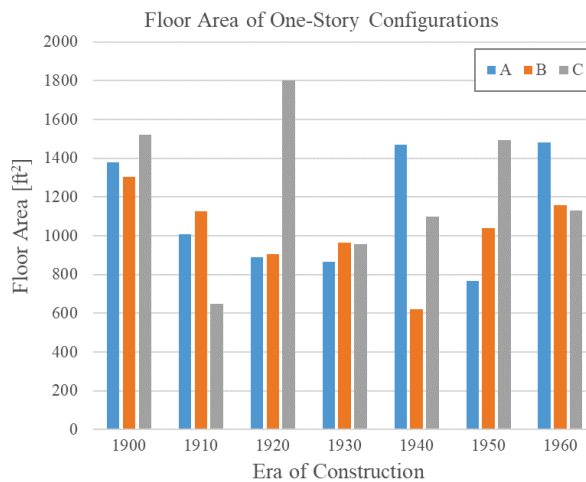


Figure 6-5 Floor areas of one-story configurations.
Average value is 1125 ft².

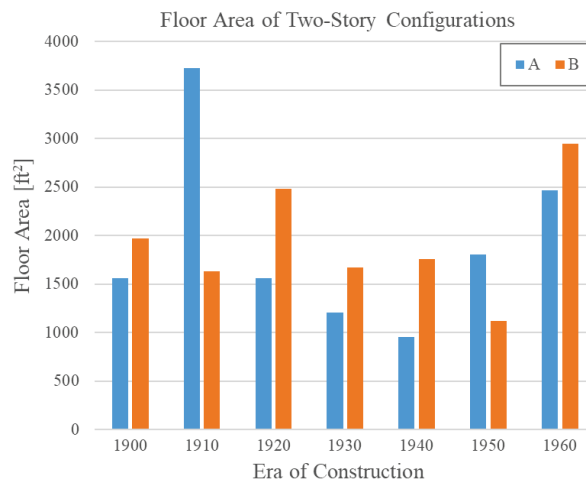


Figure 6-6 Floor areas of two-story configurations.
Average value is 1918 ft².

In order to summarize the trends in full-height exterior walls and the density of interior partitions, the wall length data is expressed in terms of four different criteria. These criteria are defined as:

- **Exterior wall density** (L_{EXT}/A): Total full-height exterior wall length divided by the floor area;
- **Maximum-to-minimum exterior wall length ratio** (L_{max}/L_{min})_{EXT}: Ratio of larger exterior wall length of two perpendicular directions to the lesser of the two perpendicular directions;
- **Interior wall density** (L_{INT}/A): Total full-height interior wall length divided by the floor area, and;
- **Maximum-to-minimum interior wall length ratio** (L_{max}/L_{min})_{INT}: Ratio of larger interior wall length of two perpendicular directions to the lesser of the two perpendicular directions.

The combination of the measured wall density with the maximum-to-minimum ratio allows definition of the total length of interior or exterior wall as well as the amount of wall expected in the two perpendicular directions of the configuration. The wall criteria summary for one-story configurations is presented in Figures 6-7 and 6-8 for exterior and interior walls, respectively. Equivalent summaries are provided for the first story of two-story configurations in Figures 6-9 and 6-10 with the second story information presented in Figures 6-11 and 6-12.

The values are presented with individual data points with the mean across all eras of construction annotated. Additionally, lognormal standard deviation bounds (i.e., $+/- \beta$) are plotted to illustrate the dispersion in the wall geometry criteria. The data was checked for both normal and lognormal distribution fitting using the Kolmogorov-Smirnov (K-S) and Lilliefors tests at 5% significance; returning the same trends for both distributions. The lognormal assumption was made after reviewing the histograms of the data. An example comparison of normal and lognormal assumptions for the interior wall density (L_{INT}/A) for the one-story configurations is shown in Figure 2-13.

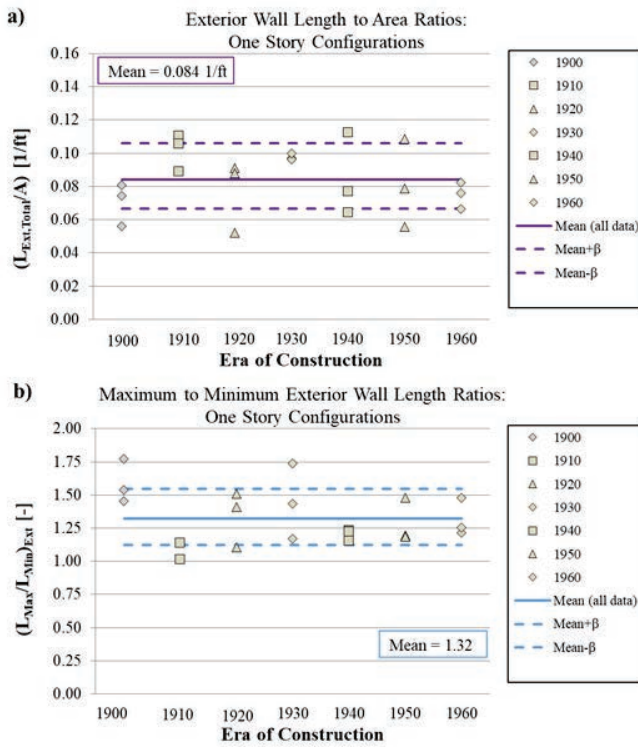


Figure 6-7 Exterior wall criteria for one-story configurations: (a) Exterior wall density, (b) Maximum-to-minimum wall length ratio.

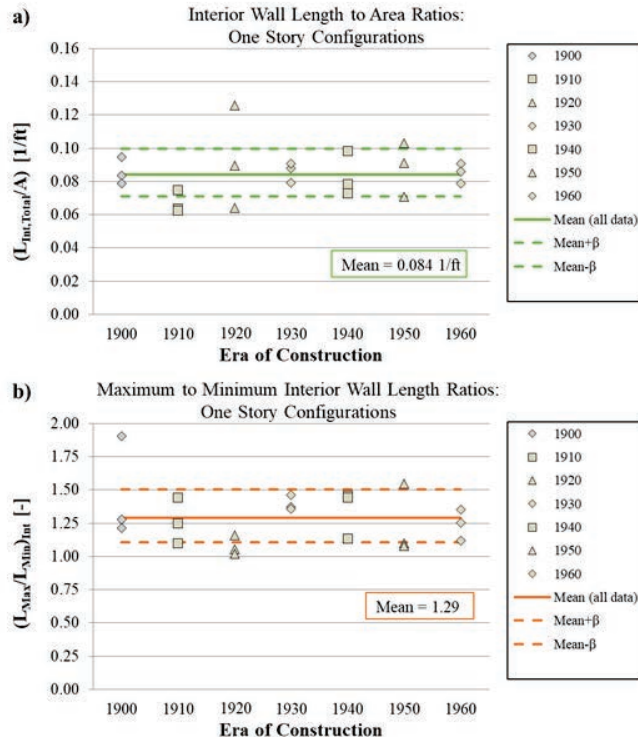


Figure 6-8 Interior wall criteria for one-story configurations: (a) Interior wall density, (b) Maximum-to-minimum wall length ratio.

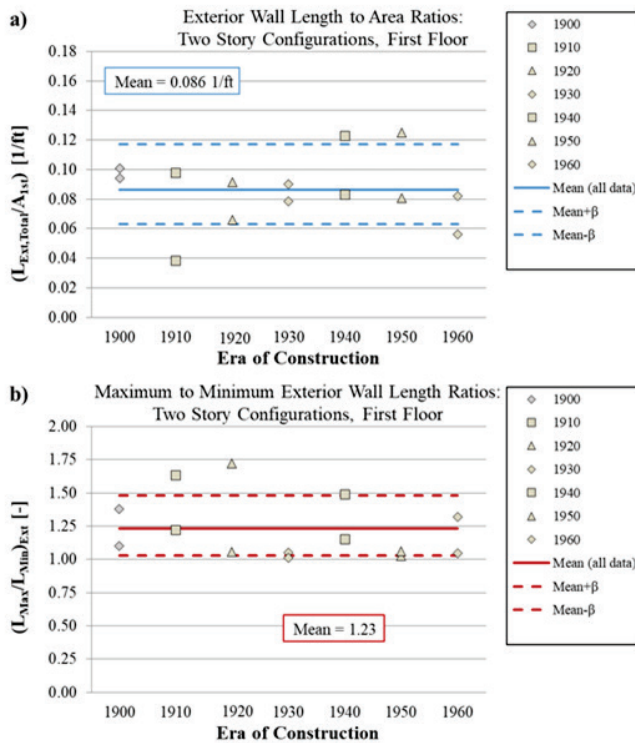


Figure 6-9 Exterior wall criteria for the first floor of two-story configurations: (a) Exterior wall density, (b) Maximum-to-minimum length ratio.

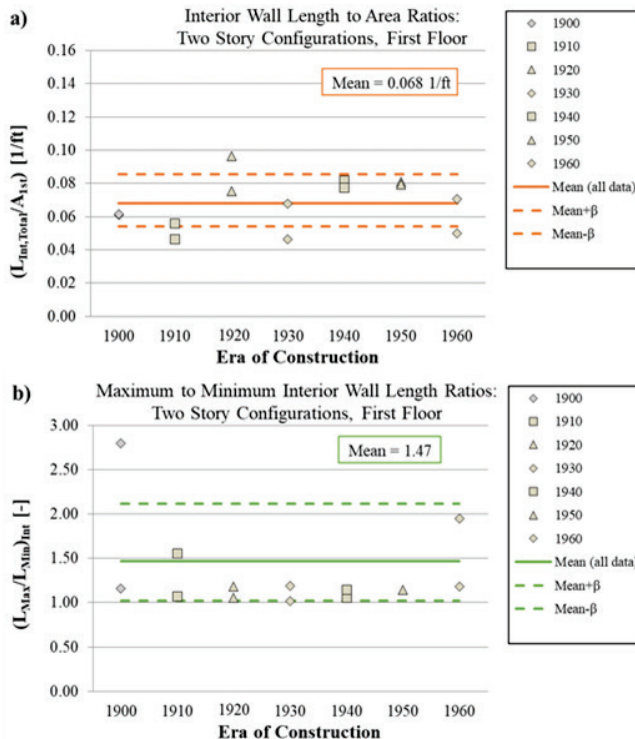


Figure 6-10 Interior wall criteria for the first floor of two-story configurations: (a) Interior wall density, (b) Maximum-to-minimum length ratio.

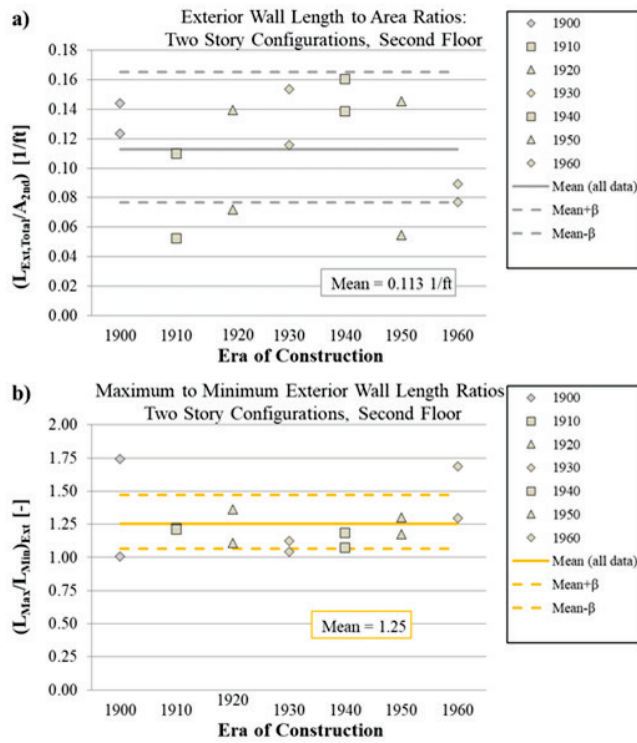


Figure 6-11 Exterior criteria for the second floor of two-story configurations:
(a) Exterior wall density, (b) Maximum-to-minimum length ratio.

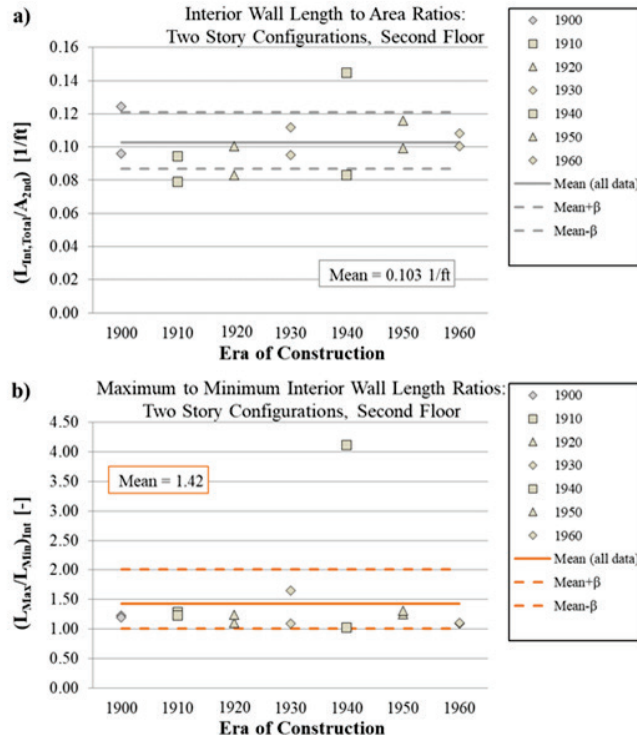


Figure 6-12 Interior criteria for the second floor of two-story configurations:
(a) Interior wall density, (b) Maximum-to-minimum length ratio.

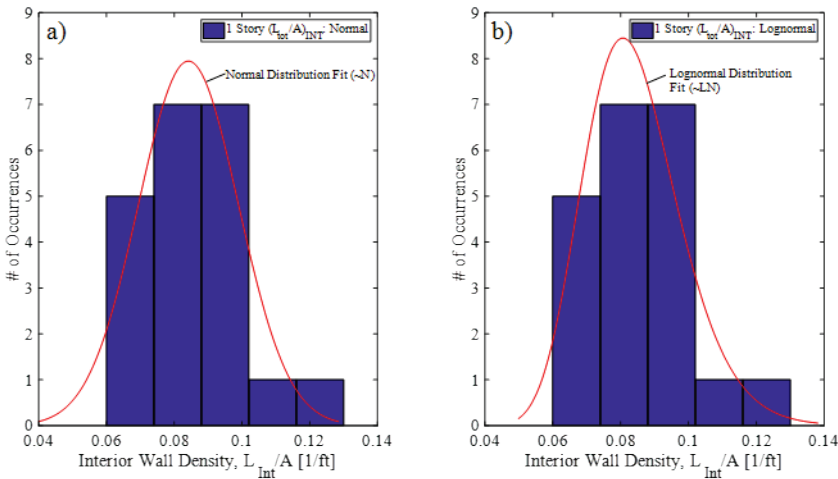


Figure 6-13 Comparing normal (a) and lognormal (b) distribution fits to interior wall density data for one-story cases.

Complete configuration geometry information is provided in Appendix A of this document.

6.3 Determining Physical Configuration Properties

The set of reviewed configurations and corresponding geometrical information is combined with physical material assumptions in order to obtain meaningful statistics on the expected range of strength and weight characteristics of older single-family dwellings. This section provides an overview on the material properties (i.e., weight and strength) assumed in order to relate the measured geometry of each configuration to physical engineering properties. Strengths are estimated using a simplified pushover approach and the resulting engineering parameters are used to define appropriate strength and weight properties in order to investigate the seismic performance of retrofitting cripple-wall dwellings.

6.3.1 Selected Physical Properties for Configuration Study

The geometrical properties were used in combination with assumed material weights (i.e., unit weights) and strengths (i.e., monotonic backbone curves) in order to obtain meaningful physical parameters for modeling representative superstructures. These parameters included:

1. Total weight-to-plan area ratios, W_T/A ;
2. Strong-to-weak direction strength ratios, $V_{\text{strong}}/V_{\text{weak}}$;
3. Average strength-to-seismic weight ratios, $(V/W_S)_{\text{Avg}}$; and,
4. Average strength-to-plan area ratios, $(V/A)_{\text{Avg}}$.

The average strength terms refer to the average strength of the two orthogonal directions of the configuration. The seismic weight (W_S) is the weight neglecting first floor diaphragms and one-half of the wall weight as if the structure was modeled on a rigid base. The total weight (W_T) includes all wall weights and first floor diaphragm weight.

For the two-story configurations, two additional parameters were calculated in order to relate the lower story to the upper story, namely:

1. Average second story-to-first story strength ratio, $(V_2/V_1)_{Avg}$; and,
2. Second-to-first story wall weight ratio, $W_{wall,2}/W_{wall,1}$.

An example illustration of the modeling parameters is shown in Figure 6-14 for the average strength-to-seismic weight ratios, $(V/W_S)_{Avg}$, for all one-story configurations.

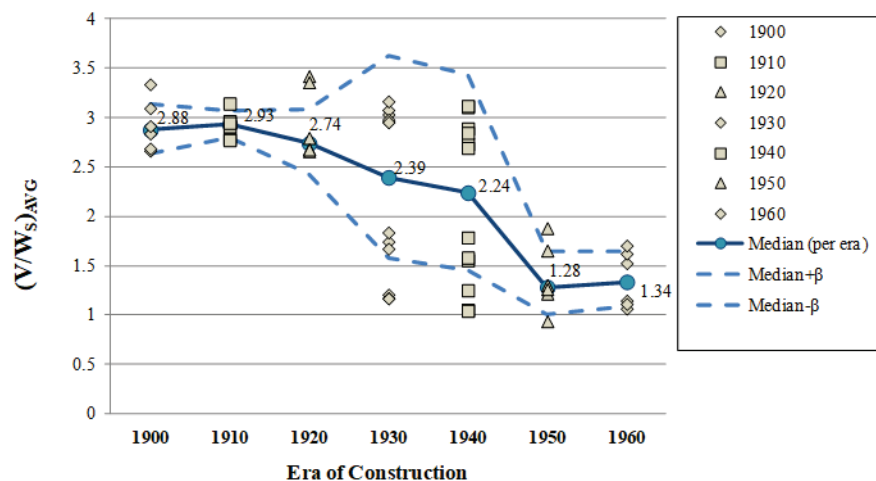


Figure 6-14 Sample of configuration data collected across different eras of construction showing the average superstructure strength to seismic weight ratios for all one-story configurations.

A number of exterior and interior materials common to the range of construction ages were considered. Stucco and horizontal wood siding were considered for exterior wall finishes. Interior gypsum and plaster on wood lath (*i.e.*, lath and plaster) were considered for interior wall finishes. The interior wall finish material assumed for each of the configurations varied as a function of the construction era. It was assumed that configurations constructed prior to 1930 exclusively had interior plaster on wood lath. Conversely, dwellings constructed in 1950 and later were assumed to have interior gypsum wallboard. The transition period of 1930 to 1949 assumed that either interior finish material could be present. The assumptions regarding era-specific materials is illustrated in Figure 6-15 for the same data provided in Figure 6-14.

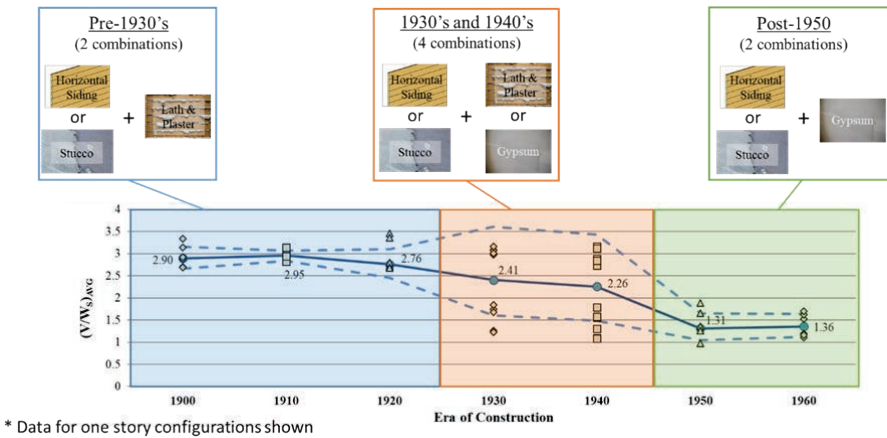


Figure 6-15 Illustration of the different building materials assumed when considering the existing building stock of cripple wall dwellings. Data shown is the average strength-to-seismic weight ratios for the one-story configurations.

The different combinations of materials require different weight and strength characteristics to be applied to each configuration. The assumed weight take-offs for the different material combinations are summarized in Table 6-2.

The weight calculations do not account for openings in the exterior walls and the estimated perimeter is used for these wall weights. For interior walls, only the weights of measured wall lengths are included and do not include weights of headers over doorways. Roof weights include additional area from eave overhang and the weight of gable ends add the exterior finish weight to the roof weight (i.e., assuming no interior finish in attic space).

Table 6-2 Summary of Weight Take-Off Assumptions for Superstructure Study for Analysis of Cripple Wall Dwellings

Exterior Material	Interior Material	1 st Floor w_{1st} [psf]	2 nd Floor w_{2nd} [psf]	Roof ¹ w_{roof} [psf]	Exterior Walls w_{ext} [psf]	Interior Walls w_{int} [psf]
Wood Siding	Gypsum	10.0	11.0	15.0	7.0	7.0
Wood Siding	Lath and Plaster	10.0	19.0	15.0	13.0	18.0
Stucco	Gypsum	10.0	11.0	15.0	14.5	7.0
Stucco	Lath and Plaster	10.0	19.0	15.0	23.0	18.0

¹ Roof loads assume asphalt shingle for all cases, reported value includes horizontal projection for 8:12 pitch

The material backbones used for the superstructure study assume the SAWS hysteresis model (MSTEW within *Timber3D* software; a.k.a. CUREE model) (Folz and Filiatrault, 2004; Christovasilis and Filiatrault, 2009) to define the monotonic capacity curves for each material. The SAWS backbone curve is defined by five parameters: (1) initial stiffness, S_0 ; (2) theoretical yield force,

F0; (3) asymptotic post-yield stiffness fraction of initial stiffness to peak strength, R1; (4) post-peak stiffness as a fraction of initial stiffness, R2; and, (5) displacement (or drift) corresponding to peak force, DU. The relationships between the different SAWS backbone parameters is illustrated in Figure 6-16. The corresponding backbone curves (in normalized units) for the best-estimate material properties used for the superstructure configuration study are shown in Figure 6-17 with corresponding input parameters provided in Table 6-3. Background and justification for the selection of superstructure material properties can be found in the FEMA P-1100 Volume 3, Part 4 document.

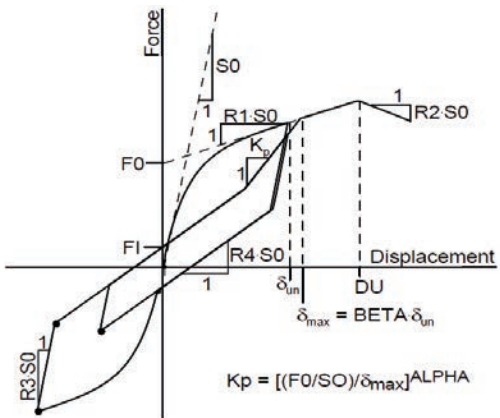


Figure 6-16 Illustration of the SAWS hysteretic model (image from Christovasilis and Filiault, 2009).

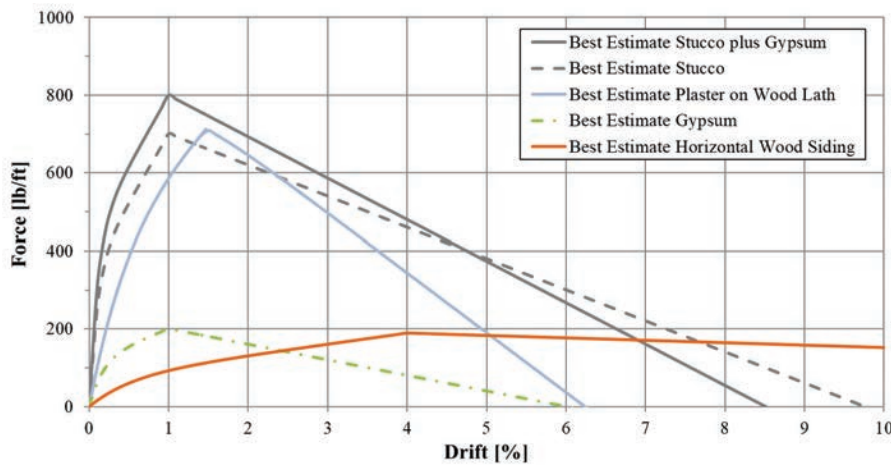


Figure 6-17 SAWS backbone curves for best-estimate materials used in superstructure study for analysis of cripple wall dwellings. Backbones reflect best-estimate properties.

Table 6-3 SAWS Backbone Parameters Used in Superstructure Configuration Study

Material ¹	S0 [lb/θ%-ft]	F0 [lb/ft]	R1	R2	DU [$\theta\%$] ²
Stucco plus Gypsum	4530.0	440.0	0.0795	-0.0235	1.00
Stucco	3750.0	350.0	0.0935	-0.0213	1.00
Lath and Plaster ³	1098.0	451.0	0.175	-0.1400	1.47
Gypsum ³	780.0	120.0	0.1030	-0.0513	1.00
Horizontal Wood Siding	169.5	75.0	0.17	-0.0370	4.00

¹ Materials reflect best-estimate properties;
² “θ%” represents drift ratio in percent;
³ Interior material properties reflect a single sided wall; the stiffness and strength properties (S0 and F0) are doubled for interior partition walls

The backbone properties of each material were used for each configuration to perform simplified pushover analysis in order to estimate superstructure strengths. The calculations were based on the assumption that all backbone curves in one direction shared the same lateral displacement, thereby neglecting torsional response. The backbone curves could be translated using expected wall lengths and wall heights to estimate the global strength properties. Most importantly, different force displacement behaviors (e.g., materials reaching peak capacity at different drift levels) were captured in the simplified pushover analysis.

The simplified technique was verified with pushover analyses of three-dimensional models for preliminary archetype configurations (see Figure 6-18) and the match proved adequate for quickly estimating peak strength. For three different control superstructures, the peak strength estimated using the simplified technique was within 2%-3% of the values obtained from explicit three-dimensional models using *Timber3D*. These discrepancies are largely due to the absence of second-order effects and gravity loading in the simplified analysis to estimate superstructure strengths. An example of one comparison case is provided in Figure 6-18.

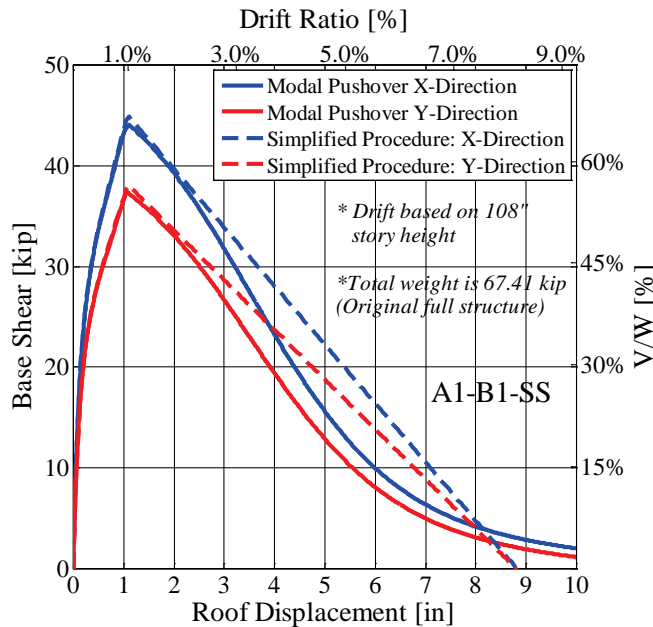


Figure 6-18 Example of simplified pushover analysis (dashed lines) and modal pushover analysis conducted in *Timber3D* using three-dimensional models (solid lines).

6.3.2 Superstructure Strength and Weight Properties from Configuration Study

The main assumption in utilizing the obtained strength and weight characteristics from the configuration sets was that two superstructure definitions would be targeted using the one- and two-story data separately. The first assumed the median properties of all configurations (of the same number of stories) from the 1900's to the 1940's (i.e., pre-1950 era). The second assumed the median minus one standard deviation (Median- β) of the strength properties for the post-1950 era, which included the configurations from the 1950's and 1960's from the configurations set. The result of this assumption was a stiff and strong superstructure controlled mostly by stucco and plaster on wood lath properties and a weak and flexible superstructure controlled by horizontal siding and gypsum properties. The logic behind the two generalized superstructure strengths is that the stronger and stiff (i.e., Median, pre-1950) superstructure will provide the greatest demands on crawlspace retrofits, while still maintaining realistic strength and mass proportions in the superstructure. Conversely, the weaker and more flexible variation (i.e., Median - β , post-1950) represents a lower bound of superstructure strength and stiffness to investigate the capability of crawlspace retrofits to "drive damage upstairs", a continuing concern with the strengthening of crawlspace dwellings. Further, the weaker variation indirectly considers the possibility of remodeling where smaller rooms may

be combined or expanded, and exterior openings may be enlarged (i.e., larger windows). Notably, the dispersion (β) represents the distribution in superstructure properties due to configuration variability only; weight take-offs and material strengths are maintained at best-estimate values.

6.3.2.1 Strength and Weight Data for One-Story Configurations

The total weight-to-plan area ratios (W_T/A) are shown for the one-story configurations in Figure 6-19. The corresponding median and dispersion values are provided in Table 6-3. The increased number of data points and scatter in Figure 6-19 for the 1930's and 1940's reflects the transition region of the era specific materials, recalling that each configuration has four combinations of interior and exterior material assumptions (see Figure 6-15).

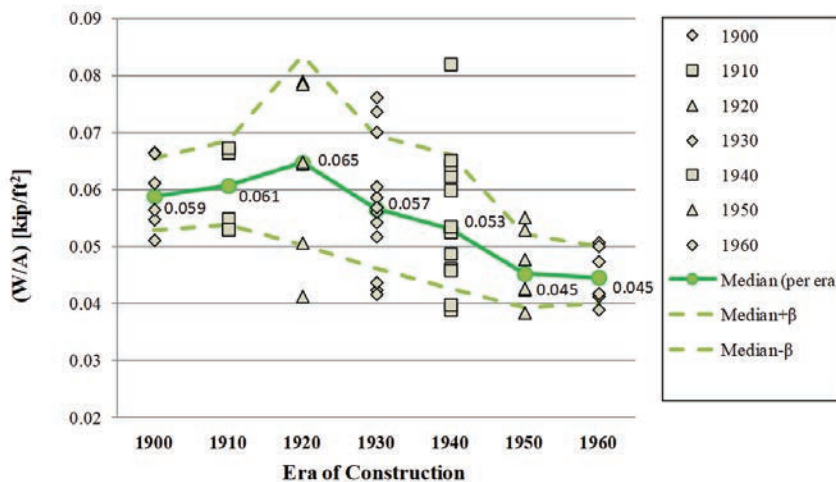


Figure 6-19 Total weight-to-plan area ratios for one-story configurations.

Table 6-4 Summary of Total Weight-to-Plan Area Ratios for One-Story Configurations

Era	1900	1910	1920	1930	1940	1950	1960	1900-1940	1950-1960	Total
Median (W_T/A)	0.059	0.061	0.065	0.057	0.053	0.045	0.045	0.057	0.045	0.054
Median+ β	0.066	0.069	0.083	0.069	0.066	0.052	0.050	0.069	0.051	0.067
Median- β	0.053	0.054	0.050	0.046	0.043	0.039	0.040	0.047	0.040	0.043
β_{LN}	0.11	0.12	0.25	0.20	0.22	0.14	0.11	0.20	0.12	0.22

The strong-to-weak-direction strength ratios ($V_{\text{strong}}/V_{\text{weak}}$) are provided in Figure 6-20 (values in Table 6-5). The median values across different eras do not fluctuate significantly. However, maximum values exceed 1.3 for a few configurations, representing a range of different plan layouts and openings when converting to estimated strength.

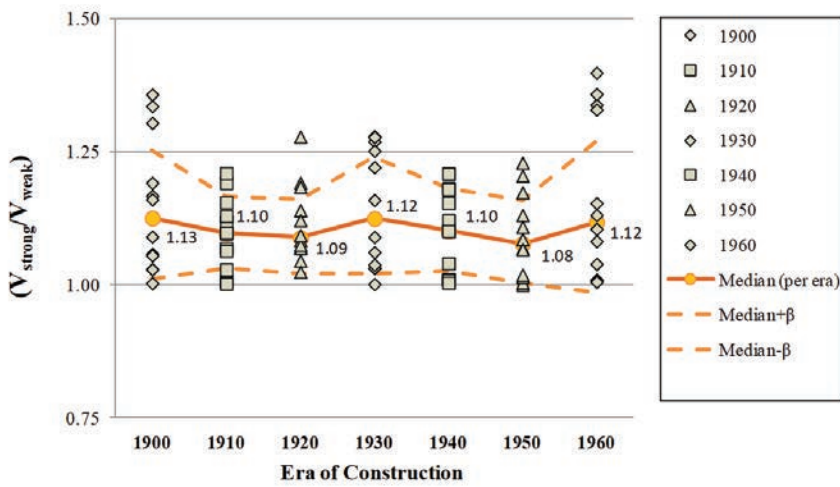


Figure 6-20 Strong-to-weak direction strength ratios for one-story configurations.

Table 6-5 Summary of Strong-to-Weak Direction Strength Ratios for One-Story Configurations

Era	1900	1910	1920	1930	1940	1950	1960	Total
Median ($V_{\text{strong}}/V_{\text{weak}}$)	1.13	1.10	1.09	1.12	1.10	1.08	1.12	1.10
Median+ β	1.25	1.17	1.16	1.24	1.18	1.16	1.27	1.20
Median- β	1.01	1.03	1.02	1.02	1.03	1.00	0.98	1.00
β_{LN}	0.11	0.06	0.06	0.10	0.07	0.07	0.13	0.09

The superstructure strength of configurations is defined by two different parameters. The average strength-to-seismic weight ratio and the strength-to-area ratio. The average strength represents the average of the two orthogonal directions of each configuration and material combination. Strength-to-weight ratios for one-story configurations are shown in Figure 6-21 (values in Table 6-6). The strength-to-area ratios are provided in Figure 6-22 and Table 6-7.

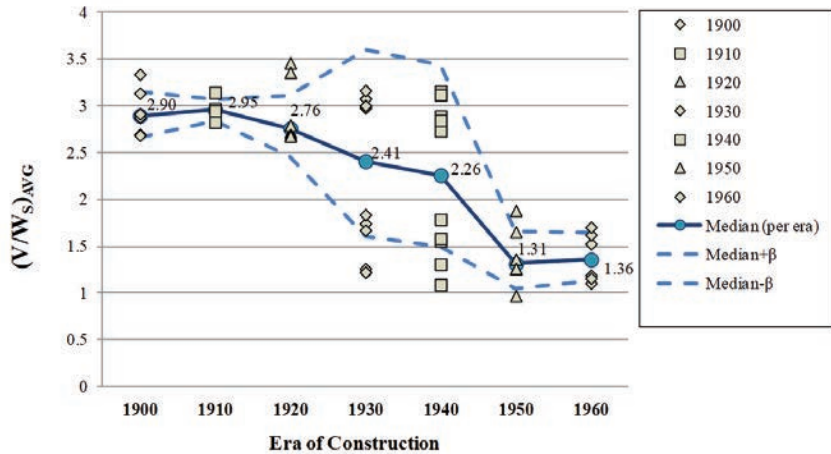


Figure 6-21 Strength-to-seismic weight ratios for one-story configurations.

Table 6-6 Summary of Strength-to-Seismic Weight Ratios for One-Story Configurations

Era	1900	1910	1920	1930	1940	1950	1960	1900-1940	1950-1960	Total
Median (V/W_s) _{Avg}	2.88	2.93	2.74	2.39	2.24	1.31	1.36	2.79	1.31	2.68
Median+ β	3.14	3.07	3.08	3.63	3.44	1.65	1.64	4.01	1.61	4.05
Median- β	2.64	2.80	2.43	1.58	1.46	1.04	1.12	1.94	1.07	1.78
θ_{IN}	0.09	0.05	0.12	0.42	0.43	0.23	0.19	0.36	0.20	0.41

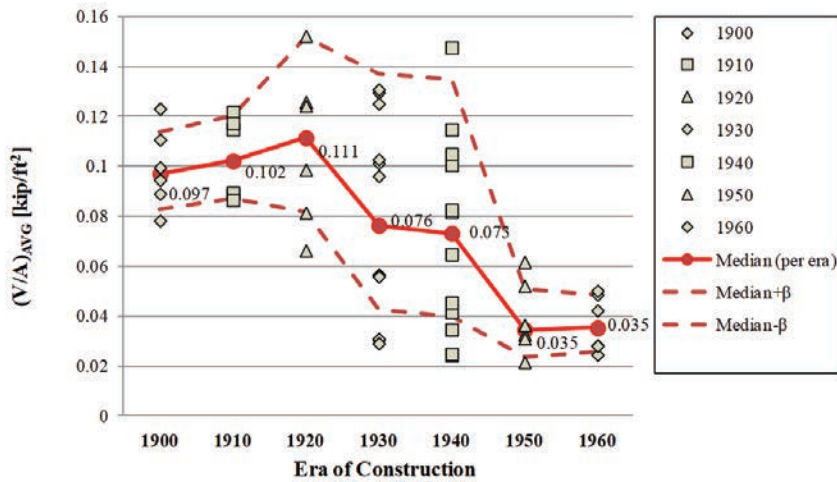


Figure 6-22 Strength-to-plan area ratios for one-story configurations.

Table 6-7 Summary of Strength-to-Plan Area Ratios for One-Story Configurations (UNITS: kip/ft²)

Era	1900	1910	1920	1930	1940	1950	1960	1900-1940	1950-1960	Total
Median (V/A) _{Avg}	0.097	0.102	0.111	0.076	0.073	0.035	0.035	0.092	0.035	0.082
Median+ β	0.114	0.120	0.152	0.137	0.135	0.050	0.048	0.153	0.048	0.146
Median- β	0.083	0.087	0.082	0.043	0.040	0.024	0.026	0.055	0.026	0.046
β_{LN}	0.16	0.16	0.31	0.58	0.61	0.38	0.31	0.51	0.33	0.57

6.3.2.2 Strength and Weight Data for Two-Story Configurations

The total weight-to-plan area ratios (W_T/A) are shown for the two-story configurations in Figure 6-23. The corresponding median and dispersion values are provided in Table 6-8. In order to monitor the weight difference between lower and upper stories, the second-to-first-story wall weight ratios ($W_{wall,2}/W_{wall,1}$) were also calculated as shown in Figure 6-24 (values in Table 6-9).

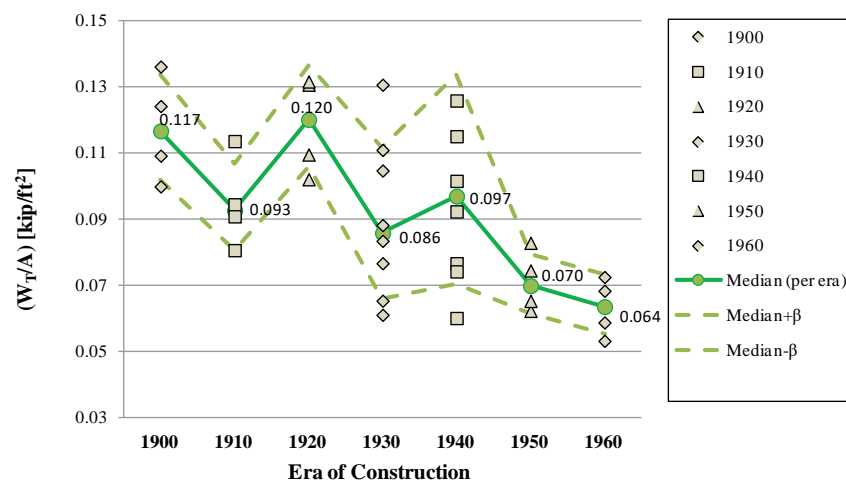


Figure 6-23 Total weight-to-plan area ratios for two-story configurations.

Table 6-8 Summary of Total Weight-to-Plan Area Ratios for One-Story Configurations

Era	1900	1910	1920	1930	1940	1950	1960	1900-1940	1950-1960	Total
Median (W_T/A) [kip/ft ²]	0.117	0.093	0.120	0.086	0.097	0.070	0.064	0.102	0.067	0.092
Median+ β	0.134	0.107	0.136	0.112	0.133	0.080	0.073	0.131	0.077	0.122
Median- β	0.102	0.080	0.106	0.066	0.071	0.061	0.055	0.079	0.058	0.069
β_{LN}	0.14	0.14	0.13	0.26	0.32	0.13	0.14	0.25	0.14	0.28

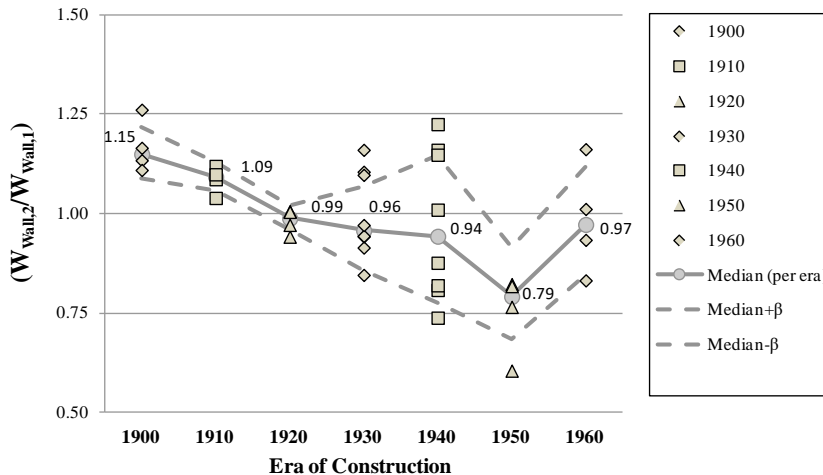


Figure 6-24 Second-to-first-story wall weight ratios for two-story configurations.

Table 6-9 Summary of Second-to-First-Story Wall Weight Ratios for Two-Story Configurations

Era	1900	1910	1920	1930	1940	1950	1960	1900-1940	1950-1960	Total
Median (W_{w2}/W_{w1})	1.15	1.09	0.99	0.96	0.94	0.79	0.97	1.02	0.83	1.01
Median+ β	1.22	1.13	1.02	1.07	1.14	0.91	1.12	1.17	1.01	1.19
Median- β	1.09	1.06	0.96	0.86	0.78	0.69	0.85	0.90	0.68	0.85
β_{LN}	0.06	0.03	0.03	0.11	0.19	0.14	0.14	0.13	0.19	0.16

The strong-to-weak-direction strength ratios ($V_{\text{strong}}/V_{\text{weak}}$) for the bottom story of two-story configurations are provided in Figure 6-25 (values in Table 6-10). Additionally, the second-to-first-story strength ratios (V_2/V_1)_{Avg} are calculated to relate bottom story strength to the upper story (see Figure 6-26; Table 6-11) which are taken as the average of the two orthogonal directions.

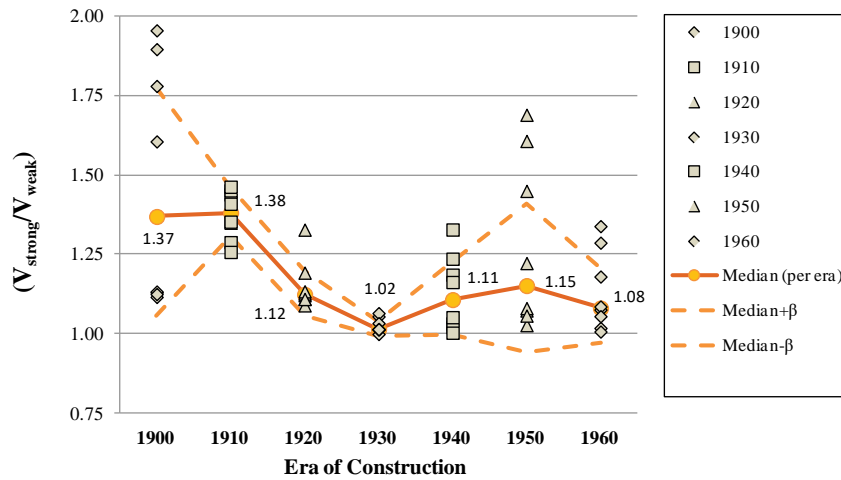


Figure 6-25 Strong-to-weak direction strength ratios for the bottom story of two-story configurations.

Table 6-10 Summary of Strong-to-Weak Direction Strength Ratios for the Bottom Story of two-Story Configurations

Era	1900	1910	1920	1930	1940	1950	1960	Total
Median ($V_{\text{strong}}/V_{\text{weak}}$)	1.37	1.38	1.12	1.02	1.11	1.15	1.08	1.13
Median+ β	1.77	1.46	1.20	1.04	1.23	1.41	1.20	1.34
Median- β	1.06	1.31	1.05	0.99	1.00	0.94	0.97	0.95
δ_{LN}	0.26	0.06	0.06	0.02	0.10	0.20	0.11	0.17

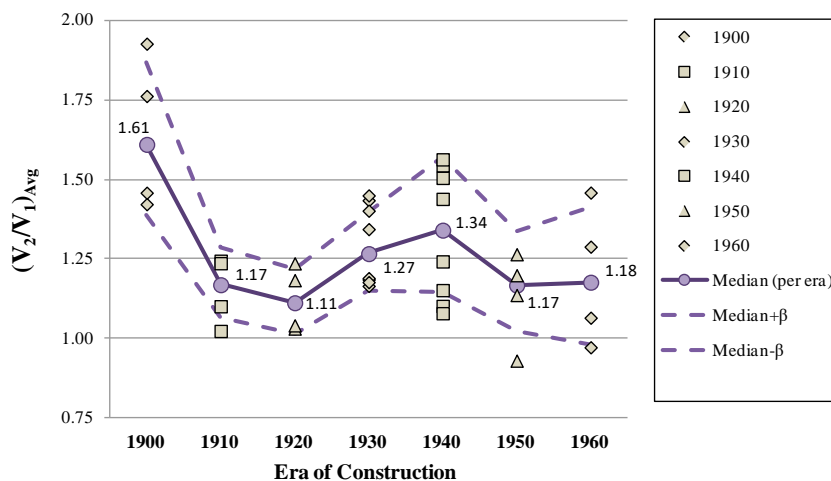


Figure 6-26 First-to-second-story strength ratios for two-story configurations.

Table 6-11 Summary of Second- to-First-Story Strength Ratios for Two-Story Configurations

Era	1900	1910	1920	1930	1940	1950	1960	Total
Median ($V_2/V_{1\text{Avg}}$)	1.61	1.17	1.11	1.27	1.34	1.17	1.18	1.24
Median+ β	1.87	1.29	1.22	1.40	1.57	1.34	1.41	1.46
Median- β	1.39	1.06	1.02	1.15	1.15	1.02	0.98	1.05
β_{LN}	0.15	0.09	0.09	0.10	0.16	0.13	0.18	0.16

The normalized superstructure strength properties of two-story configurations are defined by the average strength-to-seismic weight ratio (V/W)_{Avg} and the strength-to-area ratio (V/A)_{Avg} of the bottom story. The average strength represents the average of the two orthogonal directions of each configuration and material combination. Strength-to-weight ratios for two-story configurations are shown in Figure 6-27 (values in Table 6-12). The strength-to-area ratios are provided in Figure 6-28 and Table 6-13.

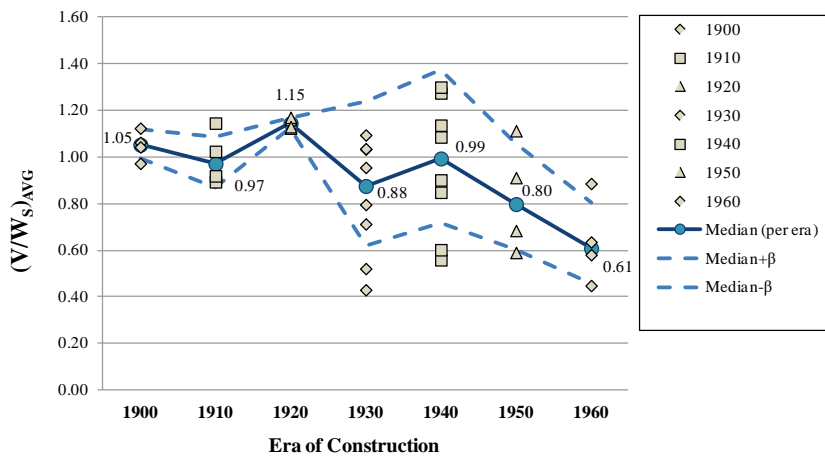


Figure 6-27 Strength-to-seismic weight ratios for the bottom story of two-story configurations.

Table 6-12 Summary of Strength-to-Seismic Weight Ratios for the Bottom Story of Two-Story Configurations

Era	1900	1910	1920	1930	1940	1950	1960	1900-1940	1950-1960	Total
Median ($V/W_{S\text{Avg}}$)	1.05	0.97	1.15	0.88	0.99	0.80	0.61	1.04	0.66	0.96
Median+ β	1.12	1.09	1.17	1.24	1.37	1.06	0.81	1.37	0.89	1.31
Median- β	0.99	0.87	1.12	0.62	0.72	0.60	0.46	0.78	0.51	0.71
β_{LN}	0.06	0.11	0.02	0.35	0.32	0.28	0.28	0.28	0.30	0.30

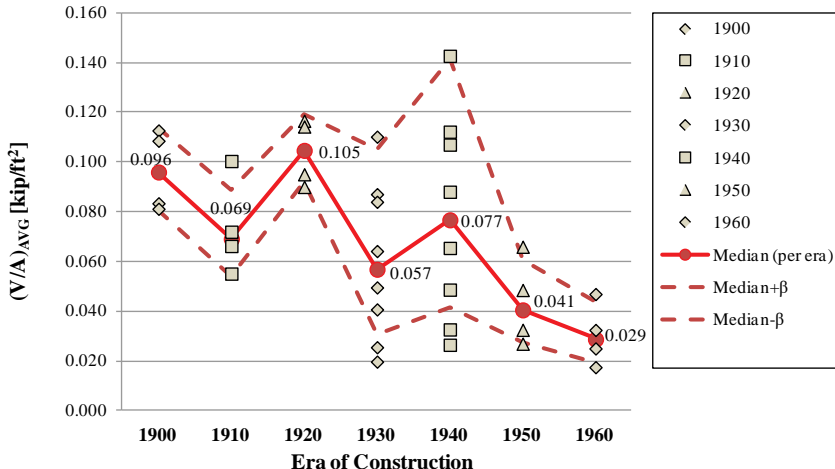


Figure 6-28 Strength-to-area ratios for the bottom story of two-story configurations.

Table 6-13 Summary of Strength-to-Area Ratios for the Bottom Story of Two-Story Configurations

Era	1900	1910	1920	1930	1940	1950	1960	1900-1940	1950-1960	Total
Median (V/A) _{Avg}	0.096	0.069	0.105	0.057	0.077	0.041	0.029	0.084	0.032	0.066
Median+ β	0.114	0.089	0.119	0.105	0.141	0.061	0.044	0.141	0.050	0.118
Median- β	0.081	0.054	0.092	0.031	0.042	0.027	0.019	0.050	0.022	0.037
β_{LN}	0.17	0.25	0.13	0.61	0.61	0.40	0.42	0.52	0.43	0.58

6.4 Developing Baseline Archetypes for Numerical Analysis

This section covers the calculations and assumptions to produce a set of four different superstructure types for the analysis of cripple wall dwellings. The baseline configurations that are modified to fit the target criteria obtained from the configuration data set are introduced. The basic numerical modeling strategy is discussed in order to illustrate how superstructure modifications were made. Finally, all necessary calculations and underlying assumptions in order to produce the archetype structures are defined.

6.4.1 Baseline Archetype Configurations

The baseline archetypes used to represent the superstructure (i.e., occupied stories above the crawlspace) of analyzed dwellings are 40 feet by 30 feet in plan dimensions (i.e., 1200 ft²). Story heights are 9 feet. Floor diaphragms are 10 inches deep. The roof geometry is assumed a hip roof with an 8:12 pitch and an 18-inch eave around the perimeter. The configuration of the

occupied stories was based on the CUREE Small House index building (Isoda *et al.* 2002) configuration with a much simpler interior partition wall layout in order to reduce torsional response and accommodate strength and mass scaling when calibrating to superstructure study results (refer Section 6.3). This small house index building was developed to exemplify post-World War II affordable housing that was constructed in large quantities, either in tracts or one-by-one by small contractors or owner builders. This was the kind of building that was originally intended for the application of the building code's (Uniform Building Code's) prescriptive construction provisions. Figures 6-29 and 6-30 show renderings of one- and two-story superstructure configurations on two-foot cripple walls.

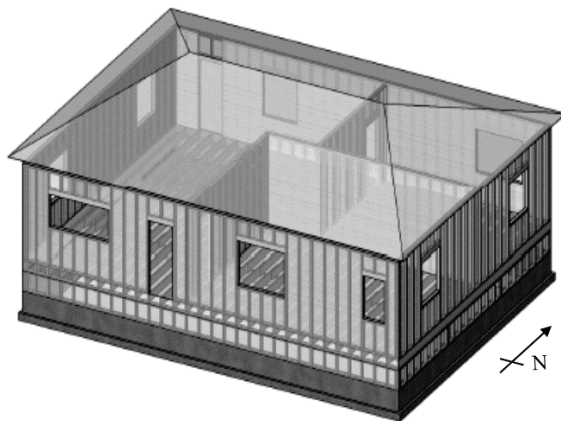


Figure 6-29 Rendering of one-story superstructure baseline configuration used in numerical modeling (rendering depicts structure on a 2-foot tall cripple-wall).

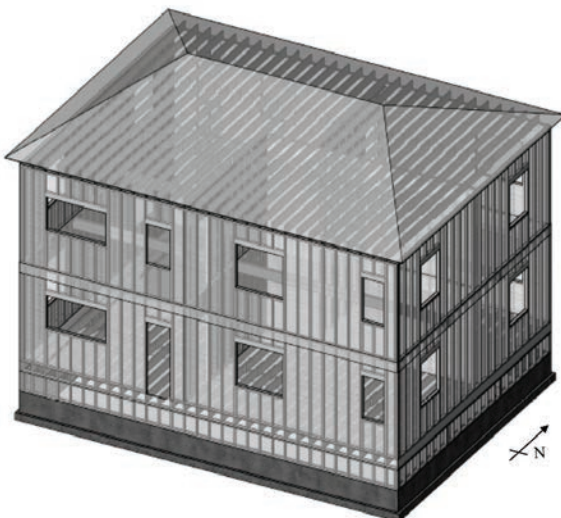


Figure 6-30 Rendering of baseline two-story superstructure configuration on two-foot cripple-wall used in numerical modeling.

Both one-story and two-story configurations assume the same layout of exterior openings and interior walls. The two-story configuration replaces doors with windows of the same width to produce a consistent full wall height distribution around the perimeter. A plan view of the one- and two-story superstructure configurations is shown in Figure 6-31.

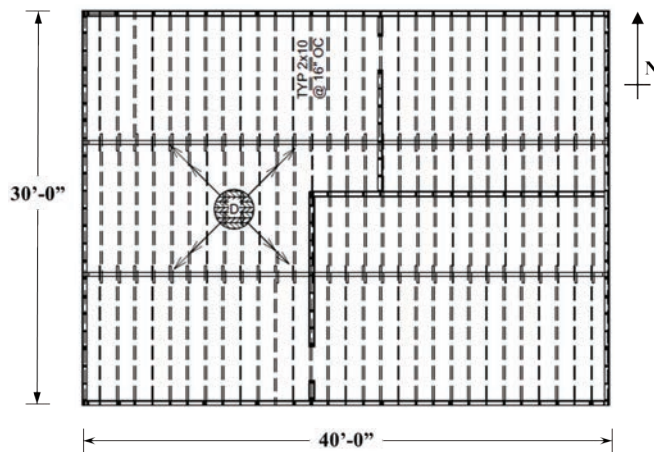


Figure 6-31 Plan view of the one- and two-story configurations selected for modeling of cripple-wall dwellings.

The baseline configurations are modeled in *Timber3D* (Pang et al., 2012) using the building block approach described in the FEMA P-1100 Volume 3, Part 5 *Protocol for FEMA P-1100 Numerical Studies* document. An example cripple-wall dwelling is compared with its equivalent modeling components within *Timber3D* in Figure 6-32.

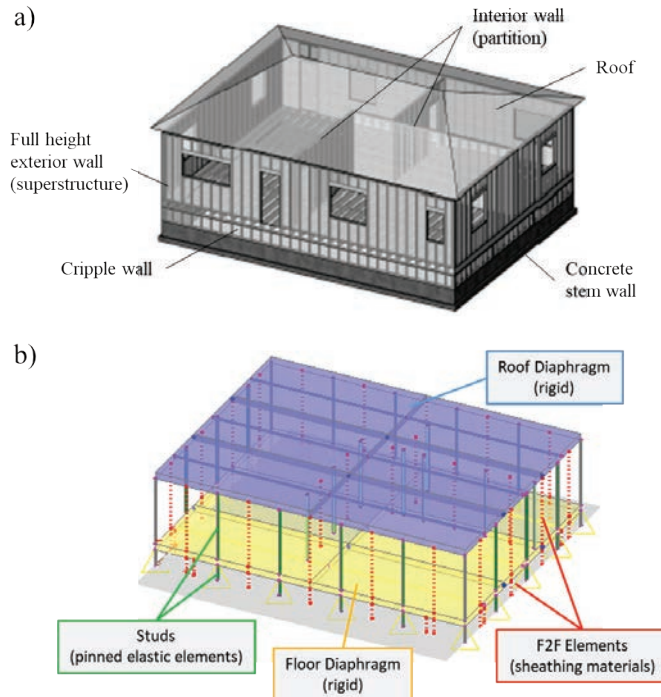


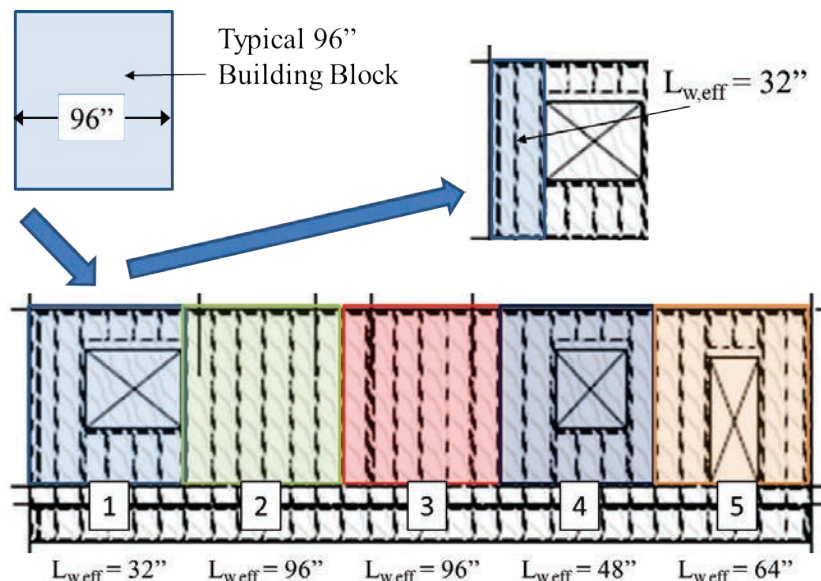
Figure 6-32 Illustration of the basic modelling components of a cripple wall dwelling: (a) Rendering and components of one-story house with two-foot tall cripple-walls; (b) Equivalent model in *Timber3D*.

Figure 6-32 shows that the floor and roof diaphragms are assembled as an array of six large elastic beam elements with a depth corresponding to the depth of the floor joists and flooring. Assuming rigid diaphragm action, the beam elements are assigned very high stiffness in both flexure and shear. The diaphragm beams are connected with rigid elastic Frame-to-Frame (F2F) link elements at the joints of adjacent beam elements to produce rigid diaphragm action. The floor and roof diaphragms are applied the corresponding flat loads for gravity and lateral mass (see Section 6.3.1).

The floor and roof diaphragms are supported vertically by pinned elastic stud elements. The stud elements are located at a spacing of 8 feet or 6 feet (around the perimeter of the house and are located at the ends and centers of interior partition walls at a spacing of 8 feet or 6.67 feet). The studs provide vertical support for the structure and provide locations for wall dead loads. The hysteretic behavior of sheathing materials is applied within F2F link elements that act as shear springs between each pair of studs.

The treatment of wall openings in exterior wall lines assumes that only full height wall sections (i.e., full wall piers) contribute to the effective length ($L_{w,eff}$) of a given building block section as proposed by Patton-Mallory *et al.* (1985). Despite numerous relationships existing in the literature for treatment

of openings of plywood shear walls (*e.g.*, Yasamura and Sugiyama, 1984; Johnson, 1997; FEMA, 2012) the full wall pier height effective length assumption was the most convenient to keep consistent when considering numerous material types and configurations for archetype development. Notably, the relationship proposed in FEMA P-807 Equation 4-3 (FEMA, 2012) was found to give similar results as those obtained using the simpler full wall pier height assumption. An example of the effective lengths used for each building block is shown in Figure 6-33. The figure shows that the 40-foot long north side of the one-story archetype configuration is broken into five separate eight-foot building blocks. The F2F link elements representing the sheathing materials will represent the annotated effective wall lengths within the numerical model. A summary of the effective wall lengths assumed for the exterior wall line building blocks is provided in Table 6-16. The same effective lengths are used for one- and two-story configurations prior to modification based on the assumed era of construction (see Section 6.4.2).



*Current example shows the North wall of the one-story house

Figure 6-33 Example of the effective length assumption used for accounting for openings within building block of exterior wall lines. Current example is for the north wall line of the one-story configuration.

The building block discretization of all exterior wall lines is illustrated in Figure 6-34 with corresponding effective lengths of each block provided in Table 6-14. Notably, the arrows and numbering in Figure 6-34 correspond to the order of building blocks presented in Table 6-14.

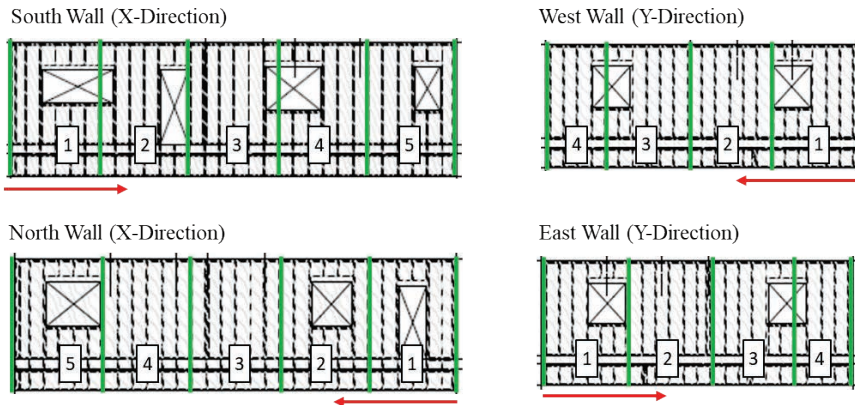


Figure 6-34 Building block discretization for exterior wall lines of archetype buildings.

Table 6-14 Effective Lengths of Exterior Building Blocks for the Superstructure Modeling of Archetype Dwellings (see Figure 6-34)

Wall Line	Block Number	L_{block} [in]	$L_{w,eff}$ [in] (%total)
South Wall (X-Direction)	1	96	32
	2	96	48
	3	96	80
	4	96	48
	5	96	64
	Total South	480	272 (57%)
North Wall (X-Direction)	1	96	64
	2	96	48
	3	96	96
	4	96	96
	5	96	32
	Total North	480	336 (70%)
West Wall (Y-Direction)	1	96	48
	2	96	96
	3	96	64
	4	72	48
	Total West	360	256 (71%)
East Wall (Y-Direction)	1	96	48
	2	96	96
	3	96	64
	4	72	48
	Total East	360	256 (71%)
Total Perimeter		1680	1120 (67%)

The interior walls are annotated in Figure 6-35 with corresponding building block discretization defined in Table 6-15. The small return walls within interior wall lines 1 and 3 are not considered for contributing to effective wall length as shown in Figure 6-35. Referring to Table 6-15, it can be seen that interior wall line 1 is broken into two separate 80-inch sections while line 3 is modeled as a single 80-inch long section. Interior wall line 2 is broken into three separate building block sections. Notably, the effective interior lengths do not account for gypsum being applied on both sides of the interior walls.

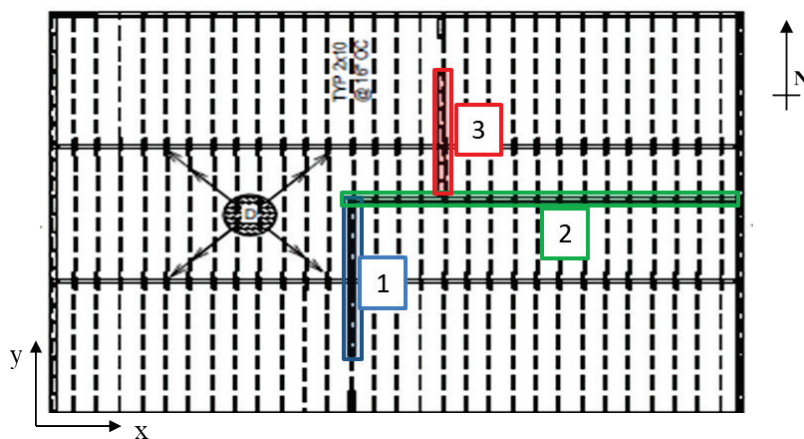


Figure 6-35 Locations of interior walls assumed in archetype configurations.

Table 6-15 Building Block Discretization and Effective Lengths for Interior Superstructure Walls (see Figure 6-35)

Interior Wall	No. of Studs	No. of Blocks	Block ID	$L_{w,eff}$ [in]
1	3	2	a	80
			b	80
2	4	3	a	96
			b	96
			c	80
3	2	1	a	80

6.4.2 Modification Factors to Represent Configuration Data

In order to incorporate the information obtained from the configuration study conducted to better represent the building stock, three modification factors (MF) were introduced to adjust the baseline superstructure models presented in Section 6.4.1. Notably, a number of parameters obtained from the configuration study described in Section 6.3 as well as subsequent calculations were used to arrive at these MFs. These final MFs are described in this section with underlying assumptions and calculations illustrated. A

full description of the configuration study calculations is provided in the FEMA P-1100 Volume 4, WG4-B5 document.

Representative vertical loading and lateral mass was obtained using a mass modification factor, MF_m , that was applied uniformly to all discrete masses within the baseline configuration model (i.e., every diaphragm mass and stud end location). The two remaining factors are the wall length modification factors, $MF_{L,X}$ and $MF_{L,Y}$, that scale the effective wall lengths of the baseline configuration to match the target strength parameters.

The incorporation of the configuration data presented in Section 6.3.2 required several assumptions. Recalling that the objective was to have a realistic range of superstructure strength and stiffness for the building archetypes, these assumptions were made toward this goal. The assumptions are outlined as follows:

- Total weight-to-area ratios (W_T/A) are taken as the median value for each era (i.e., weights are not reduced by standard deviation for the “Median- β ” cases). Baseline archetypes have mass locations scaled to meet this parameter.
- The target strength of the superstructure is based on the average value of the strength-to-seismic weight ratio and the strength-to-area ratio. Pre-1950’s Median configurations (one- and two-story) take the median values of these two parameters from the 1900 to 1940 eras. Post-1950’s Median- β configurations (one- and two-story) take the median minus one standard deviation of these parameters from the 1950 to 1960 eras.
- Strong-to-weak direction strength ratios ($V_{\text{strong}}/V_{\text{weak}}$) assume the median value for all configurations (i.e., 1900-1960) since this parameter is a function of wall and opening distribution and is not affected by era specific materials.
- Two-story configurations do not include adjustments between first and second stories (i.e., mass scaling is performed uniformly over the entire structure and first and second story strengths are assumed equal). This assumption is not expected to change the superstructure performance significantly.
- The pre-1950’s Median baseline materials and wall weights are best-estimate gypsum interior and best-estimate stucco plus gypsum exterior (refer to Section 6.3.1 and FEMA P-1100 Volume 3, Part 4 for material properties used for dynamic analysis).
- The post-1950’s Median- β baseline materials and wall weights are best-estimate gypsum interior and horizontal wood siding exterior (refer to

Section 6.3.1 and FEMA P-1100 Volume 3, Part 4 for material properties used for dynamic analysis).

The information from Section 6.3.2 that was used for the modification of baseline archetypes is presented in Table 6-16 with the corresponding table number of Section 6.3.2 annotated for reference. An example calculation is provided for the one-story pre-1950 Median superstructure is shown in Figure 6-36. All similar calculations are provided in FEMA P-1100 Volume 4, document WG4-B7.

Table 6-16 Configuration Data Used for Modification Calculations (Numbers in Parentheses Indicate Appropriate Table Number for Reference)

Superstructure Type	Total weight-to-area ratio W/A [kip/ft ²]	Strong-to-Weak Direction Strength Ratio V_{strong}/V_{weak} [-]	Average Strength-to-Seismic Weight Ratio $(V/W_s)_{Avg}$ [-]	Average Strength-to-Area Ratios $(V/A)_{Avg}$ [kip/ft ²]
1-story Median pre-1950	0.057 (Table 6-4)	1.10 (Table 6-5)	2.79 (Table 6-6)	0.092 (Table 6-7)
2-story Median pre-1950	0.102 (Table 6-8)	1.13 (Table 6-10)	1.04 (Table 6-12)	0.084 (Table 6-13)
1-story Median- β post-1950	0.045 (Table 6-4)	1.10 (Table 6-5)	1.07 (Table 6-6)	0.026 (Table 6-7)
2-story Median- β post-1950	0.067 (Table 6-8)	1.13 (Table 6-10)	0.51 (Table 6-12)	0.022 (Table 6-13)

¹ ID assumes the superstructure only on a rigid-base; ² All materials assume best-estimate properties and weight take-offs described in Section 6.2 prior to adjustment; ³ All modification factors (MF) are applied uniformly to baseline configurations

The summary of modification factors from the baseline configurations and baseline (i.e., unmodified) material assumptions for each era are presented in Table 6-17. The listed archetype ID corresponds to the cripple wall dwelling nomenclature which is described in FEMA P-1100 Volume 3, Part 11. The baseline materials listed are the starting materials applied to the baseline configurations (see Section 6.4.1). The relative magnitudes of the required scale factors are largely related to small number of interior walls assumed in the baseline plan (see Figure 6-31). For example, the post-1950's Median- β cases (one- and two-story) require modest increases in wall length modification since the baseline materials are the same as those assumed in the configurations for the 1950's and 1960's eras. The modification factors for these cases can be interpreted as being influenced by wall density alone. Conversely, the pre-1950's Median cases (one- and two-story) are based on having interior gypsum when the strength is largely controlled by the much stronger lath and plaster assumed for this era of construction. As such, the strength modification factors for these cases are much higher due to the

combined effect of representing a stronger interior and a higher wall density than the baseline interior wall layout.

<u>One-Story Pre-1950's Median Superstructure</u>	
<u>Step 1:</u> Modify total building weight based on target $W_T/A \approx 0.057 \text{ kip}/\text{ft}^2$	
Existing Baseline Structure: $A = (30\text{ft})(40\text{ft}) = 1200 \text{ ft}^2$; $W_T = 65.45 \text{ kip}$ (Total weight) $(W_T/A)_{\text{Existing}} = 65.45 \text{ kip} / 1200 \text{ ft}^2 = 0.055 \text{ kip}/\text{ft}^2$	
Required Modification: $\boxed{MF_m = (W_T/A)_{\text{Target}} / (W_T/A)_{\text{Existing}} = 0.057 / 0.055 = 1.04}$	
<u>Step 2:</u> Estimate average strength based on $(V/W_S)_{\text{Avg}} \approx 2.79$	
$W_{S,\text{Existing}} = 37.3 \text{ kip}$ (Seismic weight includes half of walls plus roof) $W_S = (W_{S,\text{Existing}})(MF_m) = (37.3 \text{ kip})(1.042) = 38.87 \text{ kip}$ $V'_w = (V/W_S)_{\text{Avg}}(W_S) = 2.79(38.87 \text{ kip}) = 108.45 \text{ kip}$	
<u>Step 3:</u> Estimate average strength based on $(V/A)_{\text{Avg}} \approx 0.092 \text{ kip}/\text{ft}^2$	
$V'_A = (V/A)_{\text{Avg}}(A) = (0.092 \text{ kip}/\text{ft}^2)(1200 \text{ ft}^2) = 110.40 \text{ kip}$	
<u>Step 4:</u> Estimate required strength based on average of steps 2 and 3	
$V'_{\text{Avg}} = (V'_A + V'_w)/2 = (110.4 \text{ kip} + 108.5 \text{ kip})/2 = 109.4 \text{ kip}$	
<u>Step 5:</u> Scale effective wall lengths to achieve desired strength properties -Required average strength of X and Y directions: $V'_{\text{Avg}} = 109.4 \text{ kip}$ -Required strong to weak direction ratio: $V_{\text{Strong}} / V_{\text{Weak}} = 1.10$	
Required Modification: $\boxed{MF_{L,X} = 2.58 \quad MF_{L,Y} = 2.77}$	

Figure 6-36 Example calculation for modifying the one-story baseline configuration with stucco and gypsum materials to the pre-1950's Median superstructure parameters.

Table 6-17 Modification Factors Applied to Baseline Superstructure Configurations to Target Era-Specific Assumptions

Superstructure Type	Archetype ID ¹	Baseline Materials ²	Mass Modification (MF_m) ³	Wall Length in X-Direction ($MF_{L,X}$)	Wall Length in X-Direction ($MF_{L,Y}$)
1-story Median pre-1950	4-1R-M-E	Stucco/ Gypsum Wallboard	1.04	2.58	2.77
2-story Median pre-1950	4-2R-M-E	Stucco/ Gypsum Wallboard	1.10	2.35	2.46
1-story Median-6 post-1950	4-1R-M6-E	Horizontal Wood Siding/ Gypsum Wallboard	1.19	1.54	1.58
2-story Median-6 post-1950	4-2R-M6-E	Horizontal Wood Siding/ Gypsum Wallboard	1.14	1.32	1.36

¹ ID assumes the superstructure only on a rigid-base; ² All materials assume best-estimate properties and weight take-offs prior to adjustment; ³ All modification factors (MF) are applied uniformly to baseline configurations

6.4.3 Summary Properties of Superstructure Configurations

The properties of the four superstructure configurations considered for the analysis of cripple wall dwellings is summarized in Table 6-18. The modal pushover curves for each of the modified superstructure configurations are presented in Figures 6-37 to 6-40. The individual pushover curves show both absolute units (i.e., kips, inches) and normalized units of roof drift ratio and strength to total weight (V/W_T). The pushover strength is normalized to total weight since this parameter is used to monitor the performance of different cripple wall dwellings (i.e., the weight that the cripple wall must resist laterally) within the numerical analysis studies (refer to FEMA P-1100 Volume 3, Part 11). A comparison of all four superstructure pushover curves is provided in Figure 6-41 to illustrate the differences between superstructure archetypes. More detailed information for each superstructure model is provided in FEMA P-1100 Volume 4, document WG-B7.

Table 6-18 Summary of Superstructure Configuration Properties for the Analysis of Cripple Wall Dwellings. Structural Models Assume A Rigid Base (Pinned Connection) to the Ground Level

Super-structure Type	Archetype ID ¹	T_1 [s] ²	T_2 [s] ²	Seismic Weight W_s [kip] ³	Total Weight W_T [kip] ³	$V_{max,X}$ [kip]	$V_{max,Y}$ [kip]
1-story Median pre-1950	4-1R-M-E	0.086	0.083	38.9	68.2	114.5	104.4
2-story Median pre-1950	4-2R-M-E	0.154	0.145	93.2	122.3	103.5	91.8
1-story Median- δ post-1950	4-1R-M δ -E	0.179	0.174	32.5	54.1	34.9	31.3
2-story Median- δ post-1950	4-2R-M δ -E	0.300	0.291	59.8	80.4	30.0	26.8

¹ ID assumes the superstructure only on a rigid-base; ² T_1 and T_2 correspond to the first translational modes in the Y- and X-directions, respectively; ³ Seismic weight (W_s) neglects first floor diaphragm and one half first story wall weight, Total weight (W_T) includes all diaphragms and wall weights

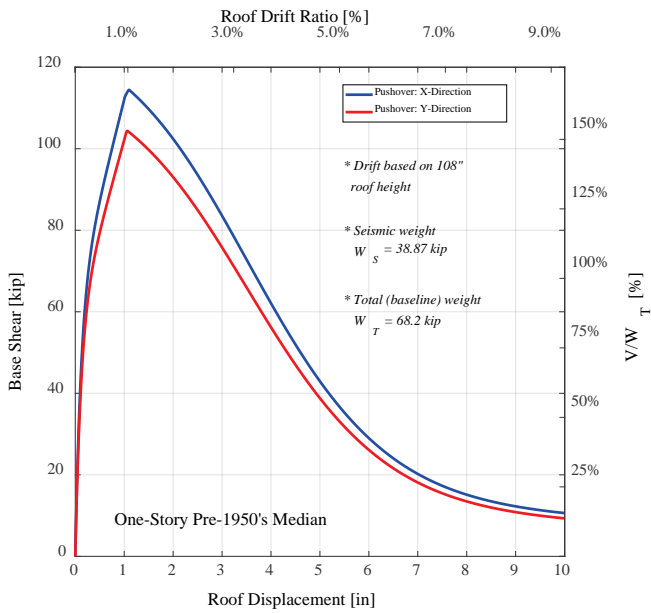


Figure 6-37 Pushover curves for the one-story pre-1950's Median Superstructure (Archetype 4-1R-M-E).

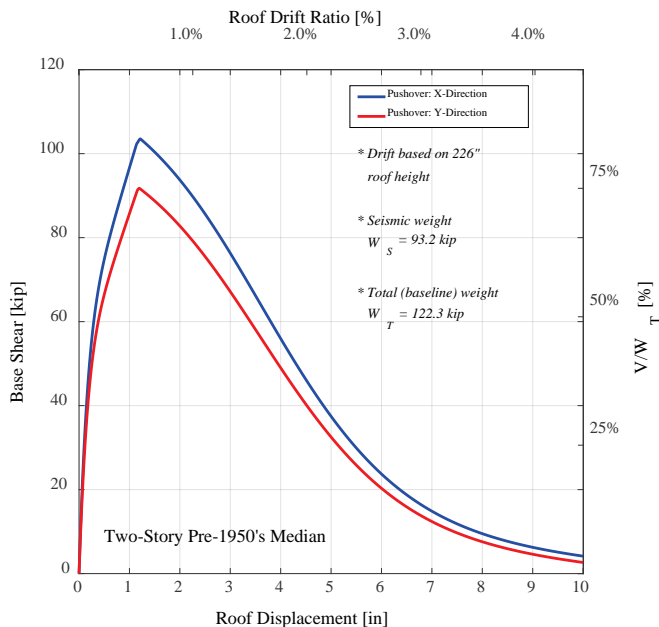


Figure 6-38 Pushover curves for the two-story pre-1950's Median Superstructure (Archetype 4-2R-M-E).

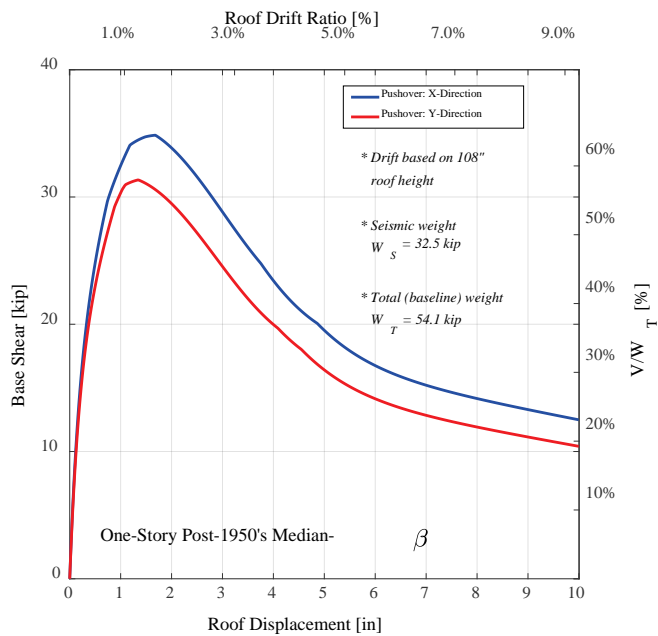


Figure 6-39 Pushover curves for the one-story post-1950's Median-6 Superstructure (Archetype 4-1R-M6-E).

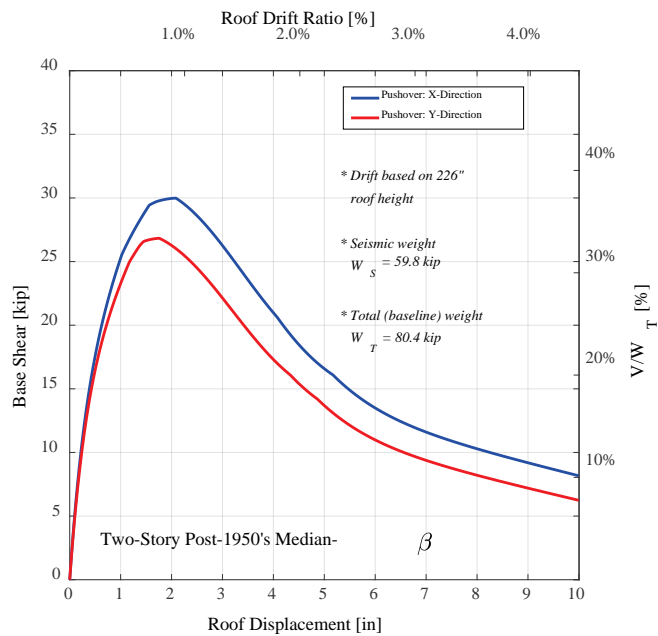


Figure 6-40 Pushover curves for the two-story post-1950's Median-6 Superstructure (Archetype 4-2R-M6-E).

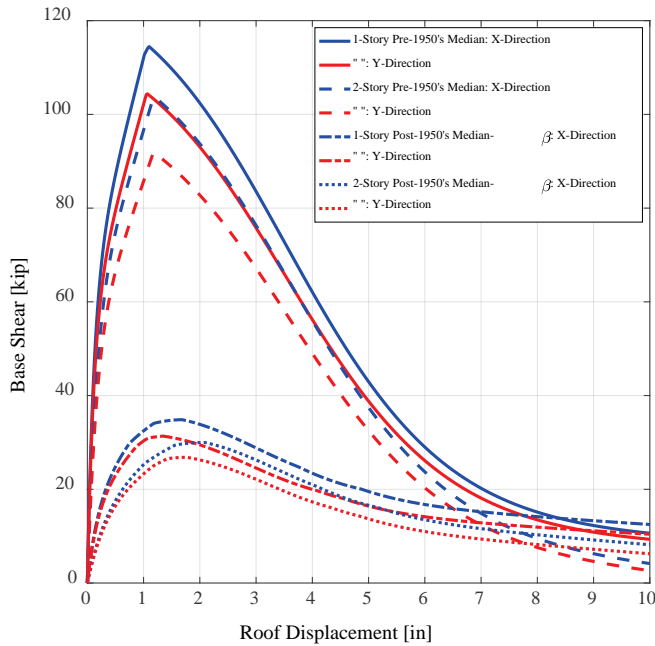


Figure 6-41 Pushover analysis comparison of all four superstructure configurations considered for cripple wall dwelling analysis.

6.5 Geometric Information Collected from All Configurations

This appendix contains all measured area and wall length information collected for each individual configuration considered within the median superstructure study.

Table 6-19 Exterior Wall Summary for One-Story Configurations

Era	Configuration	Floor Area $A [\text{ft}^2]$	Exterior Wall Length X-Direction $L_{EXT,X} [\text{ft}]^*$	Exterior Wall Length Y-Direction $L_{EXT,Y} [\text{ft}]^*$	Total Exterior Wall Length-to-Area ratio $L_{tot}/A [1/\text{ft}]$	Maximum-to-Minimum Exterior Wall Length Ratio L_{\max}/L_{\min}
1900	1A	1378	37.0	65.5	0.074	1.77
	1B	1305	62.5	43.0	0.081	1.45
	1C	1520	51.5	33.5	0.056	1.54
1910	1A	1008	42.0	48.0	0.089	1.14
	1B	1128	63.0	62.0	0.111	1.02
	1C	648	34.5	34.0	0.106	1.01
1920	1A	890	42.5	38.5	0.091	1.10
	1B	905	33.0	46.5	0.088	1.41
	1C	1800	37.5	56.5	0.052	1.51
1930	1A	864	34.5	49.5	0.097	1.43
	1B	966	34.0	59.0	0.096	1.74
	1C	955	44.0	51.5	0.100	1.17
1940	1A	1470	52.5	42.5	0.065	1.24
	1B	621	37.5	32.5	0.113	1.15
	1C	1097	38.0	46.5	0.077	1.22
1950	1A	768	38.0	45.5	0.109	1.20
	1B	1040	37.5	44.5	0.079	1.19
	1C	1494	33.5	49.5	0.056	1.48
1960	1A	1482	54.0	44.5	0.066	1.21
	1B	1157	39.0	49.0	0.076	1.26
	1C	1129	37.5	55.5	0.082	1.48

*Only full-height wall sections considered

Table 6-20 Interior Wall Summary for One-Story Configurations

Era	Config-ation	Floor Area <i>A</i> [ft ²]	Interior Wall Length X- Direction <i>L_{INT,X}</i> [ft] [*]	Interior Wall Length Y- Direction <i>L_{INT,Y}</i> [ft] [*]	Total Interior Wall Length-to- Area ratio <i>L_{tot/A}</i> [1/ft]	Maximum-to- Minimum Interior Wall Length Ratio <i>L_{max/L_{min}}</i>
1900	1A	1378	63.0	52.0	0.083	1.21
	1B	1305	42.5	81.0	0.095	1.91
	1C	1520	52.5	67.0	0.079	1.28
1910	1A	1008	39.5	36.0	0.075	1.10
	1B	1128	42.5	29.5	0.064	1.44
	1C	648	22.5	18.0	0.063	1.25
1920	1A	890	57.5	54.5	0.126	1.06
	1B	905	43.5	37.5	0.090	1.16
	1C	1800	58.0	57.0	0.064	1.02
1930	1A	864	44.0	32.0	0.088	1.38
	1B	966	52.0	35.5	0.091	1.46
	1C	955	32.0	43.5	0.079	1.36
1940	1A	1470	47.0	68.5	0.079	1.46
	1B	621	25.0	36.0	0.098	1.44
	1C	1097	42.5	37.5	0.073	1.13
1950	1A	768	42.5	27.5	0.091	1.55
	1B	1040	56.0	51.0	0.103	1.10
	1C	1494	55.0	51.0	0.071	1.08
1960	1A	1482	49.5	67.0	0.079	1.35
	1B	1157	55.5	49.5	0.091	1.12
	1C	1129	43.0	54.0	0.086	1.26

*Wall lengths consider full-height sections only

Table 6-21 Exterior Wall Summary for the First Story of Two-Story Configurations

Era	Configuration	1st Floor Area A_{1st} [ft ²]	1st Exterior Wall Length X-Direction $L_{EXT,X1}$ [ft] [*]	1st Exterior Wall Length Y-Direction $L_{EXT,Y1}$ [ft] [*]	Total Exterior Wall Length-to-Area ratio L_{tot}/A [1/ft]	Maximum-to-Minimum Exterior Wall Length Ratio L_{max}/L_{min}
1900	2A	780	33.0	45.5	0.101	1.38
	2B	984	44.0	48.5	0.094	1.10
1910	2A	1980	34.0	41.5	0.038	1.22
	2B	957	35.5	58.0	0.098	1.63
1920	2A	810	36.0	38.0	0.091	1.06
	2B	1258	30.5	52.5	0.066	1.72
1930	2A	757	30.5	29.0	0.079	1.05
	2B	850	38.5	38.0	0.090	1.01
1940	2A	477	23.5	35.0	0.123	1.49
	2B	958	42.5	37.0	0.083	1.15
1950	2A	903	37.0	36.0	0.081	1.03
	2B	560	36.0	34.0	0.125	1.06
1960	2A	1374	57.5	55.0	0.082	1.05
	2B	1616	51.5	39.0	0.056	1.32

*Wall lengths consider full-height sections only

Table 6-22 Exterior Wall Summary for the Second Story of Two-Story Configurations

Era	Config-ation	2nd Floor Area A_{2nd} [ft ²]	2nd Exterior Wall Length X-Direction $L_{EXT,X2}$ [ft] [*]	2nd Exterior Wall Length Y-Direction $L_{EXT,Y2}$ [ft] [*]	Total Exterior Wall Length-to-Area ratio L_{tot}/A [1/ft]	Maximum-to-Minimum Exterior Wall Length Ratio L_{max}/L_{min}
1900	2A	780	41.0	71.5	0.144	1.74
	2B	984	61.0	60.5	0.123	1.01
1910	2A	1744	41.0	50.0	0.052	1.22
	2B	674	33.5	40.5	0.110	1.21
1920	2A	748	55.0	49.5	0.140	1.11
	2B	1226	37.5	51.0	0.072	1.36
1930	2A	446	35.0	33.5	0.154	1.04
	2B	824	50.5	45.0	0.116	1.12
1940	2A	477	35.0	41.5	0.160	1.19
	2B	800	57.5	53.5	0.139	1.07
1950	2A	903	28.0	21.5	0.055	1.30
	2B	560	44.0	37.5	0.146	1.17
1960	2A	1094	42.5	55.0	0.089	1.29
	2B	1328	64.0	38.0	0.077	1.68

*Only full wall-heights considered

Table 6-23 Interior Wall Summary for the First Story of Two-Story Configurations

Era	Configura-tion	1st Floor Area A_{1st} [ft ²]	1st Interior Wall Length X-Direction $L_{INT,X1}$ [ft] [*]	1st Interior Wall Length Y-Direction L_{INTY1} [ft] [*]	Total Interior Wall Length-to-Area ratio L_{tot}/A [1/ft]	Maximum-to-Minimum Interior Wall Length Ratio L_{max}/L_{min}
1900	2A	780	12.5	35.0	0.061	2.80
	2B	984	28.0	32.5	0.061	1.16
1910	2A	1980	43.5	67.5	0.056	1.55
	2B	957	23.0	21.5	0.046	1.07
1920	2A	810	28.0	33.0	0.075	1.18
	2B	1258	62.5	59.0	0.097	1.06
1930	2A	757	16.0	19.0	0.046	1.19
	2B	850	29.0	28.5	0.068	1.02
1940	2A	477	20.0	19.0	0.082	1.05
	2B	958	34.5	39.5	0.077	1.14
1950	2A	903	34.0	39.0	0.081	1.15
	2B	560	11.0	33.5	0.079	3.05
1960	2A	1374	44.5	52.5	0.071	1.18
	2B	1616	27.5	53.5	0.050	1.95

*Only full wall-heights considered

Table 6-24 Interior Wall Summary for the Second Story of Two-Story Configurations

Era	Configuration	2nd Floor Area A_{2nd} [ft ²]	2nd Interior Wall Length X-Direction $L_{INT,X2}$ [ft] [*]	2nd Interior Wall Length Y-Direction $L_{INT,Y2}$ [ft] [*]	Total Interior Wall Length-to Area ratio L_{tot}/A [1/ft]	Maximum-to-Minimum Interior Wall Length Ratio L_{max}/L_{min}
1900	2A	780	53.5	43.5	0.124	1.23
	2B	984	51.5	43.0	0.096	1.20
1910	2A	1744	60.0	77.5	0.079	1.29
	2B	674	35.0	28.5	0.094	1.23
1920	2A	748	32.5	29.5	0.083	1.10
	2B	1226	68.0	55.0	0.100	1.24
1930	2A	446	26.5	16.0	0.095	1.66
	2B	824	48.0	44.0	0.112	1.09
1940	2A	477	34.0	35.0	0.145	1.03
	2B	800	13.0	53.5	0.083	4.12
1950	2A	903	58.0	46.5	0.116	1.25
	2B	560	24.0	31.5	0.099	1.31
1960	2A	1094	56.5	62.0	0.108	1.10
	2B	1328	63.5	70.0	0.101	1.10

*Only full wall-heights considered

6.6 References

B.C. Ltd. (1959). "Select Home Designs," Series 10, 1959, The Building Centre Limited, Vancouver, Canada.

Beaver Lumber. (1950). "Modern Homes," Beaver Lumber Company Limited. Digitized by the Association of Preservation Technology, Int.

Blueprints for Better Homes (BFBH). (1946). "Blueprints for Better Homes, 1946," Blueprints for Better Homes, Alderway Building, Portland, OR. Digitized by the Association of Preservation Technology, Int.

Carr and Johnston. (1926). "Practical Homes," Carr and Johnston Company, Peoria, IL.

Christovasilis, I.P., Filiastrault, A. (2009) "A Computer Program for Seismic Analysis of Woodframe Structures," *SAWS Version 2.1 User Manual*, Division of Structural Engineering, University of California, San Diego, Department of Civil, Structural and Environmental Engineering, State University of New York at Buffalo.

FEMA P807. (2012). "Seismic Evaluation and Retrofit of Multi-Unit Wood-Frame Buildings with Weak First Stories," Prepared by the Applied Technology for the Federal Emergency Management Agency, Washington, DC, 336 p.

Folz, B., Filiatrault, A. (2004). "Seismic Analysis of Woodframe Structures. I: Model Formulation," *Journal of Structural Engineering, ASCE*, 130(9): 1353-1360.

Hogdson, F.T. (1905). "Hogdson's Modern House Building – Perspective Views and Floor Plans of Fifty Low Medium Priced Houses," Frederick J. Drake and Company, Architectural Department, 350-352 Wabash Avenue, Chicago, IL. Digitized by Internet Archive.

Home Planners. (1960). "54 Homes of Distinction," Designs for Convenient Living Book No. 29, Home Planners, Inc.

Isoda, H., Folz, B., Filiatrault, A. (2002). "Seismic Modeling of Index Woodframe Buildings," *CUREE Publication W-12*, CUREE-Caltech Woodframe Project, Consortium of Universities for Research in Earthquake Engineering, Richmond, CA.

Johnson, A.J. (1997). "Monotonic and Cyclic Performance of Long Shear Walls with Openings," *MSc Thesis*, Virginia Polytechnic Institute and State University, Blacksburg, VA.

NPS. (1961). "Three Bedroom Homes," National Plan Service, Inc., Kopp's Company, Inc., Lineboro, MD. Digitized by the Association of Preservation Technology, Int.

Pang, W., Ziaeい, E., Filiatrault, A. (2012). "A 3D Model for Collapse Analysis of Soft-story Light-frame Wood Buildings," *Proceedings of the 2012 World Conference on Timber Engineering* (2012 WCTE), Auckland, New Zealand.

Patton-Mallory, M., Wolfe, R.W., Soltis, L.A. (1985). "Light-frame shear wall length and opening effects," *Journal of Structural Engineering, ASCE*, 111(10): 2227-2239.

Radford. (1908). "Radford's Artistic Bungalows – Unique Collection of 208 Designs," The Radford Architectural Company, Chicago, IL.

Sears. (2003). "Sears House Designs of the Thirties," Reprint of *Homes of Today*, Sears, Roebuck and Company, 1932.

Sears-Roebuck. (1932). "Homes of Today," Sears, Roebuck and Company.

Sears-Roebuck. (1926). “Small Houses of the Twenties,” The Sears, Roebuck 1926 Housing Catalog, Sears, Roebuck and Company.

Sears-Roebuck. (1918). “Honor Bilt Modern Homes,” Sears, Roebuck and Company, Chicago, IL.

Weyerhaeuser. (1960). “5 and 6 Room Homes,” Weyerhaeuser Sales Company, Saint Paul, MN. Digitized by the Association of Preservation Technology, Int.

Weyerhaeuser. (1957). “Selected 3-Bedroom Homes – 56 popular homes from the Weyerhaeuser 4-Square home building service,” Weyerhaeuser Sales Company, Saint Paul, MN. Digitized by the Association of Preservation Technology, Int.

Weyerhaeuser. (1958). “Attractive Multi-Level Homes,” Weyerhaeuser Sales Company, Saint Paul, MN. Digitized by the Association of Preservation Technology, Int.

Weyerhaeuser. (1940). “Weyerhaeuser 4-Square Book of Homes,” Weyerhaeuser Sales Company, Saint Paul, MN. Digitized by the Association of Preservation Technology, Int.

Yasamura, M., Sugiyama, H. (1984). “Shear properties of plywood-sheathed wall panels with opening,” *Transactions of the Architectural Institute of Japan*, 338(4): 88-98.

Part 7

Over-strength Factor for Retrofit Load Path Design

7.1 Introduction

The FEMA P-1100 prestandard has incorporated the use of over-strength factors into the simplified engineering methodologies for retrofit design, as well as the prescriptive/ plan set designs generated using these methodologies. The retrofits are vulnerability-based and will typically involve the addition of new seismic force-resisting elements.

The over-strength factors are used for design of the load path into and out of the retrofit elements. This is intended to help ensure that the peak capacity of the retrofit elements can be developed without the load path acting as a weak link. The approach taken by the prestandard differs somewhat from both the typical approach taken in design of new structures, where no over-strength factor is used, and the typical development of over-strength factors within the FEMA P-695 methodology (FEMA, 2009) where derivations include consideration of only the main structural elements and not building finishes. The choice to use an over-strength factor and go above current design practice was driven primarily by the probability of collapse (POC) basis for the retrofit design parameters; if the capacity of the retrofit element cannot be developed, results of the numerical POC studies would be invalid. Ultimately, variations from the typical FEMA P-695 derivation of the over-strength factor were incorporated to adjust both demand and capacity.

7.2 Development of Over-strength Factor

This section discusses the development of the over-strength factor used throughout the prestandard for the prescriptive and simplified engineering retrofit strategies.

7.2.1 Numerical Study Evaluation of Over-strength Factor

The ATC-110 Project studied two ways to derive the load path over-strength factor (Ω) included both a traditional FEMA P-695 approach, which suggested a factor of approximately 2.0, and a modified approach which suggested a factor of approximately 1.5. Ultimately, the modified approach factor of 1.5 was selected for incorporation. The factor of 1.5 was less

problematic in terms of implementation or constructability, and the resulting retrofit solutions still were considered to provide a reasonable safeguard against connection-level damage prior to capacity development of the main retrofit elements.

In the numerical studies used for developing the prestandard, models included a range of finish materials that could be anticipated to be present and provide additional bracing capacity. For this reason, the over-strength factor derived from the numerical studies was larger than would normally be anticipated based upon consideration of only the structural elements.

7.2.2 FEMA P-695 Approach and Discussion

Using the FEMA P-695 methodology, analysis of the pushover curves obtained from 12 retrofitted cripple wall archetypes resulted in an over-strength ratio, $\Omega_{o(total)}$, (between the peak strength of the retrofitted cripple walls, $V_{cw,u}$, and their design base shear, $\varphi V_{cw,D}$) consistently equal to 2.0. This is shown in Table 2-1. Therefore, by Equation 7-1:

$$V_{CW,u} = \Omega_{o(total)} V_{CW,D} = 2.0\varphi V_{CW,D} \quad (7-1)$$

Considering the over-strength of both the finishes and plywood separately, an omega value could also be approximated as the product of the two as follows:

$$\Omega_{o(total)} = \Omega_{o(ply)} * \Omega_{o(finishes)} \quad (7-2)$$

For this case, the over-strength of the plywood cripple wall retrofit elements, $\Omega_{o(ply)}$, from the cripple walls studied, is estimated to be approximately 1.4. This value is also approximately the ratio of the wind nominal unit shear capacities, and likely peak capacity, (column B) to the seismic nominal unit shear capacities (column A) found within Table 4.3A of the 2015 AWC NDS SDPWS [AWC, 2015]. In addition, computations presented within Section 2.3 indicate that the over-strength of the finish materials $\Omega_{o(finishes)}$, while varying widely with finish material assumptions, were on average computed to be 1.6. This then yields a total approximate omega value $\Omega_{o(total)}$ of 1.4×1.6 or 2.2. Note that this total value is slightly higher than the average value computed within Table 7-1 since the finish materials often reach peak capacity at a displacement considerably less than the plywood. This also does not adjust for the different phi factors that might be used for design of shear walls and load path connections.

**Table 7-1 Calculation of Over-Strength Factors for Work Group 4
Retrofitted Archetypes based on FEMA P-695 Methodology**

Plywood Strength Taken As Design Strength ϕV_{ns}													
Design strength is estimated by taking four times the effective brace length (four braces per direction)				Design		Pushover Strengths		Overstrength Factors					
Archetype	Superst	# of	R	h _{cw}	L _{eff} [ft]	Strength	V [kip]	V _{maxX}	V _{maxY} [kip]	Ω _{0,X}	Ω _{0,Y}	Ω _{0,Avg}	
1C2L-M-R53%WSP9-noHD	Median	1	6H	2	9.33	Low	22.7	51.7	45.7	2.28	2.01	2.15	
1C4L-M-R61%WSP6-noHD				4	10.67	Low	25.9	55.7	49.8	2.15	1.92	2.03	
1C6L-M-R61%WSP6-noHD				6	10.67	Low	25.9	59.0	53.3	2.27	2.06	2.16	
1S26L-M-R61%WSP6-noHD				S26	10.67	Low	25.9	56.8	50.7	2.19	1.95	2.07	
1C2L-MH-R70%WSP9-noHD				2H	13.33	Low	32.4	63.6	57.9	1.96	1.79	1.87	
1C6L-MH-R70%WSP6-noHD		3	6H	6H	13.33	Low	32.4	67.9	63.1	2.09	1.95	2.02	
2C2L-M-R76%WSP8-noHD				2	13.33	Medium	41.8	80.1	76.2	1.92	1.82	1.87	
2C4L-M-R76%WSP8-noHD				4	13.33	Medium	41.8	80.1	76.2	1.92	1.82	1.87	
2C6L-M-R76%WSP5-noHD				6	13.33	Medium	41.8	87.6	83.2	2.10	1.99	2.04	
1C2-Mβ-R46%WSP9-noHD				2	8.00	Low	19.5	42.1	38.0	2.16	1.95	2.06	
1C4-Mβ-R46%WSP9-noHD	Median- β	1	4	8.00	Low	19.5	42.6	39.3	2.19	2.02	2.10		
1C6-Mβ-R46%WSP6-noHD			6	8.00	Low	19.5	40.6	37.9	2.09	1.95	2.02		
										Median	2.04		
										Mean	2.02		

7.2.3 Alternate Derivation of Over-strength Factor

To supplement the P-695 over-strength factor derivation, calculations were preformed to specifically back-calculate the over-strength factor required to balance shear wall and load path capacity. These calculations were developed using both Allowable Strength Design (ASD) and Load and Resistance Factored Design (LRFD) design methods and are illustrated in Table 7-2 below.

Three factors that were considered for determining an appropriate Ω factor. These include plywood over-strength (J_1), over-strength of the existing finish materials (J_2), and connector over-strength (J_3) as well as material phi factors for the plywood $\Phi_p = 0.8$ and a phi factor for the connector $\Phi_c = 0.7$. The use of these factors to determine total overstrength are shown for ASD and LRFD in Equations 2-3 and 2-4, respectively.

$$\Omega_{0(\text{total}),\text{ASD}} = (J_1 * J_2) / J_3 \quad (2-3)$$

$$\Omega_{0(\text{total}),\text{LRFD}} = [(J_1 / \Phi_p) J_2] / (J_3 * \Phi_c) \quad (2-4)$$

For this procedure, J_1 accounts for the plywood over-strength factor. For ASD this is the ratio between an ASD allowable shear and the anticipated peak unit shear. For LRFD this is the ratio between the tabulated nominal seismic unit shear and the anticipated peak unit shear. In both cases, the anticipated peak unit shear is taken as the tabulated nominal unit shear for wind design. Using SDPWS Table 4.3A, this ratio is determined to be 2.8 for ASD and 1.4 for LRFD.

The J_2 factor accounts for the additional strength provided by inclusion of the existing finishes. To determine the capacity of the existing finish, a ratio of the peak pushover strength of nine existing representative models was divided by the corresponding nominal capacity of the plywood for retrofitted models. On average, these studies show that the finish can develop about 56% of the nominal design capacity of the plywood retrofits. Therefore, a J_2 factor of 1.6 was used.

The J_3 factor accounts for the over-strength of connectors. Published test data (Fennell et al., 2009; Mahaney and Kehoe, 2002; Ficcadenti et al., 2004) and methods for deriving design values for proprietary connectors generally support factor of safety of metal clips and anchors from concrete to mudsills of 3.0 or larger for allowable stress design (ASD). This over-strength is converted to Load and Resistance Factored Design (LRFD) by using the conversion factor Φ_c of 0.7, which results in a value of 2.1. This calculation is illustrated in Figure 7-1.

Connector Capacity Design Approach for Balanced Design

Design Notes:

- 1) Connector design shall be based upon plywood capacity approach ($J3_{ASD}=2.0$, $J3_{LRFD}=1.4$)
- 2) Design loads V_{design} (shears) shall be multiplied by Omega (' Ω ') factor.
- 3) $V_{connection} = V_{design} * \Omega$

<u>Allowable Strength Design (ASD)</u>	<u>Load and Resistance Factor Design (LRFD)</u>
$'\Omega=(J1*J2)/J3$	$'\Omega=[(J1/\Phi_p*J2)/(J3*\Phi_c)$
Plywood overstrength:	$J1=2.8$
Existing finish capacity:	$J2=1.6$
Connector overstrength:	$J3=3.0$
ASD to LRFD conversion:	$\Phi_c=0.7$
Plywood strength factor:	$\Phi_p=0.8$
$'\Omega=\Omega_{0(total)ASD}=1.49$	$'\Omega=\Omega_{0(total)LRFD}=1.33$
Use '$\Omega = 1.5$	Use '$\Omega = 1.5$

Figure 7-1 Derivation of overstrength factors for connectors.

When all the factors are multiplied using Equations 7-3 and 7-4, the final omega factor is approximately 1.5 using an ASD approach and 1.33 using a LRFD approach. The project team thought it was reasonable to use a consistent value of 1.5 for both LRFD or ASD approaches. Figure 2-1 illustrates the computation of Omega for both design approaches. Table 7-2 illustrates the method of calculation the over-strength term related to existing finishes J2.

It was originally envisioned that factors greater than 1.0 might also be used to account for round-up of the calculated required plywood lengths to lengths corresponding to the next stud bay spacing. Upon further reflection it was decided that this would make construction unnecessarily conservative, and was not warranted. It was also recognized that there are likely some existing anchors present either concealed or visible which would also provide some reserve capacity not explicitly included within the retrofit designs.

In conclusion, an over-strength factor of 1.5 was used project-wide to provide a balance between the peak capacity of retrofit elements and their load path connections. This factor has been incorporated into the engineered design methodology. This factor has also been used in derivation of the prescriptive designs. This approach to design of the load path has since been incorporated into testing of cripple wall retrofits. Component cyclic tests incorporating FEMA P-1100 retrofits on cripple walls finished with stucco and with horizontal wood siding have demonstrated that load path connections using the selected overstrength factor of 1.5 are able to develop the peak capacity of the combined finish plus retrofit sheathing (Mahdavifar and Cobeen, in progress).

Calculation of J2 (Strength of Existing Finishes as a Ratio of Nominal Design Strength)

Design strength is estimated by taking four times the effective brace length (four braces per direction) and then multiplying by the appropriate normalized strength

Archetype	Superstructure Type	# of Stories	R	h_{cw} [ft]	L_{eff} [ft]	Strength	V [kip]	Archetype	$V_{max,\chi}$ [kip]	Pushover Strengths for Comparable Existing Materials			Finish Overstrength Contribution		
										$\Omega_{0,x}$	$\Omega_{0,y}$	$\Omega_{0,Avg}$	$V_{max,\chi}/k_i$	p	
1C2L-M-R53%WSP9-noHD		1	2	9.33	Low	28.4	1C2L-M-E	27.4	20.5	0.96	0.72	0.84	0.84		
1C4L-M-R61%WSP9-noHD		4	10.67	Low	32.4	1C4L-M-E	27.4	20.5	0.84	0.63	0.74				
1C6L-M-R61%WSP6-noHD		6	10.67	Low	32.4	1C6L-M-E	27.4	20.5	0.84	0.63	0.74				
2C2L-M-R76%WSP8-noHD	Median	2	13.33	Medium	52.3	2C2L-M-E	27.4	20.5	0.52	0.39	0.46				
2C4L-M-R76%WSP8-noHD		3	13.33	Medium	52.3	2C4L-M-E	27.4	20.5	0.52	0.39	0.46				
2C6L-M-R76%WSP5-noHD		6	13.33	Medium	52.3	2C6L-M-E	27.4	20.5	0.52	0.39	0.46				
1C2-M β R46%WSP9-noHD	Median-1	2	8.00	Low	24.3	1C2-M β -E	12.9	9.1	0.53	0.38	0.45				
1C4-M β R46%WSP9-noHD		4	8.00	Low	24.3	1C4-M β -E	12.9	9.1	0.53	0.38	0.45				
1C6-M β R46%WSP6-noHD		6	8.00	Low	24.3	1C6-M β -E	12.9	9.1	0.53	0.38	0.45				
										Median	0.46				
										Mean	0.56				
										Use J2 = 1.6					

There are two aspects in which this factor has not been incorporated. Both involve design of tie-downs for overturning. These will be addressed in a separate white paper discussion.

7.3 References

AWC, 2015. Special Design Provisions for Wind and Seismic. American Wood Council, Washington, D.C.

FEMA, 2009. *Quantification of Building Seismic Performance Factors* (FEMA P695) Federal Emergency Management Agency, Washington, DC.

Fennel et al., 2009. *Report on Laboratory Testing of Anchor bolts connecting Wood Sill Plates to Concrete with Minimum Edge Distances*, Structural Engineers Association of Northern California Special Projects Initiative Report, Structural Engineers Association of California, San Francisco, CA.

Ficcadenti et al., 2004. *Cyclic Response of Shear Transfer Connections between Shearwalls and Diaphragms in Woodframe Construction* (CUREE W-28), Consortium of Universities for Research in Earthquake Engineering, Richmond, CA.

Mahaney and Kehoe, 2002. *Anchorage of Woodframe Buildings: Laboratory Testing Report* (CUREE W-14), Consortium of Universities for Research in Earthquake Engineering, Richmond CA.

Mahdavifar and Cobeen, In-Progress. Full-Scale Testing of Cripple Walls and Sill Anchorage in Existing and Retrofit Single-Family Wood-Frame Buildings, Pacific Earthquake Engineering Research Center, Berkeley, CA.

Part 8

Simplified Overturning Assumptions

8.1 Introduction

The FEMA P-1100 Prestandard has developed a simplified overturning procedure to account for a realistic level of uplift forces that would be imparted on the cripple wall level from the superstructure above during an earthquake. This procedure is based on simplified overturning assumptions and is only intended to be utilized by Work Group 4, Crawlspace Dwellings (WG4). These assumptions have been incorporated into both the simplified engineering methodologies of FEMA P-1100, Chapter 4 general retrofit design criteria as well as the prescriptive plan set designs generated using those methodologies.

8.2 Development of Simplified Overturning Assumptions

This section discusses the development of the simplified overturning assumptions used throughout this prestandard for the prescriptive and simplified engineering retrofit strategies for crawlspace dwellings.

While this prestandard utilizes a vulnerability-based approach that only addresses the strengthening of the cripple wall level, it is reasonable to assume that some degree of uplift demands could be imparted on the cripple wall level from the superstructure above. This phenomenon is very complex to evaluate as most existing dwellings were not originally engineered to have direct floor-to-floor ties as well as a full-height designated seismic force-resisting system. In practice, uplift forces that would be developed on the cripple wall from the structure above were based upon simplified engineering assumptions, varied extensively and were often either ignored or indirectly addressed by reducing the dead load resistance above. As this prestandard is vulnerability-based, it was also not deemed practical or necessary for a design professional to accurately survey the walls within the occupied levels for each particular superstructure in order to demonstrate the presence of an existing and dedicated vertical load path for these non-engineered dwellings. Rather, it was deemed appropriate to develop a reasonable and simplified engineering approach where prescriptive designs could be implemented and, if necessary, where a registered design professional could generally account

for some reasonable level of overturning forces from the superstructure into the cripple wall level. The method presented within FEMA P-1100 has been developed based upon large-scale shake table building tests conducted at University of California, San Diego (Fischer et al., 2001, 2002) in which anchors (anchor bolts and tie-downs) were directly instrumented for axial forces along wall lines. These tests concluded that the traditional force distribution imparted to the structure's base from the superstructure above, where all direct shear and overturning demands are applied only to the in-plane walls, is overly conservative. Instead, a box-type phenomenon was observed, where the majority of the tension and compression forces were resisted by the wall lines perpendicular to the direction of loading. This box-type distribution was estimated to generally have a ratio of about 70% applied to the perpendicular walls and 30% to the walls parallel to loading and at the top of the cripple wall. This leads to the use of 15% per each of the two IP exterior walls line, as illustrated in Figure 8-1.

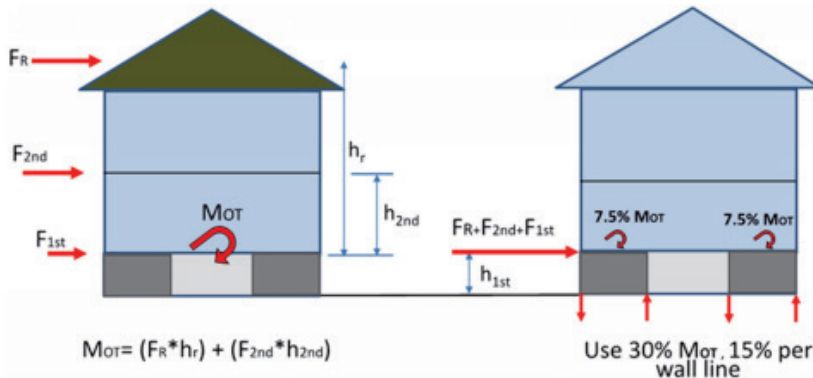


Figure 8-1 Illustration of simplified overturning assumptions for the design of cripple wall retrofit.

Figure 2-1 illustrates that the cripple wall retrofit design includes the total of lateral forces acting at each level of the building when designing for shear. However, when designing for overturning and uplift, each side of the home assumes 15% of the global overturning, which is then split evenly between the two shear wall sections (7.5%) as shown in the right portion of Figure 8-1. Additional information on this procedure is available within ATC-110 Volume 4, Background Documentation (Document WG4-B2).

8.3 Numerical Study Evaluation of Overturning Assumptions

The evaluation of overturning distributions utilizes the data from shake table testing of a full-scale two-story wood light-frame house conducted by

Fischer et al. (2001; 2002) within the CUREE-Caltech Woodframe Project. These tests were selected as the most representative, and for which the documented information permitted to the investigation of overturning assumptions.

The tested structure is 20 feet by 16 feet in plan, corresponding to the east-west and north-south directions, respectively. The shake table tests were conducted under uniaxial horizontal loading in the north-south direction of the structure. A total of eight different construction phases were considered in combination with dynamic testing following the first four phases that investigated floor diaphragm testing only. The construction phases ranged from assuming fully sheathed OSB walls on the east and west sides of the house without exterior or interior finish in Phase 5 to assuming door openings (pedestrian and garage) in these walls combined with the addition of exterior stucco, interior gypsum wallboard and windows and doors in the openings in Phase 10. An illustration of different construction and testing phases is shown in Figure 8-1 (see Table 8-1 for descriptions). Complete information on each individual testing phase is provided in Fischer et al. (2001; 2002).

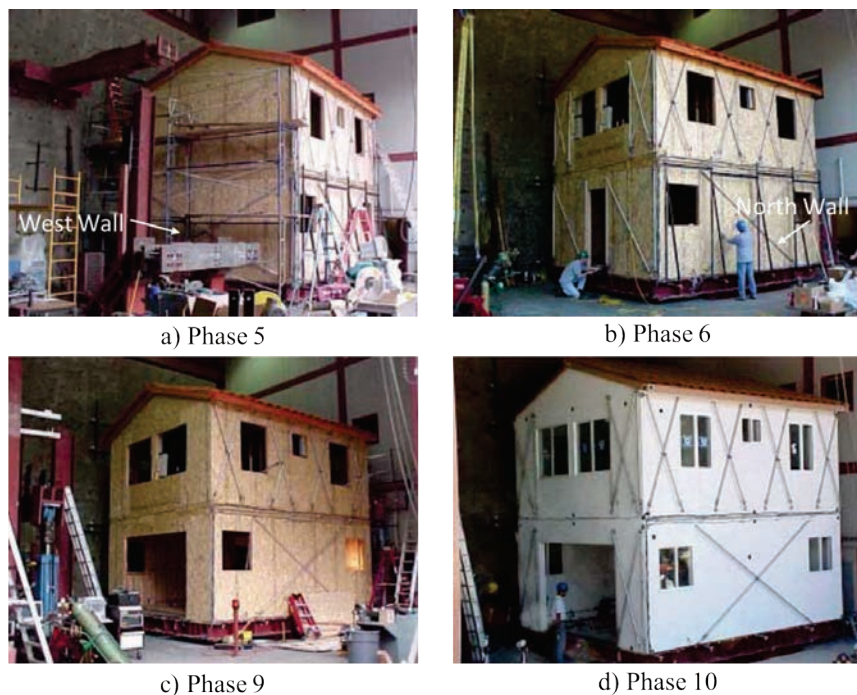


Figure 8-2 Illustration of different construction and testing phases of the two-story house tested by Fischer et al. (2001) focusing on major changes to the East and West walls: a) Fully sheathed without openings; b) Inclusion of pedestrian door openings and window openings on top story; c) Including a garage door opening (West wall only); d) Inclusion of stucco and gypsum finish materials and inclusion of windows and doors in openings.

In addition to different construction phases having different assumptions of sheathing and openings, they also have various levels of anchorage conditions. This included the use of hold-down devices at wall line ends only versus including them at each end and at each opening. Other phases looked at conventional construction where hold-downs were removed and anchor bolt spacing was increased. A brief description of each construction phase is provided in Table 8-1. See Fischer et al. (2001; 2002) for more information.

Table 8-1 Brief Description of Construction Phases in the Testing Conducted by Fischer et al. (2001; 2002)

Construction Phase	Description	Openings	Sill Anchorage
5	Fully sheathed OSB walls	No openings	Hold-downs at each end; six intermediate anchor bolts per side
6	OSB walls with symmetrical openings with hold-downs	Symmetrical pedestrian doors (1st story) and windows (2nd story)	Hold-downs at each end and at each side of door openings. Four intermediate anchor bolts per side
7	Phase 6 without hold-downs on either side of doorways	Symmetrical pedestrian doors (1st story) and windows (2nd story)	Hold-downs at each end; four intermediate anchor bolts per side; doorway hold-downs have nut removed
7A	Phase 7 with anchor bolts to replace removed hold-downs flanking doorways	Symmetrical pedestrian doors (1st story) and windows (2nd story)	Hold-downs at each end; anchor bolt added at each side of doorway
8	Phase 6 openings with conventional construction anchorage	Symmetrical pedestrian doors (1st story) and windows (2nd story)	No hold-downs; one anchor bolt at each wall segment end per side (~6ft spacing)
9	Phase 6 with unsymmetrical opening at 1st story	Large garage door opening on West wall, pedestrian door on East wall	Hold-downs at each wall end and near each opening; East wall has four intermediate anchor bolts
10	Phase 9 with the addition of exterior stucco, interior gypsum, windows and pedestrian door	Large garage door opening on West wall, pedestrian door on East wall	Hold-downs at each wall end and near each opening; East wall has four intermediate anchor bolts

Each construction phase was tested with varying levels of ground motion intensity. Phases 5 through 8 were tested with an incrementally scaled acceleration record from the Canoga Park station recorded during the 1994 Northridge earthquake. This record was scaled to four different intensities ranging from very low amplitude Level 1 (e.g., PGA = 0.05g) to an amplitude deemed appropriate to represent the 10% in 50-year hazard level (e.g., PGA = 0.5g, Level 4). Construction phases 9 (no finish) and 10 (with finish) considered a horizontal component of the Rinaldi station recording of the 1994 Northridge earthquake in addition to the first four intensity levels. This final intensity was referred to as the 2% in 50-year hazard level and was intended to represent near fault ground motions (e.g., PGA = 0.89g, Level 5). The investigative effort herein only considered the cases that were at least

tested at the “10% in 50 year” hazard level (Level 4). In some cases, the seismic test was repeated at a given intensity to study the effect of buildings subjected to repeated earthquakes, so the intensity number is followed by “R” in the nomenclature used by Fischer et al. (2001; 2002) which is maintained herein when presenting results. For example, Test “5.S.4” is construction Phase 5, a seismic test (“S”) and intensity Level 4. Additionally, Test “5.S.4R” is the same construction phase and input ground motion but represents a reproduction of the same test.

Reporting by Fischer et al. (2001; 2002) included diagrams of peak uplift forces measured from instrumented anchor bolts and hold-downs during the seismic testing. As an example, an illustration of the peak forces obtained for Test 7.S.4 is shown in Figure 8-3.

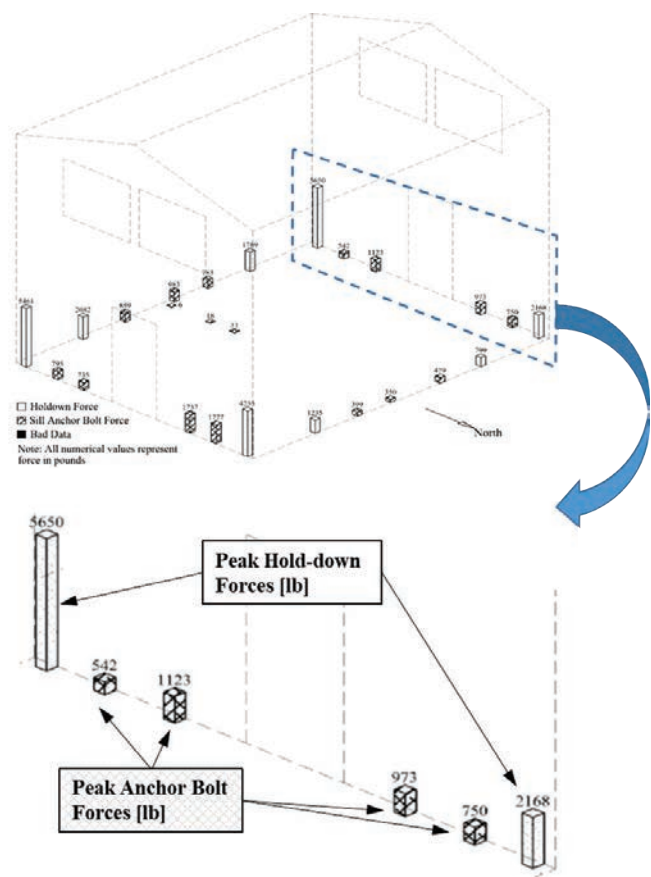


Figure 8-3 Example of documented anchorage uplift forces from the test by Fischer et al. (2001; 2002) (Current case is Test 7.S.4).

The locations of different anchor bolts and hold-downs along the east and west walls were estimated by examination of provided photos and personal communication with Andre Filiatral (Principal Investigator for the testing campaign). An illustration of the assumed anchorage locations is shown in Figure 8-4 with respect to the north side of the house.

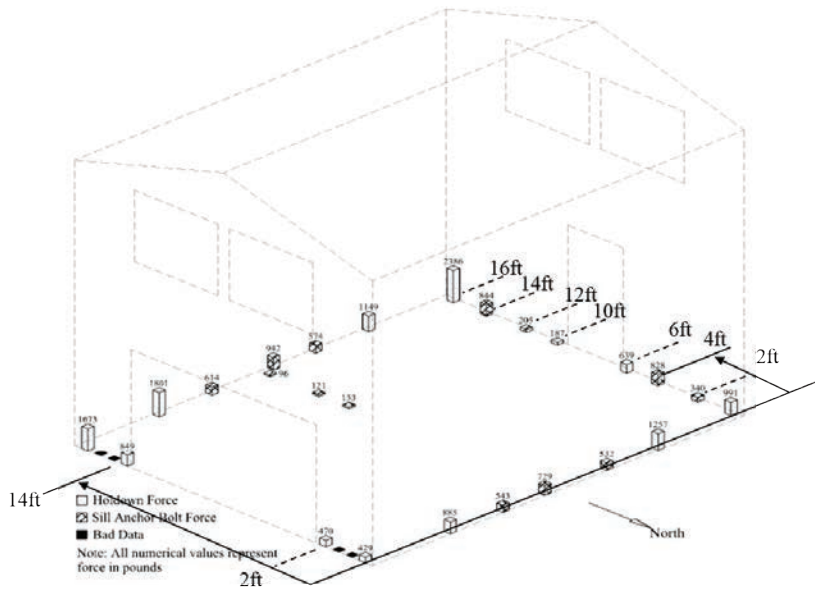


Figure 8-4 Assumed locations of anchor bolts and hold-downs for calculation of overturning moments from shake table testing by Fisher et al. (2001; 2002) (Locations for phases 9 and 10 shown).

The main purpose of the investigative effort was to understand how much of the uplift force (caused by overturning) is taken by the out-of-plane (OOP) walls perpendicular to the loading direction and the in-plane (IP) walls parallel to the loading direction. The IP portion represents the overturning that would be considered for the design of cripple wall retrofit. Since the provided uplift information represents the envelope from dynamic loading (north-south direction only), some important assumptions had to be made in order to quantify which anchorage elements were acting in tension upon north loading and south loading. These assumptions are listed as follows:

The uplift forces in the end wall perpendicular to loading and opposite to the assumed lateral loading direction (e.g., south wall for north loading) is assumed to represent the OOP overturning forces with a lever arm equal to the full depth of the house (16 feet).

The anchorage elements located in the corners of the house are assumed to equally contribute to both OOP and IP overturning and are taken as half of the reported force for each.

The neutral axis of each wall segment on each IP wall line (e.g., east and west walls) is taken at the center of each wall segment (see Figure 8-5).

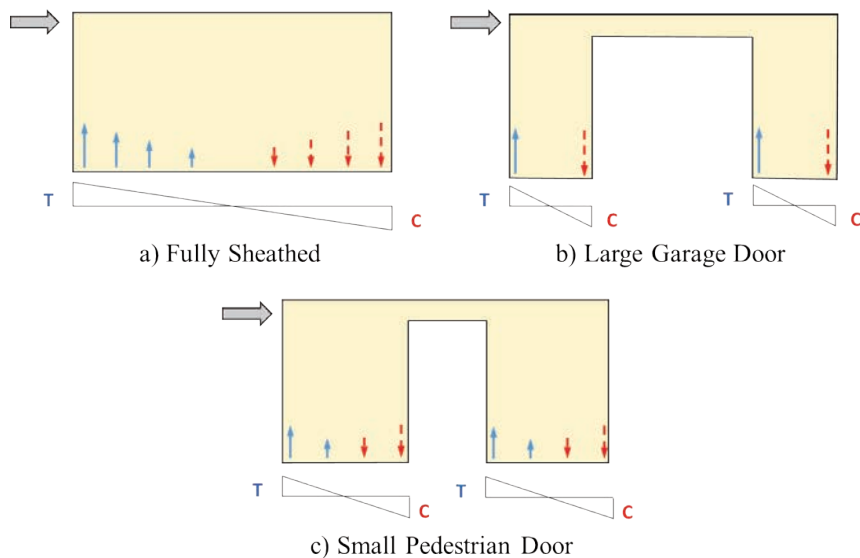


Figure 8-5 Illustration of assuming the neutral axis at the center of full-height wall segments to determine anchorage locations in tension for a direction of loading: a) fully sheathed wall, b) large garage door, c) small pedestrian door.

In-plane overturning is calculated using the assumed anchorage forces in tension multiplied by the corresponding lever arm for the assumed direction of loading (see Figure 8-5).

Three examples of assumed tension anchorage members are shown in Figures 8-6, 8-7 and 8-8 for the actual test configurations and results. Figure 8-6 shows the anchorage elements assumed in tension for north loading for Test 5.S.4R, which has continuous OSB sheathing (i.e., no openings) in the in-plane east and west walls. Figure 8-7 shows the anchorage elements assumed in tension for north loading for Test 8.S.4, which has symmetrical pedestrian door openings in the in-plane east and west walls and has conventional construction detailing with anchor bolts placed at the ends of each full-height segment (roughly 6 ft spacing). Figure 8-8 shows the anchorage elements assumed in tension for north loading for Test 9.S.4, which has unsymmetrical openings in the east and west walls and hold-downs in each end of full-height wall segments. The assumed tension elements for all cases considered are identified in the ATC-110 Volume 4, Background Documentation (WG4-B2).

A sample calculation for determining the overturning contribution is shown in Figure 8-9 for Test 10.S.5. The summary of overturning moment contribution from IP and OOP walls for all tests considered is provided in Table 8-2. The table provides the relative proportions of IP and OOP overturning (uplift) demand for each assumed direction of loading. Detailed calculation results are available in the ATC-110 Volume 4, Background Documentation (WG4-B2).

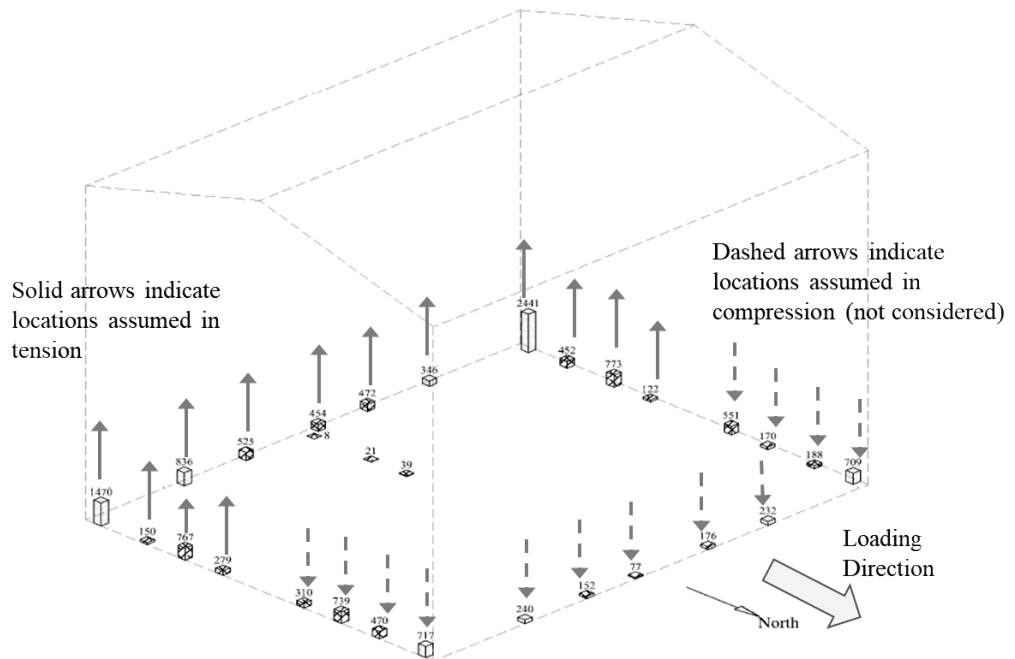


Figure 8-6 Example of anchorage elements assumed in tension for north loading: Test 5.S.4R (figure adapted from Fischer et al. (2001; 2002)).

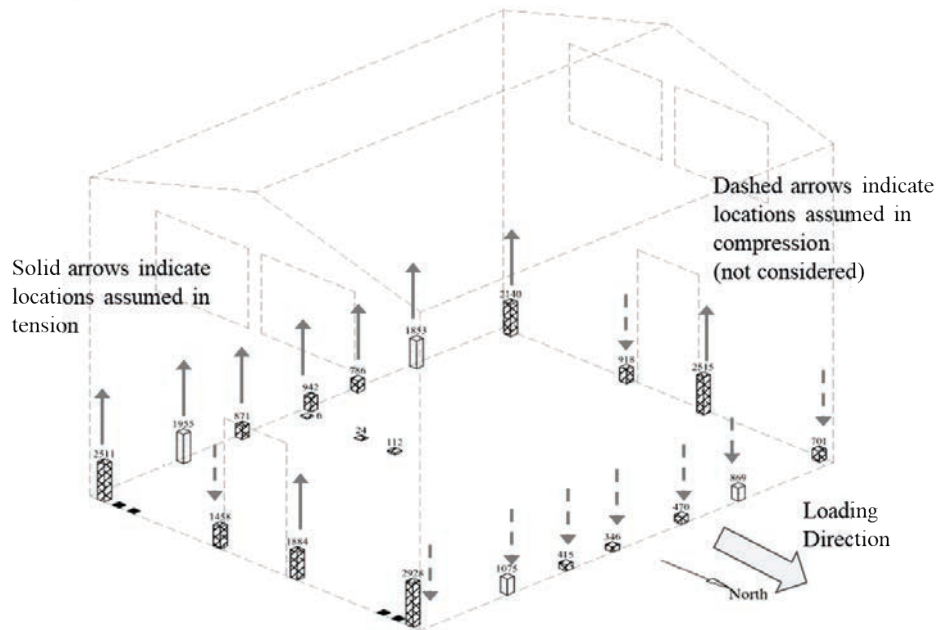


Figure 8-7 Example of anchorage elements assumed in tension for north loading: Test 8.S.4 (figure adapted from Fischer et al. (2001; 2002)).

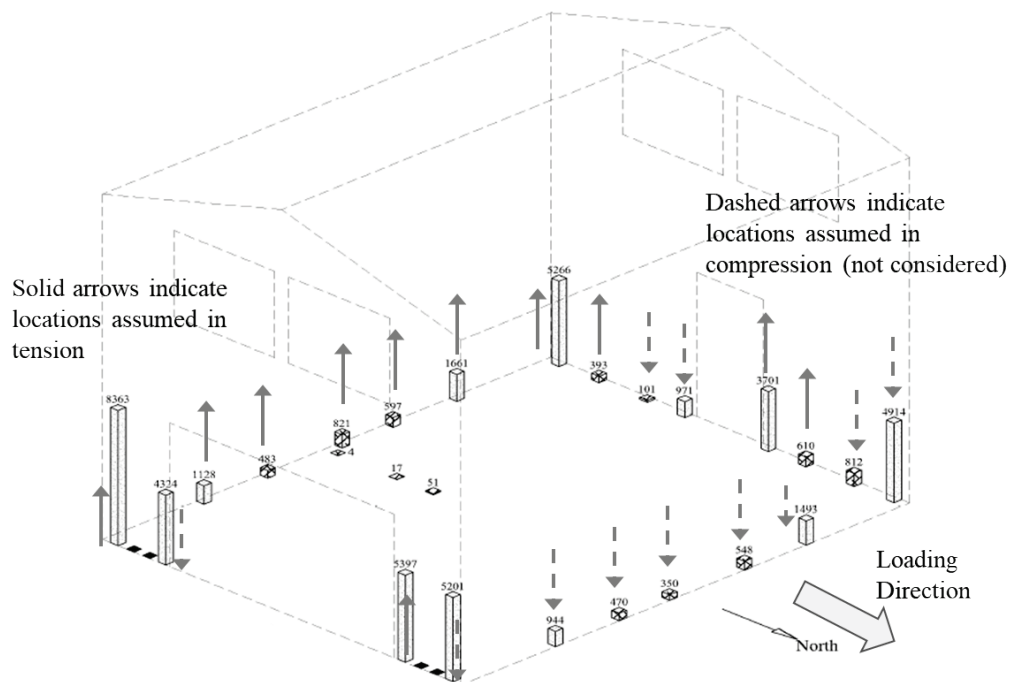
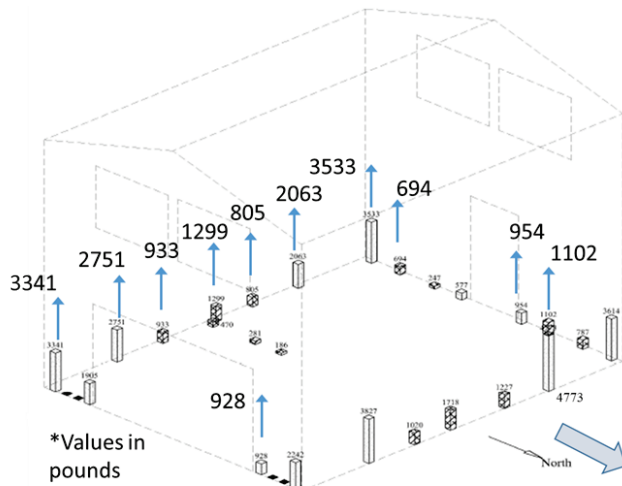


Figure 8-8 Example of anchorage elements assumed in tension for north loading: Test 9.S.4 (figure adapted from Fischer et al. (2001; 2002)).

**Test 10.S.5:
North Loading**



Test 10.S.5 Rinaldi Motion	Loading in North Direction							
	Lever arm, x [ft]	OTM _I [kip]	OTM _{OOP} [kip]	OTM _{IP} [kip]	OTM _{TOT} [kip]	OTM _{OOP} [%]	OTM _{IP} [%]	
	F [lb]	F [kip]	[kip-ft]	[kip-ft]	[kip-ft]	[%]	[%]	
16	11288	11.288	180.608	180.608	76.696	257.304	70.2%	29.8%
16	3437	3.437	54.992					
14	694	0.694	9.716					
12	0	0	0					
10	0	0	0					
6	954	0.954	5.724					
4	1102	1.102	4.408					
2	928	0.928	1.856					

Out-of-plane locations

In-plane locations

Figure 8-9 Sample calculation of overturning proportions for in-plane (IP) and out-of-plane (OOP) walls for Test 10.S.5 with north loading assumed.

Table 8-2 Summary of Overturning Proportions of In-plane and Out-of-plane Tension Demands Estimated from Shake Table Tests by Fischer et al. (2001; 2002)

Test	North Loading		South Loading	
	OOP	IP	OOP	IP
5.S.4	50%	50%	32%	68%
5.S.4R	54%	46%	36%	61%
6.S.4	56%	44%	57%	43%
6.S.4R	57%	43%	56%	44%
7.S.4	62%	38%	52%	48%
7A.S.4	59%	41%	50%	50%
8.S.4 ¹	69%	31%	65%	35%
9.S.4	55%	45%	57%	43%
9.S.5	54%	46%	64%	36%
10.S.4R ²	69%	31%	79%	21%
10.S.5 ²	70%	30%	79%	21%

⁽¹⁾ Phase 8 represents conventional construction anchorage and has symmetrical pedestrian door openings

⁽²⁾ Phase 10 is the only construction phase that represents a finished house (exterior stucco, interior gypsum wallboard, windows and pedestrian door)

Based on the results in Table 8-2, the ATC-110 Working Group 4 selected the proportions of 30% in-plane overturning and 70% out-of-plane overturning. The decision was most heavily weighted on the results of Phase 10 testing since this most closely represented a finished dwelling.

Additionally, the results from Phase 8 using conventional construction anchorage also gave similar results. These two design phases also provide the clearest paths for overturning transfer for the in-plane walls since anchorage demands are focused in the anchorage elements at the ends of each full-height segment. This is equally as important as the assumed finishes of the construction phases due to the use of envelopes of anchorage loading from dynamic shake table testing, where explicit tracking of demands in time was not feasible using published information within Fischer et al. (2001; 2002). It is possible that further investigations with different building geometries would yield different distributions, but such data was not available at the time of writing.

8.4 References

Fischer, D., Filiatrault, A., Folz, B., Uang, C-M., Seible, F. (2001) "Shake Table Tests of a Two-Story Woodframe House," *CUREE Publication No. W-06*, CUREE-Caltech Woodframe Project,

Consortium of Universities for Research in Earthquake Engineering,
Richmond, CA.

Filiatrault, A., Fischer, D., Folz, B., Uang C-M. (2002). "Seismic Testing of Two-Story Woodframe House: Influence of Wall Finish Materials", ASCE Journal of Structural Engineering, 128(10), 1337-1345.

Part 9

CrawlspacetoHillside Dwelling Transition Study

9.1 Introduction

The FEMA P-1100 Chapter 4 crawlspace dwelling retrofit with wood structural panel sheathing (WSP) and shear clips is significantly more cost effective than the FEMA P-1100 Chapter 6 hillside dwelling retrofit, with robust anchorage to the uphill foundation. This background document summarizes the information used to determine the transition point between when a dwelling with a stepped or sloped foundation can utilize a crawlspace retrofit, and when the more extensive hillside retrofit approach would be required. This transition point was of considerable interest to the ATC-110 project team, due to the significant difference in cost and construction effort between the two retrofit methodologies.

The remainder of the document is divided into four sections. Section 2 discusses the potential hillside dwelling failure modes envisioned by the project team, and the deflection limits selected in order to avoid occurrence of these failures. Section 3 outlines the numerical analysis work performed by the crawlspace dwelling working group (Working Group 4) to investigate how an increasing site slope and related change in cripple wall height from uphill to downhill side of dwelling affects the estimated deflections and resulting performance of seismic retrofitting. Section 4 outlines the numerical studies performed by the hillside dwelling working group (WG6) to investigate deflections and resulting performance. Section 5 discusses the various aspects considered when defining the crawlspace to hillside transition point, and the transition point description that was finally selected by the project team.

9.2 Potential Hillside Failure Modes

The hillside dwelling configuration identified by the project team to be of primary concern involved a dwelling with the framed floor supported directly on the foundation at the uphill side of the dwelling, and a tall cripple wall at the opposite downhill side of the dwelling. Also considered was the inclusion of a very short cripple wall at the uphill side of the dwelling in combination with the tall downhill cripple wall. In both these cases, the significantly

higher flexibility of the downhill walls will result in the floor diaphragm responding in rotation under cross-hill loading (Figure 9-1(a)) and movement of the floor diaphragm away from the uphill foundation in out-of-hill loading (Figure 9-1(b)). A primary concern was the tearing of the floor diaphragm away from the uphill foundation, as had been seen in the 1994 Northridge, California Earthquake (Figure 9-2). This resulted in loss of the gravity load path at the uphill foundation and collapses of dwellings.

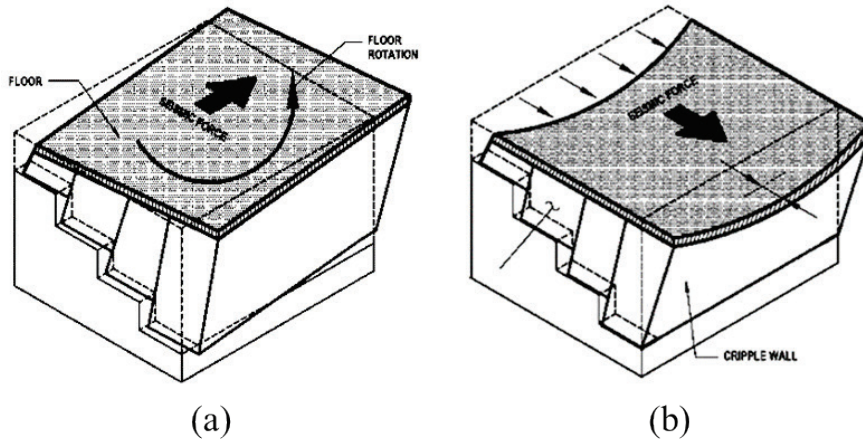


Figure 9-1

Short cripple wall at the uphill side of the dwelling in combination with the tall downhill cripple wall: (a) illustrates cross-slope loading, with rotation of the diaphragm resulting in the floor diaphragm pulling away from the uphill foundation; (b) illustrates direct out-of-hill loading.



Figure 9-2

Illustrations of hillside dwellings failing by tearing away at the uphill diaphragm connection causing global collapse following the 1994 Northridge, California earthquake. (Photo credit City of Los Angeles.)

At the uphill foundation the project team envisioned that the floor diaphragm could be sitting on top of the foundation (Case 1, Figure 9-3(a)), supported on a ledger on the face of the foundation wall (Case 2, Figure 9-3(b)), or sitting on a short cripple wall (shorter than two feet) (Case 3, Figure 9-3(c)). In each of these cases, the project team identified a displacement of the diaphragm of approximately two inches being where concern rose that the

gravity load path and in-plane shear connections at the uphill foundation might be lost. In Case 1, the floor diaphragm would be in the process of sliding off of the foundation and would have compromised shear connections. In Case 2 it is likely that the ledger connection to the wall would be failed, losing both gravity and shear connections. For Case 3, it was envisioned that the short cripple wall would have leaned (rolled) over enough in the down-hill direction that the fasteners at the top and bottom of the studs would be significantly withdrawn, and no longer able to carry horizontal load components required to stabilize the studs; this was seen to cause loss of both gravity and shear load capacity.

Based on this reasoning, the cripple wall working group (WG4) and the hillside dwelling working group (WG6) used numerical studies to provide a better understanding of what cripple wall geometries would result in this level of displacement at the uphill foundation.

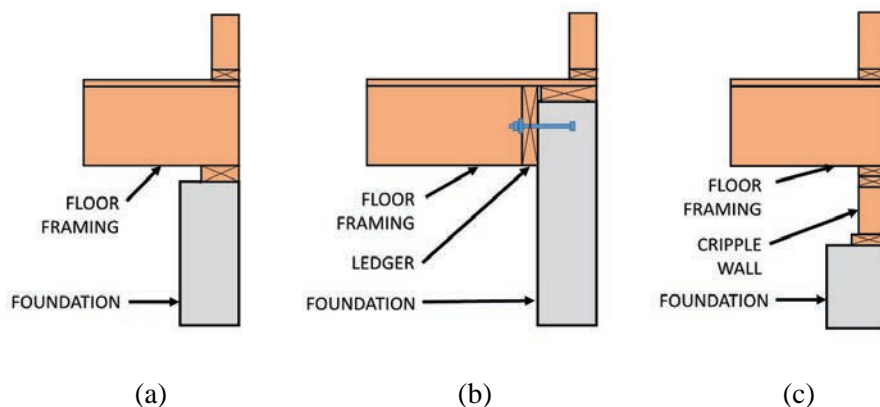


Figure 9-3 Floor diaphragm case examples: (a) illustrates Case 1 with the floor diaphragm sitting on top of the foundation, (b) illustrates Case w with the floor diaphragm supported on a ledger on the face of the foundation wall, and (c) illustrates Case 3 with the floor diaphragm sitting on a short cripple wall.

9.3 Numerical Studies by the Crawlspace Dwelling Working Group

The transition study performed by Working Group 4 aimed to quantify the seismic collapse performance of cripple wall dwellings with a stepped configuration that includes a “zero-height” condition on one side of the dwelling (i.e., one wall line where the wood framed floor sits directly on the foundation or concrete stem wall, without a cripple wall). The behavior of the “zero-height” wall was investigated in terms of likely in-plane and out-of-plane displacements, as well as global collapse performance. Various cripple wall geometries are considered in combination with different assumptions regarding the resistance provided by the connections at the

“zero-height” (i.e., uphill) wall line. Collapse performance was estimated including both global collapse and non-simulated collapse; with the latter attempting to capture likely failure of the uphill wall line and gravity load carrying capacity that is not explicitly modeled using non-linear time-history analysis.

The main objective of the study was to identify what retrofitted cripple wall geometry (e.g., height of downhill cripple wall and slope of cross-slope wall lines) generated significantly higher probabilities of collapse than for retrofitted level cripple walls. The study suggests that ATC-110 cripple wall retrofits can provide similar protection against collapse for downhill cripple wall heights up to 8 feet depending on the slope of the site. This assisted the ATC-110 teams in defining the transition point for using the hillside retrofit scheme. However, these results must be combined with additional considerations due to the complex nature of the targeted problem.

The numerical analyses performed by the crawlspace working group are discussed in this section. The archetypes considered are discussed followed by variations in numerical modelling assumptions. Results are presented and discussed.

9.3.1 Archetypes Considered for Transition Study

All of the archetypes considered for the transition study consider the WG4 one-story pre-1950 superstructure to define the properties of the model in the occupied story (see FEMA P-1100 Volume 3, Part 6 and Part 11). All archetypes are 30 feet by 40 feet in plan. The existing cripple wall finish material is taken as lower bound stucco in all cases (see FEMA P-1100 Volume 3, Part 4 for material definitions). All retrofit solutions assume wood structural panels with 8d common nails spaced at four inches on center which are designed assuming an R-factor of 3 (WG4 later selected R=4). Due to the commonalities across all archetypes considered, the nomenclature is simplified to describing only the crawlspace geometry and the anchorage assumptions pertaining to the resistance at the uphill wall line with the floor framing bearing directly on the mudsill.

Two control archetypes are used for comparison that represent level (i.e., constant height) cripple wall dwellings with heights of four and six feet, which are referred to as “Constant 4ft” and “Constant 6ft”, respectively. Notably, these archetypes correspond to “4-1C4L-M-R61%WSP9-noHD” and “4-1C6L-M-R61%WSP6-noHD” using the standard cripple wall nomenclature as discussed in FEMA P-1100 Volume 3, Part 11. An illustration of the geometry of the control archetypes is shown in Figure 9-4.

The other archetypes consider variations in the assumed downhill cripple wall height (i.e., tallest wall height) which defines the slope in the uphill/downhill direction. Two different orientations were considered for the location of the uphill wall line (i.e., wall line with the floor framing bearing directly on the mudsill). The typical orientation used for the transition study assumes the uphill wall line is located along the east side of the dwelling (30-foot dimension of plan). This orientation is referred to as “00”. The other orientation was considered in limited cases and is referred to as “90”. An illustration of the two different orientations is shown in Figure 9-5 along with helpful terminology used for the study.

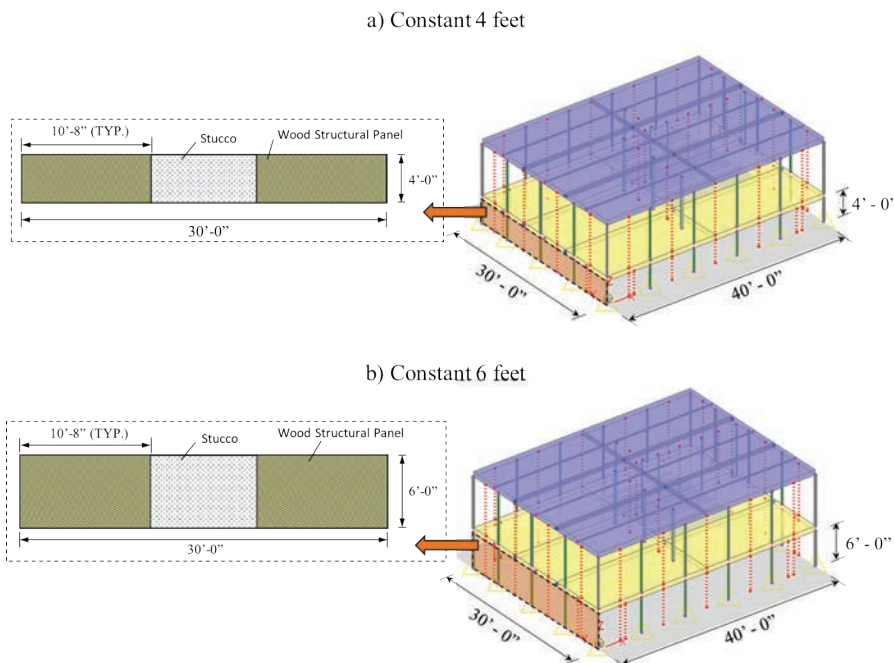


Figure 9-4 Illustration of the two control archetypes on constant height cripple walls used for comparison in the transition study: (a) four-foot cripple wall height; (b) six foot cripple wall height. Wood structural panels assume 8d common nails at 4 inches on center.

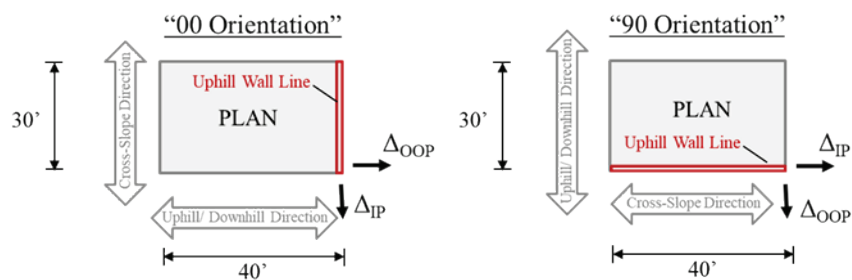


Figure 9-5 Illustration of the two orientations of the uphill wall line considered for transition study archetypes. In-plane (IP) and out-of-plane (OOP) displacements are annotated with respect to the uphill wall line.

The downhill wall heights considered were four, six and eight feet. The four and six feet cases assumed that the cross-slope walls have two equal steps in terms of height reduction and wall length. For example, the four-foot case with “00” orientation breaks the 40-foot plan dimension into two 20-foot sections with wall heights of four and two feet. In terms of wall geometry, this case is labeled as 4'-2'-0' to represent the transitions in wall height that reduce to the zero-height condition at the uphill wall line. The eight-foot cases have two different step assumptions. The first is the 8'-2'-0' case that has a large transition step from eight to two feet at the mid-point of the 40-foot dimension. The other case is denoted as 8'-6'-4'-2'-0' that assumes four equal step lengths of ten feet with a height increment of two feet along every step. Notably, all transition study cases have a total of 21'-4" of wood structural panel bracing on all sides except the uphill wall line with floor framing bearing directly on the mudsill. An illustration of the two 8-foot cases is illustrated in Figure 9-6.

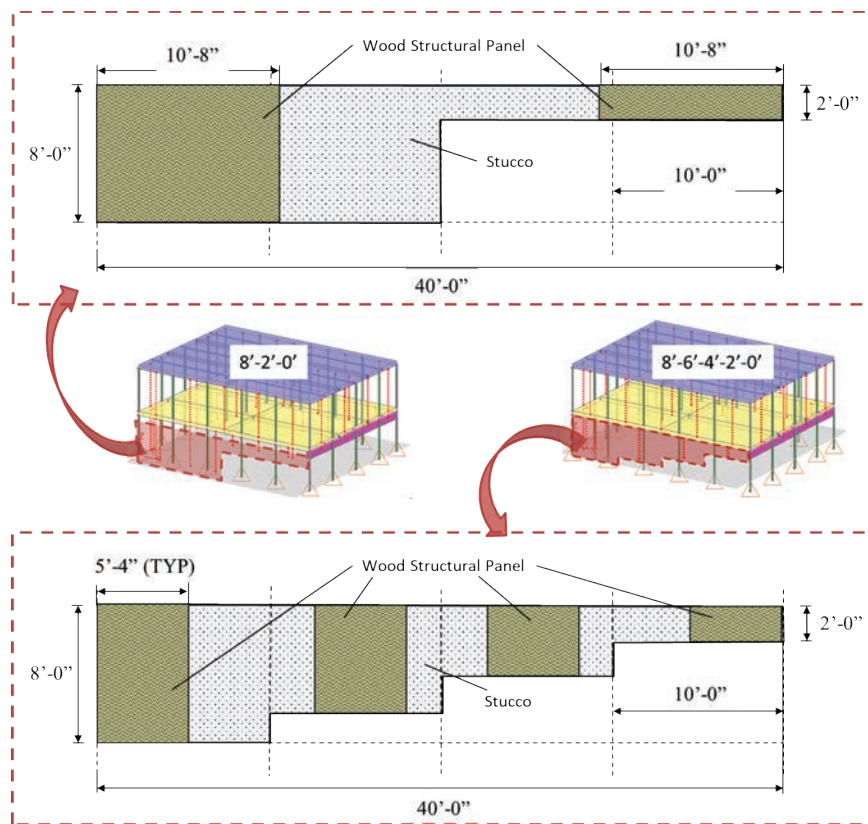


Figure 9-6 Illustration of the two variations of sloped cripple walls with a maximum downhill height of eight feet: Case 8'-2'-0' with large single transition height (above), Case 8'-6'-4'-2'-0' with evenly distributed height transition (below).

9.3.2 Considerations for Resistance at the Uphill Wall Line

The transition study aims to understand significant differences in retrofit performance when comparing constant height cripple walls to those located on a sloped lot with a zero-height condition at the uphill wall line. The assessment of the existing pre-retrofit condition of sloped cripple walls was not included in the scope of study.

The transition study considers three variations of resistance at the uphill wall line diaphragm to foundation connection:

1. In-plane resistance only
2. In-plane and out-of-plane resistance
3. Coupled in-plane and out-of-plane resistance

The modeling parameters and analysis assumptions used to create these different levels of resistance are discussed in the following sub-sections. A summary of all cases considered is provided in Section 3.3.

9.3.2.1 Modeling of In-plane Resistance at the Uphill Wall Line

Using available experimental data, A35 clips that were tested by Ficcadenti et al. (2004) within the CUREE-Caltech Woodframe Project represented the in-plane (IP) resistance and cyclic properties of sill anchorage retrofit. The behavior of the A35 clips was captured within *Timber3D* using the SAWS hysteresis model. The SAWS hysteretic model was selected to represent IP anchorage elements in order to take advantage of the ability to incorporate a failure displacement, after which the element would reduce to zero-force and essentially behave as if the element were removed. An illustration of fitting the SAWS model to A35 clips tests is provided in Figure 9-7. Notably, the figure shows that a failure displacement of 1.6 inches was sought to capture the point in the test where the clips no longer transferred appreciable load. The corresponding hysteretic properties for A35 clips are provided in Table 9-1.

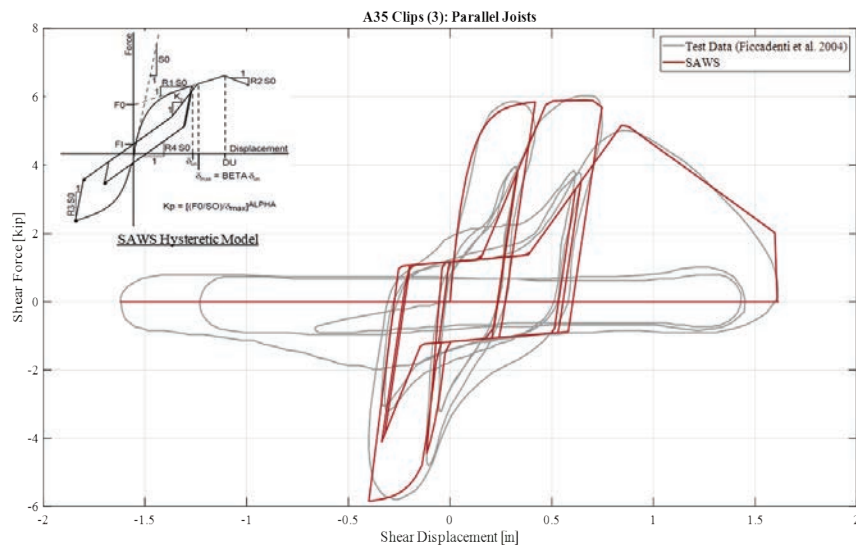


Figure 9-7 Fitting of SAWS hysteretic model to A35 clip testing conducted by Ficcadenti et al. (2004). NOTE: The test shown is for three clips in parallel.

Table 9-1 SAWS Hysteretic Parameters for A35 Clips Used for In-plane Resistance of Crawlspace Retrofit at the Joist-to-sill Connection

S ₀ [kip/in-clip]	R ₁	R ₂	R ₃	R ₄	F ₀ [kip/clip]	F ₁ [kip/clip]	D _U [in]	α	β
24.0	0.001	-0.06	0.55	0.007	1.95	0.39	0.7	0.92	1.14

9.3.2.2 Modeling of Out-of-Plane Resistance at the Uphill Wall Line

The out-of-plane (OOP) resistance at the uphill wall line was considered in some cases (see Table 9-3). Other cases neglected the OOP resistance completely. When considered, the OOP resistance at the uphill wall line was assumed to be provided by a combination of L30 clips spaced at 32 inches and $\frac{1}{2}$ " anchor bolts placed at 6 feet on center. Where included, the L30 clips for tension loads pulling away from the uphill foundation represented an additional connection that could be provided at dwellings falling under crawlspace dwelling (FEMA P-1100 Volume 1, Chapter 4) retrofit methods. In the final retrofit provisions, WG4 included detail requirement of L30 clips (or similar) spaced at 32 inches (typically at every other joist) for floor joist-to-sill connections in dwellings that had a cripple wall height of greater than four feet elsewhere in the dwelling.

Using engineering judgment and code-based design checks, the capacity of this connection was assumed to provide 275 lb/ft along the length of the sill plate. The design checks considered the ultimate capacity of the L30 clips, out-of-plane strength of $\frac{1}{2}$ " anchor bolts, bolt bearing failure at the sill plate and checking cross-grain bending of the sill. These code-based checks are

provided in Appendix A of this document. Notably, existing capacity of toenail connections from the floor joists to the mudsill were not considered for either OOP or IP loading.

In lieu of explicit experimental data for this type of connection and loading, the IP backbone curve for the A35 clips was scaled down in order to provide an equivalent element that could provide the expected resistance when spaced at 32 inches on center. The same cyclic properties as the A35 clips were assumed for the L30 elements. An illustration of the two backbone curves of uphill wall line elements is provided in Figure 9-8.

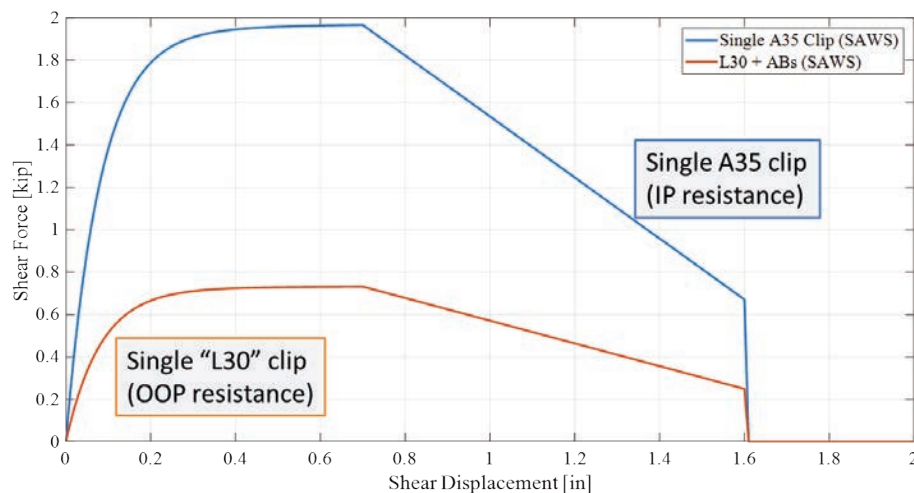


Figure 9-8 Assumed material backbones for in-plane (IP) and out-of-plane (OOP) resistance at the retrofit joist-to-sill connection at the uphill wall line of sloped cripple wall with a zero-height condition.

A scaling factor of 0.372 is applied to the parameters S0, F0 and FI in Table 9-1 in order to convert from A35 clips to the assumed L30 clip parameters. The converted L30 hysteretic parameters are provided in Table 9-2.

Table 9-2 SAWS Hysteretic Parameters for L30 Clips Used for Out-of-plane Resistance of Crawlspace Retrofit at the Joist-to-sill Connection

S0 [kip/in-clip]	R1	R2	R3	R4	F0 [kip/clip]	FI [kip/clip]	DU [in]	α	β
8.93	0.001	-0.06	0.55	0.007	0.725	0.145	0.7	0.92	1.14

When OOP resistance is considered, the equivalent L30 clip elements are attached to a foundation beam underneath the floor diaphragm elements as shown in Figure 9-9. The figure also shows that L30 clip elements are not placed in the last 4 feet of the sill plate at either end of the uphill wall line. This was done to neglect the OOP resistance in this portion due to notch shear considerations for the anchor bolts at the extreme ends.

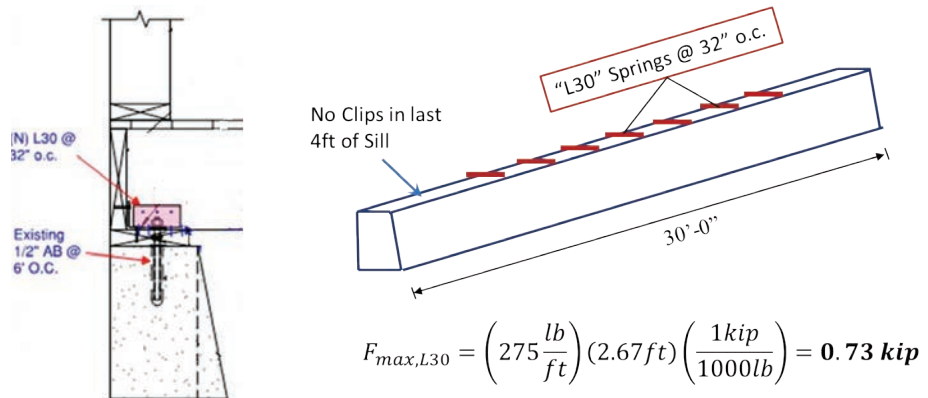


Figure 9-9 Illustration of the out-of-plane (OOP) connection at the sill plate (left) and the placement of equivalent L30 clip elements along the foundation beam (right).

The elastic foundation beam was modeled with equivalent section properties corresponding to a trapezoidal foundation beam cross section that is 18 inches high, 12 inches wide at the base and 8 inches wide at the top face (see Figure 9-10). The beam is assumed fully fixed at its ends (continuous corner to perpendicular direction) and rigid in flexure and shear. The torsional stiffness of the foundation beam assumed a concrete compressive strength of 2500 psi and an effective torsional constant of $0.1J_{gross}$. Notably, the effect of friction between the floor framing, sill and top of foundation was neglected when modeling the uphill wall line connections. The inclusion of torsional movement of the foundation beam aimed at allowing some level of differential loading of the out-of-plane anchorage when loaded purely in the uphill or downhill direction.

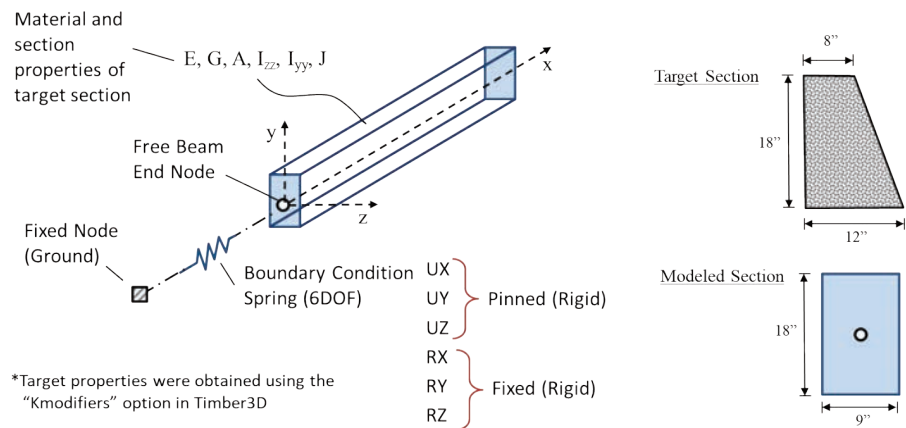


Figure 9-10 Modeling assumptions for creating the foundation beam at the uphill wall line.

An illustration of the different components used to model the uphill wall line anchorage is shown in Figure 9-11 for a zero-height cripple wall with a maximum downhill cripple wall height of 8 feet. The cripple walls on the

sides (cross slope) are reduced in height in increments of 2 feet. Notably, cripple wall perimeters with a zero-height connection were modeled with stud element heights that correspond to the tallest cripple wall height to accommodate three-dimensional diaphragm displacements without inducing axial tension in these elements undergoing large displacements. Notably, this was only found to occur for the largest height differentials with the 8-foot tall downhill wall cases. For consistency, this was also assumed for other transition study cases.

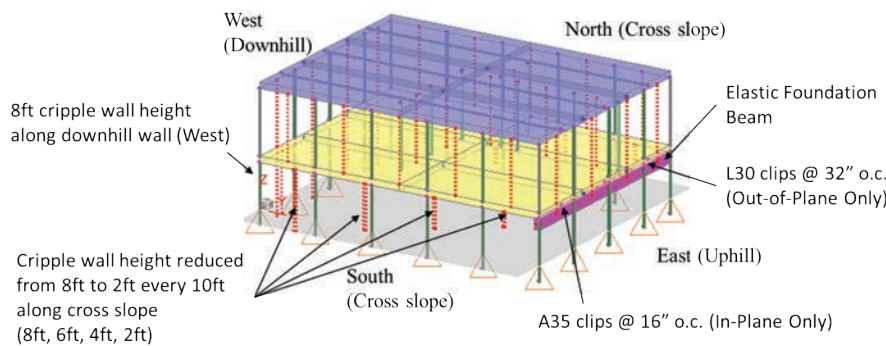


Figure 9-11 Rendering of *Timber3D* model representing a one-story cripple wall dwelling with a ‘zero-height’ condition. Current case shows both in-plane and out-of-plane resistance considered at the uphill wall line.

9.3.2.3 Coupled In-plane and Out-of-plane Resistance and Non-simulated Failure Considerations for the Uphill Wall Line

The influence of interaction between in-plane (IP) and out-of-plane (OOP) resistance at the uphill wall line was also investigated for select transition study archetypes (see Table 9-3). The main concept behind the interaction was that the IP resistance (represented by A35 clips) should be reduced or removed based on the OOP resistance (represented by L30 clips) being exceeded during previous displacement excursions during nonlinear response history analysis (NLRHA). The *Timber3D* software was updated in order to allow an interaction function to be specified between two orthogonal degrees of freedom within a non-linear frame-to-frame (F2F) element. The function assumed that the IP resistance would be reduced linearly after the OOP displacement exceeds 0.5 inches and would completely remove the IP resistance after the OOP resistance reached zero load at a displacement of 1.6 inches. The onset of IP strength reduction at 0.5 inches was selected based on judgment and group discussion. An illustration of the interaction surface and corresponding IP and OOP backbone curves are shown in Figure 9-12. Notably, the right portion of Figure 9-12 illustrates how the peak capacity of the IP resistance (dashed line) will be reduced based on a previous OOP

excursion to a given displacement. If the previous OOP displacements are less than 0.5", then the IP resistance follows the solid blue line in Figure 9-12.

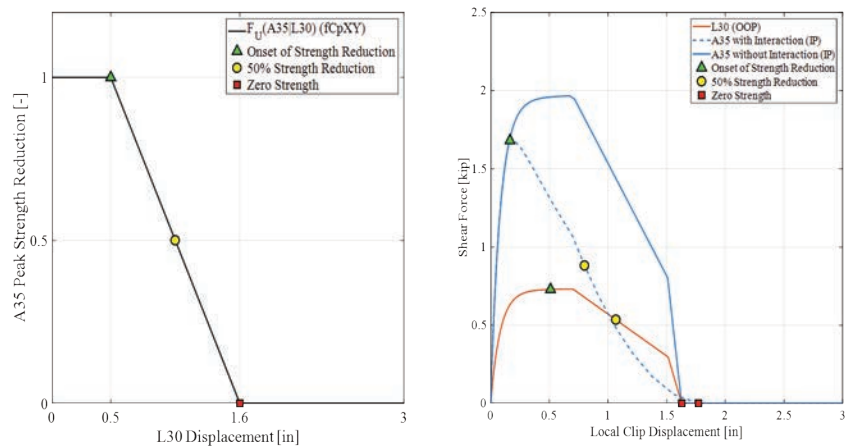


Figure 9-12 Illustration of interaction surface assumed for in-plane (IP) resistance at uphill wall line conditioned on peak out-of-plane (OOP) displacement history: example of surface (left); monotonic capacity curves (right)

To address the limitations of the numerical modeling assumptions to capture the complexity of a sloped cripple wall losing horizontal and vertical load carrying capacity, the transition study monitored the OOP displacement at the uphill wall line to represent a non-simulated collapse mode of the sill anchorage and OOP displacement of short cripple wall sections perpendicular to the uphill foundation. Two threshold displacements of 2 inches and 3.5 inches were evaluated; the exceedance of which would be treated as a non-simulated collapse that would be added to the observed global collapse of structural models. Discussion of the selected displacement thresholds is provided in Section 2. An example of how the consideration of OOP displacements can affect expected collapse probability is shown in Figure 9-13. The figure shows that for the example case, the threshold displacement of 3.5 inches gives a small increase in the expected collapse probability at MCE, and the more stringent 2-inch threshold shows a non-negligible increase in collapse probability.

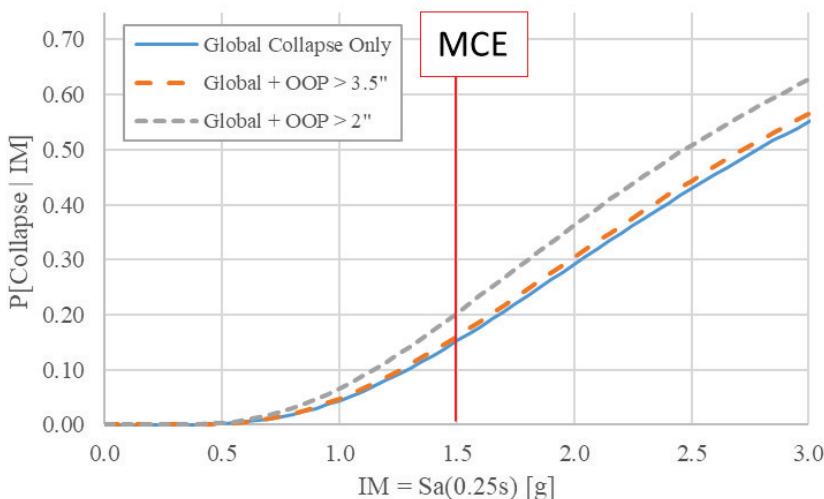


Figure 9-13 Example of using out-of-plane (OOP) displacement to relate to non-simulated collapse in addition to global collapse returned from structural analysis.

9.3.3 Analysis Results for Cripple Wall Dwellings Considered in the Transition Study

The discussion of the transition study archetype results are presented in this section. The summary of all cases considered by the cripple wall dwelling group is provided in Table 9-3. The slope of the side walls is presented as a ratio and in terms of percent grade (e.g., a slope of 1:10 has a 10% grade).

A summary of the first two modal periods and corresponding pushover strength-to-weight ratios are provided in Table 9-4. The table includes the constant height cripple wall control cases for comparison. The results of Table 9-4 illustrate that the zero-height transition study archetypes have slightly shorter fundamental periods compared to the equivalent constant height case. Similarly, the average strength to weight ratios $(V/W_{BL})_{Avg}$ are typically higher than the equivalent constant height case. This is mostly due to the increase in strength at the uphill wall line due to the addition of A35 clips at 16 inches on center. This is reflected in the larger strength ratios (i.e., greater than 1.0) estimated for the cross-slope loading direction. The uphill loading directions are very similar for the transition study archetypes when comparing to the equivalent constant height case. The eight-foot tall cases give very similar results to the corresponding six-foot case that includes OOP resistance by including L30 clips in the numerical model (e.g., comparing the "8'-2'-0' A35+L30" case to the "6'-3'-0' A35+L30" case).

Table 9-3 Summary of Different Configurations Analyzed for the Cripple Wall to Hillside Transition Study

Archetype ¹	Downhill Cripple Wall Height [ft]	Orientation	Slope (grade)	In-Plane Resistance at Uphill Wall Line ²	Out-of-plane Resistance at Uphill Wall line ³
4'-2'-0' A35	4.0	00	1:10 (10%)	A35 @ 16" o.c.	Not modeled
4'-2'-0' A35-90	4.0	90	1:7.5 (13%)	A35 @ 16" o.c.	Not modeled
6'-3'-0' A35	6.0	00	1:6.7 (15%)	A35 @ 16" o.c.	Not modeled
6'-3'-0' A35+L30	6.0	00	1:6.7 (15%)	A35 @ 16" o.c.	L30 @ 32" o.c.
8'-2'-0' A35+L30	8.0	00	1:5 (20%)	A35 @ 16" o.c.	L30 @ 32" o.c.
8'-6'-4'-2'-0' A35+L30	8.0	00	1:5 (20%)	A35 @ 16" o.c.	L30 @ 32" o.c.

¹ Initial numbers represent the stepping of cripple wall heights from downhill to uphill (0') walls;

² A35 clip properties estimated from testing by Ficcadenti et al. (2004); ³ L30 properties assume a peak strength of 275 lb/ft; last 4 feet of sill plate is neglected

Table 9-4 Modal Period and Pushover Summary for Transition Study Archetypes

Archetype ¹	Modal Periods		Pushover Strength-to-Weight Ratios (V/W _{BL}) ²		
	T ₁ [s]	T ₂ [s]	Cross-Slope	Uphill	Average
Constant 4'	0.130	0.118	0.73	0.82	0.77
4'-2'-0' A35	0.120	0.106	1.02	0.81	0.91
4'-2'-0' A35-90	0.115	0.109	1.26	0.72	0.99
Constant 6'	0.144	0.131	0.78	0.87	0.82
6'-3'-0' A35	0.128	0.118	1.05	0.83	0.94
6'-3'-0' A35+L30	0.128	0.116	1.05	0.92	0.98
8'-2'-0' A35+L30	0.134	0.110	1.05	0.89	0.97
8'-6'-4'-2'-0' A35+L30	0.136	0.114	1.04	0.91	0.97

¹ Initial numbers represent the stepping of cripple wall heights from downhill to uphill (0') walls (if applicable);

² All archetypes have the same baseline weight (W_{BL}) of 68.2 kips not including weight of cripple wall

The adjusted collapse performance at the MCE level (Primary Criterion) shown for all transition study archetypes in Figure 9-14. The two control archetypes with constant height cripple walls are shown with dark blue bars. The transition study archetypes with a zero-height condition are shown with sets of three bars that represent global collapse only and including OOP displacements that exceed 3.5 and 2.0 inches, respectively. The corresponding values in Figure 9-14 are provided in Table 9-5. The values presented in Table 9-5 do not include the collapse numbers for the 0.4MCE level (i.e., $S_a(0.25s) = 0.6g$) for brevity since none of the archetypes were found to collapse at this intensity. More complete information including modal and pushover analysis of each transition study archetype can be found in the FEMA P-1100 Volume 4 WG4-B7 document.

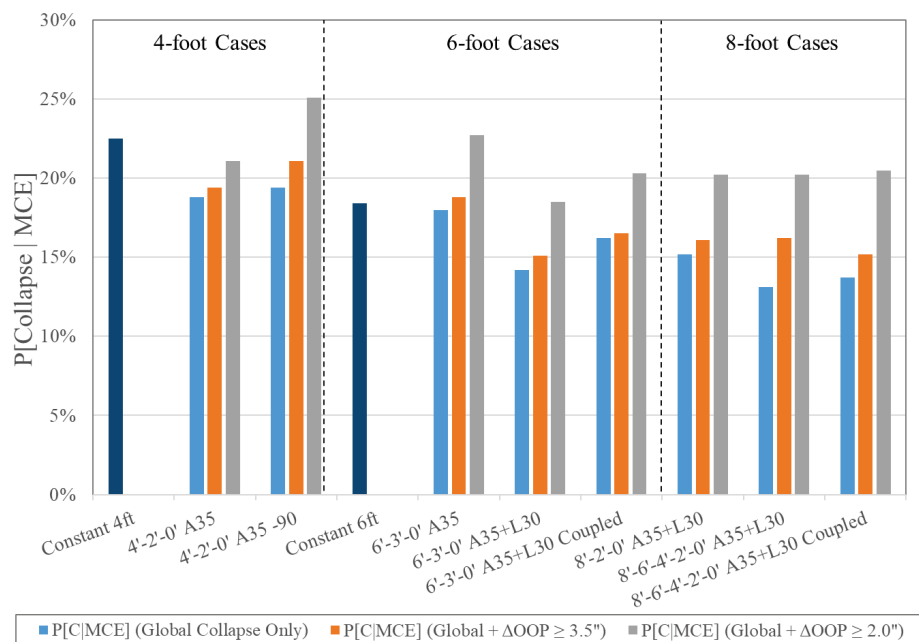


Figure 9-14 Collapse performance summary at the MCE level for all transition study archetypes. All archetypes included retrofit.

The results of Figure 9-14 can be summarized in the following observations:

- Four-foot cases: The two orientations of zero-height models without out-of-plane resistance (i.e., “4’-2’-0’ A35” and “4’-2’-0’ A35-90”) returned MCE collapse probabilities below the equivalent constant height model for all cases except the “90” orientation including the more conservative non-simulated collapse threshold of 2.0” out-of-plane displacement. Further, considering that the out-plane-resistance at the uphill wall line is completely neglected in these cases, the estimated collapse probabilities would be expected to be at or below the equivalent constant height case with any consideration of out-of-plane resistance. This is an important

Table 9-5 Collapse Performance Summary for Transition Study Archetypes—Counted Collapse Cases at the DE and MCE Intensity Levels and Adjusted Probability of Collapse at the MCE Level

Archetype	DE	MCE	P[C MCE]
	Sa=1.0g	Sa=1.5g	
<i>Global Collapse Only¹</i>			
Constant 4ft Cripple Walls	2/44	23/44	22.5%
4'-2'-0' A35 Clips (IP Only)	2/44	18/44	18.8%
4'-2'-0' A35 Clips -90 (IP Only; 90 Orientation)	3/44	19/44	19.4%
Constant 6ft Cripple Walls	0/44	18/44	18.4%
6'-3'-0' A35 Clips (IP Only)	2/44	17/44	18.0%
6'-3'-0' A35 + L30 (IP and OOP)	1/44	12/44	14.2%
6'-3'-0' A35 + L30 Coupled (IP and OOP)	1/44	14/44	16.2%
8'-2'-0' A35 + L30 (IP and OOP)	1/44	13/44	15.2%
8'-6'-4'-2'-0' A35 + L30 (IP and OOP)	1/44	11/44	13.1%
8'-6'-4'-2'-0' A35 + L30 Coupled (IP and OOP)	1/44	10/44	13.7%
<i>Including Non-simulated Collapse: $\Delta_{oop} \geq 3.5'' = \text{Collapse}^2$</i>			
4'-2'-0' A35 Clips (IP Only)	3/44	19/44	19.4%
4'-2'-0' A35 Clips -90 (IP Only; 90 Orientation)	3/44	21/44	21.1%
6'-3'-0' A35 Clips (IP Only)	2/44	18/44	18.8%
6'-3'-0' A35 + L30 (IP and OOP)	3/44	14/44	15.1%
6'-3'-0' A35 + L30 Coupled (IP and OOP)	3/44	16/44	16.5%
8'-2'-0' A35 + L30 (IP and OOP)	2/44	15/44	16.1%
8'-6'-4'-2'-0' A35 + L30 (IP and OOP)	1/44	16/44	16.2%
8'-6'-4'-2'-0' A35 + L30 Coupled (IP and OOP)	1/44	13/44	15.2%
<i>Including Non-simulated Collapse: $\Delta_{oop} \geq 2.0'' = \text{Collapse}^2$</i>			
4'-2'-0' A35 Clips (IP Only)	3/44	21/44	21.1%
4'-2'-0' A35 Clips -90 (IP Only; 90 Orientation)	5/44	26/44	25.1%
6'-3'-0' A35 Clips (IP Only)	4/44	23/44	22.7%
6'-3'-0' A35 + L30 (IP and OOP)	3/44	18/44	18.5%
6'-3'-0' A35 + L30 Coupled (IP and OOP)	3/44	20/44	20.3%
8'-2'-0' A35 + L30 (IP and OOP)	4/44	20/44	20.2%
8'-6'-4'-2'-0' A35 + L30 (IP and OOP)	4/44	20/44	20.2%
8'-6'-4'-2'-0' A35 + L30 Coupled (IP and OOP)	4/44	19/44	20.5%

¹ Vertical drop of 75% of tallest cripple wall height at the center of the roof diaphragm

² Exceedance of 3.5" or 2.0" of out-of-plane displacement at uphill wall line

finding since the maximum cripple wall height was initially set at four feet. The current results demonstrate that this would be a very conservative threshold to require a hillside retrofit.

- Six-foot cases: Similar to the four-foot cases, the six foot archetype without the inclusion of OOP resistance (i.e., “6’-3’-0’ A35”) returned similar collapse probabilities as the equivalent constant height case except the most conservative 2.0” assumption for non-simulated collapse. The increase in collapse probability versus the constant height case is much more significant when including the 2.0” non-simulated collapse criterion. However, this case still returns similar collapse probabilities as the constant four-foot case (i.e., 22.7% versus 22.5%).

The inclusion of out-of-plane resistance at the uphill wall (e.g., case “6’-3’-0’ A35+L30”) line returned a significant reduction in the MCE collapse probability when comparing to the case without OOP resistance. These trends were consistent regardless of including or excluding non-simulated collapse. The inclusion of connection coupling at the uphill wall line returned a slight increase in MCE collapse probability with respect to the uncoupled case, yet the only collapse definition to exceed the constant six-foot cripple wall archetype was the collapse case considering the 2.0” non-simulated collapse assumption (i.e., 20.3% compared to 18.4% for constant height).

- Eight-foot cases: The tallest cripple walls considered with an eight-foot downhill height returned very similar results to the six-foot cases. In terms of the assumed step layout on the cross-slope walls, the large step model (“8’-2’-0’ A35+L30”) returned a larger global MCE collapse probability compared to the more distributed step case (“8’-6’-4’-2’0’ A35+L30”). This is attributed to the larger stepped case exhausting the wood structural panel displacement capacity of the two-foot walls prior to developing the capacity of the eight-foot walls. Both cases returned similar collapse results when including non-simulated collapse cases based on OOP displacement at the uphill wall line. The inclusion of connection coupling at the uphill wall line returned marginal differences in collapse probability when compared to the uncoupled case.

9.4 Numerical Studies by the Hillside Dwelling Working Group

As illustrated in Figure 9-15, monotonic analyses were performed by the hillside dwelling working group (WG6) on a 32’x48’ dwelling with various crawl space configurations (i.e., hillside slopes). The dimension parallel to the hillside slope was consistently 32’ and the crawl space walls were

sheathed with WSP9 typically (FEMA P-1100 Volume 3, Part 4). For more information on the dwelling's floor plan and material weights, see FEMA P-1100 Volume 3, Part 13 – *Development of Vulnerability-Based Retrofit Provisions for Hillside Dwellings*.

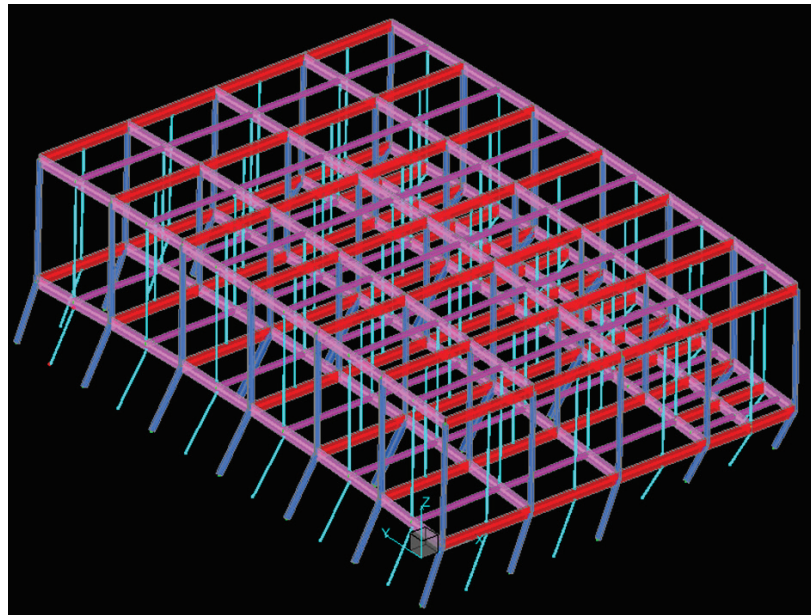


Figure 9-15 Deformed shape for monotonic uphill push (32'×48').

The following seven models with varying cripple wall configurations were evaluated: 2'-4', 2'-6', 2'-8', 2'-10', 3'-5', 3'-7' and 3'-9'. The first number is the uphill cripple wall height, and the second is the downhill cripple wall height. Each model was loaded monotonically with an incremental displacement protocol in both the out-of-hill and cross-slope directions. For each of these models, the maximum out of plane drift ratios right before P- Δ collapse is reported in Figure 9-16. These data points were enveloped in the figures provided so that each bar represents the maximum out of plane drift that would have occurred in either orthogonal direction. The drift ratios are based off the shortest cripple wall in each model (i.e., 2'-0" or 3'-0"), which occur along both the uphill foundation line and the first steps of the side foundations.

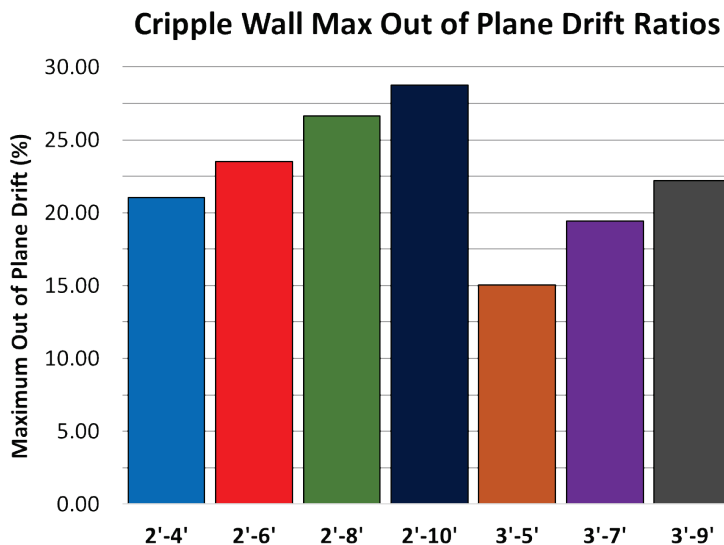


Figure 9-16 Maximum out of plane crawl space wall drift ratio (%) values for 32'×48' monotonic study.

This information can be related to the project team concern about the amount of lean that needs to occur in the uphill cripple wall studs (see Figure 9-3 (c)) in order to mobilize the capacity of retrofits that rely on sheathed cripple walls. A couple of trends are apparent in the plots that are related to hillside slope and the height of the uphill cripple walls. As shown in Figure 9-16, as the hillside slope increases, out of plane drift ratios of the shortest wall are expected to be higher due to the side and downhill walls being taller with more deformation capacity and peaking at higher drift values (i.e., more elongated stiffness curves). This would suggest that there is a transition point where the short uphill cripple walls cannot meet the drift demands of the taller cripple walls, which would be dependent on both hillside slope and the height of the uphill studs. As shown in Figure 9-16, as the height of the uphill wall studs increases from two to three feet, the expected uphill stud rotation (i.e., drift ratio) significantly lessens. This plot suggests that a small increase in stud uphill cripple wall stud height (i.e., 2'-0" to 3'-0") significantly reduces the drift ratio imposed on the uphill studs.

9.5 Transition Considerations

In addition to information from the WG4 and WG6 numerical studies, the following behavioral aspect was considered. As the dwelling is pushed uphill or downhill, the cripple walls have greater degrees of varying stiffness, which results in the shorter wall segments already entering their residual region as the taller segments reach peak capacity. As illustrated in Figure 9-17, when the dwelling is pushed in the cross-slope direction, a steeper sloped

site results in a significant stiffness difference between the uphill and downhill cripple wall. This results in significant torsion and additional stress on the cripple walls in the uphill/downhill direction. Stiff primary anchor elements at the uphill ends of base level diaphragm prevent these issues from arising, making higher sloped sites more suitable for a hillside retrofit.

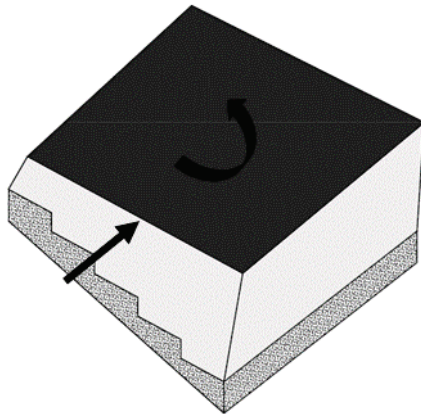


Figure 9-17 Base level diaphragm behavior for cross-slope loading.

Based on the WG4 numerical studies and the judgment of the project team, it was selected to permit use of the simpler Chapter 4 crawlspace wall retrofits up to a downhill cripple wall height of eight feet. A maximum of seven feet was eventually chosen in order to keep the height short of what might be considered a full story.

Based on WG6 numerical studies and the judgement of the project team, it was selected to require use of the Chapter 6 hillside dwelling retrofit with uphill cripple wall heights between zero and two feet. Once the cripple wall height extends above two feet, the use of the Chapter 6 retrofit is no longer mandatory. Dwellings having a cripple wall at the uphill side taller than two feet and a cripple wall at the downhill side taller than seven feet fall outside the FEMA P-1100 retrofit scope.

In summary, for a dwelling with a stepped or sloped foundation to qualify for a crawlspace retrofit, the following criteria must be satisfied:

- Cripple walls, where they occur, do not exceed 7'-0" in clear height.
- The maximum slope as measured from the top of foundations along one edge of the home to the other end does not exceed 5 to 1 (horizontal to vertical) or 20%.

The FEMA P-1100 Chapter 6 hillside dwelling retrofit is applicable when:

- The downhill cripple wall height is greater than 7'-0",

- The uphill cripple wall height is between 0'-0" and 2'-0"
- The site slope averaged over any side of the dwelling exceeds 1 vertical in 5 horizontal.

9.6 Calculations to Check Capacity of L30 Clips for Out-of-Plane Resistance at the Uphill Wall Line for Zero-height Cripple Walls

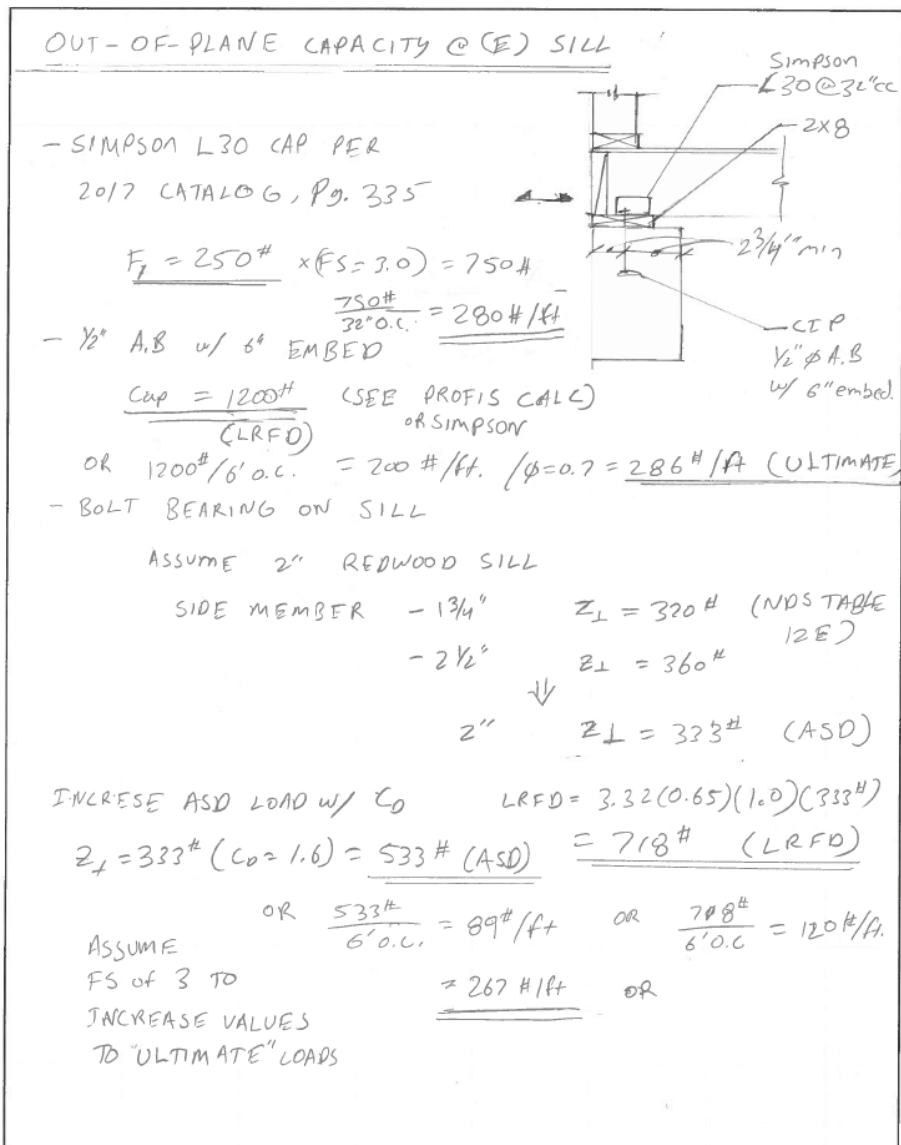


Figure 9-18 Page one of calculations for out-of-plane resistance at uphill wall line: L30 ultimate capacity, existing anchor bolt and bolt bearing on sill.

OUT-OF-PLANE CAPACITY @ (E) SILL : CONT.

- CHECK CROSS-GRAIN BENDING OF SILL

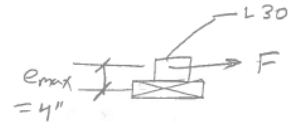
SILL BENDING CAP Y-Y

$$\sigma = \frac{M_y}{S_y}$$

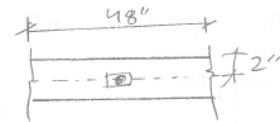
$$\sigma = 150 \text{ psi}$$

$$S_y = \frac{48(2)^2}{6}$$

$$M_{y_{max}} = 150 \text{ psi} (32 \text{ in}^3) = 32 \text{ in}^3 \\ = 4800 \text{ ft-in}$$



(CONSTRUCTION
GRADE REDWOOD)
NDS Table 4A



$$F_{max} = \frac{4800 \text{ ft-in}}{4''} = 1200 \text{ #}$$

INCREASE FOR LOAD DURATION FACTOR

$$F_{max} = 1200^L (C_D = 1.6) = 1920 \text{ # (ASD)}$$

$$F_{max} = 1200^L (K_F = 2.54)(\phi = 0.85)(\lambda = 1.0) \\ = 2590 \text{ # (LRFD)}$$

OR

$$\frac{1920 \text{ #}}{6' \text{ o.c.}} = 320 \text{ #/ft (ASD)}$$

$$\frac{2590 \text{ #}}{6' \text{ o.c.}} = 432 \text{ #/ft (LRFD)}$$

$$320 \text{ #/ft (FS = 3)} = 960 \text{ #/ft (ULTIMATE)}$$

Figure 9-19 Page two of calculations for out-of-plane resistance at uphill wall line: check for cross grain bending of sill.

9.7 References

Ficcadenti, S.J., Freund, E.J., Pardoen, G.C., Kazanjy, R.P., 2004, "Cyclic Response of Shear Transfer Connections Between Shearwalls and Diaphragms in Woodframe Construction," CUREE Publication W-28, CUREE-Caltech Woodframe Project, Consortium of Universities for Research in Earthquake Engineering, Richmond, California.

Part 10

Development of Retrofit Provisions for Masonry Chimneys and Fireplace Surrounds

10.1 Introduction

In addition to modeling vulnerable light-frame buildings, the ATC-110 Project team addressed seismic retrofit of masonry chimneys and masonry fireplace surrounds. Earthquakes constantly remind us that masonry chimneys and masonry fireplace surrounds comprise the most vulnerable elements in modern, conventionally-framed wood residences. The history of poor seismic performance of masonry chimneys in North America can be traced back to the earliest European settlers, and continues to this day as evidenced by damage in the 2014 South Napa Earthquake. Moreover, seismic damage to chimneys has proven disproportionately expensive for homeowners and insurers. While human casualties associated with collapsing chimneys and surrounds in recent earthquakes have been low (Peek-Asa 1998), the falling hazard remains and the life-safety aspects of poor masonry chimney performance cannot be ignored. In contrast, modern factory-built chimneys with metal flues enclosed in light framing present negligible economic or life-safety risks, even in strong ground shaking.

It is for these reasons that the FEMA P-1100 scope included assessment and retrofit of masonry chimneys and surrounds. The goal of the retrofit provisions is to make a substantial improvement to the expected performance. Unlike other aspects of FEMA P-1100, the retrofit provisions for chimneys and surrounds do not emerge from rigorous engineering analysis and probabilistic risk assessment. Instead these provisions rely heavily on experience, engineering judgment and perceived best practice.

This background document provides a brief overview of the retrofit provisions incorporated into FEMA P-1100, and then discusses technical background and engineering issues taken into consideration during the development of these retrofit provisions. This document is provided to serve as a record of those considerations.

10.2 Prescriptive Retrofit Provisions Based on Progressive Risk

Prescriptive retrofit methods have been developed for chimneys that the ATC-110 team considered common in California and the western U.S. Retrofits were developed for these common chimneys, with the intent of being applicable to a large majority of the existing building stock. In order to be eligible for the prescriptive procedures, the following eligibility requirements must be met:

- The dwelling is a detached one- or two-family dwelling, or the dwelling is a unit in a townhouse.
- The dwelling is of wood light-frame construction and is three stories or less above grade plane.
- The chimney is constructed of solid brick masonry.
- The chimney's largest plan dimension is not more than 40 inches.
- The chimney is either an interior chimney, or an exterior chimney engaging only one exterior wall (i.e. not at the dwelling corner).



Figure 10-1 Example of ineligible chimney—corner construction with plan dimension greater than 40 inches. (Photo by authors).

Chapter 7 of FEMA P-1100 includes progressive levels of prescriptive retrofit for eligible chimneys that are linked to increasing risk.

1. For construction considered by the project team to exhibit low relative collapse risk, retrofit is not required by FEMA P-1100. This construction includes:

- a. Chimneys or masonry surrounds constructed on or after January 1, 1995 are considered to be compliant with the minimum provisions of the standard and exempted from retrofit provisions.
 - b. Interior brick masonry chimneys of single-story dwellings that extend no more than twice the least plan dimension of the chimney above the roof, have no portion more than 6 feet tall that is not enclosed by full-height, finished walls on at least three faces, and whose greatest plan dimension does not exceed 40 inches are thought to present relatively low collapse risk and are exempted from retrofit provisions.
 - c. Masonry surrounds that extend vertically less than 4 feet above the finished floor or horizontally less than 3 feet from the edge of the firebox, are exempted from retrofit provisions.
 - d. Chimneys or masonry surrounds constructed prior to 1995 if shown by a licensed contractor or *registered design professional* to comply with the requirements of FEMA P-1100, Section 7.3.3, which are based on current building code prescriptions (ASCE 7, 2016 and IRC 2015).
2. Construction considered by the project team to be moderate collapse risk, requiring demolition to a lower roof or floor level (Figure 2) includes:
 - a. One story interior chimneys that are unbraced for more than six feet.
 - b. One story interior chimneys that extend vertically more than twice their width above the roof.
 3. Construction considered by the project team to be relatively high collapse risk, requiring demolition to the top of the firebox and reconstruction (Figure 3), includes:
 - a. Exterior chimneys of any height.
 - b. Interior chimneys more than one story tall.
 4. Tall, interior masonry fireplace surrounds are high-risk falling hazards, and are required to be fully removed or to be rebuilt and anchored to modern code requirements.



Figure 10-2 Chimney retrofit by removing masonry to the roof level and capped. (Photo by authors).



Figure 10-3 Chimney retrofit by removing masonry to the top of the smoke chamber and installing a factory-built metal flue in a light-frame chase. (Photo by authors).

The ATC-110 Project team considered the following the technical information in developing the chimney and masonry surround provisions:

- Construction of masonry chimneys common to California;
- Typical chimney failure modes;

- Literature regarding empirically based chimney seismic fragility;
- A review of historical prescriptive building code requirements for chimneys in California.

Prescriptive retrofit requirements and engineered retrofit requirements of FEMA P-1100 are based on best judgement of the authors informed by simple calculations. The provisions of FEMA P-1100 Chapter 7 focus primarily on the prescriptive retrofit of vulnerable chimneys. While engineering of residential masonry chimneys is rare (much less performance-based retrofit), FEMA P-1100 includes a brief section on engineered retrofit design. This section might be used for chimneys that exceed a plan dimension of 40 inches, where historical preservation is desired, or other circumstances.

One retrofit measure that is conspicuous by its absence is diagonal steel bracing back to the roof diaphragm. Although this is a commonly seen retrofit in California, there was no consensus among the project team that this measure would provide reliable and measurable risk mitigation; there was some concern that such measures might even result in worse performance. Similarly, while adding plywood/OSB to an attic floor to catch falling masonry might be considered a minimally expensive ways to (perhaps marginally) reduce risk, it does not provide an adequate degree of risk mitigation to be considered to be a retrofit measure, and therefore is not included in FEMA P-1100.

10.3 Technical Background

10.3.1 Description of Typical Chimney Construction

Residences constructed in the U.S. through much of the 20th century often included masonry chimneys. Typical chimney construction includes:

- An independent, shallow concrete or masonry foundation;
- A brick firebox of varying sizes;
- A tapered smoke chamber built directly atop the firebox;
- A long chimney, often composed of a single wythe brick wall surrounding a clay flue liner; and
- A cap to keep out rain and animals.

In the western U.S., chimneys constructed in the first half of the 20th century were rarely reinforced with steel and often constructed with mortar mixes that included gypsum. Early chimneys were rarely braced to roof, ceiling or

floor diaphragms. These chimneys represent the most vulnerable portion of the existing stock of residential chimneys.

Poor performance of those early designs led to implementation of progressively stronger building code requirements through the latter part of the 20th century. The progressive inclusion of seismic details, and the increased scrutiny of masonry chimneys after thousands failed in the 1994 Northridge earthquake, informed the ATC-110 Project team's decision to allow post-1994 chimneys to remain without retrofit. A summary of the evolution of code provisions appears in Section 10.5.

10.3.2 Chimney Failure Modes Considered

Implementation of chimney retrofits using progressive levels of retrofit (as discussed in Section 2) was developed based on commonly observed chimney failure modes. The ATC-110 Project team considered exterior chimneys to be more vulnerable than interior chimneys that are afforded bracing on all four sides. In addition, taller chimneys for houses greater than one story or at tall peaks of steep sloped roofs are more vulnerable than shorter chimneys (Figure 4). While chimneys of one-story houses are generally less vulnerable, failure at the roofline is often observed and remained a consideration, particularly those that cantilever above an eave (Figure 5).

Interior, one-story chimneys are considered least vulnerable and ATC-110 Project team decided to exempt them from retrofit requirements. However, failures of interior, one-story chimneys have been observed (Figure 6) and the reader should not consider such chimneys to be risk free, or even low risk relative to other residential failure modes.



Figure 10-4 Common failure of two-story exterior chimney. (Photo by authors).



Figure 10-5 Typical failure at roof line. (Photo by authors).



Figure 10-6 Atypical failure of reinforced, one-story interior chimney. Note that the chimney is fully braced on all sides at the ridge, and the rebar protruding from the remaining masonry indicates that the chimney was reinforced and did not extend very high above the roof. (Photo by authors)

10.3.3 Concepts that Guided Development of the Provisions

During the course of developing the provisions, certain guiding fundamental concepts arose from the ATC-110 Project team’s discussions.

- Homeowners with vulnerable masonry chimneys are encouraged to simply remove the entire chimney, and if desired replace it with a lightweight, factory-built flue in a light-frame chase. We understand that such comprehensive retrofit may not be feasible or affordable, and so other, less drastic prescriptive provisions are allowed.
- Any chimney or surround can be retrofit by an engineer per building code requirements in lieu of the prescriptive provisions of FEMA P-1100.
- Prescriptive retrofits herein are based on engineering judgment and experience and are intended to substantially improve performance; the prescriptions are not designed to meet performance levels used in other parts of FEMA P-1100 (such as achieving a sufficiently low probability of collapse at a given hazard).
- There was some consensus that the extent of chimney damage in the 1994 Northridge Earthquake was so extensive that chimney detailing and inspection received renewed focus. As a result, the existing stock of chimneys constructed since 1995 are thought to be of better quality and thus exempt from the retrofit provisions.

- While it is our intent to make the provisions understandable and applicable by homeowners, we do not expect an average homeowner to differentiate vulnerable construction details. As such, retrofit provisions are based on more fundamental features: age, number stories, height above the roof, basic dimensions, and location on the wall (interior or exterior). Even determination of it is a brick masonry chimney (rather than veneer or stamped concrete) can be difficult.
- The most important aspects of chimney construction quality are very difficult for professionals to ascertain, much less homeowners. These features include the presence and appropriate detailing of diaphragm anchors, reinforcement, grout and foundation anchorage. The mortar quality, including differentiation of Portland cement versus gypsum in older chimneys, requires experience or laboratory testing. Therefore determination that construction of an existing chimney has complied with prescriptive code provisions must be done by a professional.
- The masonry chimney is perhaps the most fragile component of a home, yet quantification of that fragility, pre- or post-retrofit, is not amenable to engineering calculation.
- Based on engineering judgement and observation of past performance, prescriptive code requirements and/or retrofits likely do not increase chimney performance (collapse fragility) to the performance targeted by building codes for new structures (10% probability of collapse in the risk-adjusted maximum considered earthquake).
- While not made part of the provisions in FEMA P-1100, the occupancy of the fall zone around the chimney (public space, neighbor) should be considered. An example is tall Victorian attics with tall height of unbraced masonry – these are a significant hazard because damaged chimney masonry might fall to or through the attic floor or ceiling.
- The days of the conventional masonry chimneys are numbered. Most appliance have direct vents, and many jurisdictions no longer allow wood-burning fireplaces. The demand for rebuilds or retrofits of usable masonry wood-burning fireplaces will continue to diminish.
- Previous retrofits were often done to a low standard; the simple fact that a chimney has been retrofit should not be sufficient for an exemption.
- Because of their construction detailing (or lack thereof) and their prominence location in family rooms, masonry veneer surrounds are considered a serious life-safety risk. This has been demonstrated in recent earthquakes.

10.4 Engineering Considerations

Chimneys are massive, brittle objects connected to relatively light, mostly ductile wood framing. This makes simple yet realistic modeling of earthquake performance challenging. Moreover, chimneys come in many shapes and sizes, can be interior, exterior or embedded in an exterior wall, and can be connected (or not) to the structure by widely variable connections. There is little or no test data on which to model the anchors into old masonry, diaphragm anchors or interaction between house and chimney. All of this makes it impractical to categorize chimney/construction topologies into a manageable number of well-defined archetypes that can be analyzed and assumed to perform similarly. Therefore the FEMA P-1100 retrofit recommendations are based on the combined experience and judgment of the authors, rather than nonlinear dynamic simulation and predictions of damage or collapse rates as utilized in other chapters of FEMA P1100.

The FEMA P-1100 retrofit recommendations represent a graded approach, from reducing the risk through partial removal of the masonry to eliminating the risk by full removal of the chimney and fireplace. The degree of retrofit depends on the perceived hazard (chimney characteristics and conditions) as well as level of tolerable risk. However, all unreinforced masonry chimneys, and probably many newer, reinforced masonry chimneys, represent a potential falling hazard that violate the intended performance/safety goals of modern building codes. The technical literature provides some estimates of masonry chimney fragility, which are summarized in Figure 7. The fragility estimates clearly show that collapse performance of masonry chimneys falls well below the implicit building code requirements (Maison 2018, Daniell 2015, Dorwick 2008, FEMA 2012). Masonry chimney retrofits will greatly reduce the seismic risks associated with single-family dwellings, but quantification of the improvement is not amenable to simple calculation.

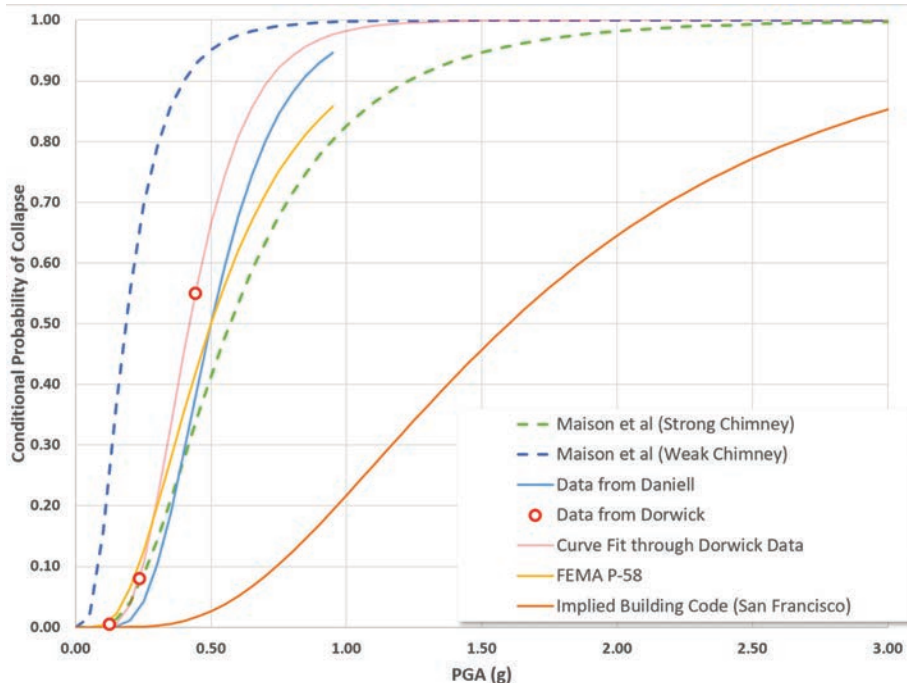


Figure 10-7 Masonry residential chimney fragility functions derived from various sources show that the collapse vulnerability is much higher than the implicit performance goal of the building code (shown for San Francisco in terms of peak ground acceleration).

Engineered retrofit of older, unreinforced masonry chimneys to meet modern seismic performance standards is generally considered to be infeasible. It is the consensus of the authors that the best practice for reducing future potential for damage is partial or complete removal of the masonry. If the functionality of the fireplace is to be maintained, then the chimney can be replaced with a metal flue in a light framed chase; if the masonry aesthetic is to be preserved, the new chimney can be finished with appropriately anchored thin brick veneer.

While all masonry chimneys pose some seismic risk, some chimneys are riskier than others. Any engineered evaluation of retrofit of a residential chimney should, at a minimum, address the following:

- Vintage. California masonry chimneys constructed before 1970 are less likely to be built using modern prescriptive techniques intended to reduce collapse risk. These more recent techniques include the use of steel reinforcement and positively tying the masonry to roof or floor framing using steel straps. In addition, many older chimneys were constructed using gypsum (rather than Portland cement) mortar, which is not as durable.

- Extension above roof: Chimneys must extend (cantilever) past the top of the roof in order to create clearance for the flue gases, but the longer the cantilever the more vulnerable they are to collapse. Exterior chimneys at the eave are required to extend several feet above the sloped roof, and are particularly vulnerable. Sometimes these chimneys are retrofit with diagonal braces back to the sloped roof surface, but the project team questions the effectiveness of such bracing absent engineering evaluation and proper detailing.
- Mortar quality: Mortar can degrade with time, and gypsum mortar degrades more quickly. Sometimes the effective quality of the mortar can be masked by shallow repointing.
- Interaction with house: Interior chimneys enjoy some degree of confinement on all sides, regardless of whether they are strapped to the framing. In addition, interior chimneys at or near the ridge line typically do not cantilever far above the roof. For these reasons, interior chimneys generally perform better than exterior.
- Chimney performance can also be affected by its interaction with the house, which has very different mass and stiffness properties. Wood light-frame houses are inherently flexible under earthquake loading while chimneys are inherently stiff. The resulting different movement due to earthquake loading is in itself a significant possible source of damage.

10.5 Summary of Key Building Code Prescriptions for Residential Masonry Chimneys

Table 10-1 History of Key Prescriptive Requirements for Masonry Chimneys in the UBC

UBC Code	Prescriptive Seismic Requirements
1927 to 1943	No requirements
1946 to 1949	UBC. Chimneys in wood frame buildings required to be laterally anchored at each floor and ceiling line which is more than six feet above grade. Los Angeles Building Code. From 1947 to 1972, every chimney to have masonry or concrete walls at least eight inches (8") in thickness not including flue lining, and to be reinforced and anchored as required for bearing walls. Also, all chimneys to be lined with fire-clay flue lining at least three-fourths inch (3/4") thick or with fire-brick lining not less than four inches (4") thick.
1952 to 1964	UBC. Chimneys shall be designed, anchored, supported, and reinforced, and no chimney shall support any structural load other than its own weight. Exception to lateral anchoring requirement for chimneys entirely within the framework.
1967	UBC. Prescriptive requirements provided in lieu of design for masonry or concrete chimneys in Seismic Zone No. 3: shall be reinforced with not less than four half-inch diameter vertical bars extending the full height of the chimney, with two additional bars for each additional flue for chimney wider than forty inches. Vertical bars shall be tied horizontally at twenty-four-inch intervals with 1/4-inch diameter steel ties.

Table 10-1 History of Key Prescriptive Requirements for Masonry Chimneys in the UBC

UBC Code	Prescriptive Seismic Requirements
1970	UBC. In Seismic Zones No. 2 and No. 3, anchorage to be designed for 900 pounds in any direction. For chimneys extending no more than 8 feet above the roof, this could be satisfied by two 3/16 square inch steel straps secured to the chimney vertical reinforcement and fastened to the structural framework of the building with six 16d common nails. Vertical tie spacing increased to 24 inches.
1973	UBC. Straps to be cast at least 12 inches into the chimney with 180-degree bend with a 6-inch extension around the vertical reinforcing bars in the outer face of the chimney. Each strap to be fastened to the structural framework of the building with two 1/2-inch bolts. Where the joists are perpendicular, they are to be connected to 2-inch by 4-inch ties crossing a minimum of four joists and connected with two 16d nails each. Tie spacing reduced back to 18 inches.
1976 to 1988	UBC. In seismic Zones No. 2, No. 3 and No. 4, all masonry and concrete chimneys shall be anchored at each floor or ceiling line more than 6 feet above grade, except when constructed completely within the exterior walls of the building. Added requirement that two ties shall also be placed at each bend in vertical bars. Los Angeles adopted the UBC language in 1987
1991 to 1997	UBC. Added requirement for masonry chimneys that vertical bars have a minimum cover of 1/2 inch of grout or mortar tempered to a pouring consistency, and that the slope of the inclined portion of vertical bars shall not exceed 1 inch horizontal in 2 inches vertical. Also added an alternative prescriptive design for perpendicular joists whereby each anchor strap could be connected to the structural framework by two 1/2-inch-diameter bolts in "an approved manner". Los Angeles adopted emergency provisions after the 1994 Northridge Earthquake: masonry chimneys shall be designed and constructed to comply with applicable sections of the UBC, but any existing masonry chimney altered or repaired more than 10 percent of its replacement cost within any 12-month period shall have its entire chimney structure comply the current requirements. Also, masonry and concrete chimney to be tied to a structural element of the building capable of providing lateral resistance for the horizontal fences [sic] specified in Section 2336 of the UBC, and anchorage of the ties to be designed for the loads specified in Section 2336 of the UBC.

10.6 References

ASCE 2016. Minimum Design Loads and Associated Criteria for Buildings and Other Structures (ASCE/SEI 7-16), American Society of Civil Engineers, Reston, VA.

Daniell, J. Schaefer, F. Wenzel, T and Kunz-Plapp, T. (2015) "The value of life in earthquakes and other natural disasters: historical costs and the benefits of investing in life safety" *Proceedings of the Tenth Pacific Conference on Earthquake Engineering, Building an Earthquake-Resilient Pacific*, 6-8 November 2015, Sydney, Australia

Dowrick, D. Hancox, G. Perrin, N. and Dellow, G. (2008) "The Modified Mercalli intensity scale – revisions arising from New Zealand experience" Bulletin of the New Zealand Society for Earthquake Engineering, Vol. 41, No. 3, September 2008.

FEMA 2012 *Seismic Performance Assessment of Buildings* (FEMA P-58-1)
Federal Emergency Management Agency, Wahsington, D.C., September 2012.

ICC 2015 “International Residential Code for One- and Two-Family Dwellings” International Code Council, Inc.

Maison, B and McDonald, B. (2018) “Fragility Curves for Residential Masonry Chimneys” *Earthquake Spectra, Volume 34, No. 3*, pp 1001–1023, August 2018

Peek-Asa, C. Kraus, J. Bourque, L. Vimalachandra, D. Yu, J and Abrams, J. (1998) “Fatal and Hospitalized injuries resulting from the 1994 Northridge Earthquake” *International Journal of Epidemiology*, 1998;27:459-465.

Part 11

Development of Vulnerability-Based Retrofit Provisions for Crawlspace Dwellings

11.1 Introduction

This white paper documents the development of the FEMA P-1100, Volume 1 (FEMA, 2018) vulnerability-based retrofit provisions for crawl space dwellings. Included is discussion of how the dwelling stock is represented, the dwellings used as the basis of numerical models, the numerical modeling and analytical procedures, selected results of analysis, their assessment and the derivations of design parameters. This white paper is intended primarily for use by engineers wanting to have a better understanding of the basis for the retrofit recommendations, and those interested in details of the numerical modeling. This paper refers to other FEMA P-1100 Volume 3 documents that provide details on specific topics. Documented in Section 8 of this white paper are additional resources providing detailed information on the numerical modeling and engineering assumptions.

11.2 Dwelling Stock Represented

The FEMA P-1100 Volume 1 definition of a crawlspace dwelling is “a dwelling in which:

1. The space below the lowest framed floor is predominantly unoccupied, including area enclosed by crawlspace walls, open areas, or a combination of the two;
2. The tallest crawlspace cripple wall clear height does not exceed 7'-0";
3. When averaged across the full length or width of the dwelling the grade slope does not exceed one vertical in five horizontal (i.e., 20% grade)."

The range of dwelling configurations that meet this description were studied early in the project, which included an initial photo set and a historical search of typical home plans from 1900 through the 1960's. This historical study was used to identify typical one- and two-story representative dwelling configurations and determine median and dispersion of structural properties that were used for numerical studies.

11.2.1 Obtaining Superstructure Strength and Mass Characteristics for Cripple Wall Dwellings

The range of ages of construction considered spanned the 1900's to the 1960's. The configuration study reviewed three one-story configurations and two two-story configurations per decade of construction. Configurations were purposefully selected to represent "stand-alone" dwellings without attached garage space. The selection criteria also aimed at minimizing the amount of plan eccentricity observed (i.e., without significant T- or L-shaped plans). The avoidance of T- and L-shapes was mostly to avoid torsional response and prevent the inclusion of eccentricity as a supplemental variable. The vulnerability caused by eccentricity is considered separately by FEMA P-1100. In total, 42 different configurations were reviewed. This consisted of 28 one-story and 14 two-story homes. A thumbnail illustration of the different plan configurations considered is provided in Figure 11-1.

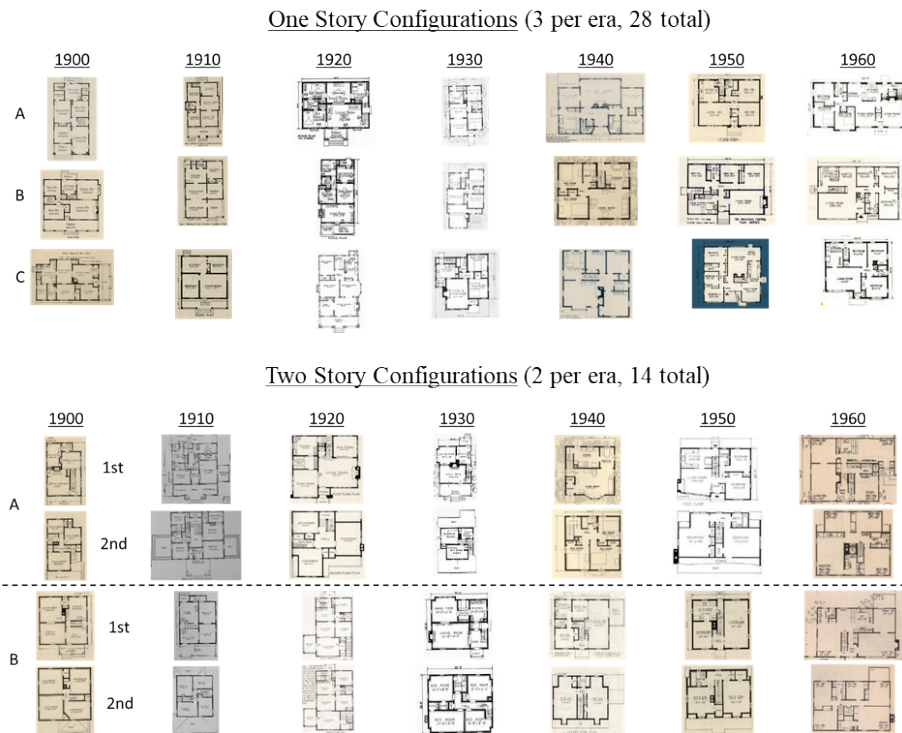


Figure 11-1 Overview of the 42 plan configurations considered in the superstructure strength study for cripple wall dwellings.

Each configuration was measured and documented for the following geometrical parameters:

- Floor area for each story;
- Length of full-height interior partition walls in each orthogonal direction;
- Length of full-height exterior walls in each orthogonal direction;

- Estimate of roof gable areas, pitch and eave overhangs (if applicable).

An example of a measured plan configuration is provided in Figure 11-2 for a 1910's one-story configuration. More detailed information on all considered configurations can be found in FEMA P-1100 Volume 3, Part 6.



Figure 11-2 Example of one-story 1910 configuration measurements within ATC-110 cripple wall dwelling superstructure study: a) Exterior view of house; b) Plan configuration; c) Plan measured for interior walls; d) Plan measured for exterior walls.

The geometrical properties were used in combination with assumed material weights and strengths (i.e., monotonic backbone curves) in order to obtain meaningful physical parameters for modeling representative superstructures. These parameters included:

1. Total weight to plan area ratios, W_T/A ;
2. Strong to weak direction strength ratios, $V_{\text{strong}}/V_{\text{weak}}$;
3. Average strength to seismic weight ratios, $(V/W_S)_{\text{Avg}}$; and,
4. Average strength to plan area ratios, $(V/A)_{\text{Avg}}$.

The average strength terms refer to the average strength of the two orthogonal directions of the configuration. The seismic weight (W_S) is the weight neglecting first floor diaphragms and one-half of the wall weight as if the structure was modeled on a rigid base. The total weight (W_T) includes all wall weights and first floor diaphragm weight.

For the two-story configurations, two additional parameters were calculated in order to relate the lower story to the upper story, namely:

1. Average second story to first story strength ratio, $(V_2/V_1)_{Avg}$; and,
2. Second to first story wall weight ratio, $W_{wall,2}/W_{wall,1}$.

An example illustration of the modeling parameters is shown in Figure 11-3 for the average strength to seismic weight ratios, $(V/W_S)_{Avg}$, for all one-story configurations. More detailed descriptions and illustrations of the calculated superstructure parameters are provided in the FEMA P-1100 Volume 3, Part 6 document.

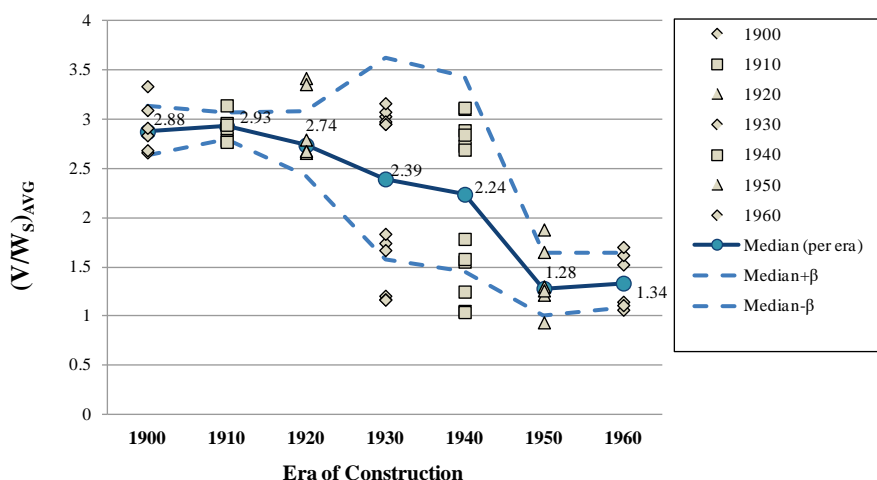


Figure 11-3 Sample of configuration data collected across different eras of construction showing the average superstructure strength to seismic weight ratios for all one-story configurations.

A number of exterior and interior materials common to the range of construction ages were considered. Stucco and horizontal wood siding were considered for exterior wall finishes. Gypsum wallboard and plaster on wood lath (i.e., lath and plaster) were considered for interior wall finishes. The interior wall finish material assumed for each of the configurations varied as a function of the construction era. It was assumed that configurations constructed prior to 1930 exclusively had interior plaster on wood lath. Conversely, dwellings constructed in 1950 and later were assumed to have interior gypsum wallboard. The transition period of 1930 to 1949 assumed that either interior finish material could be present. The assumptions

regarding era-specific materials is illustrated in Figure 11-4 for the same data provided in Figure 11-3.

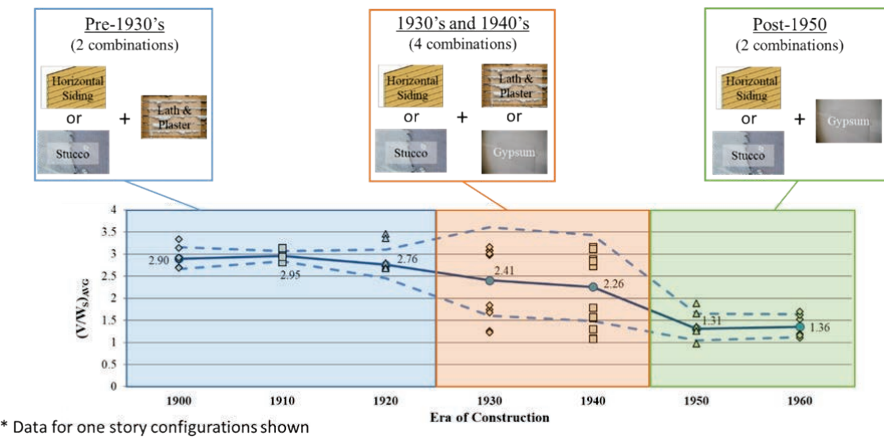


Figure 11-4 Illustration of the different building materials assumed when considering the existing one story building stock of cripple wall dwellings.

The main assumption in utilizing the obtained strength and weight characteristics from the configuration sets was that two superstructure definitions would be targeted using the one- and two-story data separately. The first assumed the median properties of all configurations (of the same number of stories) from the 1900's to the 1940's (i.e., pre-1950 era). The second assumed the median minus one standard deviation (Median- β) of the strength properties for the post-1950 era, which included the configurations from the 1950's and 1960's from the configuration sets. The generalized result of this assumption was a stiff and strong superstructure controlled mostly by stucco and plaster on wood lath properties and a weak and flexible superstructure controlled by horizontal siding and gypsum properties. The logic behind the two superstructure characteristics is that the stronger and stiff (i.e., median, pre-1950) superstructure will provide the greatest demands on crawlspace retrofits, while still maintaining realistic strength and mass proportions in the superstructure. Conversely, the weaker and more flexible variation (i.e., median - β , post-1950) represents a lower bound of superstructure strength and stiffness to investigate the capability of crawlspace retrofits to "drive damage upstairs", a continuing concern with the strengthening of crawlspace dwellings. Further, the weaker variation indirectly considers the possibility of remodeling where smaller rooms may be combined or expanded, and exterior openings may be enlarged (i.e., larger windows). Notably, the dispersion (β) represents the distribution in superstructure properties due to configuration variability and era-specific material combinations (see Figure 11-4) only; weight take-offs and material strengths are constant best-estimate values. A more complete discussion of

the use of the configuration information and underlying assumptions can be found in the FEMA P-1100 Volume 3, Part 6 document.

11.2.2 Superstructure Configurations used for Numerical Analysis

The baseline archetypes used to represent the superstructure (i.e., occupied stories above the crawlspace) of analyzed dwellings are 40 feet by 30 feet in plan dimensions (i.e., 1200 ft²). Story heights are 9 feet. Floor diaphragms are 10 inches deep representing 2x10 joists with 1" nominal flooring. The roof geometry is assumed to be a hip roof with an 8:12 pitch and an 18-inch eave around the perimeter. The configuration of the occupied stories was based on the CUREE Small House index building (Isoda et al., 2002) configuration with a much simpler interior partition wall layout in order to reduce torsional response and accommodate strength and mass scaling when calibrating to superstructure study results (see Section 2.1). This small house index building was developed to exemplify post-World War II affordable housing that was constructed in large quantities, either in tracts or one-by-one by small contractors or owner builders. This was the kind of building that was originally intended for the application of the building code's (Uniform Building Code's) prescriptive construction provisions. Figures 11-5 and 11-6 show renderings of one- and two-story superstructure configurations on two-foot cripple walls.

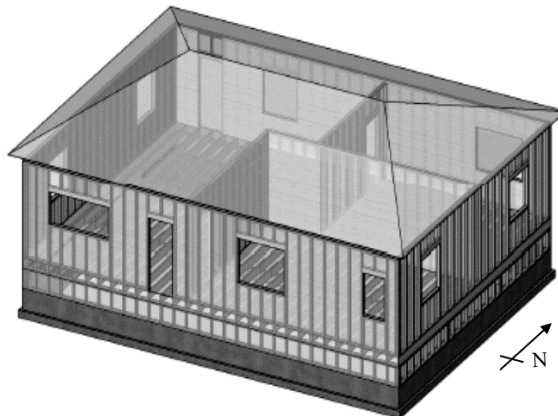


Figure 11-5 Rendering of one-story superstructure baseline configuration on two-foot cripple wall used in numerical modeling.

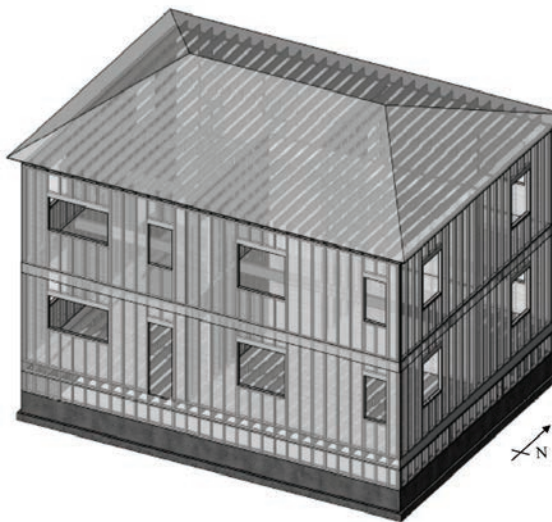


Figure 11-6 Rendering of two-story superstructure baseline configuration on two-foot cripple wall used in numerical modeling.

Both one-story and two-story configurations assume the same layout of exterior openings and interior walls. The two-story configuration replaces doors with windows of the same width to produce a consistent full wall height distribution around the perimeter. A plan view of the one- and two-story superstructure configurations is shown in Figure 11-7.

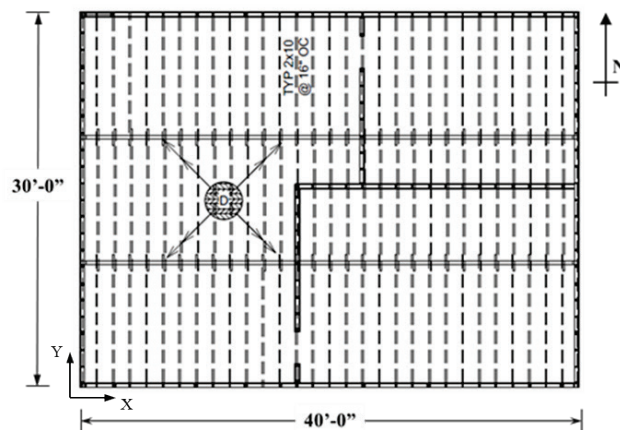


Figure 11-7 Plan view of the one- and two-story baseline configurations selected for modeling of cripple wall dwellings. Note: axes shown are used throughout the crawlspace dwelling analysis.

The configuration study strength and mass properties (Section 2.1) were incorporated into the baseline configurations using different sets of material properties for the pre-1950 median and post-1950 median- β . The final models scaled the baseline configurations according to the appropriate target statistics. Readers interested in the background of the superstructure model development can refer to the FEMA P-1100 Volume 3, Part 6 document for complete details.

The properties of the four superstructure configurations considered for the analysis of cripple wall dwellings is summarized in Table 11-1. The table provides the first two fundamental periods, lateral weight properties and peak strength obtained from modal pushover analysis. Notably, the pushover analysis was conducted assuming the superstructure is on a rigid base for comparison with the different retrofitted archetypes in Section 4.

Table 11-1 Summary of Superstructure Configuration Properties for the Analysis of Cripple Wall Dwellings

Superstructure Type	Archetype ID ¹	T ₁ [s] ²	T ₂ [s] ²	Seismic Weight W _S [kip] ³	Total Weight W _T [kip] ³	V _{max,X} [kip]	V _{max,Y} [kip]
1-story Median pre-1950	4-1R-M-E	0.086	0.083	38.9	68.2	114.5	104.4
2-story Median pre-1950	4-2R-M-E	0.154	0.145	93.2	122.3	103.5	91.8
1-story Median-β post-1950	4-1R-Mβ-E	0.179	0.174	32.5	54.1	34.9	31.3
2-story Median-β post-1950	4-2R-Mβ-E	0.300	0.291	59.8	80.4	30.0	26.8

¹ Structural models assume a rigid base (pinned connection) to the ground level

² ID assumes the superstructure only on a rigid-base (see Section 3.2); ² T₁ and T₂ correspond to the first translational modes in the Y- and X-directions, respectively; ³ Seismic weight (W_S) neglects first floor diaphragm and one half first story wall weight, Total weight (W_T) includes all diaphragms and wall weights. The total weight of the superstructure is used as the baseline weight (W_{BL}) for comparing retrofitted archetypes.

A comparison of all four superstructure pushover curves is provided in Figure 11-8 to illustrate the differences between superstructure archetypes. The pushovers are conducted using the three-dimensional models using the *Timber3D* program (see Section 3.5). The pushover curves illustrate the large range of strength defined by the pre-1950 median and post-1950 median-β variations. More detailed information for each superstructure model is provided in the FEMA P-1100 Volume 3, Part 6 document.

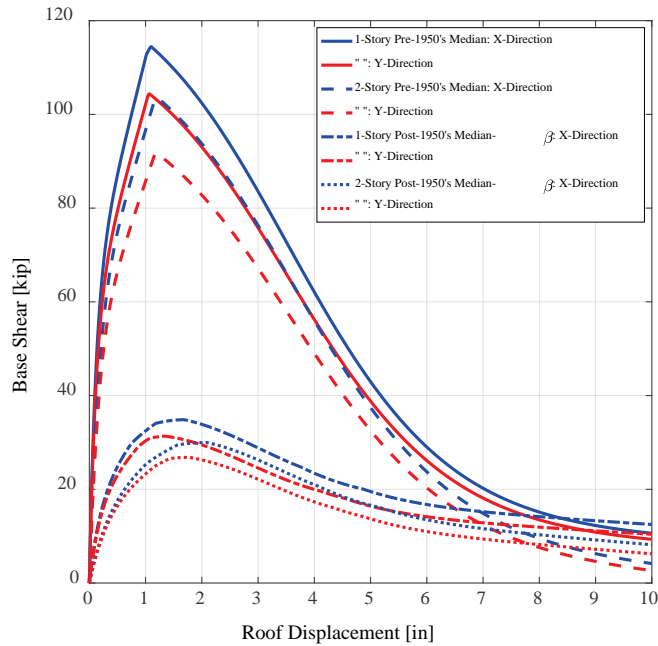


Figure 11-8 Modal pushover analysis (*Timber3D*) comparison of all four superstructure configurations considered for cripple wall dwelling analysis.

11.2.2 Geometry Variations for Archetype Models

The cripple wall dwellings analyzed assumed a range of different geometries. These are summarized as follows:

- One-and two-story superstructures.
- Three heights of uniform height cripple walls: 2 feet, 4 feet and 6 feet.
- One stepped height cripple wall with a height of 2 feet at the uphill wall line and 6 feet at the downhill wall line. Steps were reduced in increments of 2 feet (i.e., 2, 4 and 6 feet) along the sides parallel to the slope. The case study archetypes were assumed aligned with the longer 40-foot plan dimension (X-direction) parallel to the slope.

11.3 Modelling and Analysis Procedures

The general process for numerically studying dwelling archetypes within the project scope was unified across each of the three vulnerabilities studied in this project, i) cripple wall, ii) living space-over-garage, and iii) hillside dwellings. In addition to the processes that were unified for each vulnerability group, each vulnerability presented its own unique challenges when it came to the task of analyzing existing and retrofitted structures. In studying crawlspace configurations, the additional procedures used to gain understanding about this vulnerability included addressing the effect of

different aspect ratio assumptions for wood structural panels. The modelling of floor-to-sill-to-foundation connections for sloped cripple walls with a zero height condition on the uphill side of the dwelling was an additional challenge, yet this analysis is part of the cripple wall-to-hillside transition study that is described in FEMA P-1100 Volume 3, Part 9. The analysis procedures discussed herein are those related to the primary objective of understanding the relationship between retrofit parameters and the collapse performance of cripple wall dwellings. The main design consideration is the selection of the appropriate response modification factor (referred to hereafter as simply “R-factor”).

The methodologies behind these analysis procedures and the parameters associated with the implementation of the common analysis strategies are discussed in this section.

11.3.1 Overview

The following common analysis procedures, documentation and parameters provided by all working groups conducting numerical studies will be presented:

- Project nomenclature for group addressing crawlspace vulnerability.
- Assumptions regarding building and seismic weight used in analysis procedures.
- Hysteresis parameters used to define the behavior of existing building materials.
- General modeling approach and analytical assumptions for cripple wall dwellings.
- Procedure for determining median collapse intensities based on the results of non-linear response history analyses (NLRHA).

In addition, the following procedure unique to the analysis of crawlspace vulnerabilities will be reviewed:

- Treatment of strength and stiffness of wood structural panels for cripple wall retrofit.

11.3.2 Crawlspace Project Nomenclature

The following information outlines the nomenclature used to describe the numerical models that were analyzed using *Timber3D* and the methodologies outlined in FEMA P-1100 Volume 3, Part 5 – *Protocol for FEMA P-1100 Numerical Studies* and below. The general format for cripple wall dwelling

nomenclature is shown below, noting that items in parentheses do not apply to all cases:

- #-Aih(L)-S(H)-C(pW)-(noHD)
- # - describes the working group number – in case of the crawl-space analysis, this corresponds to Working Group 4 (WG4). NOTE: Analysis appendices specific to WG4 may tabulate results without the initial “#” for brevity.
- A – describes the number of occupied stories in the superstructure (e.g., 2 represents a two-story dwelling above a crawlspace, not counting the crawlspace as a story)
- i – describes the type of cripple wall. For WG4, level cripple walls are the most common and represented by “C” (for constant height). Stepped cripple walls (e.g., those with varying height) are denoted “S”. Rigid-base cases that represent control cases assuming the first occupied story is pinned to the ground (i.e., no crawl space or anchorage deficiency) are denoted “R”.
- h – describes the cripple wall *height* in feet with a single integer. In the case of stepped cripple walls, there will be two values corresponding to the tallest (downhill) and shortest (uphill) cripple wall heights. For example, a stepped cripple wall transitioning from 2-foot to 6-foot walls would be represented by “26”. NOTE: for rigid-base cases, the parameter *h* is omitted in the model name since no crawlspace exists.
- (L) – is used to denote when *lower bound* cripple wall properties are assumed for the existing material. The parentheses indicate that when “L” is not present, the existing cripple wall properties are taken as best estimate. Notably, this is only applicable to cripple walls assuming stucco as an exterior material.
- S – is used to denote the type of *superstructure* and exterior materials assumed. “M” represents the pre-1950 median superstructure strength with exterior stucco assumed for cripple walls. “M β ” represents the post-1950 median minus one standard deviation superstructure strength with horizontal wood siding assumed for cripple walls.
- (H) – is used to denote when *heavy* roof and floor diaphragm weights are assumed for the numerical model. The parentheses indicate that when “H” is not present, the roof and diaphragm weights correspond to the light weight assumptions (see Section 3.3).

- C – describes the sub-floor *condition* (e.g., below first floor diaphragm) for the numerical model. “E” represents an existing cripple wall condition, “R” represents a retrofit cripple wall condition.
- (pW) – describes the percentage p of the perimeter of the cripple wall that is braced with wood structural panel and the retrofit brace material W used for retrofitting. The parentheses indicate that p and W are only applicable to models with retrofit cripple walls. For example, if a cripple wall is retrofit with half of its perimeter sheathed with wood structural panel type 3 (i.e., WSP3; see Section 3.7 and FEMA P-1100 Volume 3, Part 4), then pW would read “50%WSP3”.
- (noHD) – is used to denote whether height-to-width (h/d) reduction factors were used to modify the strength of wood structural panel materials for cripple wall retrofits. The parentheses indicate that “noHD” is only specified when strength reduction based on aspect ratio is not included in the material properties assumed. Refer to Section 3.7 for details.

In order to illustrate the nomenclature used for constant height cripple wall dwellings, two examples are provided:

1. 1C2-M β -R38%WSP9-noHD
2. 2C4L-M-R84%WSP8

Example 1 considers a one-story median- β (post-1950) superstructure on 2-foot uniform height cripple walls with wood structural panel (WSP) retrofit. The retrofit assumes WSP type 9 (i.e., WSP9) and has 6'-8" long panels in every corner of the crawlspace. This length totals 53'-4", which is 38% of the 140'-0" perimeter. The strength properties of the WSP are not reduced according to aspect ratio.

Example 2 considers a two-story median (pre-1950) superstructure on 4-foot uniform height cripple walls with wood structural panel retrofit. The wood structural panel assumes WSP type 8 (i.e., WSP8) and has 14'-8" long panels in each direction in every corner of the crawlspace. This length totals 117'-4" which is 84% of the 140'-0" perimeter. The strength properties of the WSP are reduced to account for aspect ratio of the WSP wall panels.

11.3.3 Weight Take-off Assumptions for Cripple Wall Dwellings

The designated building weights used in all WG4 analysis and modeling are presented in this sub-section. These weight take-offs represent the baseline weights that were used prior to scaling based on configuration statistics of combined material combinations (refer to FEMA P-1100 Volume 3, Part 6).

Table 11-2 Summary of Weight Take-Off Assumptions for Analysis of Cripple Wall Dwellings

Exterior Material	Interior Material	1 st Floor w _{1st} [psf]	2 nd Floor w _{2nd} [psf]	Roof ¹ w _{roof} [psf]	Exterior Walls w _{ext} [psf]	Interior Walls w _{int} [psf]	Cripple Walls w _{CW} [psf]
Wood Siding	Gypsum	10.0	11.0	15.0	7.0	7.0	4.0
Wood Siding	Lath and Plaster	10.0	19.0	15.0	13.0	18.0	4.0
Stucco	Gypsum	10.0	11.0	15.0	14.5	7.0	14.0
Stucco	Lath and Plaster	10.0	19.0	15.0	23.0	18.0	14.0

¹ Roof loads assume asphalt shingle for all cases other than those denoted “Heavy”, reported value includes horizontal projection for 8:12 pitch

Heavy cases considered only one-story pre-1950 median superstructures. The roof weight was increased from 15 psf (asphalt shingle) to 29 psf (concrete tile). Interior walls were increased from 7 psf (gypsum) to 18 psf (plaster on wood lath).

11.3.4 Hysteretic Behavior of Existing Building Materials

This sub-section defines the material properties used to model the superstructure and exterior material of cripple walls of crawlspace dwellings archetypes with existing conditions (i.e., prior to retrofit). The materials considered are summarized for brevity, highlighting only material properties that were used by WG4 for the analysis of crawlspace dwellings. More complete information on the development and background on material properties used across all working groups can be found in the FEMA P-1100 Volume 3, Part 4 document.

The *Timber3D* analysis platform contains numerous hysteretic models for modeling wood light-frame structures. This includes the SAWS model (Folz and Filiatrault, 2004) and the EPHM (Evolutionary Parameter Hysteretic Model) (Pang et al., 2007). Additionally, the software includes the RESST (RESidual STrength) hysteretic model developed for the ATC-116: *Solutions to the Issues of Short-Period Building Seismic Performance* project. This RESST hysteretic model was selected for the modeling of most sheathing (wall) materials in the current project.

The RESST hysteretic model is an adaptation of the SAWS model and is also known as the CUREE model or Modified STEWart model (after Stewart, 1987), which includes a smooth post-peak backbone allowing for a residual strength portion of response to be defined at large displacements; similar to

the post-peak behavior using the EPHM model. An illustration of the RESST hysteretic model is shown in Figure 11-9.

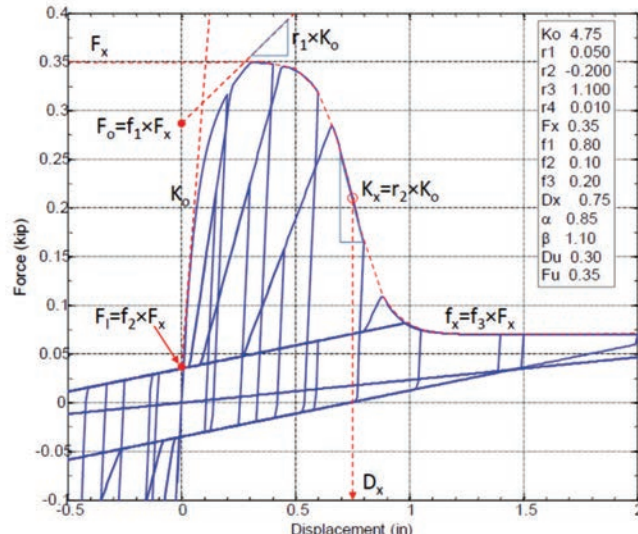


Figure 11-9 Illustration of the residual strength (RESST) hysteretic model used in *Timber3D* for modeling the behavior of wall materials.

The hysteretic behavior using the RESST model is defined by 12 parameters. The backbone is defined by the initial stiffness (K_0), peak force (F_x), post-peak displacement (D_x) and a series of force and stiffness factors (f_1 to f_3 , and r_1 to r_4) that define the backbone in terms of either K_0 or F_x as shown in Figure 11-9. Notably, D_x defines the inflection point of the exponential “S-Curve” that transitions from peak load to the desired residual strength level. Cyclic behavior is defined by a constant intercept force and stiffness to capture pinching behavior and two parameters to control stiffness degradation upon reloading from the pinched intercept to the backbone curve. The factor β defines the next reloading displacement on the backbone curve as a multiplier of the previous maximum displacement (e.g., $\Delta_{i+1}=\Delta_i\beta$). The factor α is an exponent controlling the reloading stiffness (K_p) as a function of initial stiffness (e.g., $K_p=K_0(\Delta_y/\Delta_i+1)^\alpha$). The theoretical yield displacement (Δ_y) is defined by the initial stiffness divided by the force F_0 shown in Figure 11-9.

The following existing materials were modeled using the RESST hysteretic model:

- Gypsum wallboard (interior partition walls);
- Exterior stucco (existing cripple walls); and,
- Combined stucco and gypsum wallboard (exterior superstructure walls).

The corresponding hysteretic parameters are reproduced in Table 11-3 from the FEMA P-1100 Volume 3, Part 4 document. All materials assume best estimate properties except exterior stucco that considered both best estimate and lower bound properties for cripple walls throughout the course of the numerical studies. The parameters are presented in normalized units (% drift and lb/ft). These values must be adjusted for wall height and effective wall length ($L_{w,eff}$). The parameters for gypsum wallboard represent a single-sided sheathing condition, where the effective length should be doubled when considering double-sided interior partitions. Notably, the factor f_3 representing residual strength was assumed as 10% of peak strength for all materials using the RESST model (see FEMA P-1100 Volume 3, Part 4).

Table 11-3 RESST Hysteretic Parameters for Existing Wall Materials Modeled in *Timber3D* for the Analysis of Crawlspace Dwellings

RESST Parameter ¹	Lower Bound Stucco (S1) ²	Best Estimate Stucco (S2)	Best Estimate Gypsum Wallboard (G2)	Best Estimate Stucco + Gypsum Wallboard (SG2)
K_0 [lb/%θ-ft]	3750.0	3750.0	780.0	4530.0
r_1	0.094	0.094	0.103	0.080
r_2	-0.027	-0.031	-0.074	-0.034
r_3	1.0	1.0	1.0	1.0
r_4	0.014	0.025	0.040	0.025
F_x [lb/ft]	395.6	785.3	225.9	901.6
f_1	0.442	0.446	0.531	0.488
f_2	0.051	0.128	0.068	0.141
f_3	0.1	0.1	0.1	0.1
Dx [%θ]	2.12	3.85	2.62	3.44
α	0.75	0.70	0.60	0.70
β	1.05	1.30	1.20	1.30

¹ Refer to Figure 11-9 for illustration; ² Material indices (e.g., S1) coincide with the FEMA P-1100 Volume 3, Part 4 document

The only additional existing material considered, but not modeled with the RESST hysteresis is horizontal wood siding. The hysteretic behavior of wood siding assumes the SAWS or Modified STEWart (MSTEW in *Timber3D*) model. The SAWS model exhibits the same pre-peak backbone and cyclic behavior as the RESST model, yet without the smooth post-peak backbone curve to a residual strength region of displacement. This was assumed since horizontal wood siding can be characterized by relatively low stiffness and strength, yet with very little strength degradation at very large displacements.

The SAWS parameters to represent horizontal wood siding are provided in Table 11-4. An illustration of the SAWS hysteresis model is provided in Figure 11-10.

Table 11-4 SAWS Parameters for Best Estimate Horizontal Wood Siding

SAWS Parameter	Best Estimate Horizontal Wood Siding
S0 [kip/%θ-ft]	169.5
F0 [lb/ft]	75.0
R1	0.17
R2	-0.037
DU [%θ]	4.0
FI [lb/ft]	2.5
R3	1.45
R4	0.005
α	0.38
β	1.09

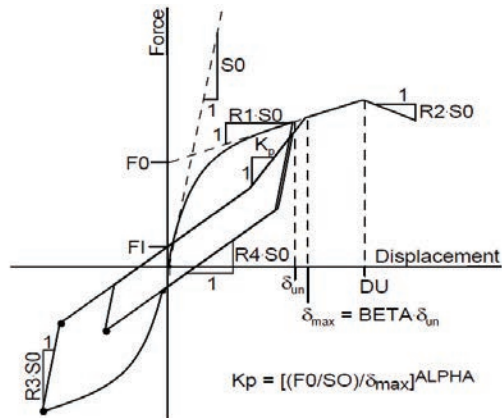


Figure 11-10 Illustration of the SAWS hysteretic model (image from Christovasilis and Filiault, 2009).

The assumed hysteretic behavior of stucco plus gypsum wallboard is provided in Figure 11-11. The comparison between best estimate and lower bound stucco is shown in Figure 11-12. Finally, the assumed hysteretic behavior of gypsum wallboard and horizontal wood siding are shown in Figure 11-13. Full discussion and justification for assumed existing material properties can be found in the FEMA P-1100 Volume 3, Part 4 document.

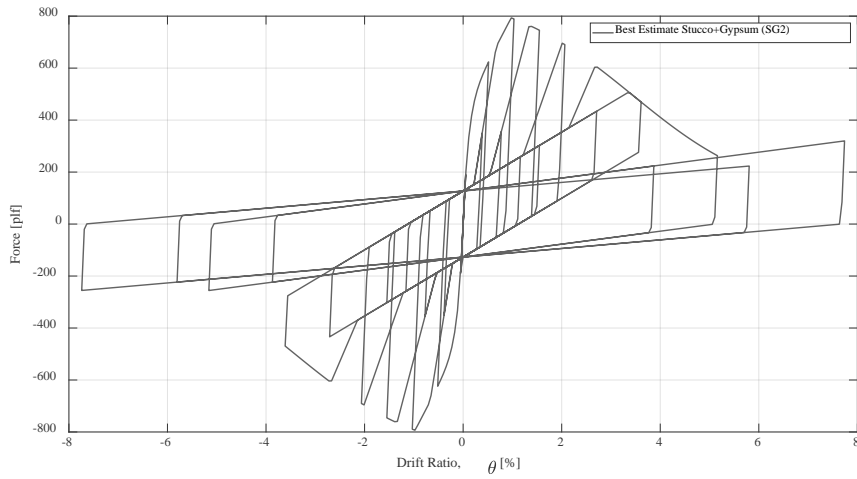


Figure 11-11 Assumed hysteretic behavior for stucco plus gypsum wallboard.

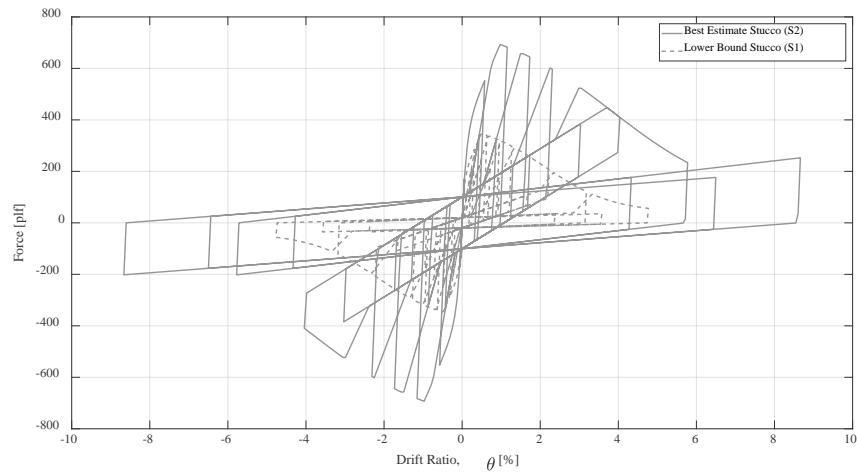


Figure 11-12 Assumed hysteretic behavior for best estimate stucco (solid line) and lower bound stucco (dashed line).

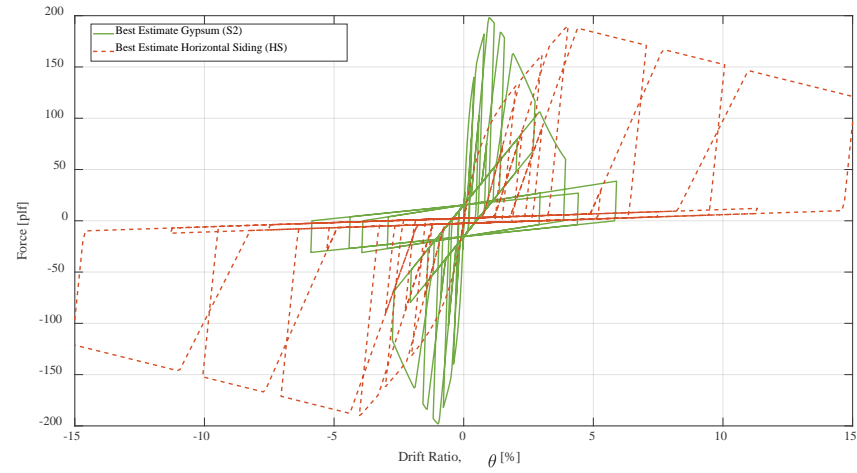


Figure 11-13 Assumed hysteretic behavior for best estimate gypsum wallboard (solid line) and horizontal wood siding (dashed line).

11.3.5 General Modeling Approach for Cripple Wall Dwellings

As recommended in the FEMA P-1100 Volume 3, Part 1 document, all cripple wall dwellings were modeled and analyzed using the *Timber3D* program (Pang et al., 2012). A “building block” modeling approach was used for representing standard length sections of interior and exterior walls. An example cripple wall dwelling is compared with its equivalent modeling components within *Timber3D* in Figure 11-14.

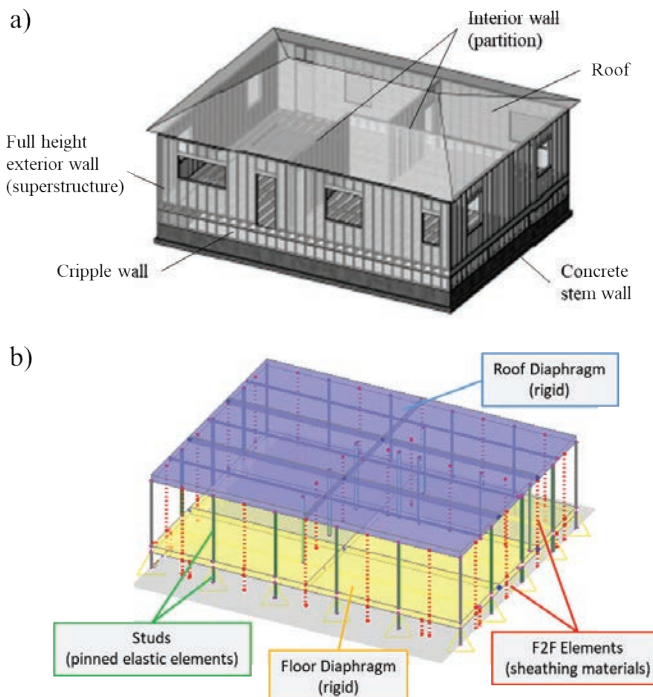


Figure 11-14 Illustration of the basic modelling components of a cripple wall dwelling: a) Rendering and components of one-story house with two-foot tall cripple walls; b) Equivalent model in *Timber3D*.

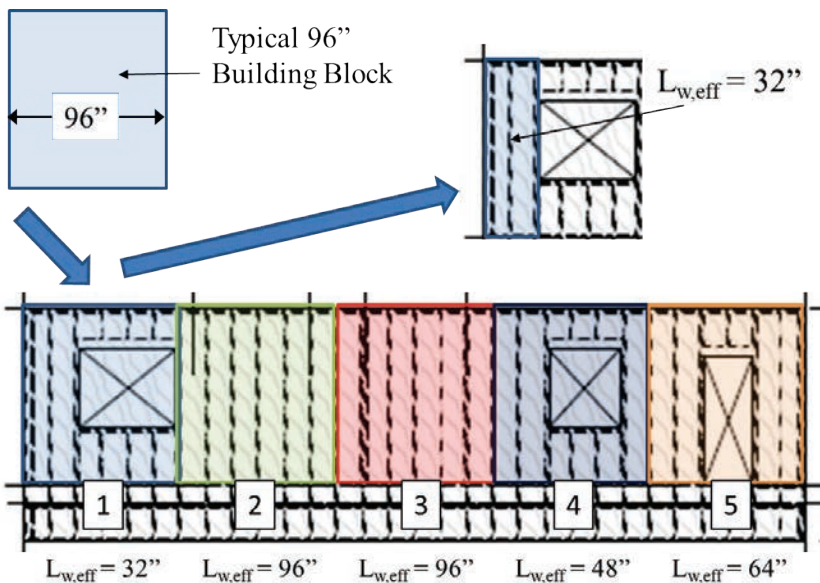
Figure 11-14 shows that the floor and roof diaphragms are assembled as an array of six large elastic beam elements with a depth corresponding to the depth of the floor joists and flooring. Assuming rigid diaphragm action, the beam elements are assigned very high stiffness in both flexure and shear. The diaphragm beams are connected with rigid elastic Frame-to-Frame (F2F) link elements at the joints of adjacent beam elements to produce rigid diaphragm action. The floor and roof diaphragms are applied the corresponding flat loads for gravity and lateral mass (see Section 3.3).

The floor and roof diaphragms are supported vertically by pinned elastic stud elements. The stud elements are located at a spacing of 8 feet or 6 feet around the perimeter of the house and are located at the ends and centers of interior partition walls at a spacing of 8 feet or 6.67 feet. The studs provide

vertical support for the structure and provide locations for wall loads. The hysteretic behavior of sheathing materials is applied within F2F link elements that act as shear springs between each pair of studs. The cripple wall F2F elements follow the same discretization as the exterior wall building blocks for the existing material. Hysteretic F2F elements representing the wood structural panel (WSP) retrofit sections of cripple walls are placed at five feet from each wall end (when applicable). The effective lengths of the retrofit elements are governed by the particular design scenario (e.g., building weight, R-factor assumed, etc.).

The treatment of wall openings in exterior wall lines assumes that only full height wall sections (i.e., full wall piers) contribute to the effective length ($L_{w,eff}$) of a given building block section as proposed by Patton-Mallory et al. (1985). Despite numerous relationships existing in the literature for treatment of openings of plywood shear walls (e.g., Yasamura and Sugiyama, 1984; Johnson, 1997; FEMA, 2012) the full wall pier height effective length assumption was the most convenient to keep consistent when considering numerous material types and generic configurations used for archetype development. Notably, the relationship proposed in FEMA P-807 Equation 4-3 (FEMA, 2012) was found to give similar results as those obtained using the simpler full wall pier height assumption. More discussion about the treatment of openings is provided in the FEMA P-1100 Volume 3, Part 4 document.

An example of the effective lengths used for each building block is shown in Figure 11-15. The figure shows that the 40-foot long north side of the one-story archetype configuration is broken into five separate eight-foot building blocks. The F2F link elements representing the sheathing materials will represent the annotated effective wall lengths within the numerical model. A summary of the effective wall lengths assumed for the exterior wall line building blocks is provided in Table 4-3. The same effective lengths are used for one- and two-story configurations prior to scaling based on the assumed era of construction (see Section 2). The building block discretization of all exterior and interior wall lines of the baseline configurations is provided in the FEMA P-1100 Volume 3, Part 6 document.



*Current example shows the North wall of the one-story house

Figure 11-15 Example of the effective length assumption used for accounting for openings within building block of exterior wall lines.

11.3.6 Determination of Median Collapse Intensity

The use of the FEMA P-695 (FEMA, 2009) methodologies to determine the probabilities of collapse at different ground-motion intensities is contingent on being able to determine the median collapse intensity. In an effort to reduce the computational demands of the project, an iterative process was performed when estimating the median collapse intensity from non-linear response history analysis (NLRHA) of cripple wall dwellings.

Each intensity used the FEMA P-695 far-field set (i.e., 22 ground motion pairs with two horizontal components) as seismic input. The records were normalized according to peak ground velocity (PGV) prior to scaling to target intensity levels (refer to FEMA, 2009 Eq. A-2). At each target intensity, the record set was scaled using median spectral acceleration at a period of 0.25s (i.e., S_a(0.25s)) as an intensity measure (IM), which is the minimum period allowed according to FEMA P-695 protocol. Each archetype model used three-dimensional analysis, with the 22 ground motion pairs run in two orthogonal orientations resulting in 44 separate analyses per intensity.

The FEMA P-1100 Volume 3, Part 5 document recommends that for each archetype building model, the incremental dynamic analyses be conducted for intensity stripes starting at S_a(0.25s) = 0.1 g. The intensity should be increased by increments of 0.1g up to an intensity level for which all (44) ground motions of the record set caused collapse of the building model.

However, in WG4, each archetype was first analyzed at three baseline intensities with $S_a(0.25s)$ values of 0.6g, 1.0g and 1.5g respectively. These are also referred to as “0.4MCE”, “DE” and “MCE” intensities within cripple wall dwelling analysis documentation. The design earthquake (DE) and maximum considered earthquake (MCE) correspond to the 10% and 2% probability of exceedance in 50-year intensities for seismic design category (SDC) D_{max}, respectively, as described in FEMA P-695. The lowest intensity, 0.4MCE, corresponds to an approximate 30% probability of exceedance in 50-year intensity estimated using Equation 3-1 within FEMA 356 (FEMA, 2000) for a site located in California. These three intensities serve as the basis for checking secondary criteria (i.e., drift response) as well as the primary intensity level of interest (i.e., MCE) for understanding collapse behavior (refer to FEMA P-1100 Volume 3, Part 2 for details on performance criteria used in the project). Using the analysis results at the first three intensities, an initial estimate of median collapse intensity (i.e., ideally the intensity where the counted median returns half of the ground motions causing collapse) is performed using the maximum likelihood approach (Baker, 2015). Based on the first estimate and judgement, one or more intensities are run in order to iterate to the counted median collapse intensity. For most cases, this typically converged with only a single iteration, yet some cases required two cycles to reliably estimate the median collapse capacity. These cases were typically for stronger archetype models that had low collapse probabilities at the three baseline intensities where data for initial maximum likelihood estimates was poorly defined. This procedure for estimating the median collapse intensity allowed for more efficient analysis of archetypes while eliminating bias due to including intensity levels scaled to extremely high (and unrealistic) levels of spectral acceleration.

As recommended in FEMA P-1100 Volume 3, Part 5, appropriate correction factors were then applied to the calculated median collapse intensity including the 3D correction factor (1.2 for all models), the spectral shape factor (1.00 for un-retrofitted structures, 1.33 for all retrofitted structures), and the pre-defined total collapse dispersion ($\beta = 0.75$ for un-retrofitted structures, $\beta = 0.6$ for retrofitted structures). Thus, overall correction factors for un-retrofitted and retrofitted structures are 1.2 and 1.6, respectively. More information on the selection and justification of adjustment factors is provided in FEMA P-1100 Volume 3, Part 5. Using the median collapse intensity, the predetermined adjustment factors, and the predetermined dispersion factors, the P-695 adjusted collapse fragility curve was obtained for each archetype model, representing the probability of collapse given an intensity expressed as $S_a(0.25s)$. An illustration of the process used to

estimate the collapse fragility curve according to FEMA P-695 is shown in Figure 11-16.

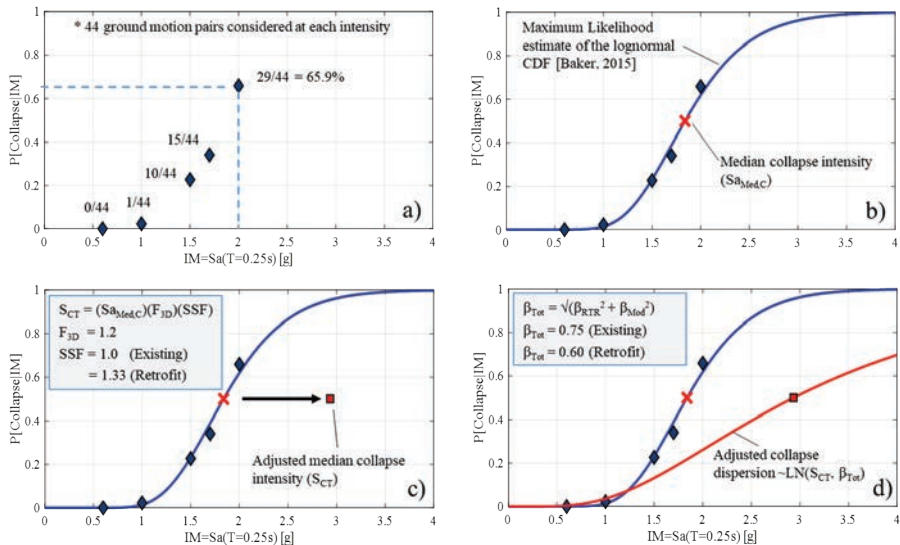


Figure 11-16 Illustration of process used for estimating the collapse fragility of a cripple wall dwelling according to the FEMA P-695 procedure: a) estimate fractions of collapse; b) maximum likelihood estimate of median collapse intensity from analysis; c) adjusted median intensity for spectral shape and 3-D effects (i.e., correction factors applied); d) adjusted collapse fragility dispersion.

11.3.7 Wood Structural Panel Materials for Cripple Wall Retrofit

The analysis work on cripple wall dwellings considered a number of different cripple wall heights to reflect expected field conditions. Due to the large variety of cripple wall heights that require retrofitting with wood structural panels, many different considerations were incorporated into modeling the seismic behavior of these materials. This sub-section outlines the different materials considered to represent WSP and subsequent material parameters used to represent them in the numerical models. More explicit information on the wood structural panel materials can be found within the FEMA P-1100 Volume 3, Part 4 document.

The initial baseline wood structural panels (WSP) are termed WSP1, WSP2 and WSP3. These baseline material properties are used across all working groups and are distinguished by the perimeter nail spacing and the type of structural sheathing (see FEMA P-1100 Volume 3, Part 4). These material properties assume that the shear wall panels are fully anchored (i.e., sill anchor bolts and tie-downs) and can develop the full capacity of the perimeter nailing (i.e., without premature uplift failure). These materials are defined as:

- WSP1: High capacity wood structural panel with 15/32-inch STR I sheathing, 8d common nails at 2 inches on center, detailing to develop full capacity of perimeter nailing through the use of tie-downs, based on fully anchored shearwalls with aspect ratio equal to one;
- WSP2: Medium capacity wood structural panel with 15/32-inch Rated sheathing, 8d common nails at 3 inches on center, detailing to develop full capacity of perimeter nailing through the use of tie-downs, based on fully anchored shearwalls with aspect ratio equal to one;
- WSP3: Low capacity wood structural panel with 7/16-inch Rated sheathing, 8d common nails at 4 inches on center, detailing to develop full capacity of perimeter nailing through the use of tie-downs, based on fully anchored shearwalls with aspect ratio equal to one.

The hysteretic behaviors of the baseline wood structural panel materials (i.e., WSP1, WSP2 and WSP3) are shown in Figure 11-17 for a shear wall having a full anchorage condition through the use of tie-downs.

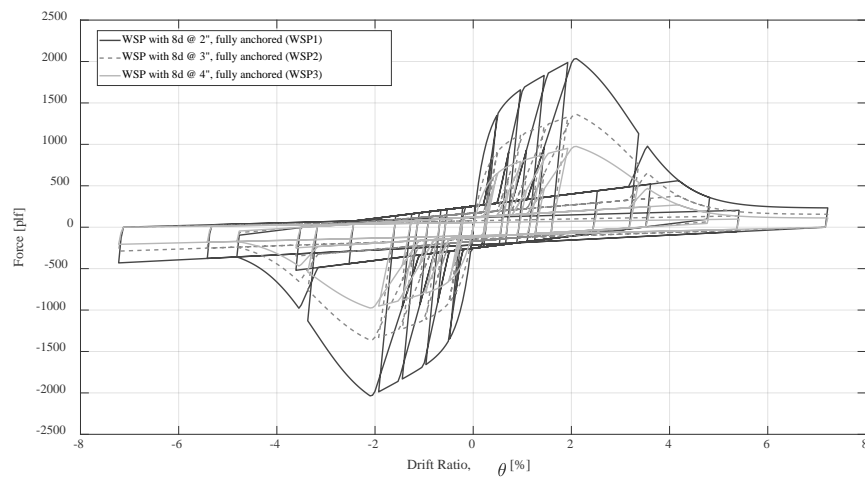


Figure 11-17 Hysteretic behavior of baseline wood structural panels assuming full anchorage conditions with tie-downs (WSP1 to WSP3).

The first specific consideration for shorter cripple walls was the expected drift capacity compared to full height (e.g., 8-foot tall) specimens. Based on the cripple wall testing conducted by Chai et al. (2002), cripple walls with a height of five feet and less was assumed to reach peak capacity at a drift ratio 1.5 times the peak assumed for the baseline WSP materials, which was termed “Capacity A” (see Figure 11-17). This increased displacement capacity was termed “Capacity B” and applied to WSPs that had a height of 5 feet or less (this is based on a limiting aspect ratio of 0.67 for an 8-foot wall length). An illustration of “Capacity A” and “Capacity B” hysteretic responses are shown for the WSP3 material (fully anchored, 8d @ 4”) in Figure 11-18.

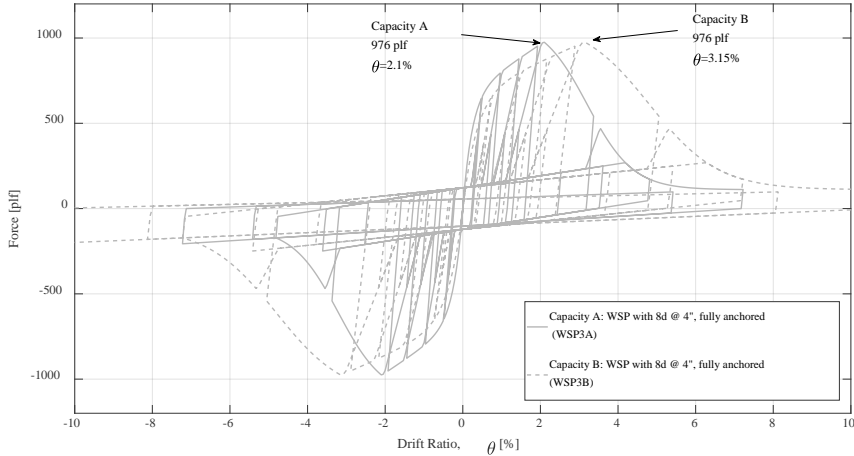


Figure 11-18 Comparison of wood structural panel displacement capacity based on cripple wall height: Capacity A (solid line) for cripple walls taller than 5 feet; Capacity B (dashed line) for cripple walls with a height of 5 feet or less.

The next consideration specific to cripple wall retrofit design was the consideration of shear wall aspect ratio. The work of Salenikovich (2000) dealt with many aspects of WSP shear walls with varying aspect ratios and anchorage conditions. A simple relationship was used to adjust the WSP capacity for intermediately anchored panels (*i.e.*, sill anchor bolts without tie-downs) according to Equation 6.36 in Salenikovich (2000) which is reproduced here as Eq. (4-1):

$$SR = v/v_{max} = 1/(1+4a_r^2)^{0.5} \quad (4-1)$$

where SR is the strength reduction factor and a_r is the aspect ratio of the shear wall panel (*i.e.*, h/d). Eq. (4-1) relates the peak strength of fully anchored shear walls (*e.g.*, sill anchor bolts and tie-downs) to unanchored shear walls of various aspect ratio assuming that a fully anchored wall will allow for the full shear capacity of the bottom fasteners (v_{max}) to be reached (*i.e.*, $v/v_{max}=1.0$ for fully anchored shear walls). The strength reduction factors for common cripple wall heights (h) are shown in Table 11-5 assuming a wall length (d) of 8 feet which was assumed in both the design and analysis processes. The table shows that a large reduction (45%) is returned using Eq. (4-1) for the taller 6-foot-high wall, which reflects that the aspect ratio reduction factors can be viewed as a conservative estimate for taller cripple walls. Salenikovich (2000) also states that the use of Eq. (4-1) is a conservative estimate.

Table 11-5 Strength Reduction Factors Based on Aspect Ratio of Wood Structural Panel Shear Walls without Tie-Downs

Wall Height, h [ft]	2	4	6
Wall Length, d [ft]	8	8	8
Aspect Ratio, a_r	0.25	0.5	0.75
Reduction Factor, SR	0.89	0.71	0.55

A total of nine WSP designations were developed for the project and defined within FEMA P-1100 Volume 3 Part 4 document. However, only six designations were used for the study of crawlspace dwellings and included WSP4 through WSP9. Each of these designations were implemented with and without consideration of the aspect ratio reduction factors. In order to include the fully anchored capacity of the WSP without aspect reduction factor for panels that do not include tie-downs, the shear wall bracing must be designed in order to prevent uplift failure due to overturning. This translates into longer WSP lengths being required in order to prevent uplift failure when compared to WSP walls including tie-downs, especially for taller cripple wall heights. Further, for cases assuming aspect ratio reduction factors (i.e., h/d factors), this reduction is applied to both the design and assessment (i.e., numerical modeling) capacities, which requires longer WSP panel lengths (and possibly tighter nail spacing) to achieve the same R-factor as cases without aspect ratio reduction. A complete discussion of these considerations is provided in Section 3.6 of the FEMA P-1100 Volume 3, Part 4 document.

The numbered WSP designations for cripple walls greater than or equal to 5 feet follow from the baseline WSP properties (i.e., WSP1, 2 and 3) that include tie-downs as follows:

- WSP4: High capacity WSP with 15/32-inch STR I sheathing, 8d common nails at 2 inches on center, design and detailing to develop full capacity of perimeter nailing without the use of tie-downs, material is applied to cripple wall heights greater than 5 feet, material assumes displacement capacity A;
- WSP5: Medium capacity WSP with 15/32-inch Rated sheathing, 8d common nails at 3 inches on center, design and detailing to develop full capacity of perimeter nailing without the use of tie-downs, material is applied to cripple wall heights greater than 5 feet, material assumes displacement capacity A;
- WSP6: Low capacity WSP with 7/16-inch Rated sheathing, 8d common nails at 4 inches on center, design and detailing to develop full capacity

of perimeter nailing without the use of tie-downs, material is applied to cripple wall heights greater than 5 feet, material assumes displacement capacity A.

For cripple walls with a height less than 5 feet without tie-downs:

- WSP7: High capacity WSP with 15/32-inch STR I sheathing, 8d common nails at 2 inches on center, design and detailing to develop full capacity of perimeter nailing without the use of tie-downs, material is applied to cripple wall heights less than 5 feet, material assumes displacement capacity B;
- WSP8: Medium capacity WSP with 15/32-inch Rated sheathing, 8d common nails at 3 inches on center, design and detailing to develop full capacity of perimeter nailing without the use of tie-downs, material is applied to cripple wall heights less than 5 feet, material assumes displacement capacity B;
- WSP9: Low capacity WSP with 7/16-inch Rated sheathing, 8d common nails at 4 inches on center, design and detailing to develop full capacity of perimeter nailing without the use of tie-downs, material is applied to cripple wall heights less than 5 feet, material assumes displacement capacity B.

The RESST hysteretic model parameters for all six of the WSP types used for retrofit of cripple wall dwellings are provided in Table 11-6. The table denotes the “-noHD” (e.g., WSP4-noHD) cases to reflect the material properties prior to considering aspect ratio reduction factors when applicable. The inclusion of aspect reduction factors scales the initial stiffness (K_0) and characteristic strength (F_x) by SR using the appropriate cripple wall height (see Table 11-5). An example of the hysteretic response of WSP6 with and without aspect ratio strength reduction is shown for a 6 feet tall wall in Figure 11-19.

Table 11-6 RESST Hysteretic Parameters for Wood Structural Panel Materials Used for Cripple Wall Retrofit without Aspect Ratio Reduction Factors Applied

RESST Parameter ¹	WSP4-noHD ²	WSP5-noHD	WSP6-noHD	WSP7-noHD	WSP8-noHD	WSP9-noHD
K ₀ [lb/%θ-ft]	6130.0	4107.0	2935.0	4086.7	2738.0	1956.7
r ₁	0.052	0.052	0.052	0.052	0.052	0.052
r ₂	-0.144	-0.144	-0.144	-0.144	-0.144	-0.144
r ₃	1.0	1.0	1.0	1.0	1.0	1.0
r ₄	0.012	0.012	0.012	0.012	0.012	0.012
F _x [lb/ft]	2309.8	1547.3	1106.7	2309.8	1547.3	1106.7
f ₁	0.595	0.595	0.595	0.595	0.595	0.595
f ₂	0.110	0.110	0.110	0.110	0.110	0.110
f ₃	0.1	0.1	0.1	0.1	0.1	0.1
Dx [%θ]	3.21	3.21	3.21	4.81	4.81	4.81
α	0.55	0.55	0.55	0.55	0.55	0.55
β	1.05	1.05	1.05	1.05	1.05	1.05

¹ Refer to Figure 11-9 for definition of parameters; ² WSP 1, 2 and 3 are not used for the analysis of cripple wall dwellings (living space-over-garage and hillside analysis only)

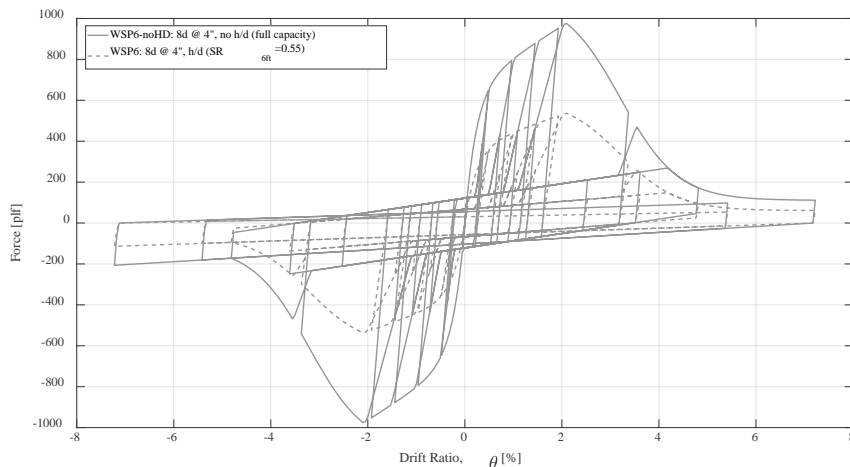


Figure 11-19 Comparison of hysteretic responses of wood structural panel WSP6 for a 6 foot tall cripple wall: No aspect ratio reduction (solid line); with aspect ratio reduction (dashed line).

11.4 Model Performance

This section provides an overview of the results of numerical analysis, and presents the figures illustrating analysis results that were used by the project team to select retrofit design parameters. The reader is reminded that, as described in FEMA P-1100 Volume 1, the numerical studies were used primarily as a tool to judge improvement in performance, rather than an

absolute indication of performance. The section first discusses the general trends in collapse performance at the MCE level (primary criterion of the project) observed for each superstructure type. This is followed by the illustration of all performance criteria for each archetype considered for decisions in retrofit guideline development.

11.4.1 General Trends in Collapse Performance

This sub-section provides an example of the documented results for each of the archetypes analyzed to support R-factor decision making. The results of all archetypes can be found in supporting background documentation (see Section 8). The estimated probability of collapse at the MCE intensity level ($P[C|MCE]$) for each archetype is plotted versus two important structural parameters:

- *Average peak strength-to-baseline weight ratio, $(V_{max}/W_{BL})_{Avg}$:* This parameter is the ratio of the peak strength obtained from a modal pushover analysis to the baseline lateral weight of the archetype. The pushovers are applied in proportion to the first elastic translational mode shape in each orthogonal direction. The average peak strength of these directions is obtained. The baseline weight (W_{BL}) is the weight of the archetype building not including the weight of the cripple walls. This parameter does not distinguish between strengths controlled by the cripple wall level or the superstructure.
- *Average cripple wall-to-superstructure strength ratio, $(V_{CW}/V_{SS})_{Avg}$:* This parameter is the average strength ratio of the cripple wall level to the superstructure level considering both orthogonal directions. These strengths are obtained through pushover analysis loading at the cripple wall only (i.e., first floor diaphragm) and the pushover obtained for each superstructure configuration located on a rigidly pinned base. This parameter illustrates the strength difference between the two stories without being dependent on load distribution as in a modal pushover analysis of the entire structure.

The $P[C|MCE]$ for one-story pre-1950 median archetypes, $P[C|MCE]$, is plotted versus $(V_{max}/W_{BL})_{Avg}$ in Figure 11-20 and $(V_{CW}/V_{SS})_{Avg}$ in Figure 11-21. These figures illustrate the existing cripple wall cases in gray and use a color gradient to illustrate changes in assumed R-factor in retrofit design (i.e., dark blue is used for the largest R-factors and red is used for the smallest R-factors). Cripple wall archetype characteristics, other than superstructure type, are shown using different symbols (e.g., 2-foot cripple walls are circles, 6ft cripple walls are triangles). For this set of archetypes with a strong and stiff superstructure, all collapses occur at the cripple wall

level which is reflected by the consistent trends of reduced P[C|MCE] with decreasing R-factor assumed in retrofit design. Notably, an increase in cripple wall height gave marginal collapse performance improvement for all archetypes within this study, regardless of superstructure type and number of stories. This was attributed to the taller (i.e., 6-foot) walls having larger global displacement capacity (displacement, not drift ratio) which allowed for somewhat longer period elongation prior to the onset of P-delta instability. This trend is clearly shown by comparing the three existing cripple wall archetypes (gray points) for three different wall heights in Figure 11-20. The figures show that retrofitting returns P[C|MCE] values that range from approximately 30% for larger R-factors (e.g., 4) to less than 10% for the smallest R-factor (e.g., 2). However, the effect of retrofitting is shown to give significant reduction when compared to the existing cases without retrofit. This is a typical observation; see Section 5 for more discussion of relative performance.

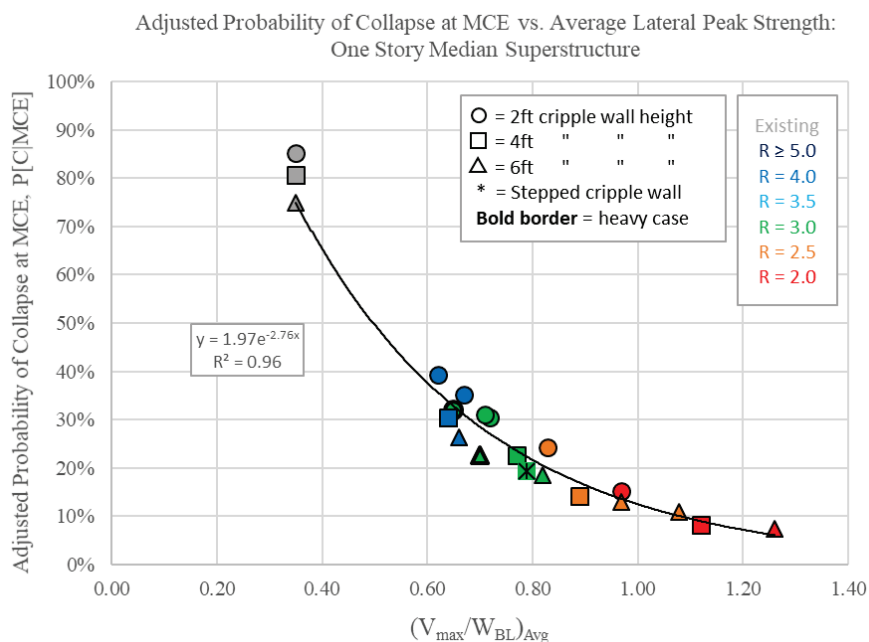


Figure 11-20 Trends of probability of collapse at the MCE intensity level versus the average peak strength-to-baseline weight ratio: One-story median pre-1950 superstructure. Note: All collapses occur at the cripple wall level.

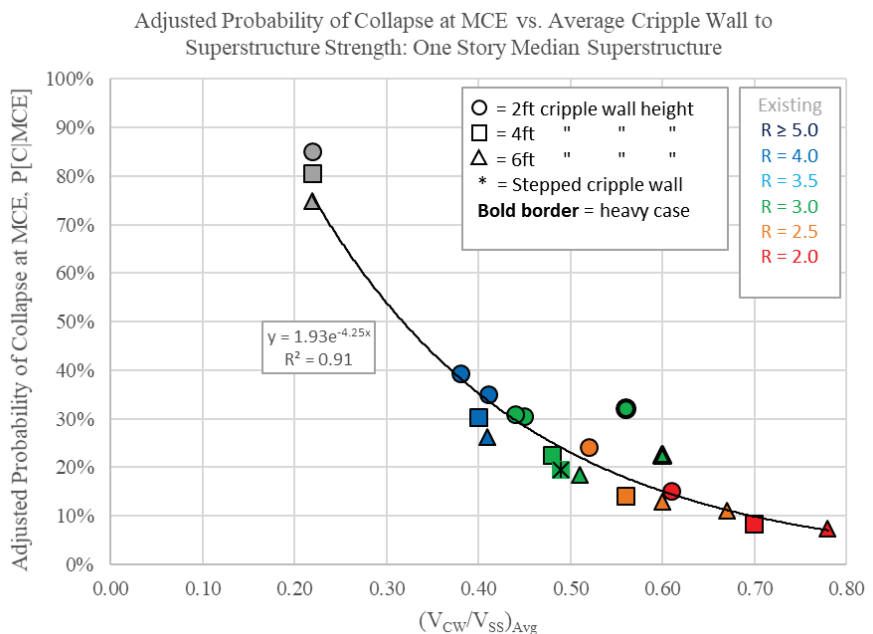


Figure 11-21 Trends of probability of collapse at the MCE intensity level versus the average cripple wall-to-superstructure strength ratio: One-story median pre-1950 superstructure. Note: All collapses occur at the cripple wall level.

The equivalent plots for the one-story post-1950 median- β archetypes are shown in Figure 11-22 ($P[C|MCE]$ versus $(V_{max}/W_{BL})_{Avg}$) and Figure 11-23 ($P[C|MCE]$ versus $(V_{CW}/V_{SS})_{Avg}$). The collapse trends in Figure 11-22 do not provide a clear trend as was observed for the pre-1950 archetypes (see Figure 11-20). This is due to the superstructure strength controlling the pushover strength for one or more directions for the calculation of $(V_{max}/W_{BL})_{Avg}$ for lower R-factors which limits the value. Conversely, Figure 11-23 illustrates the transition between collapse in the cripple wall and superstructure occurs between $R = 3.0$ and $R = 2.0$ for this superstructure. This is in good agreement in terms of reported story strength ratio of 1.3 causing this shift in collapse location reported in the FEMA P-807 project (FEMA, 2012). This value is annotated in Figure 11-23 for reference only and is not a conclusive finding between the two projects.

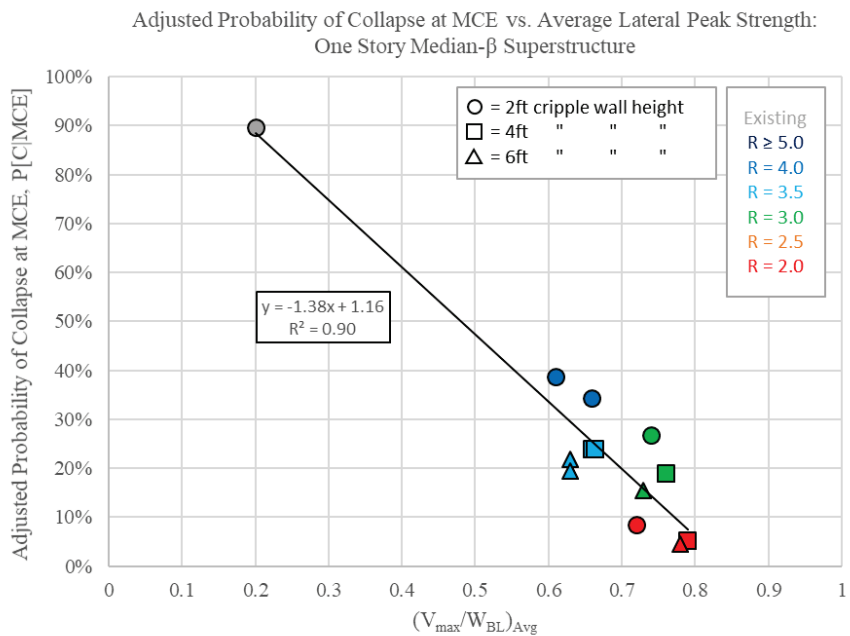


Figure 11-22 Trends of probability of collapse at the MCE intensity level versus the average peak strength-to-baseline weight ratio: One-story median- β post-1950 superstructure.

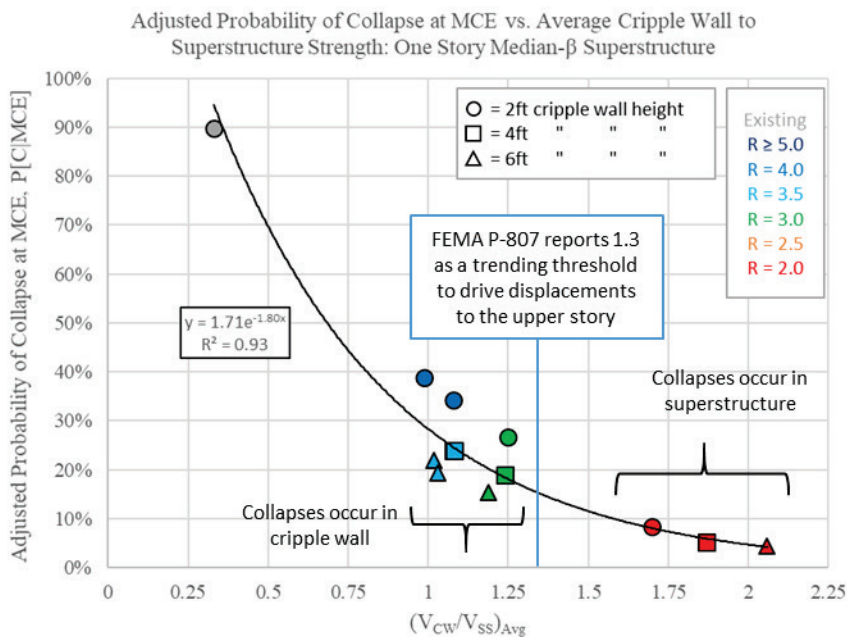


Figure 11-23 Trends of probability of collapse at the MCE intensity level versus the average cripple wall-to-superstructure strength ratio: One-story median- β post-1950 superstructure.

Similar trends between the two configuration eras were observed for two-story cases as shown in Figures 11-24 and 11-25 for pre-1950 and Figures 11-26 and 11-27 for post-1950. The largest difference between these configurations and those considered previously is the considerable weight that is added due to the second story. For the two-story pre-1950 median case, the smallest R-factor ($R = 2.5$) analyzed reached the strength ratio just before collapses would shift to the superstructure which returned a single collapse case at the MCE intensity level in the superstructure (see Figure 11-24). This is a direct result of the increased WSP retrofit brace length and added weight acting laterally on the first occupied story. Notably, this first superstructure collapse case occurred at a story strength ratio of $(V_{CW}/V_{SS})_{Avg} = 1.2$.

The two-story post-1950 median- β archetypes reached the point of superstructure strength controlling the collapse mechanism at much larger R-factor designs (i.e., weaker retrofit bracing) than the post-1950 median archetypes. This is due to the much weaker first occupied story for this set of archetypes. Figure 11-27 illustrates that $R \geq 6.0$ designs did not cause collapse to be driven into the superstructure, yet $R < 4.0$ designs forced all collapses into the first occupied story of the superstructure. This is reflected by the relatively constant $P[C|MCE]$ for $R < 4.0$ shown in Figure 11-27.

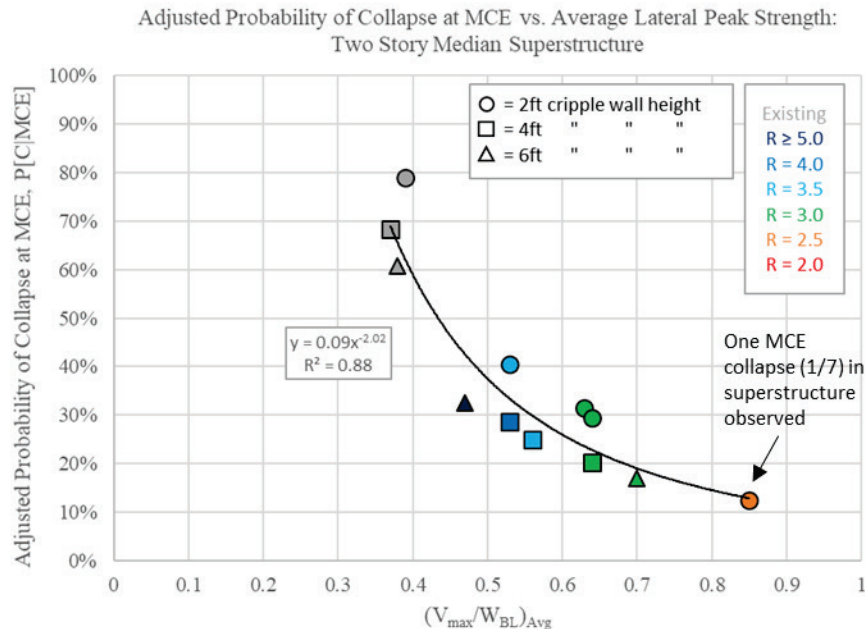


Figure 11-24 Trends of probability of collapse at the MCE intensity level versus the average peak strength to baseline weight ratio: Two-story median pre-1950 superstructure.

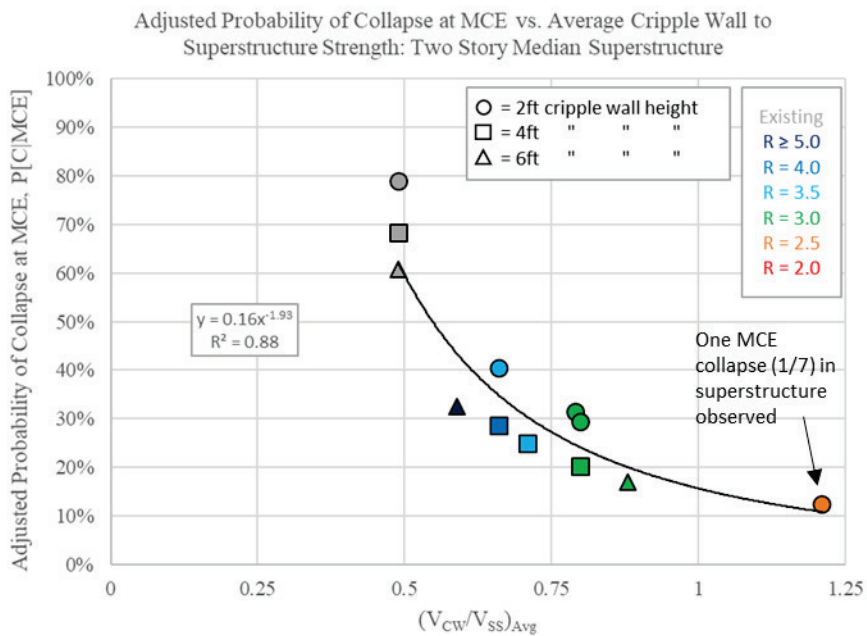


Figure 11-25 Trends of probability of collapse at the MCE intensity level versus the average cripple wall to superstructure strength ratio: Two-story median pre-1950 superstructure.

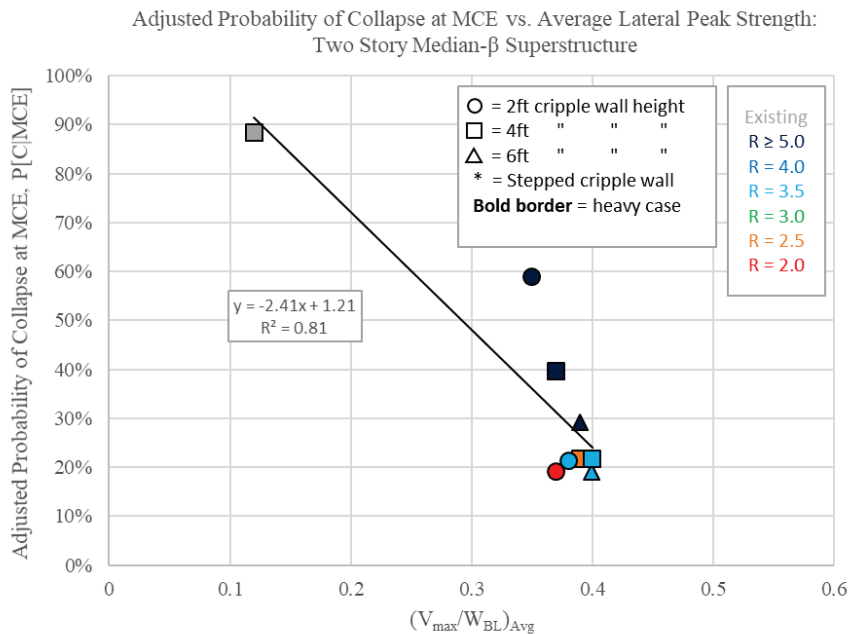


Figure 11-26 Trends of probability of collapse at the MCE intensity level versus the average peak strength-to-baseline weight ratio: Two-story median- β post-1950 superstructure. Note: Global strength controlled by superstructure strength for $R < 4$. Saturation of points near $(V/W)_{Avg} = 0.4$ reflects global collapses occurring in superstructure.

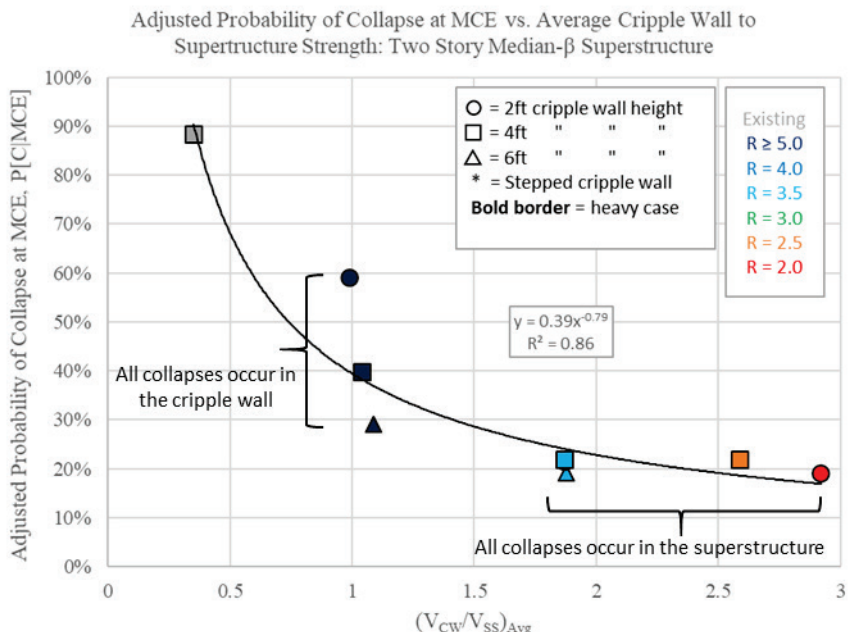


Figure 11-27 Trends of probability of collapse at the MCE intensity level versus the average cripple wall-to-superstructure strength ratio: Two-story median- β post-1950 superstructure.

11.4.2 Summary of Archetype Performance

The performance of the various retrofits was measured based on the primary and secondary criteria outlined in the FEMA P-1100 Volume 3, Part 2 document. These performance criteria are summarized as follows:

- Primary criterion: probability of collapse at the MCE intensity level ($S_a(0.25s)=1.5g$)
- Secondary criterion 1: probability of exceedance of 0.75% drift at the 0.4MCE intensity level ($S_a(0.25s) = 0.6g$)
- Secondary criterion 2: probability of exceedance of 1.5% drift at the DE ($S_a(0.25s)=1.0g$) intensity level

For each of these criteria, the probability of collapse at the MCE level (primary criterion) and the probability of exceedance of different drift and intensity combinations is shown in the following bar charts. The bar charts are grouped according to cripple wall height and provide results for all superstructure types (i.e., one- and two-story; pre-1950 and post-1950). This grouping was selected to compliment the collapse results presented in Section 4.1. Each set of bar charts provides the equivalent performance of the existing cripple wall case (labeled “Existing CW”) when possible and the performance of the superstructure modeled on a pinned base (labeled

“Superstructure Only”) for comparison. The different archetypes for the same era and configuration (e.g., one-story pre-1950 median) are sorted in order of decreasing R-factor assumed in preliminary retrofit design. R-factors are labeled near the P[C|MCE] values to quickly illustrate trends in collapse performance. R-factors labeled in blue are those that did not include the aspect ratio reduction factors in design capacities and those in red are cases that did include them.

The two-foot tall archetypes are presented in Figure 11-28. The four-foot and six-foot tall cripple wall archetypes are presented in Figure 11-29 and Figure 11-30, respectively.

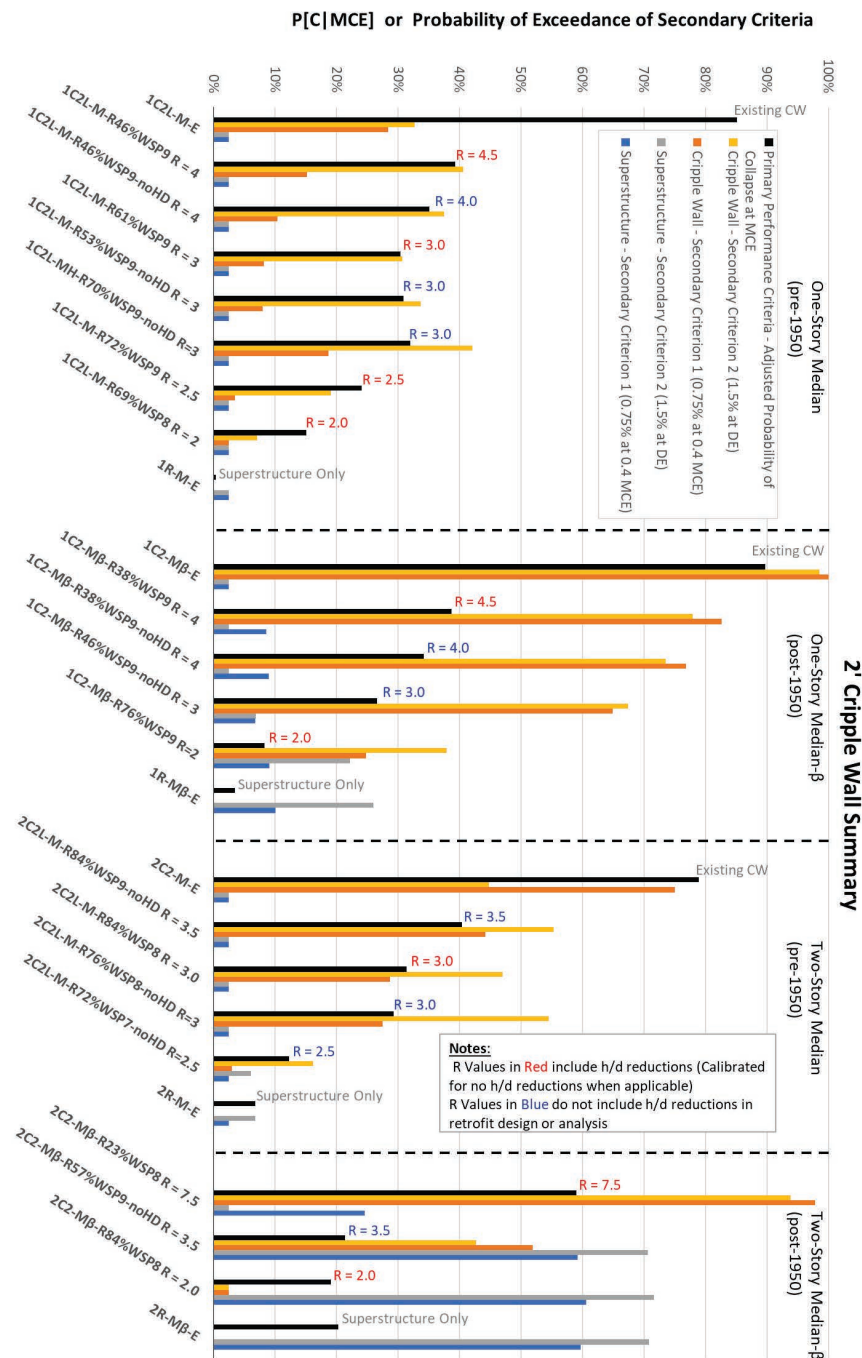


Figure 11-28

Summary of performance criteria: two-foot tall cripple wall cases. NOTE: R-factor labels are placed near the P[C|MCE] values in order to clearly illustrate its influence on collapse performance.

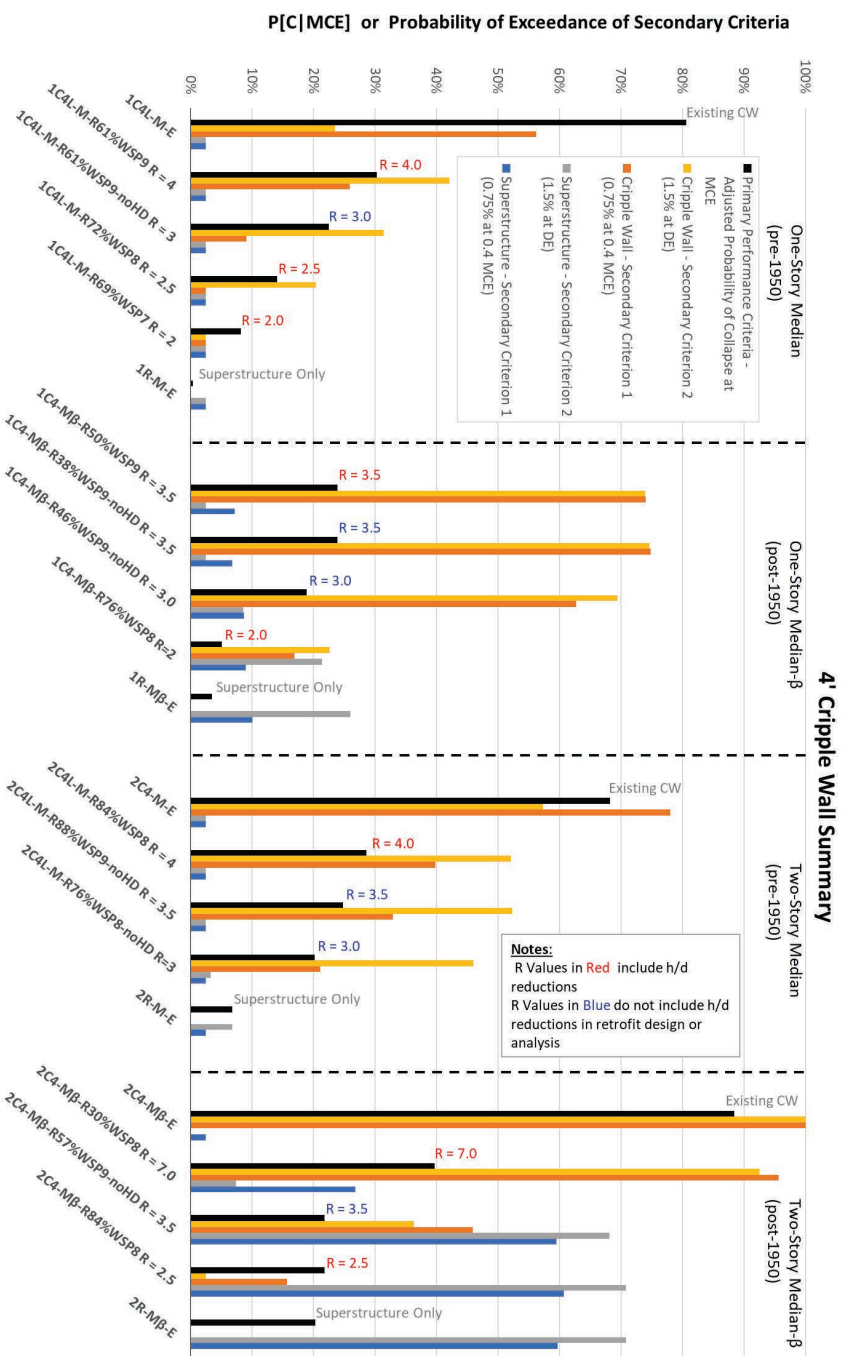


Figure 11-29 Summary of performance criteria: four-foot tall cripple wall cases. NOTE: R-factor labels are placed near the P[C|MCE] values in order to clearly illustrate its influence on collapse performance.

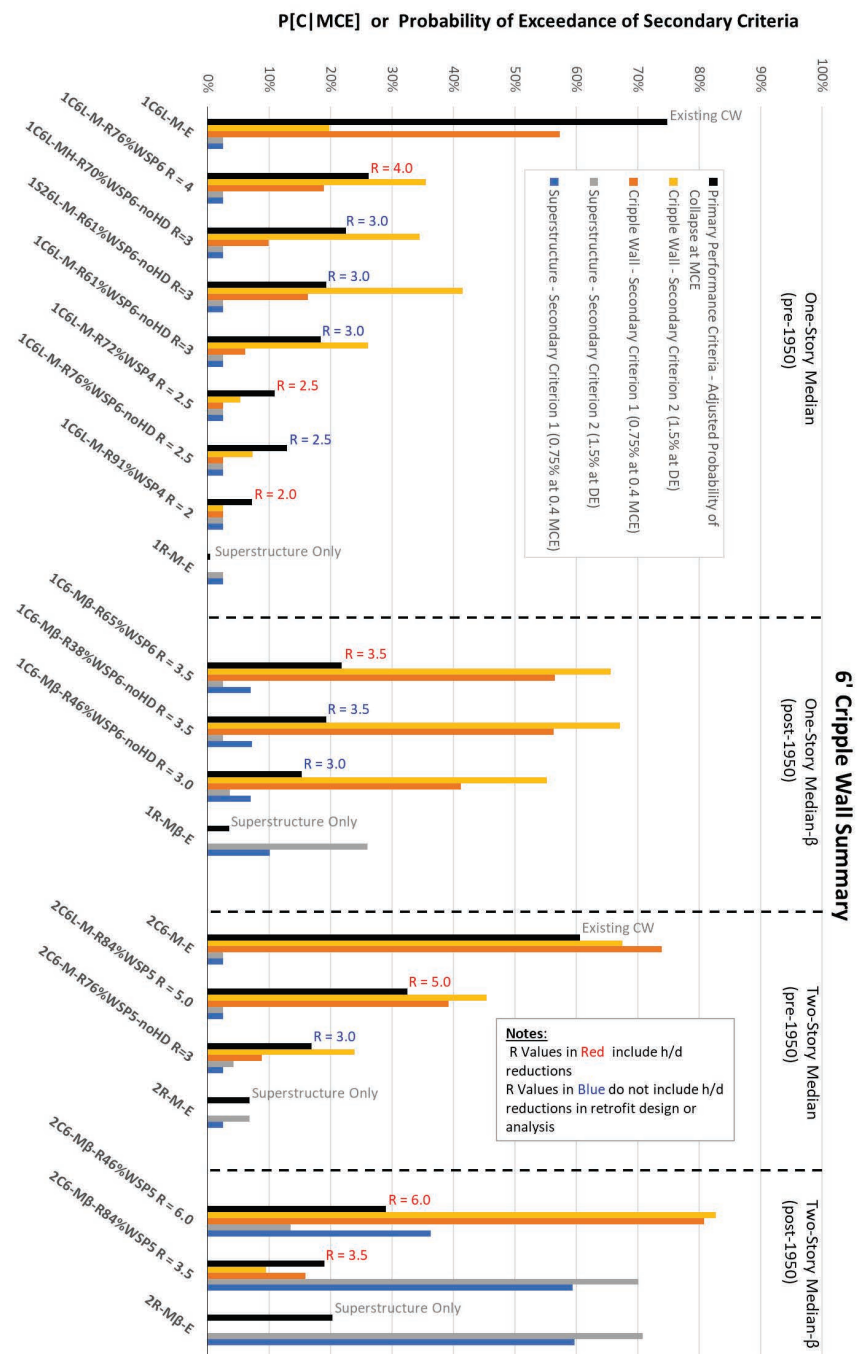


Figure 11-30 Summary of performance criteria: six-foot tall cripple wall cases.
NOTE: R-factor labels are placed near the P[C|MCE] values in order to clearly illustrate its influence on collapse performance.

11.5 Selected Retrofit Design Parameters and Methods

The fundamental design parameters of interest are the appropriate R-factor and overstrength factor “ Ω_0 ”. The selection of these parameters included consideration of both the analysis results and constructability.

Constructability was taken as the ability to practically implement the resulting design solutions to typical archetypes (e.g., one- and two-story structures with different building materials, both rectangular and irregular floor plans, different plan aspect ratios, and different height cripple walls). Analysis results were focused on the determinations of collapse probabilities for both existing and retrofit conditions. Retrofitted models included the addition of various lengths of plywood sheathing on cripple walls, which were back-calculated to corresponding approximate R-factor. While the focus was on identifying and achieving specific collapse probabilities (Section 4), the percent improvement over the un-retrofitted case was also important. Because low R-factors were required to meet the established primary performance metrics that were identified early in the studies, extensive constructability studies were undertaken. Ultimately, $R = 4.0$ was chosen as a balance between improved performance and constructability.

Tables 11-7 and 11-8 summarize the percent improvement for one- and two-story dwelling numerical studies, respectively for MCE shaking for different R-factors. The percent improvement for the one- and two-story dwellings are similar except for lower R-factors where the percent improvement for one-story buildings is larger. These percent improvements are lower bounds as they reflect only the improvement due to the added cripple wall sheathing. Larger improvements are achieved, especially for pre-1940 buildings, that are typically unanchored or inadequately anchored to the foundation.

Table 11-7 Percent Improvement in Collapse Probability for the MCE versus Computed R-Factors for One-Story Dwellings

One-Story Summary		
% Improvements in Collapse Probabilities for MCE		
	Cripple Wall Height (ft)	
R Value	2, 4, 6	2, 4
2.5	89%	89%
3	79%	79%
3.5	76%	71%
4	70%	64%

Table 11-8 Percent Improvement in Collapse Probability for the MCE versus Computed R-Factors for Two-Story Dwellings

Two-Story Summary		
% Improvements in Collapse Probabilities for MCE		
	Cripple Wall Height (ft)	
R Value	2, 4, 6	2, 4
2.5	78%	78%
3	76%	75%
3.5	70%	66%
4	67%	62%

Constructability was studied primarily by determining if the typical retrofit connectors (proprietary steel clips and anchor bolts) and plywood sheathing panels could fit within the available perimeter wall lengths of typical floor plans. This was established by developing a large spreadsheet with customized macros to perform iterative calculations required to establish retrofits satisfying both calculated shear and overturning requirements. In addition to selecting unit weights of different construction materials, several assumptions were made in order to calculate the structure's weight including:

- Eave overhang length.
- Roof pitch.
- Story height(s).
- (Interior partition length)/(perimeter wall length).
- Percentage of openings in interior and perimeter walls.
- Percentage of sheathed cripple wall.
- Percentage of floor area covered by heavy tiles.

Two different exterior wall finishes, two different interior wall finishes, and two different roofing materials were considered. This resulted in eight different possible weight combinations (e.g., one weight combination is exterior stucco, interior plaster and clay tile). In order to make the number of tables included in the prescriptive plan set reasonable, the eight different weight combinations were grouped into three different weight classifications (heavy, medium and light), with the prescriptive design details in the plan set based on the worst case in each weight classification. Assignment of weight combinations into weight classifications was based on overall calculated shear and overturning demand rather than simply an arithmetic ranking of total weights. For example, a building with weight W with stucco perimeter walls is more resistant to overturning than a building with weight W and

lighter wood panel siding because the stucco weight is directly over the perimeter foundation and thus more efficient at resisting overturning. A mapping of weight combinations into weight classifications is shown in Figure 11-31.

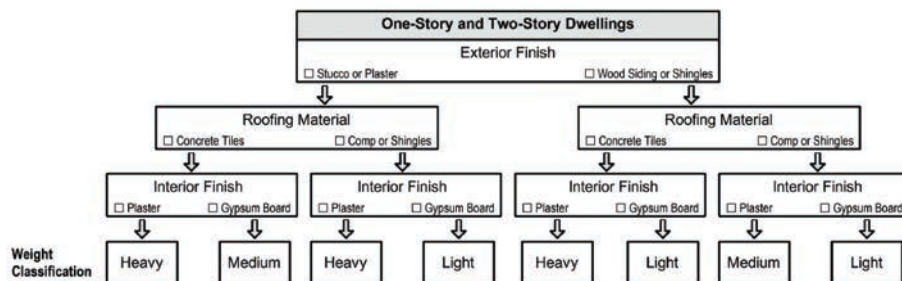


Figure 11-31 Mapping of material weight combinations into weight classifications for cripple wall constructability analysis.

During these studies the WG4 team assumed that the buildings were rectangular in plan (with identical areas for first and second floors for two-story buildings) and several plan aspect ratios were studied until the ratio of 0.75 was selected as most appropriate for study. It is recognized that plan aspect ratios significantly lower than 0.75 are problematic because of the limited length for strengthening of the cripple walls in the short direction. A range of building areas was considered; 800 to 3,000 sf for one-story buildings and 1600 to 4,000 sf for two-story buildings. Calculations were run for different levels of seismicity including $S_{DS} = 1.0$ (moderate seismicity), $S_{DS} = 1.2$ (high seismicity) and $S_{DS} = 1.5$ (very high seismicity).

The WG4 team ideally assumed that two sheathed panels would be provided along each wall line (this is not practical for irregular plan shapes with short wall line segments). Further, the WG4 team decided it impractical to assume that 100% sheathing of wall lines is possible due to obstructions, openings, etc., so a limit of 90% of the wall line length was set as an upper bound for possible sheathing for judging practicality of construction. The WG4 team did calculations for both one and two sheathed panels per wall line, and tables were generated. In order to limit the number of tables included in the plan set, only the two-wall panel solution was included.

In order to calculate the number of retrofit connectors required, the WG4 team used capacity values for representative connectors. An attempt was made to identify three different types of proprietary hardware per application (e.g., clips between top plates and blocking) to give the user choices. The hardware with the lowest capacity of the three was used in the calculations. This means that, depending on the hardware selected, the spacing specified in the table may be conservative. Note that the number of connectors required is

relatively insensitive to the height of the cripple wall. For consistency and simplicity, the team assumed a 4-foot cripple wall height for determining the number of connectors.

The WG4 team did not handle overturning in the traditional fashion. It was recognized that the structure will behave somewhat like a box to resist overturning rather than like independent wall lines parallel to the direction of load. Thus, the overturning load that was used to check foundation uplift is less than used in design of a typical wood frame structure (see FEMA P-1100 Volume 3, Part 8 for further details). Additionally, the WG4 team wanted to limit uplift loads because the typical existing foundations were not capable of resisting large loads due to quality of the concrete and the size of the foundation. In order to limit the use of tie downs, credit was given to anchor bolts with large washers based on component testing done by Mahaney and Kehoe (2002) and shake table testing conducted by Fischer et al. (2001) using conventional construction detailing. The WG4 team assumed that a pair of anchor bolts spaced at 8 inches has an uplift capacity of 2.1 kip. If it was not practical to provide a sheathed wall long enough to limit the uplift loads to 2.1 kip, the team assumed that the combination of a tie-down and anchor bolt has an uplift capacity of 4.2 kip. If uplift loads larger than 4.2 kip were calculated, the associated sheathed panel geometry was not constructible.

The overstrength factor (Ω) was used for connections to ensure the connections did not represent the weak link and the failure mode is ductile yielding of the nails in the plywood. This is discussed further in FEMA P-1100 Volume 3, Part 7.

For studying constructability a series of twelve tables (see Figure 11-32) each summarizing the results for each combination of weight classification (heavy, medium, light), number of sheathed panels per wall line (1 or 2), plan aspect ratio, R-factor and building square footage were calculated within the spreadsheet for both 1- and 2-story (24 tables total). An example of one table is reproduced below in Figure 11-33. These tables are the source of the values in the Earthquake Retrofit Schedules in the plan set.

Figure 11-32 Example of constructability tables for all weight combinations, plan dimensions, and number of sheathed panels per wall line. (Tables for two-story cases with an $S_{DS}=1.0g$ and $R=4$ shown. Only 2-Panel solutions were included in plan set.)

Construction Type		Medium		Number of Stories		2		 = Constructability Conflict																							
		Number of Panels per Wall Line		2		Aspect Ratio																									
		0.75		Minimum Total Length of Strengthening - Plywood Braced Panels (Ft)																											
		Cripple Wall Height								15/32" Plywood		Spacing of Foundation Connectors or Anchors at Each Perimeter Wall Line (in.) Assume Distributed Along Length																			
Total Floor Area in Square Feet	First Floor Area	S _{DS}	1	R	4	0' < 1'	1' < 2'	2' < 4'	4' < 6'	6' < 7'	Plywood Grade	Nailing (in.)	Type A	Type B	Type C	Type D	Type E or F	Type G	Type H												
L (ft)	B (ft)	No Tie Downs	No Tie Downs	No Tie Downs	Tie Downs	No Tie Downs	Tie Downs	No Tie Downs	Tie Downs	Tie Downs	Type A	Type B	Type C	Type D	Type E or F	Type G	Type H	Type I													
1600	800	33	24	9.3	9.3	12.0	9.3	13.3	10.7	14.7	12.0	Constr Gr	3	48	29	24	24	36	16	16	12										
2000	1000	37	27	10.7	10.7	13.3	10.7	14.7	12.0	16.0	13.3	Constr Gr	3	40	27	23	23	32	15	15	11										
2400	1200	40	30	12.0	12.0	14.7	12.0	16.0	13.3	17.3	13.3	Constr Gr	3	44	25	22	22	35	14	15	11										
3000	1500	45	34	13.3	13.3	16.0	13.3	17.3	14.7	18.7	16.0	Constr Gr	3	39	22	20	20	33	13	14	10										
4000	2000	52	39	17.3	17.3	17.3	17.3	20.0	17.3	21.3	17.3	Constr Gr	3	33	21	19	19	29	12	13	10										

Figure 11-33 Typical table for two-story structure in constructability spreadsheet. Bordered and shaded cells (pink) within required plywood bracing length and anchorage connector fields reflect constructability conflicts.

In Figure 11-33 the required length of wall panel per wall line is calculated for five different cripple wall heights (8 penny, 2 inch nail spacing was chosen for heavy construction and 8 penny, 3 inch nail spacing was chosen

for medium and 8 penny, 4 inch nail spacing for light construction) for both without and with tie-downs. The required panel wall length is rounded to the nearest 16 inches to correspond with cripple wall stud spacing. The required length in each in each cell of the table can be compared with the available exterior length available (L and B in the table), and the number of cells where insufficient length exists counted (insufficient length is defined as $(\text{required length})/(\text{available length}) > 0.9$). In the spreadsheet tables, instances with insufficient length are shaded in pink.

Similarly, for the different connectors, the required spacing can be calculated (same values required for with and without tie downs), the design is considered impractical if the connector spacing is less than 8 inches (two per stud bay). During the initial constructability studies, a spacing of 16 inches was used rather than 8 inches, as seen in Figure 11-33 and Figure 11-34. Instances where calculated spacing is less than 16 inches are also shaded in pink in the table.

The measure of constructability can be summarized by counting the pink squares in the tables and dividing by the total number of squares in the tables. For instance, use of $R = 3.0$ might result in 50% of the squares being shaded for a single table for a specific structure (say heavy construction, one story, two panels per line, plan aspect ratio = 0.75, $S_{DS} = 1.0$, $R = 3.0$), whereas use of $R = 4.0$ might result in only 25% of the squares being shaded for the same specific structure, indicating higher constructability. Figure 11-34 illustrates the counting procedure. Similarly, the data for six tables for a specific structure could be combined to give a measure of constructability for a specific R-factor for one- or two-story structures, or the data for all 12 tables combined for an overall measure of constructability for one- and two-story structures combined.

		Construction Type		Medium	Number of Stories	2			 = Constructability Conflict Minimum Total Length of Strengthening - Plywood Braced Panels (Ft)												
		Number of Panels per Wall Line		2	Aspect Ratio	0.75															
Total Floor Area in Square Feet	First Floor Area	S _{Ds}	1	Cripple Wall Height						15/32" Plywood		Spacing of Foundation Connectors or Anchors at Each Perimeter Wall Line (in.) - Assume Distributed Along Length									
		R	4	0'< 1'	1'<2'	2'<4'	4'<6'	6'<7'		Plywood Grade	Nailing (in.)	Foundation Sill Anchorage		Floor to Cripple Wall or Foundation Sill							
		L (ft)	B (m)	No Tie Downs	No Tie Downs	No Tie Downs	Tie Downs	No Tie Downs	Tie Downs	Type A	Type B	Type C	1/2" Bolt	5/8" Bolt	Type D	Type E or F	Type G				
1600	800	33	24	9.3	9.3	12.0	9.3	13.3	10.7	14.7	12.0	Constr Gr	3	48	29	24	24	38	16	16	12
2000	1000	37	27	10.7	10.7	13.3	10.7	14.7	12.0	16.0	13.3	Constr Gr	3	55	32	20	20	38	15	15	11
2400												Constr Gr	3	55	22	20	20	38	14	15	11
3000	1500	45	34	13.3	13.3	16.0	13.3	17.3	14.7	18.7	16.0	Constr Gr	3	55	22	20	20	38	13	14	10
4000	2000	52	39	17.3	17.3	17.3	20.0	17.3	21.3	17.3		Constr Gr	3	33	21	19	19	28	12	13	10

17 unacceptable solutions for panels

15 unacceptable solutions for connectors

Original measure of constructability

- Total cells = 40 for plywood braced panels + 40 for connectors = 80
- Total of unacceptable solutions = 17 for panels + 15 for connectors = 32
- Percent unacceptable = $32/80 = 40\%$

Figure 11-34 Illustration of the original measure of constructability to count conflicts for retrofit of cripple wall dwellings.

The above approach allowed comparisons of large amounts of data quickly. However, this approach was modified near the end of the study. One change was to only count the tie-down option columns for the taller cripple walls for the wall panel lengths portion of the table as it could be argued that counting the pink squares for a given cripple wall height for both with and without tie-downs is double counting (see Figure 11-35). The other change was to recognize that only one cell in each of the five columns for foundation sill anchorage needs to be acceptable for there to be a solution, and only one cell in each of the three columns for floor-to-cripple wall or foundation-to-sill needs to be acceptable for there to be a solution. In some cases, this modified approach did result in a significant change in measuring constructability. An example of this change is illustrated when comparing Figures 11-34 and 11-35.

			Construction Type		Medium	Number of Stories	2	 = Constructability Conflict (New Measure)								
			Number of Panels per Wall Line		2	Aspect Ratio	0.75									
			Minimum Total Length of Strengthening - Plywood Braced Panels (Ft)													
Total Floor Area in Square Feet	First Floor Area	SOS	R	1	Cripple Wall Height						15/32" Plywood	Spacing of Foundation Connectors or Anchors at Each Perimeter Wall Line (in.) - Assume Distributed Along Length				
L (ft)	B (ft)	No Tie Downs	No Tie Downs	No Tie Downs	Tie Downs	No Tie Downs	Tie Downs	No Tie Downs	Tie Downs	Plywood Grade	Nailing (in.)	Foundation Sill Anchorage	Floor to Cripple Wall or Foundation Sill			
Type A	Type B	Type C	Type D	Type E or F	Type G	Type 1/2" Bolt	Type 5/8" Bolt	Type D	Type E or F	Type G						
1600	800	33	24	9.3	9.3	12.0	9.3	13.3	10.7	14.7	12.0	Constr Gr	3	48 29 24 24 36	15 16 12	
2000	1000	37	27	10.7	3 unacceptable solutions for panels						16.0	13.3	Constr Gr	3	12 15 15 11	
2400	1200	40	30	12.0	12.0	14.7	12.0	16.0	13.3	17.3	13.3	Constr Gr	3	5 14 15 11		
3000	1500	45	34	13.3	13.3	16.0	13.3	17.3	14.7	18.7	16.0	Constr Gr	3	13 14 14 10		
4000	2000	52	39	17.3	17.3	17.3	17.3	20.0	17.3	21.3	17.3	Constr Gr	3	33 21 19 19 29	12 13 13 10	

New measure of constructability

- Total cells = 25 for plywood braced panels + 10 for connectors = 35
- Total of unacceptable solutions = 3 for panels + 5 for connectors = 8
- Percent unacceptable = 8/35 = 23%

Figure 11-35 Illustration of the revised or “new” measure of constructability to count conflicts for retrofit of cripple wall dwellings.

In general, the constructability studies indicated that for high and very high seismicity and heavy weight there are a relatively large number of structures that cannot be retrofitted using the prescriptive solutions in the plan set. This is in part because there are some conservatisms built into the plan set (e.g., using the most conservative connector value for the three possible proprietary hardware choices, or using a relatively steep roof pitch to calculate the seismic weight). Whether or not the prescriptive provisions can be used on an individual house must be determined by comparing the required shear panel lengths and number of connectors in the Earthquake Retrofit Schedule in the plan set and determining whether they will fit. The number of connectors used must be checked against both minimum (8 in.) and maximum spacings (64 in. and 48 in. for anchor bolts for one- and two-story buildings, respectively). If the maximum spacing is exceeded, additional connectors must be provided.

An engineer can use the Prestandard, along with actual structure weights and perhaps closer nail spacing or Struct I plywood to demonstrate that lesser wall panel lengths and larger hardware spacing are appropriate. There is also an option in the plan set to permit sheathing of 95% of the wall line length without the need for further calculations by an engineer.

11.6 Cripple Wall to Hillside Transition Based on Expert Opinion

For a dwelling with a stepped or sloped foundation to qualify for a crawlspace retrofit, the following criteria must be satisfied:

- Cripple walls, where they occur, do not exceed 7'-0" in clear height.
- The maximum slope as measured from the top of foundations along one edge of the home to the other end does not exceed 5 to 1 (horizontal to vertical) or 20%.

If the dwelling does not satisfy both above criteria, then a hillside retrofit with primary, secondary, and shear anchorage elements is required. These criteria aim to ensure that stiffness differences in the crawl space do not become too extreme and that the shorter cripple walls studs in the system can tolerate the out of plane drifts that would be expected without experiencing P- Δ collapse.

The development of these qualification criteria was largely based on engineering judgment and expert opinion. Numerical studies were conducted in order to reinforce decisions. Details of the development of the transition point criteria can be found in the FEMA P-1100 Volume 3, Part 9 document.

11.7 Archived Files

This section provides an annotated list of files developed during the course of numerical studies that have been archived for future use. More details on the archived documents for the project can be found in FEMA P-1100 Volume 4.

Document WG4-B1

- Original File Name:
ATC_110_WG4_CW_Dwelling_Analysis_Update_July_18_2019_Vol3
- Date: 7/18/2019
- Title: Analysis Update for Cripple Wall Dwellings
- Description: Results of all primary numerical models used for retrofit design decisions for cripple wall dwellings. Information includes structural geometry, material assumptions, modal analysis, pushover analysis, and nonlinear dynamic analysis results.
- Original File Format: PowerPoint (.pptx)
- Size: 637 Slides

Document WG4-B2

- Original File Name: Overturning_CUREE_Tests_11_27_2017
- Date: 11/27/2017
- Title: Overturning Results from CUREE Two-story House Tests
- Description: Summary of extracted uplift and overturning demands from the two-story shake table test series conducted within the CUREE-Caltech Woodframe Project
- Original File Format: PowerPoint (.pptx)
- Size: 29 Slides

Document WG4-B3

- Original File Name: WG4 Compiled ResultsR4-05-09-19
- Date: 5/9/2019
- Title: N/A
- Description: Bar charts showing correlations of probability of collapse at the MCE intensity level ($P[C|MCE]$) with R factors
- Original File Format: Excel (.xlsx)
- Size: 10 Worksheets

Document WG4-B4

- Original File Name: ATC110_Calc_Spreadsheet-08.04.2017-Preliminary Design for Models
- Date: 8/4/2017
- Title: N/A
- Description: Design calculations for all building configurations considered in incremental dynamic analysis.
- Original File Format: Excel (.xlsx)
- Size: 164 Worksheets

Document WG4-B5

- Original File Name:
ATC_110_WG4_Superstructure_Study_Summary_Vol4_9_5_2019
- Date: 9/5/2019
- Title: Summary of Superstructure Configuration Study for Analysis of Cripple Wall Dwellings
- Description: Overview of revised superstructure strength evaluation procedure and modification of CUREE small house for different eras of construction.
- Original File Format: PowerPoint (.pptx)
- Size: 108 Slides

Document WG4-B6

- Original File Names:
 - 2018-05-18 ATC 110 R4 SDS1 A75 70-30
 - 2018-05-18 ATC 110 R4 SDS1_2 A75 70-30
 - 2018-05-18 ATC 110 R4 SDS1_5 A75 70-30
- Date: 7/29/2019
- Title: N/A
- Description: Design and verification of constructability. Three seismic design levels (S_{DS} = 1.0g, 1.2g, 1.5g) are included.
- Original File Format: Excel (.xlsx)
- Provided File Format: PDF (.pdf)
- Size: 48 Pages

Document WG4-B7

- Original File Name: Transition_Study_Summary_Vol4
- Date: 9/2/2019
- Title: ATC-110 WG4: Analysis Summary for “Zero-Height” and Hillside Transition Study
- Description: Cripple wall to hillside transition study.
- Original File Format: PowerPoint (.pptx)
- Size: 65 Slides

11.8 References

- Baker, J.W. 2015. "Efficient Analytical Fragility Function Fitting Using Dynamic Structural Analysis," *Earthquake Spectra*, 31 (1), pp. 579-599.
- Chai, Y.H., Hutchinson, T.C., Vukazich, S.M. 2002. "Seismic Behavior of Level and Stepped Cripple Walls," *CUREE Publication W-17*, CUREE-Caltech Woodframe Project, Consortium of Universities for Research in Earthquake Engineering, Richmond, CA.
- Christovasilis, I.P., Filiatrault, A. 2009. "A Computer Program for Seismic Analysis of Woodframe Structures," *SAWS Version 2.1 User Manual*, Division of Structural Engineering, University of California, San Diego, Department of Civil, Structural and Environmental Engineering, State University of New York at Buffalo.
- FEMA. 2000. *Prestandard and Commentary for the Seismic Rehabilitation of Buildings*, FEMA 356, Prepared by the American Society of Civil Engineers for the Federal Emergency Management Agency, Washington, DC, 518 p.
- FEMA. 2009. *Quantification of Building Seismic Performance Factors*, FEMA P-695, Prepared by the Applied Technology Council for the Federal Emergency Management Agency, Washington, DC, 421 p.
- FEMA. 2011. *Quantification of Building Seismic Performance Factors: Component Equivalency Methodology*, FEMA P-795, Prepared by the Applied Technology for the Federal Emergency Management Agency, Washington, DC, 292 p.
- FEMA. 2012. *Seismic Evaluation and Retrofit of Multi-Unit Wood-Frame Buildings with Weak First Stories*, FEMA P-807, Prepared by the Applied Technology for the Federal Emergency Management Agency, Washington, DC, 336 p.
- FEMA. 2018. *Vulnerability-Based Assessment and Retrofit of One- and Two-Family Dwellings: Volume 1 – Prestandard*, FEMA P-1100, Prepared by the Applied Technology for the Federal Emergency Management Agency, Washington, DC, 290 p.
- Ficcadenti, S.J., Freund, E.J., Pardo, G.C., Kazanjy, R.P. 2004. "Cyclic Response of Shear Transfer Connections Between Shearwalls and Diaphragms in Woodframe Construction," *CUREE Publication W-*

28, CUREE-Caltech Woodframe Project, Consortium of Universities for Research in Earthquake Engineering, Richmond, CA.

Fischer, D., Filiatrault, A., Folz, B., Uang, C.M., Seible, F. 2001. "Shake Table Tests of a Two-Story Woodframe House," CUREE Publication No. W-06, CUREE-Caltech Woodframe Project, Consortium of Universities for Research in Earthquake Engineering, Richmond, CA.

Folz, B., Filiatrault, A. 2004. "Seismic Analysis of Woodframe Structures. I: Model Formulation," *Journal of Structural Engineering, ASCE*, 130 (9), pp. 1353-1360.

Isoda, H., Folz, B., Filiatrault, A. 2002. "Seismic Modeling of Index Woodframe Buildings," *CUREE Publication W-12*, CUREE-Caltech Woodframe Project, Consortium of Universities for Research in Earthquake Engineering, Richmond, CA.

Johnson, A.J. 1997. "Monotonic and Cyclic Performance of Long Shear Walls with Openings," *MSc Thesis*, Virginia Polytechnic Institute and State University, Blacksburg, VA.

Mahaney, J.A. and Kehoe, B.E. 2002. "Anchorage of Woodframe Buildings: Laboratory Testing Report," CUREE Publication No. W-14, Consortium of Universities for Research in Earthquake Engineering, Richmond, CA, 137 p.

Pang, W., Ziaeい, E., Filiatrault, A. 2012. "A 3D Model for Collapse Analysis of Soft-story Light-frame Wood Buildings," *Proceedings of the 2012 World Conference on Timber Engineering* (2012 WCTE), Auckland, New Zealand.

Pang, W.C., Rosowsky, D.V., Pei, S., van de Lindt, J.W. 2007. "Evolutionary parameter hysteretic model for wood shear walls," *Journal of Structural Engineering, ASCE*, 133 (8), pp. 1118-1129.

Patton-Mallory, M., Wolfe, R.W., Soltis, L.A. 1985. "Light-frame shear wall length and opening effects," *Journal of Structural Engineering, ASCE*, 111 (10), pp. 2227-2239.

Salenikovich, A.J. 2000. "The Racking Performance of Light Frame Shear Walls," *PhD Dissertation*, Virginia Polytechnic Institute and State University, Blacksburg, VA, 234 p.

Stewart, W.G. 1987. "The seismic design of plywood sheathed shear walls," *PhD Dissertation*, University of Canterbury, Christchurch, New Zealand, 395 p.

Yasamura, M., Sugiyama, H. 1984. "Shear properties of plywood-sheathed wall panels with opening," *Transactions of the Architectural Institute of Japan*, 338 (4), pp. 88-98.

Part 12

Development of Vulnerability-Based Retrofit Provisions for Living-Space-Over-Garage Dwellings

12.1 Introduction

This white paper documents the development of the FEMA P-1100, Volume 1 vulnerability-based retrofit provisions for living-space-over-garage dwellings. Included is discussion of the dwelling stock represented, the dwellings used as the basis of numerical models, the numerical procedures, the results of the numerical studies and the selected assessment and design parameters. This white paper is intended primarily for use by engineers who would like to have a better understanding of the basis for the retrofit recommendations, and those interested in details of the numerical modeling. Documented in Section 7 of this white paper are additional resources providing detailed information on the numerical modeling.

12.2 Dwelling Stock Represented

The Volume 1 definition of a living-space-over-garage dwelling is “a dwelling in which a primary occupied living space occurs in an upper story that extends substantially or completely over a ground story constructed primarily as a garage, including utility and storage areas.” The range of dwelling configurations that meet this description were studied early in the project. A photo set was assembled which allowed the development of a matrix of building stock that included the building age, configuration and building materials.

The range of ages of construction considered for this project included homes from the earlier 1900’s thru the 1990s. Dwelling geometries included rectangular (originally described as house-over-garage dwellings) and L-shaped (formerly described as room-over-garage dwellings). The latter residences appeared mostly after the late 1940’s and included single-story or 2-story sections adjacent to the garage. An example of the rectangular living space over garage dwellings is shown in Figure 12-1, and an example of the L-shaped configuration is shown in Figure 12-2.



Figure 12-1 Typical rectangular living-space-over-garage dwelling.



Figure 12-2 Typical L-shaped living-space-over-garage dwelling.

The range of materials of construction included a variety of wall, floor, roof and ceiling finish materials which varied in construction based on the age of the dwelling. A limited combination of the finish materials was numerically modelled to represent a sample of the building stock that would allow for decisions about the seismic design parameters to be made.

12.3 Dwelling Configurations Used in Numerical Modeling

Three basic dwelling plans were chosen to be the basis of the numerical models. This section describes the geometry and materials of these three plans.

House-over-garage without living space at ground floor

The plan for the first floor of the house over garage dwelling that does not have living space (occupied rooms) in the first story is shown in Figure 12-3. Interior walls are minimal, as this configuration was meant to represent a lower-bound of existing seismic bracing in the first story. Front and back elevations representative of the dwelling are shown in Figure 12-4.

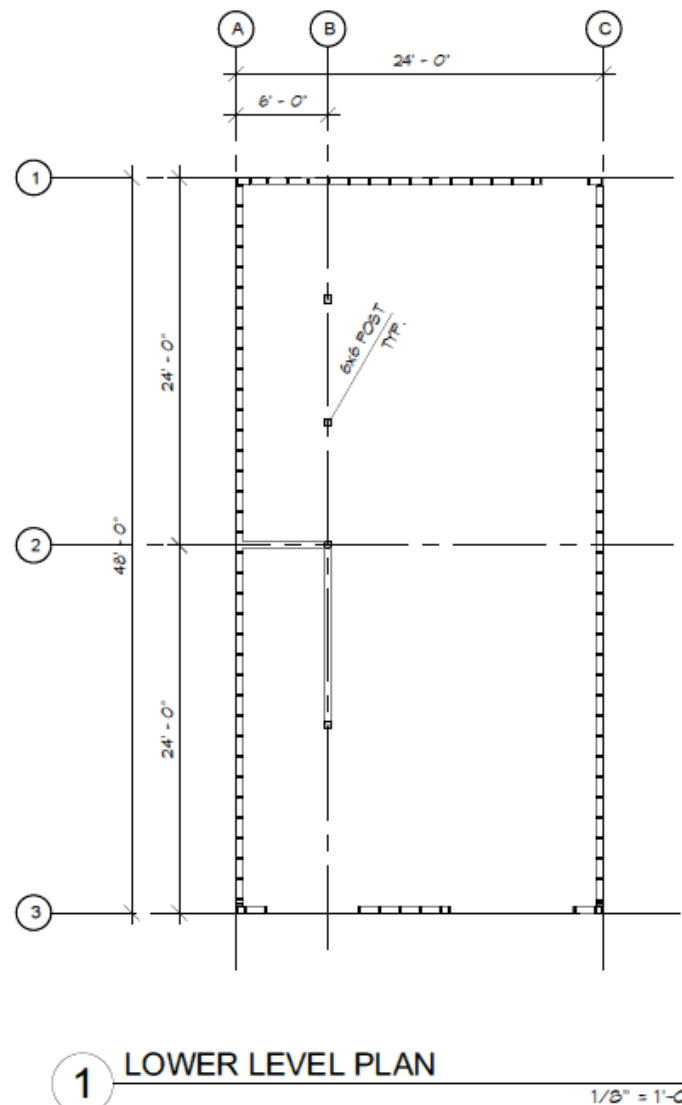
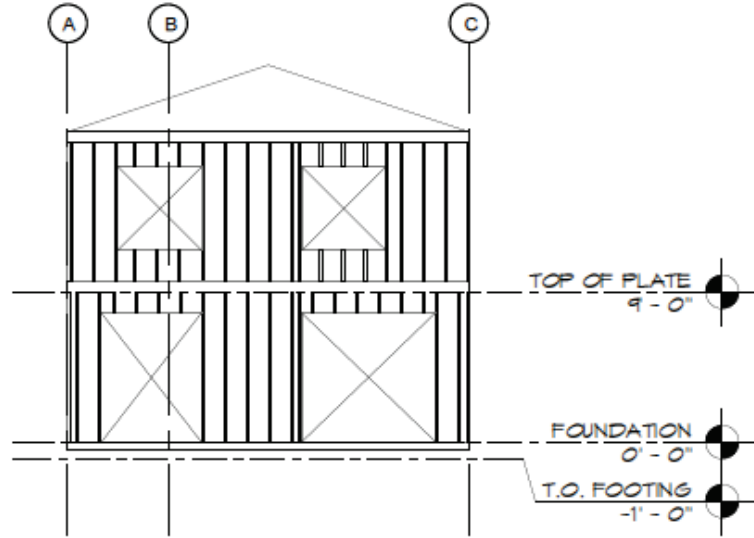
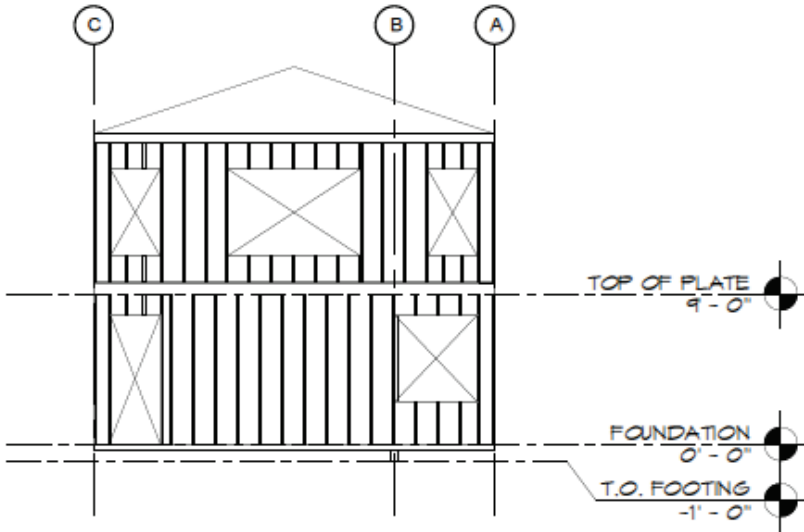


Figure 12-3 First floor plan of house-over-garage without living space at ground floor.



2 FRONT ELEVATION

$1/8'' = 1'-0''$



3 BACK ELEVATION

$1/8'' = 1'-0''$

Figure 12-4 Elevation views of house-over-garage configurations.

The range of ages of construction for these configurations included dwellings from the earlier 1900's thru the 1990s.

House-over-garage with living space at the ground floor

The plan for the first floor of the house over garage with living space dwelling is shown in Figure 12-5. The additional wall in the center of the garage and the presence of gypsum wallboard on the interior of the first story represents the finished living space at the ground floor. The added strength and stiffness

from the nonstructural elements were accounted for in the numerical modeling and when possible, location of retrofit work within finished living space was avoided. The range of ages of construction for these configurations included dwellings from the earlier 1900's thru the 1990s.

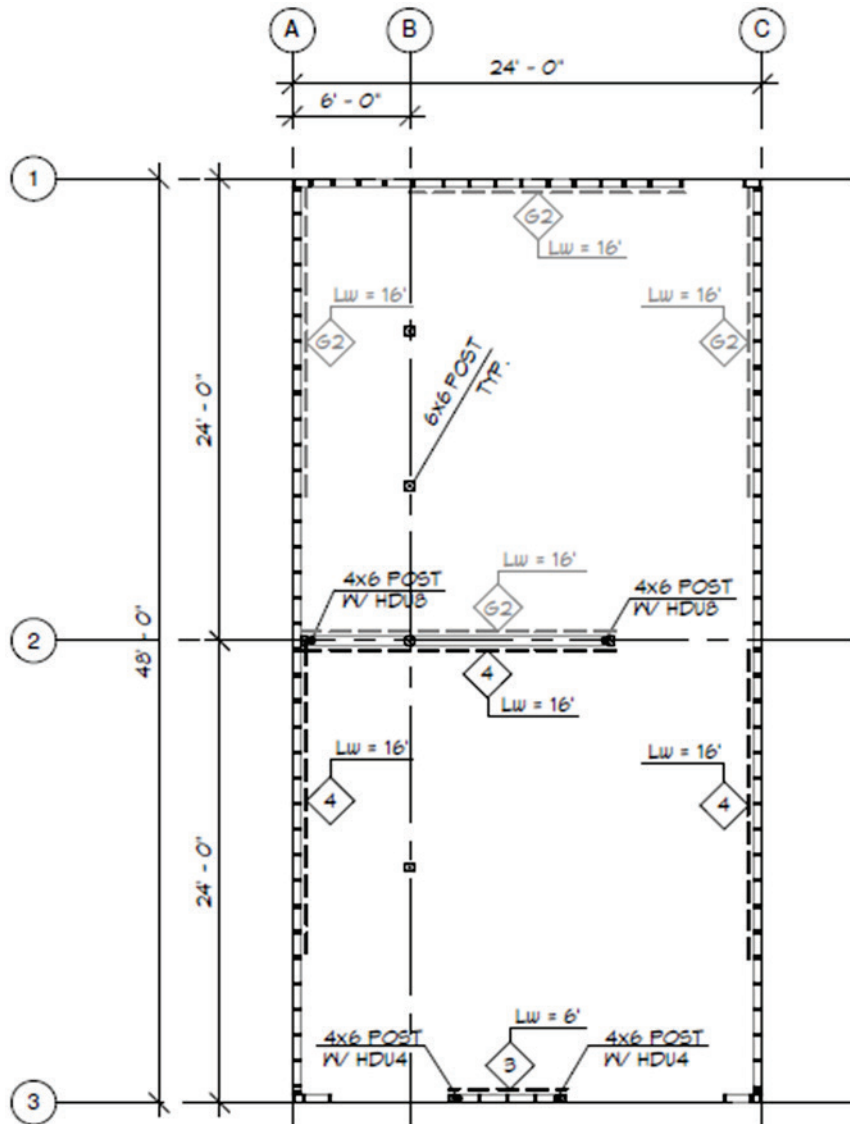


Figure 12-5 First floor plan view of house-over-garage with living space at the ground floor.

Room-over-garage with living space at the ground floor

The plan for this dwelling is shown in Figure 12-6. The non-garage portion of the structure unique to room-over-garage configurations was varied in size to determine its effect on the remaining structure. Ultimately, location of retrofit work in this portion of the structure was avoided. This dwelling is assumed to have been constructed circa 1945; however, similar structures

could be found more recently. Roof, floor, and interior finish materials were designated as light as defined in Table 12-1. Detailed descriptions of the three representative dwelling configuration including amounts of wall line and material definitions used in numerical studies is presented in Section 4.3.

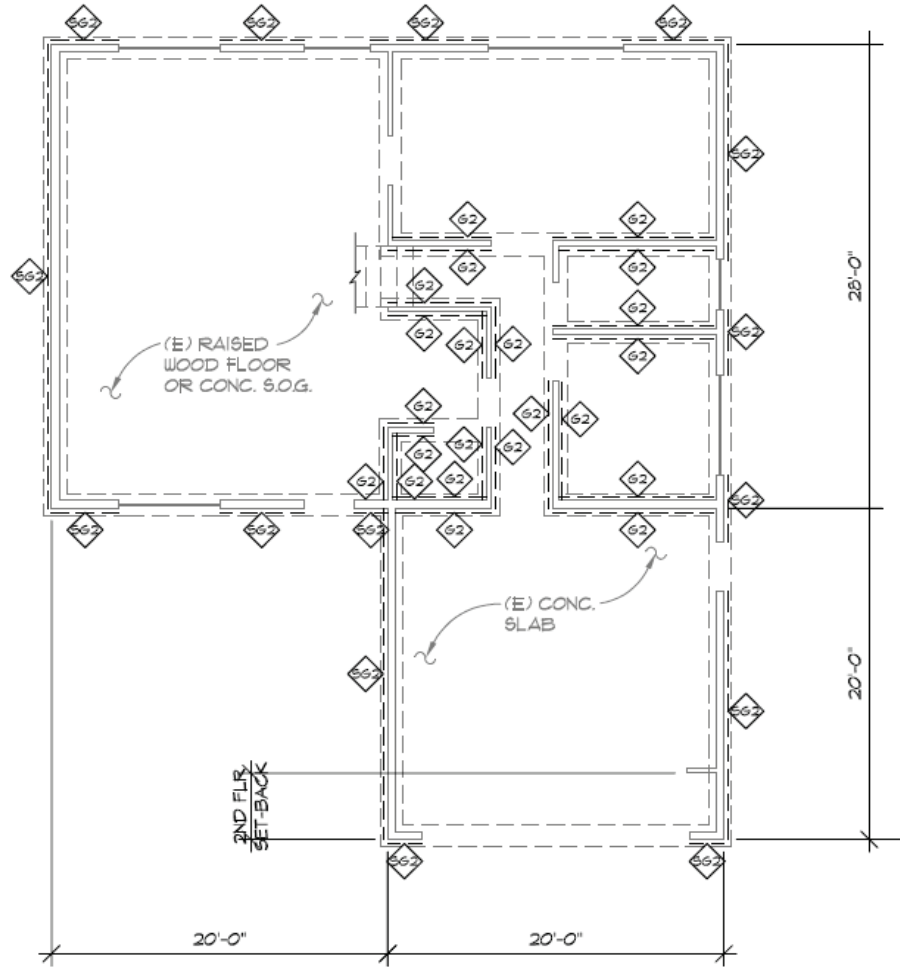


Figure 12-6 First floor plan view of existing room-over-garage configuration.

12.4 Analysis Procedures

The process for numerically studying the vulnerability was unified across each of the three vulnerabilities, cripple wall dwellings studied by Working Group 4, house- and room-over-garage dwellings, studied by Working Group 5, and hillside dwellings, studied by Working Group 6. The unified procedures for selection of software, performance criteria, material characterization, and conducting modal, non-linear static pushover and incremental dynamic analyses are described in detail in *ATC-110 Volume 3 Part 1: Software Recommendations and Applications for FEMA P-1100 Numerical Studies, Part 2: Recommendations for Performance Criteria for Numerical Studies, Part 4: Material Characterization for FEMA P-1100*

Numerical Studies, and Part 5: Protocol for FEMA P-1100 Numerical Studies.

In addition to the processes that were unified for each group, each vulnerability presented its own unique challenges when it came to the task of numerically modelling existing and retrofitted structures. In studying living-space-over-garage configurations, the additional procedures used to gain understanding about this vulnerability including addressing the modeling of the flexible diaphragms, defining the hysteresis behavior of steel W-shape column retrofits, and defining the behavior of proprietary shear wall retrofits. The methodologies behind these numerical procedures and the parameters associated with the implementation of the common numerical strategies, both common and unique to the living-space-over-garage dwellings, are discussed in this section.

12.4.1 Overview

The following are procedures and parameters that were utilized in the numerical analysis performed by this group that will be discussed in the following section. Additional assumptions and procedures used by WG5 are covered in additional ATC-110 Volume 3 documents.

- Project nomenclature for numerical study models
- Assumptions regarding building and seismic weight and un-retrofitted conditions used in numerical procedures
- Hysteresis parameters used to define the behavior of existing building materials
- Procedure for determining median collapse intensities based on the results of non-linear dynamic analyses
- Design of retrofits based on an overturning assumption where 70% of the overturning is resolved by perpendicular wall lines and 30% is resolved by parallel wall lines (more information in *ATC-110 Volume 3 Part 8: Simplified Overturning Assumptions*)

In addition, the following are procedures unique to the numerical studies of living-space-over-garage vulnerabilities:

- Hysteresis parameters developed to capture the behavior of W-shape steel retrofits
- Hysteresis parameters developed to capture the behavior of proprietary shear wall retrofits

12.4.2 Living-space-over-garage Project Nomenclature

The following information outlines the nomenclature used to describe the models that were analyzed using *Timber3D* and the methodologies outlined in *ATC-110 Volume 3 Part 5* and below.

Typical Nomenclature: #‐Ai‐j‐k (5‐HOG3‐L‐4SW)

where:

- # = describes the working group number – in case of the house- and room-over-garage numerical studies, this corresponds to working group 5 (WG5).
- A = describes the configuration of the building, either HOG for house-over-garage or ROG for room-over-garage
- i = describes the configuration number. For HOG, there are 4 configurations with various un-retrofitted first story properties.
- j = describes the weight used in the numerical model. For WG5 this was either light (L) or heavy (H)
- k = describes the retrofit/un-retrofitted condition of the model. This term takes the form of the R-factor used to design the retrofit and the retrofit type on the front (with garage door opening) and back of the building. Retrofit types include wood structural panel (W), steel retrofits (S), and proprietary wall systems (PW). For example, a building model designed with an R-factor of 5 and a proprietary retrofit on the front and a wood structural panel retrofit on the back would have a final term of 5PWW. Furthermore, existing building models were denoted with an E as the final term.

12.4.3 Weight Assumptions and Un-Retrofitted Configurations

12.4.3.1 Weight Assumptions

The designated building weights used in all WG5 modeling are shown in Table 12-2. Both the floor/roof weights and the wall weights remained constant throughout the analysis of all structures.

Assumptions about the seismic weight of the structure included the following:

- The roof was assumed to have an overhang of 18 inches on all sides
- Half of the weight of the first (ground) story walls was assumed to act as seismic mass
- Roof and floor loads were assumed to be uniformly distributed across the diaphragm while wall load acted at the locations of the walls

- Reductions in wall weights were not made for windows and doors
- Floor heights equal to 9 feet

Table 12-1 Weight (psf) Assumptions Used in WG5 Numerical Studies

ROOF Material	Light	Heavy	Floor Material	Light	Heavy
Roofing (Asphalt Shingles- max 2 layers)	4.0	11.0	Floor finish* (assumes carpet and pad)	1.4	3.6
Solar / Other	0.0	0.0	Other	0.0	0.0
Topping	0.0	0.0	Topping	0.0	0.0
1x skip sheathing + new 1/2 sheathing	2.0	2.0	Sheathing / (assume 1" horiz. Lumber)	2.3	2.3
Insulation	0.5	0.5	Insulation	0.5	0.5
M.E.P.	0.5	0.5	M.E.P.	0.5	0.5
Ceiling (1/2") gyp	2.5	8.0	1/2" Gyp. wall board	2.5	8.0
Ceiling Joists (2x6 @24")	1.0	1.0	Joists (2x8 @ 16")	2.1	2.1
Roof Rafters (2x8 @24")	1.3	1.3	Girders (4x12@ 8')	1.2	1.2
Girders (4x8 @ 8')	0.8	1.2	Columns	0.0	0.0
Columns	0.0	0.0	Tile	1.0	2.0
Misc.	0.4	0.4	Misc.	0.5	0.8
Roof Dead Load	13.0	25.9	Floor Dead Load	12.0	21.0

INTERIOR -Light*

INTERIOR - Heavy*

Material	Weight	Material	Weight
1/2" gyp. wall board (2 sides)	0.0	Wood Lath and 1" Gypsum Plaster (2 sides)	16.0
2x4 @ 16"oc	1.0	2x4 @ 16"oc	1.0
Insulation	0.0	Insulation	0.0
MEP	0.5	MEP	0.4
Misc.	0.5	Misc.	0.6
TOTAL	2.0	TOTAL	18.0

* Wall weights

12.4.3.2 Un-retrofitted Conditions (HOG)

To capture the response of a large portion of the HOG building stock, several configurations of existing conditions on the first story were studied. The second story was assumed to be the same throughout each building model. These configurations were labeled HOG1-HOG4 and each had a plan area of 24 feet by 48 feet. An example of the structural configuration with labelled wall layouts is shown in Figure 12-7 and Figure 12-8 which was modelled after the actual structure shown in Figure 12-9. A Timber3D rendering of the existing structure can be seen in Figure 12-10. Each configuration is listed in the following section with a description of the first story wall layout. A detailed description of each configuration can be found in the archived documents listed in Section 7.

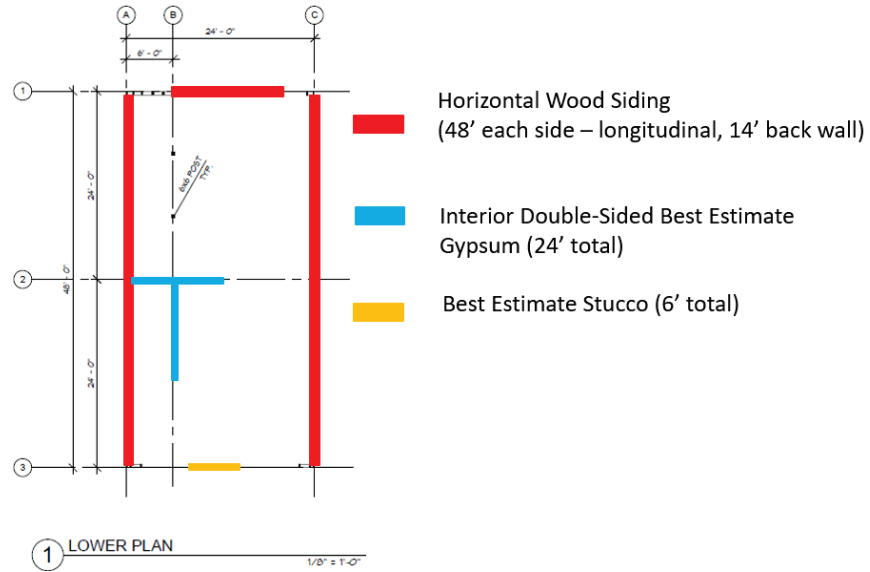


Figure 12-7 Typical existing wall layouts for the first story of HOG configurations.

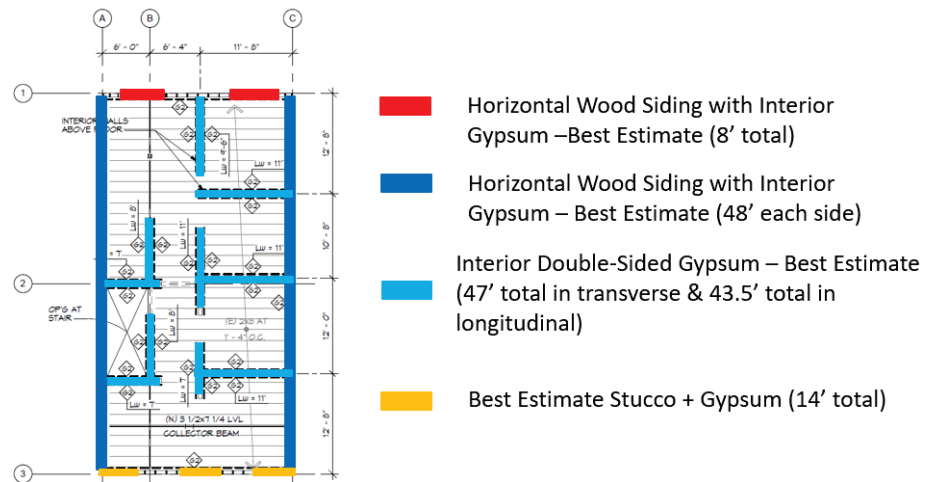


Figure 12-8 Typical existing wall layouts for the first story of HOG configurations.

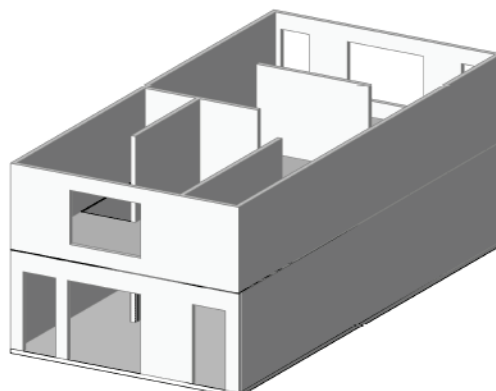


Figure 12-9 Rendering of typical HOG configuration with garage door opening.

The house-over-garage (HOG) configurations for the numerical studies are summarized in Table 12-2.

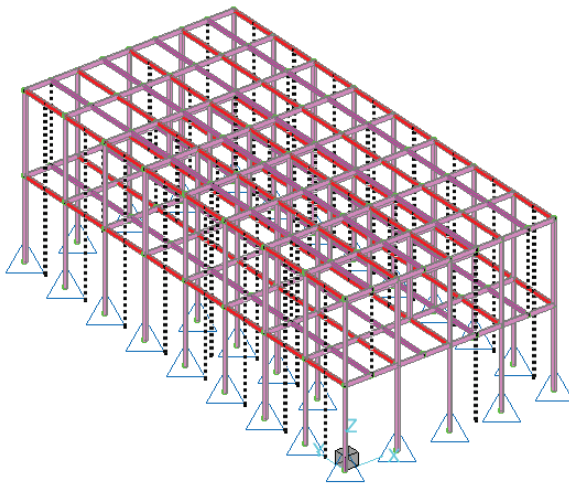


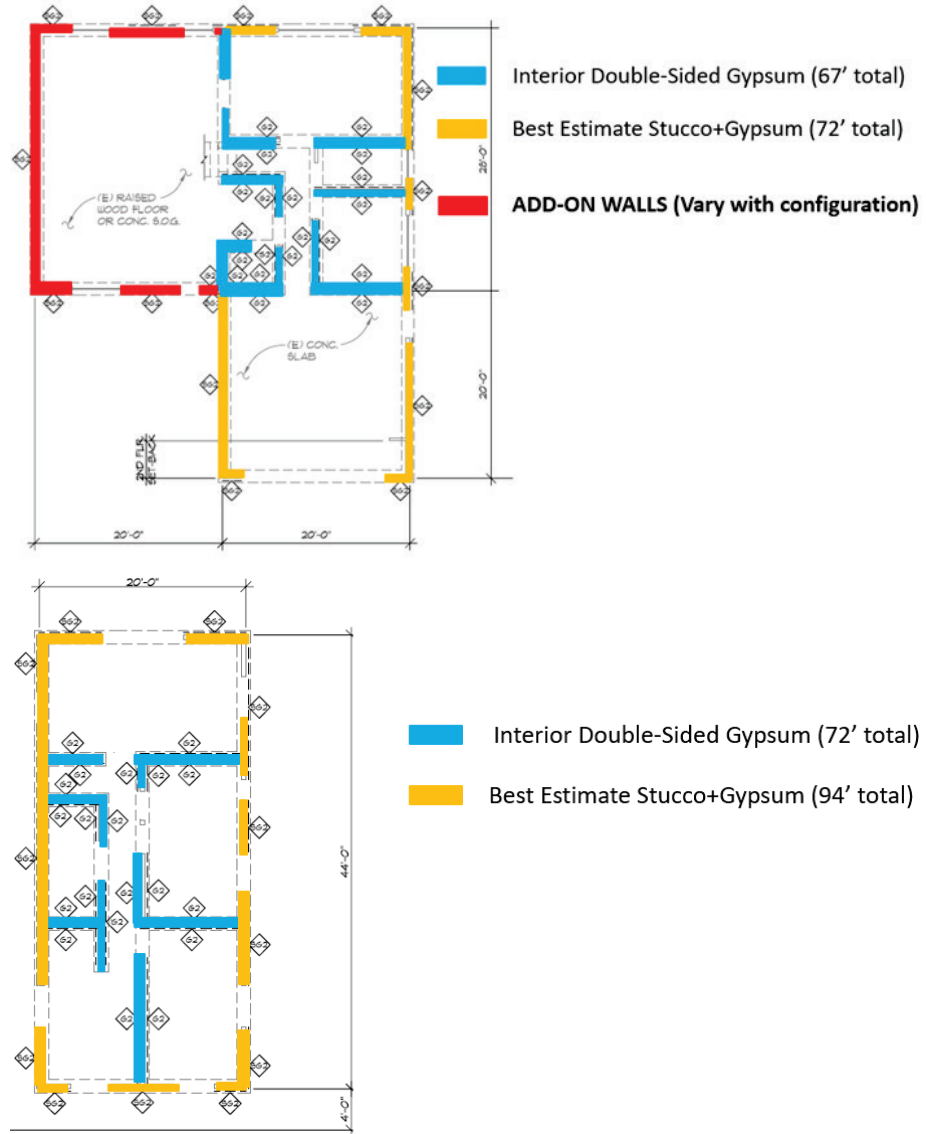
Figure 12-10 Timber3D rendering of HOG existing configuration.

Table 12-2 HOG Configuration Summary

Configuration	HOG1	HOG2	HOG3	HOG4
Exterior Wall Material - Front	Horizontal Siding	Best Estimate Stucco	Best Estimate Stucco	Best Estimate Stucco
Exterior Wall Material - Other Sides	Horizontal Siding	Best Estimate Stucco	Horizontal Siding	Horizontal Siding
Interior Walls	None	None	Stairway only	Livable space in back half of lower story
Building Weights	Light	Light	Light and Heavy	Light

12.4.3.3 Un-retrofitted Conditions (ROG)

The room-over-garage (ROG) numerical studies were performed using a building configuration similar to the HOG configuration. The building plan area was 20 feet by 48 feet with an extra 20 feet by 28 feet of building area attached. The typical configuration of the ROG numerical models is shown in Figure 12-11. To be conservative, none of the lateral strength of the additional area was considered, while all the seismic mass was assumed to contribute to the seismic demand on the main portion of the structure. Additionally, modifications were made to the second story building plan used in HOG analyses.



existing materials: best estimate stucco, horizontal siding, best estimate gypsum, horizontal siding and stucco + best estimate gypsum. Three different configurations of wood structural panel were used by WG5: 1/2 Structural grade I with 8d@2", 7/16 sheathing with 8d@3", and 7/16 sheathing with 8d@4". The hysteresis behaviors of stucco, gypsum, and wood structural panel were characterized using the RESST (RESidual STrength) model developed for the *ATC 116: Solutions to the Issues of Short-Period Building Seismic Performance* project. The RESST hysteretic model is an adaptation of the SAWS model (also known as the CUREE model or Modified STEWart model) which includes a smooth post-peak backbone allowing for a residual strength portion of response to be defined at large displacements; similar to the post-peak behavior used in the EPHM (Evolutionary Parameter Hysteretic Model) model (Pang et al. 2007). An illustration of the RESST hysteretic model is shown in Figure 12-12.

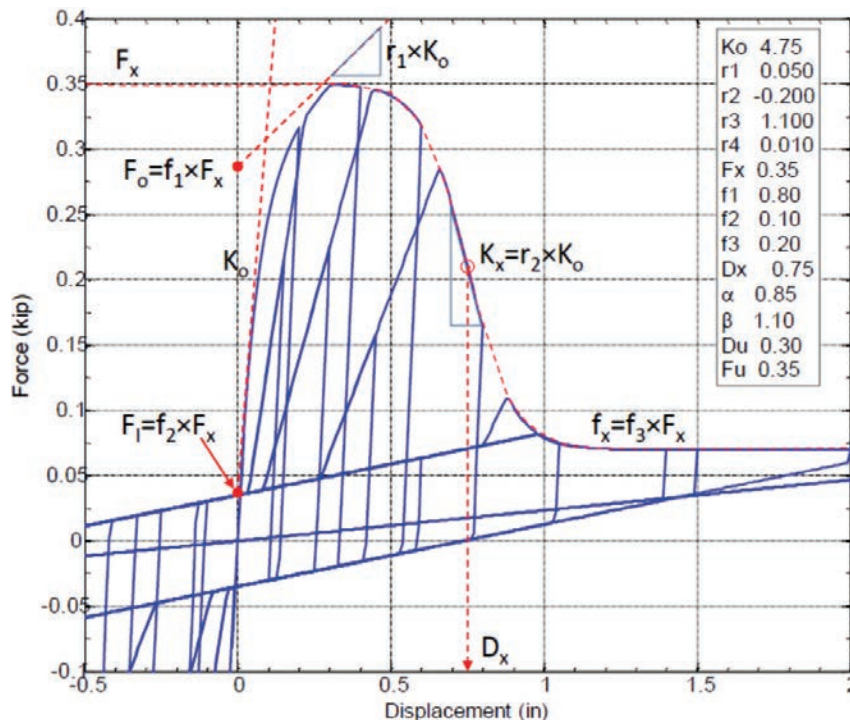


Figure 12-12 Illustration of the residual strength (RESST) hysteretic model used in *Timber3D* for modeling the behavior of wall materials.

The hysteretic behavior of the RESST model is defined by 12 parameters. The backbone is defined by the initial stiffness (K_0), peak force (F_x), post-peak displacement (D_x) and a series of normalized force and stiffness factors (f_{1-3} , r_{1-4}) that define the backbone in terms of either K_0 or F_x as shown in Figure 12-12. Notably, D_x defines the inflection point of the exponential "S-Curve" that transitions from peak load to the desired residual strength. Cyclic behavior is defined by a constant intercept force ($f_2 \times F_x$) and stiffness ($r_4 \times K_0$)

to model pinching behavior and two parameters to control stiffness degradation upon reloading from the pinched intercept to the backbone curve. The factor β defines the next reloading displacement on the backbone curve as a multiplier of the previous maximum displacement (e.g., $\Delta_{i+1} = \Delta_{i\beta}$). The factor α is an exponent controlling the reloading stiffness (K_p) as a function of initial stiffness (e.g., $K_p = K_0(\Delta_y/\Delta_{i+1})^\alpha$). The theoretical yield displacement (Δ_y) is defined by the initial stiffness divided by the force F_0 shown in Figure 12-12.

The only additional existing material considered, but not modeled with the RESST hysteresis is horizontal wood siding. The hysteretic behavior of wood siding assumes the SAWS or Modified STEWart (MSTEW in *Timber3D*) model. The SAWS model exhibits the same pre-peak backbone and cyclic behavior as the RESST model, yet without the smooth post-peak backbone curve to a residual strength region of displacement. This was assumed since horizontal wood siding can be characterized by relatively low stiffness and strength, yet with very little strength degradation at very large displacements. The SAWS parameters to represent horizontal wood siding are provided in Table 12-3. An illustration of the SAWS hysteresis is provided in Figure 12-13.

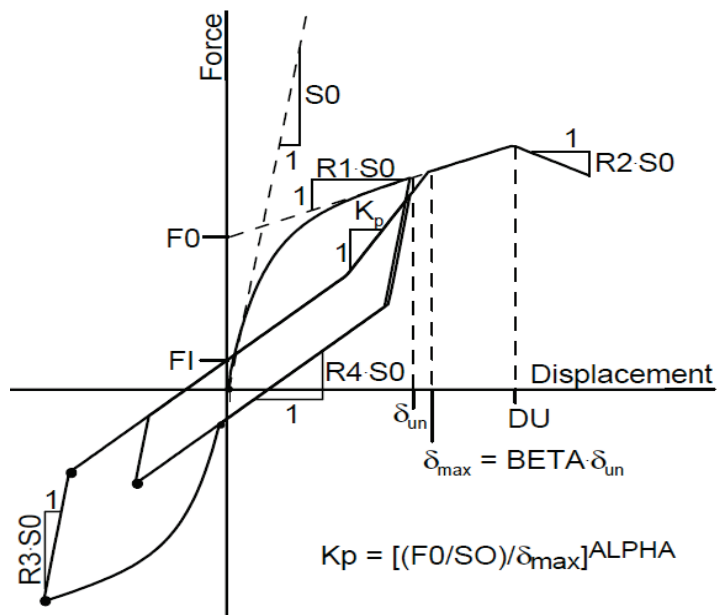


Figure 12-13 Illustration of the modified STEWart (MSTEW) hysteretic model used in *Timber3D* for modeling the behavior of wall materials.

The wall parameters presented in Tables 12-3, 12-4, and 12-5 are normalized for the length and height of the wall. The appropriate parameters (S_0 , F_0 , D_U , and F_I for SAWS and K_0 , F_x , and D_x for RESST) were scaled to create parameters that represented 9-foot-tall walls with lengths per the numerical

model. To give an indication of these material's behavior, a set of hysteresis loops has been plotted in Figure 12-14 for the existing building materials of stucco and stucco+gypsum, Figure 12-15 for the existing building materials of gypsum and horizontal siding, and Figure 12-16 for the wood structural panel materials.

Table 12-3 SAWS (or MSTEW) Parameters Used to Represent Horizontal Siding

SAWS Parameter ¹	Best Estimate Horizontal Wood Siding
S0 [kip/%θ-ft]	169.5
F0 [lb/ft]	75.0
R1	0.17
R2	-0.037
DU [%θ]	4.0
Fl [lb/ft]	2.5
R3	1.45
R4	0.005
α	0.38
β	1.09

¹ Refer to Figure 12-13 for illustration

Table 12-4 RESST Parameters for Best Estimate Stucco, Best Estimate Gypsum, and Best Estimate Stucco+Gypsum

RESST Parameter ¹	Best Estimate Stucco (S2)	Best Estimate Gypsum (G2)	Best Estimate Stucco + Gypsum (SG2)
K0 [lb/%θ-ft]	3750.0	780.0	4530.0
r1	0.094	0.103	0.080
r2	-0.031	-0.074	-0.034
r3	1.0	1.0	1.0
r4	0.025	0.040	0.025
Fx [lb/ft]	785.3	225.9	901.6
f1	0.446	0.531	0.488
f2	0.128	0.068	0.141
f3	0.1	0.1	0.1
Dx [%θ]	3.85	2.62	3.44
α	0.70	0.60	0.70
β	1.30	1.20	1.30

¹ Refer to Figure 12-12 for illustration

Table 12-5 RESST Parameters Used to Represent Wood Structural Panels

RESST Parameter ¹	Wood Structural Upper Bound (WSP1)	Wood Structural Panel Best Estimate (WSP2)	Wood Structural Lower Bound (WSP3)
K0 [lb/%θ-ft]	6130	4107	2935
r1	0.052	0.052	0.052
r2	-0.144	-0.144	-0.144
r3	1.0	1.0	1.0
r4	0.012	0.012	0.012
Fx [lb/ft]	2309.8	1547.3	1106.7
f1	0.595	0.595	0.595
f2	0.110	0.110	0.110
f3	0.1	0.1	0.1
Dx [%θ]	3.21	3.21	3.21
α	0.55	0.55	0.55
β	1.05	1.05	1.05

¹ Refer to Figure 12-12 for illustration

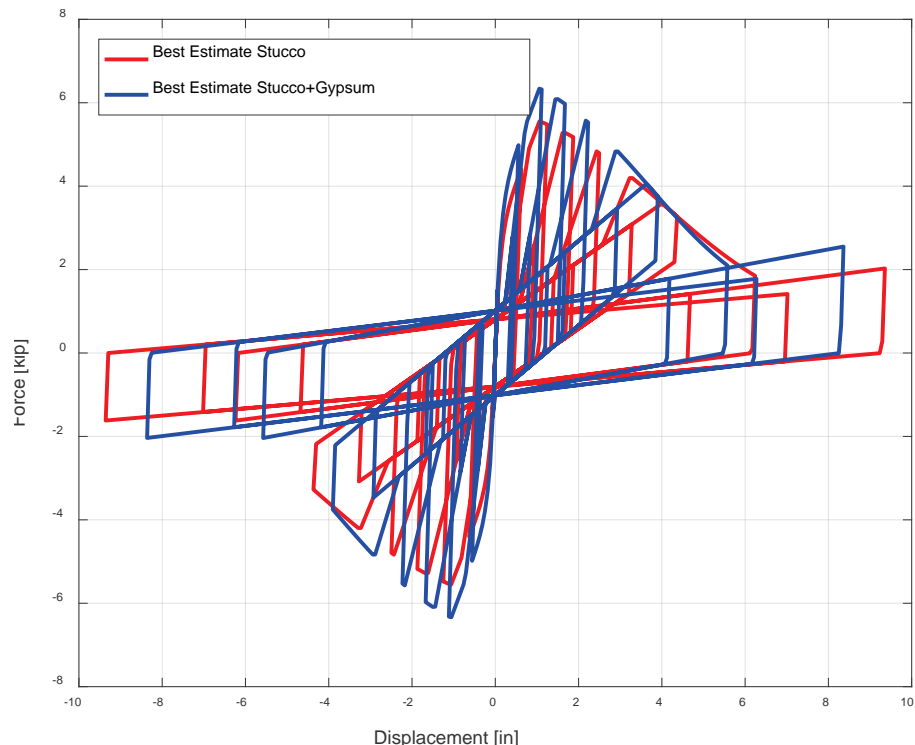


Figure 12-14 Hysteretic parameters for stucco and stucco+gypsum.

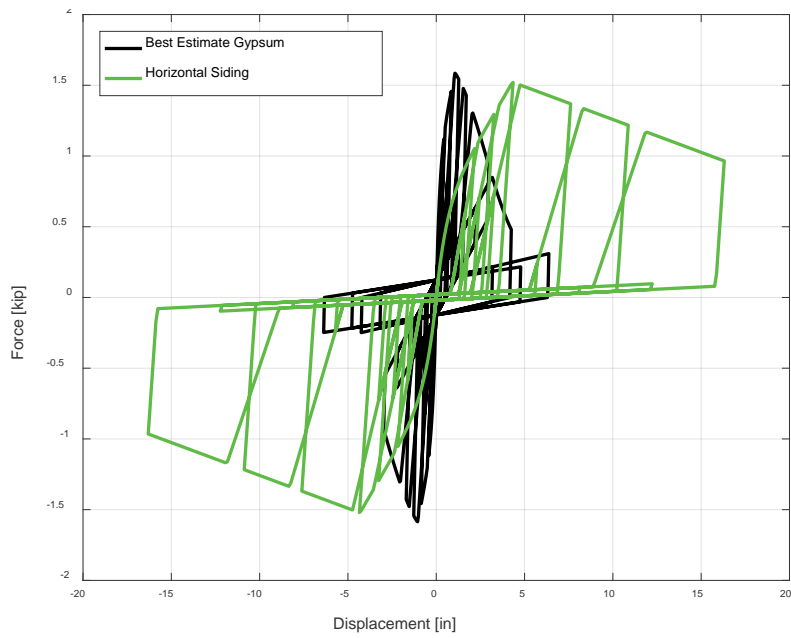


Figure 12-15 Hysteretic parameters for gypsum and horizontal siding.

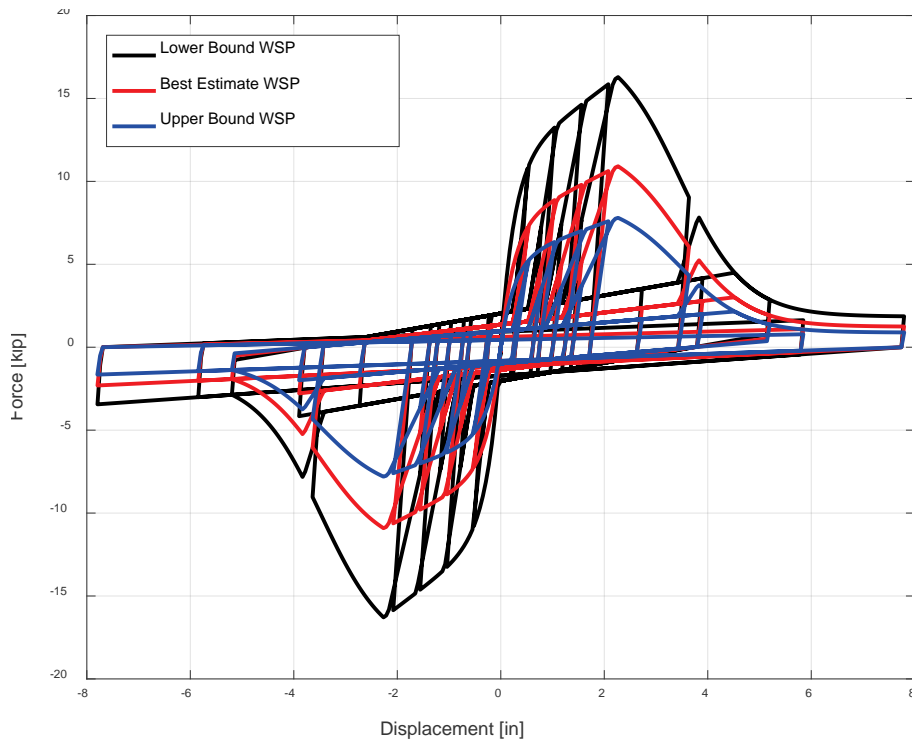


Figure 12-16 Hysteretic parameters for wood structural panels (WSP1, WSP2, and WSP3).

12.4.5 General Modeling Approach for Living-Space Over Garage dwellings

As recommended in *ATC-110 Volume 3 Part 1 - Software Recommendations and Applications*, all modeling was performed using *Timber3D* [Pang et al., 2012]. Using this program, “building blocks” were used to represent standard lengths of wall line on interior and exterior walls. Frame elements were used to model the studs and were pin-connected to the ground and the diaphragm elements. Connections between frame elements were made using Frame-to-Frame (F2F) elements. Floor and roof elements were modeled to imitate a flexible diaphragm using diaphragm boundary elements and fixed frame elements whose cross-sectional properties were modified to control the in-plane stiffness of the diaphragm. The in-plane stiffness of the diaphragm was calibrated to 8 kip/in/ft per the recommendations of *ATC-110 Volume 3 Part 4: Material Characterization for Numerical Modeling*. An example of the HOG dwelling and the equivalent modeling components is shown in Figure 12-17.

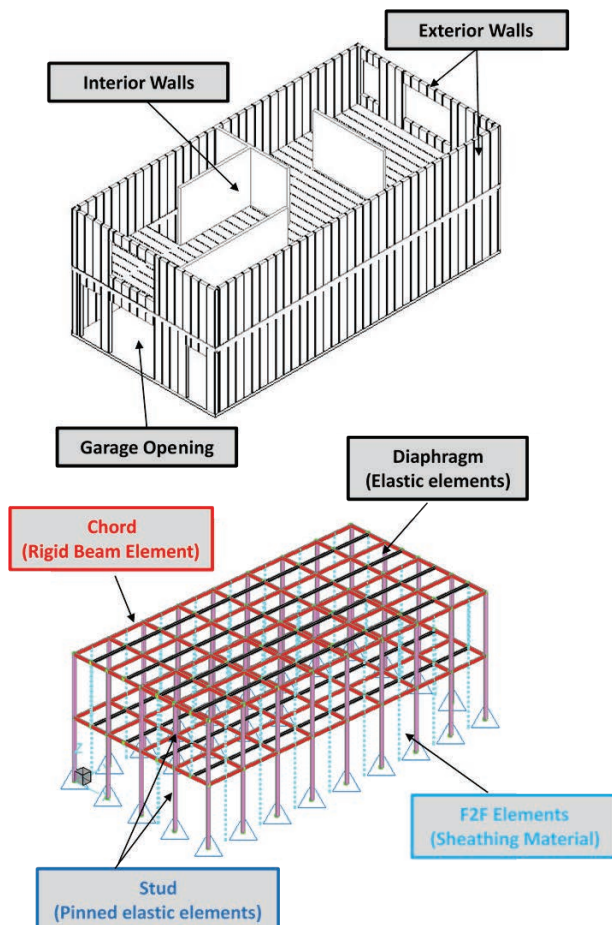


Figure 12-17 Illustration of modeling components of HOG dwelling including a rendering of actual dwelling and *Timber3D* components.

For all HOG configurations modeled, the six-foot grid of “building block” elements was used to most closely align the interior walls with the location of the interior walls in the representative dwelling. Similarly, a four-foot grid was used for the modeling of the ROG configuration as it aligned all interior walls with those in the representative dwelling.

The treatment of wall openings in exterior wall lines assumes that only full height wall sections (i.e., full wall piers) contribute to the effective length ($L_{w,eff}$) of a given building block section as proposed by Patton-Mallory *et al.* (1985). Despite numerous relationships existing in the literature for treatment of openings of plywood shear walls (e.g., Yasamura and Sugiyama 1984; Johnson 1997; FEMA 2012) the full wall pier height effective length assumption was the most convenient to keep consistent when considering numerous material types and configurations for archetype development. Notably, the relationship proposed in FEMA P-807 Equation 4-3 (FEMA 2012) was found to give similar results as that using the simpler full wall pier height assumption.

12.4.6 Determination of Median Collapse Intensity

The use of the FEMA P695 methodologies to determine the probabilities of collapse at different ground-motion intensities is contingent on being able to determine the median collapse intensity. In an effort to reduce the computational demands of the project, seven select intensities were run using the procedure outlined in FEMA P695. Each intensity included the 22 far-field ground motions specified by P695, scaled using a fundamental period of 0.25 seconds. Each 3D ground motion was run in the two orthogonal directions creating 44 unique analyses models for each of the seven intensities. Rather than using the information from an incremental dynamic analysis (IDA) where uniformly increasing intensities are run until all building models have collapsed, a maximum likelihood lognormal fitting algorithm was used in conjunction with the information from the seven intensity stripes to calculate the median collapse intensity. Appropriate correction factors were then applied to the calculated median collapse intensity included the 3D correction factor (1.2 for all models), the spectral shape factor (1.00 for un-retrofitted structures, 1.33 for all retrofitted structures), and the pre-defined dispersion factor (0.75 for un-retrofitted structures, 0.6 for retrofitted structures). The intensities used for WG5 analysis of building models were 0.6g, 1.0g, 1.2g, 1.5g, 1.8g, 2.0g, and 2.5g. These intensities were shown to provide information about the desired performance criteria and give information both below and above the median collapse intensity for retrofitted models. Previous studies have shown that using a maximum likelihood fitting method, the median collapse intensity

can be calculated with limited intensity stripes (Baker 2015). This method is illustrated in Figure 12-18. Using the median collapse intensity, the predetermined adjustment factors, and the predetermined dispersion factors, the P695 adjusted collapse fragility curve was produced for each model, giving a probability of collapse for any intensity.

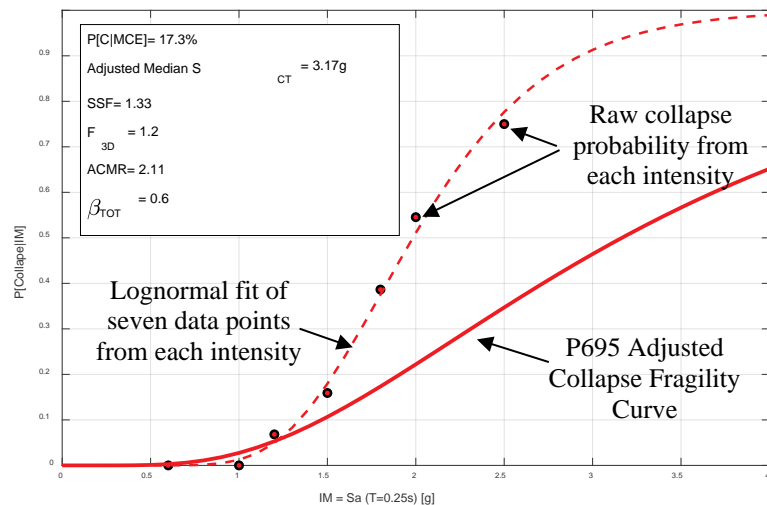


Figure 12-18 Conversion of raw collapse information to full FEMA P-695 collapse fragility curve.

12.4.7 Hysteresis Behavior of Steel Wide-Flanged Retrofits

In cases where there is not enough existing wall in the first story of a house-and room-over-garage to implement traditional wood structural panel retrofits, it was important to provide a retrofit solution that provided the shear resistance necessary to improve collapse performance. The hysteretic behavior of wide-flanged steel retrofits, sometimes referred to as cantilever column retrofits, was based on guidance from ASCE 41-13, *Seismic Evaluation and Retrofit of Existing Structures*. Because the intent of these retrofits was to connect the steel members to the existing structure in such a way that there is no transfer of gravity load to the retrofitted member, the retrofitted member was treated as a beam member. The parameters dictating the monotonic force-displacement behavior of these steel members were taken from ASCE 41-13, shown in Table 12-5. For those beams that meet the compact section requirements, points along the backbone curve were given in terms of the yield rotation angle, θ_y , and are shown in Table 12-6 and Figure 12-19. While ASCE 41-13 recommends using an increased value for the yield stress of A992 of 1.1 times the nominal yield stress of 50 ksi, all steel retrofits were modeled with a yield stress equal to 50 ksi. For the implementation of these backbone parameters into *Timber3D*, a trilinear hysteresis model was implemented, ignoring the residual strength capacity

recommended by ASCE 41-13 (DE segment of backbone curve shown in Figure 12-19).

Table 12-6 Steel Modeling Parameters from ASCE 41-13

Component or Action	Modeling Parameters		
	Plastic Rotation Angle, Radians	a	b
		c	Residual Strength Ratio
Beams—Flexure			
a. $\frac{b_f}{2t_f} \leq \frac{52}{\sqrt{F_{ye}}}$ and $\frac{h}{t_w} \leq \frac{418}{\sqrt{F_{ye}}}$	$9\theta_y$	110 θ_y	0.6

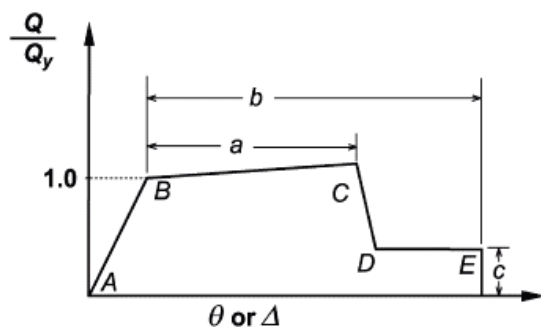


Figure 12-19 Steel backbone behavior from ASCE 41-13.

Finally, an effort was made to capture the flexibility of the connection to the concrete foundation as well as the rotational deformation of the foundation due to the moment applied at the bottom of the steel retrofit element.

Explicit modeling of the foundation with lower bound estimates for cracked concrete behavior, soil stiffness properties, and a variation of boundary conditions showed an influence of the foundation on the top of steel retrofit deflection of between 5% and 10%. In order to account for the flexibility of the foundation and the slip in the connection between the top of the steel retrofit and the existing diaphragm a reduction of 15% was taken on the stiffness of the steel column retrofits computed assuming a pinned-fix boundary condition, where the bottom of the member is fixed and the top is pin-connected. Figure 12-20 shows the comparison of a W12x35 retrofit with and without the reduction in stiffness due to the foundation flexibility.

The cyclic behavior of the steel retrofits was considered to have no strength deterioration. Other methods of modeling the non-linear cyclic behavior of steel members do include a version of cyclic strength deterioration (Lignos and Krawinkler, 2011 and Ibarra et al. 2005). Instead of implementing such deterioration models, the peak and residual deformation were monitored for each model containing a steel retrofit. Because a majority of the peak and

residual drift values occurred either on the ascending portion of the backbone (models had not yet reached yield force) or the descending portion of the backbone (models had collapsed), it was determined that the lack of strength deterioration did not significantly affect the collapse probabilities of the retrofitted models. An example of the full hysteresis behavior of a W12×35 steel retrofit is shown in Figure 12-21.

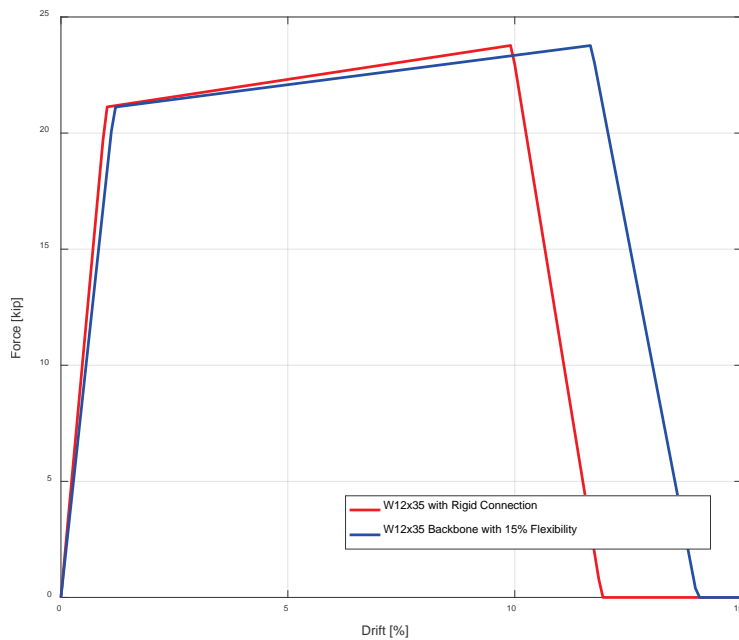


Figure 12-20 Backbone behavior of steel retrofits with and without stiffness decrease.

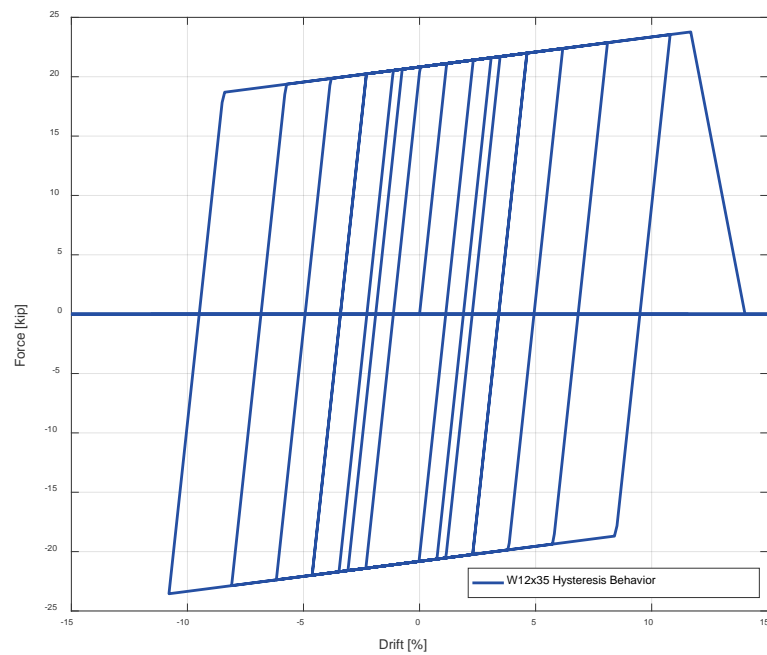


Figure 12-21 Hysteresis behavior of W12×35 steel retrofit.

12.4.8 Hysteresis Behavior of Proprietary Wall Retrofits

Similar to the steel retrofits, proprietary shear resisting elements have been used to retrofit soft-story structures where there is not enough room (full-height wall length) for traditional wood frame shear walls. Because these elements are proprietary in nature, their force-displacement response is not publicly available. Instead, the systems are often defined only by the ASD design load and the displacement at the design load. In order to build the entire backbone curve for implementation in *Timber3D*, a baseline performance standard for all proprietary retrofits needed to be considered. Currently performance benchmarks for proprietary walls are defined by the International Code Council AC 436 – *Acceptance Criteria for Establishing Seismic Equivalency to Code-Prescribed Light-Frame Shear Walls*. For proprietary manufacturers to have their products used with the same seismic design parameters as traditional light-frame wood structural panel walls, they must comply with ICC AC436, ICC AC130, or ICC AC322, depending on the type of proprietary retrofit. These acceptance criteria all reference three points denoting the minimum value of the peak force to ASD force ratio (P_{peak}/P_{ASD}), the minimum displacement for the 80% post peak force (Δ_U), and the minimum ratio of the displacement for the 80% post peak force and the drift at ASD design load (Δ_U/Δ_{ASD}). Each of these points shown in Figure 12-22.

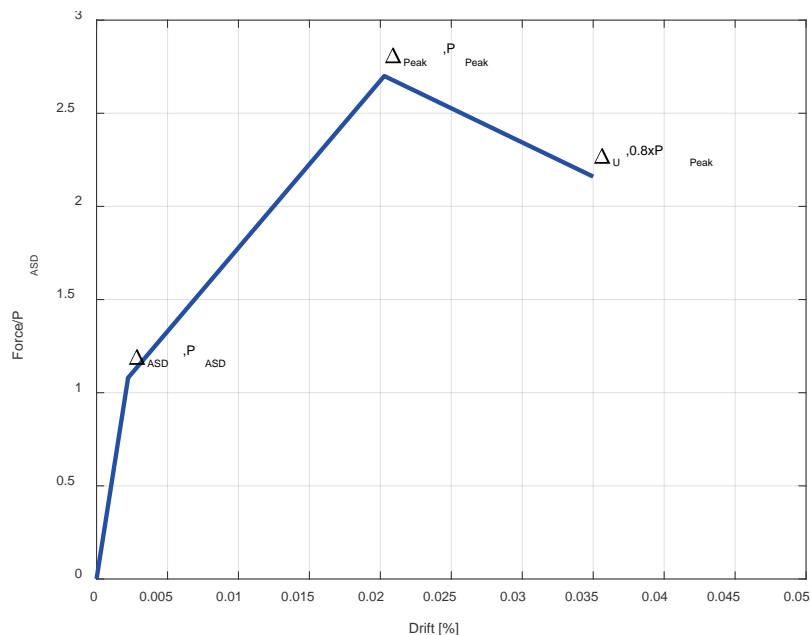


Figure 12-22 Points used for backbone of proprietary wall systems based on ICC acceptance criteria.

Using these points, additional hysteresis parameters defining the rest of the backbone and associated cyclic parameters were defined to match closely to the parameters already used to define wood structural shear panels. The behavior of the generic proprietary retrofit normalized to the ASD design load is compared to the wood structural panel retrofit behavior in Figure 12-23. The comparison of the proprietary system to the wood structural panel parameters that have been used by all WGs shows that both the initial stiffness and the peak strength of the proprietary retrofit are less than that of the wood structural panel. The backbone parameters were meant to represent the minimum level of performance needed for seismic equivalency and it was expected that the true performance of proprietary walls would exceed these minimum requirements. Using this procedure, any proprietary wall system that qualifies as seismically equivalent to wood structural panel wall systems according to the appropriate ICC Acceptance Criteria (436, 130, and 322) could be modeled in *Timber3D* with the ASD design load.

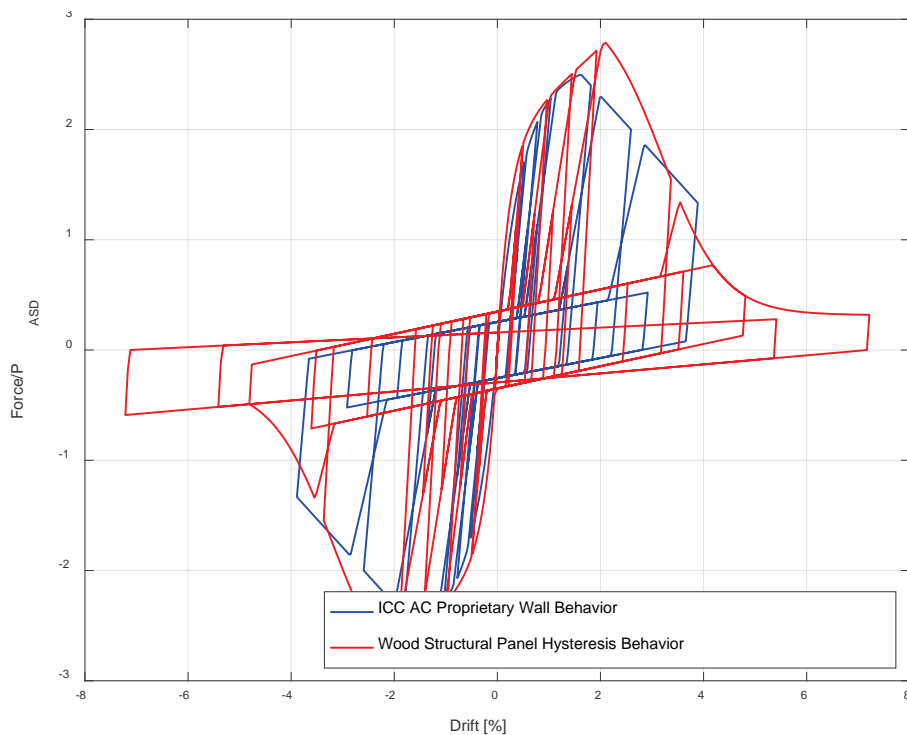


Figure 12-23 Hysteresis behavior of ICC AC proprietary and wood structural panel walls.

12.4.9 Description of Models Run by WG5

As a starting point, WG5 ran models with retrofits with R-factors equal to 2, 3, and 4 for the HOG3-L configuration. Based on the results of these models, additional models were run with R-factors of 5 and 6.5. Ultimately, each configuration had models run with R-factors of 4 and 6.5 for each

available retrofit type. All model configurations had models with steel retrofits and proprietary wall retrofits; however, for HOG3-H and ROG configurations, wood shear wall retrofits were not possible due to limited wall availability. Additional models with R-factors of 5 were run where more information was needed to make decisions about the design parameters. A complete list of models that were used to make decisions about design parameters is shown in Table 12-7.

Table 12-7 Analysis Models Run

Configuration	Retrofit Type	R-Factor
HOG3-L	Steel	2
	Steel	3
	Steel	4
	Steel	6.5
	Wood	4
	Wood	6.5
	Proprietary	3
	Proprietary	4
	Proprietary	6.5
HOG1-L	Steel	4
	Steel	6.5
	Wood	4
	Wood	6.5
	Proprietary	4
	Proprietary	6.5
HOG3-H	Steel	4
	Steel	5
	Steel	6.5
	Proprietary	4
	Proprietary	5
	Proprietary	6.5
HOG4-L	Steel	4
	Steel	6.5
	Wood	4
	Wood	6.5
	Proprietary	4
	Proprietary	6.5
ROG1-L	Steel	4
	Steel	5
	Steel	6.5
	Proprietary	4
	Proprietary	6.5

12.5 Analysis Results

This section provides an overview of a sample of the results from the numerical studies, and presents Figures 12-24, 12-25, and 12-26 illustrating numerical results that were used by the project team to inform the decision of retrofit seismic design parameters. The reader is reminded that, as described in Volume 1, the analytical studies were used primarily as a tool to judge improvement in performance, rather than an absolute indication of performance.

12.5.1 Sample Analysis Results from Model 5-HOG3-M-E

ATC-110 Volume 3 Part 5 - Protocol for FEMA P-1100 Numerical Studies describes the protocol for seismic analysis of light-frame wood residential buildings. The procedures outlined include modal analyses, non-linear static pushover analyses, and non-linear incremental dynamic analyses (IDAs) according to the FEMA P695 methodology. An example of the modal analysis results for the 5-HOG3-H-5SW model is shown in Figure 12-24 and Table 12-8. This model uses heavy model weights and uses a response modification factor of 5 to design a steel column retrofit (W10x26) with 20' of WSP3 on each side walls and 14' of WSP2 on the back wall.

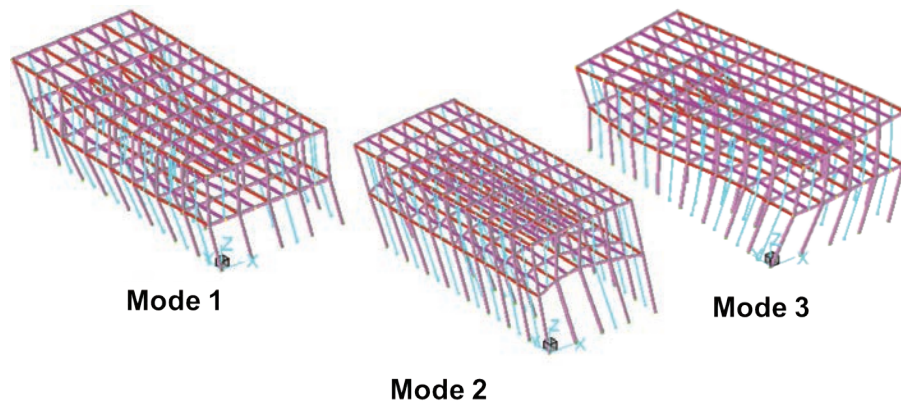


Figure 12-24 Plotted mode shapes for 5-HOG3-H-5SW configuration.

Table 12-8 Period of First Three Mode Shapes for 5-HOG3-H-5SW

Model	Period [s]	Description
Mode 1	0.416	Translation X (short direction)
Mode 2	0.341	Translation Y (long direction)
Mode 3	0.279	Torsion Z

The non-linear static pushover analyses were performed in each direction and the FEMA P795 characteristic parameters were extracted. The pushover

curves and associated with the 5-HOG3-H-5SW model are shown in Figure 12-25 and the associated FEMA P795 parameters are shown in Table 12-9.

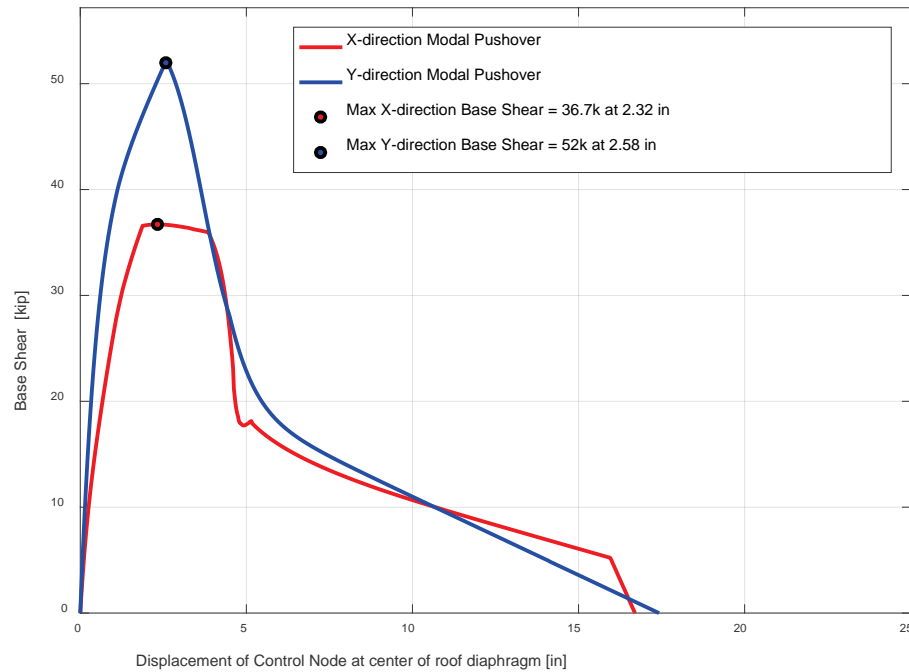


Figure 12-25 Non-linear static pushover analysis for 5-HOG3-H-5SW.

Table 12-9 FEMA P-795 Parameters of 5-HOG3-H-5SW

Direction	X	Y
K_{40} [kip/in] ¹	34.36	60.32
$\Delta_{u,80}$ [%] ²	2.0%	2.0%
$\Delta_{u,max}$ [%] ³	7.7%	8.1%

¹ Secant stiffness to 40% of peak strength

² Roof drift at 80% post-peak strength

³ Roof drift at onset of residual strength region or zero force

Non-linear time history analyses were performed at various intensity measures as described in Section 4.6. An example of the lateral displacement time history of the retrofitted 5-HOG3-H-5SW model and associated un-retrofitted model are compared in Figure 12-26. The un-retrofitted model experiences collapsed approximately 10 seconds into the ground motion record, where the retrofitted configuration survived the entire ground motion record. Collapse was detected through the vertical drop of a control node located in the center of the roof diaphragm equal to 12 inches.

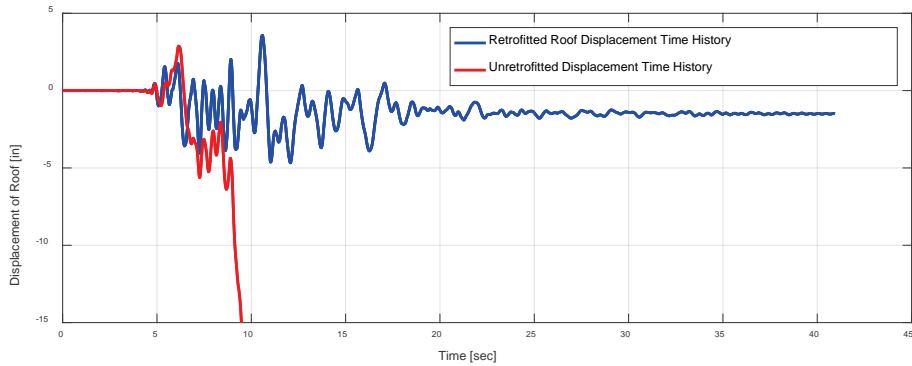


Figure 12-26 Lateral displacement time history of control roof node for retrofitted and un-retrofitted configuration of HOG3.

The non-linear time history analyses performed on HOG and ROG configurations were the primary tools used to measure performance in reference to the primary and secondary criteria outlined by FEMA P-1100 Volume 1 C.1.2. These performance measures include the probability of collapse at MCE_R as the primary performance criteria and drift limits of 0.75% at 0.4 MCE_R and 1.5% at DE as secondary performance criteria. For each of these criteria, the probability of exceedance was plotted in a bar chart for comparison with the existing conditions as well as other retrofit types. A figure is given for each of the configurations modelled by WG5, indicating the performance of both the various types of retrofits (steel column, wood structural panel, and proprietary wall retrofit) and a change in the R-factor used to design the retrofit. The purpose of testing the various configurations was to verify that retrofits that satisfied performance criteria did so for each configuration, meant to represent more of the building stock.

These figures were meant to compare the relative performance of retrofitted models with the existing building configuration and make decisions about the influence of the R-factor used in design. For all configurations, implementing retrofits reduced the probability of collapse at MCE_R by between 60% and 90%. In general, retrofits with a lower R-factor produced lower probabilities of collapse; however, they produced greater probabilities of exceeding secondary drift criteria in the upper floor, which could cause significant damages in the upper living space. In addition, the constructability of retrofits with a lower R-factor became a concern. Ultimately, retrofits with R-factors of between 4 and 6.5 produced models that significantly reduced the probability of collapse at MCE_R and limited the damage in the second story. The configuration in which heavy building materials and weight assumptions were used (HOG3-H) produced the highest probabilities of collapse; however, retrofits with R-factors of 4 and 5 still

produced acceptable levels of MCE_R collapse probabilities (13%-20%) in accordance to FEMA P695 (FEMA 2009).

When comparing the three retrofit strategies, there was not a significant difference in the probability of collapse at MCE_R. The steel retrofit did produce relatively higher drifts at the first floor due to its lower stiffness when compared to similarly designed wood or proprietary wall retrofits. In the cases of HOG3-H and ROG, wood shear wall retrofits were not considered as the design and construction of such retrofits was not feasible due to the constraints of the building configuration and available wall lengths for retrofit.

12.6 Selected Retrofit Design Parameters and Methods

The selection of design parameters included consideration of both the analysis results and the constructability of the proposed retrofits. Based on the primary and secondary performance criteria, an R-factor of 5.0 was selected for the design of both prescriptive and engineered retrofits of living-space-over-garage configurations. This selection was based on the trade-offs of a retrofit using an R-factor of 4.0 and one using an R-factor of 6.5 including increased probability of collapse, decreased damage in the occupied second story, and constructability. The selection of an R-factor of 5.0 was also determined to be independent of the retrofit type as all retrofit types performed similarly and experienced the same trends as the value of R changed. Based on the analysis results, a retrofit with an R-factor of 5 could be expected to reduce the probability of collapse at MCE_R by between 70% and 80%. Additionally, the probability of exceeding the secondary performance criteria in the first story would reduce from nearly 100% to on average 60%-70% depending on the retrofit selected. The probability of exceeding drift criteria in the second story would only increase to on average 2%-6% depending on the retrofit selected.

12.7 Archived Files

Table 12-10 provides an annotated list of files developed during the course of numerical studies that have been archived for future use.

Table 12-10 Archived Files for WG5

Document No.	Title	Description
WG5-B1	Numerical Results for HOG Configurations	Results of all incremental dynamic analyses conducted on HOG Models
WG5-B2	Primary and Secondary Performance Criteria of HOG-ROG Numerical Models	Bar charts showing the correlations of P[C/MCE] with R factors
WG5-B3	LOG Retrofit Design Calculations	Calculations used for developing the Analytical Studies and creating the Prestandard prescriptive retrofits
WG5-B4	Development of Hysteresis Behavior of Steel and Proprietary Wall Retrofits	Description of the Process Used to Model Steel Retrofits and Proprietary Retrofits based on ASCE 41 and AC436
WG5-B5	Modeling Strategies Implemented in Timber3D	Describes the comparison of simplified, intermediate, and detailed modeling strategies through the comparison of IDA and pushover results
WG5-B6	Proposal for Model Nomenclature	Development of nomenclature for numerical models
WG5-B7	Grade Beam Flexibility Results	A numerical model was developed to study the influence of the flexibility of a grade beam on the hysteresis performance of a steel column retrofit
WG5-B8	Descriptions of Model Configurations Used in WG5 Numerical Studies	Wall lengths types and retrofits implemented for each of the numerical models used by WG5
WG5-B9	Building Configuration Study	Descriptions of applicable buildings for living-space-over-garage

12.8 References

ASCE, 2010, "Minimum Design Loads for Buildings and Other Structures," ASCE Standard ASCE/SEI 7-10, American Society of Civil Engineers, Reston, VA.

Baker, J.W., 2015, "Efficient Analytical Fragility Function Fitting Using Dynamic Structural Analysis," *Earthquake Spectra*;31 (1): 579-599.

FEMA, 2000, "Prestandard and Commentary for the Seismic Rehabilitation of Buildings," FEMA 356, Prepared by the American Society of Civil Engineers for the Federal Emergency Management Agency, Washington, DC, 518 p.

FEMA P695, 2009, "Quantification of Building Seismic Performance Factors," Prepared by the Applied Technology Council for the Federal Emergency Management Agency, Washington, DC, 421 p.

FEMA P795, 2011, "Quantification of Building Seismic Performance Factors: Component Equivalency Methodology," Prepared by the Applied Technology for the Federal Emergency Management Agency, Washington, DC, 292 p.

FEMA P807, 2012, “Seismic Evaluation and Retrofit of Multi-Unit Wood-Frame Buildings with Weak First Stories,” Prepared by the Applied Technology for the Federal Emergency Management Agency, Washington, DC, 336 p.

Ibarra, L. F., Medina, R. A., and Krawinkler, H., 2005, “Hysteretic models that incorporate strength and stiffness deterioration.” *Earthquake Eng. Struct. Dyn.*, 34(12), 1489–1511

Johnson, A.J., 1997, “Monotonic and Cyclic Performance of Long Shear Walls with Openings,” *MSc Thesis*, Virginia Polytechnic Institute and State University, Blacksburg, VA.

Lignos DG and Krawinkler H. Deterioration, 2011, Modeling of steel components in support of collapse prediction of steel moment frames under earthquake loading. *Journal of Structural Engineering (ASCE)* 2011; 137(11): 1291–1302.

Pang, W., Ziae, E., Filiatrault, A., 2012, “A 3D Model for Collapse Analysis of Soft-story Light-frame Wood Buildings,” *Proceedings of the 2012 World Conference on Timber Engineering* (2012 WCTE), Auckland, New Zealand.

Pang, W.C., Rosowsky, D.V., Pei, S., van de Lindt, J.W., 2007, “Evolutionary parameter hysteretic model for wood shear walls,” *Journal of Structural Engineering, ASCE*, 133(8): 1118-1129.

Patton-Mallory, M., Wolfe, R.W., Soltis, L.A., 1985, “Light-frame shear wall length and opening effects,” *Journal of Structural Engineering, ASCE*, 111(10): 2227-2239.

Yasamura, M., Sugiyama, H., 1984, “Shear properties of plywood-sheathed wall panels with opening,” *Transactions of the Architectural Institute of Japan*, 338(4): 88-98.

Part 13

Development of Vulnerability-Based Retrofit Provisions for Hillside Dwellings

13.1 Introduction

This resource paper documents the development of the FEMA P-1100, Volume 1 (Prestandard) (FEMA, 2018) vulnerability-based retrofit provisions for hillside dwellings. Included is discussion of the dwelling stock represented, the dwelling used as the basis of numerical models, the numerical study procedures, the results of numerical studies, and the selected assessment and retrofit design parameters. This resource paper is intended primarily for use by engineers wanting to have a better understanding of the basis for the retrofit recommendations, and those interested in details of the numerical modeling. Documented in Section 7 of this resource paper are additional resources providing detailed information on the numerical modeling.

13.2 Dwelling Stock Represented

Hillside dwellings are unique both in construction and seismic response, relative to other common wood light-frame dwelling configurations. Either the dwelling recesses into the hillside slope behind it, projects out over the hillside slope below it, as shown in Figure 13-1, or in some cases, is a combination of both. Hillside dwellings that project out over the hillside often include lower partial floor levels as the dwelling steps down the slope. Foundations for such dwellings can include stepped, sloped, continuous concrete footings, with or without concrete *stem walls*, isolated spread footings, cast-in-place concrete piers or caissons, or combinations of these.

The Prestandard addresses wood light-framed hillside dwelling configurations in which the entire dwelling projects out over the hillside slope. The uphill end of the dwelling is supported either by bearing directly on top of the foundation or on a light-framed wood crawlspace wall, two feet or less in height, supported on the foundation. The retrofit provisions, in addition to relying on anchorage to the uphill foundation, also rely on support by wood light-frame crawlspace walls on the sloping sides and downhill side.

A schematic illustration of the underfloor area that is the location of greatest seismic vulnerability and the focus of retrofit for hillside dwellings is shown in Figure 13-2.



Figure 13-1 Hillside dwelling of the configuration addressed by FEMA P-1100.

The hillside dwelling crawl space may also be entirely open, as shown in Figure 13-3. While the hillside dwelling open all three sides was not explicitly modeled as part of this project, the proposed retrofit strategies presented are appropriate.

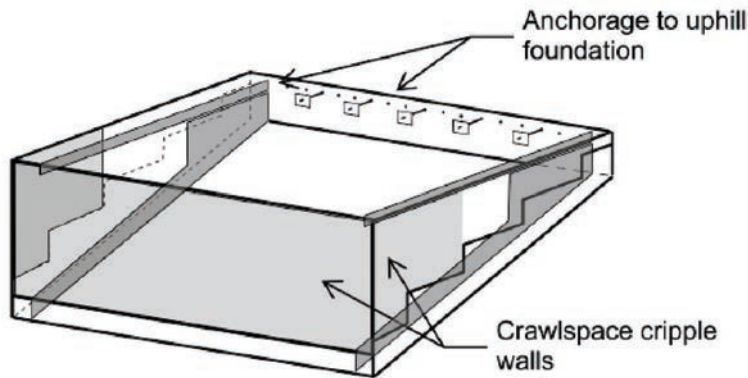


Figure 13-2 Hillside dwelling schematic illustration of the underfloor area enclosed with sheathed side walls.

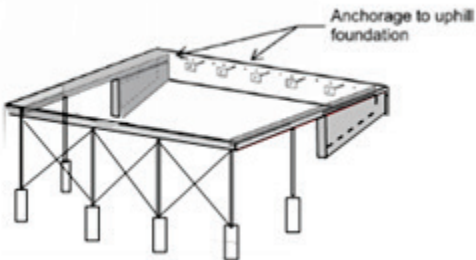


Figure 13-3 Hillside dwelling schematic illustration of the underfloor area with diagonal bracing and open area crawl space.

The general characteristics of the hillside dwelling, based on the Prestandard Chapter 2 definition are:

1. The space below the lowest framed floor is predominantly unoccupied, including area enclosed by crawlspace walls, open areas, or a combination of the two;
2. The tallest crawlspace cripple wall clear height exceeds 7'-0" (or post and beam system post height exceeds 7'-0" when underfloor area is not enclosed);
3. When averaged across the full length or width of the dwelling the grade slope exceeds 1 vertical in 5 horizontal; and
4. Where a wood light-frame crawlspace wall occurs between the base-level diaphragm and uphill foundation, the height of this crawlspace wall does not exceed 2'-0".

Hillside dwellings of this type are believed to have been constructed as long ago as the early 1900s, but became much more common in the 1950's and later. The vast majority of these dwellings are of wood light-frame construction, which is the focus of the Prestandard. The wall finish and sheathing materials that provide earthquake bracing have varied over time, and include wood siding, stucco, plywood panel exterior siding, plaster on wood or gypsum lath, gypsum wallboard, and a number of other materials. Foundation systems have also varied over time, and include simple shallow unreinforced or lightly reinforced concrete perimeter foundations that step or slope with the hillside, isolated medium or deep pier foundations, etc. Because the assessment and retrofit methods do not address behavior at the foundation to soil interface, the variation in foundation configuration does not impact the numerical studies or the resulting assessment and retrofit provisions. See Sections 6 and C6 of the FEMA P-1100 Volume 1

prestandard for discussion of the selected retrofit scope and potential behavior at the soil to foundation interface.

13.3 Dwelling Configurations Used in Analytical Modeling

The numerical studies for hillside dwellings focused primarily on a single dwelling plan. The plan was selected to be adequately representative of the group of dwellings and include the defining geometric characteristics of concern. Because the configurations of these dwellings can vary widely, it was decided to use a simple geometry in which seismic response could more easily be understood. The dwelling configuration is illustrated in Figures 13-4 through 13-6. Note that varying downhill wall heights were considered in the numerical studies. As illustrated in Figure 13-7, one additional dwelling plan (6-1H016-M-R=M1R) rotated so that the dwelling's long horizontal dimension spanned projected out over the downhill slope.

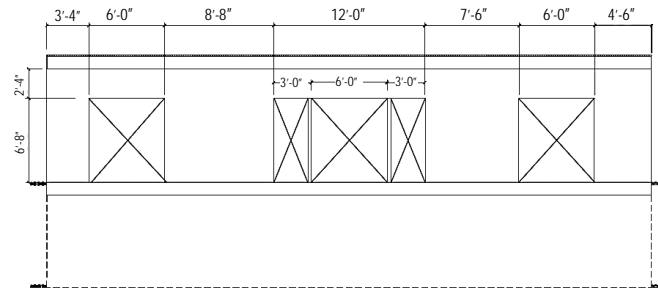


Figure 13-4 Dwelling elevation—downhill.

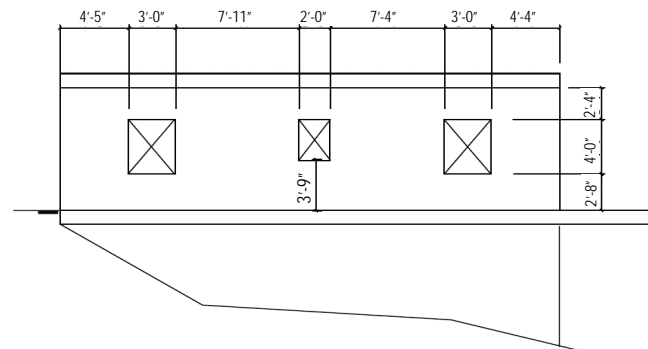


Figure 13-5 Dwelling elevation—side.

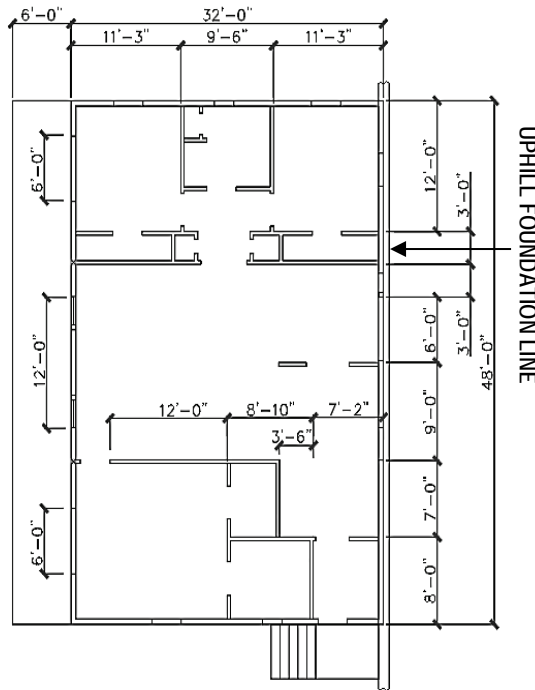


Figure 13-6 Dwelling occupied base level story plan for all models except Model 6-1H016-M-R=M1R.

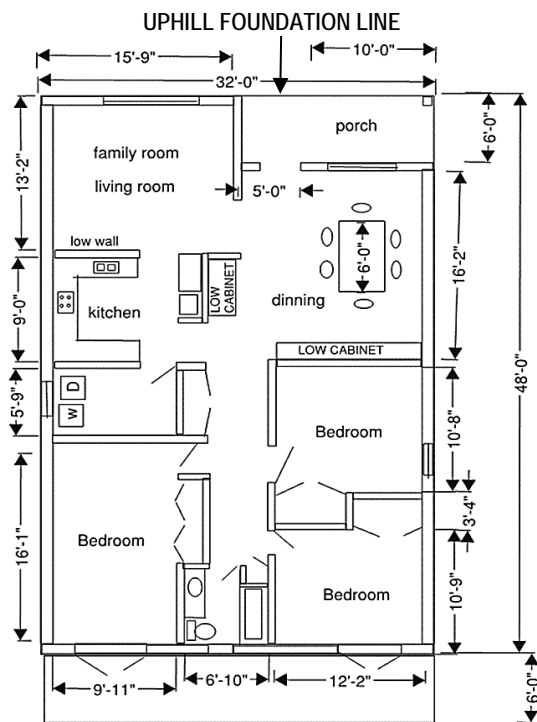


Figure 13-7 Dwelling occupied story plan for rotated model, (Model 6-1H016-M-R=M1R.)

For the purposes of trial retrofit design and assigning mass for numerical studies, the unit weights of the dwelling elements were defined. The assigned unit weights are discussed in Section 4.2. These unit weights are very close to but not exactly matching the unit weights eventually included in Appendix L of the prestandard.

Part 6 of this Volume presents the median dwelling configuration study conducted as part of the ATC-110 project. The purpose of this study was to identify the range of materials of construction and amount of wall in the occupied stories of dwellings in order to be able to speak to the range of strength and stiffness of these occupied stories. This was particularly important for crawlspace dwellings, where the choice of design parameters for the retrofit of cripple walls could affect the seismic performance of the occupied stories above. The information in the median dwelling study is informative for the performance of the superstructure in hillside dwellings, also. However, the retrofit methods selected for hillside dwellings are based on near-elastic behavior of the retrofit anchors at the base level diaphragm, with little opportunity to provide ductility. Because of this, study of the range of possible super structure strength and stiffness in the hillside dwelling was decided to be of lesser importance to the hillside dwelling numerical studies. It is believed that the hillside dwelling retrofit will substantially remove the hillside anchorage to foundation as a weak link, making the resulting performance of the dwelling a function of the performance of the superstructure, and possibly the foundation.

The terminology and design concepts used in assessment and retrofit of hillside dwellings are very unique to this dwelling type. It is helpful to become familiar with this terminology prior to proceeding with this background paper. Because of this, the following is a brief introduction of these terms and concepts. For more detail, see the prestandard provisions and commentary. The terminology is summarized below and illustrated in Figures 13-8 and 13-9.

BASE-LEVEL DIAPHRAGM. In a hillside dwelling, the framed floor at or closest in elevation to the level of the uphill foundation.

CROSS-SLOPE LOADING. In a hillside dwelling, horizontal seismic loading in the direction parallel to the uphill foundation and generally parallel to grade elevation contours. Cross-slope loading is perpendicular to out-of-hill loading.

OUT-OF-HILL LOADING (Down-hill loading). In a hillside dwelling, horizontal seismic loading parallel to the direction of descending grade, acting into or away from the hillside.

PRIMARY ANCHOR [LABC, modified]. In hillside dwellings, an anchor located at base level diaphragm ends and offsets or transitions and providing direct connection between the base-level diaphragm and the uphill foundation. Primary loading is tension in the out-of-hill direction, due to either direct tension from out-of-hill loading or torsion from cross-slope loading.

SECONDARY ANCHOR [LABC, modified]. In hillside dwellings, regularly spaced anchors providing redundant, distributed connections between the base-level diaphragm and the uphill foundation. Primary loading is in tension from downhill loading.

SHEAR ANCHOR. In hillside dwellings, an anchor connecting the base level diaphragm along the length of the uphill foundation. The primary loading is shear parallel to the uphill foundation.

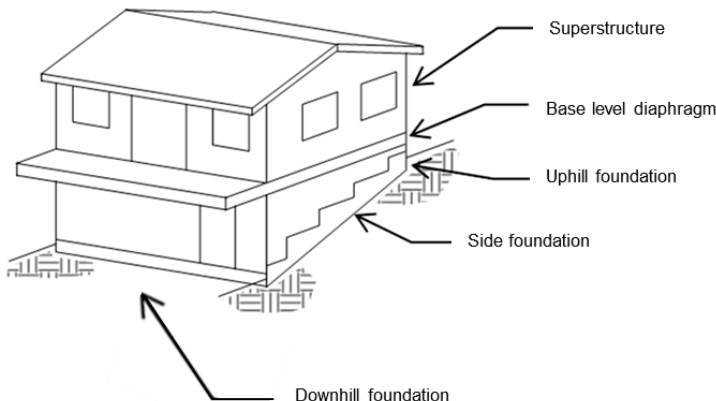


Figure 13-8 Hillside dwelling isometric with applicable terminology.

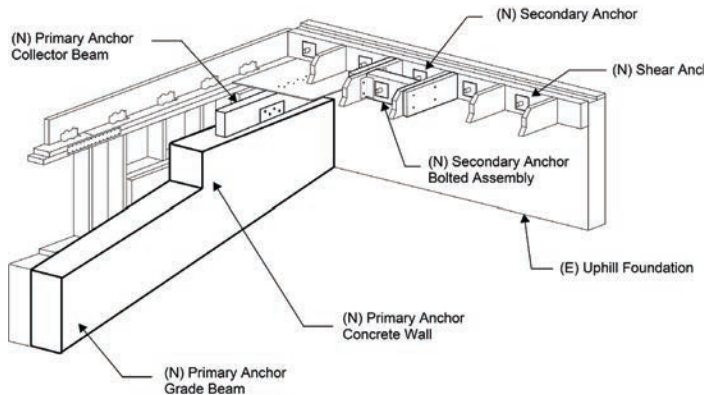


Figure 13-9 Hillside dwelling schematic illustration of retrofit elements.

13.4 Numerical Study Procedures

This section discusses modeling and analysis procedures used by the Hillside Dwelling vulnerability group (WG6). The following topics are covered: model nomenclature, seismic weight and dwelling configuration assumptions, component hysteretic behavior, diaphragm modeling and generation of collapse fragility curves. In general, numerical analyses followed the process outlined in Part 5 of this Volume, *Protocol for Numerical Studies*. Material properties used for modeling were obtained from Part 4 of this Volume, *Material Characterization for Numerical Studies* where use of materials common to all of the numerical studies was appropriate. Material characterization applicable only to the hillside dwellings is detailed in this reference paper.

13.4.1 Hillside Dwelling Numerical Study Nomenclature

The following information outlines the nomenclature used to describe hillside vulnerability models on the project. This nomenclature is similar to what was used by other groups on the project with minor variations. As illustrated in Figure 13-10, information such as the range of cripple wall height (uphill to downhill) included in the model (0'-4') and the condition modeled (i.e. existing or retrofit) can be extracted from the name of the models. Certain variables in the nomenclature, such as the working group number, number of stories in the model, and the strength properties of the superstructure remain consistent for all of the hillside vulnerability models.

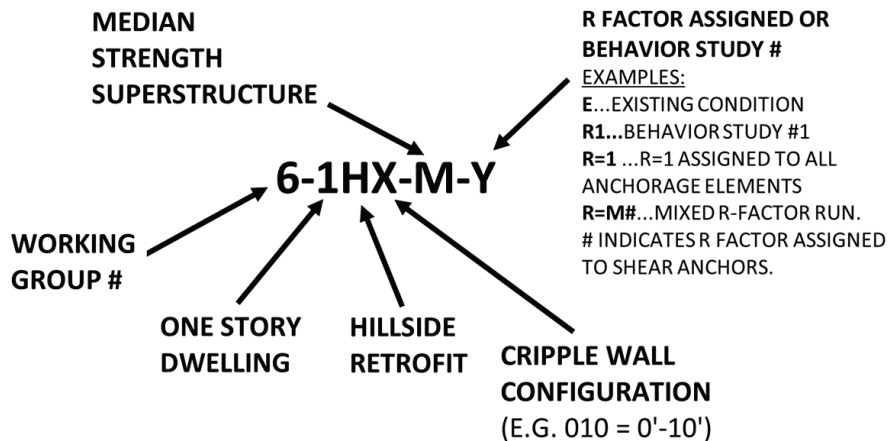


Figure 13-10 Numerical modeling nomenclature.

13.4.2 Weight Assumptions

The building material weights assumed for all hillside vulnerability analyses are shown in Table 13-1. The full seismic weight of the backyard deck was applied to the back end of the floor diaphragm, distributed over the length of the deck. A roof slope of 8:12 was assumed when obtaining the effective roof dead load value of 15 psf. All seismic weight was distributed to roof and floor level nodes, including wall weight. No reductions were made in wall weight to account for openings. In a given horizontal diaphragm, seismic weight was horizontally distributed based on the tributary area to each numerical model node. An example of the superstructure seismic weight (23k total) at the roof level diaphragm being distributed to nodes based on tributary area is illustrated in Figure 13-11.

Table 13-1 Unit Weight Summary

System	Weight Designation	Weight (psf)
Floor	Light	10
Roof and Ceiling	Light	15
Exterior Walls	Medium	14.5
Interior Walls	Light	7
Cripple Walls	Heavy	14
Deck	Medium	10

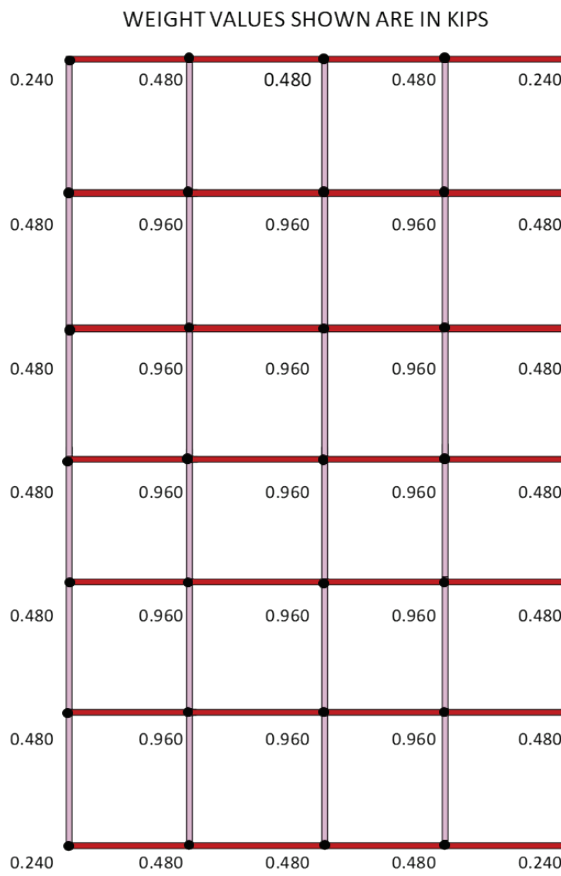


Figure 13-11 Roof diaphragm seismic weight distribution to diaphragm nodes based on tributary area.

13.4.3 Numerical Models

Seventeen hillside numerical models were produced and evaluated using methods outlined in Part 5. Model names, descriptions, reasons for why they were of interest, and references to corresponding result sections are included in Table 13-2. Models can be grouped in three categories:

- Existing (pre-retrofit) condition models that were created to establish reference points for performance. Included in this category are models 6-1H04-M-E and 6-1H0-M-S.
- Preliminary models that were investigated to gather information on hillside retrofit behavior. Included in this category are models 6-1H04-M-R1, 6-1H04-M-R2S, 6-1H04-M-R2, 6-1H04-M-R3, 6-1H010-M-R4, and 6-1H04-M-R5.
- Retrofit models that had anchorage elements (i.e. primary, secondary, and shear anchors) with peak capacities were scaled to a R value of interest. These models were compared to the existing condition model, and each other, to gather information on which R values should be

suggested for the different anchorage elements. Included in this category are models 6-1H04-M-R=1, 6-1H010-M-R=1, 6-1H010-M-R=2, 6-1H04-M-R=M2, 6-1H010-M-R=M2, 6-1H04-M-R=M1, 6-1H010-M-R=M1, 6-1H016-M-R=M1, and 6-1H016-M-R=M1R.

An example 0'-16' retrofit model (6-1H016-M-R=M1) is illustrated in Figure 13-12. Note that the uphill foundation line has stud members for vertical load path purposes even though the model's base-level diaphragm is fixed to an uphill foundation via anchorage elements (i.e. primary, secondary, and shear anchors when applies). These stud members have no lateral stiffness and, therefore, did not affect the lateral performance of the models. Each model had a footprint of 32'x48' with the short dimension spanning downhill per the configuration introduced in Figures 13-4 to 13-6. The only exception to this is Model 6-1H016-M-R=M1R, where the dwelling's orientation was rotated so that the long horizontal dimension of the dwelling was spanning downhill and a more representative superstructure configuration was developed for homes in this orientation. In the out-of-hill direction, crawl space walls typically consisted of two equal length stepped cripple walls (e.g. equal length 2' and 4' tall walls for a 0'-4' model). These crawl space walls were only sheathed for the existing (pre-retrofit) condition model and never sheathed for any of the retrofit condition models. The downhill crawl space wall (e.g. 4' tall for a 0'-4' model) was sheathed for the existing condition model, some of the preliminary models, and for all of the R-value retrofit models.

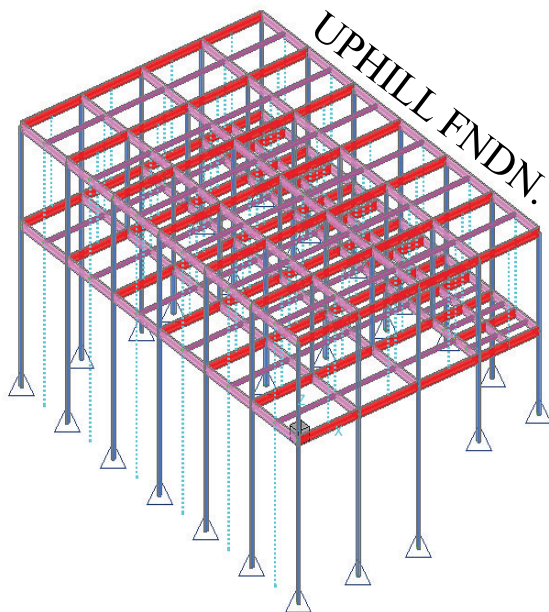


Figure 13-12 Example 0'-16' hillside retrofit model in Timber3D.

Table 13-2 Hillside Dwelling Numerical Models

Model Name	Description	Interest	Section Reference
6-1H0-M-S	Superstructure on rigid foundation model. No crawl space.	The superstructure represents the upper bound of performance. The superstructure configuration in this model was used in every other model except 6-1H016-M-R=M1R.	5.1
6-1H04-M-E	Existing condition model.	To establish the vulnerability reference point.	5.2
6-1H04-M-R1	Secondary and shear anchors only.	To evaluate performance without the use of primary anchors.	5.3
6-1H04-M-R2S	Primary and shear anchors only.	To evaluate performance without the use of secondary anchors.	5.4
6-1H04-M-R2	Primary, secondary and shear anchors.	To evaluate performance with both primary anchors and secondary anchors.	5.5
6-1H04-M-R3	Same as 6-1H04-M-R2 but with an additional primary anchor at interior grade beam.	To evaluate if additional primary anchors should be considered under concentrations of superstructure walls for further performance benefits.	5.6
6-1H010-M-R4	Primary, secondary, and shear anchors along with downhill cripple wall WSP sheathing.	To evaluate if sheathing crawl space walls with WSP sheathing results in noticeable performance benefits.	5.7
6-1H04-M-R5	Primary, secondary, and shear anchors along with downhill cripple wall WSP sheathing	To evaluate if sheathing crawl space walls with WSP sheathing results in noticeable performance benefits.	5.8
6-1H04-M-R=1	Primary, secondary, and shear anchors all scaled to R=1.	To establish retrofit performance with the lowest R-value possible (upper bound strength).	5.9
6-1H010-M-R=1	Primary, secondary, and shear anchors all scaled to R=1.	To establish retrofit performance with the lowest R-value possible (upper bound strength).	5.10
6-1H010-M-R=2	Primary, secondary, and shear anchors all scaled to R=2.	To establish retrofit performance with the second lowest whole number for an R-value.	5.11
6-1H04-M-R=M2	Secondary anchors scaled to R=1. Primary anchors and shear anchors scaled to R=2.	To see if higher R-values can be assigned to both primary and shear anchors with minimal performance loss.	5.12
6-1H010-M-R=M2	Secondary anchors scaled to R=1. Primary anchors and shear anchors scaled to R=2.	To see if higher R-values can be assigned to both primary and shear anchors with minimal performance loss.	5.13
6-1H04-M-R=M1	Secondary and shear anchors scaled to R=1. Primary anchors scaled to R=2.	To see if a higher R value can be assigned to the primary anchors only with minimal performance loss.	5.14
6-1H010-M-R=M1	Secondary and shear anchors scaled to R=1. Primary anchors scaled to R=2.	To see if a higher R value can be assigned to the primary anchors only with minimal performance loss.	5.15
6-1H016-M-R=M1	Secondary and shear anchors scaled to R=1. Primary anchors scaled to R=2.	To see if a higher R value can be assigned to the primary anchors only with minimal performance loss.	5.16
6-1H016-M-R=M1R	Rotated model with secondary and shear anchors scaled to R=1. Primary anchors scaled to R=2.	To provide information on how a hillside dwelling retrofit will perform when a dwelling's long horizontal dimension is parallel to the out-of-hill direction.	5.17

13.4.4 Hysteretic Behavior of Existing Building Materials/Fasteners

Behavior of existing building materials was standardized across all working groups and these hysteretic parameters can be obtained from Part 4. Interior superstructure walls were double sheathed with the best estimate gypsum (G2), exterior superstructure walls were sheathed with the best estimate gypsum + stucco (SG2), and cripple walls were sheathed with the lower bound stucco (S1) for the existing (pre-retrofit) condition model only.

Contributions from existing stucco sheathing were neglected at the cripple wall level for all retrofit models. As illustrated in Figure 13-13, the capacity and stiffness of superstructure walls was adjusted to account for openings as discussed in Part 4.

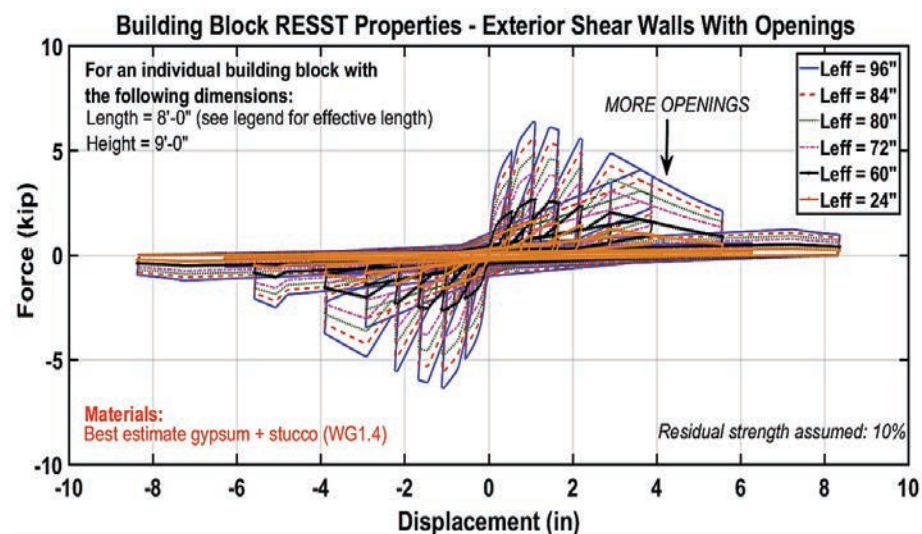


Figure 13-13 Hysteresis plots for exterior walls sheathed with best estimate gypsum and stucco (SG2). Each hysteresis is for an 8' wide x 9' tall building block, where L_{eff} represents the length of full-height pier segments after accounting for exterior wall openings.

At the uphill zero-height cripple wall, where the base-level diaphragm sits directly on the uphill foundation's sill plate, existing attachments were considered for lateral stiffness in the existing pre-retrofit model. In plane and out of plane sill bolts were modeled with capacities recommended in from Part 4 Section 3.9. A 4'-0" O.C. sill bolt schedule was assumed. Toenails from the base-level diaphragm to the uphill foundation sill plate were also modeled with capacities and hysteretic parameters recommended in Part 4 Sections 3.10 and 4.6. A nailing schedule of 3-16d common toenails at 24" O.C. was assumed across the uphill foundation sill plate. It's worth noting that either the toenails or the sill anchor bolts can be the governing failure mechanism for the base-level diaphragm detaching from the uphill

foundation. For the connection schedules discussed above, toenails were determined to be the governing connection for the pre-retrofit condition.

13.4.5 Hysteretic Behavior of Wood Structural Panel Cripple Walls

When specified for the retrofit models discussed in Section 4.3, wood structural panel (WSP) sheathing was applied to the downhill cripple wall. Modeling of this sheathing was consistent with presence of hold-downs to provide overturning restraint. The height of the downhill cripple wall varied between 4' to 16' based on the model and hillside slope being investigated. WSP3 hysteretic parameters from Part 4 Section 4.4.4 were typically used where WSP was applied in the retrofit models. These hysteretic parameters are representative of 7/16" inch rated sheathing with an 8d nails at 4" O.C. edge nailing schedule and the testing data that these parameters are based on can be found in Part 4 Section 4.3.5. Hysteretic parameters for an 8' wide x 10' tall building block are illustrated in Figure 13-14. Stepped cripple walls were conservatively treated as unsheathed for retrofit analyses, though impact would have been minimal due to the stiff and high capacity nature of the primary anchors at the ends of the uphill foundation.

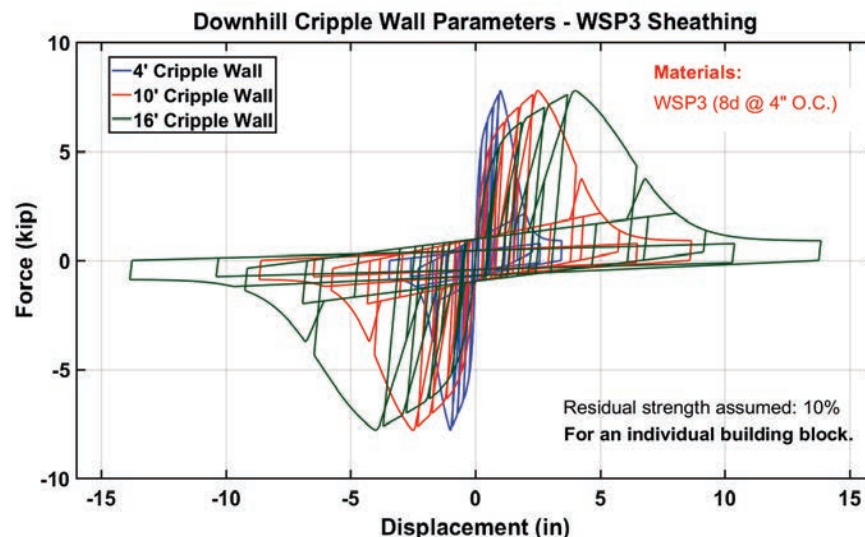


Figure 13-14 Hysteresis plots for downhill cross-slope cripple walls sheathed with WSP3 parameters.

13.4.6 Hysteresis Behavior of Anchorage Elements

Testing was performed at Washington State University's Paccar Environmental Technology Building on five Douglas Fir-Larch wood to steel ½" bolt specimens for use in developing primary and secondary anchor hysteretic parameters. Each test consisted of a singular bolt in a single shear configuration. The hysteresis curve for Test 4 is illustrated in Figure 13-15.

The connection had a peak capacity of 4000 lbs of load on average at approximately 0.35" deflection.

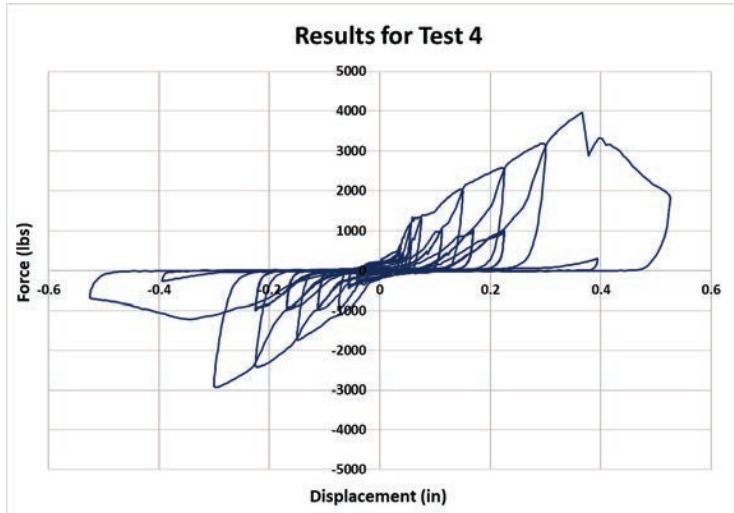


Figure 13-15 Hysterisis plots for a wood to steel 1/2" bolt specimen tested at Washington State University.

The testing data was modified to represent the secondary anchor detail illustrated in Figure 13-16. A secondary anchor assembly consisted of a threaded rod in tension, and 8 wood to sill bolts in shear from scabbed floor joists to blocking. The failure mechanism for this assembly would be tensile yielding of the threaded rod that is thru-bolted to the uphill foundation. To obtain hysteretic parameters for the secondary anchors, the RESST (Part 4 Section 4.4.1) twelve parameter hysteretic model was fitted to an average testing data specimen. The testing data was adjusted to represent a quantity of eight bolts to blocking by adjusting the K0 and F0 stiffness parameters. The testing strength data was capped to a value equal to the tensile yield force of a 3/4" threaded rod (12 kip). Springs in series concepts were then applied to account for the additional slip that would occur from the threaded rod elongating by adjusting the K0 parameter.

Primary anchor parameters were obtained by scaling the elastic stiffness and peak capacity of the secondary anchor parameters, while removing the yielding force plateau associated with the secondary anchor's tensile threaded rod. Both secondary and primary anchor hysteretic parameters were scaled based on the R-factor value that was prescribed in Section 4.3 for a given retrofit model.

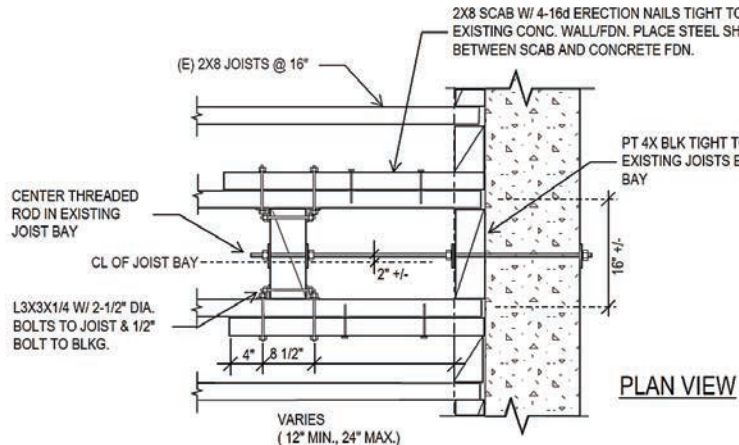


Figure 13-16 Example secondary anchor detail in plan view.

For stiffness in the cross-slope direction (parallel to the uphill foundation), the in-plane capacity of sill bolts was also considered. The CUREE/SAWS ten parameter hysteretic model was applied to the recommended testing curve in Part 4. Sill bolts were typically spaced at 4'-0" O.C. in the retrofit models.

The peak strength of the different anchorage elements (i.e. primary, secondary, and shear anchors) for modeling were determined by developing retrofit designs at the various R-factors being studied using the Equivalent Lateral Force method per Equation 12.8-1 of the ASCE 7-10 (2010). Further discussion on why this method was selected can be found in Part 3, *Assessment and Retrofit Design Criteria*. Each set of different anchorage element types (e.g. primary anchors, secondary anchors, and shear anchors) is expected to be capable of resisting the full base shear of the building for a design level event. For example, the base shear is divided by the total number of equally spaced secondary anchors to determine the required capacity of the individual secondary anchors. The same process was followed for the primary and shear anchors. Therefore, there is redundancy with this design method in the out-of-hill direction since both the primary anchors and secondary anchors are designed to resist the full base shear. Though the hillside dwelling full base shear for design of the primary anchors is 50% of the full base shear for design of the secondary anchors, the actual design forces for the primary anchors are significantly higher than for the individual secondary anchors. This was intended to account for the fact that the uphill foundation could be shallow (i.e. flexible) or deep (i.e. rigid). If the foundation is shallow, resistance from the secondary anchors would be assumed to be minimal because the uphill foundation may conform to the deformed shape of the diaphragm, resulting in the majority of the resistance to out-of-hill seismic forces coming from the side foundations at the primary

anchor locations. If the foundation is deep, resistance from the secondary anchors would be expected to be significant since the foundation would be anticipated to provide considerable resistance to out-of-hill seismic forces along its full length. Primary, secondary, and shear anchor hysteretic parameters for an example model, 6-1H04-M-R=1, are illustrated in Figures 13-17 and 13-18. For further clarification on how to obtain the required capacity of anchorage elements based on R-value, see the design example in Appendix A.

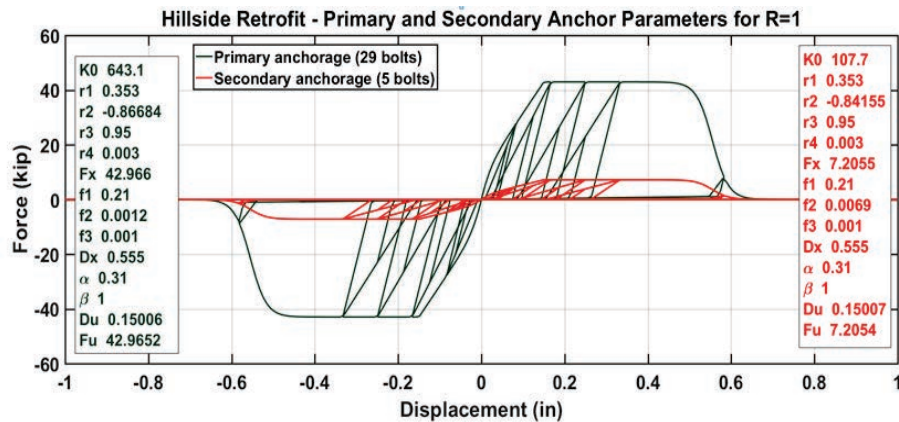


Figure 13-17 Primary and secondary anchor parameters for Model 6-1H04-M-R=1.

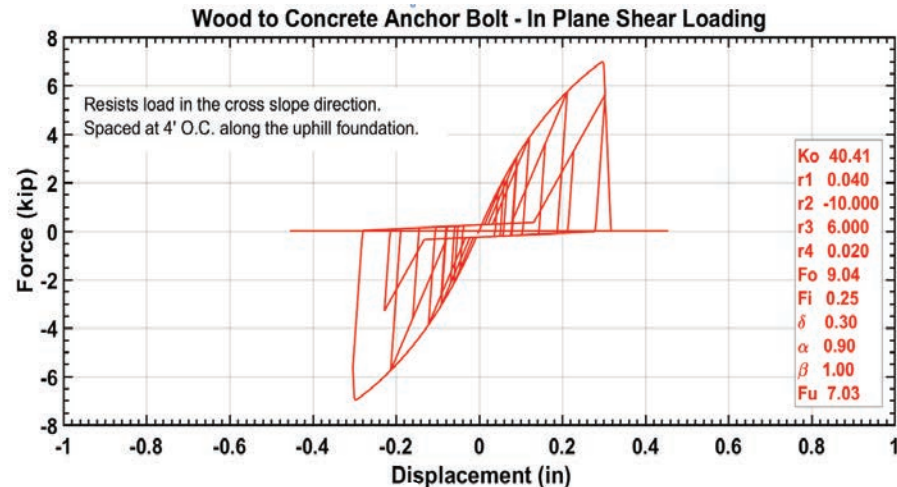


Figure 13-18 Shear anchor parameters for Model 6-1H04-M-R=1.

13.4.7 Modeling Procedures for Flexible Diaphragms

The capacity of a hillside dwelling is heavily influenced by the shear stiffness of its base-level diaphragm. The stiffness of the base-level diaphragm affects the rate that the individual anchorage elements along the uphill foundation are loaded as a function of diaphragm deformation. A

linear elastic semi-rigid diaphragm was used in the numerical studies to account for this effect.

As discussed in the Part 4, various testing data was assessed to produce a recommended value of stiffness for an unblocked wood structural panel diaphragm. The result of this effort was that all diaphragms were to be modeled with a shear stiffness (G_a) of 8.0 kip/in. Testing performed by Dolan et al. (2003) showed that diaphragm displacement components related to bending and splice slip are very small when small sections of walls are located along the perimeter of the diaphragm. For this reason, the stiffness of the diaphragms only includes the shear deformation component. This was done by manipulating the stiffness matrix of a fixed-fixed beam which is further discussed in Part 1 Section 1.3.11. This diaphragm modeling was thought to also reasonably represent lumber sheathed diaphragms with hardwood flooring, as might be common in older hillside dwellings.

The diaphragm model itself consisted of a square grid of rigid members that were modeled as rigid out of plane to avoid vertical mode shapes. These members can transfer out plane moment within the diaphragm and but do not transfer in-plane moment since only shear deformation is of interest.

Diaphragm beams calibrated to the shear stiffness of the test data recommendation were centered in each individual grid and they caused the diaphragm to experience in-plane, linear elastic shear deformation. As illustrated in Figure 13-19, a finer mesh for the diaphragm grid was applied near the uphill foundation for improved accuracy and easier extraction of displacement information for anchorage elements along this perimeter line.

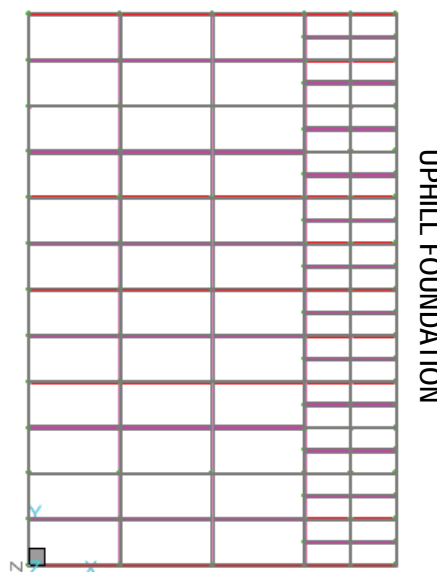


Figure 13-19 Diaphragm mesh for an example hillside model.

13.4.8 Superstructure Modeling

The superstructure was modeled by creating a slightly simplified version of the floor plan shown in Figure 13-6. Minor simplifications were necessary to allow the upper story shear walls to be attached to the square grids of the diaphragms, discussed in Section 4.7 and illustrated in Figure 13-19.

Therefore, some wall lines were shifted slightly and the closely neighboring interior walls that represented a closet space were merged to form an effective wall line. The result of this simplification process is illustrated in Figure 13-20. A merged wall line represented four panels of gypsum sheathing (two for each wall since both would be sheathed on both sides) as opposed to two for an individual wall. The total length of wall and its relative location before and after the simplification process remained the same. Therefore, the performance of the actual floor plan and the modeled floor plan would be essentially identical. A similar process was applied for the retrofit model 6-1H016-M-R=M1R, where the dwelling's footprint was rotated so that the long horizontal dimension spanned downhill.

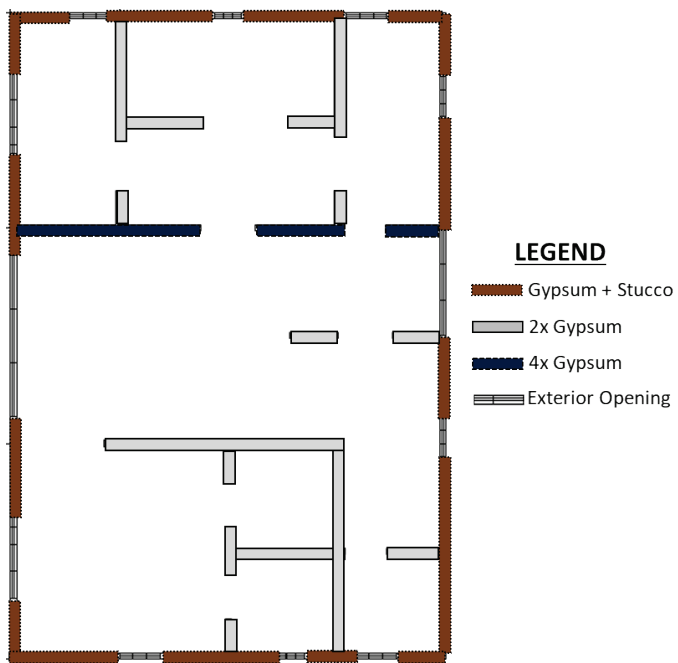


Figure 13-20 Simplified floor plan for modeling purposes. Used for all models except Model 6-1H016-M-R=M1R.

13.4.9 Concrete Foundation and Soil Assumptions

The concrete foundation was idealized as rigid with infinite stiffness for every hillside dwelling model in this project, and the interface between the foundation and soil was not modeled. This is consistent with the project's objective to address the hillside dwelling vulnerability of separation of the

dwelling from the uphill foundation. Potential sliding of the dwelling and the foundation at the soil interface is recognized as possible, but not pose as high a life-safety risk as separation of the dwelling from the foundation. The probabilities of collapse at MCE reported by this project would be anticipated to increase should significant damage occur at the foundation to soil interface. See the FEMA P-1100, Volume 1 Prestandard for more discussion.

13.4.10 Determination of Median Collapse Intensity

To determine the median collapse intensity for a given model, the FEMA P695 (2009) methodology was applied by running multiple stripe analyses as described in Part 5. As illustrated in Figure 13-21 for one earthquake record, the complete suite of 22 far-field ground motions, both horizontal components were applied to all models simultaneously for each record to perform a 3D analysis. The components were then rotated to produce a total of 44 analyses for each intensity stripe. Vertical excitation was neglected in all of the models due to the failure mechanism considered being shear based. Ground motion records were scaled with the median spectra intensity assigned at FEMA P695's minimum permitted fundamental period of 0.25s. Ground motion analyses were always run for the models at an intensity stripe of 0.4MCE ($S_a = 0.6g$), DE ($S_a = 1.0g$), and MCE ($S_a=1.5$) for Seismic Design Category D_{MAX}. An initial raw data fragility curve was then fit to the results based on these three data points to estimate a median collapse intensity. At least one additional stripe analysis was performed at the initial estimated median collapse intensity to improve the accuracy of the final median collapse intensity. The final reported median collapse intensity value was determined by fitting the fragility curve including all four-intensity stripes.

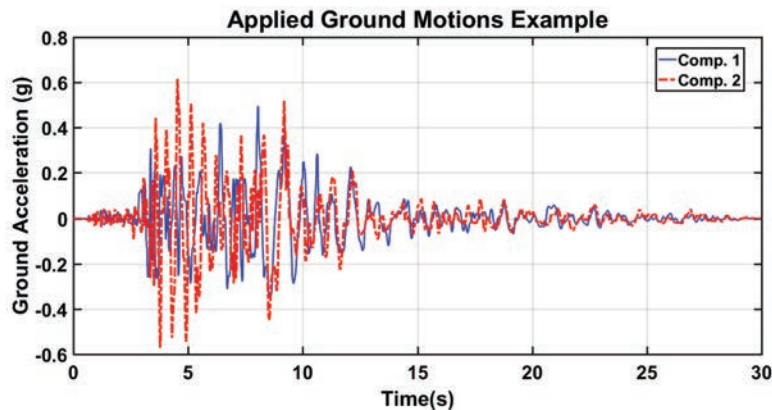


Figure 13-21 Example horizontal ground motions components shown for an earthquake included in the 22-far field ground motions.

Raw data fragility curves were modified with FEMA P695's three-dimensional, spectral shape, and correction for global dispersion factors. The three-dimensional factor of 1.2 was applied to the median of the curve and was intended to remove the conservative bias for the performance of 3D analyses when compared to 2D analyses. The spectral shape factor also was applied to the median to recognize the fact that structures with sufficient ductility will experience period elongation during a major seismic earthquake, thus reducing spectral acceleration demand. Spectral shape factors of 1.0 and 1.33 were applied to the existing and retrofit conditions, respectively. The correction for global dispersion accounts for the following sources of uncertainty: record-to-record, design requirements, testing data, and quality of modeling. Dispersion values of 0.75 and 0.60 were applied for the existing and retrofit conditions, respectively. The transformation from a raw data fragility curve to a FEMA P695 modified fragility curve is illustrated in Figure 13-22.

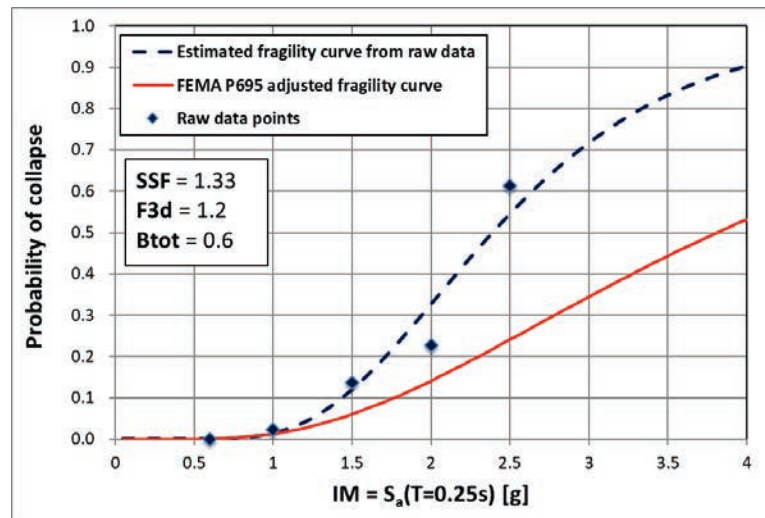


Figure 13-22 Example of an estimated raw data fragility curve being modified with FEMA P695's various seismic performance factors.

13.5 Numerical Results

This section provides an overview of the results of analysis, and presents the figures illustrating analysis results that were used by the project team to select retrofit design parameters. The reader is reminded that, as described in Volume 1, the analytical studies were used primarily as a tool to judge improvement in performance, rather than an absolute indication of performance. Results for primary criterion (reduction of probability of failure) and peak monotonic strength to weight (V/W) ratios for models introduced in Section 4.3 are tabulated in Table 13-3. Further discussion on performance goals can be found in Part 2 of this Volume, *Performance*

Criteria for Numerical Studies. Monotonic curves for models discussed in this section are included in Chapter 6 of *Seismic Retrofitting Downslope Hillside Dwellings with Uphill Anchorage and Cripple Wall Wood Structural Panel Sheathing* (Vincent, 2018). Hysteretic parameters assumed for the different elements assumed in the models can be found in Appendix A of the same document.

Table 13-3 Numerical Model Monotonic and Dynamic Results

Model	FEMA P695 adjusted P[C MCE] (%)	Reduction of P[C MCE] with Retrofit (%)	Loading Direction	V/W
6-1H0-M-S	5.8	-	Out-of-hill	1.88
			Cross-slope	1.61
6-1H04-M-E	76.9	-	Out-of-hill	0.47
			Cross-slope	0.41
6-1H04-M-R1	47.5	29.4	Out-of-hill	1.77
			Cross-slope	1.04
6-1H04-M-R2S	20.6	56.3	Out-of-hill	1.46
			Cross-slope	1.18
6-1H04-M-R2	15.5	61.4	Out-of-hill	1.88
			Cross-slope	1.18
6-1H04-M-R3	15.1	61.8	Out-of-hill	1.87
			Cross-slope	1.18
6-1H010-M-R4	6.0	70.9	Out-of-hill	1.88
			Cross-slope	1.56
6-1H04-M-R5	3.6	73.3	Out-of-hill	1.86
			Cross-slope	1.56
6-1H010-M-R=1	6.9	70.0	Out-of-hill	1.83
			Cross-slope	1.56
6-1H04-M-R=1	4.3	72.6	Out-of-hill	1.82
			Cross-slope	1.57
6-1H010-M-R=2	24.3	52.6	Out-of-hill	1.79
			Cross-slope	1.07
6-1H04-M-R=M2	6.8	70.1	Out-of-hill	1.83
			Cross-slope	1.22
6-1H010-M-R=M2	24.3	52.6	Out-of-hill	1.81
			Cross-slope	1.20
6-1H04-M-R=M1	4.8	72.1	Out-of-hill	1.78
			Cross-slope	1.58
6-1H010-M-R=M1	7.4	69.5	Out-of-hill	1.79
			Cross-slope	1.56
6-1H016-M-R=M1	10.6	66.3	Out-of-hill	1.77
			Cross-slope	1.54
6-1H016-M-R=M1R	24.5	52.4	Out-of-hill	2.16
			Cross-slope	1.00

13.5.1 Model 6-1H0-M-S

Model 6-1H0-M-S was a superstructure on rigid foundation model that was created to gain a better understanding of the capacity and behavior of the asymmetric superstructure discussed in Section 3. The hillside vulnerability exists within the crawl space, but as the crawl space is retrofitted and significantly anchored to the uphill foundation, the failure mechanism can shift to the occupied story. Due to the vulnerability-based retrofit approach applied in this project, superstructure retrofit was not considered. Therefore, this model illustrated the upper bound performance that is possible with a hillside retrofit and the dwelling discussed in Section 3. The superstructure exterior shear walls were sheathed with best estimate gypsum and stucco (SG2 per Part 4). The interior walls were double sheathed with best estimate gypsum (G2 per Part 4).

In the out-of-hill direction, the exterior wall lines and the interior wall line with the most wall had similar contributions at peak loading and similar levels of initial stiffness. The superstructure possessed a peak strength to weight ratio (V/W) of 1.88 in this direction. In the cross-slope direction, the stiffest wall line with the most capacity was as the front of the house. This indicated that a larger percentage of upper story seismic load would transfer to the uphill foundation than the downhill walls. The second stiffest wall line was at the back of the house, which was softer than the front of the house due to the presence of more openings. Interior wall contributions were less significant in the uphill-downhill direction due to the floor plan possessing less interior wall in this direction. The superstructure possessed a cross-slope peak strength to weight ratio (V/W) of 1.6, indicating that the superstructure was approximately 14% weaker when loaded in this direction. This model had a FEMA P695 adjusted probability of collapse at MCE ($S_a = 1.5g$ for SDC Dmax) of 5.8%.

13.5.2 Model 6-1H04-M-E

An existing condition (pre-retrofit) model was developed and evaluated to establish an initial performance reference point to use for comparing the performance of the retrofit models to and quantifying the improved performance. The model had a typical footprint of 32'x48' with the short dimension spanning downhill, using the configuration illustrated in Figures 13-4 to 13-6. The dwelling's crawl space consisted of a zero-height cripple wall at the uphill foundation and a 4' tall downhill cripple wall in the longitudinal/cross-slope direction. Stepped cripple walls ran parallel to the direction of the hill slope in equal length 2' and 4' tall segments. Due to its shallow hillside slope, this model would ultimately not be classified as a

hillside dwelling in the Prestandard. However, it was conservative to consider this model as the pre-retrofit condition since existing dwellings on a steeper hillside slope would be at even more susceptible to collapse. All cripple walls were sheathed with lower bound stucco (S1 per Part 4). As illustrated in Figure 13-23, at the uphill foundation (zero-height cripple wall), 3-16d nails were spaced at 24" O.C. The strength of the toenails was conservatively reduced from what testing data would suggest for strength to account for installation errors and potential decay and corrosion in the mudsill. The in-plane and out of plane capacity of 5/8" diameter uphill mudsill bolts at 4'-0" O.C. was also considered for preliminary analyses until it was discovered that the toenails were the governing failure mechanism. Similarly, an alternative uphill bearing condition with a ledger instead of a mudsill was also considered, but it was found that the mudsill condition was more vulnerable.

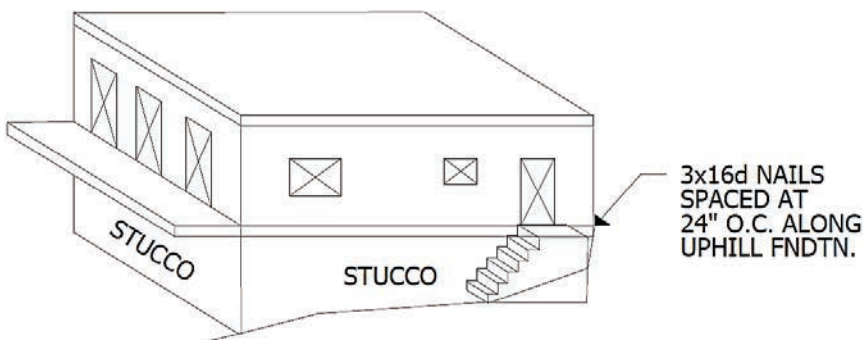


Figure 13-23 Existing model (6-1H04-M-E) crawl space configuration.

13.5.3 Model 6-1H04-M-R1

Model 6-1H04-M-R1 was the first preliminary retrofit model analyzed and it utilized anchorage to the uphill foundation via secondary anchors at 4' O.C. Primary anchors and downhill wood structural panel cripple wall sheathing was not present. The substructure utilized a 0'-4' configuration, where existing cripple wall sheathing finishes were completely neglected. This model was used to determine whether primary anchors would be necessary for a successful retrofit.

When the dwelling was loaded in the out-of-hill direction, load was resisted by ¾" threaded rod secondary anchors at 4' O.C. The failure mechanism was sequential fracture of the secondary anchors. The displacement distribution of secondary anchors at monotonic peak loading is illustrated in Figure 13-24. This model suggests that the highest force demand for uphill anchorage and this loading direction occurs below the stiffest upper story wall lines. Results from Model 6-1H04-M-R2 further suggests that primary anchors at

the ends of the uphill foundation below the exterior walls are necessary. The dwelling possesses a high strength to weight ratio (V/W) of 1.77 in this direction.

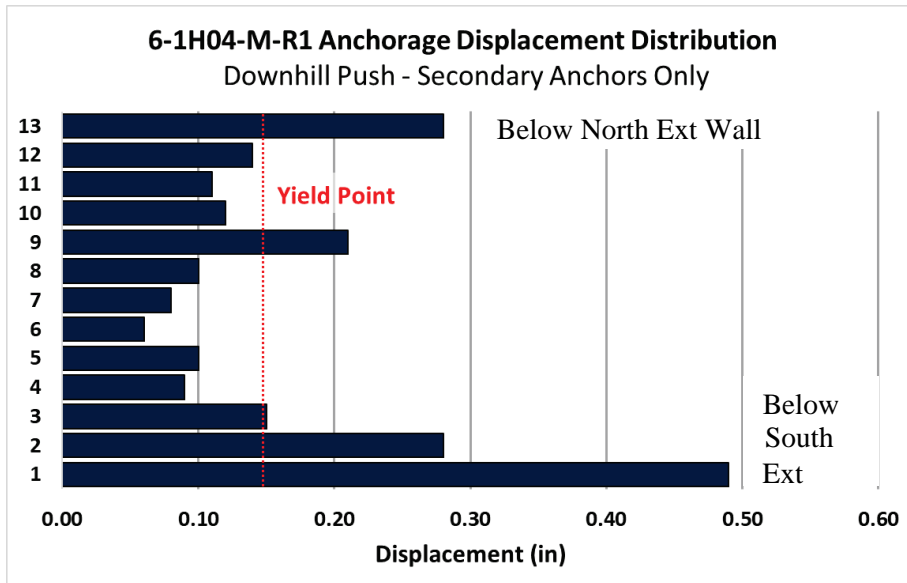


Figure 13-24 Secondary anchor displacement distribution for Model 6-1H04-M-R1 at peak loading when subjected to an out-of-hill monotonic push. The highest anchorage demand occurs near the stiffest superstructure wall lines, as discussed in Section 5.1.

When the dwelling was loaded in the cross-slope direction, load was resisted by $\frac{1}{2}$ " wood to concrete shear anchor bolts at 16" O.C. The failure mechanism occurred in the direction perpendicular to the applied load, where the secondary anchors experienced unzipping from one side to the other. This indicated that crawl space torsional behavior is not adequately addressed if primary anchors are not installed at the ends of the uphill foundation to restrict rotation of the base-level diaphragm. The dwelling possessed a low strength to weight ratio (V/W) of 1.04 in this direction. The model had a high probability of collapse at MCE (SDC Dmax) of 47.5% which was caused by a weak cross-slope direction response that was susceptibility to torsion.

13.5.4 Model 6-1H04-M-R2S

Model 6-1H04-M-R2S, which utilized anchorage to the uphill foundation via primary anchors at the ends of the uphill foundation, was intended to quantify the performance of the primary anchors. Secondary anchors and downhill wood structural panel cripple wall sheathing were not present. This model was used to determine how the retrofit would perform on a shallow foundation. Secondary anchors were conservatively removed from the uphill foundation to simulate the extreme case where the low stiffness uphill

foundation conforms to the deformed shape of the floor diaphragm during an out-of-hill push.

When the dwelling was loaded in the out-of-hill direction, load was resisted by primary anchors at the ends of the uphill foundation. The failure mechanism was fracture of the primary anchors. The dwelling possessed a high strength to weight ratio (V/W) of 1.46 in this direction. However, when the dwelling was loaded in the cross-slope direction, load was resisted by $\frac{1}{2}$ " wood to concrete shear anchor bolts at 16" O.C. The failure mechanism, when loaded in this direction, was upper story collapse. The dwelling possessed a low strength to weight ratio (V/W) of 1.18 in this direction. The superstructure caused the dwelling to perform poorly in this direction due to the upper story walls experiencing sequential collapse starting from the uphill side. This happened because the floor diaphragm cantilevers outwards from the uphill foundation and the wall lines further away from the uphill anchorage lack sufficient stiffness at the floor diaphragm level to activate the wall resistance. The model had a probability of collapse at MCE (SDC Dmax) of 20.6% which is reasonable considering the conservative secondary anchor assumptions made. The results of this model suggested that primary anchors are effective at addressing the deficiency of a dwelling with a shallow uphill foundation.

13.5.5 Model 6-1H04-M-R2

Model 6-1H04-M-R2 was the first preliminary retrofit model that utilized both primary anchors at the ends of the uphill foundation and secondary anchors at 4' O.C. Downhill wood structural panel cripple wall sheathing was not present.

When the dwelling was loaded in the out-of-hill direction, load was resisted by $\frac{3}{4}$ " threaded rod secondary anchors at 4' O.C and primary anchors at the ends of the uphill foundation. The failure mechanism was upper story collapse due to the anchors providing sufficient strength to the substructure. The dwelling possessed a high strength to weight ratio (V/W) of 1.88 in this direction. See Sections 5.3 and 5.4 for further understanding on the significance of secondary anchors and primary anchors, respectively.

When the dwelling was loaded in the cross-slope direction, load was resisted by $\frac{1}{2}$ " wood to concrete shear anchor bolts at 16" O.C. The failure mechanism was upper story collapse. The dwelling possessed a low strength to weight ratio (V/W) of 1.18 in this direction (The same as for Model 6-1H04-M-R2S.) The cause of the poor performance was the same as for the previous model. To address this issue, downhill WSP sheathing was applied

in the following preliminary retrofit model, 6-1H04-M-R4. (See Section 5.7 for further discussion.) The model had a probability of collapse at MCE (SDC Dmax) of 15.5%, with all collapses occurring in the cross-slope direction within the crawl space, as suggested by the low V/W ratio in this direction.

13.5.6 Model 6-1H04-M-R3

This subsection reviews analysis results for Model 6-1H04-M-R3 which utilized primary anchors at the ends of the uphill foundation, secondary anchors at 4' O.C, and an additional primary anchor located at an interior grade beam (below wall line I4). This model was investigated to see if adding a primary anchor to an interior grade beam would make noticeable impacts on performance. Downhill wood structural panel cripple wall sheathing was not present.

When the dwelling was loaded in the out-of-hill direction, load was resisted by $\frac{3}{4}$ " threaded rod secondary anchors at 4' O.C, primary anchors at the ends of the uphill foundation, and an additional primary anchor at interior grade beam. The failure mechanism was upper story collapse due to the anchors providing sufficient strength to the substructure. The strength of this model was essentially identical to the models without the additional primary anchor (6-1H04-M-R2S in Section 5.4 and 6-1H04-M-R2 in Section 5.5). The main difference was the distribution of anchorage forces and displacement around the interior grade beam. The neighboring secondary anchors are less likely to yield during a seismic event with the additional primary anchor. The dwelling possessed a high strength to weight ratio (V/W) of 1.88 in this direction.

When the dwelling was loaded in the cross-slope direction, load was resisted by $\frac{1}{2}$ " wood to concrete shear anchor bolts at 16" O.C. The failure mechanism was upper story collapse. The dwelling possessed a low strength to weight ratio (V/W) of 1.18 in this direction. Similar to Models 6-1H04-M-R2S (section 5.4) and 6-1H04-M-R2 (Section 5.5), the superstructure caused the dwelling to perform poorly in this direction due to the upper story walls experiencing sequential collapse starting from the uphill side. To address this issue, downhill WSP sheathing was applied in the following preliminary retrofit model, 6-1H04-M-R4. See Section 5.7 for further discussion. The model had a probability of collapse at MCE (SDC Dmax) of 15.1%, which is nearly identical to the probability of collapse of the same model without the additional interior primary anchor (6-1H04-M-R3). This suggests adding an additional primary anchor at interior grade beam has minimal effects on performance.

13.5.7 Model 6-1H010-M-R4

This subsection reviews analysis results for Model 6-1H010-M-R4 which utilized primary anchors at the ends of the uphill foundation, secondary anchors at 4' O.C., and downhill cripple wall WSP sheathing with an 8d @ 4" edge nail schedule. Various nail schedules were considered (Section B.6) but 4" O.C. was ultimately deemed adequate due to it possessing enough lateral stiffness to improve the distribution of loads and reduce the severe stiffness irregularity between the uphill and downhill wall lines below the base-level diaphragm.

This model was investigated to understand the effects of adding WSP sheathing to the downhill cripple walls. As noted for Models 6-1H04-M-R2 and 6-1H04-M-R3 (Sections 5.5 and 5.6), an apparent performance flaw was noted in the cross-slope direction that was the result of the diaphragm cantilevering from the uphill foundation with no additional stiffness or load path along the downhill perimeter. The superstructure caused the dwelling to perform poorly in this direction due to the upper story walls experiencing sequential collapse starting from the uphill side. This was also the first preliminary retrofit model to assume a 0'-10' crawlspace configuration.

When the dwelling was loaded in the out-of-hill direction, load was resisted by $\frac{3}{4}$ " threaded rod secondary anchors at 4' O.C and primary anchors at the ends of the uphill foundation. The failure mechanism was upper story collapse due to the anchors providing sufficient strength to the substructure. The strength of this model is identical to Model 6-1H04-M-R2 due to both models utilized the same anchorage configuration. The dwelling possessed the maximum (as suggested by Model 6-1H0-M-S) strength to weight ratio (V/W) of 1.88 in this direction.

When the dwelling was loaded in the cross-slope direction, load was resisted by $\frac{1}{2}$ " wood to concrete shear anchor bolts at 16" O.C along the uphill foundation and the downhill 10' WSP sheathed cripple wall. The failure mechanism was upper story collapse, but behavior was drastically improved by WSP sheathing being added to the downhill cripple wall. It allowed the superstructure to redistribute the loads and behave more like a system instead of a series of individual wall lines reaching their peak resistance one at a time, starting from the wall line nearest to the uphill foundation. This is because the WSP sheathed downhill cripple wall added stiffness to the floor diaphragm along the downhill side of the dwelling and allowed for improved activation of the upper story walls away from the uphill foundation. Essentially this provided a secondary load path for the loads to move from the base-level diaphragm to the foundation. Besides improving the

performance of the superstructure, the WSP sheathing also offered additional capacity to the dwelling's substructure in this direction. At monotonic peak loading, the uphill anchor bolts resisted approximately 90% more load than the downhill WSP sheathed cripple walls.

The model had a probability of collapse at MCE (SDC Dmax) of 6.0% which met the maximum target of 10%. Adding WSP sheathing to the downhill cripple walls allowed this retrofit technique to reach the primary criterion. Probabilities of collapse cannot be improved much further than this due to the dwelling's upper bound being dependent on the superstructure's capacity. This model experienced upper story collapse in both directions with the superstructure behaving like a system up until collapse, which is ideal behavior. Any improvements beyond this point would be from minor differences in stiffness at the downhill crawl space level (e.g. 4' downhill wall versus 10' downhill wall) impacting the drift distribution at the superstructure level.

13.5.8 Model 6-1H04-M-R5

This subsection reviews analysis results for Model 6-1H04-M-R5, which utilized primary anchors at the ends of the uphill foundation, secondary anchors at 4' O.C., and downhill cripple wall WSP sheathing with an 8d @ 4" edge nail schedule. This model was investigated for comparison against the 0'-10' model which had the same anchorage configuration (6-1H04-M-R4).

When the dwelling was loaded in the out-of-hill direction, the performance was identical to the Model 6-1H04-M-R4 due to the model's possessing identical lateral stiffness in this direction. (See Section 5.7 for out-of-hill results.) When the dwelling was loaded in the cross-slope direction, the model had superior performance when compared to 6-1H010-M-R4 due to the downhill cripple wall being stiffer from being shorter in height. The model has a probability of collapse at MCE (SDC Dmax) of 3.6%. This indicates that one of the critical objectives for retrofitting hillside buildings is to minimize the differences in wall line stiffness between the upper and lower foundation lines.

13.5.9 Model 6-1H04-M-R=1

Model 6-1H04-M-R=1 utilized primary anchors at the ends of the uphill foundation, secondary anchors at 6'-8" O.C., and downhill cripple wall WSP sheathing with an 8d @ 4" edge nail schedule. This model was designed with anchorage capacities that were scaled to an R value of 1 when using Equations 12.8-1 and 12.8-2 in ASCE 7-10 (ASCE, 2010). The primary anchors, secondary anchors, and shear anchors were each expected to be

capable of resisting the full base shear. For example, the base shear was divided by the total number of equally spaced secondary anchors to determine the required capacity of the individual secondary anchors. This model was investigated for comparison against models that assume different R values and a steeper hillside slope (i.e. 0'-10').

When the dwelling was loaded in the out-of-hill direction, load was resisted by ¾" threaded rod secondary anchors at 6'-8" O.C and primary anchors at the ends of the uphill foundation. The failure mechanism was upper story collapse due to the anchors providing significant strength to the substructure. The dwelling possessed a very high strength to weight ratio (V/W) of 1.82 in this direction, which was limited by superstructure performance.

When the dwelling was loaded in the cross-slope direction, load was resisted by ½" wood to concrete shear anchor bolts at 16" O.C and the downhill 4' WSP sheathed cripple wall. The failure mechanism was upper story collapse and the behavior was drastically improved by WSP sheathing being added to the downhill cripple wall. At monotonic peak loading, the uphill anchor bolts resisted approximately 50% more load than the downhill WSP sheathed cripple walls. The dwelling possessed a high strength to weight (V/W) ratio of 1.56 in this direction and was limited by superstructure performance. The results of this model suggested that using an R value of 1 for the design of the anchorage elements was effective. The model had a very low probability of collapse at MCE (SDC Dmax) of 4.3%. Probabilities of collapse cannot be improved much further than this due to the dwelling's upper bound being dependent on the superstructure's capacity. This model experienced upper story collapse in both directions with the superstructure behaving like a system up until collapse which is ideal behavior. %. This indicates that one of the critical objectives for retrofitting hillside buildings is to minimize the differences in wall line stiffness between the upper and lower foundation lines.

13.5.10 Model 6-1H010-M-R=1

Model 6-1H010-M-R=1 utilized primary anchors at the ends of the uphill foundation, secondary anchors at 6'-8" O.C., and downhill cripple wall WSP sheathing with an 8d @ 4" nail schedule. This model was designed with anchorage capacities that correspond with a R value of 1 per Equations 12.8-1 and 12.8-2 in ASCE 7-10 (ASCE, 2010). (See Section 5.9 for further discussion on the scaling of anchorage capacities.) This model was investigated for comparison against models that assume different R values and a more gradual hillside slope (i.e. 0'-4').

When the dwelling was loaded in the out-of-hill direction, load was resisted by $\frac{3}{4}$ " threaded rod secondary anchors at 6'-8" O.C and primary anchors at the ends of the uphill foundation. The failure mechanism was upper story collapse due to the anchors providing sufficient strength to the substructure. The dwelling possessed a very high strength to weight ratio (V/W) of 1.83 in this direction and was limited by superstructure performance.

When the dwelling was loaded in the cross-slope direction, load was resisted by $\frac{1}{2}$ " wood to concrete shear anchor bolts at 16" O.C and the downhill 10' WSP sheathed cripple wall. The failure mechanism was upper story collapse but behavior was drastically improved by WSP sheathing being added to the downhill cripple wall. The dwelling possessed a high strength to weight ratio (V/W) of 1.56 in this direction. Besides improving the performance of the superstructure, the WSP sheathing also offered additional capacity to the dwelling's substructure in this direction. At monotonic peak loading, the uphill anchor bolts resisted approximately 89% more load than the downhill WSP sheathed cripple walls. The model had a probability of collapse at MCE (SDC Dmax) of 6.9% which met the maximum target of 10%. Similar to the other model with anchorage capacities scaled to R=1 (6-1H04-M-R=1), performance cannot be improved much further than this due to the dwelling's upper bound being dependent on the superstructure's capacity. This indicates that one of the critical objectives for retrofitting hillside buildings is to minimize the differences in wall line stiffness between the upper and lower foundation lines.

13.5.11 Model 6-1H010-M-R=2

Model 6-1H010-M-R=2 utilized primary anchors at the ends of the uphill foundation, secondary anchors at 6'-8" O.C, and downhill cripple wall WSP sheathing with an 8d @ 4" nail schedule. This model was designed with anchorage capacities that correspond to a R value of 2 when using Equations 12.8-1 and 12.8-2 in ASCE 7-10 (ASCE, 2010). (See Section 5.9 for further discussion on the scaling of anchorage capacities.) For example, the base shear was divided by the total number of equally spaced secondary anchors to determine the required capacity of the secondary anchors. This model was investigated for comparison against the R=1 models (Sections 5.9 and 5.10) to see if adequate performance could still be achieved with a lower R value of 2 (i.e., assuming some inelastic response to the anchorage.)

When the dwelling was loaded in the out-of-hill direction, load was resisted by secondary anchors at 6'-8" O.C and primary anchors at the ends of the uphill foundation. The failure mechanism was fracture of the secondary and primary anchorage. The dwelling possessed a moderate strength to weight

ratio (V/W) of 1.10 in this direction, which was significantly lower than the V/W ratio of 1.83 for the R=1 model (6-1H010-M-R=1), suggesting that this model would have inferior dynamic performance in this direction.

When the dwelling was loaded in the cross-slope direction, load was resisted by $\frac{1}{2}$ " wood to concrete shear anchor bolts at 32" O.C and the downhill 10' WSP sheathed cripple wall. The failure mechanism was failure of the uphill shear anchors followed by collapse of the downhill cripple walls. The dwelling possesses a moderate strength to weight (V/W) ratio of 1.20 in this direction, which was also lower than the V/W ratio of 1.56 for the R=1 model (6-1H010-M-R=1). The model had a probability of collapse at MCE (SDC Dmax) of 24.3% which suggested that using an R value of 2 to design all the anchorage elements is not an effective retrofit approach.

13.5.12 Model 6-1H04-M-R=M2

Model 6-1H04-M-R=M2 utilized primary anchors at the ends of the uphill foundation, secondary anchors at 4'-0" O.C, shear anchors at 16" O.C., and downhill cripple wall WSP sheathing with an 8d @ 4" edge nail schedule. The primary anchors and shear anchors were designed with an R value of 2, and the secondary anchors were designed with an R of 1. This model was investigated for comparison against models that assumed different R values and a steeper sloped hillside (i.e. 0'-10').

When the dwelling was loaded in the out-of-hill direction, load was resisted by the secondary and primary anchors. The failure mechanism was fracture of the secondary anchorage starting at the center of the uphill foundation, where the stiffest interior wall line resided. The dwelling possessed a high strength to weight ratio (V/W) of 1.83 in this direction. This V/W ratio suggested that this model would perform well dynamically in this direction.

When the dwelling was loaded in the cross-slope direction, load was resisted by $\frac{1}{2}$ " wood to concrete shear anchor bolts at 32" O.C and the downhill 4' WSP sheathed cripple wall. The failure mechanism was failure of the uphill shear anchors followed by collapse of the downhill cripple walls. The dwelling possessed a low strength to weight (V/W) ratio of 1.22 in this direction, which was lower than the V/W ratio of 1.57 for the R=1 model (6-1H04-M-R=1). The model had a probability of collapse at MCE (SDC Dmax) of 6.8% which suggested that using an R value of 2 to for the shear anchors was effective for dwellings with this hillside slope. However, as discussed in Section 5.13, this was not found to be an effective assumption for dwellings with a greater hillside slope.

13.5.13 Model 6-1H010-M-R=M2

Model 6-1H010-M-R=M2 utilized primary anchors at the ends of the uphill foundation, secondary anchors at 4-0" O.C., shear anchors at 16" O.C., and downhill cripple wall WSP sheathing with an 8d @ 4" edge nail schedule. The primary anchors and shear anchors were designed with an R value of 2, and the secondary anchors were designed with an R of 1. This model was investigated for comparison against models that assumed different R values and a shallower sloped hillside (i.e. 0'-4').

When the dwelling was loaded in the out-of-hill direction, load was resisted by the secondary and primary anchors. The failure mechanism was fracture of the secondary anchorage starting at the center of the uphill foundation, where the stiffest interior wall line resided. The dwelling possessed a high strength to weight ratio (V/W) of 1.81 in this direction. This V/W ratio suggested that this model would perform well dynamically in this direction.

When the dwelling was loaded in the cross-slope direction, load was resisted by ½" wood to concrete shear anchor bolts at 32" O.C and the downhill 10' WSP sheathed cripple wall. The failure mechanism was failure of the uphill shear anchors followed by collapse of the downhill cripple walls. The dwelling possessed a low strength to weight (V/W) ratio of 1.20 in this direction, which was lower than the V/W ratio of 1.56 for the R=1 model (6-1H010-M-R=1). The model had a probability of collapse at MCE (SDC Dmax) of 24.3%, which suggested that using an R value of 2 for the shear anchors was ineffective for dwellings with this hillside slope.

13.5.14 Model 6-1H04-M-R=M1

Model 6-1H04-M-R=M1 utilized primary anchors at the ends of the uphill foundation, secondary anchors at 4-0" O.C., shear anchors at 16" O.C., and downhill cripple wall WSP sheathing with an 8d @ 4" edge nail schedule. The primary anchors were designed with an R value of 2, the secondary and shear anchors were designed with an R of 1. This model was investigated for comparison against models that assumed different R values and steeper sloped hillsides (i.e. 0'-10' and 0'-16').

When the dwelling was loaded in the out-of-hill direction, load was resisted by the secondary and primary anchors. The failure mechanism was fracture of the secondary anchorage starting at the center of the uphill foundation, where the stiffest interior wall line resided. The dwelling possessed a high strength to weight ratio (V/W) of 1.78 in this direction. This V/W ratio suggested that this model would perform well dynamically in this direction.

When the dwelling was loaded in the cross-slope direction, load was resisted by ½” uphill shear anchor bolts at 16” O.C and the downhill 4’ WSP sheathed cripple wall. The monotonic failure mechanism was upper story collapse. The dwelling possesses a high strength to weight (V/W) ratio of 1.58 in this direction. Similar to the out-of-hill direction, this V/W ratio, suggested that this model would also perform well dynamically in this direction. The model had a low probability of collapse at MCE (SDC Dmax) of 4.8%. The results of this model suggested that this assignment of R-values used for design of the different anchorage elements is optimal in terms of cost to performance.

13.5.15 Model 6-1H010-M-R=M1

Model 6-1H010-M-R=M utilized primary anchors at the ends of the uphill foundation, secondary anchors at 4-0” O.C, shear anchors at 16” O.C., and downhill cripple wall WSP sheathing with an 8d @ 4” edge nail schedule. The primary anchors were designed with an R value of 2, the secondary and shear anchors were designed with an R of 1. This model was investigated for comparison against models that assume different R values and varying sloped hillsides (i.e. 0'-4' and 0'-16').

When the dwelling is loaded in the out-of-hill direction, load was resisted by the secondary and primary anchors. The failure mechanism was fracture of the secondary anchorage starting at the center of the uphill foundation, where the stiffest interior wall line resided. The dwelling possessed a high strength to weight ratio (V/W) of 1.79 in this direction. This V/W ratio suggested that this model would perform well dynamically in this direction.

When the dwelling was loaded in the cross-slope direction, load was resisted by uphill shear anchor bolts at 16” O.C and the downhill 4’ WSP sheathed cripple wall. The monotonic failure mechanism was upper story collapse. The dwelling possessed a high strength to weight (V/W) ratio of 1.56 in this direction. Similar to the out-of-hill direction, this V/W ratio suggested that this model would also perform well dynamically in this direction. The model had a probability of collapse at MCE (SDC Dmax) of 7.4%. Similar to the 0'-4' and 0'-16' counterpart models (6-1H04-M-R=M1 and 6-1H016-M-R=M1), the results of this model suggested that this assignment of R-values to the design of the different anchorage elements is optimal in terms of cost to performance.

13.5.16 Model 6-1H016-M-R=M1

Model 6-1H016-M-R=M utilized primary anchors at the ends of the uphill foundation, secondary anchors at 4-0” O.C, shear anchors at 16” O.C., and

downhill cripple wall WSP sheathing with an 8d @ 4" edge nail schedule. The primary anchors were designed with an R value of 2, the secondary and shear anchors were designed with an R of 1. This model was investigated for comparison against models that assume different R values and lower sloped hillsides (i.e. 0'-4' and 0'-10').

When the dwelling was loaded in the out-of-hill direction, load was resisted by the secondary and primary anchors. The failure mechanism was fracture of the secondary anchorage starting at the center of the uphill foundation, where the stiffest interior wall line resided. The dwelling possessed a high strength to weight ratio (V/W) of 1.77 in this direction, suggesting that the dwelling would perform well dynamically in this direction.

When the dwelling was loaded in the cross-slope direction, load was resisted by uphill shear anchor bolts at 16" O.C and the downhill 4' WSP sheathed cripple wall. The monotonic failure mechanism was upper story collapse. The dwelling possessed a high strength to weight (V/W) ratio of 1.54 in this direction. Similar to the out-of-hill direction, this high V/W ratio suggested that the dwelling would perform well dynamically in this direction. The model has a probability of collapse at MCE (SDC Dmax) of 10.6%, which is just above the target collapse margin of 10%. Similar to the 0'-4' and 0'-10' counterpart models (6-1H04-M-R=M1 and 6-1H010-M-R=M1), the results of this model suggested that this assignment of R-values to the different anchorage elements is optimal in terms of cost to performance.

13.5.17 Model 6-1H016-M-R=M1R

Model 6-1H016-M-R=M utilized primary anchors at the ends of the uphill foundation, secondary anchors at 4-0" O.C, shear anchors at 16" O.C., and downhill cripple wall WSP sheathing with an 8d @ 4" edge nail schedule. The primary anchors were designed with an R value of 2, the secondary and shear anchors were designed with an R of 1. This model was investigated for direction comparison against Model 6-1H016-M-R=M1 to see how performance would differ if the long horizontal dimension of the dwelling was rotated to span downhill. This was the only rotated model analyzed, and used the rotated dwelling configuration discussed in Section 3 and illustrated in Figure 13-7.

When the dwelling was loaded in the out-of-hill direction, load was resisted by the secondary and primary anchors. The failure mechanism was fracture of the secondary anchorage starting at the center of the uphill foundation, where the stiffest interior wall line resided. The dwelling possessed a very

high strength to weight ratio (V/W) of 2.16 in this direction, suggesting that the dwelling would perform very well dynamically in this direction.

When the dwelling was loaded in the cross-slope direction, load was resisted by uphill shear anchor bolts at 16" O.C and the downhill 4' WSP sheathed cripple wall. The monotonic failure mechanism was upper story collapse. The dwelling possessed a very low strength to weight (V/W) ratio of 1.00 in this direction. This low V/W ratio suggested that this model would struggle dynamically in this direction. The low V/W ratio was a result of the dwelling behaving similarly to the preliminary retrofit models that did not have WSP sheathing at the downhill crawl space wall (e.g. 6-1H04-M-R-R2). The superstructure caused the dwelling to perform poorly in this direction due to the upper story walls experiencing sequential collapse starting from the uphill side. The stiffness and capacity of the downhill cripple wall was not sufficient with an 8d @ 4" O.C. nail schedule and therefore not as effective as at alleviating the superstructure behavior described in Section 5.5. The model had a probability of collapse at MCE (SDC Dmax) of 24.5%. When compared to the non-rotated counterpart model (6-1H016-M-R=M1), the results of this model suggested that this style of retrofit is not as effective for a dwelling that has its long horizontal dimension spanning downhill. The retrofit would likely require an additional line of lateral resistance halfway between the uphill and downhill foundations.

13.6 Selected Retrofit Design Parameters and Methods

Model performance was evaluated using recommendations outlined in the Part 2. In general, the most significant indicator of performance was probability of collapse at MCE for Seismic Design Category D_{MAX}. This was referred to as the primary performance criterion on the project and is based on the FEMA P695 corrected fragility curve for a model that was evaluated using the procedures outlined in Section 5.1. Additionally, Working Group 6 had a primary criterion performance target objective of less than or equal to 10% for a retrofit model's performance to be deemed adequate and a potential retrofit solution. The second most influential indicator of performance was the probability of exceeding drift thresholds of 0.75% drift at 0.4MCE ($S_a = 0.6g$) and 1.5% drift at DE ($S_a = 1.0g$). These parameters provided insight regarding the potential level of damage from a moderate to design level earthquake. See Part 2 for correspondence between drift ratios and levels of damage to finishes.

Comparing the performance (i.e. primary and secondary criteria) of the existing (pre-retrofit) model against the various R-value retrofit models provided insight for how effective an applied retrofit technique was. A

criteria plot is illustrated in Figure 13-25 that compares the primary and secondary criteria of the hillside retrofit models to the existing condition.

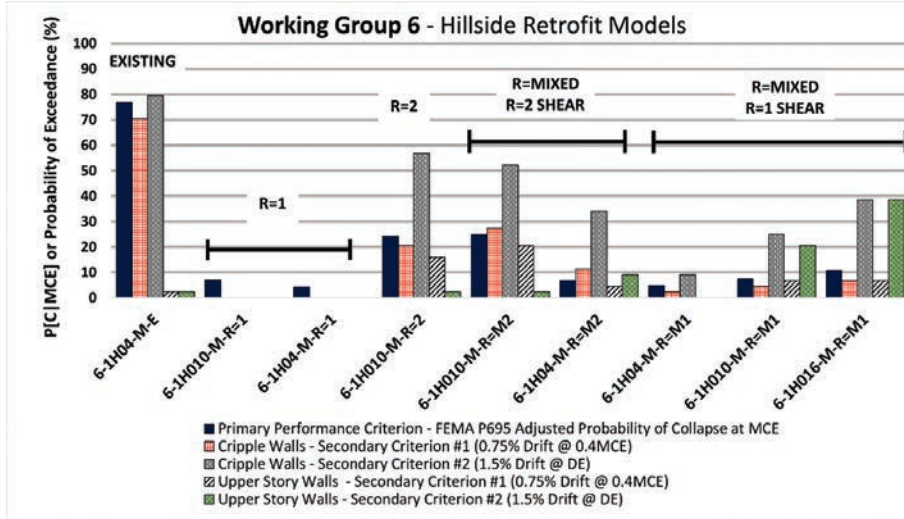


Figure 13-25 Criteria plot for the various hillside retrofit models illustrating performance criteria as discussed in Part 2.

The recommended retrofit method includes primary anchors at the ends of the uphill foundation, equally spaced secondary anchors along the uphill foundation, equally spaced shear anchors along the uphill foundation and downhill WSP sheathed cripple walls (8d at 4"). An R value of 1 was found the most effective for designing the secondary and shear anchors. An R value of 2 was selected for design of the primary anchors. This was found to provide significant improvement in performance, while balancing performance and constructability. Trial designs exploring primary anchors designs using R=1 seismic forces found the resulting anchorage configurations to be unwieldy. This assignment of anchorage R-values corresponds to Models 6-1H04-M-R=M1, 6-1H010-M-R=M1, and 6-1H016-M-R=M1.

13.7 Archived Files

Table 13-4 provides an annotated list of files developed during the course of analytical studies that have been archived for future use. Archived files are documented as FEMA P-1100 Volume 4 and are available by request from the California Earthquake Authority.

Table 13-4 Hillside Dwelling Related Archived Files

Document No.	Original File Name	Date	Title	Description	Original Format	Size
WG6-B1	WG6 Analysis Results	3/5/2018	WG6 Analysis Results	WG6 monotonic and dynamic analysis results.	Excel	2 Pages
WG6-B2	Intermediate Modeling	2/8/2017	ATC-110 Analysis Team: Intermediate Modeling/ Diaphragm Super Elements	Step by step guide on how to create an intermediate model (connectivity, etc.) and statics verification.	PowerPoint	62 Slides
WG6-B3	Cripple Wall vs Hillside Retrofit Transition	7/10/2017	Cripple Wall vs Hillside Retrofit Transition	Monotonic results for transition between cripple wall and hillside retrofit methodologies.	Excel	3 Pages
WG6-B4	Superstructure Configuration 2.22.17	2/2/2017	Working Group 6 Superstructure - Wall Configurations and Masses	Floor plan simplification for intermediate models. Segmented and perforated methods for accounting for openings in T3D.	PowerPoint	29 Slides
WG6-B5	Rob Chai Stepped Cripple Wall Verification	9/5/2016	Rob Chai Stepped Cripple Wall Verification	Stepped cripple wall verification for Timber3D.	PowerPoint	69 Slides
WG6-B6	WG6 Check in - 5.30.17	5/30/2017	Working Group 6 Effects of Downhill Sheathing and Diaphragm Stiffness	Superstructure benefits of adding downhill WSP sheathing to the crawl space. Sensitivity study for diaphragm stiffness on anchorage force distribution.	PowerPoint	47 Slides

13.8 References

ASCE 2010. "Minimum Design Loads for Buildings and Other Structures," ASCE Standard ASCE/SEI 7-10, American Society of Civil Engineers, Reston, VA.

Baker, J.W. [2015] "Efficient Analytical Fragility Function Fitting Using Dynamic Structural Analysis," *Earthquake Spectra*;31 (1): 579-599.

FEMA P1100. 2018. "Volume 1 – Prestandard, Vulnerability-Based Seismic Assessment and Retrofit of One- and Two- Family Dwellings," Prepared by the Applied Technology Council for the Federal Emergency Management Agency, Washington, DC.

FEMA P695. 2009. "Quantification of Building Seismic Performance Factors," Prepared by the Applied Technology Council for the Federal Emergency Management Agency, Washington, DC, 421 p.

FEMA P795. 2011. "Quantification of Building Seismic Performance Factors: Component Equivalency Methodology," Prepared by the

Applied Technology for the Federal Emergency Management Agency,
Washington, DC, 292 p.

Ibarra, L. F., Medina, R. A., and Krawinkler, H. (2005). "Hysteretic models that incorporate strength and stiffness deterioration." *Earthquake Eng. Struct. Dyn.*, 34(12), 1489–1511

Lignos DG and Krawinkler H. Deterioration modeling of steel components in support of collapse prediction of steel moment frames under earthquake loading. *Journal of Structural Engineering (ASCE)* 2011; 137(11): 1291–1302.

Vincent, T. C. 2018. Seismic Retrofitting Downslope Hillside Dwellings with Uphill Anchorage and Cripple Wall Wood Structural Panel Sheathing, A thesis submitted to Washington State University in partial fulfillment of the requirements for the degree of Master of Science, July, 2018.

Part 13; Appendix A

Hillside Dwelling Design Example

The following is an example of a seismic retrofit design for single-family hillside dwellings.

Overview

The following example illustrates design of seismic retrofit for hillside vulnerability in a single-family hillside home. The design example uses the simplified engineered vulnerability-based retrofit method of Section 6.5 of the FEMA P-1100 prestandard.

The vulnerability being addressed is the separation of the dwelling from the uphill foundation, potentially leading to significant damage to or collapse of the dwelling. This vulnerability occurs because the anchorage of the dwelling to the uphill foundation provides the stiffest load path for seismic loading, thus attracting most or all of the dwelling base shear. The uphill anchorage, however, is often both weak and brittle, which can lead to failure. The intent of the retrofit is to help ensure that the dwelling remains anchored to the uphill foundation. As a result, the retrofit design effort is focused on design of anchorage to the foundation and a load path into base-level diaphragm. Also included is strengthening of the side and downhill cripple walls as a secondary bracing system. Strengthening of the dwelling above the main floor, or strengthening of the foundation to soil interface are not included in the retrofit methodology. See FEMA P-1100, Volume 1 for further discussion.

The purpose of this retrofit is promote public safety and welfare by reducing earthquake-induced damage to existing hillside dwellings. Use of this retrofit method is intended to improve earthquake performance, but is not intended to prevent damage.

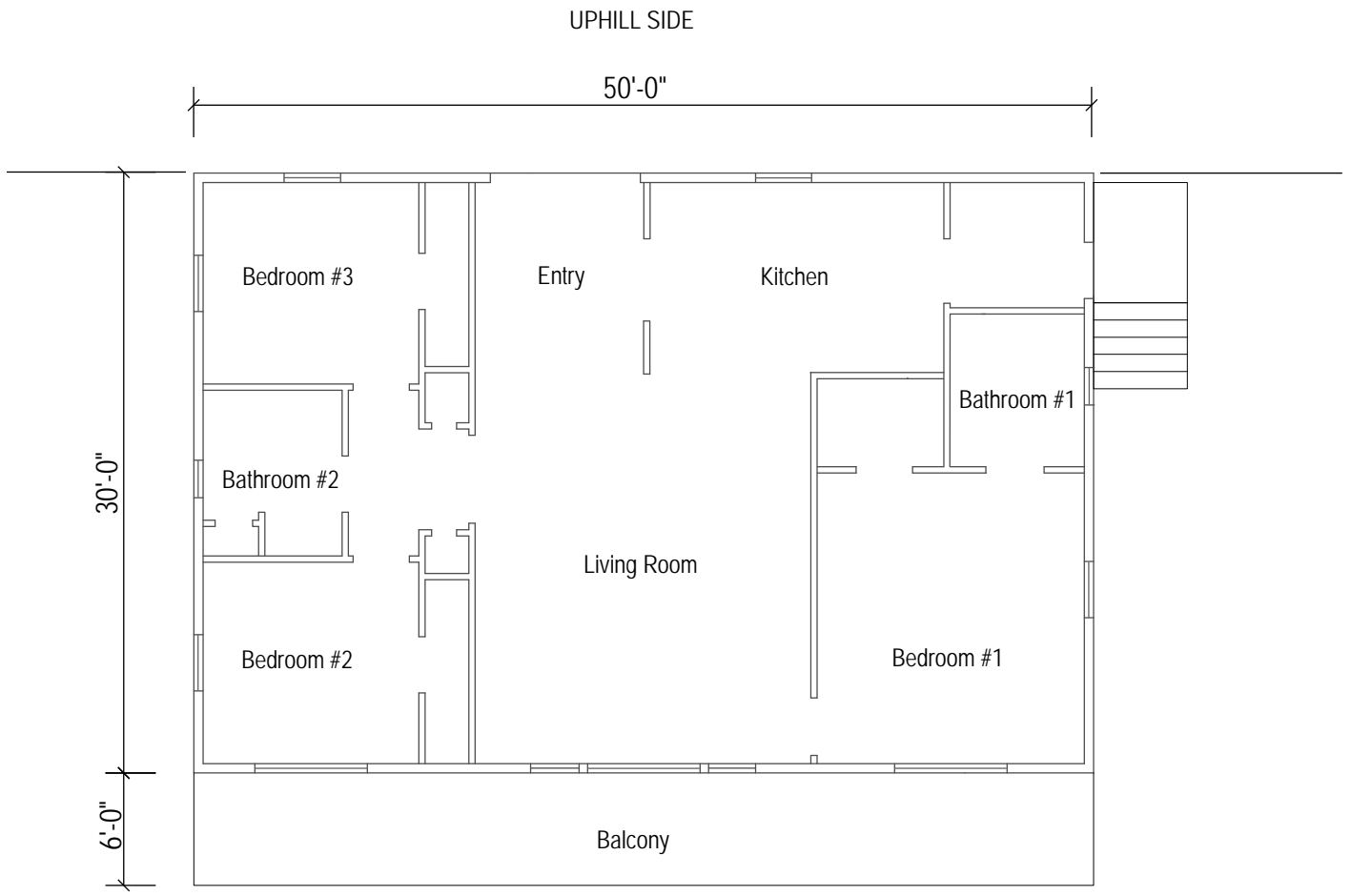
This example problem illustrates one design for hillside dwelling anchorage. A wide range of other design solutions is possible.

Outline

1. Example dwelling configuration
2. Retrofit terminology
3. Eligibility to use Chapter 6
4. Assessment
5. Simplified engineered seismic retrofit introduction
6. Construction materials and dwelling weight
7. Seismic base shears for retrofit
8. Primary anchor forces
9. Secondary anchor forces
10. Shear anchor forces
11. Crawlspace wall forces
12. Design of primary anchors
13. Design of secondary anchors
14. Design of shear anchors
15. Design of crawlspace walls

13A.1. Example dwelling configuration

Figures 13A-1 through 13A-7 show plans and details describing the example dwelling. The example dwelling is a 1500 square foot one story hillside dwelling with a gable roof. The construction materials are defined in Section 6 (construction materials and dwelling weight) of this example document.



DOWNHILL SIDE

Figure 13A-1 First floor plan

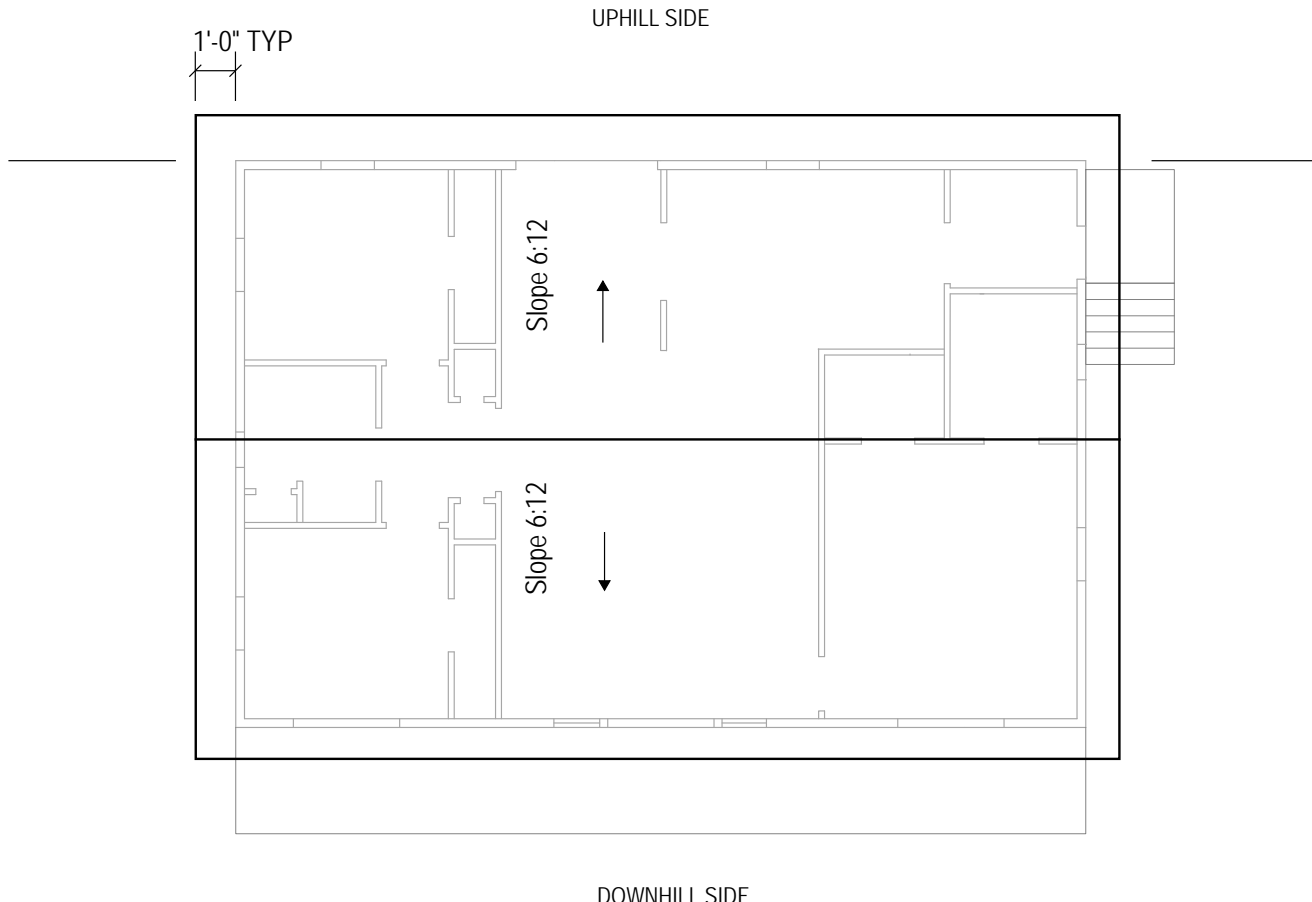


Figure 13A-2 Roof plan

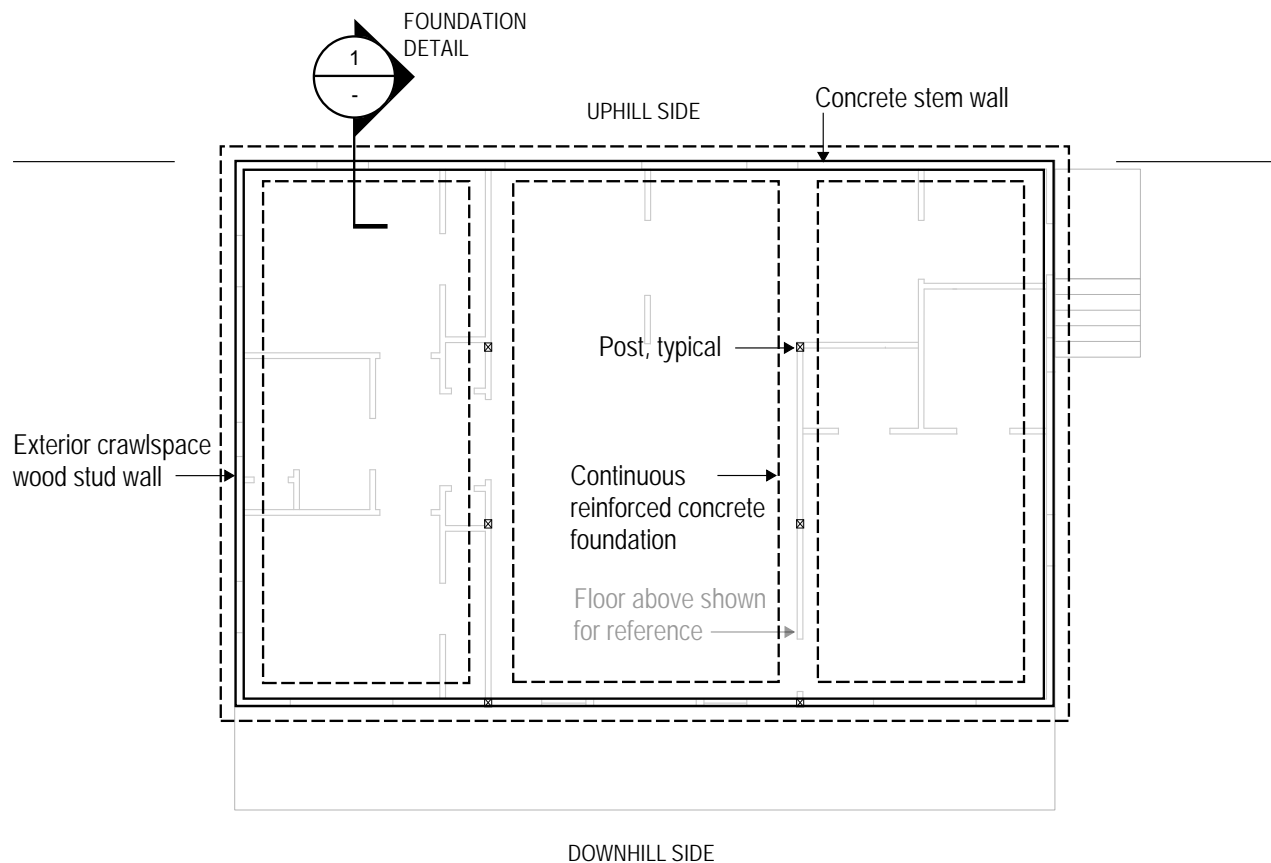


Figure 13A-3 Foundation and crawlspace plan

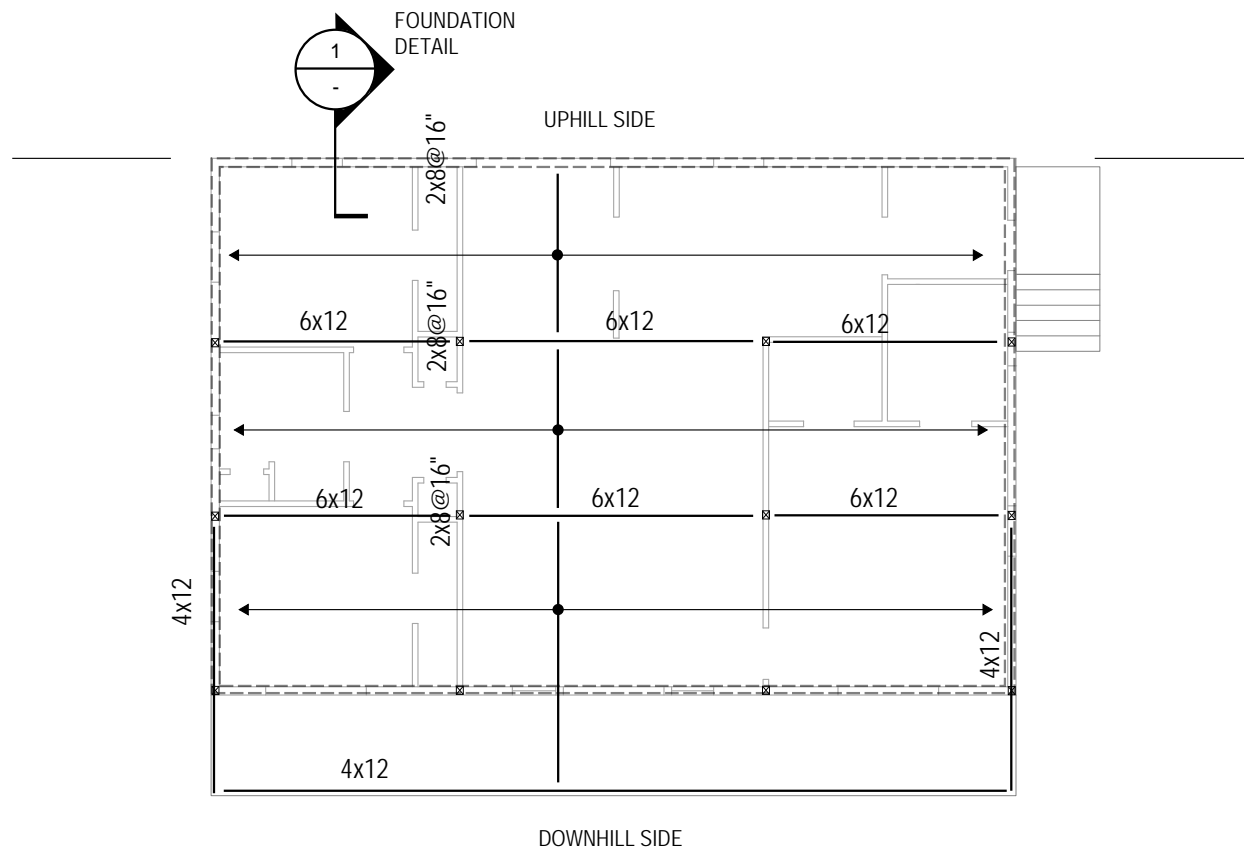


Figure 13A-4 First floor framing plan

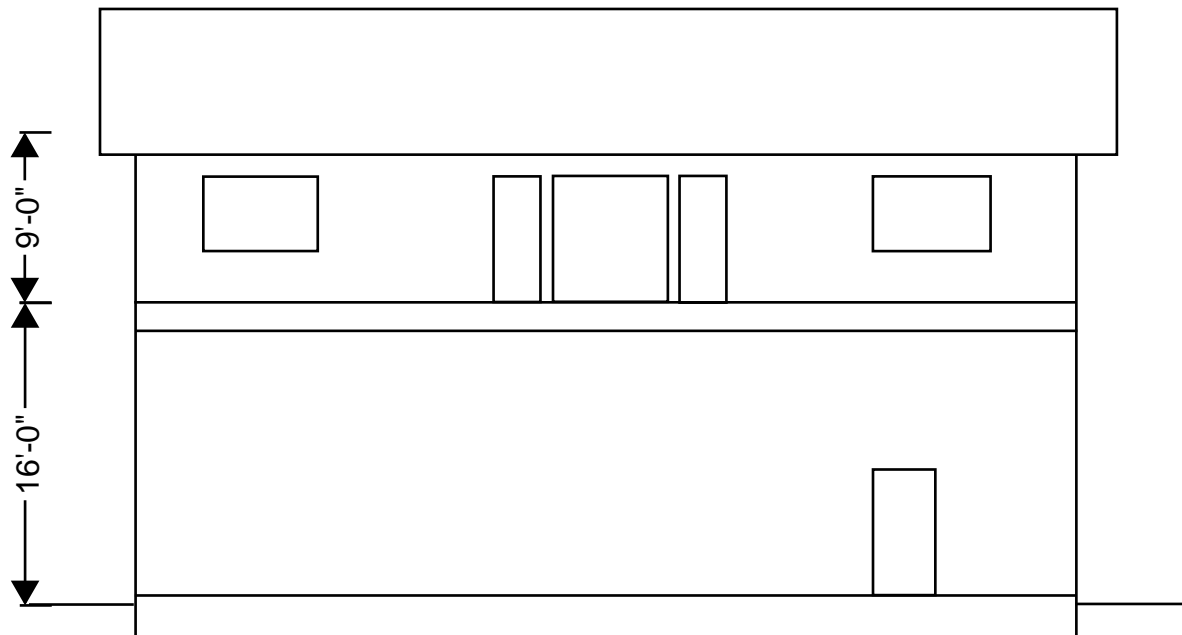


Figure 13A-5 Downhill elevation

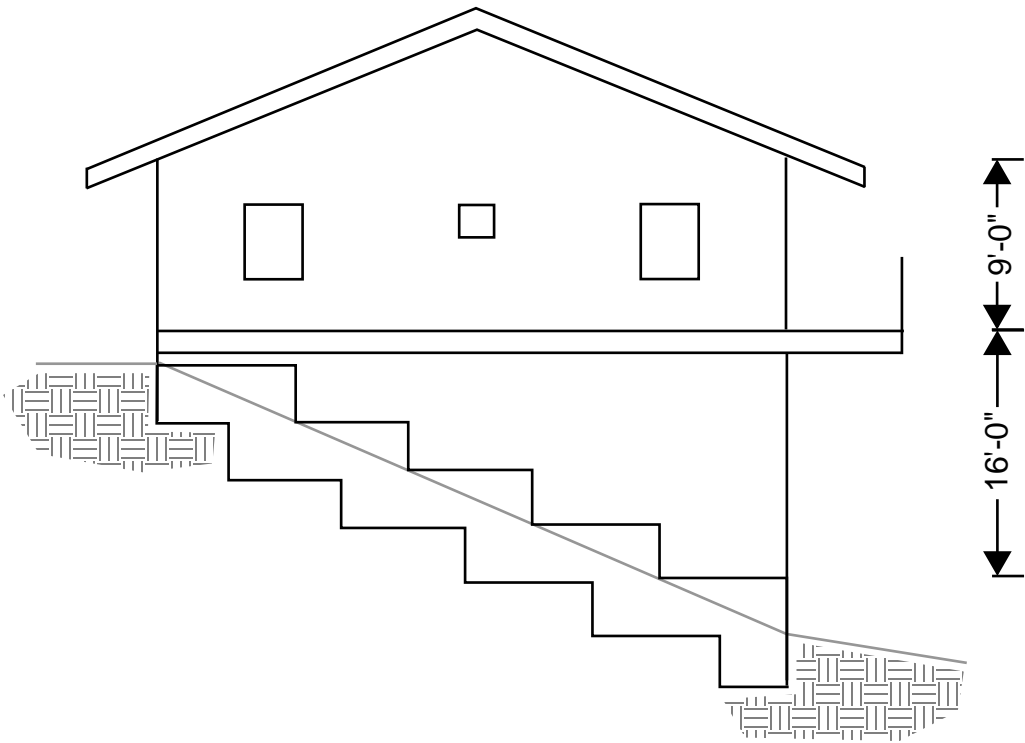


Figure 13A-6 Cross slope elevation

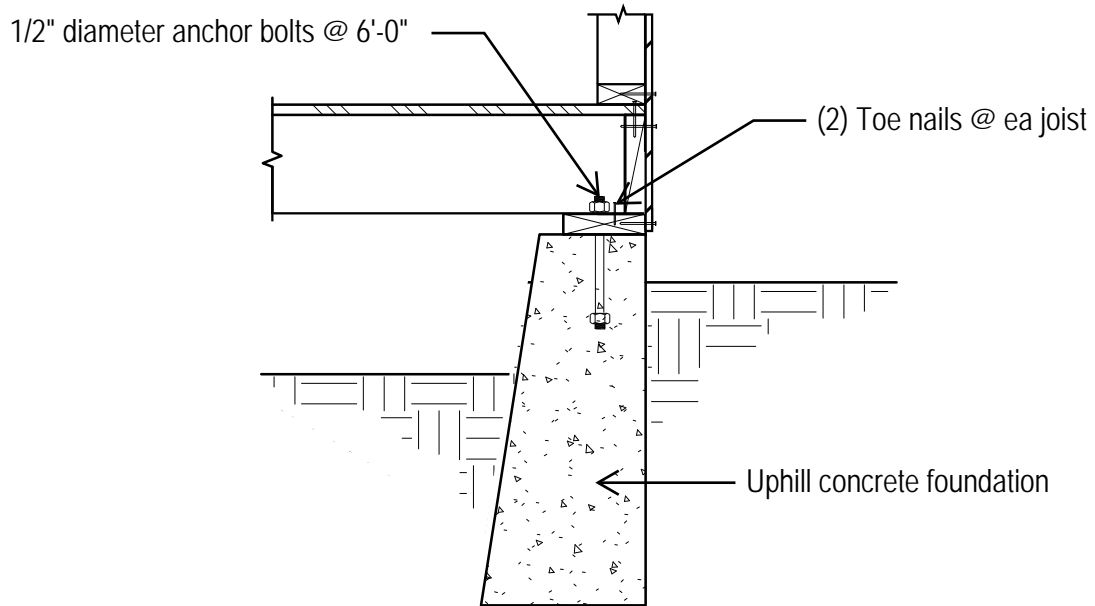


Figure 13A-7 Existing uphill foundation section

13A.2. Retrofit Terminology

The terminology and design concepts used in assessment and retrofit of hillside dwellings are very unique to this dwelling type. It is helpful to become familiar with this terminology prior to proceeding with this design example. Because of this the following is a brief introduction of these terms and concepts. For more detail see the prestandard provisions and commentary. The terminology is summarized below and illustrated in Figures 13A-8 through 13A-10.

BASE-LEVEL DIAPHRAGM. In a hillside dwelling, the framed floor at or closest in elevation to the level of the uphill foundation.

CROSS-SLOPE LOADING. In a hillside dwelling, horizontal seismic loading in the direction parallel to the uphill foundation and generally parallel to grade elevation contours. Cross-slope loading is perpendicular to out-of-hill loading.

HILLSIDE DWELLING. A dwelling in which: (1) the space below the lowest framed floor is predominantly unoccupied, including area enclosed by crawlspace walls, open areas, or a combination of the two; (2) the tallest crawlspace cripple wall clear height exceeds 7'-0" (or post and beam system post height exceeds 7'-0" when underfloor area is not enclosed); (3) when averaged across the full length or width of the dwelling the grade slope exceeds 1 vertical in 5 horizontal; and (4) where a wood light-frame crawlspace wall occurs between the base-level diaphragm and uphill foundation, the height of this crawlspace wall does not exceed 2'-0".

OUT-OF-HILL LOADING (Down-hill loading). In a hillside dwelling, horizontal seismic loading parallel to the direction of descending grade, acting into or away from the hillside.

PRIMARY ANCHOR [LABC, modified]. In hillside dwellings, an anchor located at base level diaphragm ends and offsets or transitions and providing direct connection between the base-level diaphragm and the uphill foundation. Primary loading is tension in the out-of-hill direction, due to either to direct tension or torsion from cross-slope loading.

SECONDARY ANCHOR [LABC, modified]. In hillside dwellings, regularly spaced anchors providing redundant, distributed connections between the base-level diaphragm and the uphill foundation. Primary loading is in tension from downhill loading.

SHEAR ANCHOR. In hillside dwellings, an anchor connecting the base level diaphragm along the length of the uphill foundation. The primary loading is shear parallel to the uphill foundation.

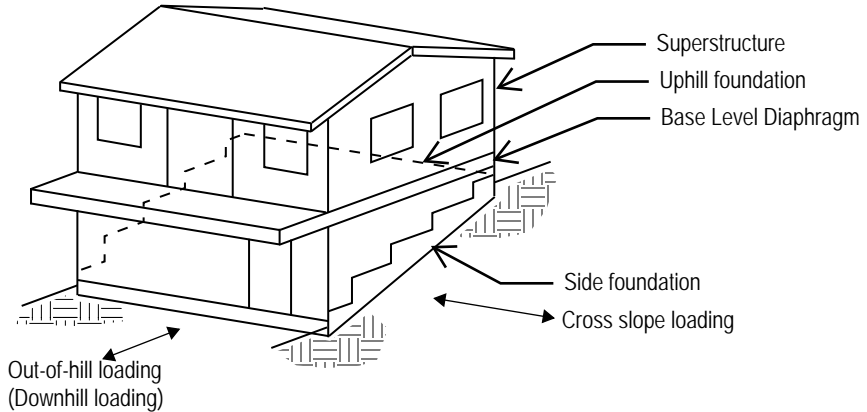


Figure 13A-8 Hillside dwelling isometric with applicable terminology

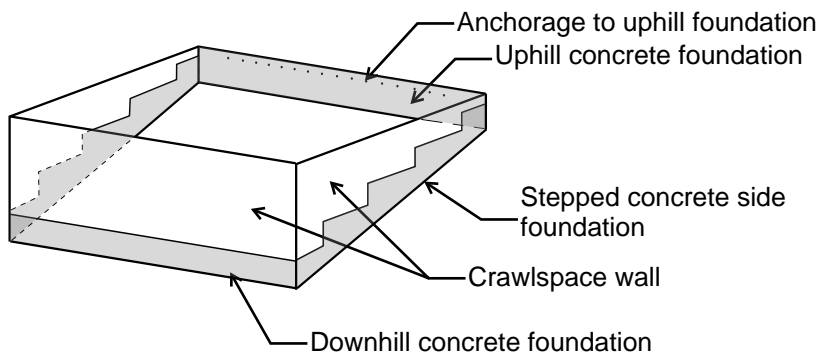


Figure 13A-9 Hillside dwelling schematic isometric of dwelling. (FEMA P-1100 Volume 1, Figure 6.1-2)

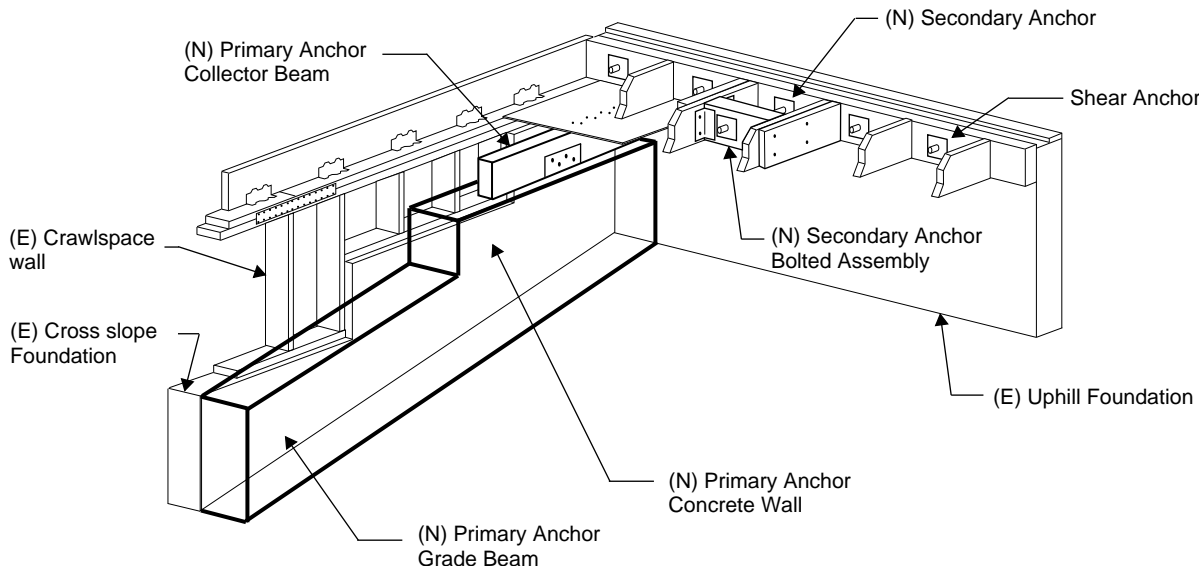


Figure 13A-10 Interior uphill foundation corner isometric showing primary anchors, secondary anchors, and shear anchors. (FEMA P-1100 Volume 1, Figure 6.5-1)

13A.3. Eligibility to Use Prestandard Chapter 6

In order to use Prestandard Chapter 6, the hillside dwelling must conform to the minimum requirements specified in Tables 1.8-1 and 6.1-1 of the Prestandard. Below are Tables 1.8-1 and 6.1-1 with qualifications for an example dwelling to be in compliance. The eligibility requirements are derived from either limitations of the study or limitations on behavior factors of a hillside dwelling.

Table 13A-1 Example Dwelling Compliance with Eligibility Requirements (from Volume 1, Table 1.8-1)

Eligibility Criteria	Compliance for Example Dwelling
1. The dwelling is a detached <i>one- or two-family dwelling</i> or the dwelling is a unit in a <i>townhouse</i> and assessment and retrofit will occur for each attached townhouse unit (the full <i>townhouse structure</i>).	The example dwelling is detached from any other structure.
2. The dwelling is of wood <i>light-frame construction</i> .	The example dwelling is of wood light-frame construction.
3. The weight of the exterior wall finish does not exceed 10 psf, except that masonry veneer wainscots supported on concrete or masonry foundations are permitted to extend up to four feet above the top of foundation	The exterior finish is stucco and weighs 10 psf.

Table 13A-2 Example Dwelling Compliance with Eligibility Requirements (from Volume 1, Table 6.1-1)

Eligibility Criteria		Compliance for Example Dwelling
1.	The dwelling is a hillside dwelling, as defined in Chapter 2.	The example dwelling is a hillside structure as defined in Chapter 2 of the Prestandard. The space below the base level diaphragm is unoccupied, the area is enclosed by crawlspace walls, the downhill wall is taller than 7 feet, the grade is 1 vertical to 2 horizontal, and there is no cripple wall on top of the uphill foundation.
2.	The dwelling is a detached <i>one- or two-family dwelling</i> or the dwelling is a unit in a <i>townhouse</i> and assessment and retrofit will occur for each attached townhouse unit (the full <i>townhouse structure</i>).	The example dwelling is detached from any other structure.
3.	The dwelling is two stories or less above the base-level diaphragm.	The example dwelling is one story above the base-level diaphragm.
4.	The dwelling is of wood <i>light-frame construction</i> .	The example dwelling is of wood light-frame construction.
5.	Existing perimeter walls below the base-level diaphragm are of wood light-frame construction, or a combination of wood light-frame and concrete construction.	The example dwelling perimeter walls below the base-level diaphragm are a combination of wood and concrete construction.
6.	Existing perimeter walls below the base-level diaphragm are supported on a continuous concrete foundation or will be retrofit to be supported on a continuous foundation. Continuous foundation includes continuous perimeter spread footing with stem wall, or continuous grade beams or tie-beams supported on pier or caisson foundations with or without continuous concrete piers.	The example dwelling exterior crawlspace walls are supported by a continuous concrete foundation.
7.	The clear height of the tallest crawlspace stud wall does not exceed 16 feet.	The example dwelling tallest wall is 16 feet.
8.	The site slope as measured along the sides of the dwelling, starting from the highest uphill point to the lowest downhill point exceeds 1 to 5 (vertical to horizontal).	The example dwelling slope is 15 feet vertical to 30 feet horizontal = 1:2, which is steeper than 1:5.
9.	The <i>base-level diaphragm</i> is of wood light-frame construction and is entirely in one plane without vertical offsets, such as a step in the floor or <i>split level</i> .	The example dwelling base-level diaphragm is in one plane. There is no split level.
10.	The garage is detached from the dwelling.	The example dwelling garage is detached.
11.	The exterior framed walls immediately above the uphill foundation sit directly above the uphill foundation for not less than 75% of the uphill foundation length.	In the example dwelling there are exterior walls directly above the uphill foundation, so 100% of the uphill foundation length has exterior framed walls immediately above them.
12.	No masonry chimney is attached to the side of the dwelling, extends through the dwelling, or sits on any floor level of the dwelling.	There is no masonry chimney in the example dwelling.

Summary of eligibility

After review of Tables 13A-1 and Table 13A-2 the example dwelling is found to comply with Section 6.2 of the Prestandard and is eligible to comply with Section 6.3 of the Prestandard.

13A.4. Assessment

Section 6.3 of the Prestandard addresses assessment of the dwelling. The dwelling is assessed to determine if retrofit is required, and what scope of retrofit is required to conform to the Prestandard. This assessment occurs in two parts: assessment of the base-level diaphragm anchorage to the uphill foundation, and assessment of the cripple walls and foundations on the other sides of the dwelling.

Assessment of the base-level diaphragm anchorage is in accordance with Section 6.3.3. This requires that a registered design professional determines if there are existing primary, secondary and shear anchors that would meet the requirements of the retrofit provisions of the prestandard. While this is not expected to commonly occur, it may occur on occasion. This will generally require that each primary anchor is capable of resisting 25 percent of the building tributary weight times the site specific spectral acceleration (S_{DS}), and secondary and shear anchors resist the tributary building weight times S_{DS} . For the purposes of this example, the registered design professional found that anchorage at the uphill foundation lacked any primary, secondary anchors, and shear anchors, and so retrofit is required.

The other portion of the assessment addresses the crawlspace walls, their anchorage to the foundation and base level diapghram, as well as sheathing of the crawlspace walls. Section 6.3.2 reviews general conditions of the dwelling below the base-level diaphragm by referencing Section 8.1 for foundation assessment, Section 8.2 for anchorage assessment, Section 8.3 for crawlspace wall sheathing assessment, and Section 8.4 for crawlspace attachment to the base level diaphragm. In this design example the crawlspace walls do not have wall sheathing, and so retrofit is required.

Summary of assessment

The example dwelling is missing primary, secondary, and shear anchors from the base level diaphragm to the foundation. The example dwelling is also lacking wall sheathing in the crawlspace walls. Retrofit is required for the example dwelling.

13A.5. Simplified Engineered Seismic Retrofit Introduction

The simplified engineering methodology outlined in Section 6.5 limits the scope to the single targeted vulnerability of connecting the base level diaphragm to the foundation as well establishing a load path for the framed crawlspace walls. The methodology requires certain elements, primary anchor, secondary anchor, shear anchors, and crawlspace walls to be designed for specific forces. The design forces are based on ASCE 7 equivalent lateral force procedure through the use of equation $V = S_{DS} * W / R$ as defined in Section 6.5.2.2. The list of specific elements requiring design are mentioned are separate Sections 6.5.4.1 through 6.5.4.3, and 6.5.5.

The following steps will demonstrate how to find the weight of the building, how to find the design load for each specific element, and provide an example on how to design the elements once the design loads are found.

13A.6. Construction Materials and Dwelling Weight

The objective is to calculate the weight of the building tributary to the base level diaphragm. This includes the weight of the superstructure, the weight of the base level diaphragm, and half the weight of the crawlspace walls.

13A.6.1. Unit Weight of Dwelling Assemblies

The first step is to determine the weight of the dwelling assemblies. Reference weights for different finishes of the roof, floor, exterior walls, and interior walls can be found in Appendix L of the Prestandard. The table's specific to the example dwelling will be selected and used to determine the weight of the dwelling's assemblies. The total load in the tables specify the total weight in pounds per square foot (psf) of the specific assemblies of the building. These tables provide a good reference point for assembly weights and can be used as a point of reference to develop loads specific to the dwelling.

This example dwelling contains the following different material finishes:

Roofing Finish = Composite or Shingle Roofing

Floor Finish = Wood flooring

Exterior Siding Finish = Stucco

Interior Wall Finish = Plaster on wood lath

The following are tables from Appendix L of the Prestandard which match the example dwelling finishes

Table 13A-3 Suggested Roof Design Dead Loads—Gravity/Seismic Flat Weight Takeoff (psf) (from Volume 1, Table L-1)

Roof Medium (Type 1)	
Material	Seismic Weight (psf)
Roofing (Asphalt Shingles- max 2 layers)	4.0
Solar / other	0.0
Topping	0.0
1x skip sheathing + new 1/2 sheathing	2.0
Insulation	0.5
M.E.P.	0.5
Wood lath and 1" gypsum plaster (1 side)	8.0
Ceiling joists (2x6 @24")	1.0
Roof rafters (2x8 @24")	1.3
Girders (4x8 @ 8')	0.8
Columns	0.0
Misc.	0.4
Dead Load	18.5

← Matches roof finish

← Matches interior finish

Table 13A-4 Suggested Floor Design Dead Loads (from Volume 1, Table L-2)

1st Floor (no ceiling finish at underside of floor framing)	
Material	Seismic Weight (psf)
Floor finish**(assumes 7/8" hardwood)	3.6
Other	0.0
Topping	0.0
Sheathing / (assume 1" horiz. Lumber)	2.3
Insulation	0.5
M.E.P.	0.5
Ceiling (unfinished)	0.0
Sprinklers	0.0
Joists (2x8 @ 16")	1.9
Girders (4x12@ 8')	1.2
Columns	0.0
Tile	2.0
Misc.	0.0
Dead Load	12.0

← Matches floor finish

* Use 6 psf for areas with tile or other heavy floor finish.

**Use 2 psf for tile (6 psf is unit weight).

Table 13A-5 Suggested Exterior Wall Design Dead Loads (from Volume 1, Table L-3)

EXTERIOR - Heavy (Type 4)	
Material	Weight (psf)
Stucco (7/8" thick one side)	10.0
1" lumber siding and waterproofing	2.7
2x4 @ 16"oc	1.0
Insulation	0.5
Wood lath and 1" gypsum plaster (1 side)	8.0
Misc.	0.8
TOTAL	23.0

← Matches exterior finish

← Matches interior finish

Table 13A-6 Suggested Exterior Cripple Wall Design Dead Loads (from Volume 1, Table L-4)

EXTERIOR Cripple Wall – Heavy Retrofitted	
Material	Weight (psf)
Stucco (7/8" thick one side)	10.0
1" lumber siding and waterproofing	2.7
2x4 @ 16"oc	1.0
1/2 in Plywood	2.0
Misc.	0.3
TOTAL	16.0

← Matches exterior finish

Table 13A-7 Suggested Interior Wall Design Dead Loads (from Volume 1, Table L-5)

INTERIOR - Heavy	
Material	Weight (psf)
Wood Lath and 1" Gypsum Plaster (2 sides)	16.0
2x4 @ 16"oc	1.0
Insulation	0.0
MEP	0.4
Misc.	0.6
TOTAL	18.0

← Matches interior finish

Summary of Unit Weights

Unit weights have been selected from Appendix L which match the example dwelling finishes. Below is a summary of unit weights selected for the example dwelling

	(psf)
Roof unit weight	18.5
Floor unit weight	12.0
Exterior wall unit weight	23.0
Exterior crawlspace wall unit weight	16.0
Interior wall unit weight	18.0

13A.6.2 Weight of Building Tributary to Base Level Diaphragm

Again, the objective is to figure out the weight of the building tributary to the base level diaphragm. The next step is finding the geometry / area of the buildings parts. For the example dwelling, the dimensions have been given in Section 13A.1. In practice, one will have to measure the building to figure out all of these dimensions. Below is a list of the example dwelling lengths.

Building Width	30 ft
Building Length	50 ft
Balcony Width	6 ft
Balcony Length	50 ft
Roof Overhang	1 ft
Floor Area	$= 30 \times 50 = 1500 \text{ sq ft}$
Balcony Area	$= 6 \times 50 = 300 \text{ sq ft}$
Roof Area	$= 32 \times 52 = 1664 \text{ sq ft}$
Length of Exterior Crawlspace wall	
Side 1	50 ft
Side 2	30 ft
Side 3	30 ft
Side 4	50 ft
Height of Exterior Crawlspace Wall*	
Side 1	16 ft
Side 2	8 ft
Side 3	8 ft
Side 4	1 ft
Length of interior walls	135 ft
Length of interior crawlspace walls	0 ft
Height of 1st Floor	9 ft

*The heights of the side walls are averaged to simply calculate the wall weight

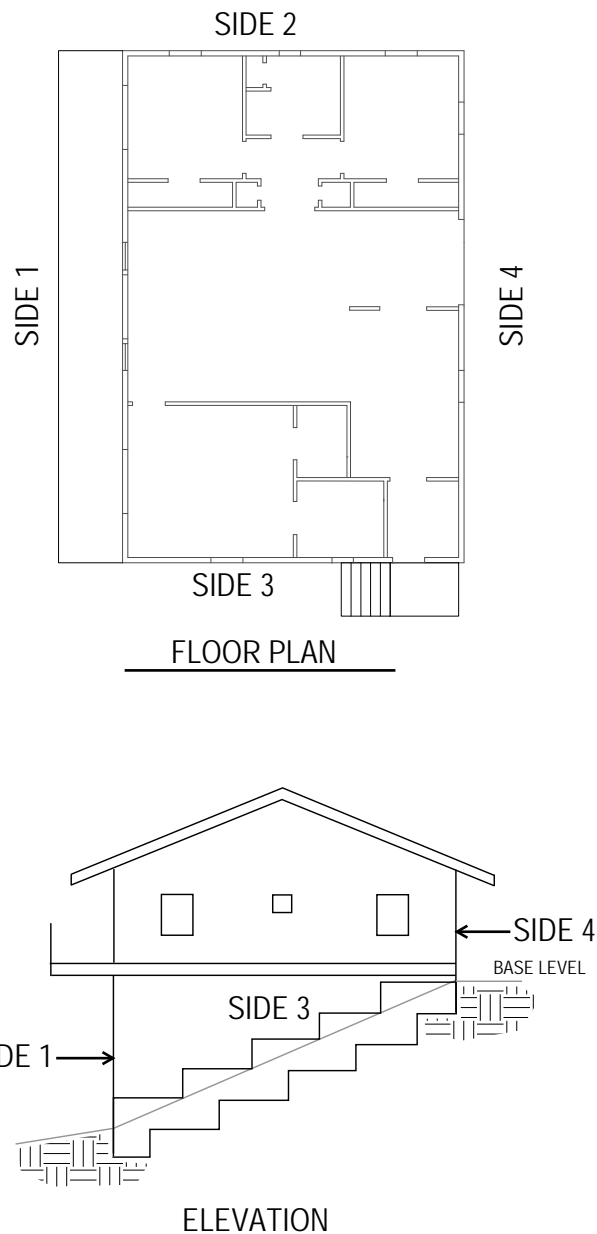


Figure 13A-11 Building wall locations

Combine unit weights of building assemblies with the corresponding building areas or wall lengths to calculate building weight.

Table 13A-8 Dwelling Weight

Wall Assembly	Unit Weight (PSF)	Area (SF)	Perimeter (Ft)	Wall Height (Ft)	Weight (kips) ⁴
Roof ¹	18.5	-	-	-	-
Roof Sloped ¹	20.7	1664 ²	-	-	34
Floor	12	1800 ³	-	-	22
Exterior Wall	23	-	160	10	37
Exterior Crawlspace Wall	16	-	160	4 ⁵	10
Interior Wall	18	-	135	10	24
Interior Crawlspace Wall	0	-	0	4 ⁵	0
Total Tributary Weight					127

Notes

- 1 The unit weight of the roof needs to be increased to account for the roof slope. Roof slope is 6:12. The hypotenuse = $(6^2+12^2)^{1/2} = 13.4$ ft. The effective weight of the sloped roof on a flat area is $18.5 * 13.4/12 = 20.7$ psf
- 2 Roof has an overhang of 1'-0" along each side. The roof area is $(30+2) * (50+2) = 1664$ sq feet.
- 3 The floor area is increased by the balcony. The floor area is $(30+6) * 50 = 1800$ sq feet.
- 4 1 kip = 1000 pounds
- 5 Crawlspace wall height has been reduced to one half the actual height to account for the force the base level diaphragm receives

13A.7 Seismic Base Shears for Retrofit

The Prestandard requires four main elements to be designed

- (1) Primary Anchors (Section 6.5.4.1, Section 13A.8)
- (2) Secondary Anchors (Section 6.5.4.2, Section 13A.9)
- (3) Shear Anchors (Section 6.5.4.3, Section 13A.10)
- (4) Crawlspace walls (Section 6.5.5, Section 13A.11)

(1) The primary anchors are designed with an $R = 2.0$. They are designed to carry the full out-of-hill base shear, and they resist the full torsional force caused by the cross-slope base shear. The primary anchors are, in addition, required to be not less than three times stronger than the secondary anchors. The primary anchor collector shall be designed with the primary anchor force. Primary anchor forces are defined in the Prestandard in Section 6.5.4.1 and are illustrated in Section 13A.8.

(2) The secondary anchors are designed with an $R = 1.0$. They cumulatively resist the base shear in the out-of-hill direction. They are required to be spaced at no more than 4'. Secondary anchor forces are defined in the Prestandard in Section 6.5.4.2 and are illustrated in Section 13A.9.

(3) The shear anchors are designed with an $R = 1.0$. They cumulatively resist the entire base shear in the cross-slope direction. Shear anchor forces are defined in the Prestandard in Section 6.5.4.3 and are illustrated in Section 13A.10.

(4) The crawlspace walls are designed with an $R = 4.0$. They resist their tributary base shear of both out-of-hill and cross-slope loading. There is also a requirement in Section 6.5.5 to design the tie-downs in the walls above the uphill foundation. Crawlspace forces are defined in the Prestandard in Section 6.5.5 and are illustrated in Section 13A.11.

Calculate base shear V

$$V = S_{DS} * W / R \quad (\text{eq. 6.5-1 of the Prestandard})$$

Where

V = Base shear

S_{DS} = Site design spectral acceleration defined in Section 1.6

The user shall determine the site specific spectral acceleration for the site. This example uses 1.2 for S_{DS}.

W = Building tributary weight

R = Seismic response modification factor as defined in Section 6.5.4 and 6.5.5

For this example

S_{DS} = 1.2

W = 127 kips

R = 2 Primary anchor (Section 6.5.4.1)

R = 1 Secondary anchor and Shear anchor (Section 6.5.4.2, Section 6.5.4.3)

R = 4 Crawlspace walls (Section 6.5.5)

$$\begin{aligned} V_{R=2} &= 1.2 * W / 2 = 0.6 W - \text{Primary anchor} \\ &= 0.6 * 127 K = 76 k \end{aligned}$$

$$\begin{aligned} V_{R=1} &= 1.2 * W / 1 = 1.2 W - \text{Secondary and shear anchor} \\ &= 1.2 * 127 k = 152 k \end{aligned}$$

$$\begin{aligned} V_{R=4} &= 1.2 * W / 4 = 0.3 W - \text{Crawlspace wall} \\ &= 0.3 * 127 K = 38 k \end{aligned}$$

Note that these are base shears that will be used for calculating forces to primary, secondary, and shear anchors. Details of forces follow.

13A.8 Primary Anchor Forces

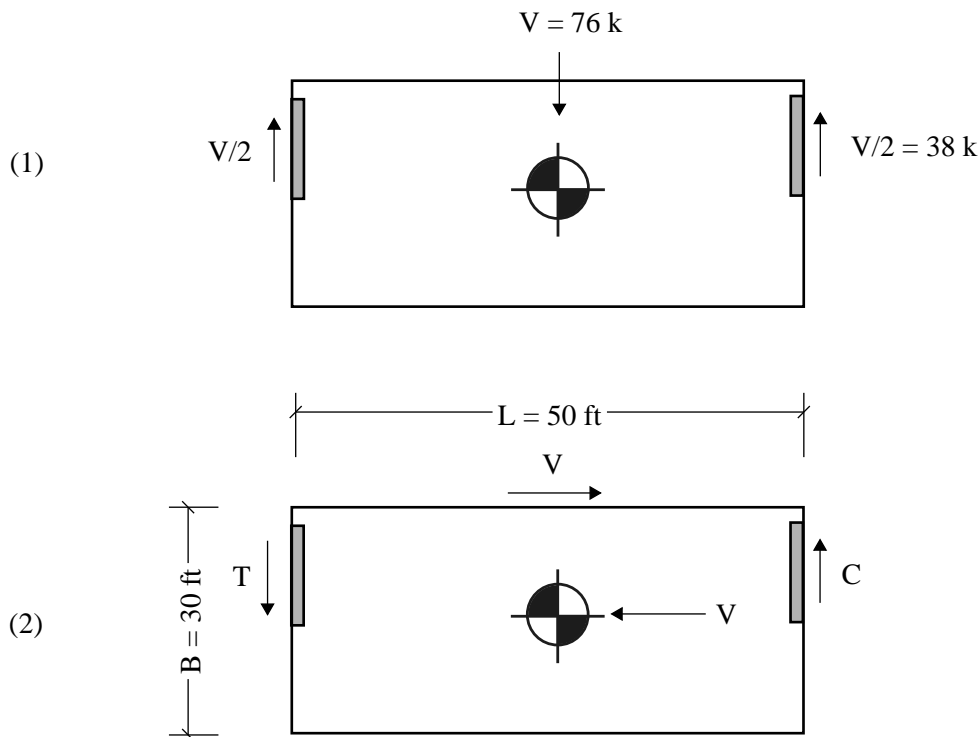
Primary anchors are located on the outside edges of the building, or where the jog (offset in the building greater than 4 feet as described in Section 6.5.4.1) in a building occurs. For simple rectangular plans, two primary anchors are required. Primary anchors are defined in Section 6.5.4.1 of the Prestandard.

Primary anchor force is the maximum of :

- (1) Tributary out-of-hill base shear, where the resisting elements are only primary anchors
- (2) The torsional force due to the cross slope base shear due to the resistance of only shear anchors
- (3) 3x the secondary anchor force

Primary anchors are designed with a response modification factor of 2 (R=2).

$$V = 76 \text{ k} \text{ (from Section 7)}$$



Note: In cases where W is greater than L, cross-slope force will be larger than item 1.

Figure 13A-12 Primary anchor configuration

$$\text{Where } T = V * (B/2) / L$$

$$T = 76 \text{ k} * (30 \text{ ft} / 2) / 50 \text{ ft} = 23 \text{ k}$$

$$(3) \quad \begin{aligned} \text{Secondary anchor force} &= 12.2 \text{ k} \text{ (from Section 9)} \\ \text{Minimum Primary anchor force} &= 3 \times 12.2 \text{ k} = 37 \text{ k} \end{aligned}$$

Summary of primary anchor forces

Primary anchor force F_1 is 38k and governed by out-of-hill loading.

13A.9 Secondary Anchor Forces

Secondary anchors are located uniformly along the uphill foundation at a spacing of 4'-0" on center maximum. Secondary anchors are defined in Section 6.5.4.2 of the Prestandard.

Each secondary anchor resists the out-of-hill base shear / building length * anchor spacing.

Secondary anchors are designed with a response modification factor of 1 (R=1).

V = 152 k (from Section 13A.7)

$$F_2 = (V/L) * t$$

$$F_2 = (152 \text{ k} / 50 \text{ ft}) * 4 \text{ ft} \\ = 12.2 \text{ k}$$

Where F_2 is a unit load based on a 4' spacing

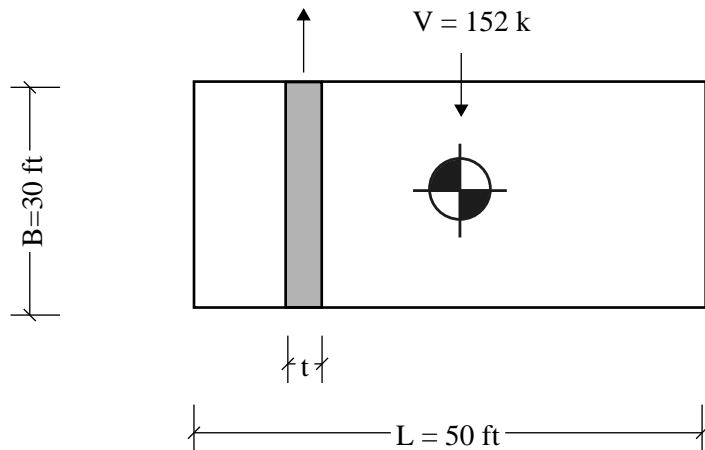


Figure 13A-13 Secondary anchor configuration

Summary of secondary anchor forces

Secondary anchor force F_2 is 12.2 k for a 4' spacing

13A.10 Shear Anchor Forces

Shear anchors are located uniformly along the uphill foundation at a spacing of 4'-0" on center maximum. Shear anchors are defined in Section 6.5.4.3 of the Prestandard.

Each shear anchor resists the cross-slope base shear / building length * anchor spacing.

Shear anchors are designed with a response modification factor of 1 (R=2).

V = 152 k (from Section 13A.7)

$$\begin{aligned} F_3 &= (V/L)*S \\ &= (152 \text{ k } /50 \text{ ft })*4 \text{ ft } \\ &=12.2 \text{ k } \end{aligned}$$

Where F_3 is a unit load based on a 4' spacing

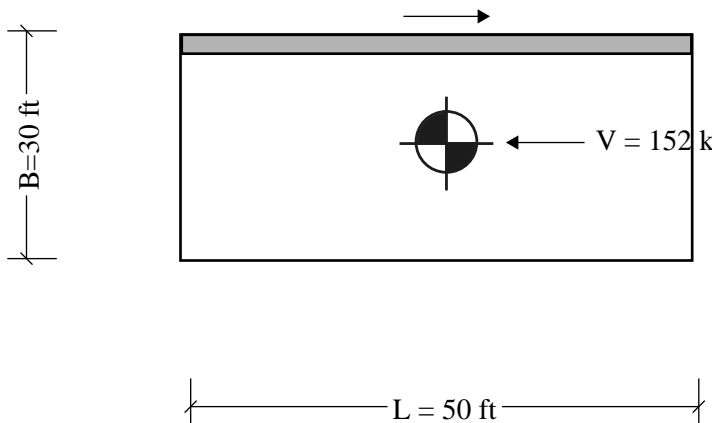


Figure 13A-14 Shear anchor configuration

Summary of shear anchor forces

Secondary anchor force F_3 is 12.2 k for a 4' spacing

13A11 Crawlspace Wall Forces

Crawlspace walls are located along the downhill foundation and can wrap around along the cross slope foundation. Crawlspace walls forces are defined in Section 6.5.5 of the Prestandard.

Crawlspace walls resist the portion of lateral force which would be distributed to them based on a flexible diaphragm. There is an exception in the Prestandard which simplifies the overturning provided:

1. Not less than 80% of the stud or crawlspace wall length is sheathed full height.
2. Ventilation and access openings in otherwise sheathed walls are permitted to be neglected for purposes of determining percent sheathed, as long as the length of the openings does not exceed 20% of the crawlspace wall's entire length.
3. A tie-down is provided at each downhill corner and at the end of each full-height sheathed segment, with an ASD capacity not less than the larger of $(1.6 * S_{DS})$ and 2.5 kips.

Crawlspace downhill walls resists half of the base shear. Crawlspace side walls resist half the base shear. The side crawlspace walls are to be designed to resist seismic forces based on tributary area, irrespective to stiffness of the primary anchor.

Crawlspace walls are designed with a response modification factor of 4 ($R=4$).

Downhill crawlspace wall design force $V = 38 \text{ k}$ (from Section 13A.7)

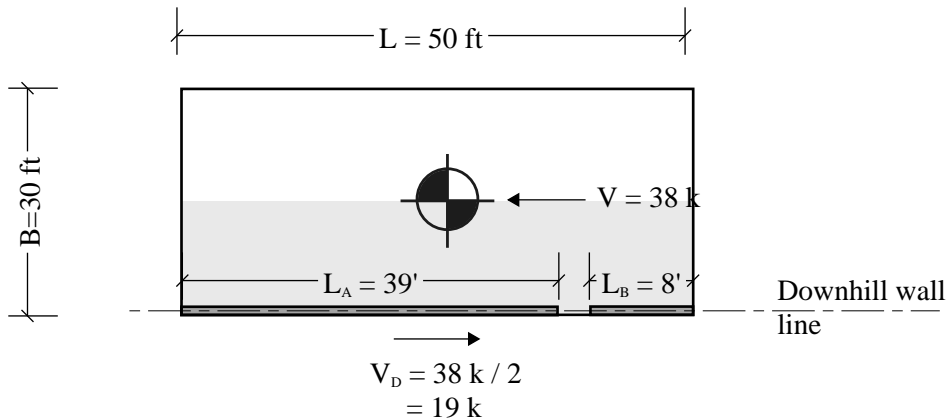
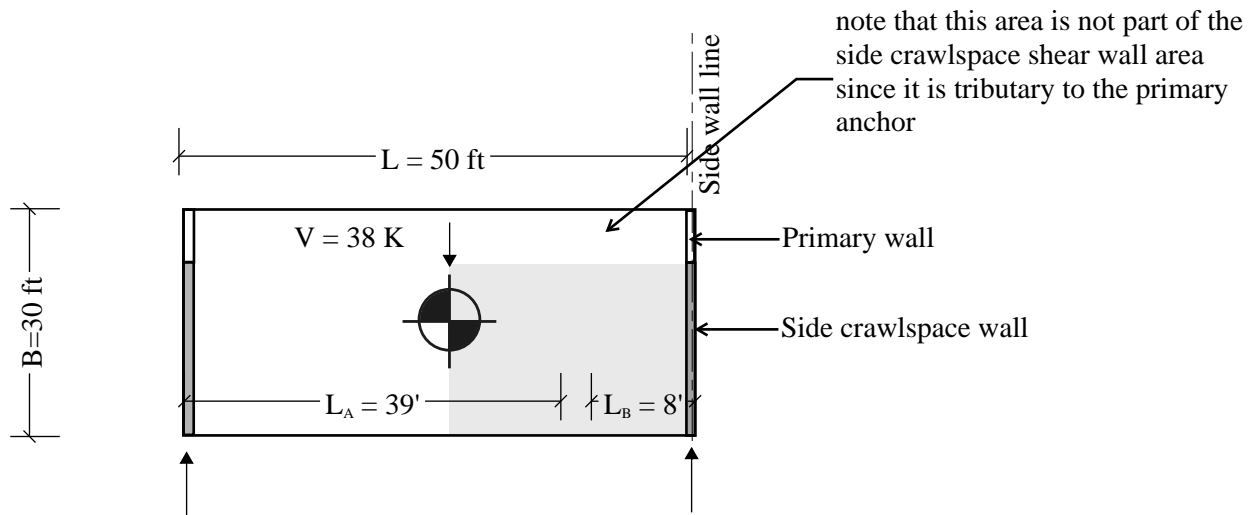


Figure 13A-15 Downhill crawlspace wall configuration

Cross slope crawlspace wall design force

$V = 38 \text{ k}$ (from Section 13A.7)



V_s is a ratio of tributary area where 5' goes to primary anchor shear wall and 25' goes to side crawlspace shear wall. Because wood crawlspace walls only extend for 25 feet of the 30 foot side wall, V_s can be reduced by the ratio of crawlspace walls to the side wall.
 $V_s = 19 \text{ k} * (25 \text{ ft} / 30 \text{ ft}) = 15.8 \text{ k}$

Figure 13A-16 Side crawlspace wall configuration

Summary of crawlspace wall forces

Downhill crawlspace wall force V_D is 19 k.
 Side crawlspace wall force V_s is 15.8 k.

13A.12 Design of primary anchors

Primary anchors are the main resistance to the building's direct tension and inherent torsional qualities due to the hillside configuration. Primary anchors forces are generally large forces in the order of half the building base shear for each anchor.

The primary anchor should be stiff as possible. Although the primary anchor could involve just a collector at the base level diaphragm and anchor to the uphill foundation, because of the large primary anchor force, it will often be necessary to provide both a continuous foundation in line with the primary anchor, and a partial length wall to transmit the primary anchor force from the base level diaphragm collector to the continuous foundation, see Figure 13A-17. Concrete shear walls, masonry shear walls, or steel brace frames are ideal to be used as part of the primary anchor load path. Wood shear walls are not strong or stiff enough to serve this purpose.

Primary Anchor Consists of three elements

- 1) Concrete shear wall or other main lateral resisting element
- 2) Concrete grade beam
- 3) Collector beam

13A.12.1 Main Lateral Load Resisting Element

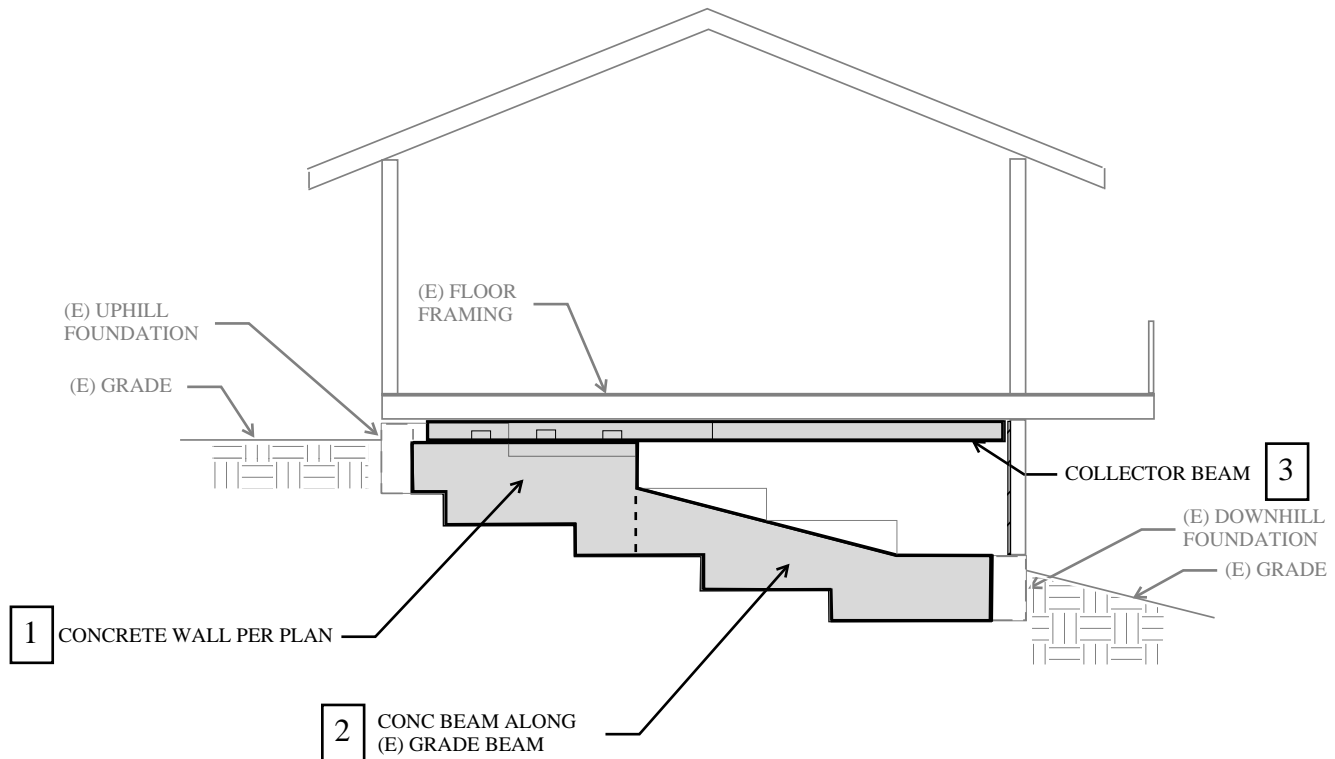


Fig 13A-17 Example dwelling elevation showing primary members

Designer notes

The existing foundation is not required to be reviewed in the Prestandard, however, in order to keep additional stresses low in the existing foundation, a grade beam is provided over the length of the cross slope foundation. The primary anchor / concrete shear wall is placed as high up the hill as possible to minimize the height of the wall. Keeping the wall height to a minimum reduces overturning moments in the wall, grade beam, foundation, and reduces the out-of-plane forces the base level diaphragm will have to resist.

The maximum collector force is at the end of the concrete wall. Shifting the splice point of the collector away from the end of the concrete shear wall will reduce the splice connection forces. Clearly locate this point in the drawings and detail the connection.

The main lateral resisting element in the example dwelling is a concrete shear wall. The concrete wall will be checked for both flexure and shear. The figure below shows outlines the concrete shear wall.

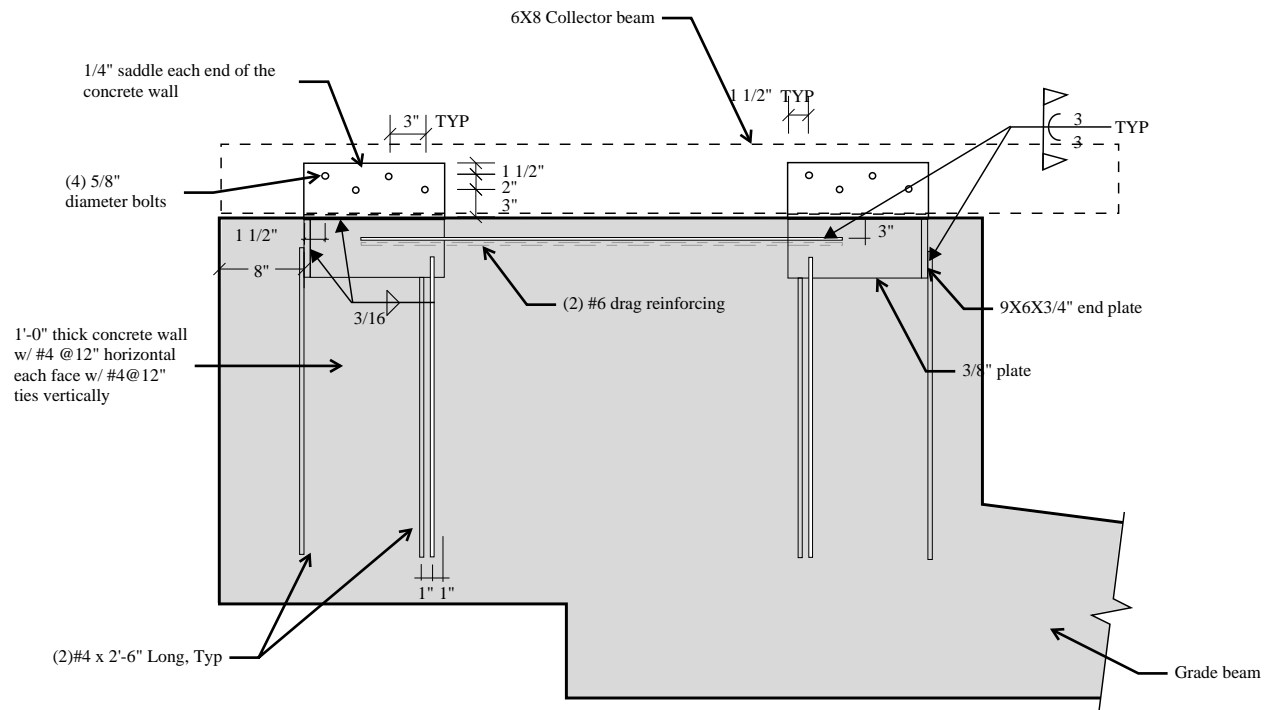


Figure 13A-18 Example dwelling concrete wall elevation

13A.12.1.1 Concrete Wall Flexural Design

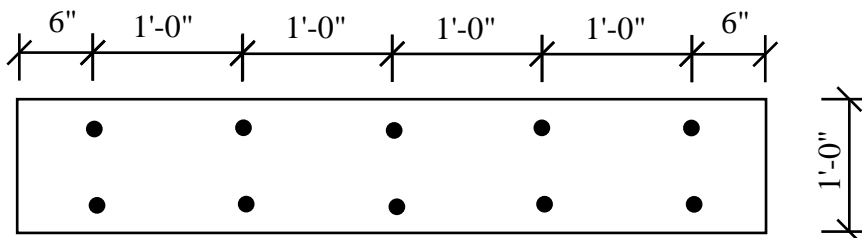
The shear demand was determined in Section 13A.8

$$Vu = 38 \text{ k}$$

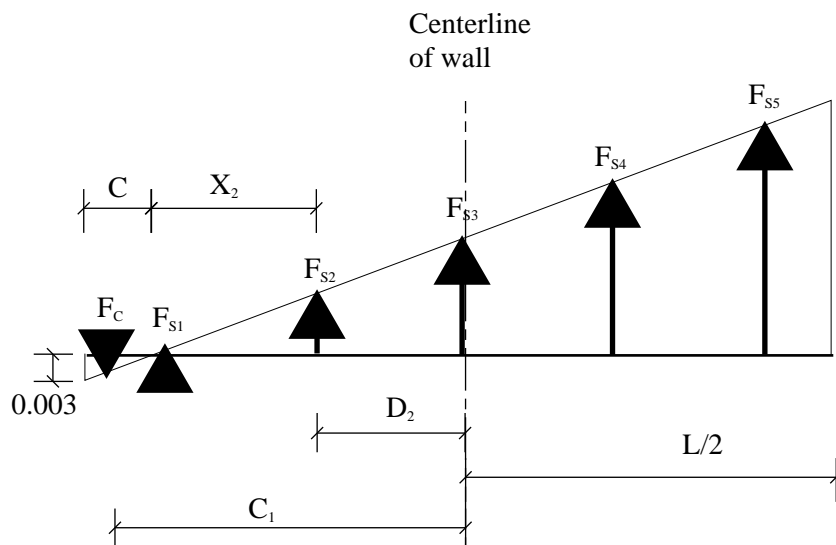
$$Mu = Vu * H = 38 \text{ k} * 4 \text{ ft} = 152 \text{ kft}$$

Where H is from the top of the diaphragm to the bottom of the concrete shear wall. In this example the bottom of the concrete wall is assumed to be at the centerline of the grade beam. The axial load on the wall is the concrete wall self (150 psf * 1 ft thick * 4 ft height * 5 ft long) weight plus the wood exterior wall self weight (23 psf * 9 ft high * 5 ft long). The total axial load $P_u = 4 \text{ K}$

Try 12" thick x 5'-0" long concrete wall with #4 ties @ 12" ($f'_c = 2.5 \text{ ksi}$)



Concrete wall plan view



Note F_{s1} and F_{s2} in this example will be negative or in the opposite direction of the rest of the forces when summing moments about the center of the wall

Figure 13A-19 Strain in wall plan view

The moment in the wall can be found by summing forces about any point.

To keep the section in equilibrium find the neutral axis, C, where $F_c + \text{Sum } (F_s) = P_u$. Use any process to find this point. For the example dwelling $C = 4.95"$

Find Strain in steel based on similar triangles with $E_c = 0.003$

$$X_1 = 1.05 \quad Es_1 = 1.05 * 0.003 / 4.95 = 0.000636 \quad Fs_1 = 0.000636 * 29000 = 18.4 \text{ ksi}$$

$$X_2 = 13.05 \quad Es_2 = 13.05 * 0.003 / 4.95 = 0.00791 \quad Fs_2 = 0.00791 * 29000 = 229 \text{ ksi (60 ksi limit)}$$

$$X_3 = 25.05 \quad Es_3 = 25.05 * 0.003 / 4.95 = 0.0152 \quad Fs_3 = 0.0152 * 29000 = 441 \text{ ksi (60 ksi limit)}$$

$$X_4 = 37.05 \quad Es_4 = 37.05 * 0.003 / 4.95 = 0.0225 \quad Fs_4 = 0.0225 * 29000 = 653 \text{ ksi (60 ksi limit)}$$

$$X_5 = 49.05 \quad Es_5 = 49.05 * 0.003 / 4.95 = 0.0297 \quad Fs_5 = 0.0297 * 29000 = 861 \text{ ksi (60 ksi limit)}$$

Any stress in the reinforcing is limited to the yield stress.

Now sum forces. In this example we are summing forces at the center of the wall. Since axial load is assumed to act in the center of the wall, the axial load does not affect the moment.

Distances of forces to center of wall

$$D_{c1} = 60"/2 - .85*4.95"/2 = 27.9"$$

$$D_{s1} = 24"$$

$$D_{s2} = 12"$$

$$D_{s3} = 0"$$

$$D_{s4} = 12"$$

$$D_{s5} = 24"$$

To calculate D_{c1} see assumed compression block geometry

Concrete Force F_c

$$F_c = a * .85 * f'_c * b = .85 * 4.95" * .85 * 2.5ksi * 12" = 107 k$$

Concrete wall flexural capacity

$$\begin{aligned}\phi M_n &= F_c * D_{c1} + A_{s1} * F_{s1} * D_{s1} + A_{s2} * F_{s2} * D_{s2} + A_{s3} * F_{s3} * D_{s3} + A_{s4} * F_{s4} * D_{s4} + A_{s5} * F_{s5} * D_{s5} \\ &= 107k * 27.9" - .2^{1/2} * 2 * 18.4ksi * 24" - .2^{1/2} * 2 * 60ksi * 12" + .2^{1/2} * 2 * 60ksi * 0" + .2^{1/2} * \\ &\quad 2 * 60ksi * 12" + .2^{1/2} * 2 * 60ksi * 24" \\ &= 3392 k" / 12"/' = 283 kft\end{aligned}$$

$$\phi M_n = .9 * 283 kft = 254 kft > M_u = 152 kft$$

Therefore wall is OK in flexure

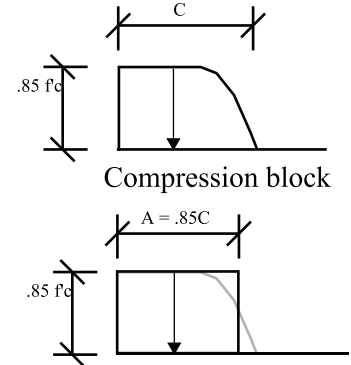


Figure 13A-20 Assumed compression block

13A.12.1.2 Concrete Wall Shear Design

The shear demand $V_u = 38 k$

Use 12" x 60" concrete wall with 2 layers of #4 @ 24" horizontal

$$\begin{aligned}\phi V_n &= \phi * A_{cv} * (a * \sqrt{f'_c} + \rho * f_y) \\ &= .75 * 12" * 60" * (3 * \sqrt{2500 \text{ psi}} / 1000 + 2 * .2^{1/2} / (12" * 24") * 60ksi) \\ &= 126 k\end{aligned}$$

$\phi V_n = 126 k > V_u = 71 k$ Therefore wall is OK in shear

13A.12.2 Grade Beam Design for Primary Anchor

13A.12.1 Grade Beam Flexural Design

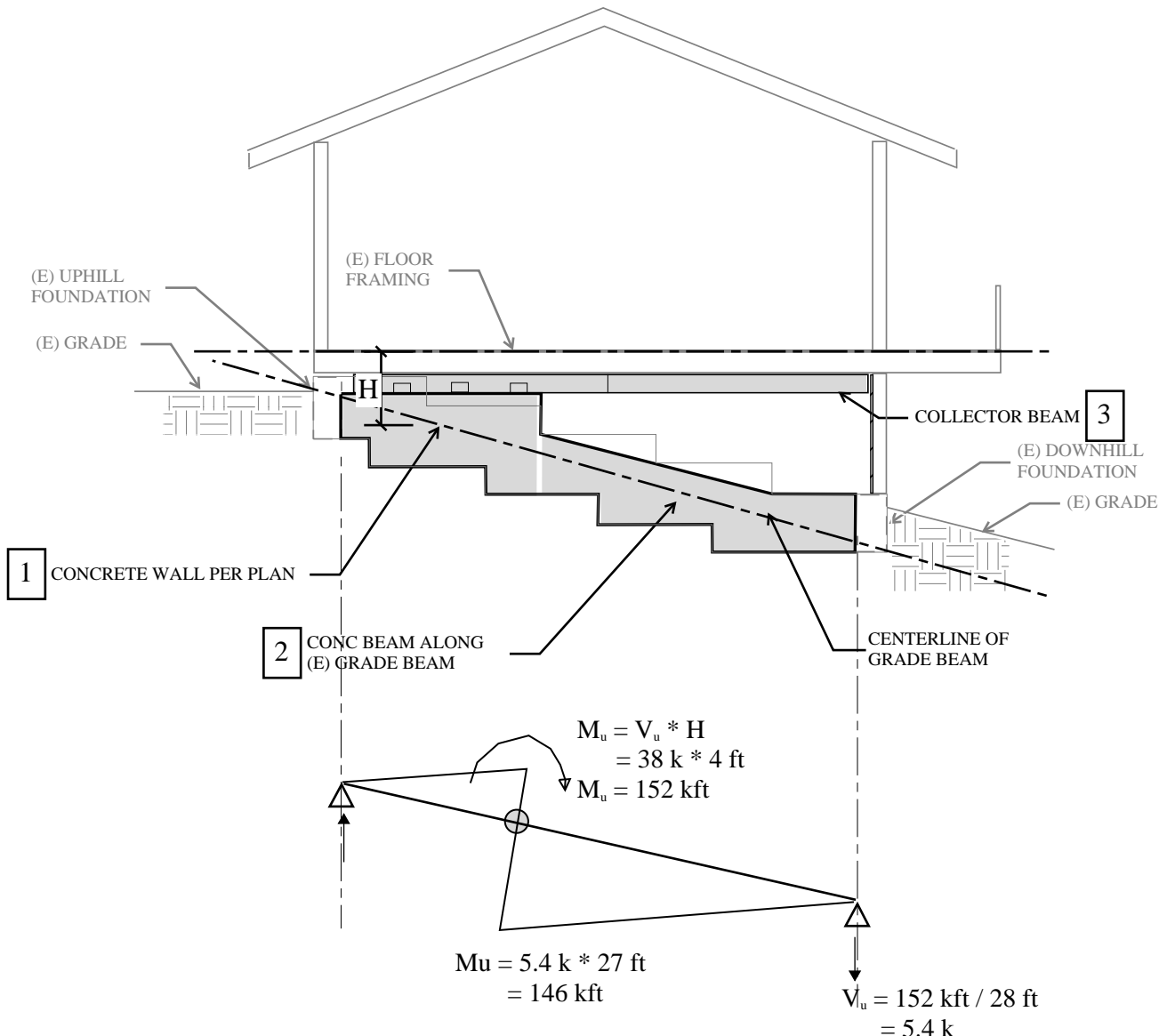


Figure 13A-21 Grade Beam

Try 12x28" grade beam w/ 3#7 T&B

$$a = A_s * F_y / (.85 * F'_c * b)$$

$$= 3 * .6^2 * 60 \text{ ksi} / (.85 * 2.5 \text{ ksi} * 12")$$

$$= 1.8"$$

$$\phi M_n = \phi * A_s * F_y (d - a/2)$$

$$= .9 * 3 * .6^2 * 60 \text{ ksi} * (24" - 1.8"/2) / 12"$$

$$= 187 \text{ kft} > 146 \text{ kft}$$

a is the assumed compression block for the concrete beam due to the moment applied.

Note that the moment diagram is a conservative approximation. Other solutions which include soil bearing maybe used when justified by the design engineer.

13A.12.2.2 Grade Beam Anchorage to Existing Footing

Anchor to existing footing = Shear + Shear due to moment

$$= 38 \text{ k} + 5.4 \text{ k}$$

$$= 44 \text{ k}$$

#4 dowel w/ epoxy w/ 5" embed = 4 k capacity in shear from Hilti software

of Dowels = $44 \text{ k} / 4 \text{ k} = 11$ dowels

Use 2#4 dowels @ 36" along the length of the grade beam

$$= 2 * 28 \text{ ft} / 3 \text{ ft} = 19 \text{ dowels} > 11 \text{ dowels}$$

13A.12.3 Collector Design

13A.12.3.1 Collector Beam Connections to Concrete Wall

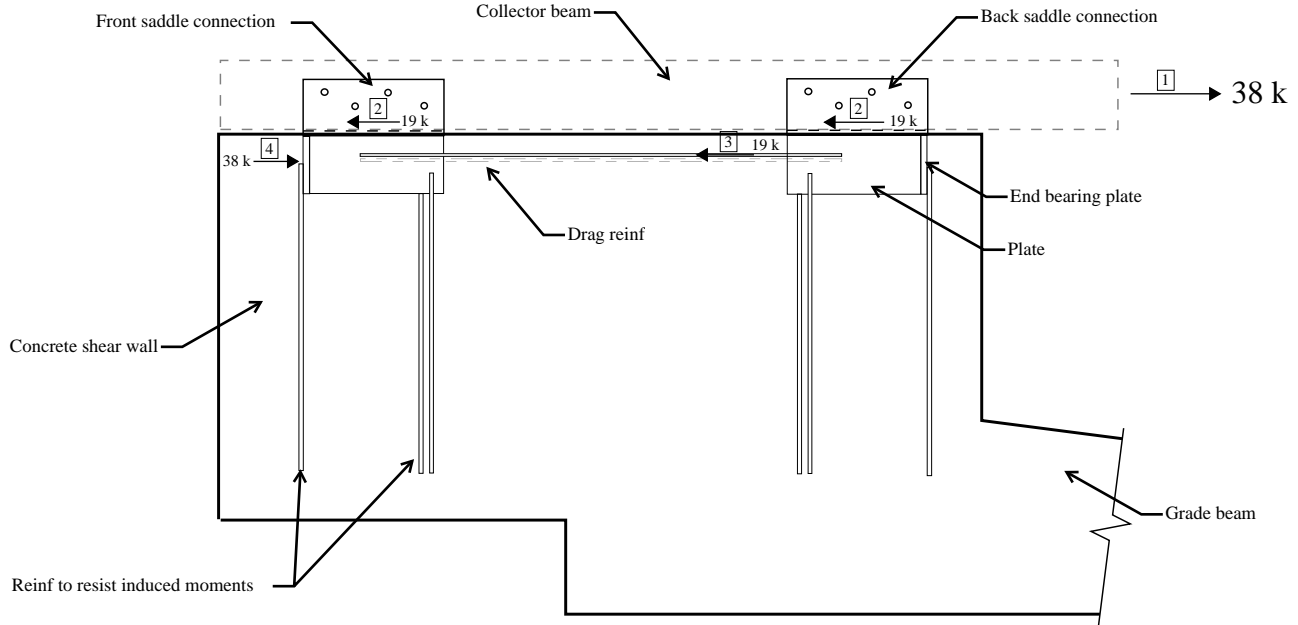


Figure 13A-22 Example dwelling concrete wall elevation

Load Path

1. From diaphragm to collector beam (required but not included in example)
2. From collector beam to saddle connection. Equal force is assumed to be transferred into each saddle connection.
3. Force from back saddle connection transfers to front saddle connection through drag reinforcing. We transfer this force to avoid a breakout failure of the bottom of the saddle connection near the end of the wall. The collected force transfers to the front saddle connection.
4. End plate of saddle connection through bearing of concrete shear wall
5. Concrete shear wall to concrete grade beam
6. Concrete grade beam to existing foundation

13A.12.3.1.1 Collector Bolt Design

$$\begin{aligned}\text{Saddle Force} &= \text{Primary anchor force} / 2 \\ &= 38 \text{ k} / 2 \\ &= 19 \text{ k}\end{aligned}$$

Design bolts in double shear
 $5/8"$ Diameter Bolt $Z' = 2410 * 3.32 * .65 = 5200\#$
Bolts per saddle = $19 \text{ k} / 5.2 \text{ k} = 4$

$3/4"$ Diameter Bolt $Z' = 3340 * 3.32 * .65 = 7208\#$
Bolts per saddle = $19 \text{ k} / 7.21 \text{ k} = 3$

Bolts in double shear are used in the saddle connection instead of lags or nails to increase the stiffness of the primary anchor connection. In this particular example dwelling, most of the flexibility from the primary anchor is from the bolted connection.

13A.12.3.1.2 Collector Drag Reinforcing Design

Drag Reinforcing
Demand = 19 K
Required Steel = $F/\phi * F_y$
 $= 19 / (.9 * 60 \text{ ksi})$
 $= .35^{\prime\prime 2}$

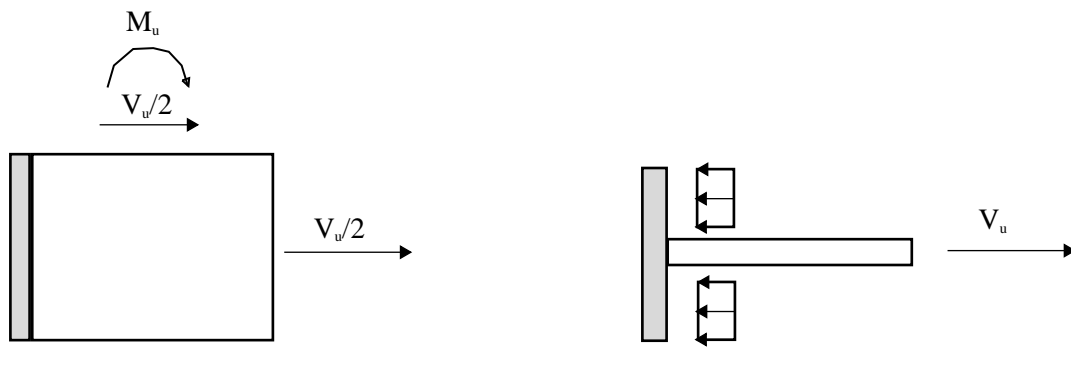
Use (2) #5 = $2 * .31^{\prime\prime 2} = .52^{\prime\prime 2}$

Check Weld of drag reinforcing

$$\begin{aligned}V_u &= 20 \text{ k} \\ \phi R_n &= f * F_w * A_w \\ &= .75 * (.6 * 70 \text{ ksi}) * .707 * .25^{\prime\prime 2} \\ &= 5.5 \text{ k/in} \\ \text{Length Required each end of both reinf} &= 19 \text{ k} / 5.5 \text{ k/in} = 4" \\ \text{Use } 12" &(\text{3 inches ea side ea reinf})\end{aligned}$$

Since the radius of the $5/8"$ reinf is smaller than $3/8"$ a reinforced fillet weld is required and the flare bevel cannot be used in the calculation (footnote a of Table J2.2 AISC)

13A.12.3.1.3 Design of Saddle Plates Embedded in the Concrete Shear Wall



Saddle Connection Elevation

Saddle Connection Plan View

Figure 13A-23 Saddle embed plates

Plate Design

Find minimum area of plate required for concrete bearing

$$\begin{aligned} \text{Area required} &= F / (\phi * .85 * f'_c) \\ &= 38 \text{ k} / (.65 * .85 * 2.5 \text{ ksi}) \\ &= 28''^2 \end{aligned}$$

use 9x6" plate

Find required thickness of plate

$$\begin{aligned} \text{first calculate uniform load} \\ \text{uniform pressure} &= 38 \text{ k} / (9'' * 6'') \\ &= 0.7 \text{ ksi} \end{aligned}$$

Find moment in plate

$$\begin{aligned} M_u &= w * l^2 / 2 \\ &= 0.7 * 3^2 / 2 \\ &= 3.15 \text{ k"} \end{aligned}$$

Find required thickness of plate

$$\begin{aligned} D_{req} &= \sqrt{(4 * Z / B)} \\ &= \sqrt{(4 * (M_u / (\phi * F_y)) / B)} \\ &= \sqrt{(4 * (3.15 / (.9 * 36)) / 1)} \\ &= 0.62" \end{aligned}$$

Use 3/4" thick plate ($f_y = 36$ ksi)

The end plate in this case is governed by detailing constraints, by trying to fit the drag reinforcing in combination to the additional reinforcing resisting the moments

Resolve the eccentricity of the plates embedded in concrete shear wall

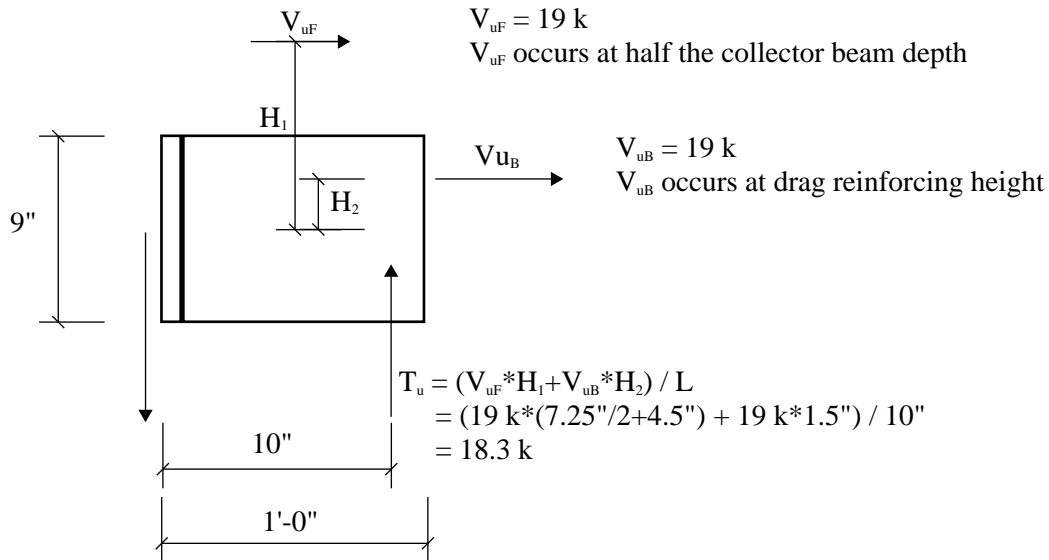


Figure 13A-24 Saddle Connection Elevation

$$\begin{aligned} \text{As Req} &= T / (\phi * F_y) \\ &= 18.3 \text{ k} / (.9 * 60 \text{ ksi}) \\ &= .34 \text{ in} \end{aligned}$$

$$\text{Use (2) } \#4 = 2 * .2 \text{ in} = .4 \text{ in}$$

Eccentricity of the connection is resolved in this example by reinforcing which is placed near the edges of the embedded plates.

Required weld of reinf to pl

$$T_u = 18.3 \text{ k}$$

Capacity of 1/4" fillet

$$\begin{aligned} \phi R_n &= \phi * F_w * A_w \\ &= .75 * (.6 * 70 \text{ ksi}) * (.707 * .25) \\ &= 5.56 \text{ k/in} \end{aligned}$$

$$\text{Length of weld} = 18.3 \text{ k} / 5.56 \text{ k/in} = 3.5 \text{ in}$$

use 12" (3" of weld ea side ea reinf)

Check weld length of stiffener plate to saddle

$$V_u = 19 \text{ k}$$

Capacity of 3/16" fillet

$$\begin{aligned} \phi R_n &= \phi * F_w * A_w \\ &= .75 * (.6 * 70 \text{ ksi}) * (.707 * .1875) \\ &= 4.17 \text{ k/in} \end{aligned}$$

$$\text{Length Required} = 19 \text{ k} / 4.17 \text{ k/in} = 4.6 \text{ in}$$

Use 12" of weld ((2) 3" 3/16" fillet welds each end of each side of the stiffener plate)

13A.12.3.2 Collector Beam Design

6x8 DFL#1 Collector Beam

Assume Fully Braced, This assumption should be checked base on the actual condition

V_u = Primary anchor collector force = Primary anchor force

$$V_u = 38 \text{ k}$$

Check beam

$$F_t = 675 \text{ psi}$$

A = Area of beam minus one bolt hole

$$A = 5.5" * 7.25" - 5.5" * .75" = 34.25"$$

$$\begin{aligned} \text{Tension} &= 675\text{psi} * 34.25"^2 * 2.7 * .8 \\ &= 50 \text{ k} > 38 \text{ k} \end{aligned}$$

6x8 Collector Ok

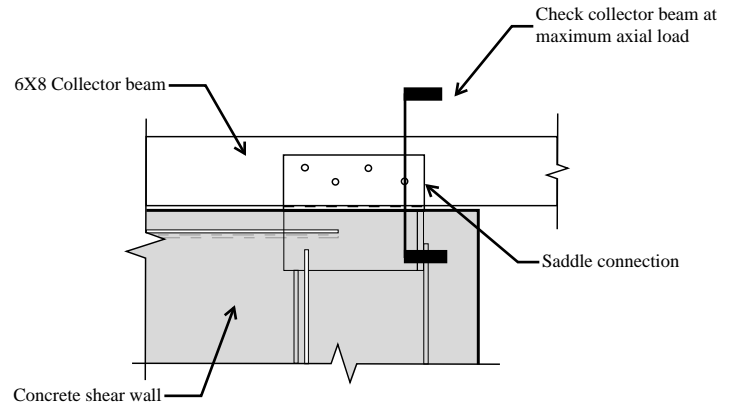


Figure 13A-25 Collector beam to saddle connection diagram

Check Splice Connection

Splice location 15 feet from downhill foundation

$$V_u = 38 \text{ k} / 30\text{ft} * 15\text{ft} = 19 \text{ k}$$

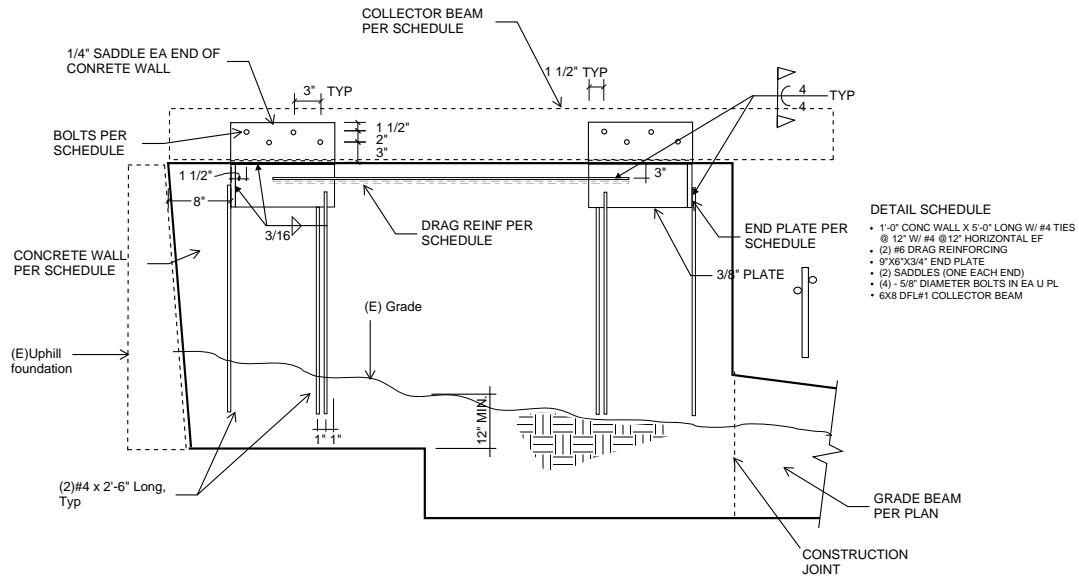
Design Bolts in double Shear

$$5/8" \text{ Diameter Bolt } Z' = 2410\# * 3.32 * .65 = 5200\#$$

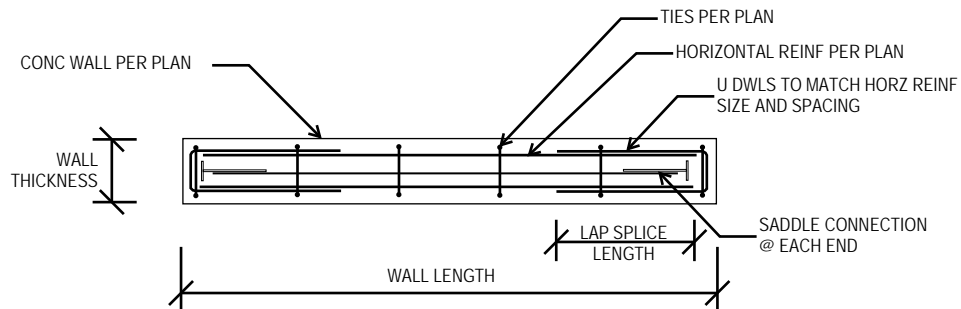
$$\# \text{ Bolts} = 19 \text{ k} / 5.2 \text{ k} = 4$$

Use 1/4" plate on each side of collector beam with (4) 5/8" diameter thru bolts each side of the splice. Specify maximum distance from the downhill foundation = 15'-0" on the drawings

Following are some examples of primary anchor details

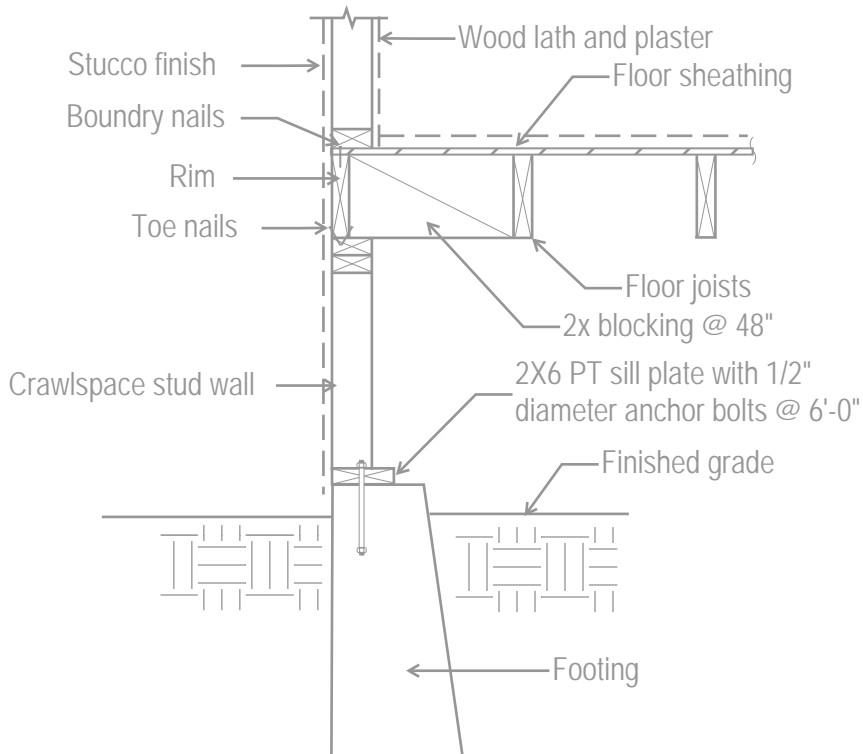


Elevation of primary anchor shear wall

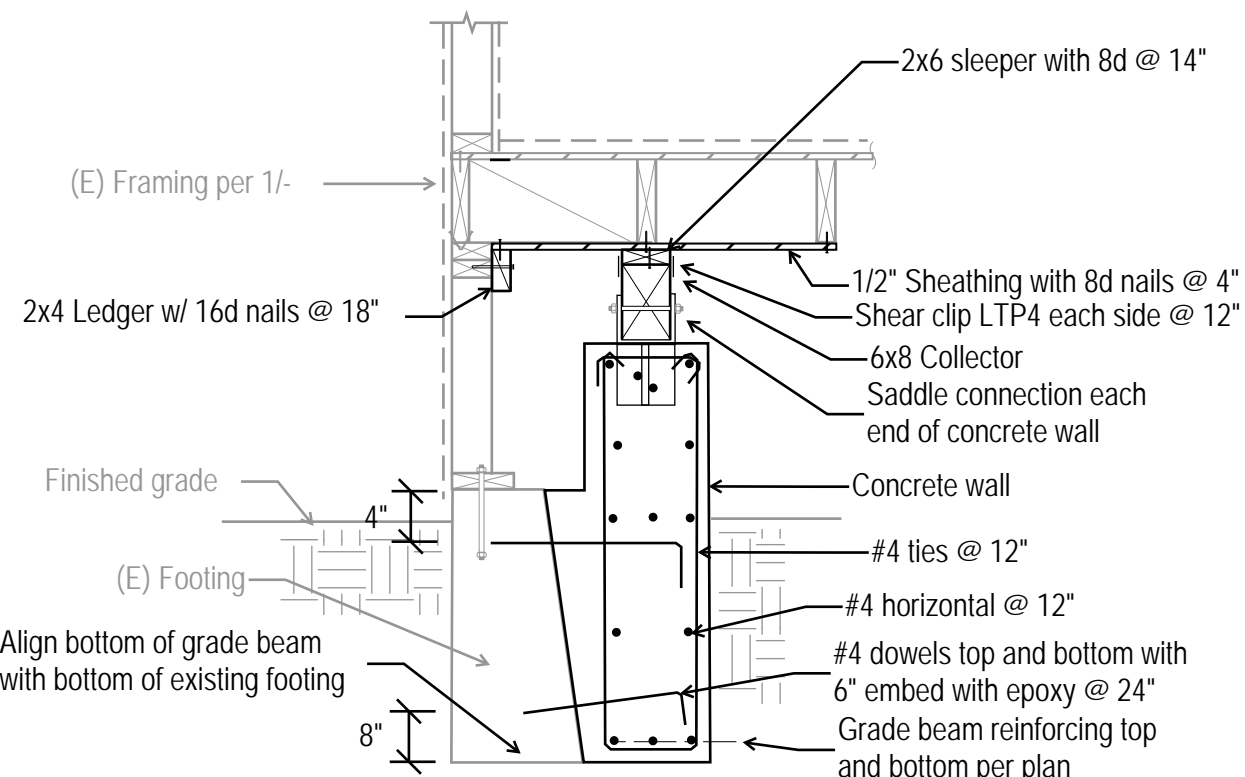


Plan view of primary anchor shear wall

Figure 13A-26 Primary anchor detail

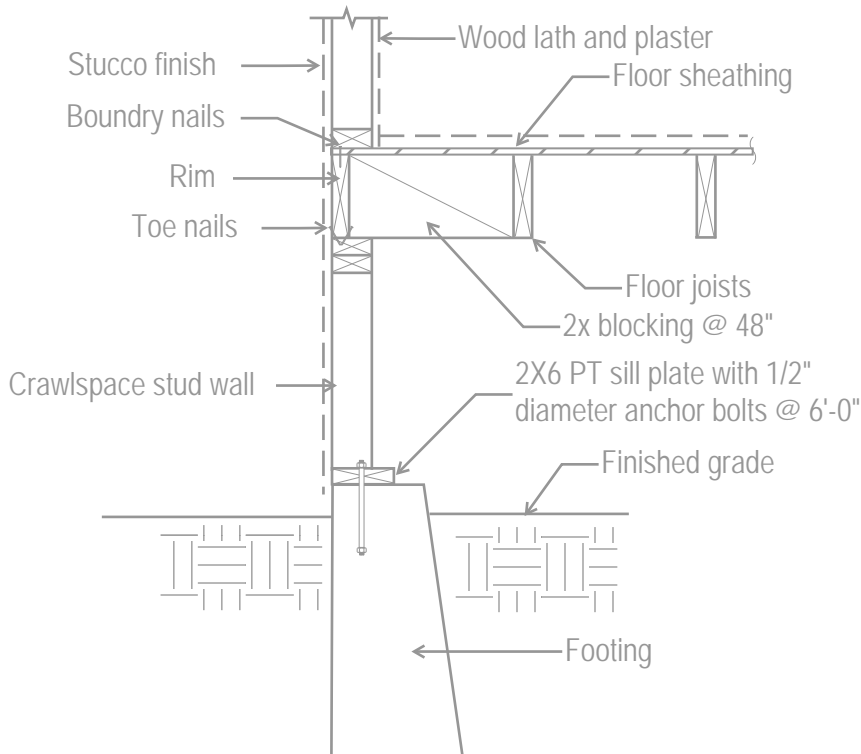


Existing section @ side foundation

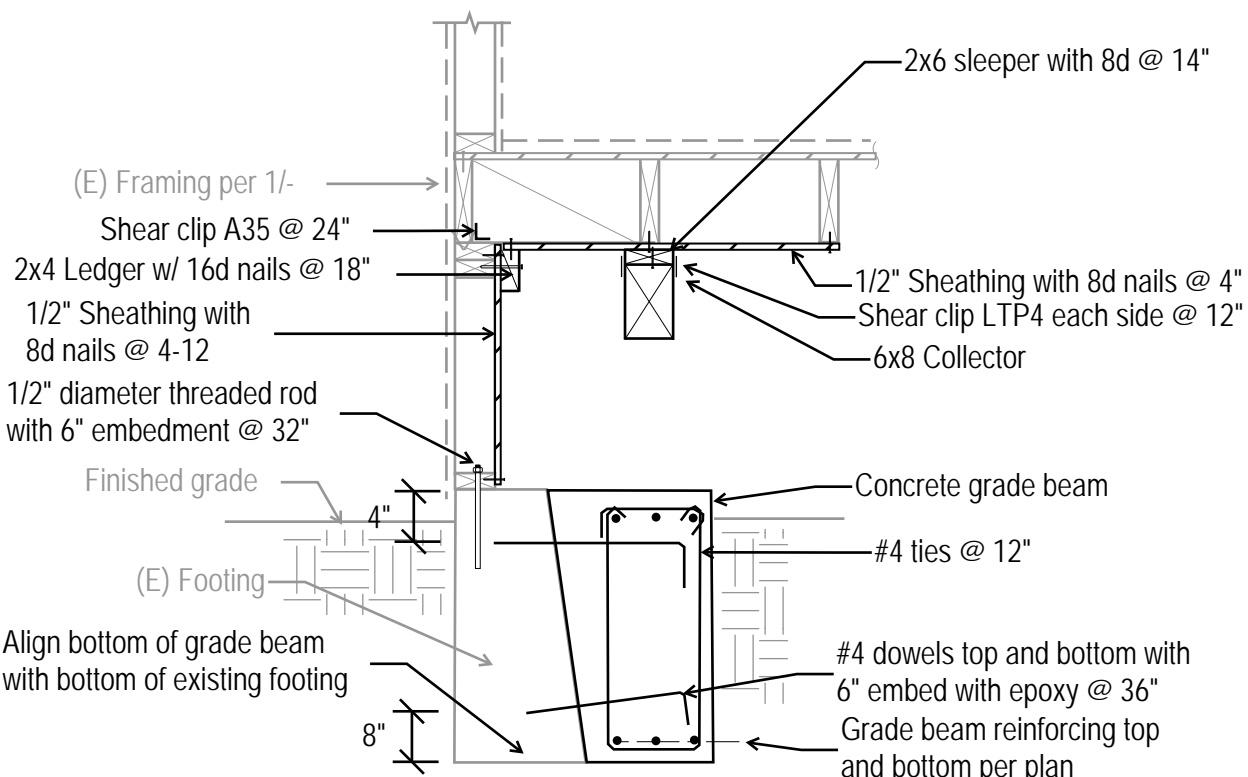


Retrofit section of Primary anchor concrete shear wall at side foundation

Figure 13A-27 Primary anchor detail at concrete wall

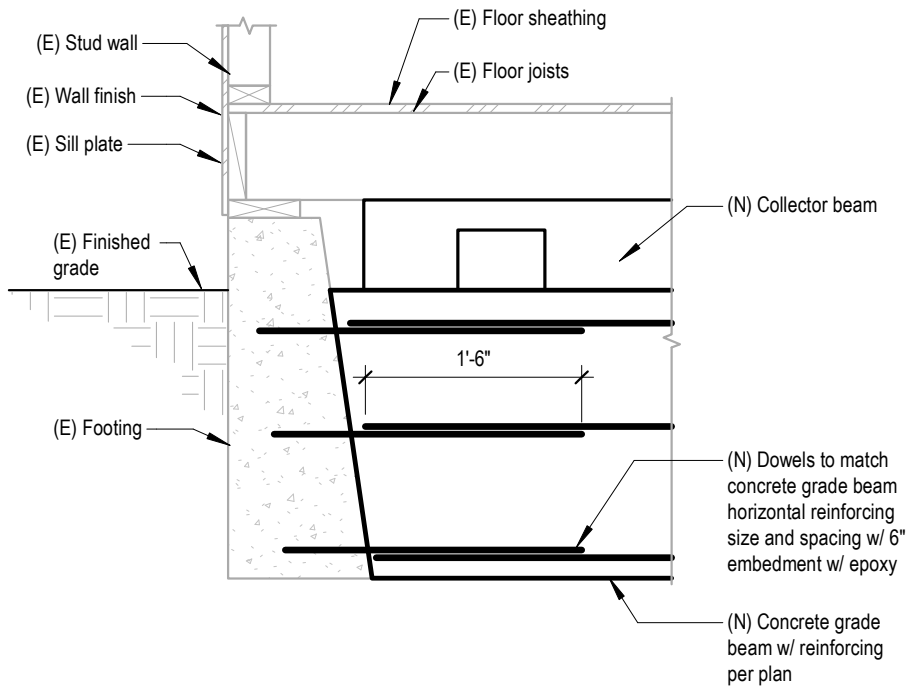


Existing section @ side foundation



Retrofit section of Primary anchor concrete grade beam at side foundation

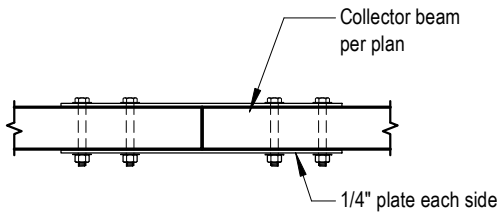
Figure 13A-28 Primary anchor detail at grade beam



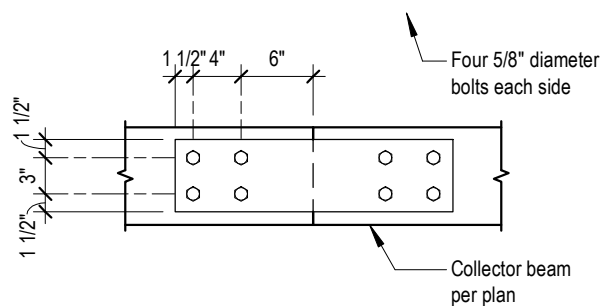
3 Detail at uphill wall foundation

$3/4" = 1'-0"$

Figure 13A-29 Primary anchor grade beam to uphill foundation



A Plan view



2 Collector beam splice
3/4" = 1'-0"

Figure 13A-30 Collector beam splice detail

13A.13 Design of Secondary Anchors

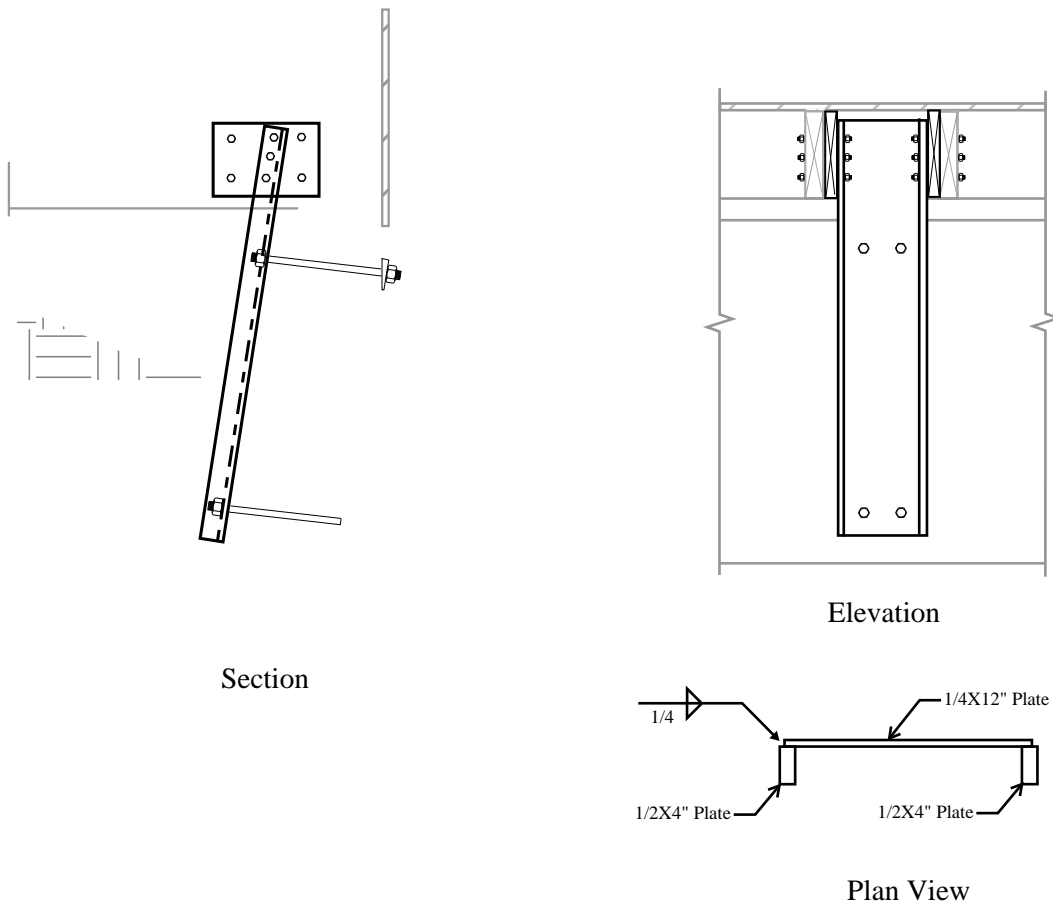


Figure 13A-31 Secondary anchor

The secondary and shear anchor will be one combined anchor in the example dwelling. Secondary anchor forces occur during out-of-hill lateral loads and shear anchors forces occur during cross slope loading. Since this element will resist both forces it shall be designed for 100% in both directions according to the last paragraph in Section 6.5.4.3 of the Prestandard.

The channel we will be using in this example dwelling is a built-up section consisting of plates welded together, defined in the figure above.

13A.13.1 Design of Channel for Secondary Anchor

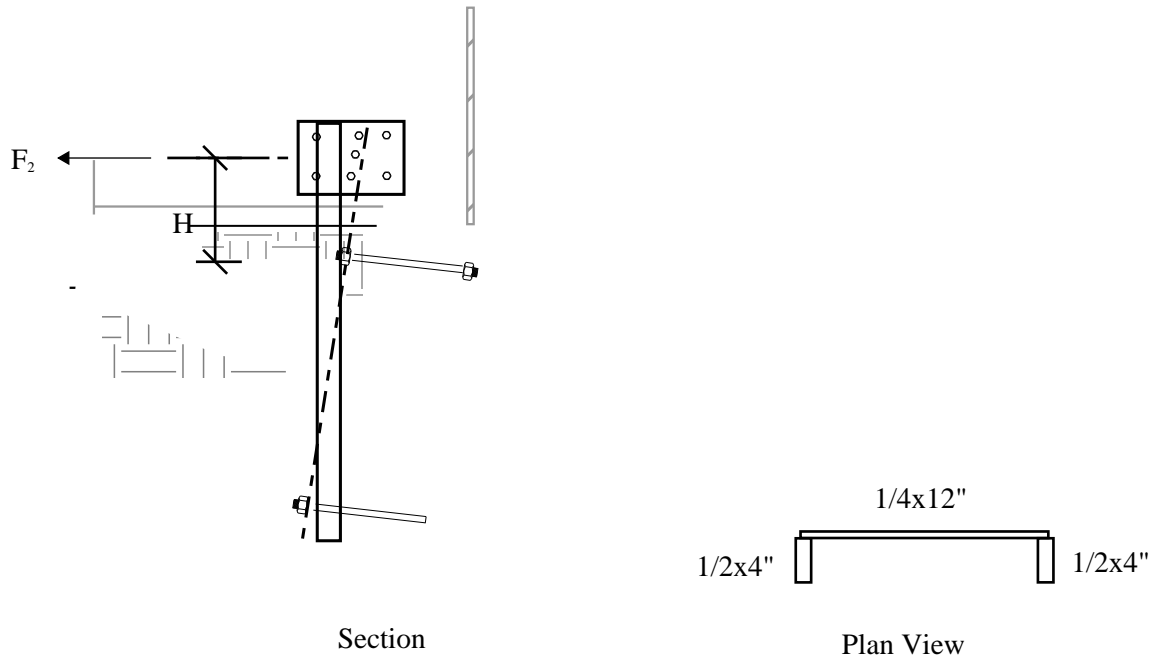


Figure 13A-32 Secondary anchor

Channel Demand

$V_u = 12.2 \text{ k}$ (from Section 13A.9 secondary anchor force)

$$M_u = V_u * H \text{ (where } H \text{ is the distance from the center of the joist to the location of the first anchor)}$$

$$= 12.2 k * 9"$$

$$= 110 \text{ kin}$$

$$= 12.2 \text{ k} * 9''$$

$$= 110 \text{ kin}$$

$$\begin{aligned}\bar{Y} &= \text{Sum of } A^*D / \text{Sum of } A \\ &= .5^{*4}*2^{*2}^{*2} + .25^{*12}^{*4.125} / (.5^{*4}^{*2} + .25^{*12}) \\ &\equiv 2.91\end{aligned}$$

$$I = \text{Sum of } bh^3/12 + \text{Sum of AD}^2$$

$$= .5*4^3/12*2 + 12*.25^3/12 + 4*.91^2 + 3*1.2^2$$

$$= 13.1^{in^4}$$

$$\begin{aligned} Sy &= I / Y \\ &= 13.1''^4 / 2.91'' \\ &\equiv 4.5''^3 \end{aligned}$$

$$\begin{aligned}\phi M_n &= \phi S_{Fy} * S_y \\ &= .9 * 36 \text{ksi} * 4.5^{in^3} \\ &\equiv 130 \text{ kip} \geq 110 \text{ kip}\end{aligned}$$

Compact Check

Flanges

$$B/t = 3/.5$$

= 6

Flange Limit

.38 * sqrt (E/Fy)

$$= .38 * \sqrt{29000/36}$$

$$= 10.8$$

Flange Compact

Web

$$H/t = 11/.25$$

= 44

Web Limit

$$3.76 * \text{sqrt}(E/F_y)$$

$$= 3.76 * \sqrt{29000/36}$$

$$= 106.7$$

Web Compact

13A.13.2 Design of Anchor Bolts for Secondary Anchors

The uphill and downhill actions of the out-of-hill lateral loading will create different forces in the anchor bolts. We will go through the different directions to collect all the forces in the anchor bolts.

Force in the uphill direction will create compression on the top of the stem wall and create a tension force in the bolts in the bottom of the stem wall.

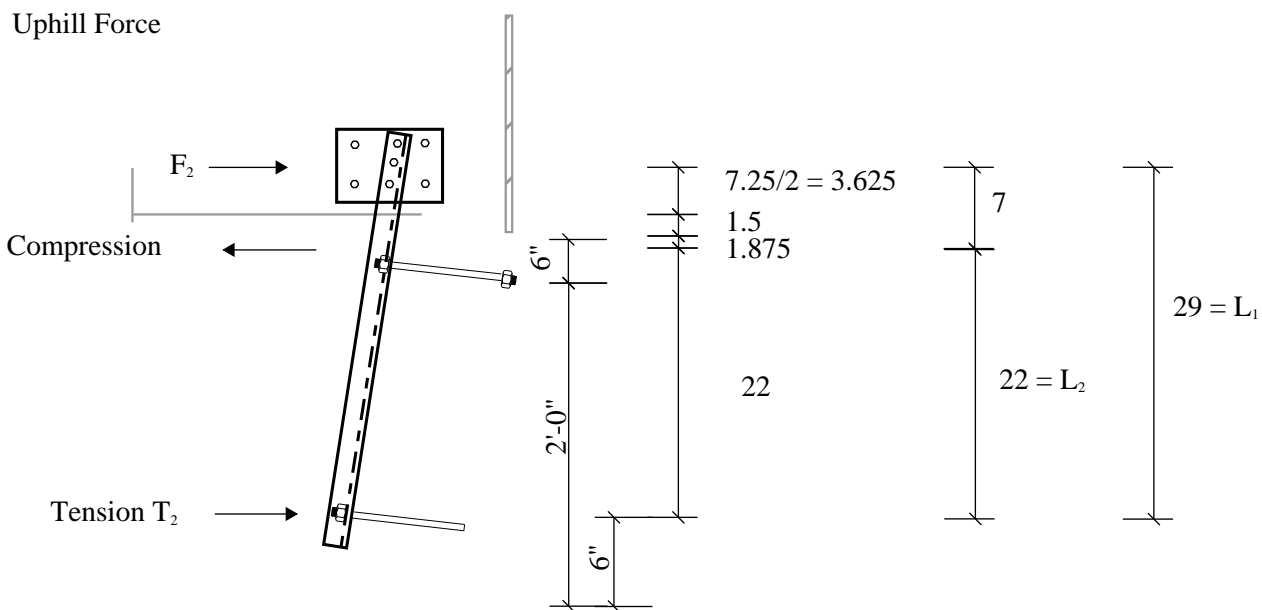


Figure 13A-33 Secondary anchor uphill force diagram

$$\text{Compression} = F_2 * L_1 / L_{12}$$

$$T_2 = C - F_2$$

$$= (F_2 * L_1 / L_{12}) - F_2$$

$$= 12.2 \text{ k} * (29" / 22" - 1)$$

$$= 3.9 \text{ k}$$

Notes

The secondary anchor force (F_2) is assumed to act at the centroid of the joist.

The Tension forces are dependent on the geometry of the section, some exploration of the existing will be required find the dimensions of the existing foundation.

The anchor bolts and built up section shall be protected from the environment as required by the IBC
For this example we will use A193-B8 class 2 stainless steel, AISI 304

The force in the downhill direction will create compression on the bottom of the stem wall (due to prying action) and will create a tension force in the top of the stem wall.

Downhill force

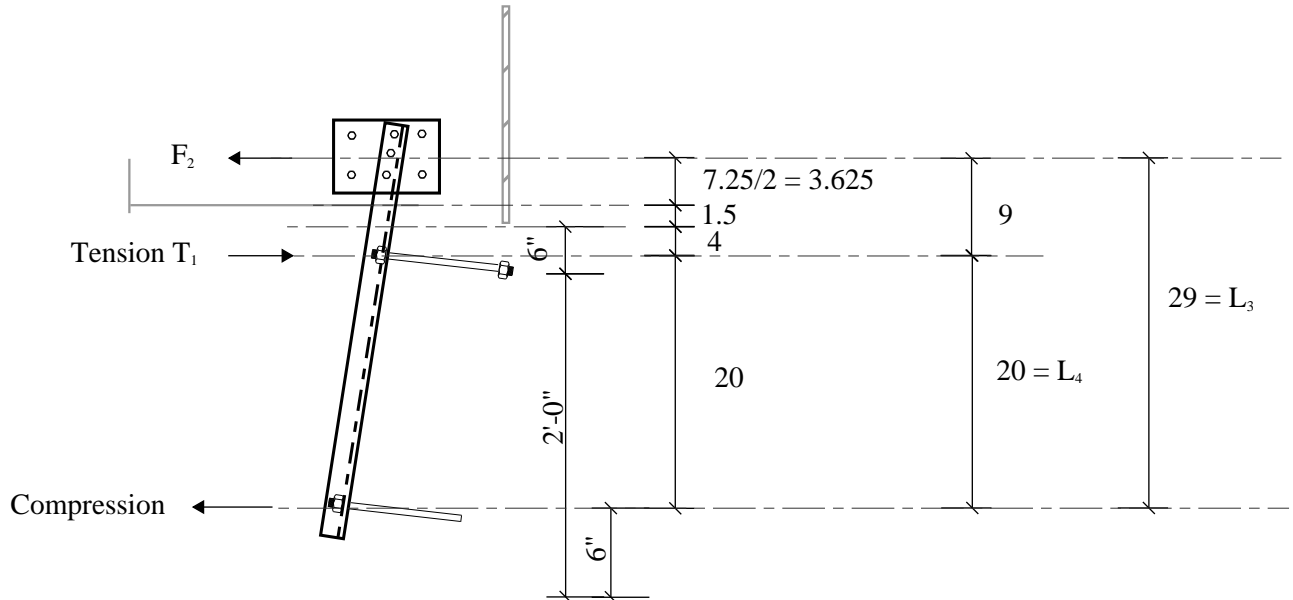


Figure 13A-34 Secondary anchor downhill force diagram

$$\begin{aligned}\text{Tension} &= F_2 * L_3 / L_4 \\ &= 12.2 \text{ k} * 29" / 20" \\ &= 17.7 \text{ k}\end{aligned}$$

Summary of Secondary anchor forces
The anchor forces due to both uphill and downhill forces create tension in the top anchor bolts of 17.7k and a tension in the bottom anchor bolts of 3.9k. Since these forces will need to be checked in combination with the shear anchor forces we will check the anchor bolts in the next section (Section 13A.14)

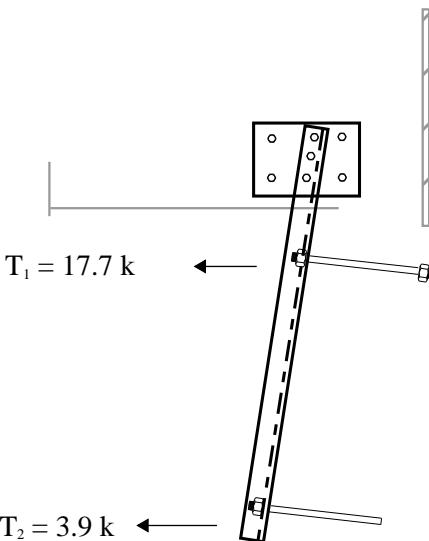


Figure 13A-35 Secondary anchor force summary

13A.13.3 Check Floor Joists for Secondary Anchor Force

The existing joists are 2x8 @ 16"

The floor dead load is 12 psf from the assembly weight in Section 13A.6.

The length of joists are 10 feet

The axial load due to out-of-hill lateral loading is shown in the figure below.

For point 1 (see Figure 13A-36) use (2) 2x8 DFL-2 each side of the channel anchor.

Use Section 3.9.2 of the NDS to check the capacity of the existing floor joists

$$(f_c/F'_c)^2 + f_b/(F'_b(1-(f_c/F_{cE1}))) \text{ and } f_c/F_{cE2} + (f_b/F_{bE})^2$$

$$\begin{aligned} f_c &= P / A \\ &= 12200\# / 2 * 1.5" * 7.25" \\ &= 560 \text{ psi} \end{aligned}$$

$$\begin{aligned} F'_c &= F_c * C_p * 2.4 * .9 \\ C_p &= (1+(F_{cE}/F_c))/2c - ((1+(F_{cE}/F_c))/2c)^2 - F_{cE}/F_c * c/c^{1/2} \\ F_{cE} &= 0.822 E_{min}' / (I_e/d)2 \\ I_e &= 1.33 \text{ in} \\ &= 1.33 * 10 \text{ ft} * 12 \text{ "/} \\ &= 160" \text{ (assume the beam is unbraced for} \\ &\quad \text{axial load, but braced continuously for bending)} \\ E_{min}' &= E_{min} * 1.76 * 0.85 \\ &= 580000 \text{ psi} * 1.76 * 0.85 \\ &= 867680 \text{ psi} \\ F_{cE} &= 0.822 * 867680 \text{ psi} / (160"/7.25")^2 \\ &= 1464 \text{ psi} \\ F_c^* &= F_c * 2.4 * .9 \\ &= 1350 \text{ psi} * 2.4 * .9 \\ &= 2916 \text{ psi} \\ F_{cE} / F_c^* &= 1464 \text{ psi} / 2916 \text{ psi} \\ &= .504 \\ c &= .8 \\ C_p &= (1+.504) / (2*.8) - ((1+.504) / (2*.8))^2 - .504/.8^{1/2} \\ &= 0.434 \\ F'_c &= 2916 \text{ psi} * .434 \\ &= 1266 \text{ psi} \end{aligned}$$

Continuation for checking drag for secondary anchor

$$(f_c/F'_c)^2 + f_b/(F'_b(1-(f_c/F_{ce}))) \text{ and } f_c/F_{ce} + (f_b/F_{be})^2$$

$$f_b = M_u / S$$

$$M_u = wl^2/8$$

$$= (1.2*12+1.6*40)*16/12 * 10^2/8$$

$$= 1307 \text{ lb-ft}$$

$$S = bd^2/6$$

$$= 1.5" * 7.252 "^2/6$$

$$= 13.1 "$$

$$f_b = 1307 \text{ lb-ft} * 12"/13.1" = 1194 \text{ psi}$$

$$F_{be} = 1.2 E_{min}' / R_b^2$$

$$R_b = (le*d/b^2)^{1/2}$$

$$= (12" * 7.25" / (1.5")^2)^{1/2}$$

$$= 6.218$$

$$F_{be} = 1.2 * 867680 \text{ psi} / 6.218^2$$

$$= 26930 \text{ psi}$$

$$F'_b = F_b * C_f * C_r * 2.54 * 0.85$$

$$= 900 \text{ psi} * 1.2 * 1.15 * 2.54 * 0.85$$

$$= 2681 \text{ psi}$$

$$f_c = 561 \text{ psi}$$

$$F_{ce} = 0.822 * E_{min}' / (le / d)^2$$

$$= 0.822 * 867680 \text{ psi} / (12" / (7.25"))^2$$

$$= 260342 \text{ psi}$$

$$(f_c/F'_c)^2 + f_b/(F'_b(1-(f_c/F_{ce})))$$

$$(561 \text{ psi} / 1269 \text{ psi})^2 + 1194 \text{ psi} / (2681 \text{ psi} * (1 - 561 \text{ psi} / 1464 \text{ psi}))$$

$$.195 + .721 = .916$$

$$f_c/F_{ce} + (f_b/F_{be})^2$$

$$(561 \text{ psi} / 1464 \text{ psi}) + (1194 \text{ psi} / 26930 \text{ psi})^2$$

$$.442 + .044 = .486$$

$0.92 < 1$ therefore (1) 2x8 each side of the channel anchor for point 1 is acceptable

Design the strap at point 2 due to the secondary anchor force described in Figure 13A-36

Tension at point 2 = 8.1 k over 2 beams

Tension per beam = $8.1 / 2 = 4.1$ k

Tension force in ASD = $4.1 * .7 = 2.9$ k

Use a coil strap to resist the tension force

Use Simpson CMSTC16 with (32) 0.148" diameter x 2

1/2" long nails over each beam

The allowable strap capacity = 3.1 k > 2.9 k

Tension at point 3 = 4.1 k over 2 beams

Tension per beam = $4.1 / 2 = 2.1$ k

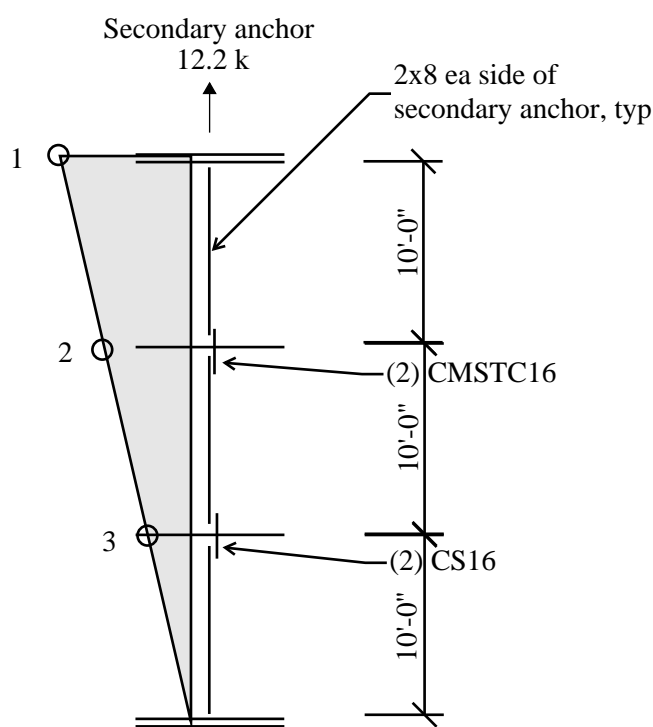
Tension force in ASD = $2.1 * .7 = 1.5$ k

Use a coil strap to resist the tension force

Use Simpson CS16 with (18) 0.148" diameter x 2 1/2" long

nails over each beam

The allowable strap capacity = 1.8 k > 1.5 k



Point	Force
1	12.2 K
2	$8.1 \text{ K} = 12.2 * 20 / 30$
3	$4.1 \text{ K} = 12.2 * 10 / 30$

Figure 13A-36 Secondary anchor collector diagram

13A.14. Design of Shear Anchors

13A.14.1 Design of Anchor Bolts for Shear Anchors

The next force applied to the anchor bolts is due to cross-slope loading.

Cross-slope shear force F_3 is 12.2 k from Section 13A.10

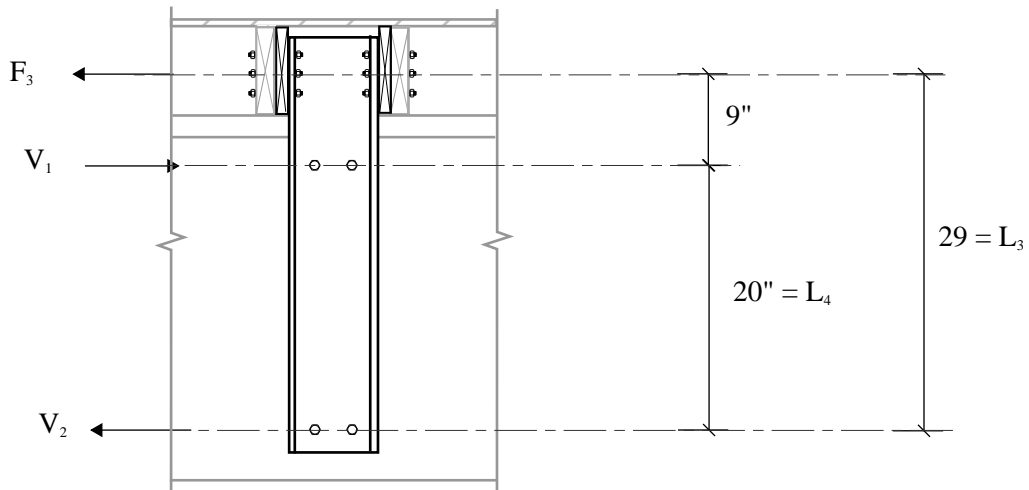


Figure 13A-37 Shear anchor elevation

$$\begin{aligned}V_1 &= F_3 * L_3 / L_4 \\&= 12.2 \text{ k} * 29'' / 20'' \\&= 17.7 \text{ k}\end{aligned}$$

13A.14.2 Check Bolts for Combined Shear and Tension

Check anchors in combined shear and tension due to a combination of secondary and shear anchor forces due to out-of-hill and cross-slope lateral forces, respectively.

The top anchor has a tension from out-of-hill loading of $17.7 \text{ K} / 2 = 8.7 \text{ K}$ and a shear force from cross-slope loading of $17.7 \text{ K} / 2 = 8.9 \text{ K}$.

Try 3/4" diameter threaded rod A193-B8 Class 2 Stainless Steel, AISI 304 $F_y = 100 \text{ ksi}$, $F_u = 125 \text{ ksi}$

Combined tension and shear bearing connection

$$\begin{aligned}\phi R_n &= \phi * F'_{nt} * A_b \\ F'_{nt} &= 1.3F_n - F_n/\phi F_{nv} * f_v \\ F_{nt} &= .75 * F_u \\ &= .75 * 125 \\ &= 93.8 \text{ ksi} \\ F_{nv} &= .4 * F_u \\ &= .4 * 125 \\ &= 50 \text{ ksi} \\ f_v &= V / A_g \\ &= 8.7 \text{ k} / (\pi * .75^2 / 4) \\ &= 19.7 \text{ ksi} \\ F'_{nt} &= 1.3 * 93.8 - 93.8 / (.75 * 50) * 19.7 \\ &= 72.7 \text{ ksi} \text{ (not to exceed } F_{nt} = 93.8 \text{ ksi)} \\ &= 72.7 \text{ ksi} \\ A_b &= \pi * d^2 / 4 \\ &= \pi * 1^2 / 4 \\ &= .785 \text{ in}^2 \\ \phi R_n &= .75 * 72.7 * .785 \text{ in}^2 \\ &= 42.8 \text{ k}\end{aligned}$$

Tension anchor capacity = 42.8 k > 8.7 k therefore anchor is adequate in tension.

Check anchor shear capacity

$$\phi R_u = \phi * F_{nv} * A_{SE}$$

$$\begin{aligned}\phi &= .75 \\ F_{nv} &= .4 * F_u \\ &= .4 * 125 \\ &= 50 \text{ ksi} \\ A_{SE} &= \pi / 4 * (D_{th} - .9743/n_t)^2 \\ &= \pi / 4 * (.75 - .9743/10)^2 \\ &= 0.334 \text{ in}^2\end{aligned}$$

$$\Phi R_u = .75 * 50 \text{ ksi} * 0.334 \text{ in}^2 = 12.5 \text{ k}$$

Shear anchor capacity = 12.5 k > 8.7 k therefore anchor is adequate in shear

Throughbolts shall be tight to the hole in order work in shear. The hole shall be oversized and filled with non-shrink grout.

13A.14.3 Check Concrete Pullout of Bolts

In the example dwelling we have run the top anchor bolts thru the stem wall because of insufficient embedment length. We will check for punching failure in the wall.

Concrete punching shear for two bolts

$$\phi P_n = \phi * 4 * (f_c)^{1/2} * b_o * d$$

$$\phi = .75$$

$$f_c = 2500 \text{ psi}$$

$$D = 8"$$

$$b_o = 2 * D/2 + S + D/2 + C_1$$

$$= 2 * 8"/2 + 6" + 8"/2 + 4"$$

$$= 22"$$

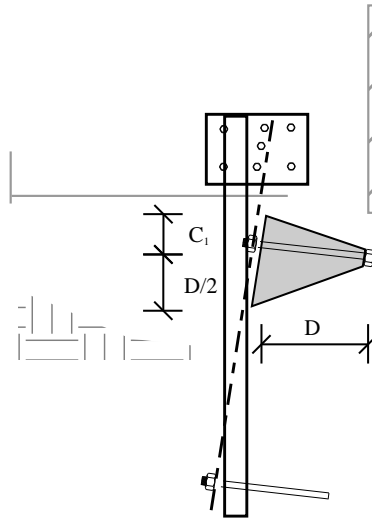
$$\phi P_n = .75 * 4 * (2500 \text{ psi})^{1/2} * 22" * 8" / 1000$$

$$= 26.4 \text{ k}$$

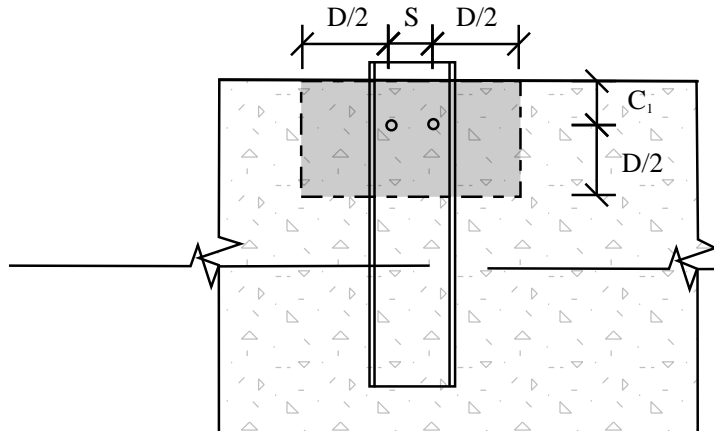
$\phi P_n = 26.4 \text{ k} > 17.7 \text{ k}$ therefore the stem wall is adequate for punching shear

note

if C_1 is smaller than $D/2$, the depth in the formula should be reduced to $2*C_1$



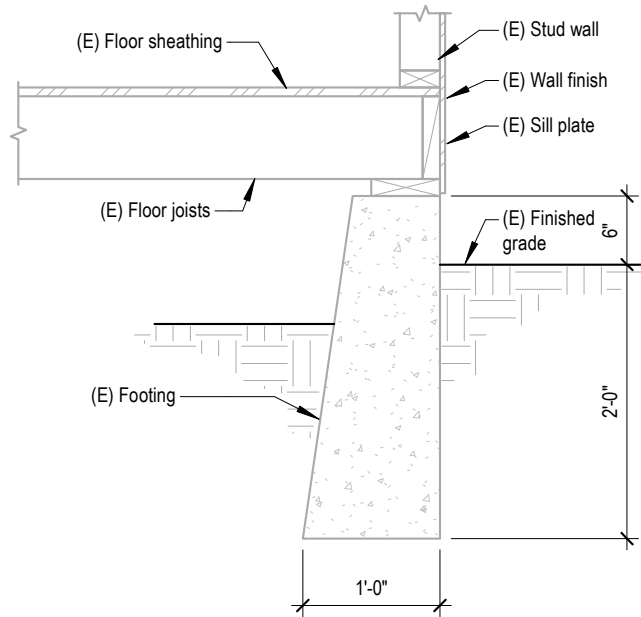
Section



Elevation

Figure 13A-38 Secondary anchor punching shear

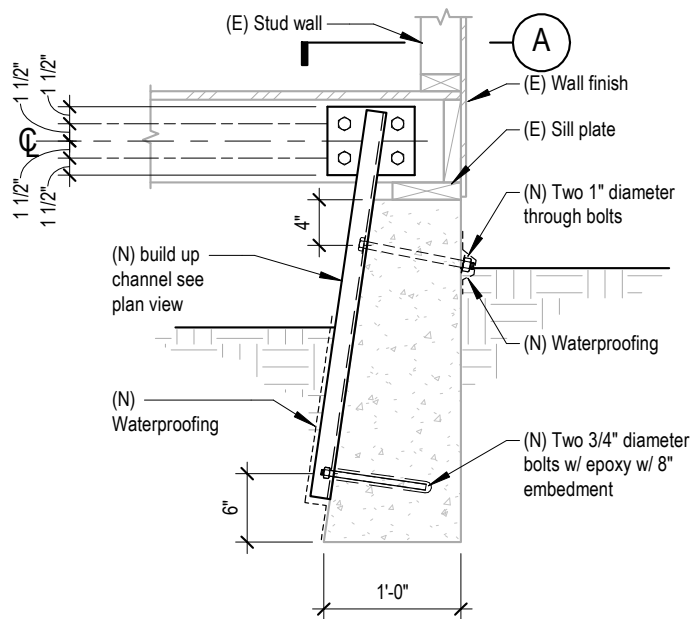
Following are some examples of secondary and shear anchor details



1 Existing section @ uphill foundation

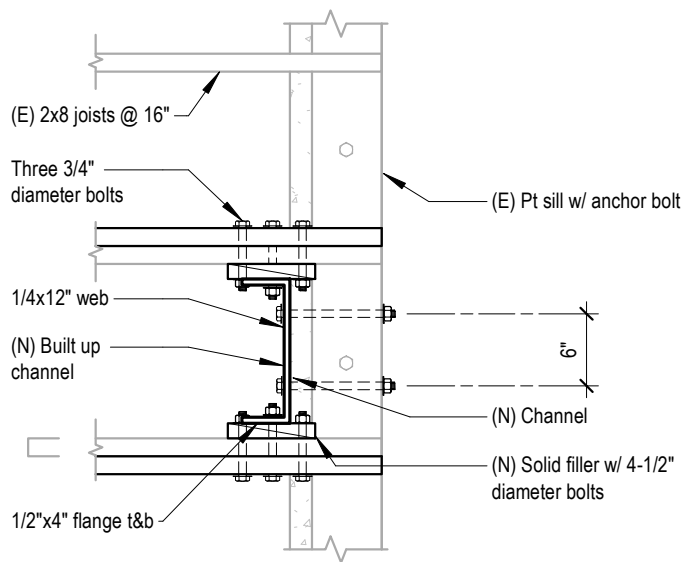
$\frac{3}{4}'' = 1'-0''$

Figure 13A-39 Existing uphill foundation detail



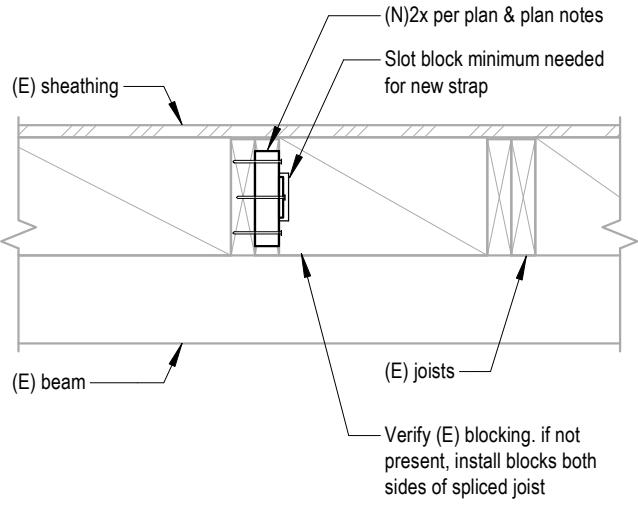
(1R) Retrofit section for secondary and shear anchor

3/4" = 1'-0"



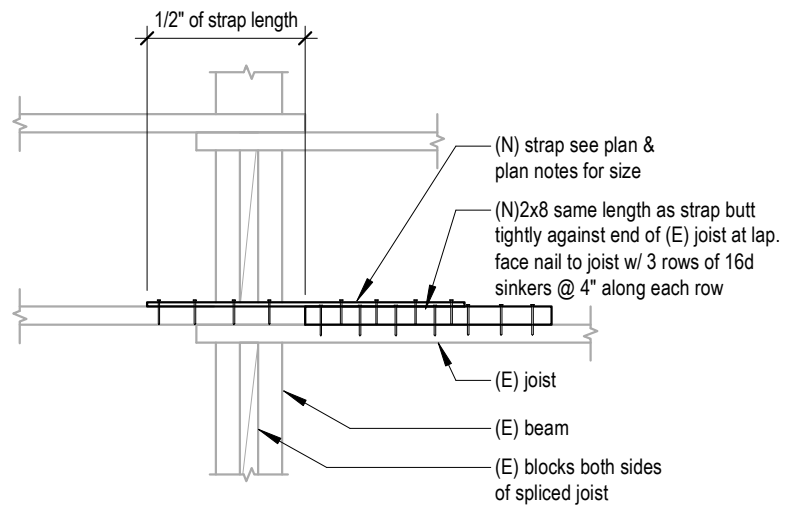
A Plan view

Figure 13A-40 Secondary and shear anchor detail



① Joist Splice Connection

3/4" = 1'-0"



A Plan view

Figure 13A-41 Secondary anchor collector detail

13A.15 Design of Crawlspace Walls

The sheathing of the crawlspace walls main purpose is to help the structural become more regular. This can be achieved by installing wood sheathing to the interior face of the wall and providing attachment to the base level diaphragm and to the foundation.

13A.15.1 Downhill Crawlspace Wall

The downhill crawlspace wall demand is 19 k from Section 13A.11.

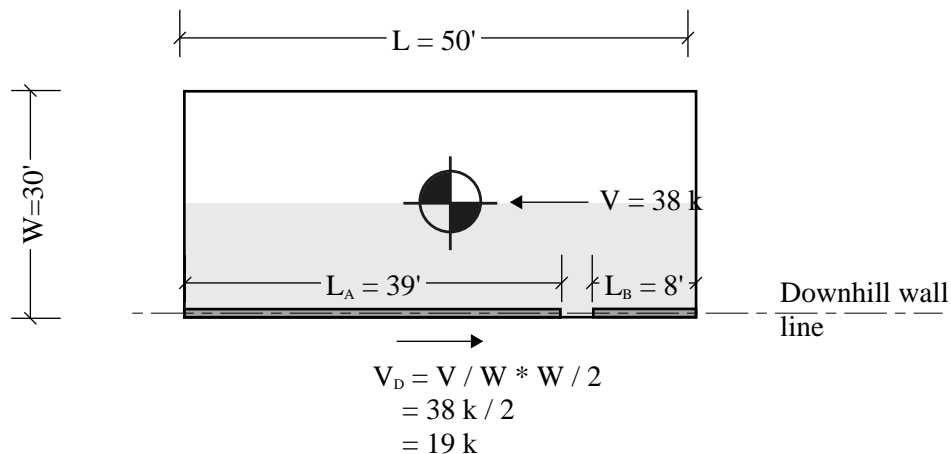


Figure 13A-42 Downhill crawlspace wall force diagram

Since there is door (3'-0" x 7'-0") in the wall, we will use the perforated shear wall method, see SDPWS 4.3.3.5.

$$C_o = (r/(3-2r) * (L_t / \Sigma L_i))$$

$$r = 1 / (1 + A_o / (h * \Sigma L_i))$$

$$= 1 / (1 + 3 \text{ ft} * 7 \text{ ft} / (16 \text{ ft} * 47 \text{ ft}))$$

$$= .973$$

$$C_o = (.973 / (3-2*.973) * (50 \text{ ft} / 47 \text{ ft}))$$

$$= .982$$

$$L_{EFF} = \Sigma L_i * C_o$$

$$= 47 \text{ ft} * .982$$

$$= 46 \text{ ft}$$

$$\text{unit shear (v)} = 19 \text{ k} / 46 \text{ ft} = 413 \text{ plf}$$

Use 15/32" Structural 1 sheathing with 8d common nails @ 4". The unit shear capacity is 860 plf * .8 = 688 plf which is greater than the demand of 413 plf.

13A.15.2 Side Crawlspace Wall

The side wall crawlspace wall demand is 15.8 k from Section 13A.11.

It is the Prestandard's intent to ignore the steps in the foundation and design the side stepped crawlspace shear walls using the design force divided by the length of the sum of cross slope walls along each line.

Side wall demand = 15.8 k

unit shear demand = $15.8 \text{ k} / 25 \text{ ft} = 632 \text{ plf}$

Use 15/32" Structural 1 sheathing with 8d common nails @ 4". The unit shear capacity is $860 * .8 = 688 \text{ plf}$ which is greater than the demand of 632 plf.

The Prestandard's intent is to provide some form of lateral resistance, without getting too caught up in the details, and is not meant to be a comprehensive design. If this was a new design, one would not be able to ignore the step in the foundation and would require the design to incorporate the steps in the foundation. The steps in the foundation cause the side wall to be designed as separate walls at each step. Since the heights are different for each wall, they will have different stiffness. Typically the differences in stiffness are so significantly different that it causes shortest wall to be required to resist the entire loading, since the other walls will not start resisting the load before the failure of the shortest wall.

For detailing of the crawlspace walls see Chapter 4 of the Prestandard.

13A.15.3 First Story Wall Above Uphill Foundation

Tie-downs are required at the first story walls above the uphill foundation per Prestandard Section 6.5.5, second to last paragraph. The tie-down strength needs to be equal to the smaller of the shear in the wall based on ASCE 7 Section 12.4 or 12.8 using $R = 4.0$ or the overturning strength capacity of the existing first floor shear wall above. We will review the overturning due to the strength capacity of the existing exterior wall.

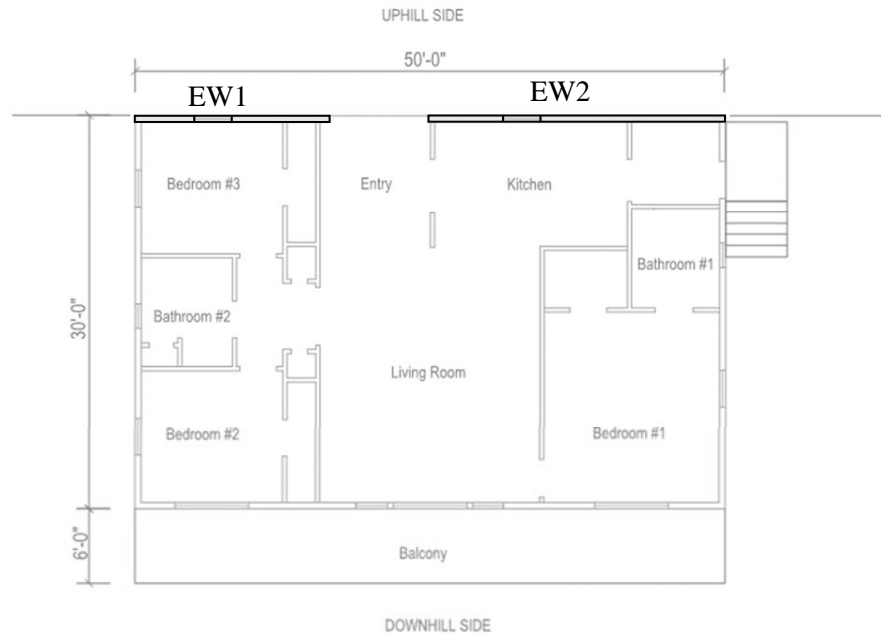


Figure 13A-43 Uphill superstructure wall location

Exterior wall 1 is 16.5 ft long. It has a 3'-0" x 3'-0" window in the bedroom, which is 5'-0" away from the edge of the wall. The existing unit shear capacity (v) is 350 plf per ASCE 41 Table 12-1.

Verify the effects of the 3' opening using perforated wall method specified in the SPDWS

$$C_o = (r/(3-2r)) * (L_t / \Sigma L_i)$$

$$\begin{aligned} r &= 1 / (1 + A_o / (h * \Sigma L_i)) \\ &= 1 / (1 + 3 \text{ ft} * 3 \text{ ft} / (9 \text{ ft} * 13.5 \text{ ft})) \\ &= .931 \end{aligned}$$

$$\begin{aligned} C_o &= (.931 / (3-2*.931)) * (16.5 \text{ ft} / 13.5 \text{ ft}) \\ &= 1.0 \end{aligned}$$

$$\begin{aligned} L_{eff} &= \Sigma L_i * C_o \\ &= 13.5 \text{ ft} * 1 \\ &= 13.5 \text{ ft} \end{aligned}$$

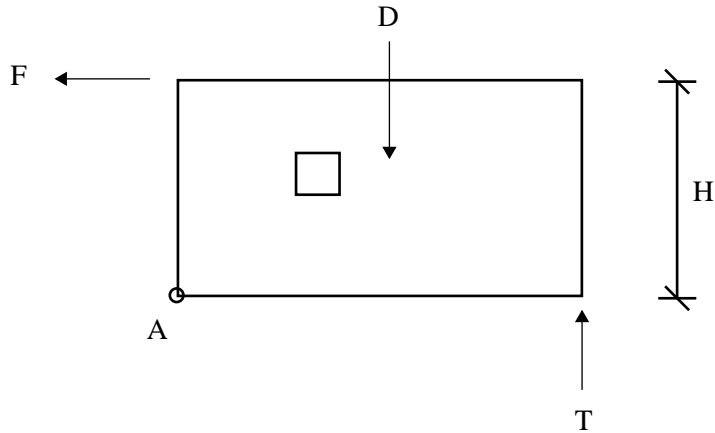


Figure 13A-44 Exterior wall 2 elevation

Solve for the wall uplift by summing moments at point A in Figure 13A-44

$$\begin{aligned}
 F &= \text{force of exterior shear wall using existing wall capacity} \\
 &= 350 \text{ plf} * 13.5 \text{ ft} \\
 &= 4725 \text{ pounds (expected force level)}
 \end{aligned}$$

$$\begin{aligned}
 D &= \text{wall self weight} \\
 &= 23 \text{ psf} * 9 \text{ ft} * 16.5 \text{ ft} \\
 &= 2795 \text{ pounds}
 \end{aligned}$$

$$\begin{aligned}
 T &= (F * H - D * L / 2) / L \\
 &= (4725 \text{ lb} * 9 \text{ ft} - 2795 \text{ lb} * 16.5 \text{ ft} / 2) / 15.5 \text{ ft} \\
 &= 1256 \text{ pounds (expected force level)}
 \end{aligned}$$

Use a factor of 3 to get the expected force into a ASD level for the purposes of specifying tie-down hardware, this is due to the assumption that the testing requirements for the manufacturer are on the order of 3.

$$T = 1256 \text{ lbs} / 3 = 420 \text{ lbs}$$

Use Simpson HD2 at each end of the exterior wall. The tie-down capacity of the HD2 = 3075# > 420#



FEMA

FEMA P-1100-3